



Cardiff School of Pharmacy and Pharmaceutical Sciences
Cardiff University

Synthesis and Biological Evaluation of Novel Nucleosides and Nucleotides as Potential Therapeutic Agents

A thesis submitted *in accordance with the conditions governing
candidates* for the degree of
Philosophiae Doctor in Cardiff University

Valentina Ferrari

Supervisor: Prof. C. McGuigan

Supervisor: Dr. A. Brancale

September 2015

DECLARATION

This work has not been submitted in substance for any other degree or award at this or any other university or place of learning, nor is being submitted concurrently in candidature for any degree or other award.

Signed ...*Valentina Ferron*... (candidate) Date 15.1.2016

STATEMENT 1

This thesis is being submitted in partial fulfillment of the requirements for the degree of PhD.

Signed...*Valentina Ferron*... (candidate) Date 15.1.2016

STATEMENT 2

This thesis is the result of my own independent work/investigation, except where otherwise stated.

Other sources are acknowledged by explicit references. The views expressed are my own.

Signed ...*Valentina Ferron*... (candidate) Date 15.1.2016

STATEMENT 3: PREVIOUSLY APPROVED BAR ON ACCESS

I hereby give consent for my thesis, if accepted, to be available for photocopying and for inter-library loans after expiry of a bar on access previously approved by the Academic Standards & Quality Committee.

Signed ...*Valentina Ferron*... (candidate) Date 15.1.2016

Acknowledgements

I would like to thank my supervisor Prof. Chris McGuigan for the possibility he gave me to be part of his research team, and for all that I have learnt from him throughout my PhD.

Thanks to NuCana and the President Research Scholarship for funding.

I am thankful to my second supervisor Dr. Andrea Brancale, and to Marcella and Salvo for their support with the molecular modelling.

My sincere thanks to Prof. Chris Pepper for his help with the in vitro biological assays on KG1a cell line.

Thanks to Helen and Julie for their guidance and support.

I will never thank my friends Michaela and Fabrizio enough for all the precious help and teachings they have given me in these three years, and for having contributed in making this experience more enjoyable.

Thanks to Chiara, Jenny, Davide, Silvia, Marco, Marcella, Michela, Salvo and Karen, and all the people I met during my PhD and enriched my life with their beautiful friendship.

And finally thank you to my family who were always there and supported me during these years, and especially to Rob for his patience, friendship and love.

Abstract

Nucleoside analogues are an important class of antimetabolites, used both as anticancer and antiviral agents for their resemblance to endogenous nucleosides, and their capacity to inhibit metabolic pathways in which these substrates are involved, leading to therapeutic potential. The need for both new anticancer and antiviral cures is significant, and often caused by the emergence of resistance to the available therapies. In the case of therapies with nucleoside analogues, the delivery of a nucleoside monophosphate prodrug inside the cell has potential to overcome resistance to treatment, and proved successful especially with the application of the ProTide approach. This strategy led to the progression into clinical trials of numerous antiviral and anticancer agents.

This work focused on the synthesis of novel ProTide prodrugs to different nucleoside analogues that are involved in clinical trials, such as cordycepin, 8-chloroadenosine, CNDAC and the recently approved agent trifluorothymidine. This strategy was also applied to 2'-mercapto-2'-deoxyuridine and 2'-trifluoromethyl-2'-deoxyuridine, whose *in vitro* evaluation has never been reported. The synthetic strategies to prepare each nucleoside analogue are also reported.

The *in vitro* evaluation of novel nucleotide prodrugs as anticancer and antiviral agents is described and discussed. Moreover the mechanism of activation of the ProTides is supported by studying their bioactivation to the corresponding monophosphate forms, through enzymatic NMR studies and molecular modeling simulations.

Modifications on the scaffold of the two most promising families of ProTides of cordycepin and 8-chloroadenosine were also performed, leading to the introduction of groups on the nucleobase or alteration of the sugar moiety. Moreover, the phosphate group was also modified, with the application of alternative phosphorodiamidate and phosphonoamidate prodrug approaches, with the aim of improving the biological profile.

Cordycepin and 8-chloroadenosine families of compounds emerged as the most potent prodrugs. Selected analogues from these two families were evaluated on resistant cancer cell lines, retaining better potency compared to the parent nucleoside. Moreover these analogues are stable in human plasma, serum and liver microsomes. Furthermore, the most promising ProTides showed selective targeting of the stem cell population of the KG1a leukaemic cell line.

Finally, two candidates in the cordycepin family of ProTides were tested *in vivo* on a mouse model of human non-Hodgkin lymphoma, leading to promising results.

Further investigations on these analogues are currently ongoing.

Table of Contents

1	Nucleoside analogues as anticancer agents	1
1.1	The structure of endogenous nucleosides.....	1
1.2	Modified nucleoside analogues as therapeutic agents.....	2
1.2.1	Mechanism of action of nucleoside analogues.....	2
1.2.2	Anticancer nucleoside analogues	4
1.2.3	Antiviral nucleoside analogues	7
1.3	Resistance and limitations to nucleoside analogue treatment.....	8
1.4	Strategies to overcome NA resistance.....	9
1.5	Monophosphate prodrugs.....	10
1.5.1	Bis(POM) and Bis(POC) approach	10
1.5.2	Bis(SDTE)- and Bis(SATE) Approach	11
1.5.3	CycloSal approach.....	12
1.5.4	Phospholipid conjugates approach	13
1.5.5	HepDirect approach.....	14
1.5.6	Phosphoramidate diester approach.....	14
1.5.7	Aryloxy phosphoramidate approach	15
1.5.8	Cyclic phosphate prodrugs	18
1.5.9	Phosphorodiamidate approach	19
1.6	Summary of the phosphate prodrug technologies.....	20
1.7	Aim of the work.....	21
2	Synthesis of nucleotide prodrugs	23
2.1	ProTide synthesis.....	23
2.1.1	Phosphorodichloridate synthesis	24
2.1.2	Amino acid ester synthesis	26
2.1.3	Phosphorochloridate synthesis	27
2.2	Phosphoramidate synthesis	28
2.3	Phosphorodiamidate synthesis	29
3	3'-Deoxyadenosine analogues.....	31
3.1	3'-Deoxyadenosine prodrugs.....	31
3.1.1	Background	31
3.1.2	Synthesis of 3'dA	34
3.1.3	Prodrug synthesis	40
3.1.3.1	Synthesis of 3'dA ProTides.....	40

3.1.3.2	Synthesis of 3'dA phosphorodiamidates	44
3.1.4	Biological evaluation of 3'dA prodrugs	45
3.1.4.1	<i>In vitro</i> cytotoxic screening of 3'dA prodrugs	45
3.1.4.2	Antiviral screening on 3'dA derivatives.....	49
3.1.4.3	Additional cytotoxic screening of 3'dA prodrugs	50
3.1.4.4	<i>In vitro</i> screening of 3'dA ProTides on additional cell lines	51
3.1.4.5	Evaluation of intracellular 3'dA triphosphate levels after treatment with 3'dA ProTides	54
3.1.4.6	Selective cytotoxicity of 3'dA analogues on cancer stem cells.....	56
3.1.4.6.1	The concept of cancer stem cells (CSCs)	56
3.1.4.6.2	Characterisation of KG1a stem cell phenotype	58
3.1.4.6.3	Analysis of LSC targeting after treatment with 3'dA and relative ProTides at the LD ₅₀ concentration	59
3.1.4.6.4	Analysis of LSC targeting after treatment with 3'dA and relative ProTides at a range of concentrations.....	61
3.1.4.6.5	Effect of 3'dA and ProTides on β -catenin levels of the KG1a cell line	
	62	
3.1.5	Mechanistic investigations on the metabolic activation of 3'dA derivatives..	65
3.1.5.1	Carboxypeptidase Y (CPY) enzymatic NMR assay.....	65
3.1.5.1.1	Enzymatic CPY processing of 3'dA 5'-phosphoroamidates	65
3.1.5.1.2	Enzymatic experiment on 2'-phosphoramidate.....	68
3.1.5.1.3	Enzymatic experiment on diamidate	71
3.1.5.2	Docking studies.....	73
3.1.5.2.1	Docking of compounds in the active site of Hint-1	73
3.1.6	Stability studies.....	75
3.1.6.1	Stability to adenosine deaminase-mediated catabolism	75
3.1.6.1.1	UV assay.....	75
3.1.6.1.2	Docking within the ADA active site.....	76
3.1.6.2	Stability of 3'dA ProTides in Mice and Human plasma	77
3.1.6.3	3'dA ProTides stability in human hepatocytes	80
3.1.7	Conclusions	81
3.2	2-Modified cordycepin analogues and their prodrugs	83
3.2.1	Background.....	83
3.2.2	Synthesis of 2-fluorocordycepin.....	84
3.2.3	Synthesis of 2-modified cordycepin ProTides.....	93

3.2.4	Cytotoxic <i>in vitro</i> screening	95
3.2.4.1	In vitro evaluation of 2F3'dA ProTides.....	95
3.2.4.2	In vitro screening of 2(CH ₃ O)3'dA ProTides	98
3.2.4.3	Leukaemic stem cells selectivity.....	100
3.2.5	Adenosine deaminase (ADA) stability of 2-modified 3'dA analogues	102
3.2.5.1	ADA UV assay	102
3.2.5.2	Docking of 2-modified 3'dA analogues within the ADA active site..	103
3.2.6	Mechanistic investigations	104
3.2.6.1	Enzymatic NMR experiments.....	104
3.2.6.2	Docking studies	106
3.2.7	Conclusions	107
3.3	Further preclinical investigations on 3'dA and 2F3'dA prodrugs	109
3.3.1	Separation of isomers of ProTides 30a and 49b.....	109
3.3.1.1	Rationale behind diastereoisomer separation	109
3.3.1.2	Attempt to separate diastereoisomers via silylation/desilylation methods	110
3.3.1.3	Separation of ProTides 30a and 49b diastereoisomers via reverse phase chromatography.....	112
3.3.2	<i>In vitro</i> testing of separated isomers	117
3.3.3	<i>In vivo</i> evaluation of ProTides 30a and 49b in a lymphoma mouse xenograft	119
3.3.4	Stability NMR assays	123
3.3.5	Conclusions	125
3.4	5'-Modified 3'dA prodrugs	126
3.4.1	Introduction on rationale for 5'-modification	126
3.4.2	Synthesis of 5'-modified 3'dA ProTides	127
3.4.2.1	Attempts to introduce an alkyl group in the 5'-position.....	127
3.4.2.2	Synthesis of phosphonate bond containing analogue of ProTide 32a	129
3.4.3	Biological evaluation.....	133
3.4.4	Mechanistic studies	135
3.4.5	Conclusions	137

4	8-Chloroadenine nucleoside derivatives	139
4.1	8-Chloroadenosine	139
4.1.1	Background.....	139
4.1.2	Preliminary biological evaluation of 8ClA ProTides	142
4.1.3	Synthesis of 8ClA	144
4.1.4	Synthesis of 8ClA prodrugs.....	146
4.1.4.1	8ClA phosphoramidates.....	146
4.1.4.2	8ClA phosphorodiamidates.....	147
4.1.5	Biological evaluation of 8ClA prodrugs.....	148
4.1.5.1	Cytotoxic screening of the newly synthesised 8ClA prodrugs	149
4.1.5.2	Cytotoxic screening of 8ClA prodrugs on a broader panel of malignant cell lines.....	151
4.1.5.3	Biological evaluation of selected ProTides on resistant cell lines....	156
4.1.5.4	ATP assay on 8ClA ProTides	159
4.1.6	8ClA and prodrug stability	162
4.1.6.1	8ClA ProTides stability in plasma.....	162
4.1.6.2	8ClA ProTide stability in human hepatocytes.....	163
4.1.7	Evaluation of 8ClA ProTides on the CSC compartment of the KG1a cell line	163
4.1.8	Mechanistic investigations	165
4.1.8.1	CPY NMR assays	166
4.1.8.2	Molecular modelling studies.....	168
4.1.8.2.1	Docking of ProTides in the active site of CPY	168
4.1.8.2.2	Docking of compounds in the active site of Hint-1.....	170
4.1.9	Conclusions	172
4.2	5'-Modified 8-chloroadenosine analogues.....	174
4.2.1	Rationale behind the 5'-modification on 8ClA ProTides.....	174
4.2.2	Synthesis of 8ClA phosphonate ProTides	175
4.2.3	Biological evaluation.....	176
4.2.4	Mechanistic studies.....	178
4.2.5	Conclusions	180
4.3	8-Chloro-2'-deoxyadenosine	181
4.3.1	Background.....	181
4.3.2	Synthesis of 8-chloro-2'-deoxyadenosine	182
4.3.3	Synthesis of 8ClA prodrugs.....	183

4.3.3.1	Schwartz's reagent as dephosphorylating agent.....	186
4.3.4	Cytotoxic <i>in vitro</i> screening of 8CIdA prodrugs.....	187
4.3.5	Mechanistic investigations.....	191
4.3.5.1	Docking in CPY active site.....	191
4.3.5.2	Docking in Hint active site.....	193
4.3.6	Conclusions.....	194
5	CNDAC.....	195
5.1	Background.....	195
5.2	Synthesis of CNDAC.....	198
5.3	Synthesis of sapacitabine (CYC682).....	203
5.4	Synthesis of CNDAC ProTides.....	204
5.5	<i>In vitro</i> anticancer screening of CNDAC ProTides.....	207
5.6	Mechanistic investigations.....	209
5.6.1	CPY enzymatic assay.....	210
5.6.2	Docking in the active site of Hint1.....	210
5.7	Conclusions.....	211
6	Trifluorothymidine ProTides.....	213
6.1	Background.....	213
6.2	Synthesis of TFT ProTides.....	216
6.3	Biological evaluation.....	218
6.4	Mechanistic investigations on TFT ProTides.....	220
6.4.1	CPY enzymatic assay.....	220
6.5	Docking in the Hint enzyme.....	221
6.6	Biological evaluation on HSV infected cells.....	222
6.7	Conclusions.....	223
7	2'-SCF₃ deoxyuridine and 2'-SH deoxyuridine.....	225
7.1	Background.....	225
7.2	Synthesis of nucleosides 2'-SH-2'-dU and 2'-SCF₃-2'-dU.....	227
7.3	Synthesis of 2'-SCF₃-2'-dU and 2'-SH-2'-dU ProTides.....	230
7.3.1	Synthesis of 2'-SCF ₃ -2'-dU ProTides.....	230
7.3.2	Synthesis of 2'-SH-2'-dU prodrugs.....	231
7.4	Biological evaluation of 2'-SCF₃-2'-dU ProTides.....	234
7.4.1	<i>In vitro</i> cytotoxicity assay.....	234
7.4.2	Mechanistic investigations.....	235

7.4.2.1	Enzymatic CPY experiment	235
7.4.2.2	Docking into Hint active site	237
7.5	Biological evaluation of 2'-SH-2'-dU ProTides.....	238
7.5.1	<i>In vitro</i> cytotoxicity evaluation.....	238
7.5.2	Mechanistic investigations on the processing of 2'-SH-2'-dU derivatives...	241
7.5.2.1	CPY docking of ProTide 120a in CPY.....	242
7.5.2.2	CPY docking of 2'-SH-2'-dU intermediate 120a ^c in Hint.....	243
7.6	Conclusions.....	243
8	Conclusions.....	245
9	Experimental part.....	246
9.1	General experimental details.....	246
9.2	Molecular modelling studies	247
9.3	Enzymatic and stability assays	248
9.3.1	Carboxypeptidase Y assay	248
9.3.2	Adenosine deaminase UV assay.....	248
9.3.3	Serum stability assay	249
9.3.4	KG1a cell culture conditions	249
9.3.5	Measurement of <i>in vitro</i> apoptosis	249
9.3.6	Immunophenotypic identification of the leukaemic stem cell compartment	250
9.3.7	Identification of β -catenin levels in the leukaemic stem cell compartment..	250
9.4	Standard synthetic procedures.....	250
9.4.1	Standard procedure A ₁ for synthesis of amino acid esters hydrochloride salt	250
9.4.2	Standard procedure A ₂ for synthesis of amino acid esters <i>p</i> -toluene sulfonate salt	250
9.4.3	Standard procedure B for synthesis of aryl phosphorodichloridate	251
9.4.4	Standard procedure C for synthesis of aryl amino acid ester phosphorochloridates from amino acid hydrochloride or <i>p</i> -toluene sulfonate salt ...	251
9.4.5	Standard procedure D for the synthesis of 2',3'-anhydrous adenosine analogues	251
9.4.6	Standard procedure E for the synthesis of 3'-deoxyadenosine analogues...	252
9.4.7	Standard procedure F ₁ for the synthesis of ProTides	252
9.4.8	Standard procedure F ₂ for the synthesis of ProTides	253
9.4.9	Standard procedure G for the synthesis of phosphorodiamidates.	253

9.5	Experimental details	254
9.5.1	Synthesis of aryl alcohol	254
9.5.2	Synthesis of aryl phosphorodichloridates	254
9.5.3	Synthesis of amino acid ester salts	255
9.5.4	Synthesis of aryl amino acid phosphorochloridates	258
9.5.5	Synthesis of 3'-deoxyadenosine	266
9.5.6	Synthesis of 3'-deoxyadenosine prodrugs	268
9.5.7	Synthesis of 2'-modified 3'-deoxyadenosine analogues	280
9.5.8	Synthesis of 2'-fluoro-3'-deoxyadenosine ProTides	284
9.5.9	Synthesis of 2'-methoxy-3'-deoxyadenosine ProTides	289
9.5.10	Synthesis of 5'-modified 3'-deoxyadenosine analogues	293
9.5.11	Synthesys of 8-chloroadenosine	302
9.5.12	Synthesis of 8-chloroadenosine ProTides	304
9.5.13	Synthesis of 5'-modified 8-chloroadenosine analogues	323
9.5.14	Synthesis of 8-chloro-2'-deoxyadenosine	327
9.5.15	Synthesis of 8-chloro-2'-deoxyadenosine prodrugs	329
9.5.16	Synthesis of CNDAC and sapacitabine	338
9.5.17	Synthesis of CNDAC ProTides	343
9.5.18	Synthesis of TFT ProTides	350
9.5.19	Synthesis of 2'-SCF ₃ -2'-deoxyuridine and 2'-SH-2'-deoxyuridine	357
9.5.20	Synthesis of 2'-SCF ₃ -2'-dU ProTides	359
9.5.21	Synthesis of 2'-SH-2'-dU ProTide dimers	363
10	References	367

Abbreviations

- 1-Naph	1-Naphthyl
- 2(CH ₃ O)3'dA	2-Methoxy-3'-deoxyadenosine
- 2'-C-Me-C	2'-C-methylcytidine
- 2'-C-Me-G	2'-C-methylguanine
- 2'-SCF ₃ -2'-dU	(2'-trifluoromethylthio-2'-deoxyuridine)
- 2'-SH-2'dU	2'-mercapto-2'-deoxyuridine
- 2F3'dA	2-Fluoro-3'-deoxyadenosine
- 3'dA	3'-deoxyadenosine, cordycepin
- 3'dAMP	3'-deoxyadenosine-5'-monophosphate
- 3'dATP	3'-deoxyadenosine-5'-triphosphate
- 3'dIno	3'-deoxyinosine
- 3TC	Lamivudine
- 5'-NT	5'-nucleotidase
- 5FU	5-fluorouracil
- 6-MP	6-mercaptopurine
- 8ClA	8-Chloroadenosine
- 8ClIdA	8-Chloro-2'-deoxyadenosine
- 8ClIno	8-Chloroinosine
- A-134974	N ⁷ -[(1'R,2'S,3'R,4'S)-2',3'-dihydroxy-4'-iodopyrrolopyrimidine dihydrochloride
- ABC	Abacavir
- ACV	Acyclovir
- ADA	Adenosine deaminase
- Ade	Adenine
- AMPK	Adenylate kinase
- Ado	Adenosine
- ADP	Adenosine diphosphate
- AK	Adenosine kinase
- AMPK	Adenosine monophosphate kinase
- Ara-C	Cytarabine
- Ara-G	9-β-D-Arabinofuranosyl guanine

- ATP	Adenosine triphosphate
- AZT	zidovudine
- Bn	Benzyl
- BNF	British national formulary
- BSA	<i>N,O</i> -bis(trimethylsilyl)acetamide
- cAMP	Cyclic adenosine monophosphate
- catA	Cathepsin-A
- CDA	Cytidine deaminase
- cGMP	Cyclic guanosine monophosphate
- cHex	Cyclohexyl
- CMV	Cytomegalovirus
- CNDAC	2'- <i>C</i> -cyano-2'-deoxy-1- β -D- <i>arabino</i> - pentofuranosylcytosine
- CNDAU	2'- <i>C</i> -cyano-2'-deoxy-1- β -D- <i>arabino</i> - pentofuranosyluridine
- CPE	Cytophatic effect
- CPY	Carboxypeptidase Y
- CSC	Cancer Stem Cells
- Cyd	Cytidine
- Cyt	Cytosine
- CV	Column volumes
- d4T	Stavudine
- dAdo	2'-Deoxyadenosine
- dCF	Deoxycoformycin, pentostatin
- dCK	Deoxycytidine kinase
- DCM	Dichloromethane
- dCyt	2'-Deoxycytidine
- ddAMP	Dideoxyadenosine monophosphate
- ddATP	Dideoxyadenosine triphosphate
- ddI	Didanosine
- DDQ	2,3-Dichloro-5,6-dicyano-1,4- benzoquinone)
- ddU	Dideoxyuridine
- dGK	Deoxyguanosine kinase

- dGuo	2'-Deoxyguanosine
- DIPEA	Diisopropyl ethyl amine
- DLP	Dilauroyl peroxide
- DMA	Dimethylacetamide
- DMAP	Dimethylamino pyridine
- DMF	Dimethylformamide
- DMG	Dimethylglycine
- DMP	Dess-Martin periodinane
- DNA	Deoxyribonucleic acid
- dNTP	Deoxynucleoside triphosphate
- DTT	Dithiothreitol
- dTTP	Thymidine triphosphate
- dUTP	Deoxyuridine triphosphate
- ED ₅₀	Median effective dose
- EHNA	Erythro-9-(2-hydroxy-3-nonyl) adenine
- ES/MS	Electrospray mass spectrometry
- Et	Ethyl
- EtOAc	Ethyl acetate
- EtSCSCL	Ethyl chlorodithioformate
- ETV	Entecavir
- FAD	Flavin adenine dinucleotide
- FCV	Famciclovir
- FDA	Food and Drug Administration
- FdT	3'-Fluoro-3'-deoxythymidine
- FE	Fast eluting
- FTC	Emtricitabine
- FUdR	Floxuridine
- GCV	Ganciclovir
- Gly	Glycine
- Gua	Guanine
- Guo	Guanosine
- HBV	Hepatitis B virus
- HCV	Hepatitis C virus

- hENT transporter 1	Human equilibrative nucleoside
- Hint	Hystidine triad nucleoside-binding protein
- HSV	Herpes simplex virus
- <i>i</i> Bu	Isobutyl
- IBX	2-Iodoxybenzoic acid
- IPA	Isopropanol
- L-Ala	L-Alanine
- LD ₅₀ viability	50% Inhibitory concentration of cell
- LDA	Lithium diisopropyl amide
- L-Leu	L-leucine
- L-Phe	L-phenylalanine
- LSC	Leukemic Stem Cells
- MDS	Myelodisplastic syndrome
- Me	Methyl
- <i>m</i> CPBA	<i>meta</i> -chloroperbenzoic acid
- MHz	Mega Hertz
- NAD	Nicotinamide adenine dinucleotide
- NBTI	S-(4-Nitrobenzyl)-6-thioinosine
- NCS	N-chlorosuccinimide
- NDPK	Nucleoside diphosphate kinase
- NDPK	Nucleoside diphosphate kinase
- NDPK	Nucleoside diphosphate kinase
- Neop	Neopentyl
- <i>n</i> -Hex	Normal-hexyl
- NMI	N-methylimidazole
- NMPK	Nucleoside monophosphate kinase
- NMR	Nuclear magnetic resonance
- <i>n</i> -Pen	Normal-pentyl
- P	Phosphate group
- PARP	Poly (ADP) ribose polymerase
- PCV	Penciclovir
- Ph	Phenyl

- PLC	Phospholipase C
- POC	(isopropoxyloxycarbonyloxymethyl)
- POM	(pivaloyloxymethyl)
- PTC-Cl	Phenoxythiocarbonyl chloride
- <i>p</i> -TSA	<i>para</i> -toluene sulfonic acid
- Pyr	Pyridine
- RBV	Ribavirin
- RNA	Ribonucleic acid
- RNR	Ribonucleotide reductase
- ROS	Reactive oxygen species
- RSV	Respiratory syncytial virus
- S-8ClAMP	Succinyl-8ClA monophosphate
- SATE	<i>S</i> -acyl-2-thioethyl
- SDTE	<i>S</i> -[2-hydroxyethylsulfidyl]-2-thioethyl
- SE	Slow eluting
- Ser	Serine
- TBAF	Tetrabutylammonium fluoride
- TBAN	Tetrabutylammonium nitrate
- TBDMSCl	<i>Tert</i> -butyl dimethylsilyl chloride
- <i>t</i> Bu	<i>Tert</i> -butyl
- TEA	Triethylamine
- TFA	Trifluoroacetic acid
- TFAA	Trifluoroacetyl anhydride
- TFT	Trifluorothymidine
- TG	Thioguanine
- Thd	Thymidine
- THF	Tetrahydrofuran
- Thy	Thymine
- TIPSCl	1,3-Dichloro-1,1,4,4-
	tetraisopropylidisiloxane
- TK1/2	Thymidine kinase ½
- TLC	Thin layer chromatography
- TMSCN	Trimethylsilyl cyanide
- TMSOMe	Trimethylmethoxysilane

- TMSOTf	Trimethylsilyl trifluoromethanesulfonate
- TP	Thymidine phosphorylase
- TsCl	Tosyl chloride
- UCK1/2	Uridine-cytidine kinase1/2
- Ura	Uracil
- Urd	Uridine
- UV	Ultraviolet
- VACV	Valaciclovir
- VGCV	Valganciclovir
- α -AIBBr	α -Acetoxyisobutyryl bromide

1 Nucleoside analogues as anticancer agents

1.1 The structure of endogenous nucleosides

Nucleosides are endogenous metabolites formed by a heterocyclic purine or pyrimidine ring called “base” linked to a pentose carbohydrate through a β -*N*-glycosidic bond.¹

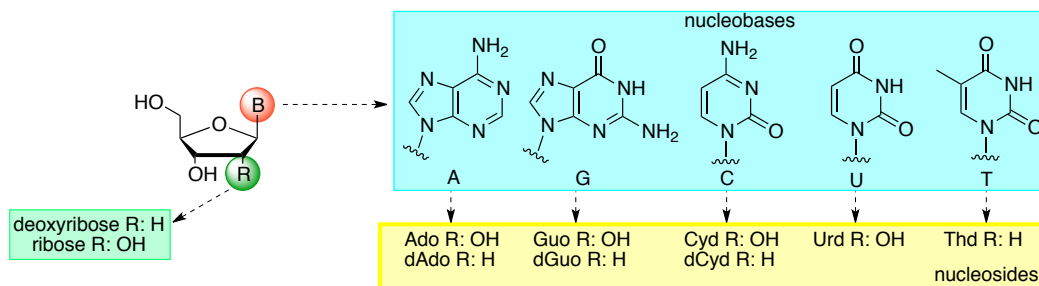


Figure 1.1: Purine and pyrimidine deoxyribonucleoside and ribonucleoside structures.

The five major bases found in nature are the purines adenine (A) and guanine (G) and the pyrimidines cytosine (C), uracil (U) and thymine (T) (Figure 1.1).

The sugar can be either a D-ribose or a 2-deoxy-D-ribose. The nucleosides containing D-ribose are called ribonucleosides and are represented by adenosine (Ado), guanosine (Guo), cytidine (Cyd), and uridine (Urd). The presence of 2-deoxy-D-ribose generates deoxynucleosides such as deoxyadenosine (dAdo), deoxyguanosine (dGuo), deoxycytidine (dCyt) and thymidine (Thd) (Figure 1.1).

Nucleotides are the 5'-mono-, di- or triphosphorylated forms of nucleosides and are primarily found in the organism as units of the major nucleic acids of the cell, DNA and RNA.² DNA is a polymer formed by deoxyribonucleoside monophosphate monomers linked together via a phosphodiester bond between the 3'-OH of one nucleotide and the 5'-OH of the second nucleotide (Figure 1.2).

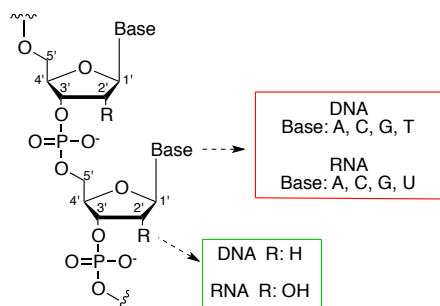


Figure 1.2: Structural components of nucleic acids.

RNA has a similar structure but the nucleotide thymidine 5'-monophosphate is replaced by a uridine 5'-monophosphate and the deoxyribose sugar by ribose (Figure 1.2).

Nucleosides and nucleotides are involved in other crucial processes such as neurotransmission,³ regulation of cardiovascular activity,⁴ and cell signaling as cyclic phosphates, such as cyclic adenosine monophosphate (cAMP) and cyclic GMP (cGMP).⁵⁻⁷ Furthermore, ATP involved in energy storage and liberation via hydrolysis of the phosphodiester bonds.⁸ Nucleoside analogues, linked to other moieties, especially in the form of adenosine diphosphate (ADP), are also involved in enzyme regulation as enzyme cofactors, such as nicotinamide adenine dinucleotide (NAD), flavin adenine dinucleotide (FAD) and coenzyme A.^{2,9}

1.2 Modified nucleoside analogues as therapeutic agents

Nucleoside and nucleotide analogues are structurally related to the endogenous counterparts, hence can exploit cellular metabolism and subsequently be incorporated into DNA and RNA to inhibit cellular division¹⁰ and viral replication.¹¹ Therapeutic properties of these molecules could also derive from the interaction with both human and host polymerase enzymes, responsible for the synthesis of nucleic acids (DNA-dependent DNA polymerases,¹² RNA-dependent DNA polymerases or RNA-dependent RNA polymerases).¹³ Furthermore, ribonucleotide reductase (RNR), responsible for deoxyribonucleoside pool homeostasis, is recognised as a target of antitumour agents.¹⁴ Additional targets for treatment with anticancer nucleoside analogues are DNA methyltransferase,¹⁵ purine nucleoside phosphorylase¹⁶ and thymidylate synthase.¹⁷

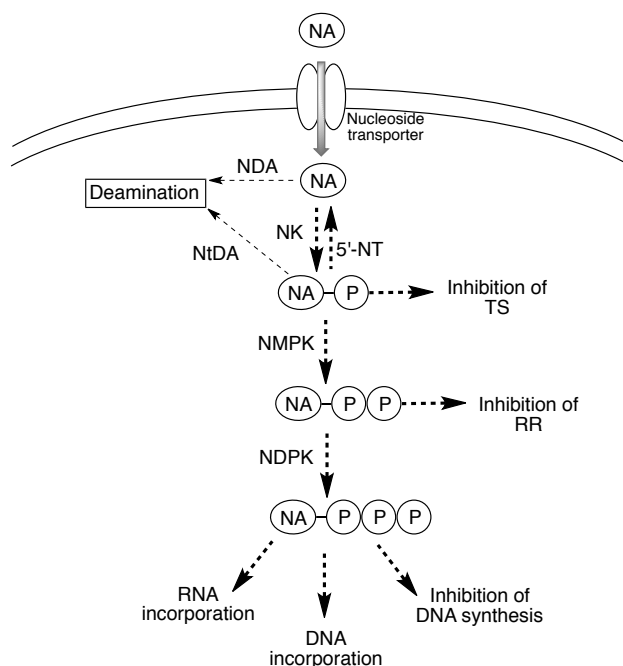
Nucleoside and nucleotide analogues used in antiviral treatment are structurally more diverse than anticancer nucleosides (such as the acyclic sugar moiety in acyclovir, an antiviral agent used as a treatment against herpes infections); this difference causes antiviral agents to be less active on mammalian enzymes, leading to better tolerance profile than anticancer analogues.⁹

1.2.1 Mechanism of action of nucleoside analogues

Presently used nucleoside analogues exploit the same metabolic pathways as endogenous nucleosides and nucleotides, and compete with them acting as antimetabolites.^{9,18}

Nucleosides depend on transporter proteins on the cell membrane to enter the cell, because their polarity inhibits passive diffusion through the lipophilic cell membrane.^{19,20}

Once inside the cell, nucleosides are phosphorylated to their corresponding active 5'-O-triphosphate forms in three consecutive enzymatic steps.²¹ The nucleoside kinase (NK) enzymes involved in the first phosphorylating step, active on deoxyribonucleosides are: deoxycytidine kinase (dCK), deoxyguanosine kinase (dGK) and thymidine kinase 1 and 2 (TK1 and TK2). The known NK responsible for the phosphorylation of ribonucleosides are adenosine kinase (AK) and uridine-cytidine kinase 1 and 2 (UCK1, 2).^{22,23}



Scheme 1.1: Nucleoside analogues intracellular mode of action. NK: nucleoside kinase, NA: nucleoside analogue, 5'-NT: 5'-nucleotidase, NDA: nucleoside deaminase, NtDA: nucleotide deaminase, P: phosphate group, TS: thymidylate synthase, NMPK: nucleoside monophosphate kinase, RR: ribonucleotide reductase, NDPK: nucleoside diphosphate kinase.

These enzymes are also involved in the first phosphorylation of most nucleoside drugs that are currently used.²⁴ This step is often rate-limiting.²⁵ The other two steps are catalysed by nucleoside monophosphate kinases (NMPKs),²⁴ and nucleoside diphosphate kinases (NDPKs).²⁶

There are also nucleoside and nucleotide deaminase enzymes (respectively NDA and NtDA) that deactivate nucleoside drugs. Cytidine deaminase (CDA),²⁷ and adenosine deaminase (ADA),²⁸ perform hydrolytic deamination of cytidine and adenosine derivatives, to the corresponding uridine or inosine derivatives. On the monophosphate level, adenosine monophosphate deaminase carries out similar conversions.²⁹ Furthermore, the enzyme 5'-nucleotidase (5'-NT) catalyses the conversion of nucleoside monophosphates to nucleosides.³⁰

As mono, di and triphosphorylated forms, nucleoside analogues can accumulate inside the cell and inhibit intracellular enzymes, while as the triphosphate form they can be incorporated into DNA and/or RNA, leading to inhibition of chain growth,¹¹ accumulation of mutations in the viral progeny,³¹ and induction of apoptosis.³²

1.2.2 Anticancer nucleoside analogues

Nucleoside analogues represent some of the oldest treatments in the anticancer and antiviral fields. Despite being old treatments, they still represent a cornerstone in these diseases, and research is still ongoing to improve the therapeutic profile of such agents. The British National Formulary (BNF) lists 14 anticancer agents with a nucleobase or nucleoside structure that are currently used in the clinic (Figure 1.3).³³

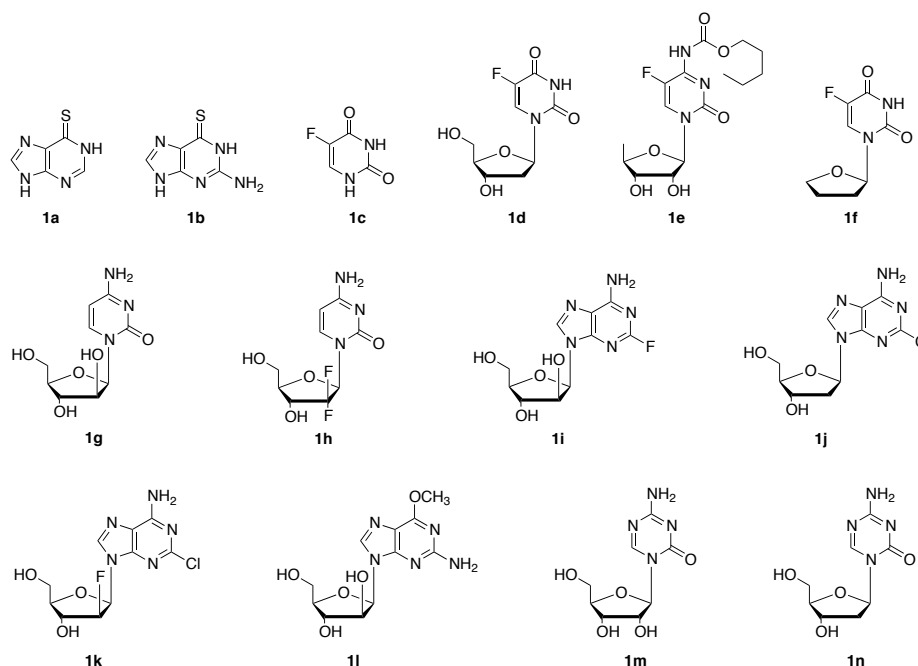


Figure 1.3: Anticancer nucleobase and nucleoside analogues currently used in the clinic (BNF 2014). 6-Mercaptopurine (**1a**), thioguanine (**1b**), 5-fluorouracil (**1c**), floxuridine (**1d**), capecitabine (**1e**), tegafur (**1f**), cytarabine (**1g**), gemcitabine (**1h**), fludarabine (**1i**), cladribine (**1j**), clofarabine (**1k**), nelarabine (**1l**), azacitidine (**1m**), decitabine (**1n**).

The nucleobases 6-mercaptopurine (6-MP, **1a**) and thioguanine (TG, **1b**) are thiopurines and some of the oldest cytotoxic agents.³⁴ These structures require the activity of the salvage enzyme hypoxanthine-guanine phosphoribosyl transferase for the formation of respectively thioinosine monophosphate and thioguanosine monophosphate. These molecules are then converted to their nucleoside triphosphate forms and integrated into nucleic acids, leading to inhibition of DNA polymerases, ligases and endonucleases. Other

effects on *de novo* enzymes were documented, such as inhibition of 5-phosphoribosyl-1-pyrophosphate amidotransferase, inosine monophosphate dehydrogenase and ribonucleotide reductase. Thiopurines are used against acute leukaemias, alone or more often in combination with other antineoplastic agents.³⁵

5-Fluorouracil (5FU, **1c**) is a derivative of uracil and initially synthesised in the 1950s and used in the treatment of several solid tumours including colorectal cancer.¹⁷ Floxuridine (FUdR, **1d**) is the deoxynucleoside derivative of 5FU. Both drugs are in equilibrium in cancer cells due to the activity of the enzyme thymidine phosphorylase, which catalyses the coupling of 5FU with deoxyribose and the cleavage of the glycosidic bond in floxuridine.³⁶

Floxuridine monophosphate irreversibly inhibits thymidylate synthase, which catalyses the reductive methylation of deoxyuridine monophosphate into thymidine monophosphate. This causes an imbalance in the thymidine triphosphate/deoxyuridine triphosphate ratio (TTP/dUTP), leading to an increase of dUTP which is integrated into DNA and excised by the enzyme uracil-DNA glycosylase, with consequent DNA strand breaks and apoptosis. Moreover, after conversion into floxuridine triphosphate, this drug is integrated into RNA and DNA affecting intracellular metabolism.³⁶

Capecitabine (**1e**) and tegafur (**1f**) are both 5-fluorouracil prodrugs to be administered orally.³⁷ Tegafur is part of a combination with uracil called UFT. Both drugs share structural similarities and activation processes. After oral administration, both compounds cross the intestinal mucosa. Capecitabine undergoes metabolism with first cleavage of the amidic bond, followed by conversion into the uridine derivative by cytidine deaminase. The product is then finally converted into 5FU by thymidine phosphorylase activity, which catalyses the same conversion on tegafur.

Cytarabine (**1g**) is a deoxycytidine analogue with activity on haematologic malignancies, especially against acute myeloid leukaemia and no effect on solid tumours.³⁴ This nucleoside is phosphorylated by dCK and inactivated by conversion to the uracil derivative by CDA. In the triphosphate form, it is integrated into DNA leading to chain termination and it directly inhibits DNA polymerase.³⁴ Unlike cytarabine, the deoxycytidine derivative gemcitabine (**1h**) has activity on solid tumours such as pancreas, breast, lung and ovaries.³⁸ The mechanism of action of this nucleoside analogue differs from cytarabine as after incorporation into DNA, an endogenous nucleotide is added, thus preventing DNA repair by base-pair excision. Gemcitabine diphosphate also has inhibitory activity on ribonucleotide reductase, blocking the *de novo* DNA synthesis pathway and determining a

self-potentiating effect of the drug, as dCTP levels decrease. This leads to an increase of gemcitabine intracellular activation and integration into both DNA and RNA.³⁸

Fludarabine (**1i**) and cladribine (**1j**) are deoxyadenosine analogues.³⁹ The former is orally administered as the 5'-monophosphate to improve solubility, and its approved application is against chronic lymphocytic leukaemia.³⁹ Cladribine was approved against hairy cell leukaemia, and similarly to fludarabine, its triphosphate form is integrated in DNA stopping the elongation by DNA polymerases in the S phase of the cell cycle causing apoptosis.⁴⁰ Both compounds also inhibit RNR and are toxic on resting cells, a feature that was suggested to derive from inhibition of DNA repair. Both nucleosides are integrated into RNA, causing premature termination of RNA transcription.⁴⁰

More recently approved nucleoside analogues are the deoxyadenosine derivative clofarabine (**1k**) and the deoxyguanosine derivative nelarabine (**1l**). Clofarabine was approved in 2004 for the treatment of acute myeloid leukaemia.⁴¹ The triphosphate form inhibits DNA polymerase enzymes and RNR. These effects cause a self-potentiating profile with improved integration of clofarabine triphosphate into DNA and induction of apoptosis.

Nelarabine (**1l**) was approved in 2005 for the treatment of T-cell acute lymphoblastic leukaemia and T-cell lymphoblastic lymphoma.⁴² This guanosine analogue was initially developed to improve the poor pharmacokinetic profile of 9-β-D-arabinofuranosyl guanine (Ara-G), as the introduction of a methoxy moiety in position 6 on the guanine portion improved the water solubility approximately 10-fold. Both drugs were found to be integrated into DNA as their triphosphate form, inhibiting DNA synthesis and leading to apoptosis.⁴²

Azacitidine (**1m**) and decitabine (**1n**) are respectively cytidine and deoxycytidine analogues. Both drugs were approved respectively in 2004 and 2006 for the treatment of myelodysplastic syndrome (MDS). The development of these drugs was initially due to their cytotoxic profile, and only several years later the epigenetic properties of both compounds were confirmed.¹⁵ Azacytidine and decitabine are inhibitors of the enzyme DNA methyltransferase and have shown substantial potency in reactivating epigenetically silenced tumour suppressor genes. In fact, DNA methyltransferase inhibition reverts hypermethylation induced gene silencing, which in turn causes silencing of tumour suppressor genes, which are responsible for human tumourigenesis. Azacytidine is integrated into RNA, although 10-20% of it is converted by RNR into decitabine, which is, instead, integrated into DNA.⁴³

1.2.3 Antiviral nucleoside analogues

Nucleoside analogues were broadly explored in the antiviral field, and Figure 1.4 shows the compounds still used in the clinic in the UK (**2a-2p**).⁴⁴ The nucleoside analogues zidovudine (**2a**), didanosine (**2b**), lamivudine (**2c**), emtricitabine (**2d**), stavudine (**2e**) and abacavir (**2f**) are active as anti-HIV reverse transcriptase inhibitors and HIV-DNA chain terminators.⁴⁵

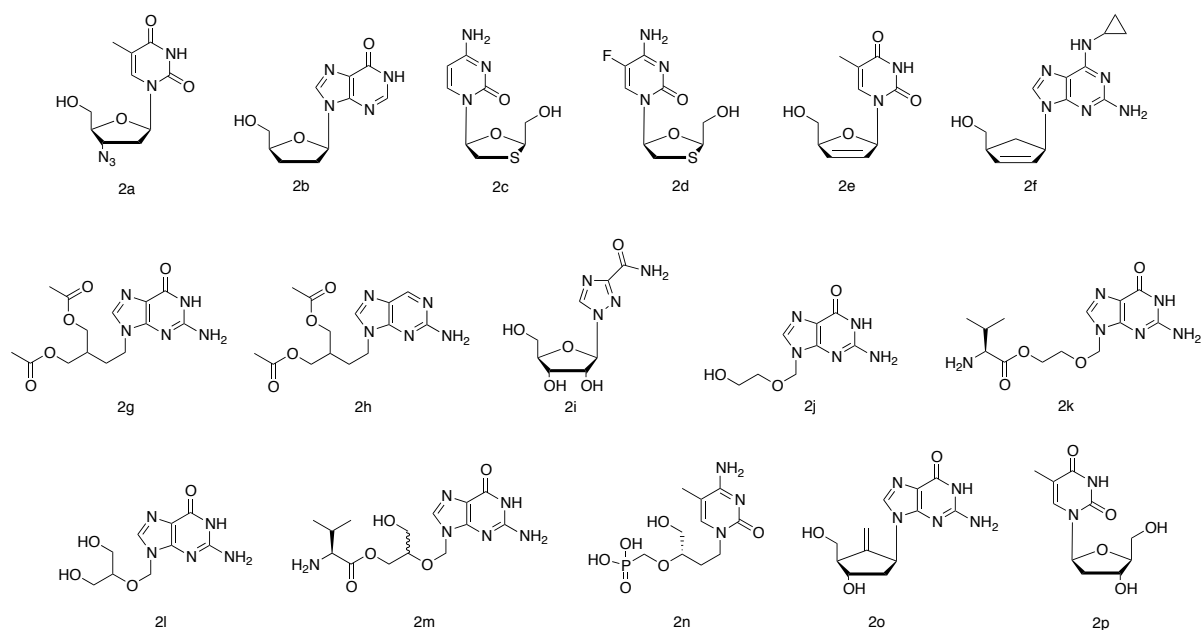


Figure 1.4: Antiviral nucleoside analogues. Zidovudine (**2a**), didanosine (**2b**), lamivudine (**2c**), emtricitabine (**2d**), stavudine (**2e**), abacavir (**2f**), penciclovir (**2g**), famciclovir (**2h**), ribavirin (**2i**), acyclovir (**2j**), valaciclovir (**2k**), ganciclovir (**2l**), valganciclovir (**2m**), cidofovir (**2n**), entecavir (**2o**), telbivudine (**2p**).

Zidovudine (AZT, **2a**), first approved as an anti-HIV nucleoside analogue in 1987, is active as the nucleoside triphosphate by inhibiting viral reverse transcriptase and HIV-DNA chain growth.⁴⁶

Didanosine (ddI, **2b**), approved as an anti-HIV agent in 1991, is converted to dideoxyadenosine monophosphate (ddAMP) by the action of first a phosphotransferase enzyme and secondly by adenylosuccinate lyase and adenylosuccinate synthetase. After two additional phosphorylation steps, ddATP represents the final active metabolite.⁴⁷

Lamivudine (3TC, **2c**) and emtricitabine (FTC, **2d**) are anti-HIV agents approved respectively in 1995 and 2003, as L-isomers.⁴⁸ Lamivudine is also used as an anti-hepatitis B virus (HBV) agent, at a lower dosage.

Stavudine (d4T, **2e**) is a thymidine derivative approved in 1995 as an anti-HIV agent.⁴⁵

Abacavir (ABC, **2f**) was approved in 1998 as an anti-HIV agent and acts after conversion into the guanosine analogue carbovir triphosphate, which was initially synthesised and

biologically evaluated as an anti-HIV agent but poor pharmacokinetics halted its progression into the clinics.⁴⁸

Penciclovir (PCV, **2g**), is an acyclic nucleoside analogue approved in 1996 for the topical treatment of herpes simplex virus (HSV), followed in 1997 by its prodrug famciclovir (FCV, **2h**), used also against herpes zoster virus.⁴⁹ Both drugs act as chain terminators after intracellular phosphorylation and integration into the DNA growing chain. Famciclovir additionally requires an initial step of conversion into penciclovir after first-pass metabolism in intestine and liver.⁴⁹

Ribavirin (RBV, **2i**) is a guanosine analogue inhibitor of RNA synthesis and metabolism,⁵⁰ which was approved in 1986 for the treatment of respiratory syncytial virus (RSV), and in 2001 against hepatitis C virus (HCV) in combination with interferon.⁵¹

Acyclovir (ACV, **2j**) is an acyclic adenosine analogue approved in 1982 for the treatment of HSV,⁵² and later also as an anti-varicella zoster virus agent.⁴⁶ The valine prodrug valaciclovir (VACV, **2k**), was approved in 1995 with the same purpose, due to increased bioavailability.⁵²

Ganciclovir (GCV, **2l**), an acyclic guanosine analogue, was approved as an anti cytomegalovirus agent (CMV) in 1989, followed by its valine prodrug valganciclovir (VGCV, **2m**), approved in 2001 for the same application due to increase in bioavailability compared to the parent nucleoside, as in the case of valaciclovir.⁵²

Cidofovir (CDV, **2n**) is an acyclic cytidine derivative bearing a phosphonate group, which allows bypassing of the first monophosphorylation step as this group is recognised as a phosphate group although endowed with increased stability.⁵³ This nucleotide analogue was approved in 1996 for the treatment of CMV.

Entecavir (ETV, **2o**) is a RT and DNA replication inhibitor, approved in 2010 for the treatment of HBV, similar to the thymidine L-isomer telbivudine (**2p**) approved in 2006.^{54,55}

1.3 Resistance and limitations to nucleoside analogue treatment

Resistance to the anticancer activity of NAs can arise after modification in the tumour cell functions and genome mutations.⁴⁰ Resistance to antiviral NAs could similarly derive from mutations in the host cells or from specific mutations in the viral genome.⁹ The rate of mutations in the viral genome is higher than in mammalian genomes due to limited proof reading capacities of viral polymerases, and this provides avenues to overcome resistance to such drugs. Such mutations could affect the interaction between the nucleoside analogue and viral polymerase enzymes.⁵⁶

Cell mutations affect the insurgence of metabolic resistance that might cause insufficient intracellular concentration of the active triphosphate.⁵⁷ This was reported to be due to deficiency in nucleoside transporters, such as the human equilibrative nucleoside transporter 1 (hENT1), which affects the sensitivity to cytarabine (ara-C), fludarabine and cladribine.¹⁹ Moreover, decreased activity of intracellular nucleoside kinase enzymes has been associated with resistance to NA treatment.²⁵ In the case of dCK, an enzyme responsible for the phosphorylation of many NAs, such as cladribine, gemcitabine, fludarabine and ara-C, reduced enzyme activity could derive from either decreased expression of dCK gene or from inactivating mutations in the gene, such as hypermethylation of the promoter region of the gene.⁴⁰ An alternative factor affecting the intracellular concentration of the active NA triphosphates is the increased expression of deactivating enzymes. High levels of 5'-nucleotidase enzymes have consistently been associated with poor response to anticancer NAs.³⁰ This enzyme hydrolyses the phosphate bond of NA monophosphates, thus counteracting the activity of kinase enzymes. Furthermore, cytidine and adenosine derivatives can be substrates of cytidine or adenosine deaminase enzymes, which catalyse the conversion respectively into inactive uridine or inosine derivatives, as documented after treatment with gemcitabine, Ara-C or Ara-A.⁴⁰ Once in their active triphosphate form, NAs could cause insufficient alterations in nucleic acid strands or to the nucleoside triphosphate pools, i.e. by altered interaction with DNA or RNA polymerases,⁵⁸ or by ineffective inhibition of the RNR enzyme,⁵⁹ responsible for the dNTP pool. Finally, NA treatment failure might derive from defective cell death pathways and p53 exonuclease activity.⁶⁰ The p53 protein possesses exonuclease activity, and is able to excise DNA-incorporated NA. Alterations in the expression of such protein has been related *in vitro* to resistance to NAs. DNA damage caused by NA can induce the expression of p53, causing induction of pro-apoptotic molecules such as Bax and down regulation of anti-apoptotic proteins such as Bcl-2.⁴⁰

1.4 Strategies to overcome NA resistance

Overcoming the dependency of nucleoside analogues on cell mediated activation pathways could lead to a reduction in resistance to therapy.⁶¹ One of the main documented factors affecting the activity of NA is the dependency on nucleoside kinase enzymes for the first, often rate-limiting, phosphorylation step.^{40,62} Nucleotides could be administered instead of nucleosides, hence bypassing this limiting stage.⁶¹ However, the much higher hydrophilic nature of the nucleotide (related to the phosphate group, which is acidic and thus

negatively charged at physiological pH) would decrease its bioavailability and inhibit cell penetration. Moreover, the phosphate group is metabolically labile and could rapidly be cleaved by ecto-5'-NT enzymes, such as in the case of fludarabine monophosphate. One strategy to increase the stability of nucleotides is the use of nucleoside phosphonates, where the replacement of the phosphate O-P bond with a phosphonate C-P bond greatly increases the chemical and enzymatic stability of this moiety, still representing a moiety generally recognised by the nucleotide kinase enzymes.⁶³⁻⁶⁵ However, these molecules are often poorly bioavailable, due to the negative charges on the phosphonate.

A better strategy may be the use of lipophilic substituents to mask the charges on the phosphate and phosphonate groups, and different approaches are detailed in several reviews.^{61,66-69} This could additionally bypass the dependency on nucleoside transporters for cell penetration, due to increased lipophilicity, which would allow passive diffusion through cell membranes. Moreover, some of these strategies were found to inhibit NA inactivation by deaminase enzymes. The attached moieties should be then either chemically or enzymatically cleaved inside the cell, representing prodrugs of the corresponding nucleoside monophosphate analogue.

1.5 Monophosphate prodrugs

To overcome the previously mentioned issues correlated with the use of nucleosides as anticancer therapeutics, different approaches have been developed, and some of the most established ones will be described here.

1.5.1 Bis(POM) and Bis(POC) approach

Farquhar *et al.* were the first to use the *bis*(pivaloyloxymethyl) (POM) approach for the preparation of pro-nucleotides.⁷⁰ The intracellular activation of the prodrug moiety depends on carboxyesterase enzymes yielding the free nucleotide.

This approach was used as a phosphate prodrug motif in the antiviral setting, on nucleosides such as dideoxyuridine (ddU) and AZT,^{71,72} although it proved more efficient on phosphonate substrates with *bis*(POM) adefovir dipivoxil (**3a**) approved as an anti-HBV agent,^{73,74} and LB80380 (**3b**) in clinical trials as an anti-HBV agent (Figure 1.5).^{75,76} The methodology was also applied to FUdR (**3c**, Figure 1.5) with the aim of improving anticancer activity, but was not progressed in the clinic.⁷⁷

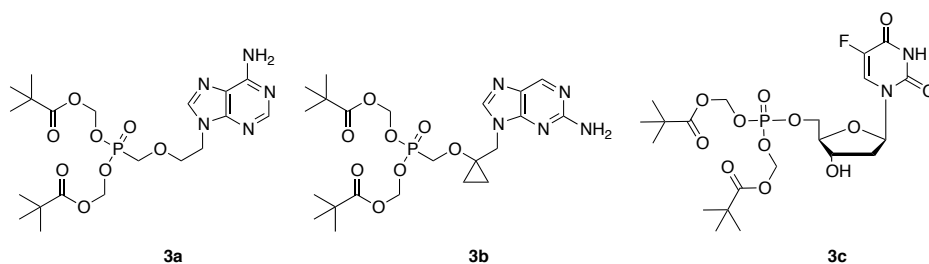


Figure 1.5: Structures of the anti-HBV agents *bis*(POM) adefovir dipivoxil (**3a**), LB80380 (**3b**) and the anticancer agent *bis*(POM) FUDR (**3c**).

A modification of this strategy consisted of the introduction of *bis*(isopropoxycarbonyloxymethyl) esters (POC). Similar intracellular conversions as for the *bis*(POM) prodrugs affords the desired nucleotide inside the cell. The application of this prodrug approach yielded the approved anti-HBV agent *bis*(POC) tenofovir (**3d**, Figure 1.6).^{78,79}

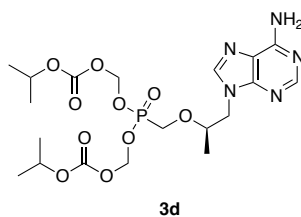


Figure 1.6: Structure of the anti-HBV agent *bis*(POC) tenofovir (**3d**).

1.5.2 Bis(SDTE)- and Bis(SATE) Approach

Imbach and Gosselin explored the application of *bis*(*S*-[2-hydroxyethylsulfidyl]-2-thioethyl)- [*bis*(SDTE)] and the *bis*(*S*-acyl-2-thioethyl)- [*bis*(SATE)] nucleotide prodrug approaches.⁸⁰⁻⁸³ Both prodrug approaches require intracellular enzymatic cleavage of the pronucleotide moieties, catalysed by a reductase enzyme in the case of the *bis*(SDTE) and a carboxyesterase enzyme for the *bis*(SATE), similar to the *bis*(POM) and *bis*(POC) approaches. The *bis*(SATE) approach was applied to the anti-HIV nucleoside analogue AZT (**4a**, Figure 1.7), retaining good activity in a TK-deficient strain. The *bis*(SDTE) approach was applied to AZT (**4b**), yielding lower *in vitro* anti-HIV activity compared to the *bis*(SATE) approach.⁸⁴

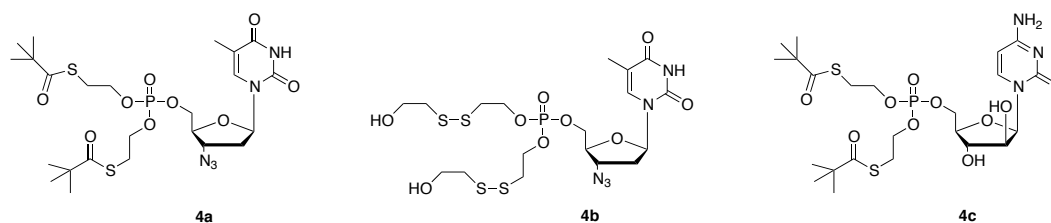


Figure 1.7: Structures of the anti-HIV agents *bis*(SATE) AZT (**4a**), *bis*(SDTE) AZT (**4b**), and the anticancer agent UA911 (**4c**).

Furthermore, the application of the *bis*(SATE) approach to Ara-C generated the agent UA911 (**4c**), currently involved in anticancer preclinical studies due to better activity on deoxycytidine kinase (dCK)-deficient cells than cytarabine.⁸⁵

This prodrug approach was modified with the introduction of an aromatic or aliphatic amine or an amino acid ester in place of one of the two SATE chains.⁸⁶ The activation of such prodrugs requires one esterase step followed by a putative phosphoramidase-mediated cleavage of the phosphoramidate bond.

One of the most important examples of such a prodrug approach was IDX184, a 2'-C-methylguanosine prodrug that entered phase IIb clinical evaluation as an anti-HCV agent.⁸⁷

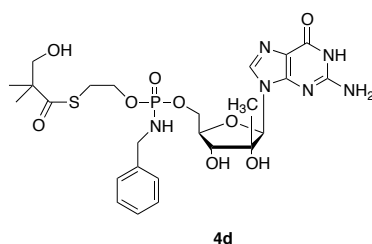


Figure 1.8: Structure of the anti-HCV agent IDX184.

Although the progression in the clinic was halted, IDX184 is the only example of a SATE derivative reaching clinical investigations.⁸⁸

1.5.3 CycloSal approach

Meier *et al.* developed this approach and it consists of masking the phosphate group on nucleotides with salicylic alcohols. The prodrug then requires a pH (acid) sensitive chemical hydrolysis mechanism of activation.^{66,89} This method was applied to different NAs, such as d4T (**5a**, Figure 1.9),^{90,91} AZT,⁹² etc.⁹³ Second and third generations of cycloSal analogues have also been developed. The second generation of prodrugs has an esterase cleavable moiety on the aromatic ring that is a substrate of an esterase enzyme inside the cell (**5b**). This enzyme releases the more polar product, and hence traps it within

the cell. The third generation cycloSal prodrugs contain a geminal carboxylate attached to the aromatic ring, *para* to the phenoxy phosphate ester (**5c**). Upon enzymatic ester hydrolysis, this breaks down to an aldehyde, which is electron withdrawing and thus speeds up the chemical hydrolysis to release the nucleotide. The three prodrug approaches are described on the anti-HIV agent d4T in Figure 1.9.

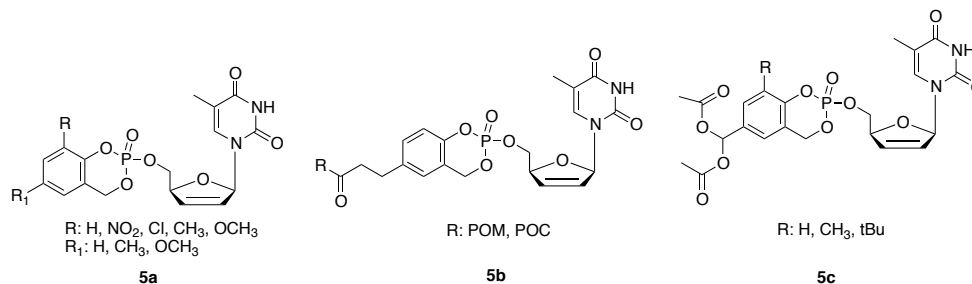


Figure 1.9: Structures of first (**5a**), second (**5b**) and third (**5c**) generation cycloSal prodrugs on the anti-HIV agent d4T.

Moreover, the approach was also applied to the anticancer NA cladribine, yielding a compound more active than the parent nucleoside in dCK deficient cells.⁹⁴ So far, none of these agents have progressed to clinical trial.

1.5.4 Phospholipid conjugates approach

This prodrug strategy has been developed by Hostetler *et al.*³⁴ and applied to some acyclic nucleoside phosphonates, enhancing their antiviral potency. In this approach, one of the phosphonate negative charges is masked with a phospholipid moiety, such as hexadecyloxypropyl or octadecyloxyethyl groups. This phospholipid moiety mimics lysophosphatidylcholine, a naturally occurring phospholipid, and is hence recognised and cleaved intracellularly by phospholipase C (PLC). In the case of cidofovir, this approach increased the uptake inside the cell by 100-fold,⁹⁵ and this prodrug is currently involved in a phase III clinical trial study under the name of brincidofovir (**6a**, CMX001, Figure 1.10) on CMV infected patients. The application of this prodrug approach to tenofovir afforded derivative CMX157 (**6b**), which was terminated after phase I clinical study having been developed as an anti-HIV agent.^{96,97}

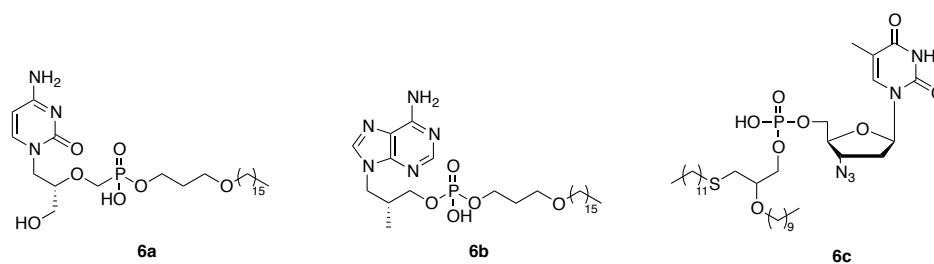


Figure 1.10: Phospholipid conjugate approach applied to cidofovir (**6a**), tenofovir (**6b**) and AZT (**6c**).

This structure was also modified yielding fozivudine tidoxil, a thioether lipid prodrug of AZT, which reached phase II clinical trial for the treatment of HIV.⁹⁸

1.5.5 HepDirect approach

This method consists of the introduction of a 1-aryl-1,3-propanyl ester (HepDirect) on the monophosphate group of the nucleotide. This group allows the monophosphate nucleoside analogue to be delivered in the liver *via* cytochrome P₄₅₀ (CYP450) oxidation of the prodrug moiety.⁹⁹ An important application of such a prodrug approach is pradefovir (**7a**, Figure 1.11), a derivative of adefovir that was successfully developed to overcome the renal toxicity derived from treatment of HBV affected patients with adefovir dipivoxil.¹⁰⁰ Moreover, the approach was applied to cytarabine, yielding the phosphate prodrug MB07133 (**7b**), that has completed phase II clinical studies against primary liver cancer,¹⁰¹ and was granted orphan drug designation for the treatment of this malignancy.¹⁰²

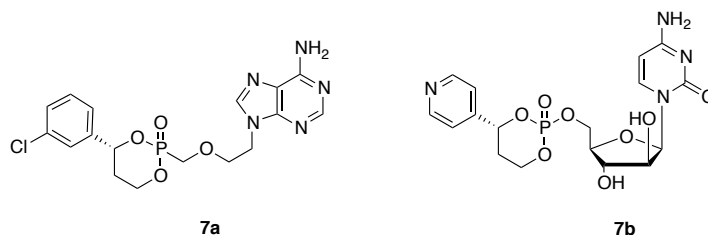


Figure 1.11: Structures of HepDirect prodrugs of adefovir (**7a**) and cytarabine (**7b**, MB07133).

1.5.6 Phosphoramidate diester approach

In this approach, developed by Wagner *et al.*, only one of the two negative charges on the phosphate group of a nucleotide is masked by an aminoacyl methyl ester. The intracellular bioactivation of this prodrug involves the cleavage of the P-N bond by a phosphodiesterase or phosphoramidase enzyme. This approach has been applied to different nucleoside analogues, such as the anticancer agents FUDR (**8a**) and ara-C (**8b**),¹⁰³ and the antiviral

analogue AZT (**8c**),¹⁰⁴ which was endowed with a better pharmacokinetic profile compared to the parent nucleoside (Figure 1.12).

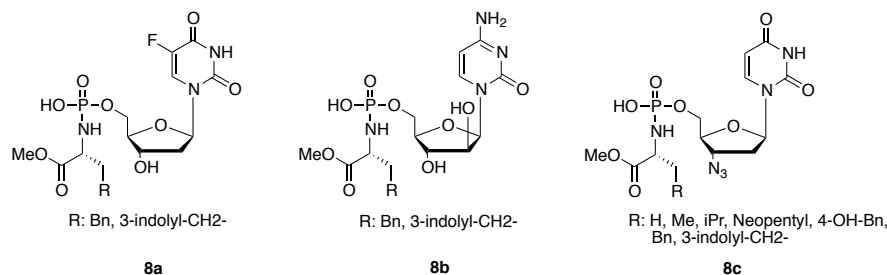


Figure 1.12: Structures of phosphoramidate diesters derivatives of FUDR (**8a**), Ara-C (**8b**) and AZT (**8c**).

1.5.7 Aryloxy phosphoramidate approach

First developed by McGuigan and co-workers, the aryloxy phosphoramidate nucleotide prodrug (ProTide) approach^{105,106} involves masking of the negative charges on the monophosphate group by an aryloxy and an amino acid ester group.

The development of this prodrug strategy followed different steps, described in Figure 1.13 on AZT. At first, the prodrug structure was characterised by the presence of bis(alkyloxy) and haloalkyloxy substituents on the phosphate group (**9a**), which conferred stability but also prevented the bioactivation inside the cell, thus showing less activity than the parent nucleoside.¹⁰⁷⁻¹¹³ The introduction of either an amino acid ester in place of one of the two alkyl chains (**9b**),¹¹³ or two aryl moieties (**9c**),¹¹⁴⁻¹¹⁶ were reported to lead to release of free nucleoside inside the cell, and not the desired nucleotide.

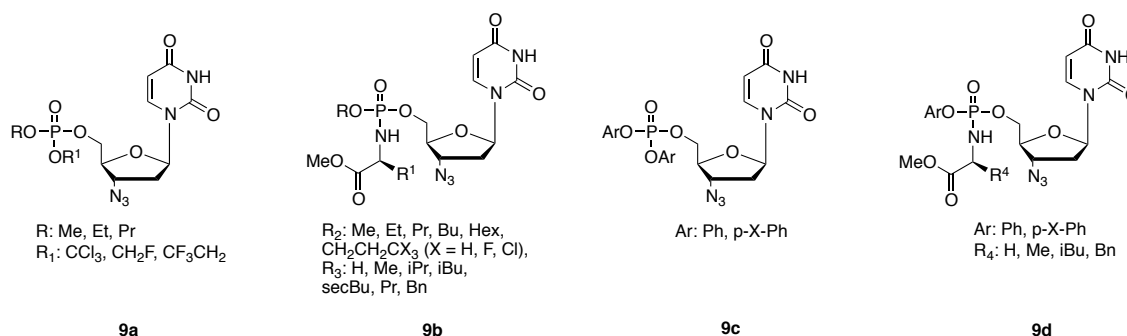


Figure 1.13: Development of the aryl phosphoramidate (ProTide) approach using AZT.

The final step was the introduction of an aryloxy group and an amino acid ester moiety on the phosphate group (**9d**), which led to structures with improved *in vitro* antiviral activity in comparison to AZT.¹¹⁷ Application of the ProTide technology in the antiviral and anticancer settings, led to numerous examples of compounds endowed with better potency,

compared to the parent nucleoside. A pivotal example is represented by sofosbuvir (**9e**, Figure 1.14), approved in 2013 for the treatment of HCV.¹¹⁸

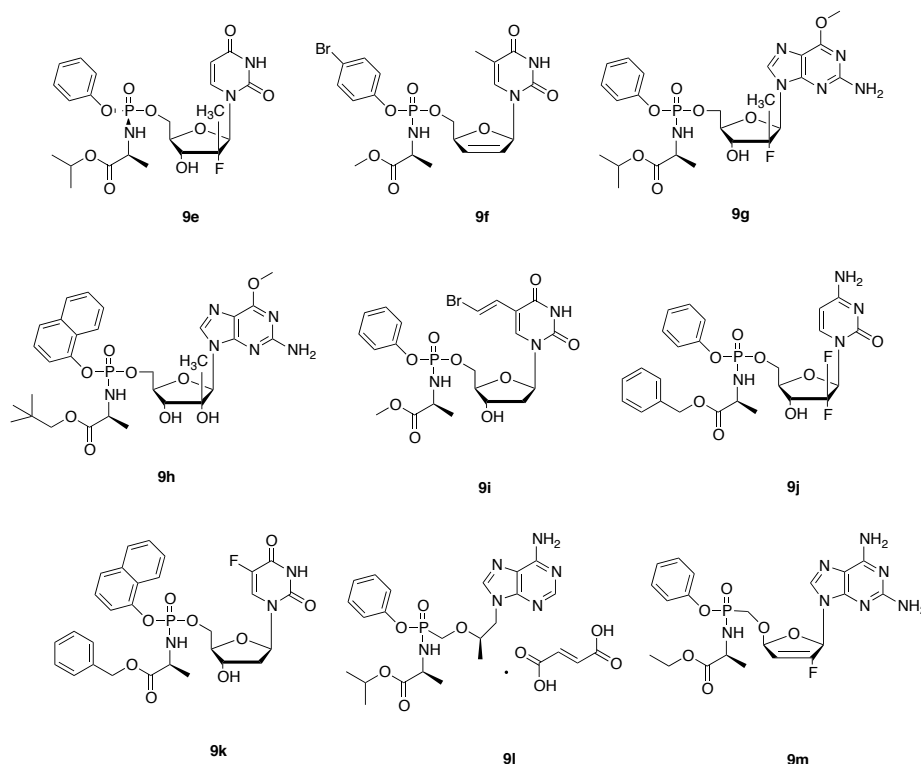


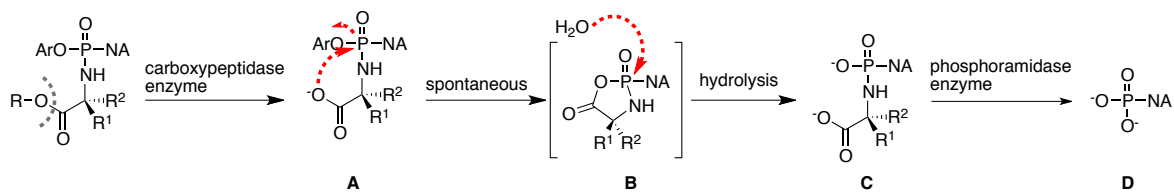
Figure 1.14: Structures of ProTide analogues that have entered clinical evaluation: sofosbuvir (**9e**), stampidine (**9f**), PSI-353661 (**9g**), INX-08189 (**9h**), thymectacin (**9i**), NUC-1031 (**9j**), NUC-3373 (**9k**), GS-7340 (**9l**), GS9131 (**9m**).

Many ProTides have entered clinical trials, such as the anti-HIV agent stampidine in phase I (**9f**),¹¹⁹ the anti-HCV agents PSI-353661 in phase I (**9g**),¹²⁰ and INX-08189 (**9h**),¹²¹ in phase II. Despite progression into phase II clinical trials, the development of INX-08189 was halted in 2012 due to the development of severe cardiotoxicity in patients.¹²² The development of PSI-353661 was halted concomitantly, due to structural similarities to INX-08189 and the danger of development of similar toxicity.⁸⁸

Within the anticancer setting, thymectacin has entered phase I/II (**9i**),¹²³ and NUC-1031 is in phase III (**9j**),¹²⁴ along with FUDR ProTide NUC-3373 (**9k**), which is currently in preclinical development and was announced to enter phase I in 2015.¹²⁵

Moreover, tenofovir alafenamide fumarate (**9l**, TAF, formerly known as GS-7340), ProTide of the antiviral acyclic nucleoside analogue tenofovir has also reached phase I/II development for the treatment of HIV and HBV viruses,¹²⁶ and the phosphonate ProTide GS9131 (**9m**) has reached phase II clinical development as an anti-HIV agent.¹²⁷

The initial step of the ProTide putative activation consists of the cleavage of the ester moiety by an enzyme with esterase-type activity, such as lysosomal carboxypeptidase A (cathepsin A, catA),¹²⁸⁻¹³⁰ yielding the intermediate **B** (Scheme 1.2).



Scheme 1.2: ProTide activation pathway.

The initial ester cleavage is believed to be followed by an intramolecular attack of the newly formed carboxylate anion on the phosphorus atom, with formation of a putative five membered cyclic carboxylic phosphorus mixed anhydride, and resulting in elimination of the aryloxy group.¹³¹⁻¹³³ Due to the likely instability of such an intermediate, hydrolysis of the five membered ring may be spontaneous, with water attack on the phosphorus centre, and opening of the ring.¹³¹ Finally, the cleavage of the P-N bond, mediated by an intracellular phosphoramidase-type enzyme, releases the monophosphate.^{103,104,134} This step may be performed by histidine triad nucleoside-binding protein 1 (Hint enzyme 1), which belongs to the HIT superfamily.¹³⁵

The modifiable ProTide moieties are represented by the aryl group (Ar), the amino acid (R_1 , R_2) and the ester (R), giving rise to vast sets of combinations.

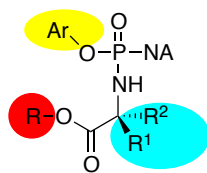


Figure 1.15: Common structure of ProTide nucleotide prodrugs with highlighted key modifiable residues.

Concerning the ester moiety (moiety **R**, Figure 1.15), many different linear (such as methyl, ethyl, pentyl) and branched (such as isopropyl, *tert*-butyl, neopentyl) groups were used, along with the benzyl group. In most programs, the benzyl moiety proved to yield the most active prodrugs, whilst in the case of *tert*-butyl group, the prodrugs were found to be mostly inactive.^{62,106} Aryl moieties (**Ar**) such as differently substituted phenol groups were investigated and good results were obtained when using electron-withdrawing groups such as *p*-Br. The naphthol functionality was used in many different programs, yielding promising activity as in the case of NUC-3373. The amino acids (R^1 , R^2) were extensively

explored, with a key moiety represented by L-alanine, used so far in all ProTides in clinical development. The use of unnatural D-alanine and other D-amino acids usually yielded inactive ProTides. ProTides bearing glycine were usually poorly active, while the alkylation to dimethylglycine afforded more potent analogues.¹³⁶

1.5.8 Cyclic phosphate prodrugs

3',5'-Cyclic phosphoramidate prodrugs were developed with the intent of reducing the potential toxicity arising from the release of an aryloxy moiety via the ProTide approach. This method was applied to 2'-C-methylcytidine (**10a**, 2'-C-Me-C) and FUDR (**10b**) (Figure 1.16), but was not progressed further.^{137,138}

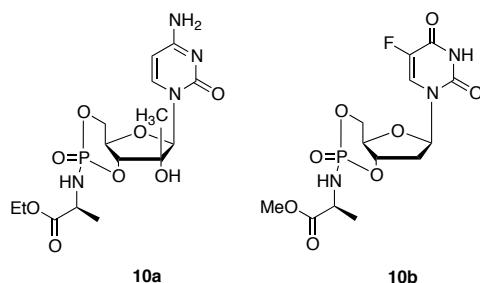


Figure 1.16: Structures of 3',5'-cyclic phosphoramidate prodrugs of 2'-C-Me-C (**10a**) and FUDR (**10b**).

Interesting results were obtained with 3',5'-cyclic ester prodrugs, reported to be activated by enzymatic P-O-dealkylation catalysed by CYP3A4 and then cleavage of the 3'-P-O bond by phosphodiesterase enzymes.¹³⁹

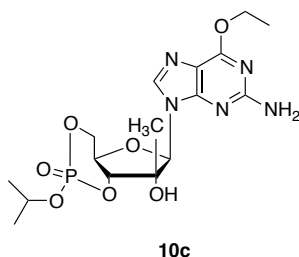
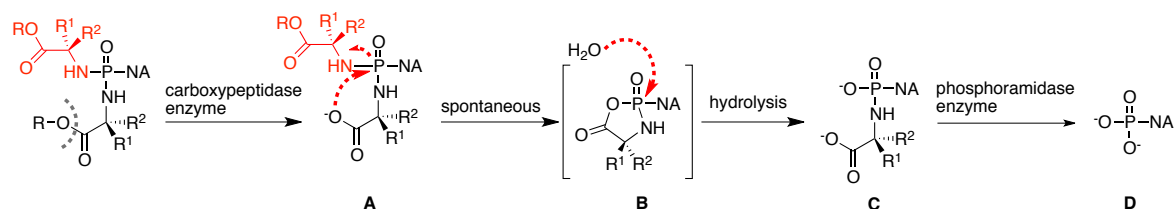


Figure 1.17: Structure of the anti-HCV agent PSI-352938 (**10c**).

The application of this prodrug approach yielded PSI-352938 (**10c**, Figure 1.17), an anti-HCV agent that entered phase I trials,¹³⁹ although its progression into the clinic was halted due to hepatic side effects.¹⁴⁰

1.5.9 Phosphoramidate approach

McGuigan *et al.* synthesised phosphoramidate derivatives of AZT and 3'-fluoro-3'-deoxythymidine (FdT) by using two amino acid groups,^{141,142} which allowed the presence of an achiral phosphorus center, therefore a single isomer. The proposed activation of such prodrugs is similar to the ProTide approach, requiring initial step of cleavage of the ester moiety catalysed by a carboxypeptidase enzyme, inducing spontaneous cyclisation into a five membered ring (Scheme 1.3).¹⁴³ Attack of the carboxylate ion to the phosphorus center triggers the release of one amino acid. A phosphoramidase enzyme finally catalyses the release of the nucleoside monophosphate. One additional positive aspect of this prodrug strategy is the release of two amino acid ester moieties during the activation process, avoiding the generation of potentially toxic aryloxy groups.



Scheme 1.3: Mechanism of activation of phosphoramidate nucleoside prodrugs.

Our group was involved in the synthesis of phosphoramidates of 6-*O*-alkyl-2'-*C*-methylguanosine (6-*O*-alkyl-2'-*C*-Me-G) as anti HCV-agents, and different compounds such as **11a** gave similar results to the phosphoramidate INX189 in *in vitro* assay against HCV replication (Figure 1.18).¹⁴³

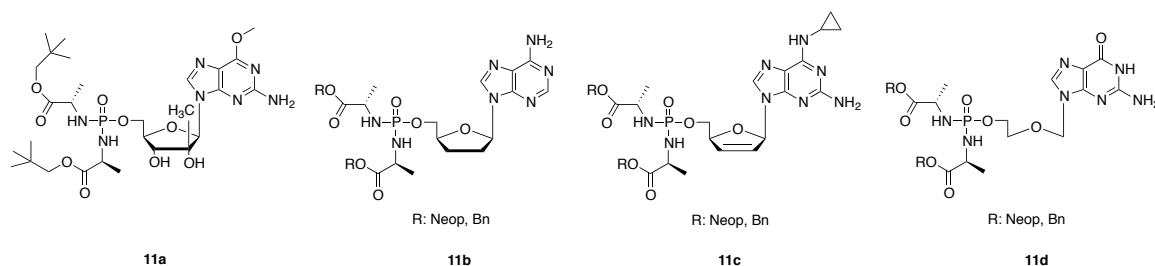


Figure 1.18: Structures of phosphoramidate prodrugs of 6-*O*-alkyl-2'-*C*-Me-G (**11a**), ddA (**11b**), ABC (**11c**), ACV (**11d**).

A more recent study focused on the application of this approach on a broad selection of antiviral and anticancer nucleoside analogues,¹⁴⁴ with improvement of the *in vitro* anti-HIV activity of phosphoramidates of ddA (**11b**), ABC (**11c**) and ACV (**11d**), compared to the parent nucleosides.

1.6 Summary of the phosphate prodrug technologies

A summary of all the different monophosphate prodrug approaches described is reported in Table 1.1, along with the activation pathway required and whether any analogue has been taken to human trials.

Prodrug class	Activation step required	Taken to human trials
Bis(POM)/(POC)	Esterase	✓
Bis(SATE)/(SDTE)	Esterase/(reductase + esterase)	✗
SATE phosphoramidate	Esterase + amidase	✓
CycloSal	Chemical	✗
Phospholipid conjugate	Phospholipase C	✓
HepDirect	CYP450	✓
Phosphoramidate diester	phosphoramidase	✗
ProTide	Carboxypeptidase + phosphoramidase	✓
Cyclic phosphoramidate	Phosphoramidase + phosphodiesterase	✗
Cyclic phosphate ester	CYP3A4 + phosphodiesterase	✓
Phosphorodiamidate	Carboxypeptidase + phosphoramidase	✗

Table 1.1: Summary of the phosphate prodrug approaches.

1.7 Aim of the work

Nucleoside analogues are therapeutics with a wide application in anticancer and antiviral therapies. Their use is often limited by the emergence of resistance to the treatment, due to different factors such as the down-regulation of activating pathways, or transporter proteins and up-regulation of inactivating enzymes. Many limiting steps can be overcome by the use of a lipophilic nucleotide prodrug, and our aim was to improve the biological profile of already known nucleoside analogues by applying the ProTide approach.

The synthesis of ProTides of different nucleoside analogues was planned, along with the evaluation of each analogue *in vitro* as anticancer agents. Selected compounds were also tested as antiviral agents.

NMR and molecular modelling studies on the enzymatic activation of selected compounds were planned in order to further validate the biological data, and respectively involved carboxypeptidase-Y and Hint enzymes.

Assays of the stability of promising derivatives were also considered, in mammalian plasma, serum and liver microsomes and against deactivating enzymes such as adenosine deaminase.

On the most promising ProTides families of known nucleoside analogues, modifications of the nucleotide structure at the nucleobase, sugar and phosphate level were also designed in order to gain an advantage over the already active analogues.

Anticancer evaluation of the most active derivatives was planned on the cancer stem cell population of the KG1a cell line.

The target nucleoside for the application of prodrug approaches were (Figure 1.19):

- 3'-Deoxyadenosine (chapter three).
- 2-Fluoro-3'-deoxyadenosine (chapter three).
- 8-Chloroadenosine (chapter four).
- 8-Chloro-2'-deoxyadenosine (chapter four).
- 2'-C-cyano-2'-deoxy-1- β -D-*arabino*-pentofuranosylcytosine (chapter five).
- Trifluorothymidine (chapter six).
- 2'-Mercapto 2'-deoxyuridine (chapter seven).
- 2'-Trifluoromethylthio 2'-deoxyuridine (chapter seven).

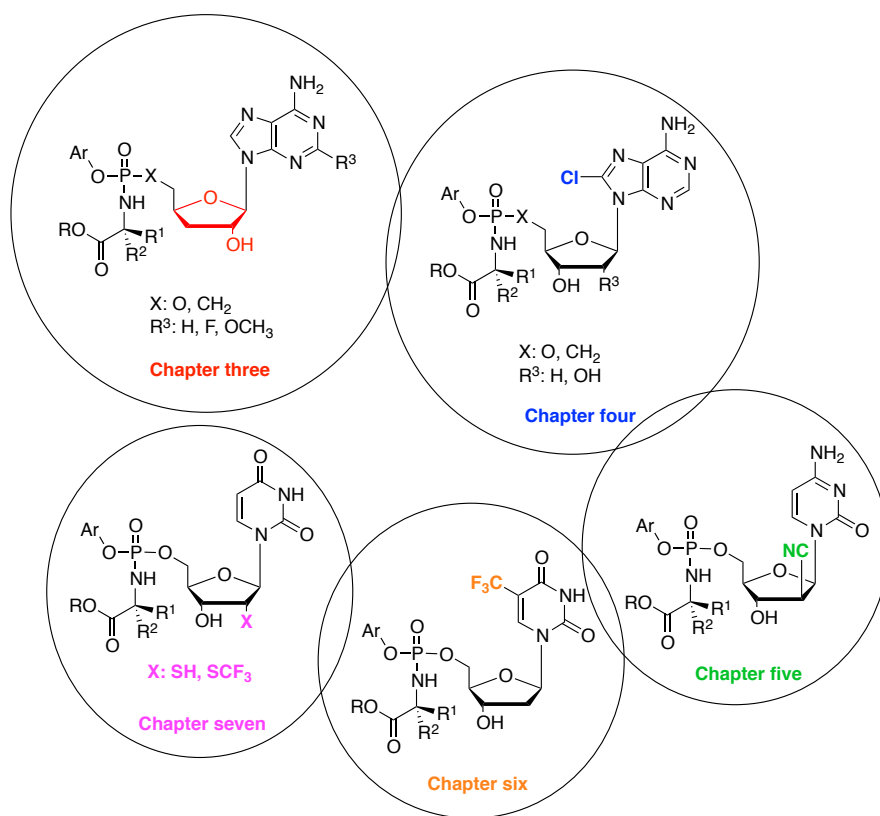


Figure 1.19: Visual outline of the content of each chapter.

2 Synthesis of nucleotide prodrugs

2.1 ProTide synthesis

The ProTide approach was elected as our primary nucleotide prodrug method and applied to different nucleoside analogues. As already mentioned in Chapter 1, ProTides consist of a nucleoside monophosphate bearing different substituents on the phosphate group. One of these substituents is an aromatic moiety and the other is an amino acid ester, linked to the phosphorus through a phosphoramidate bond (**12**, Figure 2.1).^{62,105,106}

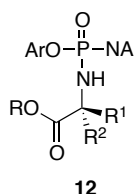
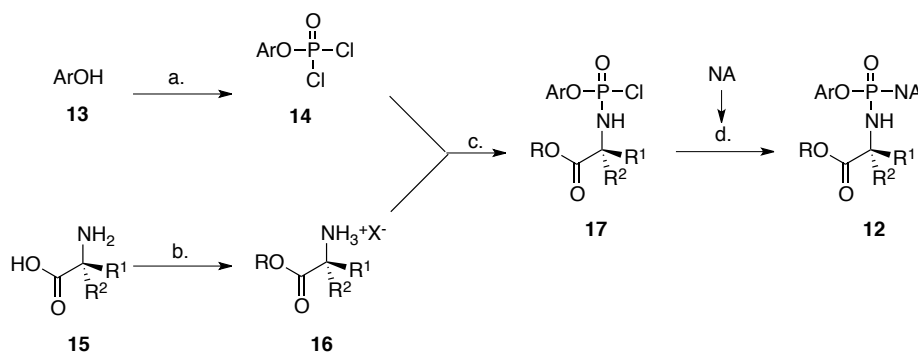


Figure 2.1: ProTide general structure (**12**).

Different methodologies were reported for the synthesis of ProTides, although the most commonly used one is the coupling of the nucleoside analogue (NA) with a phosphorochloridate reagent, reported in Scheme 2.1.¹⁴⁵



Scheme 2.1: Synthetic pathway to ProTide (**12**). Reagents and conditions: (a.) POCl_3 (1 eq), Et_3N (1 eq), Et_2O , -78°C to rt, 3h (90-91%); (b.) [i] ROH (15 eq), SOCl_2 (2 eq), toluene, reflux, 16h, (88-98%); [ii] ROH (5 eq), *p*TSA (1.1 eq), toluene, reflux, 16h, (40-96%); (c.) Et_3N (2 eq), CH_2Cl_2 , -78°C to rt, 2-4 h. (75-99%) (d.) *t*BuMgCl (1M in THF, 1-3 eq), THF, rt, overnight or NMI (5 eq), THF, rt, 16h (see yields throughout the work). NA: nucleoside analogue.

The key moiety is the phosphorochloridate (**17**) that is coupled with the nucleoside analogue only in the last step (d.). The phosphorochloridate is synthesised by coupling aryl phosphorodichloridates (**14**) and amino acid ester salts (**16**). The aryl

phosphorodichloridate is obtained by reacting aryl alcohol (**13**) and phosphorus oxychloride (POCl_3), while the amino acid ester (**16**) is synthesised by esterification of the amino acid (**15**) with an alcohol.

All these different moieties can vary greatly, leading to a broad variability of ProTide structures and to the modulation of both biological activity and chemical stability of the structures. In this work, different modifications were attempted on the general ProTide structure, as reported in Figure 2.2.

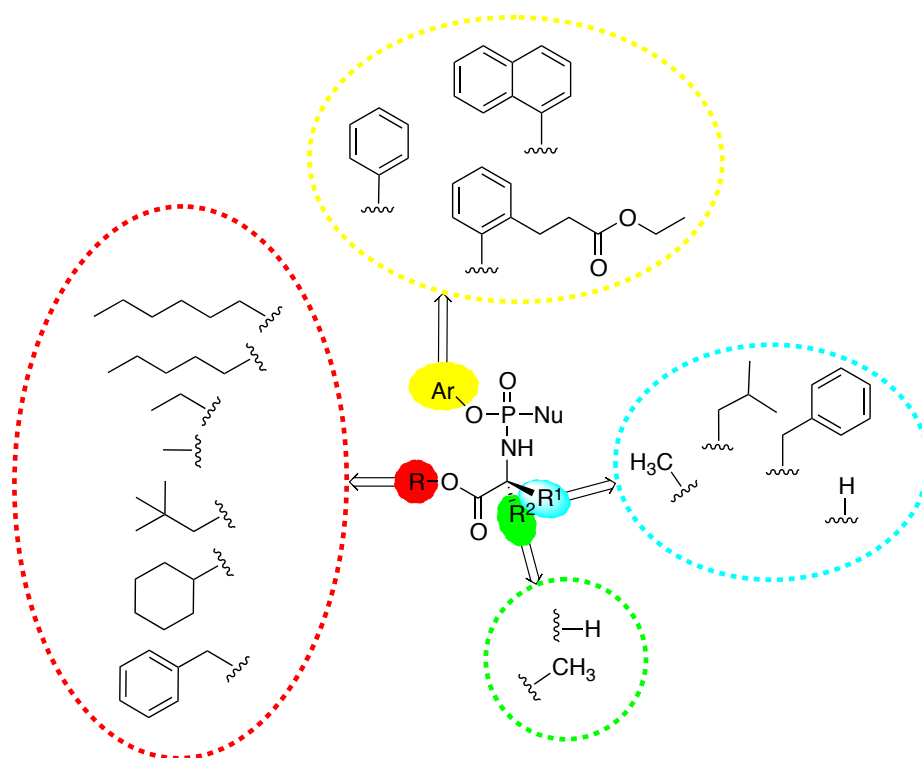


Figure 2.2: Different modifications of ProTides developed in this work.

2.1.1 Phosphorodichloridate synthesis

Phosphorochloridates were synthesised in a coupling reaction between an amino acid ester salt (**15**) and an appropriate phosphorodichloridate (**14**) in the presence of triethylamine (Et_3N) as a base (Scheme 2.1, step c.).¹⁴⁶

The phosphorodichloridate is the phosphorylating agent, which determines the properties of the aryl moiety in the final ProTide. Phenyl- (**14a**), 1-naphthyl- (**14b**) and the *o*-ethyl-3-(2-hydroxyphenyl)propanoylphenyl phosphorodichloridate (**14c**) were used in this work (Figure 2.3); unlike **14a**, both **14b** and **14c** are not commercially available and were synthesised according to Scheme 2.1 (step a.), in approximately 90% yields (Table 2.1).

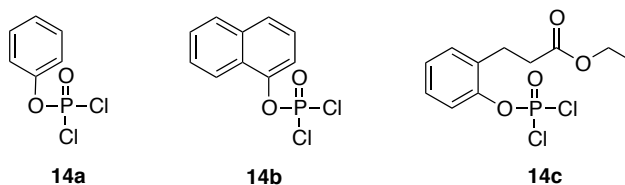


Figure 2.3 Aryloxy phosphorochloridate moieties (**14a-c**) used within this work as ProTide building blocks.

In order to obtain compounds **14b** and **14c**, phosphorus oxychloride (POCl_3) was added to a stirred solution of the aryl alcohol (respectively 1-naphthol **13b**, and ethyl 3-(2-hydroxyphenyl)propanoate **13c**, Figure 2.4) in diethyl ether, in the presence of triethylamine at $-78\text{ }^\circ\text{C}$ (Scheme 2.1, a.) and the reaction was monitored by ^{31}P NMR.

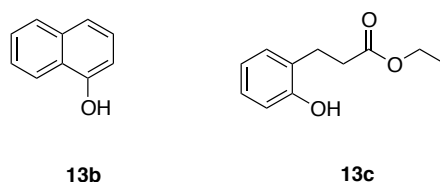


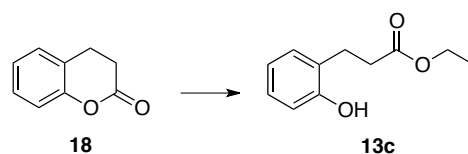
Figure 2.4: Structures of aryl alcohols used for the synthesis of phosphorodichloridates **13b** and **13c**.

The reaction was complete with the disappearance of the ^{31}P NMR peak corresponding to POCl_3 ($\delta\text{P} = 4.27$, CDCl_3 , 202 MHz), paralleled by only the presence of the peak corresponding to the appropriate phosphorodichloridate (Table 2.1).¹⁰⁵ Once the reaction was complete the triethylammonium chloride salt was filtered off and the solvent was removed *in vacuo* to give compounds **14b** and **14c** as clear oils, which were used in the next step without further purification.

Compound	Ref.	Aryl	Yield %	^{31}P -NMR δ
14b	¹⁴⁷	1-Naphthol	91 %	3.69
14c	¹⁴⁸	Ethyl 3-(2-hydroxyphenyl)propanoate	90 %	3.22

Table 2.1 Reaction yields for the synthesis of phosphorodichloridates (**14b** and **14c**).

Ethyl 3-(2-hydroxyphenyl)propanoate (**13c**) was synthesised in quantitative yield by treating 3,4-dihydrocoumarin (**18**) with a catalytic amount of 2,3-dichloro-5,6-dicyano-1,4-benzoquinone (DDQ) in ethanol (Scheme 2.2).¹⁴⁹



Scheme 2.2: Synthesis of ethyl 3-(2-hydroxyphenyl)propanoate (**13c**). *Reagents and conditions*: DDQ (0.07 eq), EtOH, rt, 8h, 100%.

This specific aryl group was chosen because ProTides bearing this moiety were shown to have good antiviral activity, suggesting efficient processing to the monophosphate.¹⁵⁰ Moreover, the introduction of an ethyl propanoic ester side chain at the *ortho* position of the phenol portion is supposed to release during the ProTide activation hydroxyphenyl propanoic acid, which is a known non-toxic metabolite of dihydrocoumarin, a common flavouring agent widely used in food and cosmetics.¹⁵⁰

2.1.2 Amino acid ester synthesis

The synthesis of amino acid esters that were not commercially available was performed according to two different synthetic routes, depending on the nature of the alcohol used for the esterification reaction.

In the first method, the amino acid and the appropriate alcohol were heated under reflux overnight in the presence of thionyl chloride. After evaporation of volatiles, pure amino acid esters were obtained as white hydrochloride salts (**16a-c**, Table 2.2, Scheme 2.1, b.[i]). This method is preferred when using low boiling point alcohols for the esterification, because it is easier to reach the reflux temperature required to promote the reaction.

Common structure	Cpnd	Ref.	R ¹	R ²	AA	R (ester)	Yield %	X
	16a	¹⁵²	<i>i</i> Bu	H	L-Leu	<i>n</i> -Pen	98 %	Cl ^{-a}
	16b	-	<i>i</i> Bu	H	L-Leu	Et	94 %	Cl ^{-a}
	16c	-	Bn	H	L-Phe	Et	88 %	Cl ^{-a}
	16d	¹⁵¹	Me	H	L-Ala	<i>n</i> -Pen	80 %	<i>p</i> TSA ^b
	16e	¹⁵¹	Me	H	L-Ala	cHex	88%	<i>p</i> TSA ^b
	16f	-	H	H	Gly	<i>n</i> -Pen	96 %	<i>p</i> TSA ^b
	16g	-	H	H	Gly	cHex	88 %	<i>p</i> TSA ^b
	16h	-	<i>i</i> Bu	H	L-Leu	cHex	40 %	<i>p</i> TSA ^b
	16i	¹⁵²	Bn	H	L-Phe	<i>n</i> -Pen	95 %	<i>p</i> TSA ^b
	16j	-	Bn	H	L-Phe	cHex	83 %	<i>p</i> TSA ^b

Table 2.2: Summary of amino acid esters synthesised (**16a-j**) using the two methods described above and isolated yields. ^a amino acid ester synthesised through procedure [i]. ^b amino acid ester synthesised through procedure [ii].

In the second method, the amino acid and the appropriate alcohol were suspended in toluene and heated at reflux overnight, in the presence of *para*-toluenesulfonic acid monohydrate (*p*-TSA, Scheme 2.1, b[ii]).

A Dean-Stark apparatus was fitted to the reaction flask to remove the water produced in the reaction. The corresponding pure amino acid esters were obtained through partial evaporation of the volatiles and diethyl ether-induced precipitation as white tosylate (*p*TSA) salts (**16d-j**, Table 2.2). A smaller volume of alcohol is used in comparison to the previous method and therefore this procedure is preferred when using high boiling point alcohols, in order to ease the evaporation work-up.

All newly synthesised amino acid esters, were used for the preparation of some of the synthesised phosphorochloridates (**17c, d, f-h, j-l, n-p**).

2.1.3 Phosphorochloridate synthesis

Phosphorodichloridates were coupled at low temperature (-78 °C) in the presence of Et₃N in anhydrous CH₂Cl₂, with the different amino acid ester hydrochlorides or tosylate salts (Scheme 2.4, c.). After 1 hour the reaction mixture was allowed to reach room temperature. The formation of phosphorochloridate was monitored by ³¹P NMR. The phosphorochloridates derived by tosylate amino acid salts were purified from the triethylamine tosylate salt by flash chromatography using a mixture of hexane/ethyl acetate as an eluent system. A simple filtration was sufficient to purify the phosphorochloridates derived by hydrochloric amino acid salts from the triethylamine chloridate salt.

Most of the phosphorochloridates obtained during the coupling method were represented by diastereomeric mixtures. ³¹P NMR of synthesised compounds showed signal splitting except for the glycine and dimethylglycine species, which were obtained as a mixture of enantiomers and therefore showed only one single peak in the phosphorus spectra (Table 3.3).

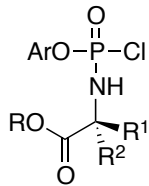
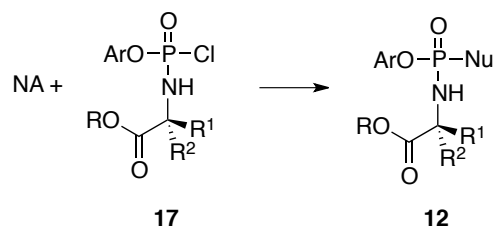
Common structure	Cpnd	Ref.	Ar	R ¹	R ²	AA	R	Yield	³¹ P NMR δ
	17a*	¹⁴⁷	1-Naph	Me	H	L-Ala	Bn	87 %	8.2; 8.0
	17b*	¹⁴⁷	1-Naph	Me	H	L-Ala	Et	99%	8.3; 8.0
	17c	¹⁵¹	1-Naph	Me	H	L-Ala	cHex	92 %	8.3; 7.9
	17d	¹⁵¹	1-Naph	Me	H	L-Ala	<i>n</i> -Pen	85 %	8.6; 8.7
	17e*	¹⁵²	1-Naph	<i>i</i> Bu	H	L-Leu	Bn	89 %	8.3; 8.0
	17f	¹⁵²	1-Naph	<i>i</i> Bu	H	L-Leu	<i>n</i> -Pen	89 %	8.8; 8.5
	17g	-	1-Naph	<i>i</i> Bu	H	L-Leu	cHex	90 %	8.8; 8.5
	17h	-	1-Naph	<i>i</i> Bu	H	L-Leu	Et	85 %	8.7; 8.5
	17i*	-	1-Naph	H	H	Gly	Et	95 %	9.3 ⁱ
	17j	¹⁴⁸	1-Naph	H	H	Gly	Bn	80 %	8.9 ⁱ
	17k	-	1-Naph	H	H	Gly	<i>n</i> -Pen	88 %	9.1 ⁱ
	17l	-	1-Naph	H	H	Gly	cHex	77 %	9.0 ⁱ
	17m*	¹⁴⁸	1-Naph	Bn	H	L-Phe	Bn	87 %	8.29; 8.17
	17n	¹⁵²	1-Naph	Bn	H	L-Phe	<i>n</i> -Pen	82 %	8.35; 8.25
	17o	-	1-Naph	Bn	H	L-Phe	cHex	86 %	8.45; 8.35
	17p	-	1-Naph	Bn	H	L-Phe	Et	90 %	8.36; 8.23
	17q**	¹⁵⁴	1-Naph	Me	Me	DMG	Me	75 %	6.02 ⁱ
	17r*	¹⁴⁷	Ph	H	H	Gly	Bn	80 %	9.04 ⁱ
	17s*	¹⁴⁷	Ph	Me	H	L-Ala	Bn	82%	7.5; 7.8
	17t**	-	Ph	Me	H	L-Ala	Neop	79%	7.5; 7.8
	17u**	¹⁵¹	Ph	Me	H	L-Ala	<i>n</i> -Hex	82%	7.6; 7.9
	17v*	¹⁵⁰	<i>o</i> -C ₂ H ₅ CO ₂ EtPh	Me	H	L-Ala	Bn	92 %	7.70; 7.53

Table 2.3: Yields and ³¹P NMR shifts of synthesised phosphorochloridates (**17a-v**). ^aSpectra were performed in CDCl₃, 202 MHz. *Amino acid ester was purchased (SigmaAldrich/Fisher) ** Amino acid esters were provided by NuCana Biomed (as HCl salts). ⁱNo diastereomeric splitting ³¹P NMR as compounds are a mixture of enantiomers.

2.2 Phosphoramidate synthesis

The phosphoramidates were obtained by coupling of nucleoside analogues with the appropriate phosphorochloridates in the presence of either *tert*-butyl magnesium chloride (*t*BuMgCl)⁶ or *N*-methylimidazole (NMI)¹⁷ in anhydrous THF, at room temperature, over 12-16 hours (Scheme 2.1). The use of *t*BuMgCl aimed at the deprotonation of the 5'-hydroxyl group on the sugar, which would then react with the phosphorochloridate. NMI, instead, functioned as an activator of the phosphorochloridate by replacing chlorine as a leaving group.



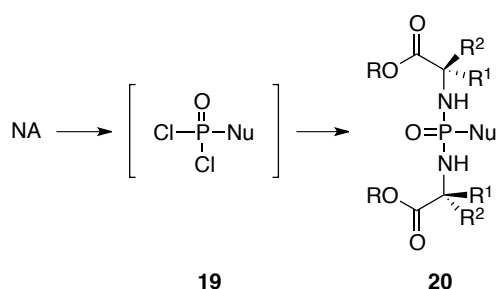
Scheme 2.3: General synthesis of phosphoramidates (**12**). *Reagents and Conditions*: a) *t*-BuMgCl (1-3 eq), THF, rt, overnight/ NMI (5 eq), THF, rt, overnight.

The Grignard reagent *t*BuMgCl was reported to act as a specific activator for *O*-selective phosphorylation.¹⁵⁴ Despite the selectivity towards the alcohol groups, *t*BuMgCl mediated coupling reactions target both the primary and the secondary alcohols on unprotected nucleosides. NMI mediated coupling reactions favour the primary alcohol, although in some cases leading to poor reaction yields, caused either by poor solubility of the substrate in the reaction solvent, or by parallel formation of side products from the coupling on secondary hydroxyl functions. Strategies involving initial protection of the secondary hydroxyl groups on the sugar moiety, followed by coupling reaction and final deprotection step, often improved the reaction outcome, and will be described in the next chapters.

2.3 Phosphorodiamidate synthesis

The phosphorodiamidate approach is an alternative method to the already mentioned aryl phosphoramidate to mask the negative charges on the nucleotide molecule (chapter 1). The synthetic strategy applied in this work was adapted from work by Yoshikawa *et al.*^{144,155,}

156



Scheme 2.4: General synthesis of phosphorodiamidates. *Reagents and Conditions*: a) POCl₃ (1 eq), trialkylphosphate (b) amino acid ester *p*-TSA or HCl salt (10 eq), anhydrous DIPEA (5 eq), anhydrous CH₂Cl₂.

According to the mentioned studies, in a one pot reaction the unprotected nucleosides were suspended in trialkyl phosphate, and phosphorus oxychloride is added in order to obtain

predominantly the 5'-phosphorodichloridate (**19**). The formation of this intermediate is monitored by ^{31}P -NMR (appearance of a peak ~ 7 ppm corresponding to the 5'-dichlorophosphate, disappearance of the ~ 4.27 ppm peak of POCl_3). Due to the relative instability of these intermediates, the isolation was not accomplished, and the compounds were immediately coupled with the appropriate amino acid ester salts in the presence of diisopropyl ethyl amine (DIPEA). The progression of the reaction was monitored again by ^{31}P -NMR: the appearance of a single peak in the range of 13-17 ppm, depending on the amino acid used for the synthesis, indicated the formation of the product **20**.

3 3'-Deoxyadenosine analogues

3.1 3'-Deoxyadenosine prodrugs

3.1.1 Background

3'-Deoxyadenosine (3'dA, cordycepin, **21**) is a nucleoside analogue of adenosine that lacks the 3'-hydroxyl group on the ribose moiety (Figure 3.1).

3'dA is one of the major bioactive substances produced by *Cordyceps militaris*, a parasitic fungus used for traditional Chinese medicine because of its activity on the immune system, and anti-aging and anti-tumour effects.^{157,158,159,160}

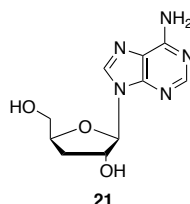
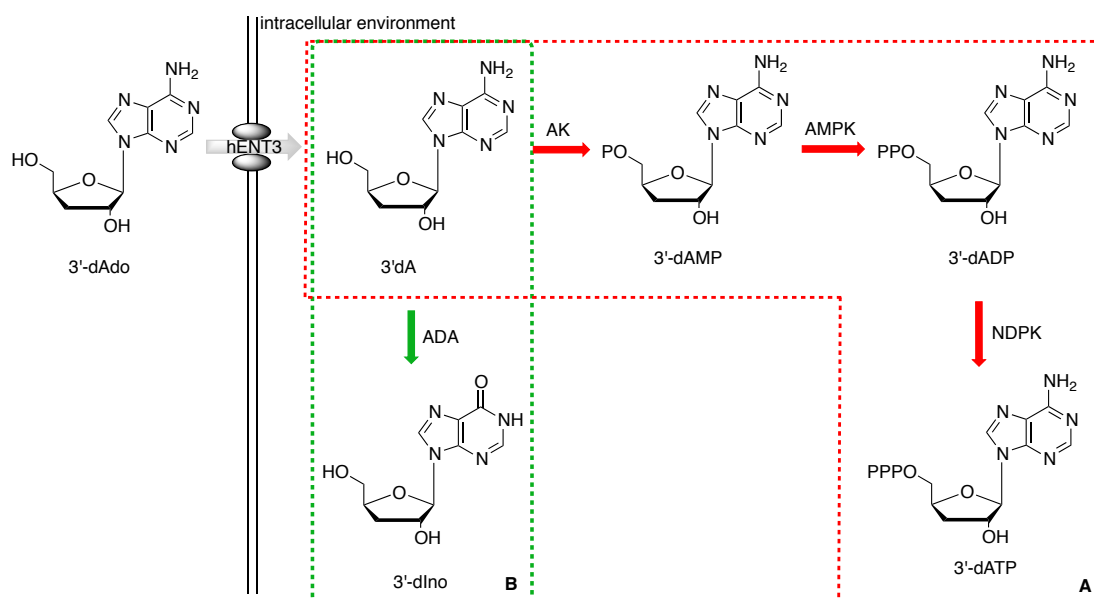


Figure 3.1: Structure of 3'dA (**21**).

Because of its structure, 3'dA and its triphosphate form could potentially interfere with any process respectively requiring adenosine or adenosine triphosphate (ATP), 3'dA was suggested to enter the cell via the equilibrative nucleoside transporter 3 (hENT3),¹⁶¹ and to be phosphorylated by adenosine kinase (AK) to 3'-deoxyadenosine monophosphate (3'-dAMP) and then to the active metabolite 3'-adenosine triphosphate (3'-dATP) by the combined actions of adenosine monophosphate kinase (AMPK) and nucleoside diphosphate kinase (NDPK) (Scheme 3.1, **A**).¹⁶²

In addition, 3'dA is known to be quickly deaminated by adenosine deaminase (ADA), and rapidly metabolised to an inactive metabolite, 3'-deoxyinosine (3'-dIno, Scheme 3.1, **B**).^{163,164}



Scheme 3.1: (A) Mechanism of intracellular activation of 3'dA. (B) Inactivation of 3'dA by ADA enzyme.

Following 3'dA intracellular phosphorylation, 3'-dATP was proposed to be a chain terminator for transcription, but it was reported that total nuclear mRNA precursors are less affected than cytoplasmic mRNA.^{165,166} In contrast, it has been demonstrated to be an efficient chain terminator for mRNA polyadenylation by poly (A) polymerases, thus causing mRNA instability.^{167,162,168,166} In addition, some studies indicate that 3'dA may act through adenosine receptors^{169-171,172} causing overproduction of reactive oxygen species (ROS) and apoptosis induction or cause inhibition of poly (ADP) ribose polymerase (PARP).^{173,167}

The molecular effects generated by 3'dA translate into numerous biological applications of this nucleoside analogue reported to date, including anti-inflammatory activity.^{174,167,175} inhibition of platelet aggregation¹⁷⁶ and anti-fungal¹⁷⁷ and anti-trypanosomal activity,^{178,179,180} along with antiviral properties.¹⁸¹⁻¹⁸³ However, this nucleoside has been studied most extensively as an anti-cancer agent. As such, 3'dA was reported to induce cytotoxic activity in various types of human cancer cells such as breast cancer,¹⁷³ head and neck,¹⁸⁴ colorectal,^{185,186} thyroid carcinoma cells,¹⁸⁷ multiple myeloma cells,¹⁸⁸ leukaemia^{171,189} and lymphoma cells.¹⁹⁰ In addition, the inhibitory effect was demonstrated on haematogenic metastasis of mouse melanoma cells¹⁷⁰ and lung carcinoma cells.^{169,191} Importantly, 3'dA has completed two phase I clinical studies in patients with refractory acute lymphocytic or chronic myelogenous leukaemia.¹⁹² Because of the very quick inactivation by ADA, during this study the administration of 3'dA was combined with the ADA-inhibitor pentostatin (deoxycoformycin, dCF, Figure 3.2) and the same combination

was involved in a phase I/II clinical trial in patients with refractory terminal deoxynucleotidyl transferase (TdT)-positive leukaemia, although the status of the study is currently unknown.¹⁹³

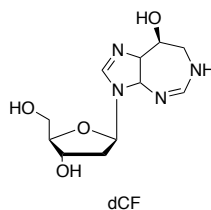


Figure 3.2: Adenosine deaminase inhibitor deoxycoformycin (dCF).

Although the combination of 3'dA and dCF was reported as effective both *in vivo* and *in vitro*,^{179,189} toxicity studies revealed that dogs treated with this combination of drugs presented toxicities to lymphoid tissue (lymphopenia and thymus lymphoid depletion), thrombocytopenia, and decreased food consumption.¹⁹⁴

The aim of this work is to apply a nucleotide prodrug approach to 3'dA in order to enhance the anticancer potential of this nucleoside. Some research groups have worked on the synthesis of 3'dA prodrugs with the aim of bypassing the ADA-catalysed catabolism affecting the activity of this nucleoside analogue and enhance the pharmacokinetic properties.^{195,196} A patent disclosed the synthesis and anticancer evaluation of different N-6 thioaminal prodrugs of 3'dA with the aim of bypassing ADA catabolism.¹⁹⁷ In addition, some dinucleoside phosphate prodrugs of cordycepin and AZT were also synthesised as prodrugs of both 3'dA and AZT and proved to be weak HIV agents.¹⁹⁸

This work focussed on the application of the ProTide¹⁰⁵ and phosphorodiamidate⁶⁷ phosphate prodrug approaches to 3'dA (Figure 3.3). Nucleosides bearing substitutions on the 5'-OH group of the sugar moiety were already reported to be immune to ADA-catabolism.¹⁹⁹ Moreover ProTides were proved not to be substrates of nucleoside deaminase enzymes,¹⁵¹ and therefore this approach can be an interesting way to bypass ADA-deamination, along with the increasingly well established ability of ProTides to overcome the dependency on AK for the first phosphorylation step, whose down-regulation was reported to induce resistance to 3'dA.²⁰⁰

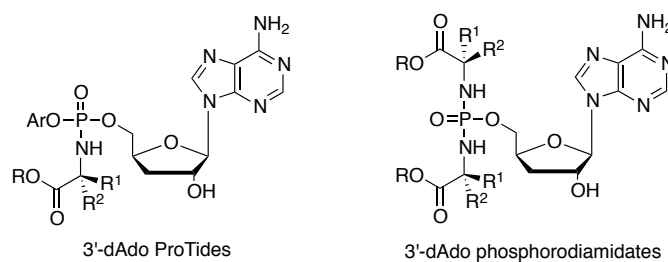
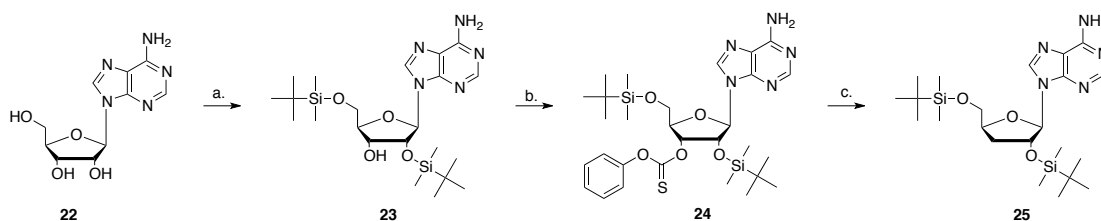


Figure 3.3: General structure of cordycepin prodrugs: ProTides and phosphorodiamidates.

In conclusion, the ProTide approach would make unnecessary the combination of dCF, therefore avoiding the toxicity risks connected with this treatment and the dosing and pharmacokinetic complications of dual drug administration.

3.1.2 Synthesis of 3'dA

Many different strategies for the synthesis of cordycepin are reported in the literature. In some reports 3'dA is synthesised starting from non-nucleoside derivatives;²⁰¹⁻²⁰⁴ however the synthesis requires multiple steps and is often low yielding. Other research groups developed a methodology requiring adenosine (Ado) as a starting material. The methodology by Meier *et al.* was initially applied in this work. This procedure involved a 4 step synthesis with an overall 55% yield,²⁰⁵ and was adapted from a similar procedure for the synthesis of 2'-deoxynucleosides.²⁰⁶ This procedure requires the selective protection of the 2'- and 5'-hydroxyl groups in the riboside moiety of adenosine (**22**) with *tert*-butyldimethylsilyl chloride (TBDMSCl) (Scheme 3.2). This intermediate (**23**) is then converted into the 3'-phenoxythiocarbonyl derivative (**24**) by treatment with phenoxythiocarbonyl chloride (PTC-Cl) and dimethylaminopyridine (DMAP) in acetonitrile (CH₃CN). In the final step this product is transformed into protected 3'dAdo (**25**) by radical deoxygenation (Barton-McCombie reaction) with azobisisobutyronitrile (AIBN) and tributyltinstannane (*n*-Bu₃SnH).^{205,207,208}



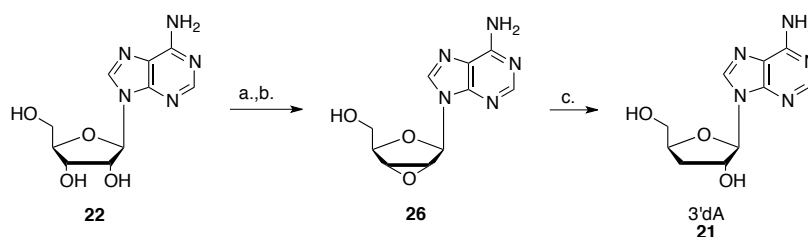
Scheme 3.2: First synthetic strategy for the synthesis of TBDMS-protected 3'dA (**25**). *Reagents and conditions:* (a.) see Table 3.1 (b.) PTC-Cl, DMAP, CH₃CN, rt, 16h. (c.) AIBN, *n*-Bu₃SnH, toluene, 3h, 75 °C.

For the first selective protection step,^{205,207} adenosine (**22**) was treated with 2.2 equivalents of TBDMSCl and an equimolar amount of AgNO₃ in THF in the presence of 5 equivalents of pyridine (Table 3.1. entry 1). This procedure was reported by Ogilvie *et al.* to yield 2',5'-bis-*O*-TBDMS-adenosine as the main product,^{209,210} but in our hands this attempt yielded only 5'-TBDMS-adenosine in quantitative yield. In order to improve the reaction outcome, the solubility of the reagents was enhanced by the use of a 1:1 v/v mixture of THF and DMF and warming up the suspension to 30 °C until the formation of a clear solution.

Entry	Reagents	Pyridine	Solvent	T	Yield
1	TBDMSCl (2.2 eq), AgO ₃ (2.2 eq)	5 eq	THF	rt	-
2	TBDMSCl (2.2 eq), AgO ₃ (2.2 eq)	-	THF/DMF (1:1)	30 °C	15%

Table 3.1: Reagents and conditions for the selective 2',5'-TBDMS-protection of adenosine.

Although allowing the formation of the desired product (**23**), the yield was still low (15%), and the 3',5'-regioisomer and 5'-silylated derivative could be recovered in lower yields (Table 3.1. entry 2). This step was not optimised further, and compound **23** was used for the second step (Scheme 3.2. step b.) of 3'dA synthesis. This intermediate was treated with 3 equivalents of phenoxythiocarbonyl chloride (PTC-Cl) in the presence of 6 equivalents of DMAP. The reaction was attempted in different scales but never yielded sufficient amounts of the desired product **24** but only traces of compound whose purification was difficult due to similar retention factor (R_f) on silica gel to other impurities and the starting material. Because of the lack of success of this strategy, an alternative strategy reported by Robins *et al.* was followed, requiring first conversion of adenosine (**22**) into 9-(2,3-anhydro-β-D-ribofuranosyl)adenine (**26**), with final metal hydride mediated reductive opening of the epoxide ring, which was reported to afford 3'dA (**21**) in 91% yield (Scheme 3.3).²¹¹⁻²¹⁴ Following this procedure, adenosine (**22**) was reacted with α-acetoxyisobutyryl bromide (α-AIBBr) in acetonitrile at room temperature for 1 hour (Scheme 3.3, step a).



Scheme 3.3: Synthesis of 3'dA. (a.) α -AIBr (4 eq), H₂O/CH₃CN, rt, 1h; (b.) Amberlite (IRN78) (8 mL/mmol), CH₃OH, rt, 16 h; (c.) conditions reported in Table 3.3.

The reaction described was first used by Moffatt and coworkers²¹⁵ who applied the Mattocks reaction of diols with α -AIB halides to nucleosides.²¹⁶ The products of this reaction were reported to be a mixture of more lipophilic intermediates as shown in Figure 3.4;²¹² these intermediates were not isolated in this work, but the following step was performed on the crude after neutralisation and extraction with ethyl acetate.

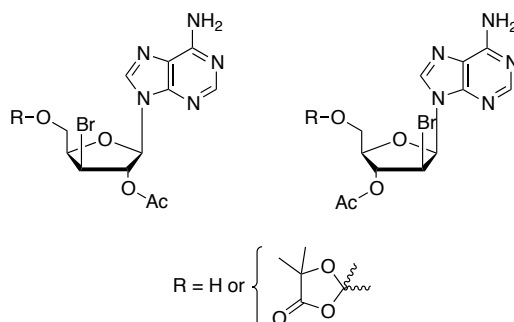


Figure 3.4: Lipophilic intermediates of reaction of Ado with α -AIBr in CH₃CN/H₂O.²¹²

The crude mixture thus obtained was treated with Amberlite (IRN78) resin in methanol for 1 hour, yielding intermediate **26** in 40% yield (Table 3.2, entry 1). This outcome differed from the reported 93% yield; however, the reaction yield was improved to 98% by adding Amberlite (IRN78) in separate portions, and allowing the reaction to stir for 16 hours (Table 3.2, entry 2).

Entry	Reagents and conditions	yield
1	Amberlite (IRN78) (4 mL/mmol), CH ₃ OH, 1h, rt	40%
2	Amberlite (IRN78) (8 mL/mmol in two portions), CH ₃ OH, 16h, rt	98%
3	NaOMe (4 eq), CH ₃ OH, up to 72h, rt	-
4	K ₂ CO ₃ (4 eq), CH ₃ OH, 48h, rt	67%

Table 3.2: Reagents and conditions for the synthesis of intermediate **26**.

Very careful washing of the resin with methanol ensured the product was completely extracted. Since the use of basic Amberlite is required to cleave the acetyl group in position 2' or 3' of the starting material and thereafter trigger the intramolecular cyclisation with release of Br⁻, the use of alternative basic conditions was attempted, with the aim of reducing the reaction time and avoiding the tedious washing of the resin. When sodium methoxide (NaOMe) was used in CH₃OH, only traces of the desired product could be formed (Table 3.2, entry 3). As an alternative, K₂CO₃ in CH₃OH was used and, along with the long reaction times required, filtration through celite pad yielded only 68% of the product **26**, due to some degradation already noticed on TLC (Table 3.2, entry 4).

Therefore the method involving the use of basic resin was considered the most successful. The identity of 2',3'-anhydro intermediate **26** was confirmed by NMR, and Figure 3.5 shows the ¹H-NMR of this product, performed in DMSO-*d*₆, characterised by the presence of the 5'-OH proton but lacking any other hydroxyl group. Moreover, from the distinctive coupling pattern, already described in the literature,^{212,217} it is evident that the H1' is not coupled with the H2', and the two signals appear respectively as a singlet and as a doublet, the latter due to the coupling with the H3'.

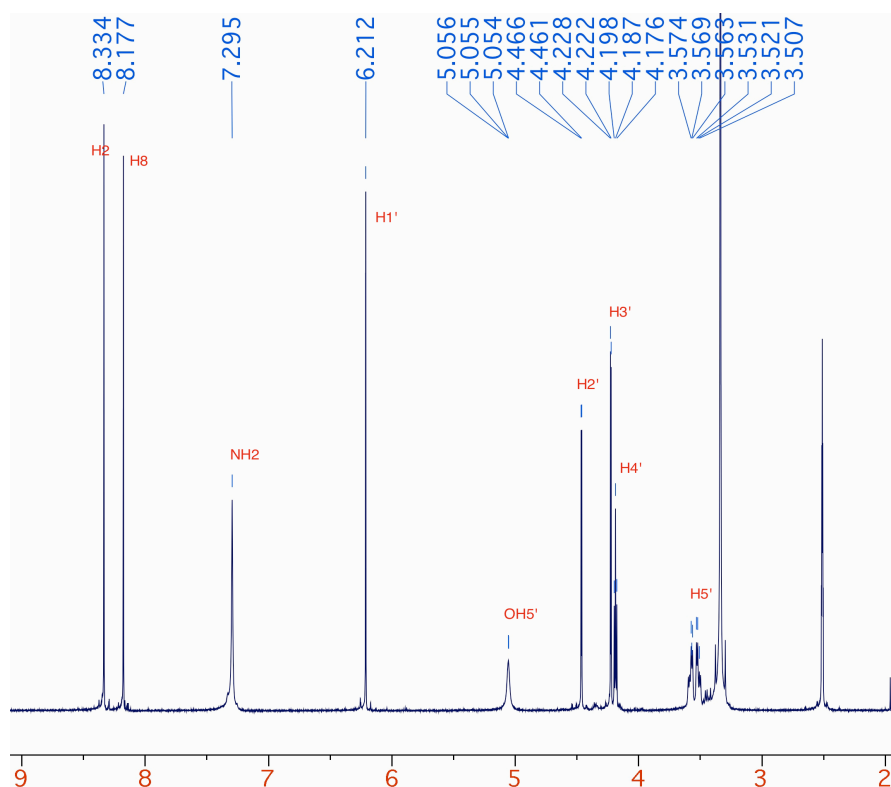


Figure 3.5: ¹H NMR (DMSO-*d*₆, 500 MHz) spectrum of 2',3'-anhydroadenosine **26**.

For the last step of 3'dA synthesis, Robins *et al.* reacted **26** with 12.5 equivalents of lithium triethylboron hydride (superhydride, LiEt₃BH) in anhydrous DMSO. In our hands, this procedure was initially attempted on a small scale (0.50 g of starting material), yielding 3'dA (**21**) in 23% yield due to incomplete conversion of the starting material (Table 3.3. entry 1), in contrast with the reported 98% yield.

Entry	Reagents and conditions			Yield
	LiEt ₃ BH*	Solvent	Temperature.	
1	12.5 eq (one portion)	DMSO (15 mL/mmol)	0 °C to rt. 16h	23%
2	4.5 eq (two portions)	DMSO (4 mL/mmol). THF (10 mL/mmol)	0 °C to rt. 16h	95%
3	4.5 eq (two portions)	THF (15 mL/mmol)	0 °C to rt. 16h	-

Table 3.3: Reagents, conditions and yields of the different attempts to synthesise 3'dA (**21**). * LiEt₃BH was used as a 1M solution in THF.

Following this procedure, no 2'-deoxyadenosine (2'dA, **27**) was synthesised, and the identity of the product was confirmed by both monodimensional and bidimensional NMR experiments, and by comparison with NMR characterisation reported in the literature (Figure 3.6, Figure 3.7). The ¹H NMR spectra of 3'dA yielding from this reaction method can be compared to commercially available 2'dA, and the most evident difference lies in the chemical shifts of H2' and H3' groups of signals, which are the most upfield signals respectively in 2'dA and 3'dA (Figure 3.6).

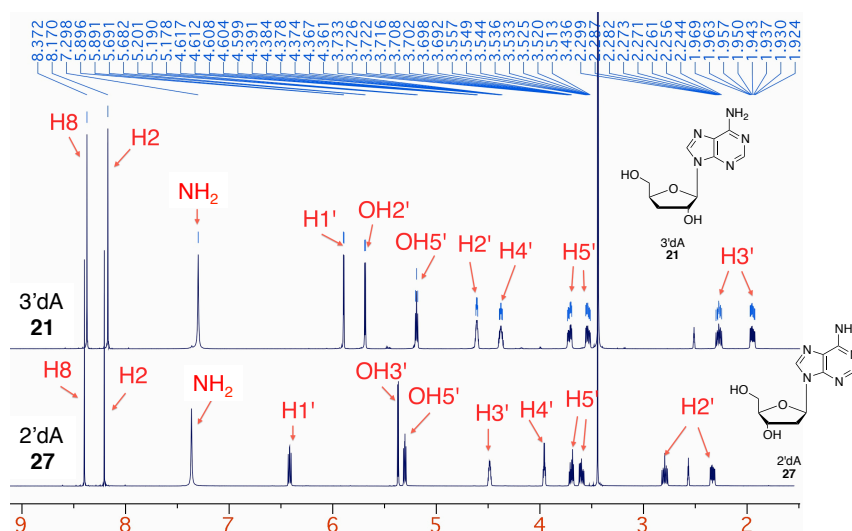


Figure 3.6: ¹H NMR (DMSO-*d*₆, 500 MHz) spectra of overlaid 3'dA (**21**) and 2'dA (**27**).

Moreover, analysis of the COSY 2D NMR experiment shows characteristic coupling patterns relative to 3'dA (Figure 3.7).

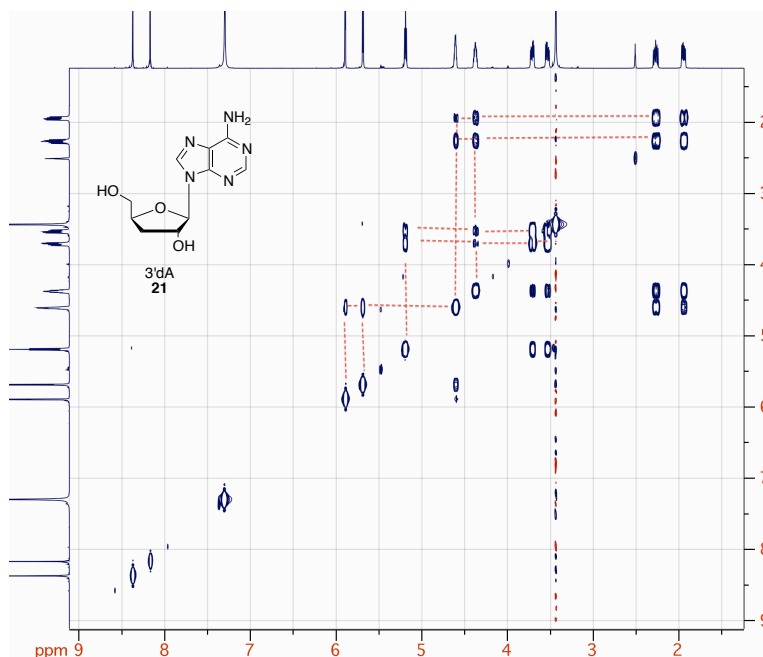


Figure 3.7: COSY NMR (DMSO-*d*₆) spectrum of 3'dA (**21**).

When the reaction was performed on a bigger scale (1.5 g), with the same reaction conditions, the yield was similar (28%) and the removal of the large volume of DMSO proved tedious. In order to improve both the reaction yield and purification step, when the reaction was carried out on 9 g of intermediate **26**, a reduced amount of anhydrous DMSO (4 mL/mmol) was used and anhydrous THF was added (10 mL/mmol). Furthermore, a reduced amount of LiEt₃BH (3 eq.) was added, followed by an additional portion (1.5 eq.) after 16 hours.

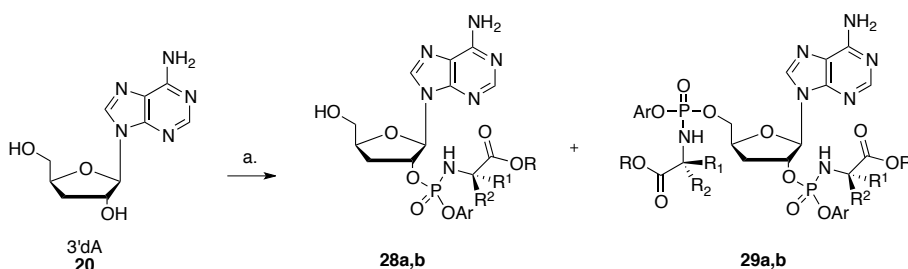
This resulted in 95% final yield of 3'dA (Table 3.3, entry 2). The mixture of a small amount of DMSO in THF does not allow the starting material to dissolve completely, but addition of the 1M solution of LiEt₃BH in THF allows the solid to dissolve and the solution to turn from clear to a dark orange colour. The attempt to completely avoid the use of DMSO as a solvent was unsuccessful: the reaction mixture of **26** in THF turned into a clear dark orange solution after addition of LiEt₃BH but even after 16 hours no conversion to 3'dA was noticed on TLC (Table 3.3, entry 3). A small amount of DMSO was added along with other 3 eq. of LiEt₃BH and the conversion happened within 3 hours. This proves that although not crucial as a solvent, DMSO may participate in the reaction mechanism.

3.1.3 Prodrug synthesis

The phosphoramidate (ProTide) and phosphorodiamidate phosphate prodrug technologies were applied to cordycepin, generating a family of nucleotide analogues for *in vitro* testing, primarily as anticancer agents. The following paragraphs will report synthetic methodologies and biological evaluation of 3'dA derivatives.

3.1.3.1 Synthesis of 3'dA ProTides

The first synthetic strategy for the synthesis of 5'-phosphoramidates implied the treatment of 3'dA with 1.1 equivalents of *t*BuMgCl and 3 equivalents of the appropriate phosphorochloridate under argon atmosphere overnight (Scheme 3.4).¹⁵⁴ The initially promising conversion of 3'dA into two other main species, as detected by TLC, resulted in the undesired synthesis of 2'-phosphoramidate (**28a,b**) and 2',5'-bis-phosphoramidate (**29a,b**) products (Table 3.4).



Scheme 3.4: First attempt of the synthesis of 3'dA ProTides using Grignard reagent. Reagents and conditions: a. *t*BuMgCl (1.1 eq), appropriate phosphorochloridate (3 eq), anhydrous THF, rt, 16 h.

Compound	Ar	R ¹ , R ²	Amino acid	Position	R	Yield
28a	Ph	CH ₃ , H	L-Ala	2'	Bn	5 %
28b	Nap	CH ₃ , H	L-Ala	2'	Bn	13%
29a	Ph	CH ₃ , H	L-Ala	2', 5'	Bn	35 %
29b	Nap	CH ₃ , H	L-Ala	2', 5'	Bn	11 %

Table 3.4: First family of cordycepin phosphoramidates synthesised through *t*BuMgCl-mediated coupling reaction.

Figure 3.8 and Figure 3.9 report the ³¹P NMR spectra of the products of the reaction of 3'dA with 3 equivalents of L-alanine benzyloxy naphthyl phosphorochloridate in the presence of *t*BuMgCl, and it is clear that this method yields only 2'-phosphoramidate (**28b**) and 2',5'-phosphoramidate (**29b**) products. In fact, the ³¹P NMR spectrum of **29b**

shows the presence of 8 peaks in a range between 4.5 and 2.5 ppm, corresponding to the 4 different isomers synthesised, each one containing two phosphoramidate moieties.

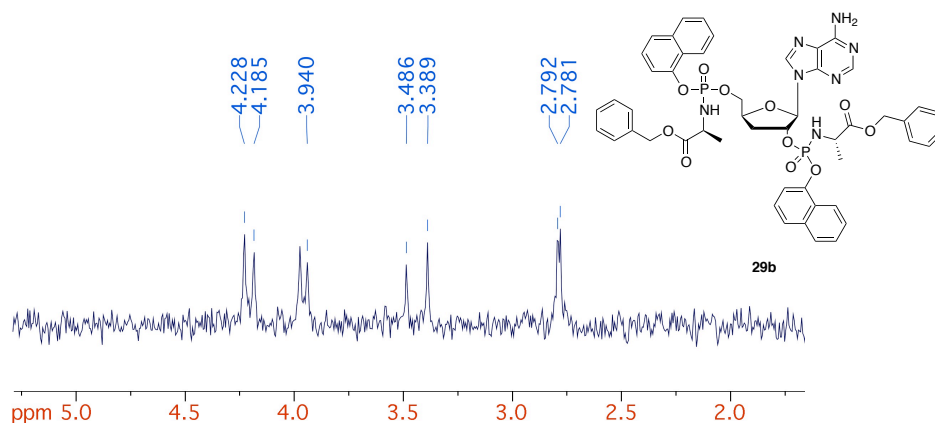


Figure 3.8: ^{31}P NMR (202 MHz, CD_3OD) spectrum of **29b**.

The ^{31}P NMR spectrum of the 2'-phosphoramidate **28b**, on the other hand, is not confirmative of the presence of the phosphoramidate moiety in position 2' or 5', with two peaks corresponding to the two diastereoisomers with chemical shifts in the region where 5'-phosphoroamidates should also be expected.

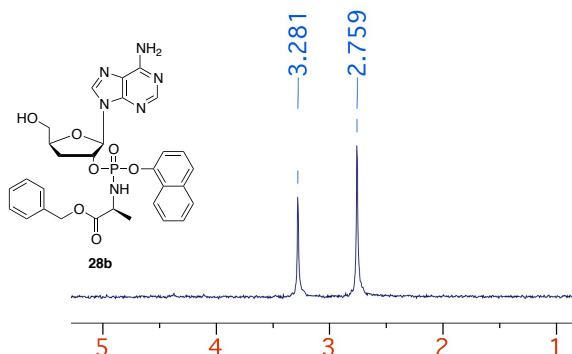
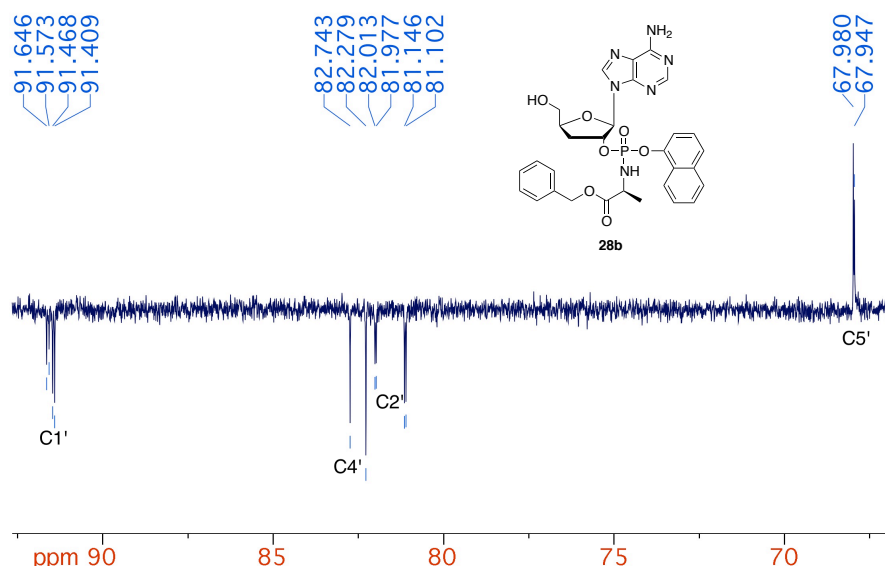


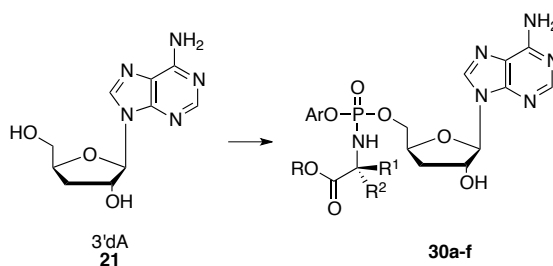
Figure 3.9: ^{31}P NMR (202 MHz, CD_3OD) spectrum of **28b**.

However, from the analysis of the ^{13}C NMR spectrum (Figure 3.10) it becomes evident that the structure of **28b** corresponds to a 2'-phosphoramidate, because of the splitting of the two diastereomeric peaks of the C1' into 4 peaks, due to a three bond coupling constant with phosphorus ($^3J_{\text{CCOP}} = 7.5$ Hz).

Figure 3.10: ^{13}C NMR spectrum of **28b**.

Another characteristic of the presence of a 2'-phosphoramidate moiety consists of the splitting of the carbon signals of the C2' due to the two bond coupling constant with phosphorus ($^2J_{\text{COP}} = 5.5$ Hz). On the other hand, the C4' and C5' signals are not split (Figure 3.10).

When the coupling reaction was performed with NMI and the appropriate phosphorochloridate in THF, the 5'-phosphoroamidates of 3'dA were synthesised as major products in moderate yields, although the 2',5'-bis-phosphoroamidate side products were nevertheless formed (Figure 3.5, Table 3.5).

Scheme 3.5: Synthesis of cordycepin ProTides (**30a-f**) via the NMI method. Reagents and conditions: NMI (5eq), appropriate phosphorochloridate (3 eq), anhydrous THF, rt, 16h.

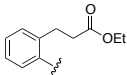
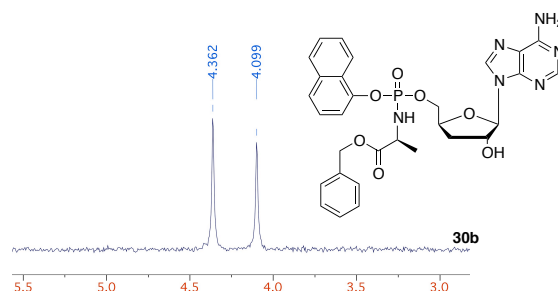
Cpnd	Ar	R ¹ /R ²	AA	R	Yield
30a	Ph	Me/H	L-Ala	Bn	28 %
30b	1-Naph	Me/H	L-Ala	Bn	12 %
30c	Ph	H/H	Gly	Bn	19 %
30d	1-Naph	<i>i</i> Bu/H	L-Leu	<i>n</i> -Pen	25 %
30e		Me/H	L-Ala	Bn	22 %
30f	1-Naph	Me/Me	DMG	Me	18 %

Table 3.5: 3'dA ProTides (**30a-f**) structures and yields.

Similar to the case of the 2'-phosphoramidates, confirmation of the presence of the 5'-phosphoramidate moiety is given primarily by the analysis of the signal splitting pattern of the ¹³C NMR spectrum. In fact, the ³¹P NMR spectrum of compound **30b** presents two peaks corresponding to the two diastereoisomers in the same region as for the 2'-phosphoramidate regioisomer **28b** (Figure 3.11).

Figure 3.11: ³¹P NMR (202 MHz, CD₃OD) spectrum of **30b**.

On the other hand, the ¹³C NMR spectrum presents crucial differences because of the splitting of the C4' and C5' signals respectively due to three and two bond coupling constant (³J_{COP} = 2.7 Hz and ²J_{COP} = 5.2 Hz), while in this case the C1' and C2' signals appear as two peaks due to the presence of two diastereoisomers (Figure 3.12).

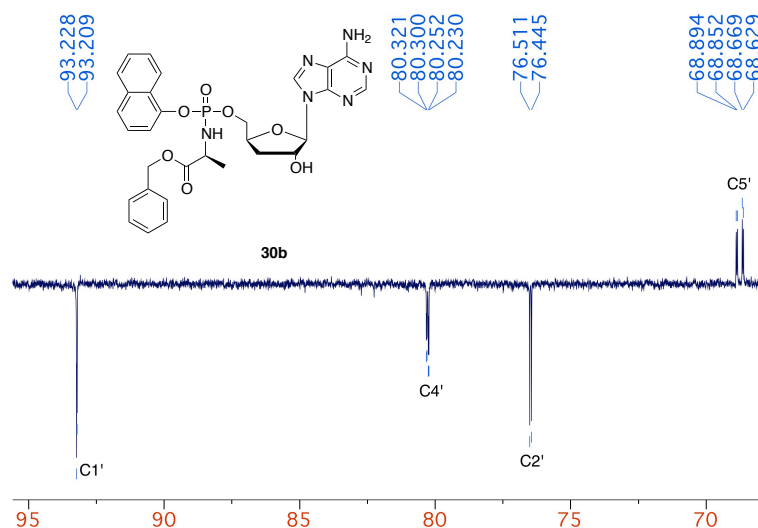
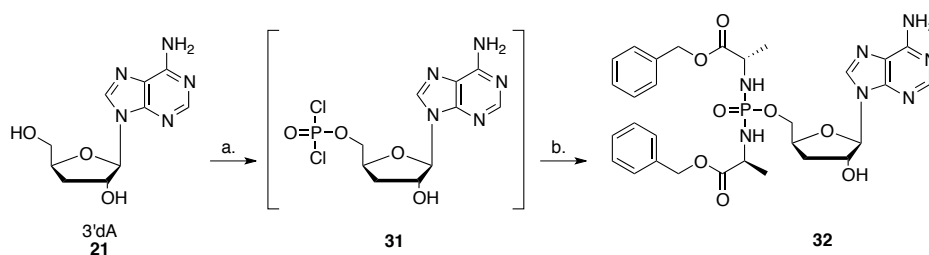


Figure 3.12: ^{13}C NMR (125 MHz, CD_3OD) spectrum of **30b**.

3.1.3.2 Synthesis of 3'dA phosphorodiamidates

The phosphorodiamidate approach was the second nucleotide prodrug system applied to 3'dA.^{67,156,218} In the present work, the Yoshikawa¹⁵⁶ procedure was adopted to obtain 5'-phosphorylated nucleoside analogues using unprotected 3'dA. According to the cited study, in a one pot reaction the unprotected nucleoside is suspended in trimethyl phosphate (TMP), and phosphorus oxychloride is added in order to obtain the 5'-phosphorodichloridate (**31**, Scheme 3.6) *in situ*.¹⁵⁵ The formation of this intermediate was monitored by ^{31}P -NMR (appearance of a peak ~ 7 ppm corresponding to the 5'-dichlorophosphate). Intermediate **31** was not isolated but immediately coupled with the appropriate amino acid ester salt in the presence of anhydrous diisopropyl ethyl amine (DIPEA). The progression of the reaction was monitored again by ^{31}P -NMR: the appearance of a single peak in the range of 13-17 ppm, depending on the amino acid used for the synthesis, indicated the formation of the product. The synthesis of the benzyloxy-L-alaninyl phosphorodiamidate **32** was accomplished in 49% (Scheme 3.6).



Scheme 3.6: Synthesis of 3'dA phosphorodiamidate **32**. Reagents and conditions: (a.) POCl_3 (1 eq), TMP 0°C -rt, 4h. (b.) L-AlaOBn-HCl (5 eq), DIPEA (10 eq), CH_2Cl_2 , 0°C -rt, 16h.

The product identity was confirmed by NMR characterisation and Figure 3.13 shows the characteristic ^{31}P NMR spectrum of compound **32** with only one peak due to the lack of chirality at the P centre.

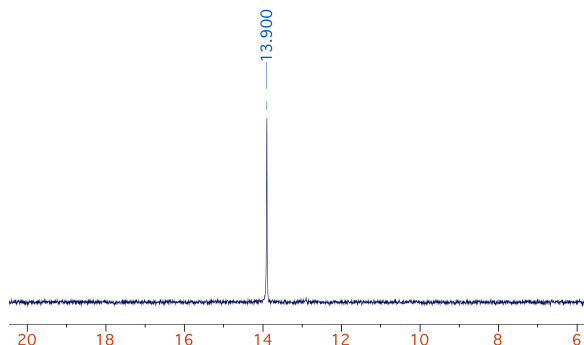


Figure 3.13: ^{31}P NMR (202 MHz, CD_3OD) spectrum of **32**.

3.1.4 Biological evaluation of 3'dA prodrugs

3.1.4.1 *In vitro* cytotoxic screening of 3'dA prodrugs

An initial cytotoxicity screening on a selection of cell lines was performed by WuXi AppTech on the synthesised ProTides (**30a-f**) and the 5'-phosphorodiamidate (**32**) prodrug of 3'dA. Moreover, the 2'-phosphoroamidates (**28a,b**), and one example of 2',5'-bisphosphoroamidate (**29b**) were included in this preliminary evaluation (Table 3.6).

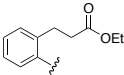
Comp.	Position	Ar	R ¹ ,R ²	AA	R	CLogP
3'-dA	-	-	-	-	-	- 2.36
28a	2'	Ph	CH ₃ , H	L-Ala	Bn	1.12
28b	2'	Nap	CH ₃ , H	L-Ala	Bn	2.30
29a	2',5'	Ph	CH ₃ , H	L-Ala	Bn	4.42
30a	5'	Ph	CH ₃ , H	L-Ala	Bn	0.93
30b	5'	Nap	CH ₃ , H	L-Ala	Bn	2.10
30c	5'	Ph	H, H	Gly	Bn	0.81
30d	5'	Nap	<i>i</i> Bu, H	L-Leu	<i>n</i> -Pent	3.97
30e	5'		CH ₃ , H	L-Ala	Bn	1.60
30f	5'	Nap	CH ₃ , CH ₃	DMG	CH ₃	0.70
32	5'	- (phosphorodiamidate)	CH ₃ , H	L-Ala	Bn	2.91

Table 3.6: Compounds tested on cancer cell lines by WuXi AppTech. CLogP calculated *via* ChemDraw program.

The selected cell lines derive mainly from haematologic malignancies (MOLT-4, KG-1, HL-60, CCRF-CEM, K562), since 3'dA has been involved in clinical trials against acute myeloid leukaemia (AML). Moreover, two solid tumour-derived cell lines (MCF-7, HepG2) were considered in light of the activity of 3'dA reported on breast cancer cell lines^{219,220} and hepatocellular carcinoma cell lines (Table 3.7).²²⁰

Cell lines	Malignancy
MOLT-4	Acute T lymphoblastic leukaemia
KG-1	Acute myelogenous leukaemia
HL-60	Acute promyelocytic leukaemia
CCRF-CEM	Acute lymphoblastic leukaemia
K562	Chronic myelogenous leukaemia
MCF-7	Breast adenocarcinoma
HepG2	Hepatocellular carcinoma

Table 3.7: Malignant cell lines selected for the cytotoxic screening of 3'dA prodrugs by WuXi AppTech.

This screening aimed to provide an initial understanding of whether 3'dA prodrugs would bring advantage over the parent nucleoside in terms of cytotoxic activity on the considered cell lines.

Table 3.8 reports the cytotoxic activities of 3'dA prodrugs as μM IC_{50} values, the concentration of compound leading to a 50% reduction in cell viability and percentage of maximum inhibition ($\text{MI}_{\%}$).

Across all range of cell line considered, 3'dA does not represent a potent anticancer drug, due both to the high IC_{50} values and the inability to reach 100% inhibition of viability. Particularly striking is the effect of cordycepin on the CCRF-CEM cell line, in which the maximum inhibition of viability reaches only 12% (Figure 3.14).

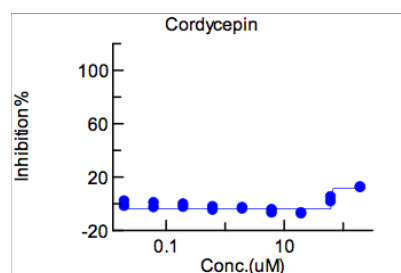


Figure 3.14: Cordycepin activity in CCRF-CEM cell line, reported as a set of data points corresponding to effect on cell viability of the different concentrations of drug. Screening performed by WuXi AppTech.

3'dA does not lead to a measurable 50% inhibition of cell growth in most of the cell lines, in fact the IC_{50} is reported as a predicted value ($>100 \mu\text{M}$) on most cell lines. On the cells

in which 3'dA exerts inhibition of cell viability higher than the 50%, the IC₅₀ concentrations range from 34.23 μM on the MCF-7 cell line and 151.92 μM on the MOLT-4 cell line.

3'dA derivatives, on the other hand, bring an advantage over the parent nucleoside in terms of cytotoxicity in almost all cell lines (Table 3.8).

Cpnd	CCRF-CEM		HL-60		KG-1		MOLT-4		K562		HepG2		MCF-7	
	IC ₅₀	MI%	IC ₅₀	MI%	IC ₅₀	MI%	IC ₅₀	MI%	IC ₅₀	MI%	IC ₅₀	MI%	IC ₅₀	MI%
3'-dA	>198	12	76.84	88	70.82	78	151.92	52	59.31	88	142.47	66	34.23	78
28a	64.83	65	143.47	57	111.95	63	62.86	75	26.3	78	85.5	667	10.35	97
28b	27.14	99	78.59	99	66.28	93	14.78	100	25.35	87	30.16	90	5.05	99
29a	17.63	99	31.09	80	79.44	69	18.62	100	26.87	89	83.06	55	5.06	94
30a	2.36	100	17.78	97	17.36	92	0.51	98	6.1	92	18.73	76	3.07	94
30b	1.17	100	6.37	100	11.03	100	0.32	100	4.93	97	11.53	95	1.39	99
30c	14.93	94	45.23	82	136.56	65	3.55	93	15.42	92	142.35	59	15.46	87
30d	4.72	100	8.9	100	12.02	99	1.46	100	11.7	99	9.53	99	2.48	100
30e	40.09	90	78.51	74	102.14	69	12.62	97	174.71	61	96.11	59	15.78	78
30f	4.92	99	24.08	98	>198	29	1.4	100	10.69	91	70.22	84	9.10	99
32	7.03	100	16.53	100	34.13	98	3.52	100	24.34	97	156.87	55	12.97	97
PTX	0.003	95	0.004	96	0.07	89	0.002	97	0.008	94	#Intersect	54	0.003	79

Table 3.8: *In vitro* cell viability evaluations after treatment with 3'dA and 3'dA prodrugs. Cytotoxicity data reported as μM IC₅₀ values (concentration of drug causing 50% of cell viability inhibition) and MI% values (maximum inhibitory effect of the drug at the range of concentration considered). PTX: paclitaxel (control). Screening performed by WuXi AppTech.

The derivatives emerging as the most active on the majority of cell lines tested were 5'-phosphoramidates **30a** (L-alanine-*O*-benzyl phenyl derivative), **30b** (L-alanine-*O*-benzyl naphthyl derivative) and **30d** (L-leucine-*O*-pentyl naphthyl derivative) (Table 3.8, Figure 3.15).

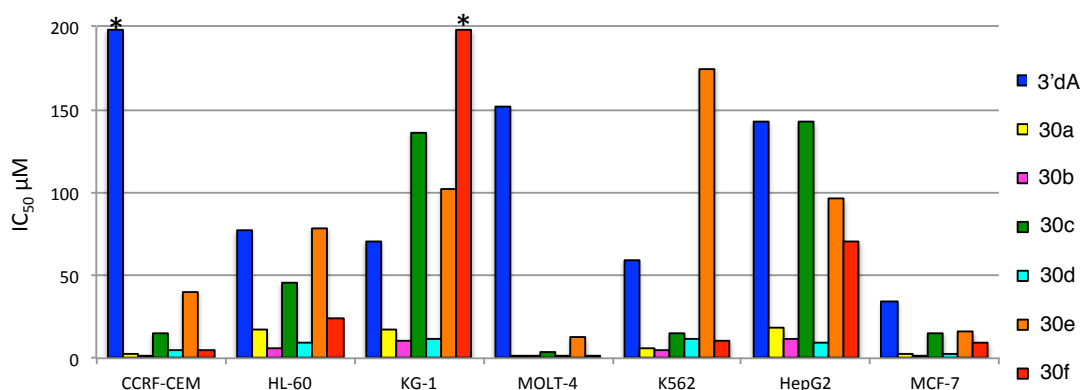


Figure 3.15: Cytotoxic activity of 3'dA and 5'-phosphoramidates **30a-f**. *IC₅₀ > 198 μM.

However, replacing the amino acid portion with glycine (**30c**) or dimethylglycine (**30f**) caused a drop in anticancer activity, especially in the case of compound **30f**, bearing a methyl ester instead of a benzyl ester. The introduction of a new moiety in place of the most frequently used phenyl or naphthyl group, represented by the ethyl 3-phenyl propanoate group in compound **30e**, generated a compound with lower activity on KG-1 and HepG2 cell lines, compared to the naphthyloxy and phenoxy-bearing compounds **30a**, **30b** and **30d**. However, **30e** had similar IC_{50} values to **30a** and **30b** when tested on the other cell lines.

The 2'-phosphoroamidates **28a** and **28b** and the *bis*-phosphoroamidate **29b** usually represent side products of the coupling reaction to synthesise the desired 5'-phosphoroamidate prodrugs.

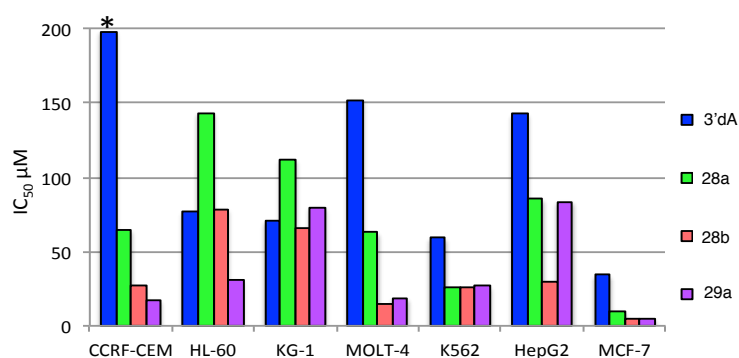


Figure 3.16: Cytotoxic activity of 3'dA and 2'-phosphoroamidates **28a** and **b**, and 2',5'-bisphosphoramidate **29a**. * $IC_{50} > 198 \mu\text{M}$.

However, some results generated in the McGuigan group²²¹ reported that some examples of 3'-phosphoroamidate prodrugs of cladribine were more cytotoxic than the 5'-regioisomers, and this bizarre result stimulated the investigation on the cytotoxic potential of alternative phosphoroamidate derivatives (such as 2'-phosphoramidates **28a** and **28b** and 2',5'-*bis* phosphoramidates **29a**), especially in situations where as was the case of 3'dA ProTides synthesis, these side products could be generated in relatively large amounts. Although not as potent as the most active ProTides **30a**, **30b** and **30d**, the naphthyl derivatives **28b** and **29a** were several-fold more potent than 3'dA, while **28a** performed less efficiently, despite retaining higher potency than 3'dA on most cell lines (Table 3.8, Figure 3.16).

The 5'-phosphorodiamidate **32** was more active than 3'dA and the ProTides **30c**, **30e** and **30f** but less active than the lead ProTides **30a**, **30b** and **30d** (Figure 3.17 shows the comparison between **32** and **30a**, along with the parent nucleoside).

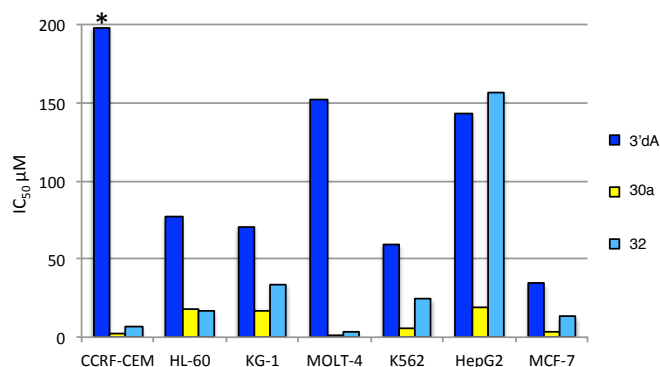


Figure 3.17: Cytotoxic activity of 3'dA and phosphorodiamidate **32**, compared to the 5'-phosphoramidate **30a**. *IC₅₀ > 198 μM.

In conclusion, this initial cytotoxicity screening was aimed at understanding whether the ProTide and phosphorodiamidate prodrug approaches could generate potential anticancer agents by enhancing the potency of 3'dA. All the derivatives tested showed improved cytotoxicity on all cell lines considered, and some ProTides, such as the L-alanine derivatives **30a** and **30b**, reaching 2.6 log lower IC₅₀ values (on MOLT-4 cell line), were considered as lead candidates for further preclinical development.

3.1.4.2 Antiviral screening on 3'dA derivatives

3'dA, the intermediate in 3'dA synthesis 9-(2,3-anhydro-β-D-ribofuranosyl)adenine **27**, the 2'-phosphoramidate derivatives **28a** and **28b**, the 2',5'-bis-*O*-phosphoramidate **29a** and ProTides **30a** and **30d** were tested on yellow fever virus (YFV) infected cells by Dr. J. Bugert (School of Medicine, Cardiff University). The rationale behind this screening was that in the early literature reports, 3'dA was found to have some activity on both RNA and DNA viruses.^{182,183}

Compound	TOX +/-	CPE +/-
3'dA	-	+
27	-	+
28a	-	+
28b	-	+
29b	-	+
30a	-	+
30d	-	+

Table 3.9: Anti-YFV activity and toxicity profile of prodrugs **28a**, **28b**, **29b**, **30a** and **30d** plus the parent nucleoside 3'-dA and **27**. Antiviral activity and cytotoxicity were determined at 10 μM concentration. Assays performed by Dr. Joachim Bugert (School of Medicine, Cardiff University).

In an attempt to investigate the possible antiviral activity of 3'dA derivatives, they were sent for testing against YFV, a RNA virus of the Flaviviridae family that can cause devastating epidemics of potentially fatal, hemorrhagic disease.²²² Although YFV vaccination exists, there is no approved treatment for infected patients.²²³

The compounds were first screened at a fixed concentration of 10 μM to detect activity on YFV infected Vero and BSC-1 cells (both kidney epithelial cells extracted from an African green monkey) and the toxicity on these cells.

The antiviral activity was measured by analysis of the cytopathic effect (CPE) on the infected cells: this effect refers to the damage to the host cells during virus invasion that can be studied in tissue culture. A positive CPE value means the cells are infected and the tested compounds are not showing any effects, whereas a negative CPE value means the compounds are effective at the given concentration.²²⁴

As evident from Table 3.9, none of the compounds showed any interesting activity on yellow fever viruses infected cells; on the other hand the compounds are not toxic at 10 μM concentration on non malignant Vero and BSC-1 cell lines, and this could be positive data in terms of selective toxicity of compounds **30a** and **30d** (3'dA ProTides) on cancer cells at that same concentration (compounds **30a** and **30d** showed activity at lower concentrations on almost all cancer cell lines shown in Table 3.8).

3.1.4.3 Additional cytotoxic screening of 3'dA prodrugs

The parent nucleoside 3'dA, ProTide **30b** and the intermediate **27** were tested for their activity on L1210 (murine lymphocytic leukaemia), CEM (acute lymphoblastic leukaemia) and HeLa (cervical adenocarcinoma) cell lines by Prof. Balzarini group at the Rega Institute (Leuven, Belgium). The results are shown in Table 3.10.

Compound	L1210	CEM	HeLa
3'dA	39 \pm 9	50 \pm 14	85 \pm 15
30b	5.2 \pm 1.6	1.7 \pm 0.6	7.4 \pm 4.4
27	> 250	> 250	> 250

Table 3.10: Compounds tested on cancer cell lines by Prof. Balzarini group at the Rega Institute (Leuven, Belgium), (IC_{50} μM activity).

The 5'-phosphoramidate **30b** retains better activity than 3'dA on these cell lines, confirming the data previously generated (Table 3.8). Compound **27** was previously tested as an anti-trypanosome agent,²²⁵ and anti-HIV agent,²²⁶ but was inactive. However, tested

as the triphosphate on different viral DNA-polymerase enzymes, it proved an efficient inhibitor.²²⁷ Compound **27** was never reported as potentially active as anticancer agent, and from this cytotoxic screening the compound was inactive.

3.1.4.4 *In vitro* screening of 3'dA ProTides on additional cell lines

The favourable activity profile of ProTides **30a**, **30b**, **30d**, **30e** prompted further testing of these compounds on additional cell lines (Table 3.11) by WuXi AppTech, in order to confirm the potency of the compounds and select a candidate for the preclinical studies. The parent nucleoside 3'dA was tested in parallel, along with ProTide **30f**, selected as a negative control, due to the lower cytotoxic potential demonstrated in the previous assays.

	Cell line	Malignancy
Haematologic malignancies	RL	non-Hodgkin's lymphoma
	HS445	Hodgkin lymphoma
	RPMI-8226	human multiple myeloma
	THP-1	acute monocytic leukaemia
	Z-138	mantle cell lymphoma
	MV4-11	biphenotypic B myelomonocytic leukaemia
	NCI-H929	plasmacytoma
	HEL92.1.7	erythroleukaemia
	Jurkat	acute T cell leukaemia
Solid tumours	BxPC-3	Pancreas carcinoma
	HT29	Colon adenocarcinoma
	MIA PaCa-2	Pancreas adenocarcinoma
	SW620	Colon adenocarcinoma

Table 3.11: Cell lines selection for the second anticancer evaluation of 3'dA ProTides by WuXi AppTech.

As shown in Table 3.12, the lack of potency of 3'dA was confirmed in this second screening on different cell lines by the inability to reach 100% inhibition of cell viability up to the highest concentration considered (198 μ M).

Cpnd	MV4-11		THP-1		RL		HS445		HEL92.1.7		NCI-H929		RPMI-8226	
	IC ₅₀	MI%	IC ₅₀	MI%	IC ₅₀	MI%	IC ₅₀	MI%	IC ₅₀	MI%	IC ₅₀	MI%	IC ₅₀	MI%
3'dA	>198	1	>198	-3	>198	17	>198	2	68.9	88	>198	24	>198	1
30a	2.1	99	65.45	74	3	93	30.53	98	8.07	100	6.07	100	14.72	96
30b	1.48	99	46.47	99	1.68	96	10.18	96	2.94	98	3.38	99	9.48	102
30d	8.78	106	68.91	99	11.61	100	39.53	102	4.23	99	7.21	104	24.06	103
30e	3.27	100	36.66	100	7.26	90	42.73	92	14.49	99	7.57	100	31.05	106
30f	8.71	101	>198	43	13.54	88	54.98	85	15.42	101	16.11	98	46.7	89
PTX	0.01	99	0.03	72	0.003	83	0.01	74	0.02	83	0.003	82	0.003	91

Table 3.12: *In vitro* cell viability evaluation after treatment with 3'dA and selected ProTides. Cytotoxicity data reported as μM IC₅₀ values (concentration of drug causing 50% of cell viability inhibition) and MI% (maximum inhibitory effect of the drug at the range of concentration considered). PTX: paclitaxel (control). Screening performed by WuXi AppTech.

3'dA exerted measurable cell viability inhibition (MI% = 88%) at high concentration (IC₅₀ = 68.9 μM) only on the erythroleukaemia cell line HEL92.1.7, and performed distinctively well on the mantle cell lymphoma cell line Z138,²²⁸ a unique example where 3'-dA could reach 95% of cell viability inhibition with an IC₅₀ value of 12.15 μM . The cell line Z138 also represented an exception because ProTides **30b** and **30d**, usually many times more active than the parent nucleoside, were in this case only two-fold more active than 3'dA and more strangely **30a** was two-fold less active than 3'dA (Table 3.13).

Cpnd	Jurkat		Z138		BxPC-3		HT29		MIA PaCa-2		SW620	
	IC ₅₀	MI%	IC ₅₀	MI%	IC ₅₀	MI%	IC ₅₀	MI%	IC ₅₀	MI%	IC ₅₀	MI%
3'dA	>198	20	12.15	95	>198	22	>198	44	>198	35	>198	10
30a	1.44	100	26.97	95	23.59	81	13.42	93	6.85	96	24.94	85
30b	0.9	100	6.32	100	13.36	90	7.52	98	3.73	98	11.41	93
30d	7.15	100	5.65	100	65.46	99	16.06	99	14.69	106	35.48	100
30e	4.75	100	68.18	76	60.92	78	25.24	89	12.09	101	43.4	90
30f	7.01	95	43.84	93	76.18	71	37.94	76	17.55	91	56.48	74
PTX	0.005	97	0.002	99	>0.5	42	0.004	75	0.002	87	0.02	96

Table 3.13: *In vitro* cell viability evaluation after treatment with 3'dA and selected ProTides. Cytotoxicity data reported as μM IC₅₀ values (concentration of drug causing 50% of cell viability inhibition) and MI% (maximum inhibitory effect of the drug at the range of concentration considered). PTX: paclitaxel (control). Screening performed by WuXi AppTech.

No explanation for this peculiar result could be found in the literature, therefore one could only speculate that this cell line may down-regulate ADA, therefore there may be a reduction in deamination of 3'dA that could prolong and enhance the activity of this nucleoside. Alternatively, enzymes responsible for the ProTide activation

(carboxypeptidase/phosphoramidase enzymes) could be down-regulated, leading to a reduced activity of these molecules. However, this was an isolated event, as ProTides **30a**, **30b**, **30d**, **30e** and **30f** were consistently more active than 3'dA on all the other cell lines considered, the only exception being the negative control ProTide **30f** that did not lead to 50% of inhibition of cell viability on THP-1 cell line.

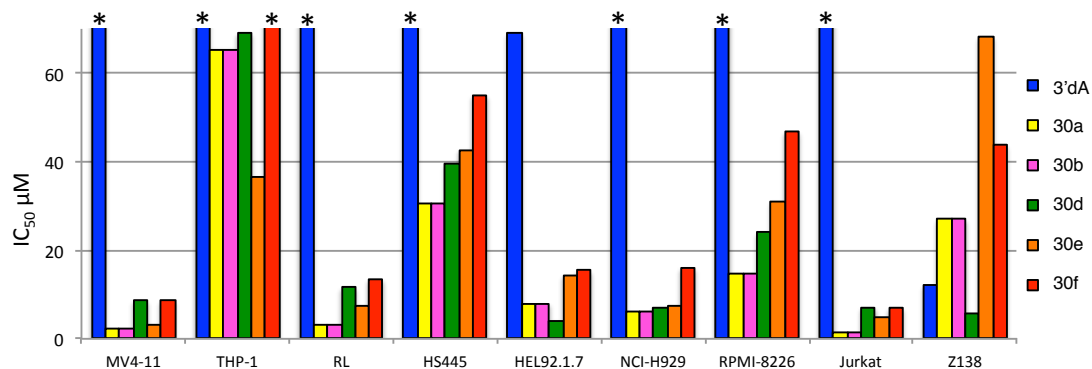


Figure 3.18: Cytotoxic activity of 3'dA and selected ProTides, on haematologic malignancies. *IC₅₀ > 198 μM.

ProTides **30a** and **30b** were the most active compounds in most of the considered cell lines, **30b** being usually 1 or 2 fold more active than **30a**. The best results were achieved on Jurkat cell line (acute T-cell leukaemia), where **30b** reached 100% of cell viability inhibition at a concentration of 0.9 μM, and **30a** performed similarly at a concentration of 1.44 μM (Table 3.13, Figure 3.18).

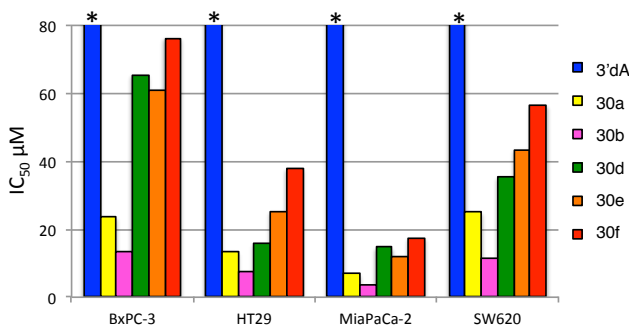


Figure 3.19: Cytotoxic activity of 3'dA and selected ProTides, on solid tumours *IC₅₀ > 198 μM.

Compounds **30e** and **30d** had similar potencies in most cell lines, although with higher IC₅₀ values than **30a** and **30b**. On solid tumours (Table 3.13, Figure 3.19) the compounds were generally less active than in other settings, however with activity still in the μM range.

In conclusion, this second set of cytotoxic data demonstrated again the superior activity of 3'dA ProTides compared to the parent nucleoside, and the L-alanine benzyloxy compounds **30a** and **30b** proved the most potent derivatives in the series.

3.1.4.5 Evaluation of intracellular 3'dA triphosphate levels after treatment with 3'dA ProTides

The anticancer activity of 3'dA is primarily generated by the intracellular triphosphate metabolite (3'-dATP). In order to investigate whether the superior cytotoxic activity of 3'dA ProTides could be a consequence of increased intracellular 3'dATP levels, a selection of cell lines were treated with 3'dA and the ProTides which emerged as most active in the previous screenings performed by Barts Institute (London). ProTide **30f** was selected as a poorly performing analogue in order to have a negative control (Table 3.14).

General Structure	Cpnd	Ar	R	R ₁ /R ₂	AA
	3'dA	-	-	-	
	30a	Ph	Bn	H/H	Gly
	30b	Nap	Bn	Me/H	L-Ala
	30d	Nap	<i>n</i> -Pen	Me/H	L-Ala
	30e		Bn	Me/H	L-Ala
	30f	Nap	Me	Me/ Me	DMG

Table 3.14: Compound selected for *in vitro* evaluation of 3'dATP intracellular levels on CEM, K562 and HL-60 cell lines. Screening performed by Barts Institute (London).

The cell line selection includes the acute lymphoblastic leukaemia cell line CEM, the chronic myelogenous leukaemia cell line K562 and the acute promyelocytic leukaemia cell line HL-60. Cells were treated with concentrations of the selected compounds ranging from 10 nM to 20 μ M and were incubated for 2 hours at 37 °C. The results reported in Table 3.15 as IC₅₀ values confirm the better activity profile of 3'dA ProTides compared to the parent nucleoside, with the exception of compound **30f**, which was chosen as a negative control, and emerged again as a poorly active compound.

Compound	CEM	K562	HL-60
3'dA	19.5	10.9	11.4
30a	0.87	2.4	4.6
30b	0.13	0.21	2.6
30d	6.1	4.2	5.4
30e	4.3	6.3	8.3
30f	10	13.9	10.2

Table 3.15: Evaluation of concentration inhibiting 50% of cell viability (IC_{50} , μM) on CEM, K562 and HL-60 cell lines. Assays performed by Barts Institute (London).

With IC_{50} activity ranging from 4- to 15-fold lower than 3'dA, naphthyl L-alaninyl-benzyloxy ProTide **30b** emerged as the most potent compound, followed by the phenyl-bearing counterpart, compound **30a**.

The analysis of 3'dATP levels generated in the intracellular environment after treatment with the selected compounds at a fixed concentration was performed at Barts Institute (London) via LC-MS. Table 3.16 shows these results as mean concentrations of intracellular 3'dATP expressed in $\mu g/mL$.

Compound	CEM	K562	HL-60
3'dA	0.2	1.7	1.7
30a	3.7	2.6	3.2
30b	11.5	6.2	5.1
30d	2.9	0.9	0.7
30e	1.1	1.3	1.2
30f	0.2	0.2	0.2

Table 3.16: 3'dATP intracellular levels generated after treatment of malignant cell lines with selected 3'dA ProTides. Values expressed as $\mu g/mL$ concentrations. Assays performed by Barts Institute (London).

The low levels of intracellular 3'dATP generated after treatment with 3'dA, ranging from 0.2 to 1.7 $\mu g/mL$, suggest that the low cytotoxicity of this compound derives from a poor intracellular processing to the active metabolite, which could depend on either an inefficient phosphorylation by nucleoside kinase enzymes or the catabolism into inactive intracellular species such as 3'dIno. The 3'-dATP levels generated after treatment with the least active ProTide **30f** was comparable, potentially because of an inefficient intracellular processing to 3'dAMP. On the other hand, the levels of 3'dATP produced by the intracellular processing of the most active compound **30b** are significantly higher, and range from 5.1 to 11.5 $\mu g/mL$. High levels of intracellular active metabolite are similarly generated by treatment with compound **30a**. Cell treatment with ProTides **30e** and **30f**, on the other hand, led to intracellular 3'dATP levels 5 to 15-fold higher than the parent

nucleoside on CEM cell line, and lower levels of HL-60 and K562 cells, despite the similar IC_{50} values of these compounds on all cell lines.

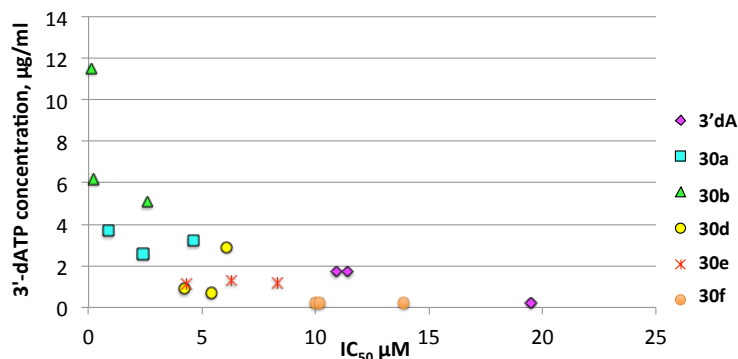


Figure 3.20 Correlation between cytotoxic IC_{50} values (μ M) of selected compounds and intracellular 3'-dATP concentrations (μ g/mL) after treatment with 3'dA and ProTides **30a,b,d-f**.

Figure 3.20 shows a correlation between the cytotoxic activity (IC_{50} values) of drugs (3'dA and selected ProTides **30a,b,d-f**), and the intracellular levels of 3'dATP measured. A link between activity of drug and level of putative intracellular metabolite (3'dATP) emerged from these studies.

3.1.4.6 Selective cytotoxicity of 3'dA analogues on cancer stem cells

3.1.4.6.1 The concept of cancer stem cells (CSCs)

Cells with stem-cells characteristics have been identified in haematological malignancies and in the vast majority of solid tumours, such as breast cancer,²²⁹ lung cancer,²³⁰ colon cancer,²³¹ prostate cancer,²³² ovarian cancer,²³³ melanoma²³⁴ etc. These cells are considered responsible for cancer initiation, progression, metastasis, recurrence and drug resistance.²³⁵⁻²³⁸ These cells share normal stem cells features such as the ability to self-renew, proliferate and differentiate in a pluripotent manner.^{236,238} Two different models have been proposed in order to explain the heterogeneous cell phenotypes that constitute a tumour.^{237,239} According to the cancer stem cell model, rare cancer stem cells are responsible for the initiation and development of cancer, along with features such as recurrence and metastasis.^{239,240} Moreover the heterogeneity and hierarchy between cells in the tumour depend on CSCs asymmetric division, generating an identical cell clone and a differentiated daughter cell. A second theory, named the clonal evolution model considers all tumour cells responsible for the maintenance of the tumour, and the heterogeneity

derived from genetic and/or epigenetic modifications during cancer development.^{239,240} Understanding important features of these cells can help identify new anti-cancer therapeutics able to eradicate the tumour by targeting not only the bulk cells but also CSCs.^{235,236,241} The identification of CSCs from other cancer cells is based on the presence of specific CSCs biomarker phenotypes that can be used in fluorescence-activated cell sorting (FACS) to identify these populations and separate them from other cells. As an example, the leukaemia stem cells (LSC) were the first to be identified, due to the presence of a CD34⁺/CD38⁻ surface marker phenotype.²³⁷ The lower expression of CD38 distinguished LSCs from normal hematopoietic stem cells, while the presence of CD34 is a feature of both cell types. Aside from extracellular and intracellular markers, CSCs appear to express high levels of ATP-binding cassette (ABC) transporters such as P-glycoprotein (P-gp), involved in the extracellular efflux of small molecules such as anti-tumour drugs, and contributing to the multidrug-resistance (MDR).^{239,242,243} Moreover, the up-regulation of self-renewal pathways and down-regulation of apoptotic pathways are features of CSCs.²³⁹ Examples of this are the up-regulation of PI3K/AKT signalling pathway causing cellular transformation and tumourigenesis in acute myeloid leukaemia (AML) and chronic myeloid leukaemia (CML).²³⁹ Moreover, aberration of the JAK/STAT pathway involved in tumour initiation through activation of several oncogenes was described in many tumours, including leukaemias.²³⁹ Aberrant activation of the transcription factor nuclear factor kappa B (NF- κ B), affects the expression of several apoptosis-related proteins and causes cancer development, progression and chemo-resistance.²³⁹ Other important affected pathways are the Notch, Hedgehog²³⁸ and Wnt pathways, responsible for the CSCs self-renewal capacity and differentiation.²³⁹

Resistance to chemotherapy and radiotherapy causes recurrence of malignancies, and this has been linked with the inability to eradicate CSCs through conventional therapy.^{237,244} For this reason, new therapeutic strategies are evolving in order to target the features of CSCs, exemplified by ligands or antibodies to target extracellular markers and agents capable of down-regulating the expression or inhibiting the activity of ABC-transporters.^{235,242} In addition, many agents were developed with the purpose of affecting the altered key signalling pathways in CSCs or to alter the tumour microenvironment responsible for promoting the CSCs development.²³⁹ Given that cells with a stem cell phenotype persist and are enriched in patients who have been treated with conventional therapies,²⁴⁵⁻²⁴⁷ there is a strong rationale for using stem cell targeting therapies in frontline therapy. This has the potential to induce more durable remissions and even cures.

3.1.4.6.2 Characterisation of KG1a stem cell phenotype

The effect of 3'dA and some of the most active prodrugs was assessed on the CSC compartment of the acute myelogenous leukaemia cell line KG1a by Prof. C. Pepper (School of Medicine, Cardiff University). A minor stem cell-like compartment is present in this cell line, with a distinct immunophenotype (CD34⁺/CD38⁻/CD123⁺).^{248,249}

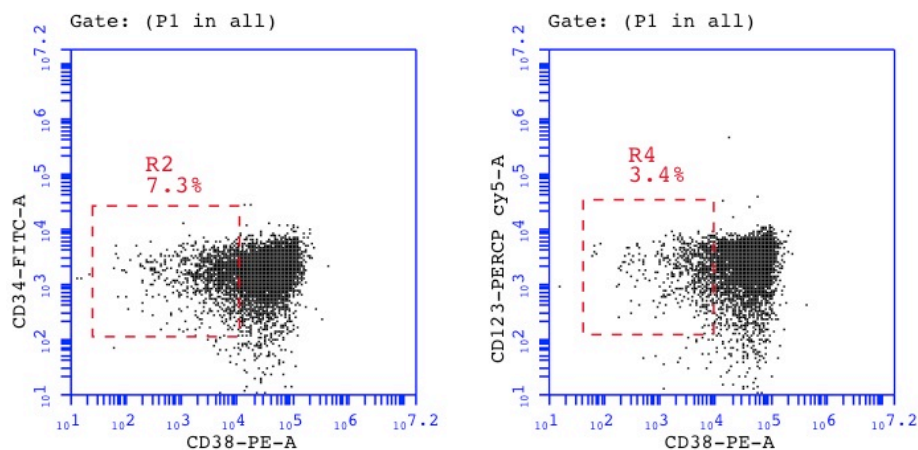


Figure 3.21: Gating strategy to define the LSC sub-population in the KG1a cell line. Analysis performed by Prof. C. Pepper (School of Medicine, Cardiff University).

This immunophenotype is evident through fluorescence-activated cell sorting (FACS) analysis of the cells after labelling with a cocktail of anti-lineage antibodies (PE-cy7), anti-CD34 (FITC), anti-CD38 (PE) and anti-CD123 (PERCP cy5). The subpopulation expressing a leukaemic stem cell (LSC) phenotype can be identified and expressed as a percentage of all viable cells in the culture (Figure 3.21).

Furthermore, in the KG1a cell line, both the ATP-binding cassette sub-family G member 1 and 2 (ABCB1 and ABCG2) appear to be upregulated in the LSC portion of cells and the comparison between LSC and bulk tumour cells expression is given in Figure 3.22.

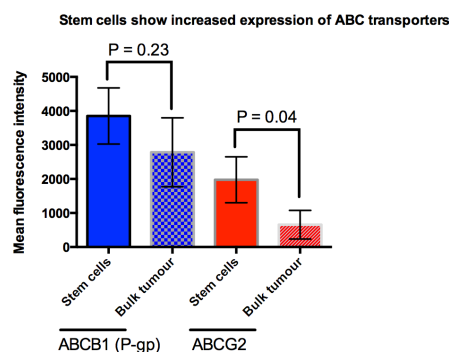


Figure 3.22: Increased expression of ABC transporters in the stem cell population of KG1a. Analysis performed by Prof. C. Pepper (Cardiff University).

Hypoxic conditions, such as the tumour environment, are well known to induce stem cell phenotype.²⁵⁰⁻²⁵³ Analysis of the effect of these conditions on the KG1a cell line clearly showed that the percentage of cells expressing the distinct CD34⁺/CD38⁺/CD123⁺ phenotype was increased (Figure 3.23).

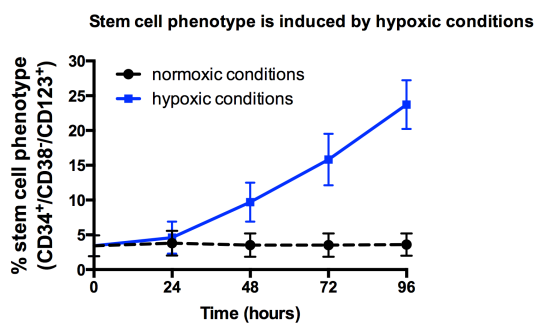


Figure 3.23: Induction of cancer stem cell phenotype in hypoxic condition in the KG1a cell line. Analysis performed by Prof. C. Pepper (Cardiff University).

3.1.4.6.3 Analysis of LSC targeting after treatment with 3'dA and relative ProTides at the LD₅₀ concentration

The KG1a cell line was treated with 3'dA and some of the most active ProTides (**30a-d**) (Table 3.17).

Common structure	Cpnd	Ar	R	R ₁	AA
	3'dA	-	-	-	-
	30a	Ph	Bn	Me	L-Ala
	30b	Nap	Bn	Me	L-Ala
	30c	Ph	Bn	H	Gly
	30d	Nap	<i>n</i> -Pen	<i>i</i> Bu	L-Leu

Table 3.17: Compound selected for evaluation on the KG1a cell line by Prof. C. Pepper (Cardiff University).

Cell apoptosis was measured after 72 hours *via* the Annexin V/propidium iodide assay²⁵⁴ by dual-colour immunofluorescent flow cytometry. The phenyl L-alanine benzyl ester ProTide **30a** emerged as the most active compound, with an LD₅₀ value of 4.3 μM, 100-fold lower than the value reported for the parent nucleoside (Table 3.18). The naphthyl L-leucine pentyl ester derivative **30d** performed similarly to **30a**, while on this cell line the naphthyl derivative **30b** performed poorly, in contrast with the data reported on the other cell lines. The glycine analogue **30c**, on the other hand, was already reported as not very potent, and the poor activity was confirmed with the KG1a cell line (Table 3.18).

Compound	KG1a	
	LD ₅₀ μM	% stem cells
3'dA	500	3.1
30a	4.3	3.6
30b	140	3.5
30c	220	3.3
30d	7.8	2.9
Control	-	3.3

Table 3.18: Cytotoxicity values and percentage of LSC in KG1a after treatment. Analysis performed under the supervision of Prof. C. Pepper (Cardiff University).

The LD₅₀ values were calculated and the same concentrations were used to treat the cell lines and determine the effect of the selected compounds on the LSC compartment (CD34⁺/CD38⁻/CD123⁺) after 72 hours of incubation.

This effect was analysed via FACS after labelling of the mentioned cell surface markers with specific luminescent antibodies: CD34-FITC, CD38-PE and CD123 PERCP-cy5. The effect of each compound on the stem cell compartment was compared with untreated cultures labelled with the same antibodies and was expressed as a proportion of the total cells analysed (Table 3.18). 3.3% of cells express the LCS phenotype, and is reported as the control percentage. The parent nucleoside appears to selectively target this population by decreasing the percentage to 3.1%, and this seems to be contrasted by ProTides **30a** and **30b**, which led to an increase in LCS population up to respectively 3.6 and 3.5%. ProTide **30c** leaves the percentage unaffected, while the leucine ProTide **30d** decreases this percentage to 2.9%.

These results could derive from an actual selective killing of the LSC population performed moderately by 3'dA and more significantly by ProTide **30d**. Alternatively, these agents could lead to a differentiation of LSC cells into bulk tumour cells, which would not

express the typical extracellular phenotype and therefore this effect would lead to a decrease in the detected LSC population *via* FACS analysis.

3.1.4.6.4 Analysis of LSC targeting after treatment with 3'dA and relative ProTides at a range of concentrations

The evaluation of the preferential LSC targeting of 3'dA and relative ProTides on the KG1a cell line was improved by the generation of a more complete dose-response curve for each compound and the evaluation of the effect on the LSC compartment at each concentration used, performed by Prof. C. Pepper (School of Medicine, Cardiff University).

Cpnd	LD ₅₀ μ M
3'dA	120
30a	4.2
30b	90
30c	110
30d	8.2

Table 3.19: LD₅₀ values for 3'dA, and selected prodrugs. All assays were carried out using KG1a cells and data are presented as mean of five independent experiments. Analysis performed under the supervision of Prof. C. Pepper (Cardiff University).

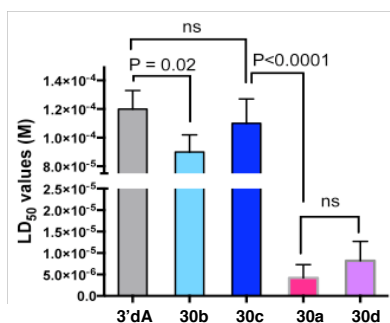


Figure 3.24: Comparison of the LD₅₀ values for 3'dA, and selected prodrugs. All assays were carried out using KG1a cells and data are presented as mean (\pm SD) of five independent experiments. Analysis performed under the supervision of Prof. C. Pepper (Cardiff University).

The LD₅₀ values were newly measured, and did not differ significantly from the previous data, with compounds **30a** and **30d** still emerging as the most active in this series (Table 3.19, Figure 3.24). The analysis of the LSC population percentage after treatment with compounds at different concentrations is reported in Figure 3.25.

Once again, treatment with both compounds **30b** and **30c** did not lead to any significant alteration of the LSC compartment, and this is confirmed throughout all the range of

concentrations. On the other hand, 3'dA and ProTides **30a** and **30d** appear to reduce this population at concentrations ranging from high micromolar to millimolar. At very high concentrations (10^{-3} - 10^{-2} M), 3'dA seems to revert the pattern and leave the percentage unaffected. In contrast, **30a** and **30d** appear to consistently reduce the population even at the highest doses. However, only compound **30a** can be considered to significantly reduce the LSC population to a larger extent than the parent nucleoside at concentrations above 1mM (Figure 3.25).

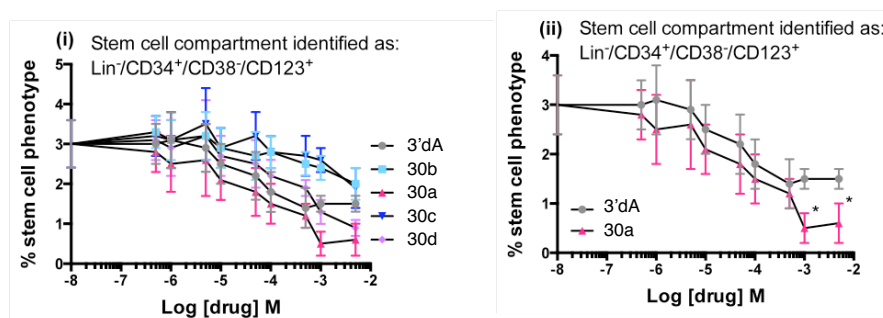


Figure 3.25: Analysis of the LSC targeting capacity of 3'dA and selected prodrugs. All data are the mean (\pm SD) of three independent experiments. Analysis performed under the supervision of Prof. C. Pepper (Cardiff University).

Although a clear correlation between selective targeting of the LSC population and a potential mechanism of action could not be identified, at a broad range of concentrations compound **30a** appears to clearly affect this subset, which is in contrast with the apparent increase in LSC population noted in the previous studies at LD₅₀ dose. However, the selective cytotoxic effect of compounds **30a** and **30d** on LSC population becomes significant at concentrations 1 to 2 log higher than the LD₅₀ (which is around 10^{-6} M, Figure 3.25).

3.1.4.6.5 Effect of 3'dA and ProTides on β -catenin levels of the KG1a cell line

The nucleoside 3'dA was reported to suppress cell proliferation affecting GSK-3 β / β -catenin signalling through down-regulation of the β -catenin intracellular levels in leukaemic cells.²²⁰ β -Catenin is involved in the Wnt pathway, involved in LSCs self-renewal capacity.^{255,256,257} Glycogen synthase kinase 3 β (GSK-3 β) regulates the stability of β -catenin by phosphorylation.²⁵⁸ At the cellular basal level, β -catenin is part of a complex of proteins and undergoes phosphorylation by GSK-3 β , which activates β -catenin degradation via the proteasome-dependent pathway.^{220,259} Signalling through the Wnt pathway causes inactivation of GSK-3 β , resulting in β -catenin dissociation from the complex and

translocation to the nucleus, where it regulates the expression of self-renewal genes.²²⁰ The expression of β -catenin in AML cells was associated with clonogenic capacities and poor prognosis.²⁶⁰ Treatment of leukaemic cell lines K562, THP1 and the lymphoma cell line U937 with 3'dA was reported to cause a dramatic reduction in β -catenin intracellular levels, that was paralleled by a significant reduction of the colony forming capacity of these cell lines.²²⁰ These effects were reported to derive from increase in proteasome-dependent degradation of β -catenin, which was in turn dependent on modulation of the Wnt/GSK-3 β signalling.

These intriguing results prompted us to study the effects of 3'dA and relative ProTides on the intracellular levels of β -catenin in the KG1a cell line. First, the expression of β -catenin was assessed both in bulk tumour cells and in the stem-cell population within the KG1a cell line. Secondly, our goal was to understand whether these levels were modulated by the treatment with 3'dA and/or 3'dA ProTides and if the effects were similar on all cells or if the alteration was only visible in one cell population. The final aim was to understand whether the potential LSC targeting of 3'dA and ProTide **30d** could derive from a perturbation of β -catenin levels.

Cells were treated with LD₅₀ concentrations of both 3'dA (LD₅₀ = 500 μ M) and ProTides **30a** (LD₅₀ = 4.3 μ M) and **30d** (LD₅₀ = 7.8 μ M). Subsequently, cells were stained with both the already mentioned cocktail of antibodies useful to detect the presence of the distinctive extracellular markers (CD34⁺/CD38⁻/CD123⁺) and with Anti- β -catenin-FITC. Before adding the last β -catenin specific antibody, cell permeability was increased by incubation with PBS-Tween. This step was necessary for the intracellular binding of the selective antibody to intracellular β -catenin.

Figure 3.26 reports the analysis of the β -catenin levels in the bulk subset of KG1a cells and in the (CD34⁺/CD38⁻/CD123⁺) population, measured as fluorescent intensity related to β -catenin intracellular levels. Increased levels of β -catenin appear to be present in the LSC population, which is in accordance with the characteristics of other leukaemic cells,^{220,249} confirming its interest as a target of investigation.

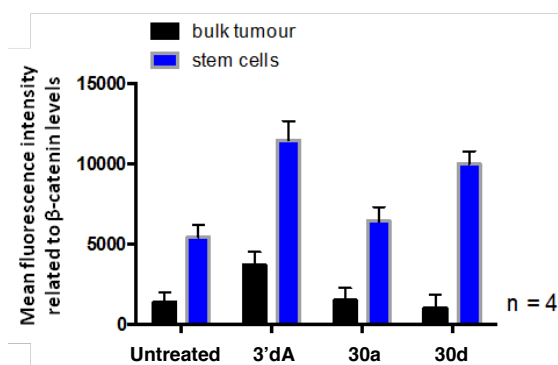


Figure 3.26: Effect of treatment with 3'dA and ProTides **30a** and **30d** on the β -catenin intracellular levels of the KG1a cells leukaemic stem cell compartment. Analysis performed under the supervision of Prof. C. Pepper (Cardiff University).

Treatment of leukaemic cell lines such as U937, K562 and THP1 was reported to lead to a decrease in the levels of intracellular β -catenin.²²⁰ Our results are in contrast to the previous reports, as we observed an increase in such levels both in the LSC compartment and in the bulk tumour cells. This may suggest that, although at the LD₅₀ value 3'dA seems to reduce the amount of cancer stem like cells within the cell line, the treatment may select for cells with a higher amount of intracellular β -catenin, hence the higher levels detected via FACS analysis (Figure 3.26). On the other hand, at LD₅₀ concentrations, both ProTides **30a** and **30d** were found not to significantly reduce the LSC population, although it should be highlighted that this population was not enriched either. Therefore, the activity of both compounds at LD₅₀ concentrations was not selective for the LSC compartment over the bulk tumour cells. The effect of both compounds on the β -catenin levels in the bulk tumour cells was not leading to a significant decrease compared to the untreated cells. On the other hand, a difference could be noticed on the effect of ProTides **30a** and **30d**, on the β -catenin levels in the LSC compartment, which seemed to be increased in comparison to the control after treatment with compound **30d**, while compound **30a** did not significantly alter such levels. This might suggest that ProTide **30d**, similarly to 3'dA, enriched the LSC population with cells expressing higher levels of β -catenin, in contrast to the effects of **30a**. Although still preliminary, the reported data show that unlike other nucleoside based treatment, which lead to an enrichment in the cancer stem cell population within treated tumour, 3'dA and ProTides seem to avoid the enrichment of the cell line with cells with potentially more aggressive LSC characteristics. Moreover, at high concentrations both parent nucleoside and ProTides **30a** and **30d** appear to selectively target the LSC population in the KG1a cell line, leading to its reduction in percentage within all the cells. Analysis of the β -catenin levels after treatment with 3'dA and ProTides **30a** and **30d** did

not show a reduction in the levels of the intracellular mediator, however, seemed to indicate that only **30a** over the other compounds does not lead to an increase in β -catenin levels, highlighting the intriguing potential of such compound.

3.1.5 Mechanistic investigations on the metabolic activation of 3'dA derivatives

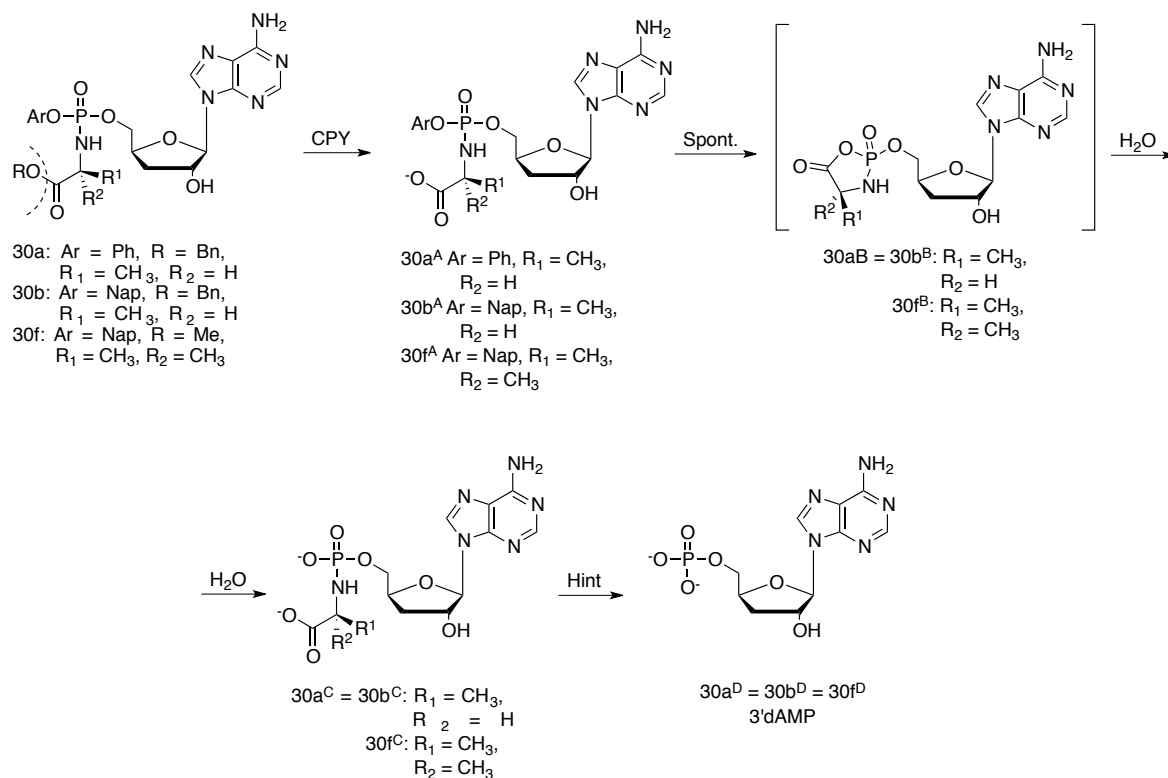
3.1.5.1 Carboxypeptidase Y (CPY) enzymatic NMR assay

ProTides are activated inside the body in 4 steps, as discussed in Chapter 1. The process of intracellular activation involves a first step catalysed by a carboxyesterase enzyme (Cathepsin A),²⁶¹ which is believed to be responsible for the cleavage of the amino acid ester moiety.^{129,130,261} Ester hydrolysis studies can be performed in order to gather information on these first steps in the activation of ProTides, and carboxypeptidase Y (CPY) can be used as a surrogate of cathepsin A enzyme, since it belongs to the same family of C-type carboxypeptidases and was reported to share similarities in the active site.²⁶² The enzymatic reaction can be monitored by ³¹P NMR, according to a procedure developed in the McGuigan group: the ProTide is dissolved in acetone-*d*₆ and trizma buffer (pH 7.6) is added to the solution.¹⁴⁷ A blank spectrum is recorded. The enzyme CPY, previously dissolved in trizma buffer (pH 7.6), is added to the ProTide mixture (1 U per mmol of ProTide), and ³¹P NMR experiments are recorded.

CPY experiments were carried out on different 3'dA derivatives, namely 5'-phosphoramidates **30a**, **30b** and **30f**, in order to understand whether the better cytotoxic profile of **32a** and **32b** in comparison to **30f** could derive from better intracellular processing, relative to the first activation step. Comparison between the processing rates of 2'-phosphoramidate **28b** and 2,5'-bisphosphoramidate **29b**, against the 5'-phosphoramidate counterpart **30b** was also assessed. Moreover, the 5'-phosphorodiamidate **32** was processed by CPY and the rate compared to the 5'-ProTide counterparts **30a** and **30b**.

3.1.5.1.1 Enzymatic CPY processing of 3'dA 5'-phosphoramidates

Simulation of the intracellular processing of 5'-phosphoramidates **30a**, **30b** and **30f** was performed via CPY NMR assay, in order to monitor the conversion into final aminoacyl metabolites **30a^C**, **30b^C** and **30f^C**.



Scheme 3.7: Conversion of ProTides **30a**, **30b** and **30f** into amino acyl phosphate monoester intermediates **30a^C**, **30b^C** and **30f^C**.

The final conversion into 3'dAMP (metabolites **30a^D**, **30b^D** and **30f^D**) can be simulated by docking of intermediates **30a^C**, **30b^C** and **30f^C** into the active pocket of the Hint enzyme, which was recognised as the enzyme responsible for the phosphoramidate bond cleavage.¹²⁸ These assays will be described below.

Phenyl L-alanine benzyl ester ProTide **30a** was treated with CPY enzyme and Figure 3.27 shows the stacked ³¹P NMR spectra that were recorded overnight. Two peaks resonating at 3.71 and 3.53 ppm, corresponding to the two diastereoisomers, were processed into two more downfield peaks corresponding to intermediate **30a^A** (Scheme 3.7). Complete conversion of **30a** into **30a^C** happened within 1 hour from enzyme addition and was confirmed both by the presence of a ³¹P NMR peak at 7.30 ppm, and by ES/MS analysis of the crude mixture, showing a predominant peak corresponding to the structure of **30a^C** (calculated: $m/z = 402.11$ [M], found: $m/z = 401.08$ [M - H⁺]).

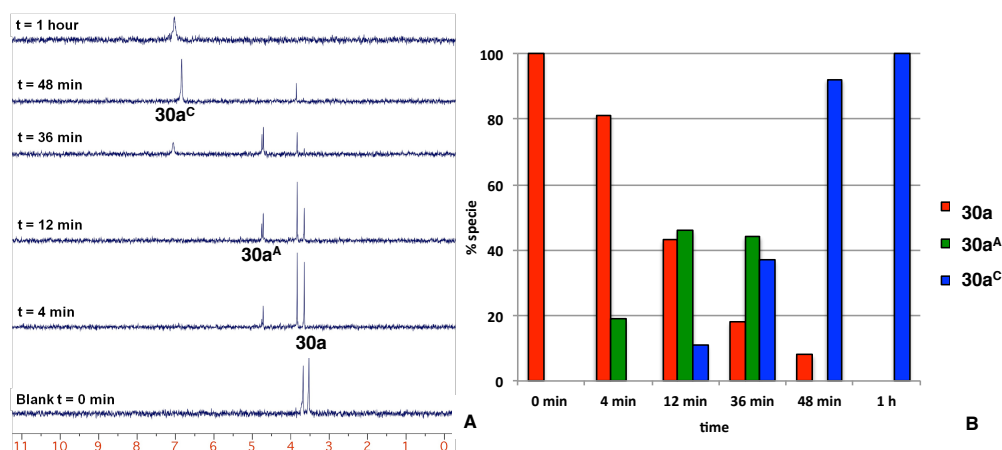


Figure 3.27 (A) ^{31}P NMR spectra (202 MHz, acetone-*d*₆) showing conversion of ProTide **30a** to intermediate **30a^C**. (B) % variation of ^{31}P NMR integrals of each species over the time.

The same assay was performed on ProTide **30b**, the naphthyl counterpart of **30a**. Two peaks corresponding to **30b** are visible in the blank experiment at 4.02 and 3.84 ppm (Figure 3.28). After 7 minutes from the enzyme addition, the two diastereoisomers are converted almost entirely into two peaks corresponding to intermediate **30b^A** (4.92, 4.96 ppm) and the simultaneous appearance of a peak at 7.30 ppm indicates the immediate formation of the metabolite **30b^C** (Scheme 3.7). The complete conversion to intermediate **30b^C** takes approximately 56 minutes, and is confirmed by mass analysis on the centrifuged mixture, showing a prevalent peak corresponding to compound **30b^C** with the same *m/z* as for **30b^C**. These results suggest that the anticancer activity of both compounds **30a** and **30b** in the *in vitro* assay could be a consequence of rapid intracellular metabolism to the active species.

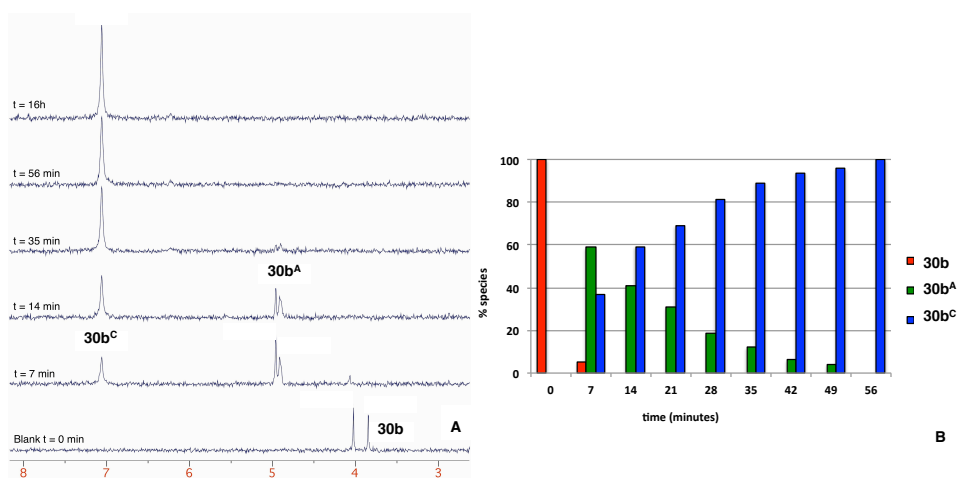


Figure 3.28: (A) ^{31}P NMR spectra (202 MHz, acetone-*d*₆) showing conversion of ProTide **30b** to intermediate **30b^C** in 56 minutes. (B) Variation of ^{31}P NMR integrals of each species over the time.

Notably, the **30b** diastereoisomers are processed at a similar speed, with no apparent difference in the metabolic stability of the two species, in contrast with the behaviour of the two diastereoisomers of **30a**, which are converted more slowly (Figure 3.27).

The CPY assay, applied to the poorly active 3'dA ProTide **30f** (Scheme 3.7), bearing naphthyl dimethylglycine methyl ester, showed that conversion into intermediate **30f^C**, (³¹P NMR signal at 5.08 ppm; calculated m/z : 416.12 [M], found m/z = 415.13 [M – H⁺]) was very slow and not complete after 14 hours (Figure 3.29).

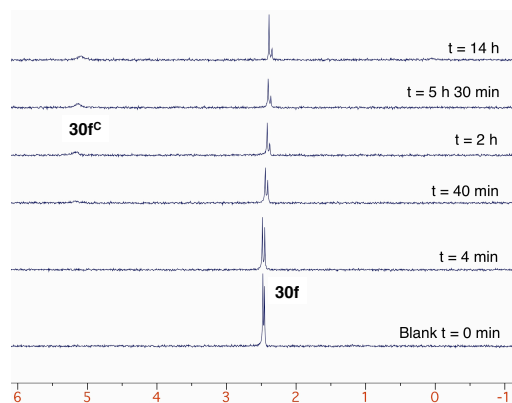
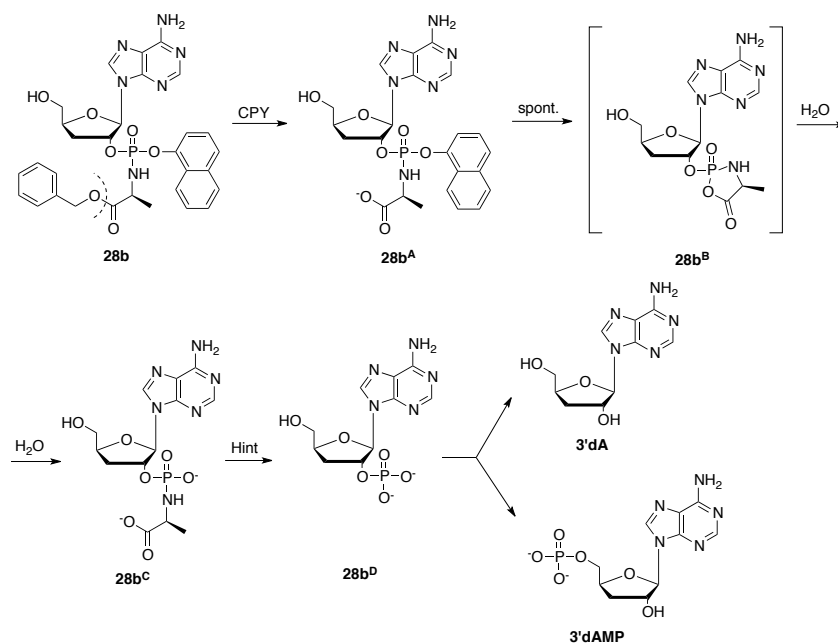


Figure 3.29 ³¹P NMR spectra (202 MHz, acetone-*d*₆) showing slow processing of ProTide **30f** to intermediate **30f^C**.

Moreover, one of the two diastereoisomers (at 2.59 ppm) appeared to be more stable than the other (at 2.56 ppm). These results strongly suggested that the low cytotoxic profile of this compound might derive from inefficient intracellular processing of the ProTide moiety.

3.1.5.1.2 Enzymatic experiment on 2'-phosphoramidate

To the best of our knowledge, the synthesis and biological evaluation of phosphoramidate prodrugs of 3'-deoxynucleosides has never been reported before, nor the evaluation of the 2'-phosphoroamidate regioisomers. Although demonstrating lower anticancer activity compared to their 5'-regioisomers, compounds **28a** and **28b** still proved more potent than the parent nucleoside in most of the cell lines. These results could be due to their lipophilicity, that would allow cell entering by passive diffusion, and once within the cell these derivatives could be metabolically activated to 3'dA-2'-monophosphate (**28b^D**, Scheme 3.8), and exert their activity with an unknown mechanism of action.²⁶³



Scheme 3.8: Putative bioactivation of 2'-phosphoramidate **28b**.

Alternatively, once inside the cell, these compounds could undergo cleavage of the phosphate moiety catalysed by nucleotidase enzymes, with release of the parent nucleoside 3'dA. These enzymes have already been reported to be responsible for resistance to the treatment with anticancer nucleoside analogues such as gemcitabine and cytarabine.^{264,265} A third more complex mechanism could be the isomerisation of the released 2'-monophosphate to the 5'-position, generating 3'dAMP.

Presently, no clear mechanism of action could be confirmed. However, in an attempt to explain the activity of compound **28b**, the 2'-regioisomer of ProTide **30b**, a CPY-mediated enzymatic assay was performed (Figure 3.30).

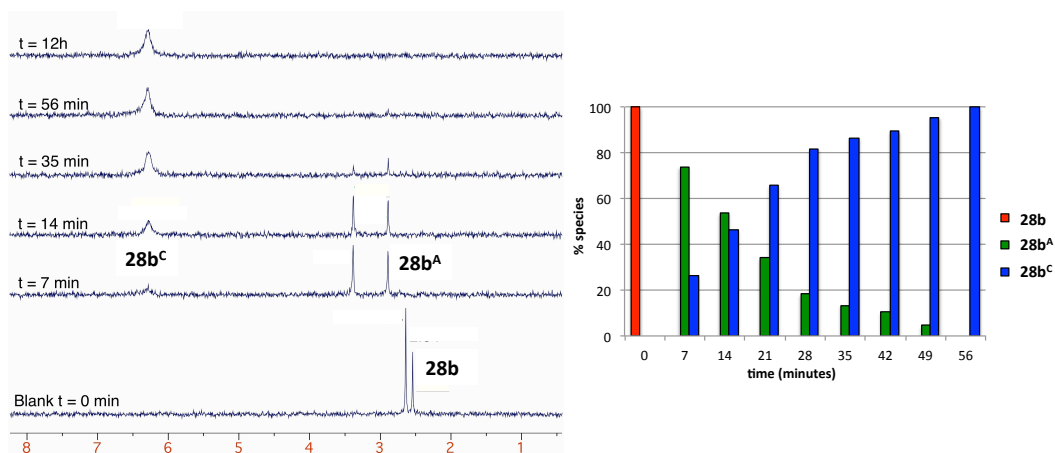


Figure 3.30: (A) ³¹P NMR spectra (202 MHz, acetone-*d*₆) showing complete conversion of compound **28b** to intermediate **28b^C**. (B) Variation of ³¹P NMR integrals of each species over the time.

Compound **28b** peaks appear in the blank experiment at 2.63 and 2.54 ppm. After 7 minutes from the addition of CPY, the conversion to intermediate **28b^A** is complete, with the comparison of two peaks at 3.39 and 2.89 ppm. In 20 minutes, the peak corresponding to compound **28b^C** could be seen at 6.28 ppm, and the complete conversion happens in 70 minutes. As for compound **30b^C**, a mass experiment of the final solution from enzymatic reaction on compound **30b** confirmed the final peak at 6.28 ppm corresponded to intermediate **28b^C** (calculated $m/z = 400.09$ [M], found $m/z = 402.12$ [M + 2H⁺]). This result suggests that ProTide 2'-regioisomes could be processed by similar enzymes involved in the metabolism of the 5'-counterparts, and release the 2'-monophosphate inside the cell.

In addition to the reported data, the metabolism of 2',5'-bisphosphoramidate **29a** by CPY was assessed, in order to gather information on the putative mechanism of intracellular activation. A bulk molecule such as **29a** was hypothesised to be processed less efficiently by CPY.

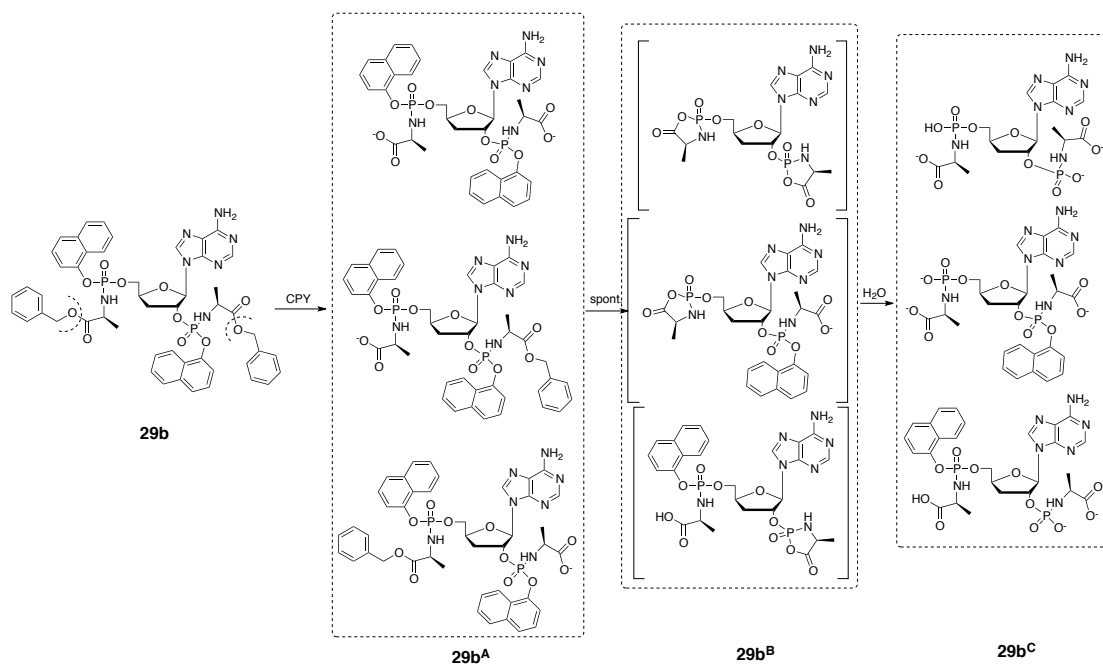


Figure 3.31: Putative conversion of bis-phosphoramidate **29b** into amino acyl phosphate monoester intermediates **29b^C**.

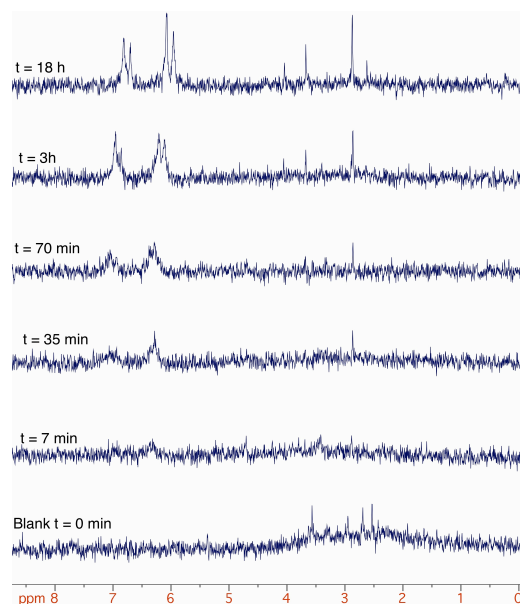
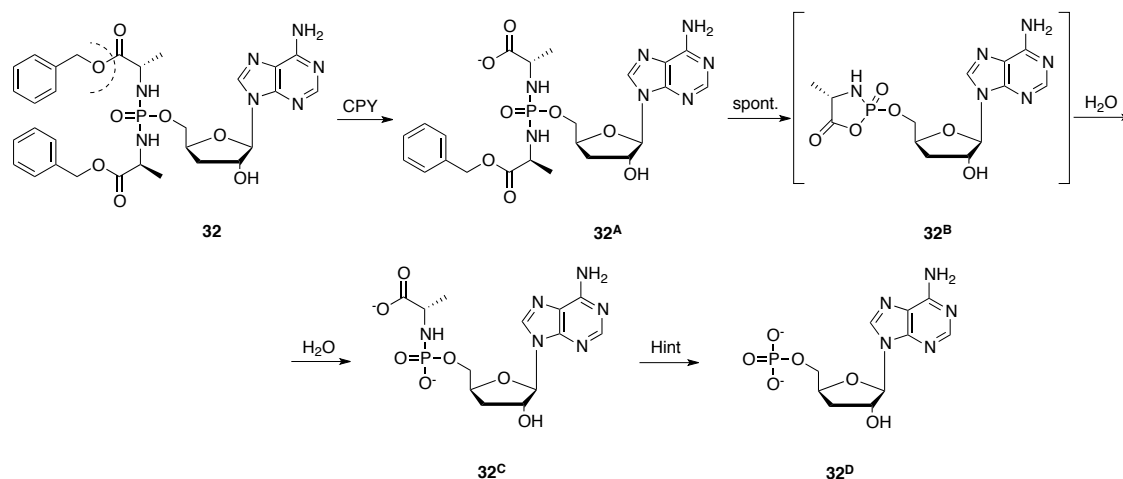


Figure 3.32: (A) ^{31}P NMR spectra (202 MHz, acetone- d_6) showing processing of **29b** by CPY.

However, the result of the CPY assay, shown in Figure 3.32 through the stacked ^{31}P NMR spectra relative to the overnight assay, suggest that **29b** is potentially processed by the enzyme into the putative metabolites represented in Figure 3.31. The peaks corresponding to **29b** are not clearly visible in the blank spectrum, due to low solubility of the molecule in acetone- d_6 and trizma buffer (pH 7.6), in fact the spectra appears as a broad peak in the area between 2 and 4 ppm. However, once the processing by CPY begins, some more downfield peaks appear, potentially corresponding to the structures **29b^A** (Figure 3.31), as a mixture of isomers either totally or partially lacking the ester moieties. Concomitantly, peaks in the area between 6 and 7 ppm also develop, potentially corresponding to the different isomers **29b^C**. These results suggest that **29b** is processed by CPY to some extent, although at a slower rate than the 2'-phosphoramidate or 5'-phosphoramidate counterpart, and this could explain the activity of such prodrug inside the cell.

3.1.5.1.3 Enzymatic experiment on diamidate

The 5'-phosphorodiamidate of 3'dA **32** did not show similar anticancer potency as seen for 3'dA ProTides, although was still more potent than 3'dA in the cytotoxicity screenings. In order to get an insight into the possible reason why this phosphate prodrug did not show the same anticancer potential as other prodrugs, such as the ProTides **30a** and **30b**, a CPY assay was performed.



Scheme 3.9: Conversion of diamidate **32** into intermediate **32^C**.

After addition of CPY, **32** (^{31}P NMR peak at 13.77 ppm) was converted to intermediate **32^A** (Scheme 3.9, Figure 3.33), lacking the ester moiety therefore presenting two diastereomeric peaks at 14.36 and 14.59 ppm. Finally the formation of the metabolite lacking one of the amino acids (**32^C**) was confirmed by comparison of the peak at 7.04 ppm and by mass analysis of the centrifuged crude (calculated $m/z = 400.09$ [M], found $m/z = 402.1$ [M + 2H⁺]).

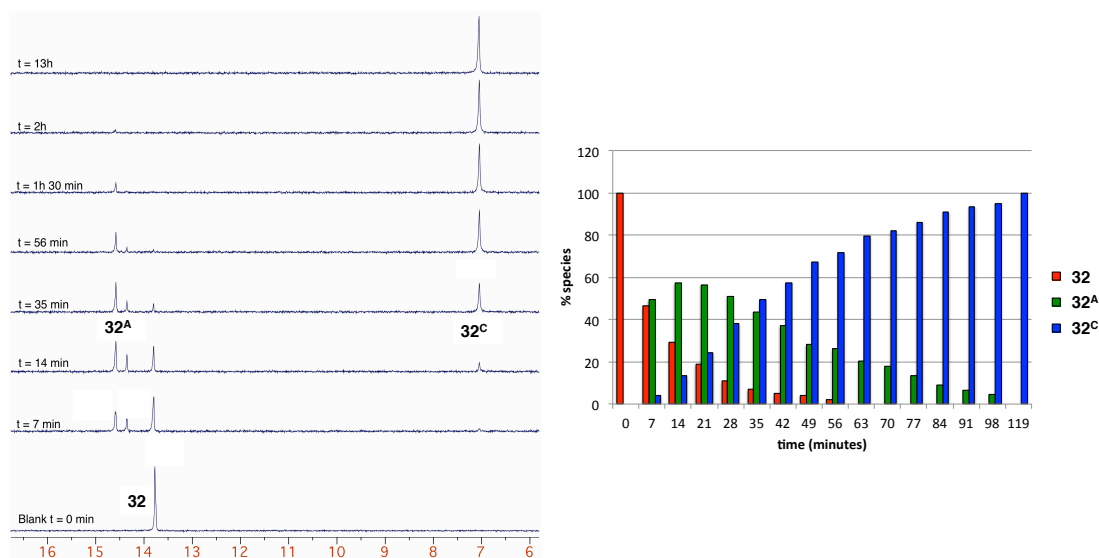


Figure 3.33: (A) ^{31}P NMR spectra (202 MHz, acetone-*d*₆) showing complete conversion of compound **32** to intermediate **32^C** in 120 minutes. (B) Variation of ^{31}P NMR integrals of each species over the time.

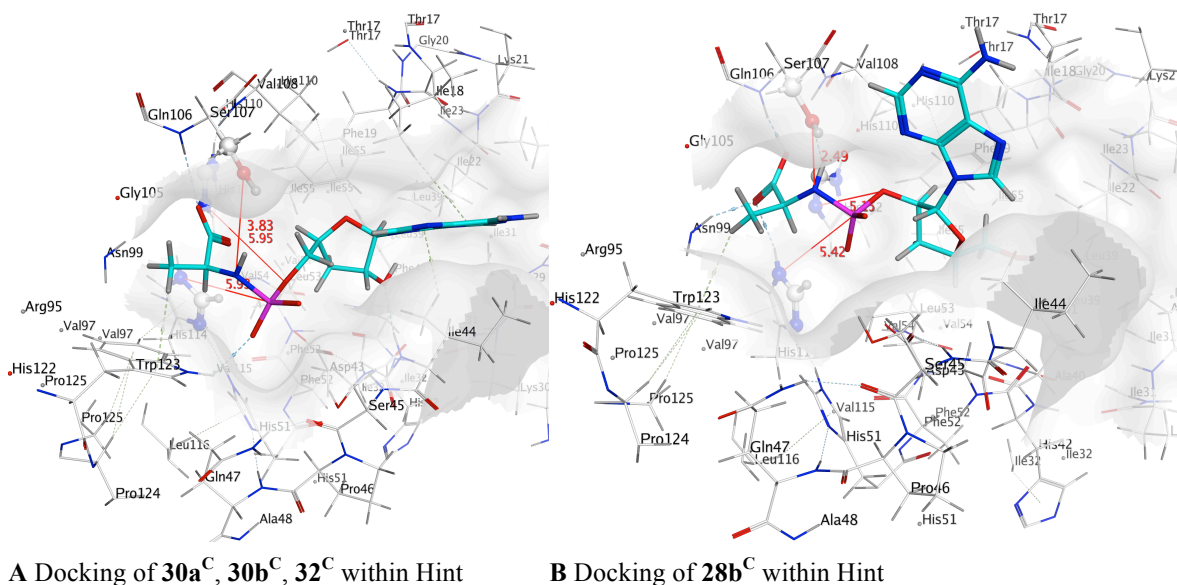
The activation of **32** into intermediate **32^C** is slower than the conversion of **30b** into **30b^C**, as it happens within 2 hours (Figure 3.33), instead of 56 minutes. The slower activation of

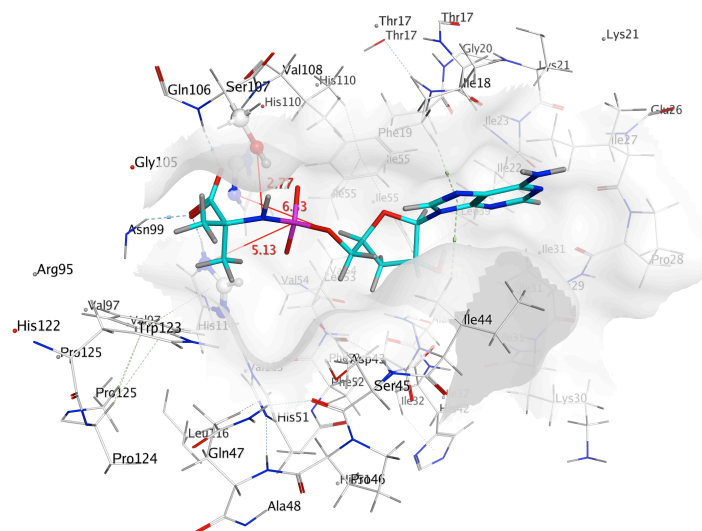
the phosphoramidate derivative could thus be the reason for the lower anticancer potency of this derivative, compared to **30b**.

3.1.5.2 Docking studies

3.1.5.2.1 Docking of compounds in the active site of Hint-1

The second enzymatic step required for the activation of ProTides is the phosphoramidate bond cleavage, and the enzyme responsible for this step was reported to belong to the human histidine triad nucleotide-binding protein (Hint).^{135,261} In order to predict the likelihood of processing of 3'dA prodrugs by Hint, docking studies within the enzyme active site were carried out using PLANTS. The crystal structure of Hint was downloaded from the protein data bank (PDB 1RZY),²⁶⁶ and the interaction between each selected aminoacyl phosphate monoester intermediate and the crucial residues within the active pocket (Ser107, His 112 and His114), implicated in the P-N bond cleavage, were analysed with MOE software.





C Docking of **30f^C** within Hint

Figure 3.34 Docking of compounds (A) **30a^C**, **30b^C**, **32^C**, (B) **28b^C** and (C) **30f^C** within the active pocket of Hint enzyme.

Comparison between the intracellular metabolic activation processes of the 5'-phosphoroamidate **30a^C** (corresponding to the same structure as **30b^C** and **32^C**), and the 2'-regioisomer **28b^C** was carried out by docking the L-alaninyl phosphate monester metabolites of both compounds within Hint (Figure 3.34, **A** and **B**). Similar positioning of the phosphoroamidate moiety close to the residues responsible for the phosphoramidase activity could be noticed for both compounds. However the positioning of the 5'-regioisomer seemed to allow better interaction of the nucleobase with the active site, which suggests more efficient positioning of the moiety within the pocket. However, the two moieties interact very similarly with Hint, therefore the P-N bond cleavage step should not represent a limiting step for the activation of compound **28b^C** over **30a^C**. Very similar positioning could be observed for compound **32^C** (Figure 3.34, **C**), therefore suggesting that the lower activity of the dimethylglycinyl compound **32** should not result from a lower activation step catalysed by Hint, but more likely by a slower processing by CPY, as suggested by the NMR assay performed (Figure 3.29).

3.1.6 Stability studies

3.1.6.1 Stability to adenosine deaminase-mediated catabolism

3.1.6.1.1 UV assay

The poor activity of cordycepin in the *in vitro* assays could derive primarily from a quick intracellular metabolism to inactive inosine, catalysed by adenosine deaminase enzyme, as already extensively reported.¹⁸⁹ In order to have a proof of the quick metabolism of the nucleoside, and confirm the stability of 3'dA ProTides in the same conditions, an enzymatic assay was designed. In the first assay, 3'dA was treated with a solution of adenosine deaminase from calf and the UV absorbance was recorded over time.

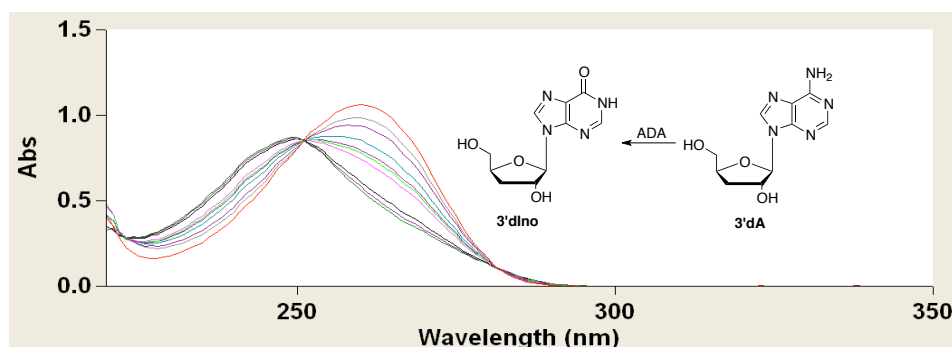


Figure 3.35: Change in UV absorbance spectra of 3'dA after addition of a solution of ADA (in phosphate buffer pH 7.4).

Figure 3.35 reports the UV spectrum of 3'dA (red line) and the shift of the maximum wavelength of absorption from 259 nm to lower wavelengths of the other curves describes the appearance of the metabolite 3'-deoxyinosine (3'-dIno), characterised by a maximum absorbance wavelength of 249 nm.²²⁵ The metabolic deamination is complete within 2 minutes from the enzyme addition.

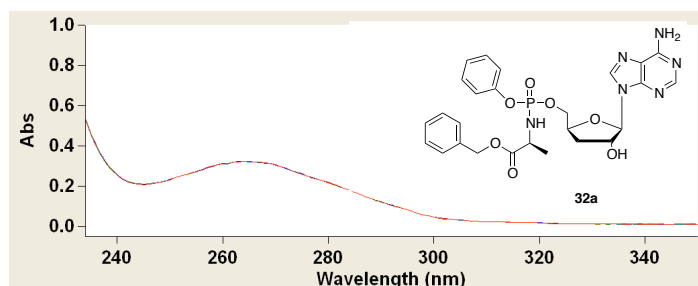


Figure 3.36: UV absorbance spectra of **30a** after addition of a solution of ADA.

On the other hand, ProTide **30a**, treated under the same conditions, was stable to deamination up to 2 hours from the addition of the enzyme solution, confirming the stability of 3'dA ProTides to deamination.

3.1.6.1.2 Docking within the ADA active site

In order to have an additional indication of the stability of 3'dA prodrugs to ADA-mediated catabolism, we docked the parent nucleoside, 5'-phosphoroamidate **30a** and the 2'-regioisomer **28a** within the ADA active site (ADA crystal structure was downloaded from the protein data bank, PDB 3IAR).

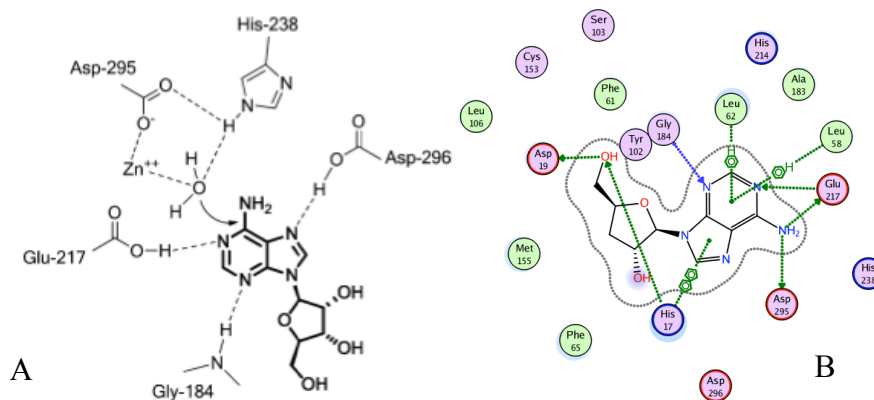


Figure 3.37 **A**. Interaction of adenosine with catalytic residues within the ADA enzyme (image from Vodnala et al.).²²⁵ **B**. Docking interaction of 3'dA within the ADA active site.

Figure 3.37**A** shows the key interactions of the natural substrate adenosine within ADA, involving the crucial residues Glu217, Asp295, His238, Gly184 and Asp296. Figure 3.37**B** shows the interaction of 3'dA in ADA, involving directly Glu217, Asp295, Gly184 and the close proximity to His238. The correct positioning resulting from docking confirms the very quick processing of this substrate by ADA, noticed in the UV assay. On the other hand, when both ProTide **30a** and 2'-phosphoraminate **28a** were docked within the ADA active pocket, these structures could not properly fit in the enzyme, due to the much larger dimensions compared to the natural substrates (Figure 3.38).

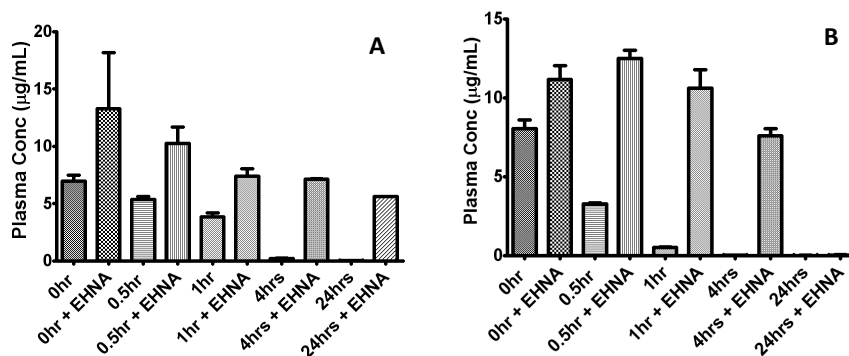


Figure 3.39: Stability assay of 3'dA in human plasma (A) and mouse plasma (B). Assays performed by Essam Ghazaly (Barts Institute, London).

When 3'dA was incubated in human plasma (Figure 3.39, A), without the addition of EHNA the concentration of compound decreased immediately and gradually, until completely metabolised after 4 hours. When EHNA was added, the stability of 3'dA was significantly increased, and the compound could still be detected in plasma after 24 hours. The metabolism of 3'dA in mouse plasma was similar although the nucleoside was completely metabolised after 1 hour of plasma incubation without the presence of ENHA.

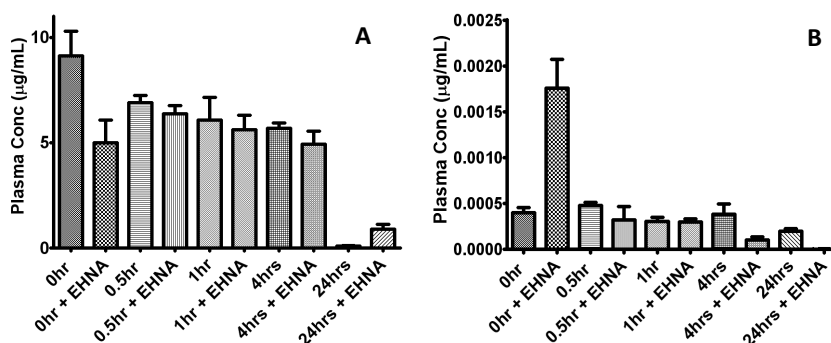


Figure 3.40: Stability assay of ProTide 30a in human plasma (A) and mouse plasma (B). Assays performed by Essam Ghazaly (Barts Institute, London).

The incubation of ProTide 30a in human plasma showed increased stability compared to the parent nucleoside, due to stable concentration up to 4 hours from the beginning of the assay. Moreover, the addition of EHNA does not significantly affect the compound stability. Conversely, the stability of ProTide 30a in mouse plasma was poor; in fact the concentration of compound dropped immediately down to ng/mL concentrations after 30 seconds from the incubation. Moreover the presence of EHNA did not significantly affect these results, suggesting that the compound was not metabolised by ADA (as expected) but through other pathways, potentially involving esterase enzymes. In fact, higher levels of carboxylesterase enzymes were reported in rodents,²⁶⁷ compared to human, monkey and

dogs, and were suggested to induce reduced stability of ProTides in *in vivo* mouse xenografts.^{151,268}

Similar outcomes resulted from ProTide **30b** incubation, with noticeable stability in human plasma, which was unaffected by addition of EHNA; on the other hand, the compound was rapidly metabolised in mouse plasma, down to ng/mL concentration immediately after incubation.

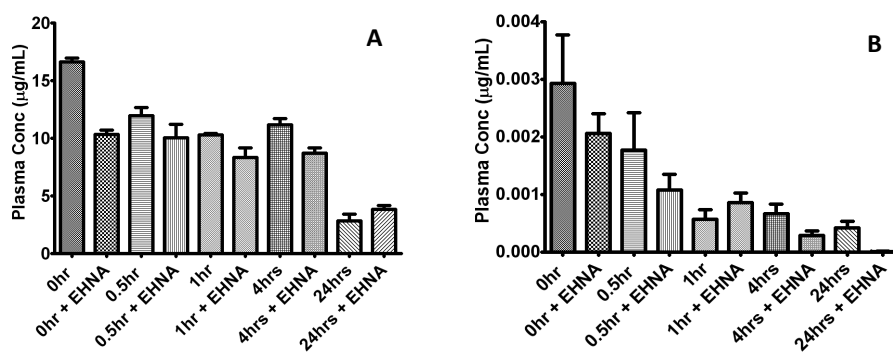


Figure 3.41: Stability assay of ProTide **30b** in human plasma (A) and mouse plasma (B). Assays performed by Essam Ghazaly (Barts Institute, London).

ProTide **30f** emerged as very stable in human plasma, and more stable than the other ProTides in mouse plasma, with concentrations in the µg/mL range still after 1 hour after the beginning of the assay (Figure 3.42).

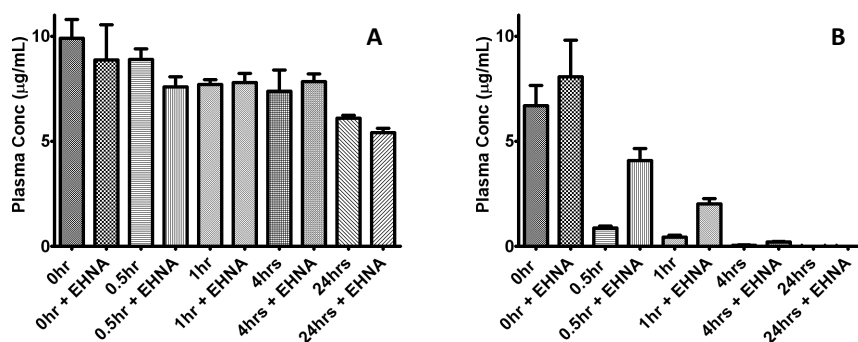


Figure 3.42: Stability assay of ProTide **30f** in human plasma (A) and mouse plasma (B). Assays performed by Essam Ghazaly (Barts Institute, London).

These results, along with the poor activity noticed in *in vitro* assays and the slow activation in the CPY assay, suggest that the lack of anticancer activity of this derivative may derive from poor processing of the ProTide moiety.

3.1.6.3 3'dA ProTides stability in human hepatocytes

The optimal metabolism of ProTides depends on their enzymatic and chemical stability. Upon administration, the circulating ProTides are exposed to challenging conditions, such as catalytic enzymes in the liver and should resist long enough to enter tumour cells before being degraded. Conversely, ProTides unaffected by enzymatic digestion might not be efficiently converted into active compounds inside the cancer cells. To further select the lead candidates with suitable chemical stability, five ProTides were incubated with human hepatocytes, performed by Eurofins CEREP USA laboratories. In the human hepatocyte extracts the half-lives of the six compounds varied from 24 minutes for compound **30e** up to 99 min for compound **30f**. The selection criteria included identifying a compound with a mid-range half-life in human hepatocytes. The short half-life of 3'dA (48 min) may be an indication of quick conversion into 3'dIno due to the activity of ADA. The very quick metabolism of **30e**, resulting in the highest clearance, may be due to the presence of a second ester moiety attached to the aryl group, that, along with the ester attached to the amino acid group as in each ProTide, would increase the susceptibility to esterase-mediated processing.

Common structure	Cpnd	Ar	R	R ₁ /R ₂	AA	t _{1/2}	Cl _{int}
	3'dA	-	-	-	-	48	20.70
	30a	Ph	Bn	Me/H	L-Ala	44	22.60
	30b	Nap	Bn	Me/H	L-Ala	48	20.80
	30d	Nap	<i>n</i> -Pen	<i>i</i> Bu/H	L-Leu	63	15.80
	30e		Bn	Me/H	L-Ala	24	41.10
	30f	Nap	Me	Me/Me	DMG	99	10.00

Table 3.20 Incubation of 3'dA and selected ProTides in human cryopreserved hepatocytes. Half life (t_{1/2}) expressed in minutes, intrinsic clearance (Cl_{int}) expressed as μL/min/10⁶cells. Assays performed by Eurofins CEREP USA laboratories.

In contrast, compound **30f** shows higher t_{1/2} value, and this, along with the poor cytotoxicity profile of this compound, could indicate slow processing. Compounds **30a** and **30b** (44-48 min) show very similar stability profiles, with favourable t_{1/2} values, indicating a good balance between appropriate speed of processing and extracellular stability. Compound **30e** has an intermediate stability profile (63 min). From these stability studies, compounds **30a** and **30b** result again as promising 3'dA derivatives, with stability in human hepatocytes comparable to ProTides already progressing in the clinic.¹⁵¹

3.1.7 Conclusions

The synthesis of 3'dA after optimisation of the literature reports was accomplished, and allowed the generation of a family of nucleoside derivatives through the ProTide and phosphoramidate prodrug approaches. 5'-Monophosphate prodrugs were produced along with 2'-monophosphate and 2',5'-bis-*O*-phosphate prodrugs. All the synthesised derivatives proved to be more effective cytotoxic agents than the parent nucleoside on a broad selection of malignant cells. In particular 5'-phosphoramidates of 3'dA resulted as the most potent anticancer agents, with IC₅₀ values in the low μM range especially on cells derived from haematologic malignancies and the ProTides emerging as the most active were the L-alanine benzyloxy derivatives **30a** and **30b**. The IC₅₀ values of some of the most active compounds and 3'dA were assayed on a small selection of leukaemic cell lines (CEM, K562 and HL60), and the 3'dATP levels were subsequently measured on these cells. The intracellular levels of 3'dATP, the active intracellular metabolite, were found to be higher after treatment with compounds **30a** and **30b**, correlating with the better cytotoxicity profile of these drugs. The most active compounds were also assayed, along with the parent nucleoside, on the KG1a cell lines, possessing a distinct sub-population endowed with cancer stem cells characteristics. At high concentrations, ProTide **30a** was found to selectively target this population with higher efficiency compared to the other derivatives.

The metabolism of 3'dA prodrugs was assayed first with a NMR CPY assay, predicting quick intracellular processing for the active ProTides **30a** and **30b** and diamidate **32** and slow for the poorly active derivative **30f**, therefore confirming that quick intracellular processing is a determinant for the intracellular activity of 3'dA prodrugs. CPY was also found to potentially process the 2'-phosphoramidate derivative **28b** at a similar speed as the ProTide counterpart **30b**, and to process the bis-phosphoramidate derivative **29b** to some extent. Docking into the Hint enzyme, responsible for the last step in 3'dA prodrugs activation, appeared to be similar with different intermediate structures, suggesting that this is not a limiting step in 3'dA prodrug activation. Metabolism by ADA was evaluated, and was found to be very quick in the case of 3'dA, while not significant in the case of one example of ProTide (**30a**). Docking studies within the ADA active site correlated these results to the bulkier structure of 3'dA prodrugs, impeding a correct positioning of these compounds inside the pocket. The stability of 3'dA was assayed in human and mouse plasma, and was found to be similar in both assays and strongly dependent on ADA activity, as evaluated after addition of EHNA, an ADA inhibitor. On the other hand, for

ProTides **30a** and **30b**, the stability was found not to be significantly affected by the presence of EHNA, although considerably lower in mouse compared to human plasma, potentially due to higher expression of carboxyl esterase enzymes in rodent plasma. Stability evaluation in human hepatocytes confirmed a suitable pharmacokinetic profile for ProTides **30a** and **30b**, comparable to ProTides in clinical development such as NUC-1031.¹⁵¹ In conclusion, combining all stability and cytotoxicity data, ProTides **30a** and **30b** emerged as the most intriguing 3'dA prodrugs, deserving further evaluation. ProTide **30a**, although endowed with lower cytotoxicity compared to **30b** on some cell lines, was capable of selectively targeting the leukaemic stem cell compartment of KG1a cell line. This result was considered potentially useful for the *in vivo* application of such drug, as it could potentially overcome relapse to anticancer treatment. For this reason, ProTide **30a** was included in further preclinical investigations.

3.2 2-Modified cordycepin analogues and their prodrugs

3.2.1 Background

The synthesis and biological evaluation of prodrugs of 3'dA has never been thoroughly investigated, and there is no literature report on the application of monophosphate prodrug approaches to any 3'-deoxynucleoside. Considering the intriguing results of the application of the ProTide approach to 3'dA, investigations on other 3'dA derivatives were carried out, with the aim of improving the activity of this family of ProTides. In this sense, the work by Vodnala *et al.* was of interest. This group recently published the synthesis and anti-trypanosomal evaluation of different 3'dA analogues.²²⁵ The anti-trypanosomal activity of 3'dA had already been described both *in vitro* and *in vivo*.^{178-180,269} The most promising modification was represented by the introduction of a fluorine atom in position 2 on the nucleobase and resulted in increased metabolic stability of this derivative. In fact, the resistance of 2-fluorocordycepin (2F3'dA, **33**, Figure 3.43) to ADA-mediated catabolism was already reported in 1967.²⁷⁰

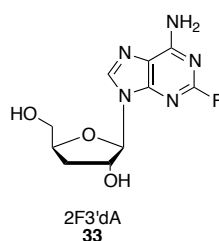


Figure 3.43: Structure of 2-fluorocordycepin (2-fluoro-3'-deoxyadenosine, 2F3'dA, **33**).

Similarly, the presence of such modification on 2-fluoroadenosine (2FA, **34**)²⁷¹ and fludarabine (2FAraA, **1i**),²⁷² is responsible for increased metabolic stability to ADA-deamination (Figure 3.44).

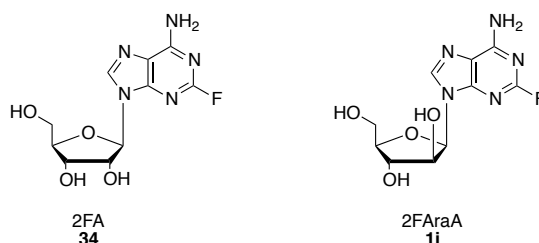


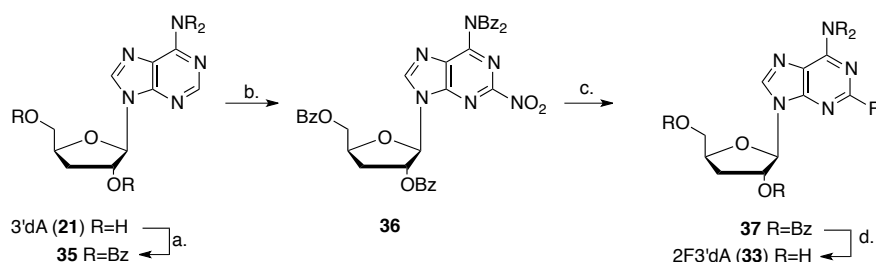
Figure 3.44: Structure of 2-fluoroadenosine (2FA, **34**) and fludarabine (2FAraA, **1i**).

Base modifications in position C2 and C8 have been reported to cause ADA-inhibition or, as in the case of small C2 substitution, simply lack in recognition by the enzyme.²⁷³ Introduction of a halogen substitution in C2 was reported to reduce the partial negative charges on N1 and N3 and therefore the capability of behaving as H-bond acceptors and the overall pKa, crucial features for interaction with ADA.²²⁵

Despite the increased metabolic stability of 2F3'dA and the more favourable activity profile on trypanosome-infected models, the activity of this nucleoside analogue as anticancer agent was not extensively investigated. In 1969 the cytotoxic screening of 2F3'dA resulted in an ED₅₀ (median effective dose) concentration of 2 μM on the hepatocellular carcinoma Hep-G2 cell line, compared to ED₅₀ 80 μM concentration of 3'dA.²⁷⁴ Considering the interest in these reported results, investigation of the anticancer activity of both 2F3'dA and a family of ProTides was carried out on a broader selection of cell lines. In fact, although 2F3'dA represents a 3'dA derivative less prone to ADA-mediated inactivation, this nucleoside analogue might still benefit from the application of a monophosphate prodrug approach in order to bypass potential limiting steps such as the dependency on a kinase enzyme for the first phosphorylation step,²⁷⁵ or inefficient transport-mediated cell penetration.

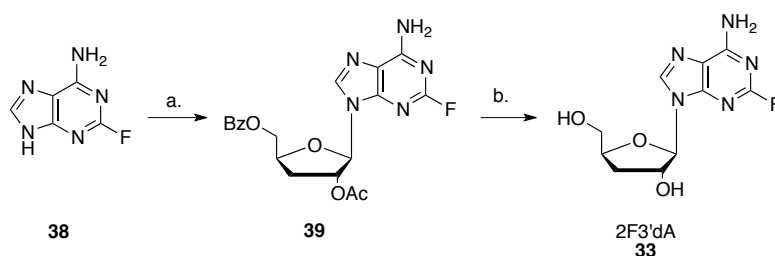
3.2.2 Synthesis of 2-fluorocordycepin

One reported procedure for the synthesis of 2F3'dA requires a four-step route starting from 3'dA (**21**, Scheme 3.10), which is first protected on the amino and hydroxyl groups via benzoyl chloride (**35**), to allow introduction of a nitro group in position 2 on the adenine moiety (**36**) by means of tetrabutylammonium nitrate (TBAN) and trifluoroacetic anhydride (TFAA). The NO₂ group is finally replaced by fluorine by treatment with tetrabutylammonium fluoride (TBAF) in CH₃CN (**37**) and de-benzoylation in methanolic ammonia to give the desired 2F3'dA (**33**).²²⁵



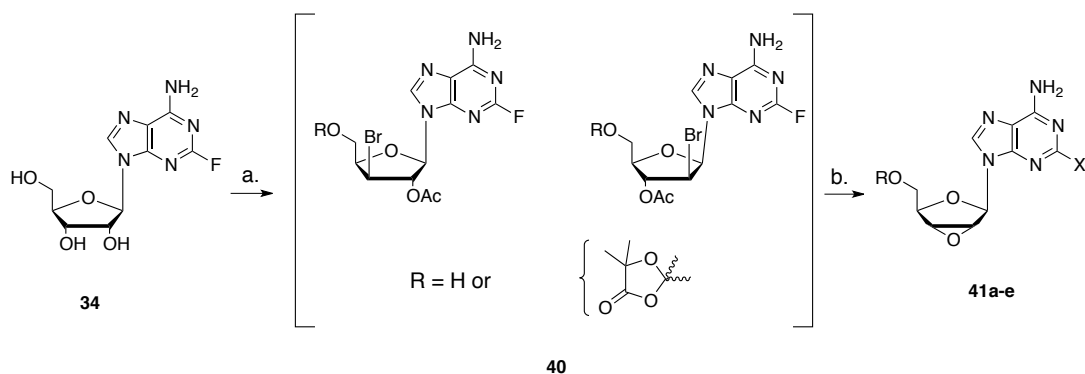
Scheme 3.10: Synthesis of 2F3'dA (**33**).²²⁵ Reagents and conditions: (a.) BzCl, pyr; (b.) TBAN, TFAA; (c.) TBAF, CH₃CN; (d.) NH₃, CH₃OH. (Overall yield of 4 steps from 3'dA = 7%)

In an alternative methodology, the desired 2F3'dA is synthesised via Vorbrüggen-type glycosylation between 2-fluoroadenine (2FAde, **38**) and 5-*O*-benzoyl-1,2-di-*O*-acetyl-3-deoxy-D-ribose in the presence of *N,O*-bis(trimethylsilyl)acetamide (BSA) and trimethylsilyl trifluoromethanesulfonate (TMSOTf) (Scheme 3.11) with a final deprotective step in methanolic ammonia yielding the desired 2F3'dA (**33**).²⁷⁶

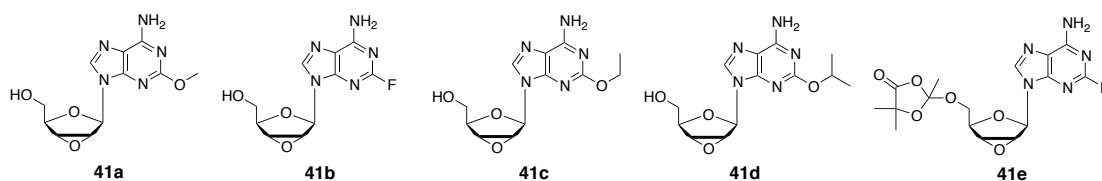


Scheme 3.11: Synthesis of 2F3'dA (**33**).²⁷⁶ Reagents and conditions: (a.) BSA, 5-*O*-benzoyl-1,2-di-*O*-acetyl-3-deoxy-D-ribose, TMSOTf; (b.) NH₃, CH₃OH. (Overall yield 2 steps from 2FAde = 35%)

Considering both the numerous steps required and the low yield reported for the first strategy (7%, 4 steps), and both high cost of intermediates and moderate yield (35%, 2 steps) needed for the second methodology, a different procedure was applied. The synthetic procedure successfully used for the synthesis of 3'dA (93% yield, 2 steps) was adapted, using 2FA as a starting material. Commercially available 2FA (**34**) was reacted with 4 equivalents of α -AIBBr in a mixture of CH₃CN and water. TLC monitoring of the crude confirmed the formation of more lipophilic species similarly to the reaction of adenosine in the same conditions. These intermediates were not isolated as the crude could be directly subjected to the next step after extraction of the mixture with EtOAc, washing of the organics with NaHCO₃ (saturated solution) and evaporation of the organic phase. However, similarly to the intermediates isolated by Robins *et al.*²¹² during the synthesis of 3'dA, the putative structures of the intermediates of this reaction were drawn as products of step a in Scheme 3.12.



Scheme 3.12: Attempted synthesis of 2',3'-dehydro-2FA (**41a-e**). Reagents and conditions: (a.) α -AIBBr (4 eq), CH₃CN/H₂O; (b.) see Table 3.21. X: see Table 3.21.



Entry	Scheme 2.5. Step b. Reagents and Conditions			Product 1 (yield)	Product 2 (yield)
	Amberlite	Solvent	Time		
1	8mL/mmol	CH ₃ OH.	16 h	41a (89%)	-
2	5mL/mmol	CH ₃ OH	1h 30min	41a (11%)	41b (54%)
3	6mL/mmol	EtOH	16 h	41c (83%)	-
4	6mL/mmol	<i>i</i> PrOH	16 h	41d (*)	-
5	8mL/mmol	THF	16 h	41b (traces)	-
6	8mL/mmol	H ₂ O	16 h	-	-
7	8mL/mmol	THF/H ₂ O (4:1 v/v)	96 h	41b (31%)	41e (17%)

Table 3.21: Reaction conditions and relative products and yields corresponding to step b. in Scheme 3.12. (*) Conversion confirmed via TLC and ES/MS. ^aAll volumes (mL/mmol) of Amberlite were added in 2-3 portions over the time. ^bReactions were performed at rt.

The crude from step a (**40**, Scheme 3.12) was treated with Amberlite (IRN78, 8 mL/mmol) in two portions in CH₃OH over 16 hours (Table 3.21, entry 1), following the procedure adopted previously in this work for the synthesis of 3'dA. The starting material **40** was completely converted into a less lipophilic spot on TLC that after filtration of the resin and evaporation of the solution was confirmed to be 2-methoxy-2',3'-anhydroadenosine **41a**, by analysis of ¹H NMR (Figure 3.45), ¹³C NMR, ES/MS and lack of peaks in the ¹⁹F NMR spectrum.

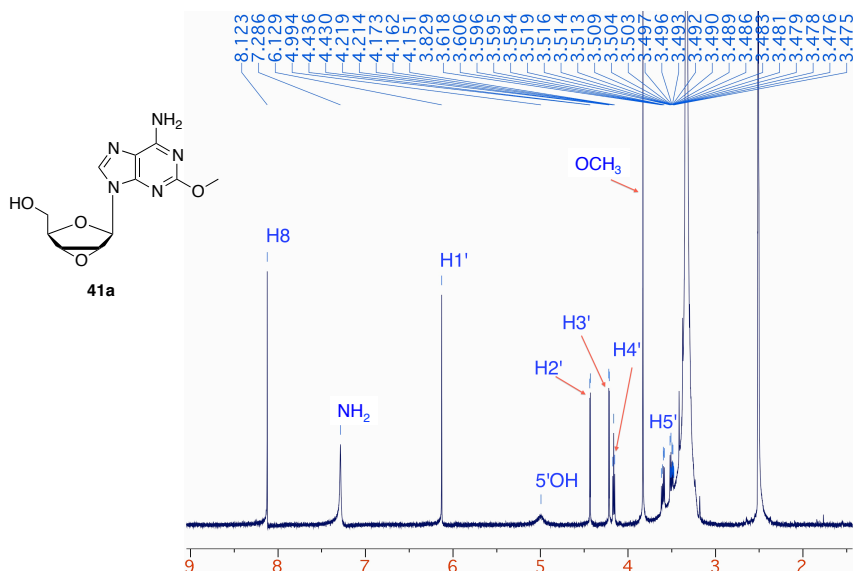


Figure 3.45: ^1H NMR of **41a** in CD_3OD (500 MHz).

Nucleophilic substitution of the fluorine in position 2 on the nucleobase was caused by reaction with methanol in basic conditions. In an attempt to limit this side reaction, the crude **40** was dissolved in CH_3OH and 4 mL/mmol of Amberlite ($2 \times \text{OH}^-$) were added (Table 3.21, entry 2).

The reaction was carefully monitored and after only 1 hour a less lipophilic spot appeared on TLC, with a different R_f when compared to **41a**. The conversion was not complete, however only traces corresponding to undesired **41a** were noticed. An additional portion of Amberlite ($2 \times \text{OH}^-$, 1 mL/mmol) was added, and the reaction was stirred for an additional 30 minutes, until the starting material **40** was present only in traces and the spot corresponding to undesired **41a** became more intense on TLC. The resin was immediately filtered and washed with CH_3OH and isolation of products by flash column chromatography yielded the desired 2-fluoro intermediate **41b** in 54% yield, along with 11% of **41a** and traces of starting material (**40**), as confirmed by NMR analysis of the products (^1H NMR and ^{19}F NMR of desired **41b** are reported in Figure 3.46).

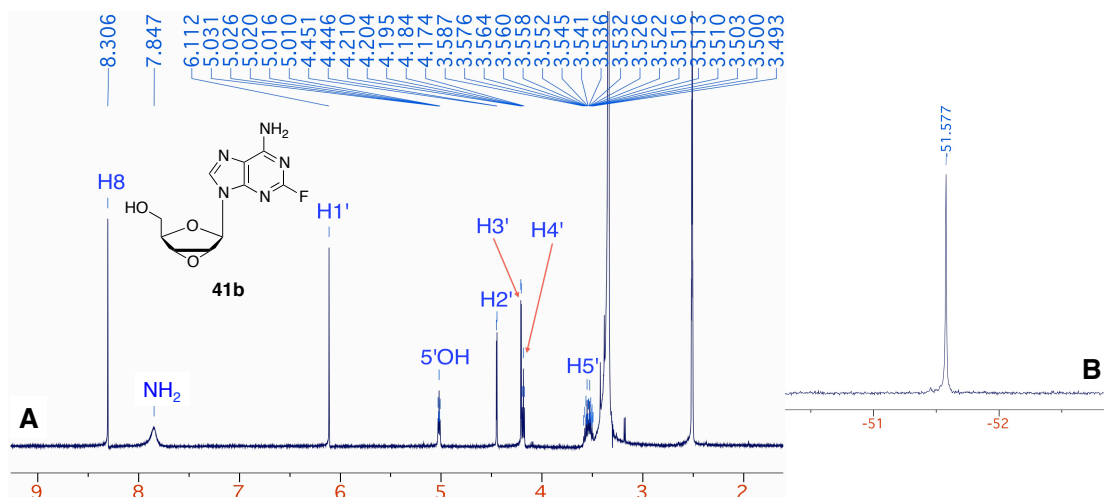


Figure 3.46: (A) ^1H NMR (500 MHz) and (B) ^{19}F NMR (470 MHz) spectra of compound **41b** in $\text{DMSO-}d_6$.

In an attempt to improve the yield of the reaction, identification of a solvent for the reaction that could avoid risk of the aromatic nucleophilic substitution was necessary. At the same time, the solvent should have allowed the resin to behave as an ion exchanger. In fact, ion-exchange with conventional resins is frequently unsuccessful if anhydrous solvents of low polarity are used,²⁷⁷ due to the inability of the resin matrix to swell sufficiently in the solvent. If the resin is not swollen or is only partially swollen, the ion-exchange rate-process or the penetration of the non-electrolyte or electrolyte into the resin will be limited.²⁷⁸⁻²⁸⁰

Our first attempt in replacing CH_3OH as a solvent involved the use of EtOH (Table 3.21, entry 3), and 6 mL/mmol of Amberlite ($2 \times \text{OH}^-$), reasoning that the increase in bulk of the alcohol could avoid or reduce the nucleophilic substitution.

However, 2-ethoxy-2',3'-anhydroadenosine (**41c**) was recovered from resin filtration after 16 hours. The presence of an ethyl chain is clear from ^1H NMR spectrum (Figure 3.46) and the splitting pattern of the sugar moiety confirms the presence of the epoxide ring.

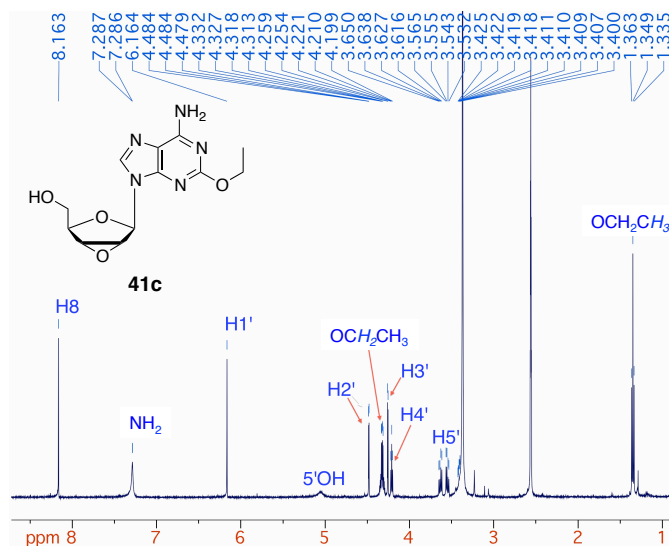


Figure 3.47: ^1H NMR of 2-*O*-ethyl-2',3'-anhydroadenosine **41c** in $\text{DMSO-}d_6$.

Increasing the bulk of the alcohol with isopropanol (*i*PrOH), (Table 3.21, entry 4) as a solvent led to conversion into 2-isopropoxy-2',3'-anhydroadenosine **41d** as confirmed by TLC and ES/MS. Replacing the use of an alcohol with THF (Table 3.21, entry 5) caused a considerable reduction of the reaction rate, with only a small extent of conversion into desired **41b** on TLC after 16 hours. The reaction attempted in water was unsuccessful due to the insolubility of the starting material in the solvent (Table 3.21, entry 6). Consequently, the use of a mixture of water in THF was attempted (Table 3.21, entry 7). Although the conversion into **41b** appeared to be faster after 16 hours compared to the use of pure THF as a solvent, the reaction was pushed by stirring for 96 hours. Finally, complete conversion into **41b** was obtained and a more lipophilic spot that was isolated and characterised as compound **41e**, which was confirmed by ^1H NMR (Figure 3.48), ^{19}F NMR and ES/MS analysis. Intermediates with the same 2,4,4-trimethyl-5-oxo-1,3-dioxolane ring in position 5' on the sugar moiety were already reported by Robins *et al.*²¹² during the synthesis of 3'dA (possible structures of such intermediates, which were not isolated, were reported in Scheme 3.12), however **41e** can be considered as a partial product, because the formation of the epoxide ring on the sugar has happened.

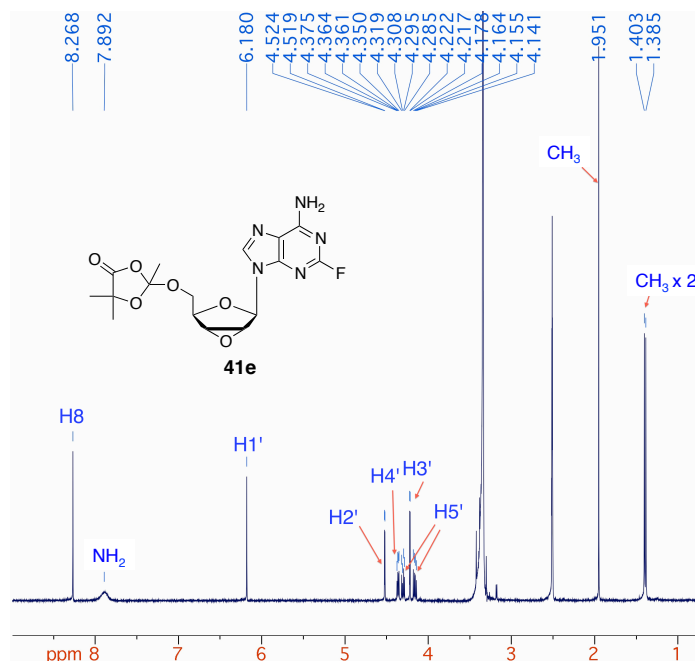
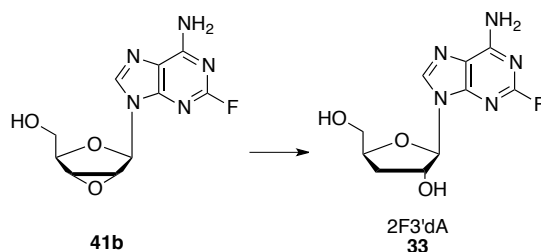


Figure 3.48: ¹H NMR (500 MHz) spectra of **41e** in DMSO-*d*₆.

Therefore, these latter reaction conditions are too mild to complete the reaction with the total cleavage of this 5'-ring, although favourably not leading to nucleophilic substitution of the fluorine on the adenine ring. However, considering the results of these attempts, the best yields achieved are represented by entry 2, with 54% yield of desired product and 11% yield of side product **41a** in 1 hour 30 minutes of reaction time.

The final step for the synthesis of 2F3'dA was performed on **41b**, which was subject to reductive opening of the epoxide ring via treatment with 4 equivalents of LiEt₃BH (1M solution in THF) portioned in 2 additions: the first addition of 3 equivalents of the reagent was performed at 0 °C and after overnight stirring at room temperature the mixture was brought to 0 °C a second time to allow the addition of the final equivalent of reagent (Scheme 3.13).



Scheme 3.13 Final step to the synthesis of 2F3'dA (**33**). Reagents and conditions. (a.) LiEt₃BH (1M sol. in THF, 4 eq), DMSO (4 mL/mmol), THF (10 mL/mmol), 0 °C to rt, 16h (82%).

Stirring of the mixture for an additional 5 hours at room temperature led to complete conversion of the starting material into desired 2F3'dA (**33**) (as confirmed by $^1\text{H-NMR}$ and $^{19}\text{F-NMR}$ analysis (Figure 3.49), which was isolated in 82% yield, reaching a 3-step yield of 45%.

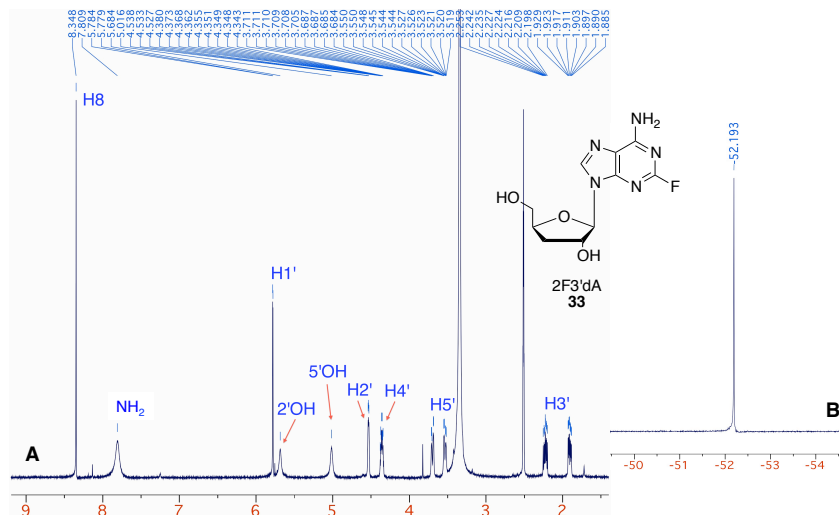
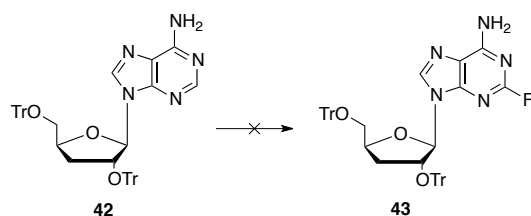


Figure 3.49: (A) $^1\text{H NMR}$ (500 MHz) and (B) $^{19}\text{F NMR}$ (470 MHz) spectra of 2F3'dA (**33**) in $\text{DMSO-}d_6$.

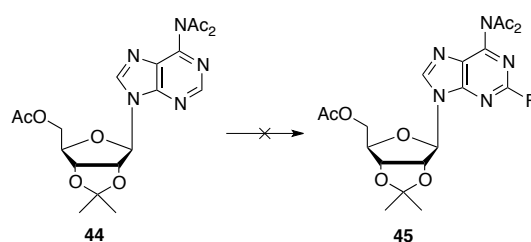
Not completely satisfied with the yield of synthesis of 2F3'dA, a different synthetic strategy was attempted. Hartwig *et al.* described the fluorination of multi-substituted pyridines and diazines at the position α to nitrogen accomplished by the use of silver fluoride (AgF_2) in CH_3CN , at rt for 3 hours.²⁸¹ This mild methodology was applied to a variety of pyrimidine rings. Moreover, in a more recent publication by the same group, the introduction of a fluorine group α to nitrogen containing heterocycles was described as valuable for late-stage functionalisation of such substrates with oxygen, nitrogen and carbon-bearing nucleophiles, confirming the easy nucleophilic substitution on the 2-fluoroadenine ring noticed in this work.²⁸² The fluorination methodology required protection of both free hydroxyl and amino groups of the substrate.

When the reaction on 2',5'-*O*-bistrityl-3'-deoxyadenosine (**42**) was carried out, the result was unsuccessful, with no trace of desired fluorinated product (**43**) detected (Scheme 3.14). The starting material (**42**) was recovered.



Scheme 3.14: Attempted fluorination of **43**. *Reagents and conditions*: AgF₂ (3 eq), CH₃CN, rt, 3h.

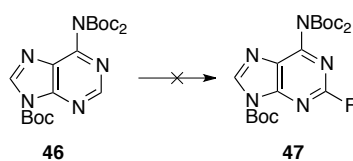
The same reaction procedure was performed on fully protected *N,N*-5'-*O*-triacetyl-2',3'-isopropylidene adenosine (**44**) (Scheme 3.15), in an attempt to avoid any potential side reactions caused by the free amino group in substrate **42**.



Scheme 3.15: Attempted fluorination of **44**. *Reagents and conditions*: AgF₂ (3 eq), CH₃CN, rt, 3h.

TLC analysis of the mixture showed the presence of a less lipophilic spot that was then confirmed by mass to be a side product lacking one acetyl group.

Therefore, the reaction on a simpler substrate such as fully protected adenine *via* di-*tert*-butyl dicarbonate (**46**) was attempted (Scheme 3.16).

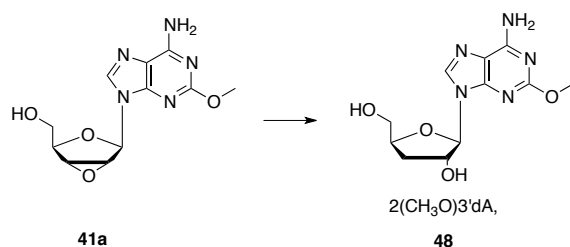


Scheme 3.16: Attempted fluorination of **46**. *Reagents and conditions*: AgF₂ (3 eq), CH₃CN, rt, 3h.

The reaction mixture visibly changed colour to yellow suggesting conversion of AgF₂, although analysis of the crude *via* TLC revealed complete degradation into more hydrophilic products that could not be identified, with no trace of fluorinated product **47**.

Despite not being able to improve the reaction yield for the synthesis of 2F3'dA over 45%, this still represented a significant improvement over the yields that were previously reported through different methodologies (7%²²⁵ and 35%²⁷⁶).

Due to the amount of 2-*O*-methyl-2',3'-anhydroadenosine **41a** synthesised in the attempts for the synthesis of **41b**, conversion of this side-product into an alternative 3'-deoxyadenosine analogue by treatment with LiEt₃BH (4 equivalents in two portions) was carried out in a mixture of DMSO and THF.



Scheme 3.17: Final step of the synthesis of 2(CH₃O)3'dA (**48**). Reagents and conditions: LiEt₃BH (1M sol. in THF, 4 eq), DMSO (4 mL/mmol), THF (10 mL/mmol), 0 °C to rt, 16h (85%).

This reaction led to the synthesis of 3'-deoxy-2-*O*-methyladenosine (2(CH₃O)3'dA, **48**) in 85% yield (Scheme 3.17), as confirmed in Figure 3.50.

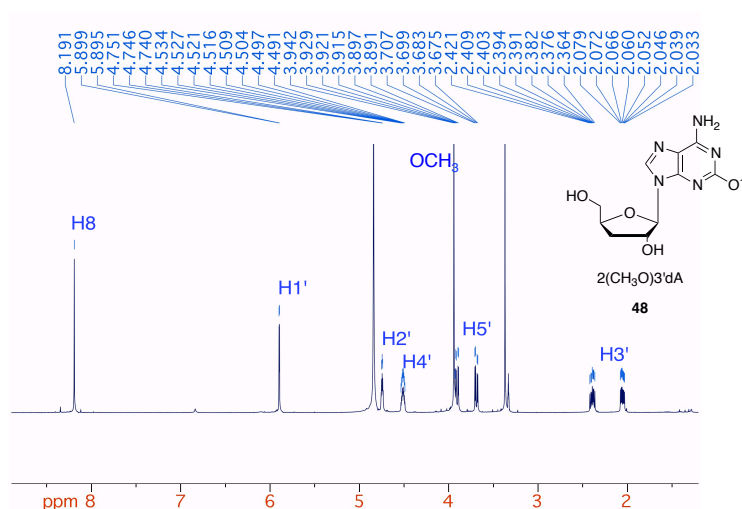


Figure 3.50: ¹H NMR (500 MHz) spectrum of 2(CH₃O)3'dA (**48**) in DMSO-*d*₆.

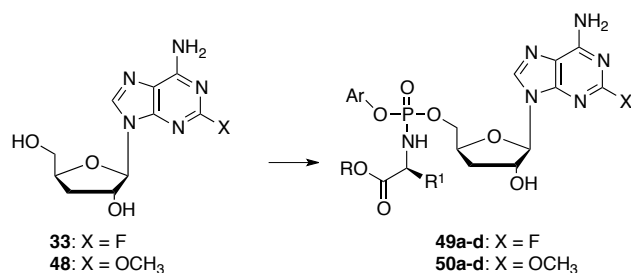
The biological activity of this nucleoside analogue has never been reported, therefore the synthesis of a small family of ProTides of **48** was accomplished in order to investigate the potential anticancer activity of both the nucleoside and its ProTides.

3.2.3 Synthesis of 2-modified cordycepin ProTides

The synthesis of ProTides of both 2F3'dA and 2(CH₃O)3'dA was accomplished via treatment of the nucleoside analogue with 5 equivalents of *N*-methylimidazole (NMI) and

3 equivalents of the appropriate phosphorochloridates in anhydrous THF over 16 hours, at rt (Scheme 3.18).

Similarly to the synthesis of 3'dA ProTides, the NMI method applied to 2F3'dA and 2(CH₃O)3'dA also yielded 2'-phosphoramidate and 2'-5'-bis-*O*-phosphoramidate side products. However, these compound were not isolated, and the desired 5'-phosphoramidates were obtained in yields ranging from 7% to 28% and 9 to 60% respectively for the 2F3'dA and 2(CH₃O)3'dA families of ProTides.



Scheme 3.18: Synthesis of ProTides of 2F3'dA (**49a-d**) and 2(CH₃O)3'dA (**50a-d**). *Reagents and conditions:* NMI (5 eq), appropriate phosphorochloridate (3 eq), THF, rt, 16h.

Cpnd	Nucleoside	Ar	R	R ^I	AA	yield
49a	2F3'dA (X = F)	Nap	Bn	Me	L-Ala	15 %
49b	"	Ph	Bn	Me	L-Ala	7%
49c	"	Nap	<i>n</i> -Pen	<i>i</i> Bu	L-Leu	16 %
49d	"	Ph	<i>n</i> -Hex	Me	L-Ala	28 %
50a	2(CH ₃ O)3'dA (X = OCH ₃)	Nap	Bn	Me	L-Ala	9 %
50b	"	Ph	Bn	Me	L-Ala	60%
50c	"	Nap	<i>n</i> -Pen	<i>i</i> Bu	L-Leu	15%
50d	"	Ph	<i>n</i> -Hex	Me	L-Ala	18%

Table 3.22: Structures and yields of ProTides of 2F3'dA (**49a-d**) and 2(CH₃O)3'dA (**50a-d**).

3.2.4 Cytotoxic *in vitro* screening

3.2.4.1 *In vitro* evaluation of 2F3'dA ProTides

The cytotoxic activity of 2F3'dA and 2(CH₃O)3'dA and relative prodrugs was tested on a panel of blood tumours and solid cancers (Table 3.23), by WuXi AppTech.

	Cell line	Malignancy	Cell line	Malignancy
Blood tumours	MOLT-4	acute lymphoblastic	HEL92.1.7	erythroleukaemia
	CCRF- RL	acute lymphoblastic non-Hodgkin's lymphoma	HL-60	promyelocytic leukaemia
	K562	chronic myelogenous	Z-138	mantle cell lymphoma
	KG-1	acute myelogenous leukaemia	Jurkat	acute T cell leukaemia
	THP-1	acute monocytic leukaemia	HS445	hodgkin lymphoma
	NCI-H929	plasmacytoma	RPMI-8226	human multiple myeloma
			MV4-11	biphenotypic B myelomonocytic
Solid cancers	BxPC-3	pancreas adenocarcinoma	HT29	colon adenocarcinoma
	SW620	colon adenocarcinoma	MCF-7	breast adenocarcinoma
	Cal 27	oral adenosquamous	MIA PaCa- 2	Pancreas adenocarcinoma
	HepG2	hepatocellular carcinoma		

Table 3.23: Malignant cell lines selected for the cytotoxic screening of ProTides of 2F3'dA and 2(CH₃O)3'dA (performed by WuXi AppTech).

The selection of cell lines used for the cytotoxic evaluation of 2F3'dA (reported only on HepG2 cells) was broadened.²⁷⁰ Secondly, fewer cells were selected to test 2(CH₃O)3'dA and derivatives, since there was no report in the literature of any potential anticancer activity of such compound.

Cpnd	CCRF-CEM		MOLT-4		K562		HEL92.1.7		KG-1		MV4-11		HL-60	
	IC ₅₀	MI%	IC ₅₀	MI%	IC ₅₀	MI%	IC ₅₀	MI%	IC ₅₀	MI%	IC ₅₀	MI%	IC ₅₀	MI%
2F3'dA	15.23	101	8.82	99	16.83	97	10.9	99	10.85	99	2.76	99.5	10.64	96
49a	0.62	99	0.5	98	3.86	99	3.41	100	6.48	99	0.43	99.8	1.78	101
49b	0.41	99	0.32	96	2.63	97	2.91	99	2.6	97	0.61	99.9	2.04	100
49c	0.35	101	0.25	97	1.66	100	0.7	99	6.07	103	0.32	99.7	2.74	99
49d	0.37	100	0.25	97	14.7	96	2.52	99	2.15	96	0.53	99.4	1.99	100
PTX	0.003	98	0.003	95	0.01	91	0.02	83	0.08	88	0.003	98.2	0.003	85

Table 3.24: *In vitro* cytotoxicity screening of parent nucleoside 2F3'dA and ProTides **49a-d** on selected cell lines. Cytotoxicity data reported as μ M IC₅₀ values (concentration of drug causing 50% of cell viability inhibition) and MI% (maximum inhibitory effect of the drug at the range of concentrations considered). PTX: paclitaxel (control). Assays performed by WuXi AppTech.

Treatment of blood cancer cells with 2F3'dA shows good values of IC₅₀, consisting in low micromolar concentrations of 3.49 μM on the plasmacytoma cell line NCI-H929, and 8.82 μM on the leukaemic cell line MOLT-4.

Cpnd	Thp-1		Z-138		RL		Jurkat		Hs-445		RPMI-8226		NCI-H929	
	IC ₅₀	MI%	IC ₅₀	MI%	IC ₅₀	MI%	IC ₅₀	MI%	IC ₅₀	MI%	IC ₅₀	MI%	IC ₅₀	MI%
2F3'dA	140.15	65	12	100	29.18	100	59	96	25	102	34	97	3.49	102
49a	17.72	100	1.07	99	3.95	102	2.83	96	11	100	7.98	100	1.47	101
49b	17.49	99	1.41	99	1.25	101	3.84	93	31	106	9.83	95	1.12	102
49c	17.2	104	2.84	103	2.23	105	8.02	103	14	102	10	101	0.27	99
49d	35.37	99	1.59	98	2.64	99	7.87	94	72	87	38	98	1.25	100
PTX	0.03	72	0.003	99	0.003	83	0.003	82	0.004	84	0.003	96	0.003	82

Table 3.25: *In vitro* cytotoxicity screening of parent nucleoside 2F3'dA and ProTides **49a-d** on selected cell lines. Cytotoxicity data reported as μM IC₅₀ values (concentration of drug causing 50% of cell viability inhibition) and MI% (maximum inhibitory effect of the drug at the range of concentrations considered). PTX: paclitaxel (control). Assays performed by WuXi AppTech.

The treatment of the same cells with 3'dA gave IC₅₀ values of 151.92 μM and >198 μM respectively on MOLT-4 and NCI-H929 cells.

Cpnd	MIA PaCa-2		BxPC-3-Luc		HT29		SW620		HepG2		MCF-7		Cal 27	
	IC ₅₀	MI%	IC ₅₀	MI%	IC ₅₀	MI%	IC ₅₀	MI%	IC ₅₀	MI%	IC ₅₀	MI%	IC ₅₀	MI%
2F3'dA	32.44	100	38	70	54.19	73	23	95	17	82	51.48	97	35	99
49a	3.31	100	23	95	18.21	84	7.73	99	13	83	3.24	95	9.09	101
49b	2.42	98	32	78	14.83	87	15	97	5.88	74	1.53	95	11	95
49c	4.88	100	55	90	16.54	88	12	104	4.02	94	1.32	99	35	101
49d	5.82	98	34	67	35.36	92	37	89	5.3	82	1.17	87	32	86
PTX	0.002	87	0.016	51	0.004	75	0.011	84	0.04	50	0.01	65	0.002	92

Table 3.26: *In vitro* cytotoxicity screening of parent nucleoside 2F3'dA and ProTides **49a-d** on selected cell lines. Cytotoxicity data reported as μM IC₅₀ values (concentration of drug causing 50% of cell viability inhibition) and MI% (maximum inhibitory effect of the drug at the range of concentrations considered). PTX: paclitaxel (control). Assays performed by WuXi AppTech.

This improvement in cytotoxic activity is similar on all the other cell lines, including those from solid tumours: although in some cases generating IC₅₀ values as high as 54.19 μM (on the colon adenocarcinoma cell line HT29). 2F3'dA had a significant cytotoxic effect on all cell lines, leading to inhibition of cell viability higher than 73%.

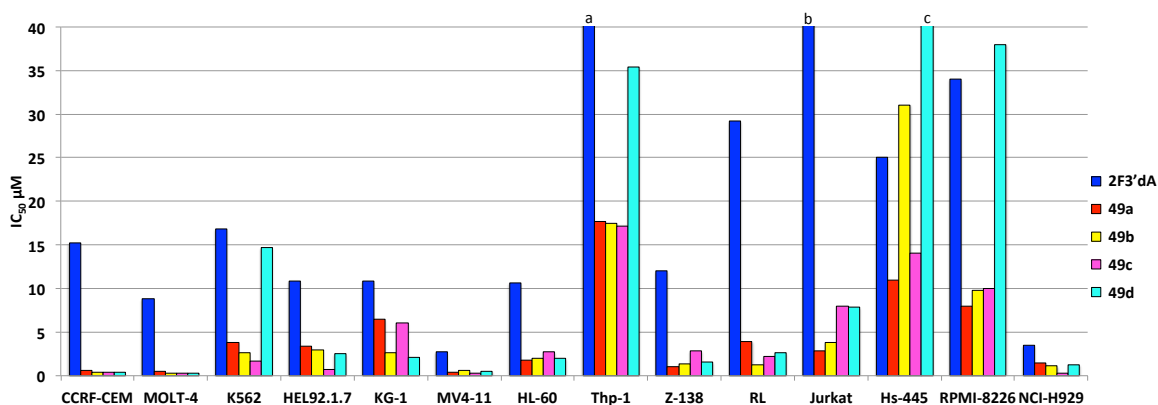


Figure 3.51: Activity of 2F3'dA and ProTides **49a-d** on blood cancer cell lines. ^aIC₅₀ = 29.18 µM; ^b IC₅₀ = 140.15 µM; ^c IC₅₀ = 35.37 µM.

ProTides of 2F3'dA are more active than the parent nucleoside, the pentyloxy-L-leucine naphthyl phosphate derivative **49c** being consistently the most potent derivative, with IC₅₀ values in the submicromolar range (0.25-0.7 µM) on the blood cancer cell lines MOLT-4, NCI-H929, CCRFCEM and HEL92.1.7. The L-alanine phenyl benzyloxy derivative **49b** was similarly potent on most cell lines, and this trend was generally maintained by all 2F3'dA prodrugs.

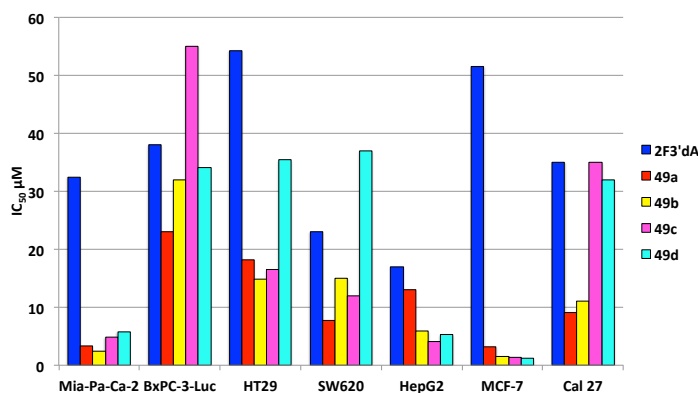


Figure 3.52: Activity of 2F3'dA and ProTides **49a-d** on solid cancer cell lines.

Comparable results were gathered after treatment of solid tumour cell lines with 2F3'dA and relative prodrugs, with the parent nucleoside being moderately active. The activity of 2F3'dA ProTides was, in this case, overall very similar, with IC₅₀ values rarely higher than 15 µM and ranging between 1.17 µM (IC₅₀ value of compound **49d** on MCF-7 cell line) and 35.36 µM (IC₅₀ value of compound **49d** on HT29 cell line).

3.2.4.2 *In vitro* screening of 2(CH₃O)3'dA ProTides

The introduction of a 2-methoxy group in place of fluorine on the adenine ring generated an inactive nucleoside analogue, as shown in Table 3.27, Table 3.28 and Figure 3.53.

Cpnd	CCRFCEM		KG-1		K562		MOLT-4	
	IC ₅₀	MI%	IC ₅₀	MI%	IC ₅₀	MI%	IC ₅₀	MI%
2(CH ₃ O)3'dA	>198	-4	>198	1	>198	40	>198	1
50a	22.2	100	106.4	92	42.1	104	29	101
50b	12.9	102	86.6	99	29.6	100	17.9	104
50c	10.6	100	20.6	102	13.7	100	6.5	101
50d	75.5	93	82.9	96	84.4	78	58.1	97
PTX	0.003	98	0.08	88	0.01	91	0.003	95

Table 3.27 *In vitro* cytotoxicity screening of parent nucleoside 2(CH₃O)3'dA and ProTides **50a-d**. Cytotoxicity data reported as μ M IC₅₀ values (concentration of drug causing 50% of cell viability inhibition) and MI% (maximum inhibitory effect of the drug at the range of concentrations considered). PTX: paclitaxel (control). Assays performed by WuXi AppTech.

2(CH₃O)3'dA did not significantly affect the growth of the considered cell lines, up to the highest concentration assayed (198 μ M). Conversely, ProTides of 2(CH₃O)3'dA reached approximately 100% of inhibitory effect on almost all treated cell lines, with IC₅₀ values ranging within the high micro-molar range.

Cpnd	RL		NCI-H929		HT29		MCF7	
	IC ₅₀	MI%	IC ₅₀	MI%	IC ₅₀	MI%	IC ₅₀	MI%
2(CH ₃ O)3'dA	>198	0	>198	51	>198	19	>198	8
50a	35.8	97	22	104	94.1	81	44.1	90
50b	24.5	104	12.4	102	75.8	98	38.1	99
50c	11.6	100	10.5	99	24.4	100	13.9	100
50d	60.2	88	41.6	99	98.3	69	96.6	73
PTX	0.003	83	0.003	82	0.004	75	0.01	65

Table 3.28: *In vitro* cytotoxicity screening of parent nucleoside 2(CH₃O)3'dA and ProTides **50a-d**. Cytotoxicity data reported as μ M IC₅₀ values (concentration of drug causing 50% of cell viability inhibition) and MI% (maximum inhibitory effect of the drug at the range of concentrations considered). PTX: paclitaxel (control). Assays performed by WuXi app. Tech.

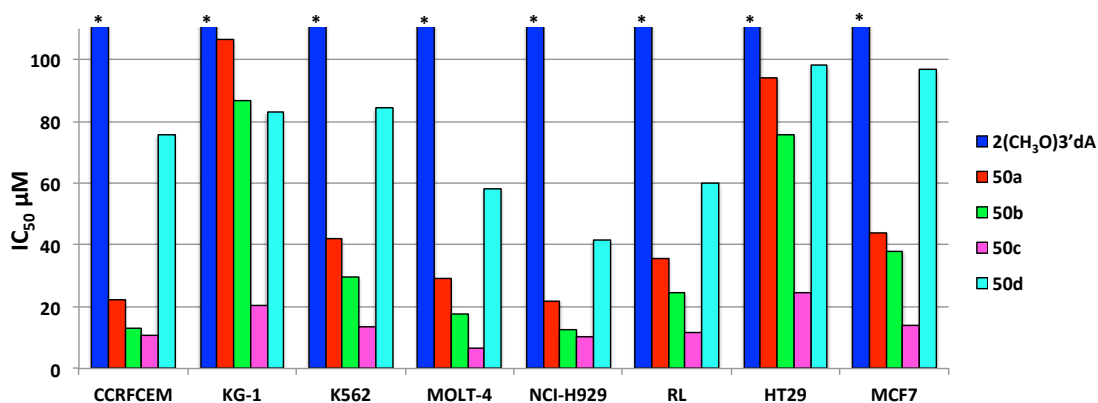


Figure 3.53: Cytotoxic activity of 2(CH₃O)3'dA and ProTides **50a-d**. *IC₅₀ > 198 μM.

The L-leucine derivative **50c** was the most active derivative in this series, with an IC₅₀ of 6.51 μM on MOLT-4 cell line and similar activity profile on colorectal and breast solid tumour cell lines (HT29 and MCF7).

In conclusion, the *in vitro* evaluation of 2-modified 3'dA analogues and relative ProTides confirmed the superior cytotoxic activity of 2F3'dA over 3'dA. Comparison between the cytotoxicity data relative to 3'dA, 2F3'dA and 2(OCH₃)3'dA is given in Figure 3.54. On this selection of cell lines, 3'dA was more active than 2(OCH₃)3'dA, although 2F3'dA emerges as consistently the most active nucleoside.

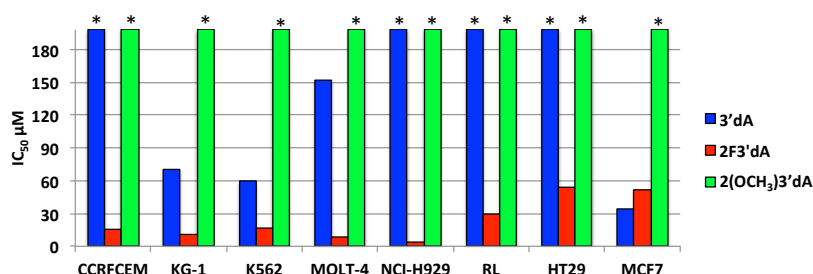


Figure 3.54 Comparison between cytotoxicity (μM IC₅₀) values of 3'dA, 2F3'dA and 2(OCH₃)3'dA. *IC₅₀ > 198 μM.

Figure 3.55 shows a comparison between the most active ProTides of the three families of 3'dA derivatives, namely the phenyl L-alanine benzyl ester ProTides of 3'dA (**32a**), 2F3'dA (**51a**) and 2(OCH₃)3'dA (**50a**), naphthyl L-alanine benzyl ester ProTides of 3'dA (**30b**), 2F3'dA (**49a**) and 2(OCH₃)3'dA (**50b**) and naphthyl L-leucine *n*-pentyl ester ProTides of 3'dA (**30d**), 2F3'dA (**49c**) and 2(OCH₃)3'dA (**50c**). Despite the significant improvement in activity of 2F3'dA in comparison to 3'dA, ProTides of 2F3'dA are endowed with similar cytotoxicity as the 3'dA counterparts. The same moieties applied to 2(OCH₃)3'dA, on the other hand, generate less active compounds, apart from the naphthyl

L-leucine *n*-pentyl ester moiety, which generate three compounds with very similar cytotoxicity (**30d**, **49c**, **50c**).

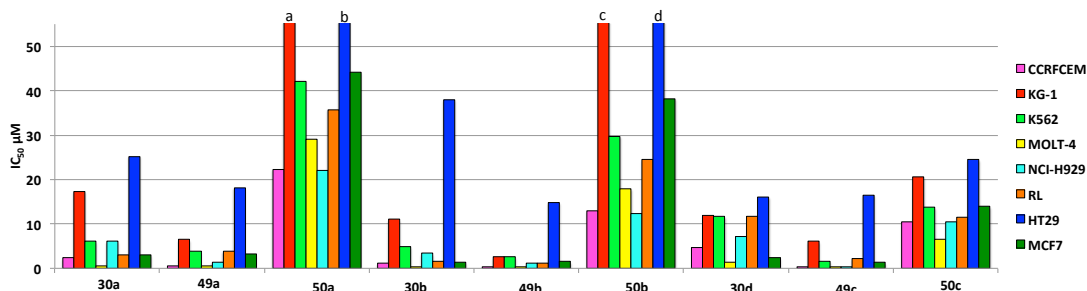


Figure 3.55: Comparison between cytotoxicity ($\mu\text{M IC}_{50}$) values of phenyl L-alanine benzyl ester ProTides of 3'dA (**30a**), 2F3'dA (**49a**) and 2(OCH₃)3'dA (**50a**), naphthyl L-alanine benzyl ester ProTides of 3'dA (**30b**), 2F3'dA (**49b**) and 2(OCH₃)3'dA (**50b**) and naphthyl L-leucine *n*-pentyl ester ProTides of 3'dA (**30d**), 2F3'dA (**49c**) and 2(OCH₃)3'dA (**50c**). ^aIC₅₀ = 106.41 μM , ^bIC₅₀ = 94.09 μM , ^cIC₅₀ = 86.58 μM , ^dIC₅₀ = 75.81 μM .

The cytotoxic evaluation of new 2-modified 3'dA and related ProTides led to the identification of promising new derivatives within the 2F3'dA family of prodrugs, which were further investigated.

3.2.4.3 Leukaemic stem cells selectivity

The intriguing anticancer activities of both 2F3'dA and relative ProTides prompted us to investigate the potential selective targeting of the LSC population present within the KG1a cell line. Initially, the LD₅₀ values of these compounds were evaluated on KG1a cell line (Table 3.29) by Prof. C. Pepper (School of Medicine, Cardiff University).

Common structure	Cpnd	Ar	R	R ₁	AA	LD ₅₀
	2F3'dA	-	-	-	-	11
	49a	Nap	Bn	Me	L-Ala	7.1
	49b	Ph	Bn	Me	L-Ala	3.9
	49c	Nap	<i>n</i> -Pen	<i>i</i> Bu	L-Leu	3.3
	49d	Ph	<i>n</i> -Hex	Me	L-Ala	3.5

Table 3.29 Structures of 2F3'dA ProTides assayed for cytotoxicity on KG1a cell line, reported as LD₅₀ values (μM). Assays performed by Prof. C. Pepper, Cardiff University.

Consistently with the data previously reported, 2F3'dA results indicated a good anticancer agent, with LD₅₀ value in the micromolar range. ProTides **49a-d** were more active than the

parent nucleoside, although by only 1.5 to 3.3-fold. The most active compound on the KG1a cell line was the naphthyl L-leucine pentyl derivative **49c** (Table 3.29).

The KG1a cell line was then treated with a range of concentrations of 2F3'dA and ProTides **49a-d**, and the effect on the LSC population within this cell line was evaluated via FACS analysis. Figure 3.56 reports a comparison between the LD₅₀ values of 2F3'dA and ProTides **49a-d**, also in relation to the LD₅₀ values of 3'dA and 3'dA ProTide **30a** on the same cell line.

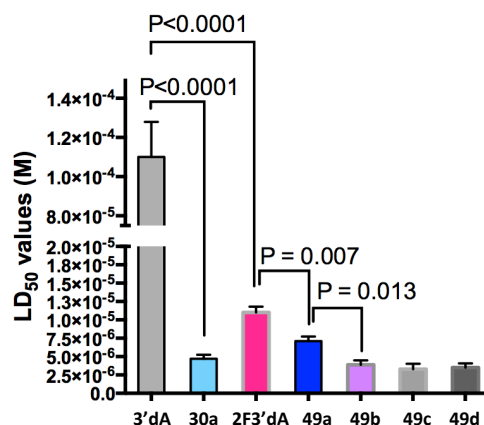


Figure 3.56: LD₅₀ (M) values of 3'dA and 2F3'dA and ProTides **30a** and **49a-d**. Assays performed by Prof. C. Pepper, Cardiff University.

As noted from the previous *in vitro* screening, 2F3'dA appears to be a much more cytotoxic agent than 3'dA. However, the LD₅₀ values of 2F3'dA ProTides were lower than the parent nucleoside, but not significantly different from ProTide **30a**.

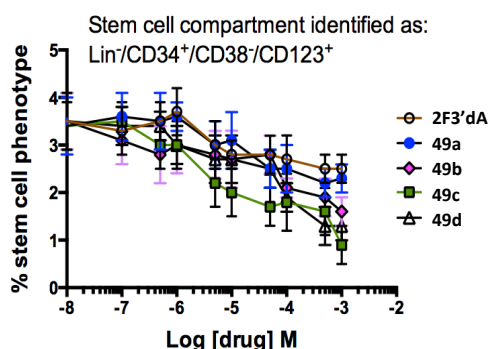


Figure 3.57 Effect on LCS population after treatment with 2F3'dA and ProTides at a range of concentrations. Assays performed by Prof. C. Pepper, Cardiff University.

When the LSC targeting was analysed after treatment with 2F3'dA derivatives at a broad dose range, both compound **49a** and the parent nucleoside seemed to leave the percentage of this population unaffected (Figure 3.57, Figure 3.58). On the other hand, ProTides **49b**,

49c and **49d** led to selective targeting of the stem cell population at concentrations higher than 10^{-4} M.

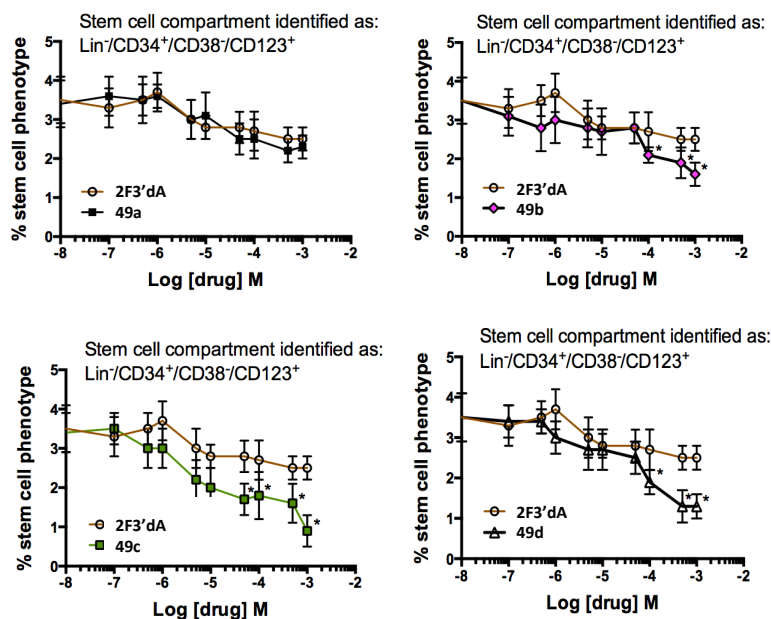


Figure 3.58: Effect on LCS population after treatment with 2F3'dA and ProTides at a range of concentrations. Assays performed by Prof. C. Pepper, Cardiff University.

3.2.5 Adenosine deaminase (ADA) stability of 2-modified 3'dA analogues

3.2.5.1 ADA UV assay

The presence of a fluorine substituent in position 2 on the 3'dA structure was already reported to induce resistance to ADA-mediated catabolism.^{225,270}

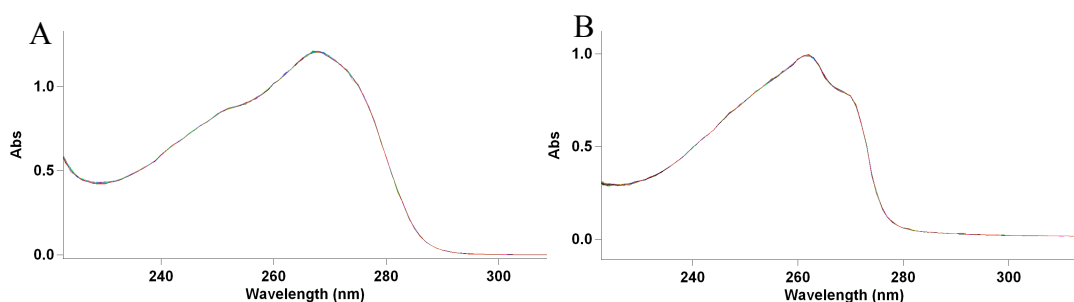


Figure 3.59 Stability of 2(CH₃O)3'dA (A) and 2F3'dA (B) to ADA mediated deamination. Spectra recorded every 0.1 minute for 10 minutes. No significant transformation into the respective 2-modified inosine derivative was noticed for either substrates.

Therefore, the stability of 2(CH₃O)3'dA to ADA was assayed, due to the presence of a 2-methoxy functionality. The introduction of a methoxy group in position 2 on the adenine ring would be expected to lead to an opposite effect compared with the 2-fluoro

substituent, owing to electron donation of the methoxy group. In fact, the introduction of a halogen in C2 was reported to reduce the partial negative charges on N1 and N3 and therefore the capability of behaving as H-bond acceptors and the overall pKa, crucial features for interaction with ADA.²²⁵ On the other hand, the CH₃O- group should have an opposite electron donating effect, hence enhancing the partial negative charges on N1 and N3.

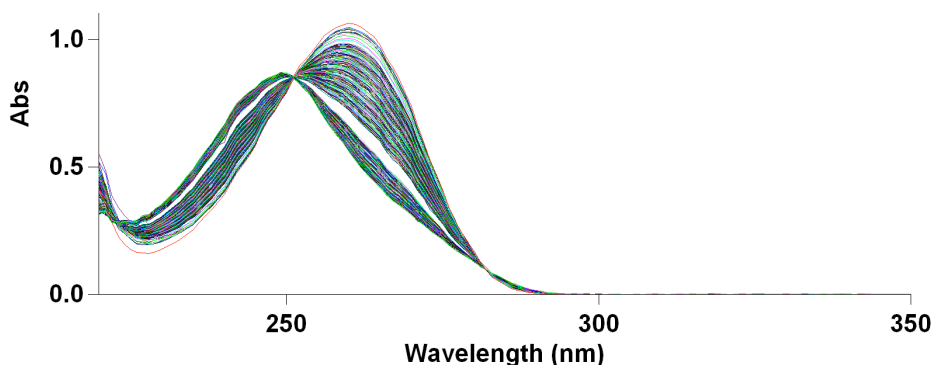


Figure 3.60: Stability of 3'dA to ADA mediated deamination. Spectra recorded every 0.1 minute for 10 minutes. 3'dA (UV_{max} = 259 nm) was converted into 3'dIno (UV_{max} = 249 nm) in the presence of ADA over 10 minutes (A).

However, ADA UV assay performed by treating both 2F3'dA and 2(CH₃O)3'dA nucleosides with bovine adenosine deaminase in phosphate buffer (pH 7.6) showed that both compounds are resistant to ADA-mediated catabolism over 10 minutes (Figure 3.59), while 3'dA was completely converted into the inosine counterpart within 5 minutes (Figure 3.60), as noticeable from the shift in λ_{max} from 259 nm (corresponding to 3'dA) to 249 nm (corresponding to 3'dIno).²²⁵

Since the electronic effect would not explain the stability of 2(CH₃O)3'dA resistance to ADA, other factors may contribute to stability of compounds to deamination such as the steric hindrance, as already noted for 3'dA prodrugs.

3.2.5.2 Docking of 2-modified 3'dA analogues within the ADA active site

In order to understand whether steric factors could affect the recognition of 2-modified 3'dA analogues by ADA, hence the deamination of the considered compounds, docking studies were performed within the active site of ADA (crystal structure PDB 3IAR).

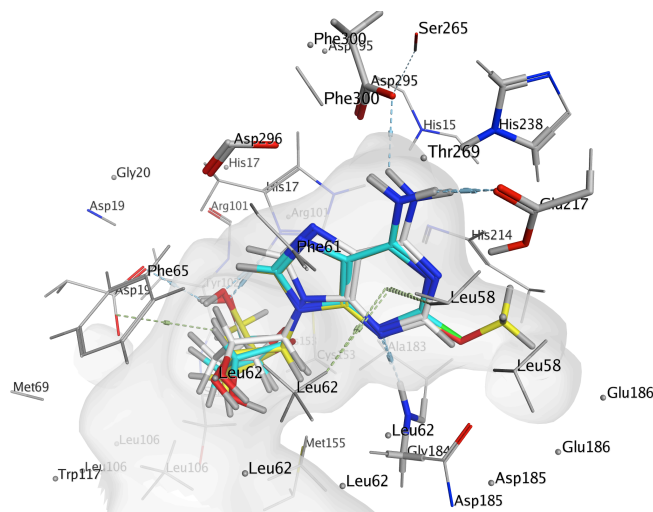


Figure 3.61 Overlap of 2F3'dA (blue), 2(CH₃O)3'dA (yellow) and 3'dA (white) within the ADA active site.

Although overlapping almost entirely with 3'dA, both 2F3'dA and 2(CH₃O)3'dA seemed to interact differently with the active site. This was suggested by the lack of interaction with the Asp295 residue. Moreover, the space around position 2 on the adenine ring is close to the substrate, and seems not to allow any bulky group in this position. In contrast there is a larger area around the amino group and position 8. This may suggest that the lack of processing of 2(CH₃O)3'dA by ADA derives from a clash within the active site residues, leading to incorrect positioning of the molecule.

3.2.6 Mechanistic investigations

3.2.6.1 Enzymatic NMR experiments

A NMR enzymatic assay involving CPY enzyme was carried out on the phenyl L-alanine benzyl ester ProTide of 2F3'dA (**49b**), and on the 2(CH₃O)O3'dA ProTide (**50b**), which is endowed with significantly lower activity, as evident from Figure 3.55.

The aim was to compare the metabolism by CPY of these two prodrugs and predict whether the lower cytotoxic activity of **50b** could derive from a less efficient processing by this enzyme.

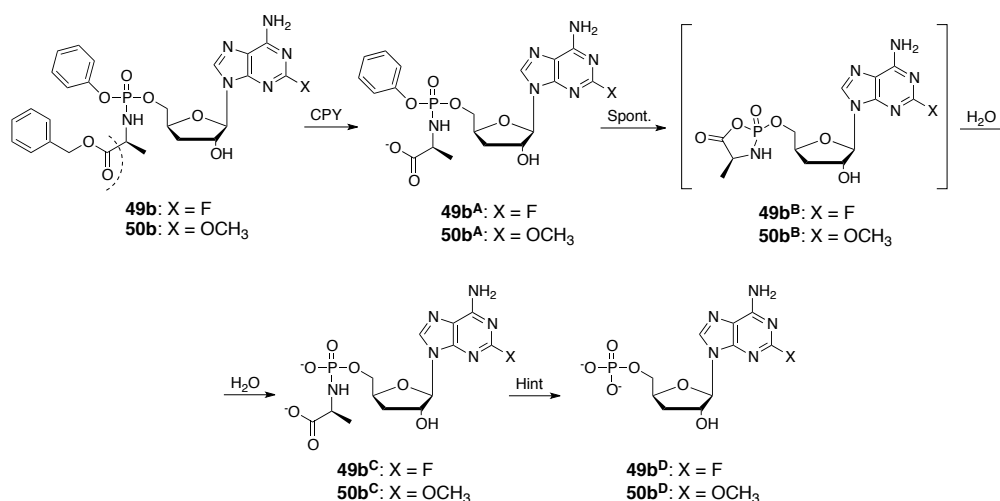


Figure 3.62 Putative metabolic processing by CPY/Hint of ProTides **49b** and **50b** to final release of 5'-monophosphate nucleosides **49b^D** and **50b^D**.

Conversion of ProTide **49b** into L-alanyl phosphate monoester intermediate **49b^C** was rapid and complete after 48 minutes, as described in Figure 3.63.

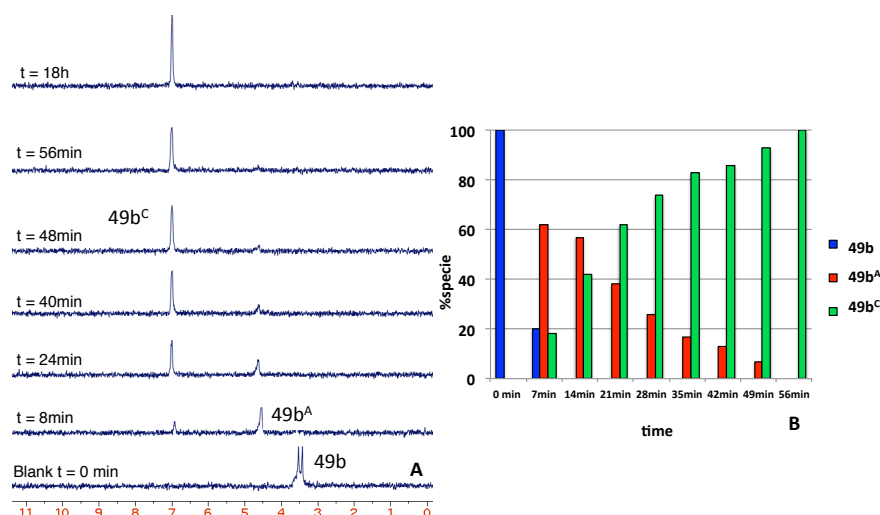


Figure 3.63: (A) Stacked ³¹P NMR spectra (acetone-*d*₆, 202 MHz) monitoring the conversion of ProTide **49b** into metabolite **49b^C**. (B) Graph describing the conversion of **49b** into metabolite **49b^C** over time, as percentage of ³¹P NMR integral of each species.

Similarly, compound **50b** was processed very quickly by CPY, with complete disappearance of the initial peaks within 7 minutes from the enzyme addition. The ³¹P NMR peak of the final compound resulting from CPY metabolism (**50b^C**), appears as a broad peak. However the positioning of the peak in the appropriate range of ppm (6-8 ppm), and ES/MS analysis of the final solution (calculated *m/z* = 432.12 [M], found 431.09 [M - H⁺]) confirmed the presence of the expected metabolite **50b^C**.

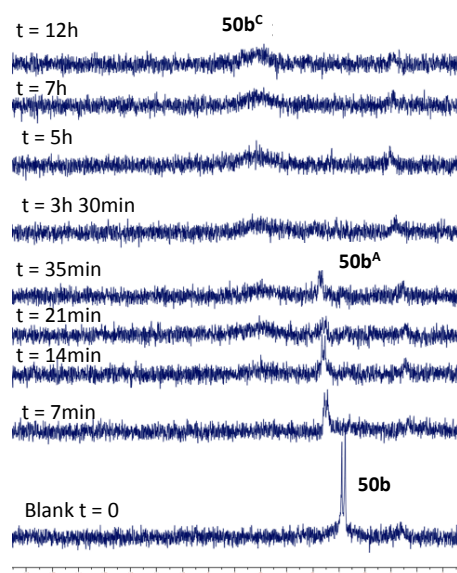


Figure 3.64 Stacked ^{31}P NMR spectra (acetone- d_6 , 202 MHz) monitoring the conversion of ProTide **50b** into metabolite **50b^C**.

Therefore, the CPY assay suggests that the cleavage of the ester moiety of compound **50b** with release of metabolite **50b^C** after intracellular rearrangements might not be a limiting step affecting the low activity of compound **50b**. This assay also suggests that the promising anticancer activity of compound **49b** might be a consequence of quick intracellular release of intermediate **49b^C**. Metabolite **49b^C**, along with the L-alaninyl intermediate **50b^C**, were docked into the active site of Hint, in order to predict the likelihood of processing to respectively 2F3'dAMP (**49b^D**) and 2(CH₃O)3'dAMP (**50b^D**) by this enzyme.

3.2.6.2 Docking studies

Prediction of the intracellular metabolism of compounds **49b** and **50b**, regarding the last step of ProTide activation, catalysed by Hint enzyme, was carried out through docking simulations of intermediates **49b^C** and **50b^C** within the active pocket of the enzyme.

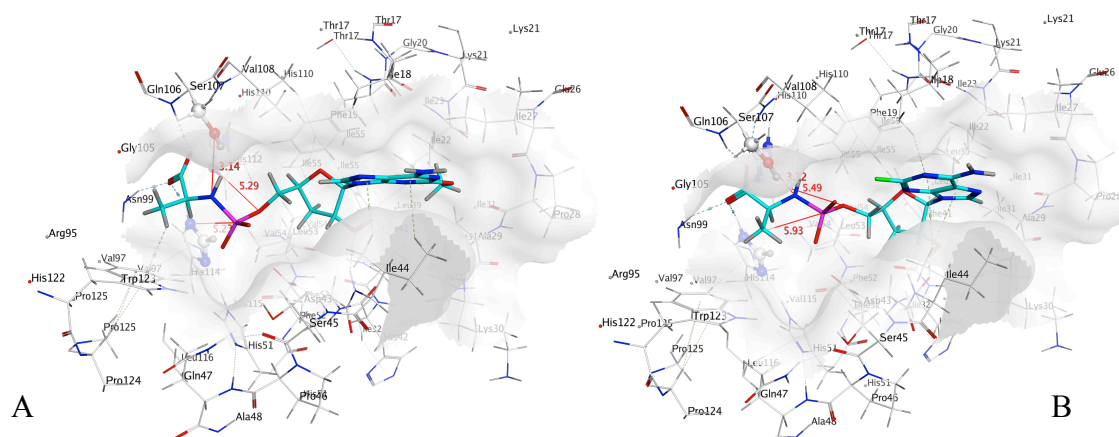


Figure 3.65 Docking of metabolic intermediates **50b^C** (A) and **49b^C** (B) in the active site of the Hint enzyme.

Both intermediates appear to interact very similarly in the active site, with both phosphoramidate moieties closely positioned to the catalytic residues and the nucleobase interacting with additional residues and allowing a correct positioning of both structures. Consequently, Hint enzyme does not appear to discriminate between the two compounds; hence it should not be responsible for the differences in cytotoxic profiles of the two compounds.

3.2.7 Conclusions

The already optimised strategy for the synthesis of 3'dA was modified and applied to the preparation of 2F3'dA, yielding as side product 2(CH₃O)3'dA. 2-Modified analogues of 3'dA were already reported as more stable to ADA-catabolism compared to 3'dA, although were not thoroughly investigated as anticancer agents. In this work both the already reported 2F3'dA and the newly synthesised 2(CH₃O)3'dA along with some ProTide examples of these two families were tested, in search of modified 3'dA ProTides endowed with potentially improved anticancer activity. The introduction of fluorine on the adenine ring generated a nucleoside analogue with significantly improved cytotoxicity compared to 3'dA. On the other hand the presence of a 2-CH₃O group on the adenine moiety was not beneficial in terms of anticancer activity. This was potentially due to a lack of recognition from adenosine kinase, as suggested by the significant improvement in activity when the ProTide moiety was applied to 2(CH₃O)3'dA. ProTides of 2F3'dA were potent derivatives, with IC₅₀ values ranging within sub-micromolar and low-micromolar range. In particular, compound **49b** emerged as both one of the most active 2F3'dA ProTides on a vast selection of malignant cell lines and as a selective cytotoxic agent against the LSC population of the KG1a cell line. On the basis of these promising *in vitro*

results, a new set of preclinical investigations were performed, aimed at comparing the activities of the lead candidates **30a** and **49b**, respectively within the 3'dA and 2F3'dA families of ProTides.

3.3 Further preclinical investigations on 3'dA and 2F3'dA prodrugs

The cytotoxic *in vitro* screening of 3'dA ProTides showed the anticancer potential of this family of prodrugs. In particular, the L-alanine benzyl ester phenyl ProTide **30a**, emerged as one of the most active derivatives in the *in vitro* screening on a broad selection of cell lines. In addition, this derivative was capable of targeting the LSC population within the KG1a cell line, which could potentially offer an advantage *in vivo*. Based on the intriguing activity of 3'dA ProTides, 2F3'dA derivatives were synthesised and proved to be endowed with potent cytotoxic activity.

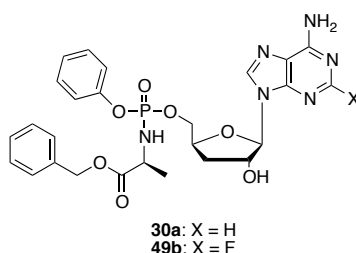


Figure 3.66: Structure of compounds **30a** and **49b**.

Therefore, the separation of the two diastereoisomer of the most promising derivatives **30a** and **49b** (Figure 3.66) was carried out, with the aim of separately evaluating their cytotoxicity on a selection of cell lines. Furthermore, *in vivo* anticancer studies on mice inoculated with RL non-Hodgkin's lymphoma cells were performed by WuXi AppTech, along with additional stability assays in human and rat serum.

3.3.1 Separation of isomers of ProTides **30a** and **49b**

3.3.1.1 Rationale behind diastereoisomer separation

As mentioned in the previous chapters, the two commonly used procedures for the synthesis of nucleoside ProTides consist of the NMI or *t*BuMgCl-mediated coupling reaction between the nucleoside and a phosphorochloridate. These reactions result in the generation of roughly a 1:1 mixture of two diastereoisomers (*S*_p and *R*_p), due to the non-stereoselective formation of a new chiral center at the phosphorus atom.

Difference in the stereochemistry of drugs has often led to compounds with dissimilar activity, toxicology and metabolism, hence the preference for the use of a single isomer in the clinics.^{283,284} In the case of ProTides, the separation is not always straightforward, nor is the preparation of one single diastereoisomer, due to the lack of control of the

stereochemistry at the phosphorous centre during the coupling reaction.²⁸⁵ However, when the separation was successful, the different isomers were often found to be endowed with differences in the biological profile.²⁸⁶⁻²⁸⁸ Crucial examples are the marketed anti-HCV drug sofosbuvir (**9e**, Figure 3.67), whose *Sp* isomer was 18 fold more active than the *Rp*,²⁸⁷ or the anti-HIV acyclic phosphonate analogue GS7340 (**9l**, Figure 3.67),²⁸⁶ currently in phase III clinical trials as the *Sp* isomer, which was found to be 10-fold more active than the *Rp* isomer.

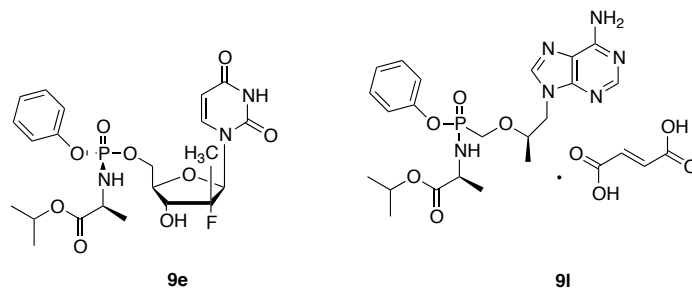


Figure 3.67: Structures of sofosbuvir (**9e**) and GS7340 (**9l**).

A similar pattern was observed also in the family of cytostatic [5-(*E*-bromovinyl)]-2'-deoxyuridine ProTides, whose separated diastereoisomers showed different activity profiles, with *Sp* isomers 10 times more active and *Rp* isomers slightly less active than the mixture.¹⁵³ Moreover, phosphoro(no)amidate diastereoisomers were found to be processed by carboxypeptidase enzyme,^{151,152,289} or be transported through intestinal absorption cell models (Caco-2 and MDCK cells), at different rates.^{290,291}

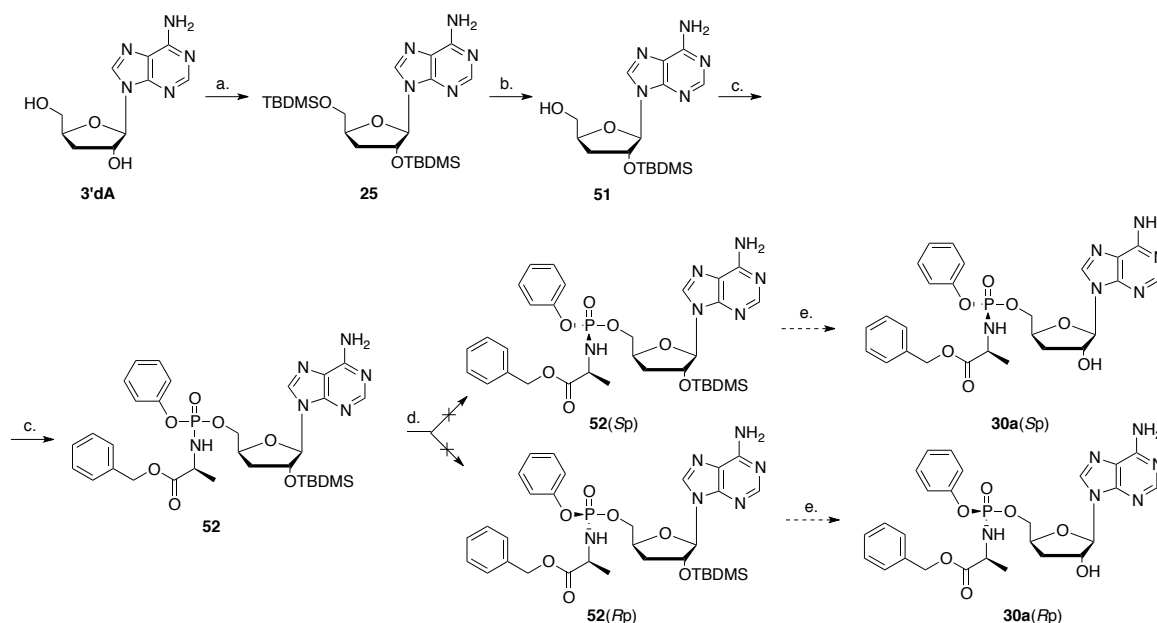
Separation of nucleoside phosphoramidates is generally considered as a difficult task, however was reported as feasible on some substrates by means of reverse phase HPLC,^{286,290-293} molecularly imprinted stationary phase,²⁹⁴ capillary electrophoresis with chiral sectors^{295,296} and normal phase chiral HPLC.^{286,292,296-298} Nonetheless, the separation of diastereoisomers *via* reported methods is not always successful.

3.3.1.2 Attempt to separate diastereoisomers via silylation/desilylation methods

The attempts to separate the diastereoisomers of ProTides **30a** and **49b** via direct phase silica gel column chromatography were unsuccessful, due to the very close retention factor of both isomers on silica.

A recently developed method within the McGuigan group involved direct phase silica gel chromatography separation of sugar TBDMS protected ProTides of the anticancer agent

FUdR, due to different affinity for the stationary phase. Initially this method was applied to 3'dA ProTide **30a**, in order to obtain the desired separated isomers **30a** (*Rp*) and **30a** (*Sp*) and be able to individually evaluate their potentially different cytotoxicity profile.



Scheme 3.19: Attempt to separate **30a** diastereoisomers via silylation/desilylation method. *Reagents and conditions:* (a.) [1] TBDMSCl (3 eq), pyridine, rt, 16h, 50%; [2] TBDMSCl (3 eq), DMAP (0.6 eq), imidazole (6 eq), DMF, rt, 16h, 100%; (b.) THF:H₂O:THF (1:1:4), 5h, 0 °C, 98% (c.), phosphorochloridate (3 eq), NMI (5 eq), THF, 16h, rt, 62%. (d.) chromatographic separation. (e.) TFA, CH₂Cl₂, rt.

This step was performed initially by treatment of the nucleoside analogue with *tert*-butyl dimethylsilyl chloride (TBDMSCl) in pyridine at room temperature for 16 hours, yielding compound **25** in 50% yield (Scheme 3.19).²⁰⁸ Dissolving unprotected 3' dA in DMF and adding imidazole and DMAP to the mixture, followed by addition of the silylating agent, generated a significant improvement of this reaction to quantitative yield.²⁹⁹ Derivative **25** was subject to selective 5'-deprotection of the silyl group after treatment with a 1:1:4 mixture of trifluoroacetic acid (TFA) in water and THF,³⁰⁰ yielding 98% of desired product **51**.

Coupling of the intermediate **51** with phenyl L-alanine benzyl ester phosphorochloridate by means of NMI in THF yielded 62% of 2'-TBDMS protected ProTide **52**. However, efforts to separate by silica gel TLC using different binary and ternary eluent systems did not result in positive outcome.

A more hindered silyl protecting group was believed to allow a separation *via* the same method, therefore **30a** was treated with *tert*-butyldiphenylsilyl chloride (TBDPCI), imidazole and DMAP in DMF, to yield compound **53** in 76% yield.

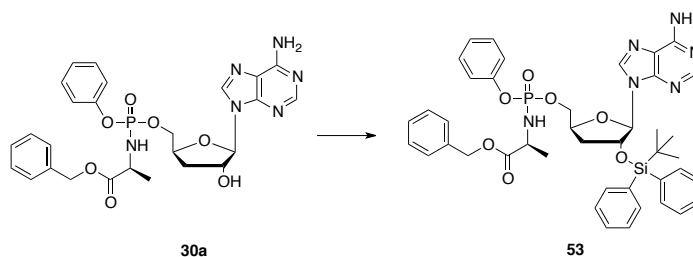


Figure 3.68 Synthesis of 2'-TBDPS protected ProTide **53**. Reagents and conditions: (a.) TBDPSCl (3 eq), DMAP (0.6 eq), imidazole (6 eq), DMF, rt, 16h, 76%.

Attempted methods to separate the two diastereoisomers of compound **53** on TLC yielded only modest differences in R_f between the two isomers. The outcome was not positive enough to promise good separation through flash chromatography.

The separation of **30a** isomers was therefore attempted *via* reverse phase chromatography.

3.3.1.3 Separation of ProTides **30a** and **49b** diastereoisomers via reverse phase chromatography

Only a few milligrams of each separated isomer were required for preliminary *in vitro* testing, therefore preparative HPLC was initially used as a separating tool. The optimal elution method was firstly investigated on analytical HPLC, and at the beginning a gradient of CH_3CN in water from a mixture of 40:60 to 70:30 in 30 minutes was used as eluent system (Figure 3.69, A), then a gradient of CH_3CN in water 30:70 to 70:30 (Figure 3.69, B) and finally a gradient of CH_3CN in water 10:90 to 90:10 (Figure 3.69, C).

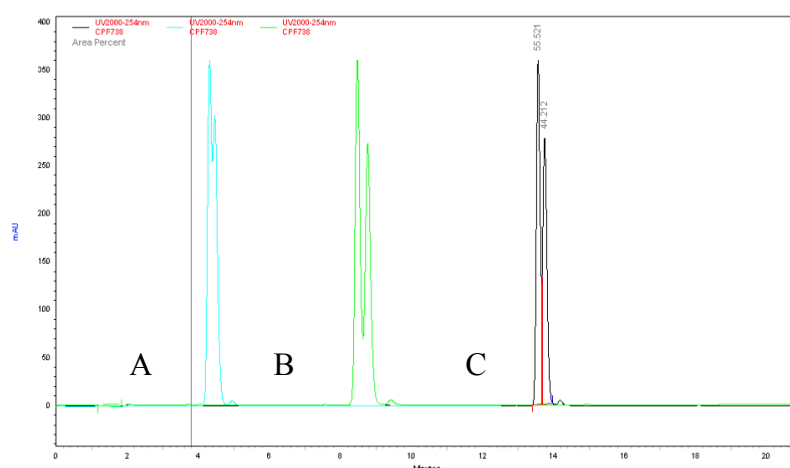


Figure 3.69: Overlaid HPLC traces of **30a** diastereomeric mixture in different solvent gradients. (Blue, **A**) HPLC conditions: 40 : 60 $\text{CH}_3\text{CN}:\text{H}_2\text{O}$ to 70 : 30 $\text{CH}_3\text{CN}:\text{H}_2\text{O}$ in 30 min. Flow = 1 mL min^{-1} ; $\lambda = 254 \text{ nm}$; (green, **B**) HPLC conditions: 30 : 70 $\text{CH}_3\text{CN}:\text{H}_2\text{O}$ to 70 : 30 $\text{CH}_3\text{CN}:\text{H}_2\text{O}$ in 25 min. Flow = 1 mL min^{-1} ; $\lambda = 254 \text{ nm}$; (black, **C**) HPLC conditions: 10 : 90 $\text{CH}_3\text{CN}:\text{H}_2\text{O}$ to 90 : 10 $\text{CH}_3\text{CN}:\text{H}_2\text{O}$ in 25 min. Flow = 1 mL min^{-1} ; $\lambda = 254 \text{ nm}$.

The second eluent system method was believed to be the most suitable for the separation of **30a** diastereoisomers *via* preparative HPLC. The separation of 15 milligrams of mixture was carried out, and two fractions of partially separated fast eluting (FE) and slow eluting (SE) isomers were collected. The FE fraction contained a 93:7 mixture of FE:SE isomers (Figure 3.70, **A** and **B**), whereas the SE fraction contained a 22:77 mixture of FE:SE (Figure 3.70, **C**). Thus, the separation was evidently inefficient in yielding isomers characterised by a purity higher than 95%.

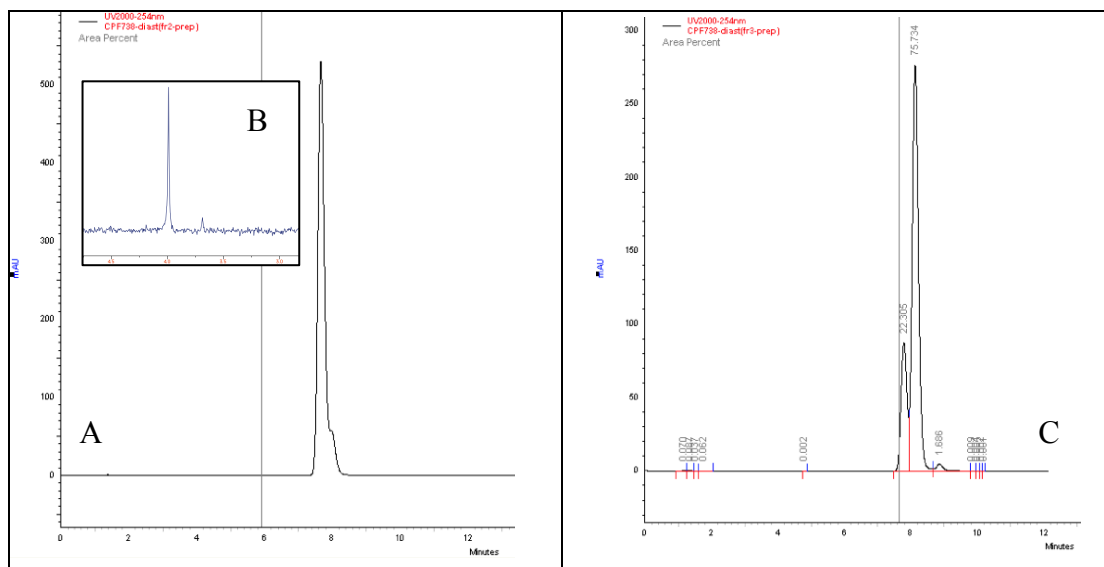


Figure 3.70 (**A**) HPLC trace of **30a** diastereomeric mixture enriched of FE isomer. HPLC conditions: 30:70 CH₃CN:H₂O to 70:30 CH₃CN:H₂O in 25 min. Flow = 1 mL min⁻¹; λ = 254 nm; (**B**) ³¹P NMR (CD₃OD, 202 MHz) of diastereomeric mixture depicted in (**A**), FE : SE = 93 : 7. (**C**) HPLC trace of **30a** diastereomeric mixture enriched of SE isomer (FE : SE = 22.3 : 75.7), HPLC conditions: 30 : 70 CH₃CN:H₂O to 70 : 30 CH₃CN:H₂O in 25 min.

Consequently, the replacement of CH₃CN with CH₃OH, which by analytical HPLC seemed to improve the separation via the same gradient method (CH₃OH in H₂O from 30:70 to 70:30 in 30 minutes, Figure 3.71), was attempted.

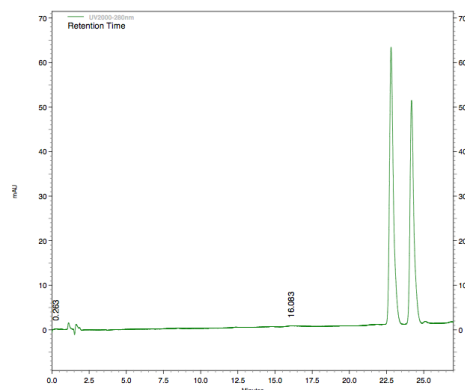


Figure 3.71: Analytical HPLC trace of **30a** diastereomeric mixture. HPLC conditions: 30 : 70 CH₃OH:H₂O to 70 : 30 CH₃OH:H₂O in 25 min. Flow = 1 mL min⁻¹; λ = 280 nm.

Separation via preparative HPLC of 25 mg of **30a** mixture yielded 8 mg of each isomer characterised by a purity higher than 98% (Figure 3.72). Some material was collected as a mixture.

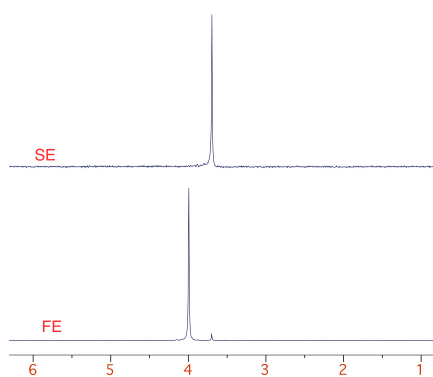


Figure 3.72: ³¹P NMR spectra (CD₃OD, 202 MHz) of fast eluting (FE) and slow eluting (SE) isomers of ProTide **30a**.

With the aim of identifying a possible scalable process for isomer separation, the gradient reverse phase method was applied to Biotage Isolera One flash chromatography system. The same gradient system (CH₃OH in H₂O from 30:70 to 70:30 in 30 minutes) that was successful in yielding pure isomers *via* preparative HPLC was applied to the separation of 50 mg of mixture using a Snap C18 12 g cartridge. Unfortunately, no separation was achieved *via* this method, due to a solvent mixing issue in the build up of the gradient system.

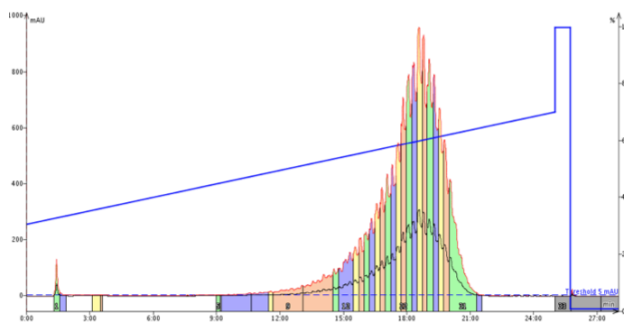


Figure 3.73: Biotage Isolera One chromatogram of the elution of **30a**. Run conditions: cartridge SNAP-Ultra 12g. flow: 12 mL/min. gradient eluent system: water methanol A/B 30% to 70% in 25 min. 50 mg sample. $\lambda = 280$ nm (black). 254 nm (red).

Consequently, an isocratic eluent system that could allow separation was thought to provide a solution to this issue, avoiding automatic mixing of the solvent by the instrument. In addition, cartridges characterised by smaller particle size were used.

SNAP ultra C18 cartridges (with particle size of 25 μm of spheric silica) were therefore used in place of SNAP C18 (with particle size of 50 μm of irregular silica).

Analytical HPLC was initially used to identify a suitable isocratic method. Different isocratic eluent mixtures of CH_3OH in water (60:40, 55:45, and 40:60) were attempted (Figure 3.74).

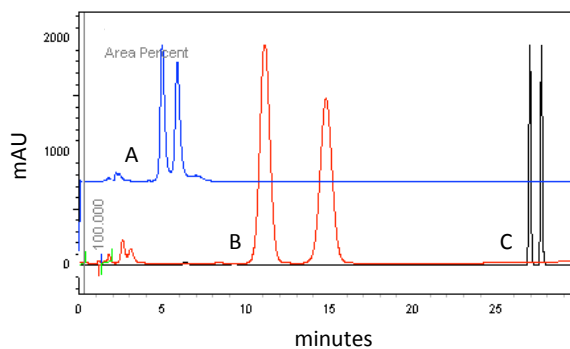


Figure 3.74: analytical HPLC trace of **30a** diastereomeric mixture. HPLC isocratic conditions: (A) 60:40 $\text{CH}_3\text{OH}:\text{H}_2\text{O}$ in 30 min. (B) 55:45 $\text{CH}_3\text{OH}:\text{H}_2\text{O}$ in 30 min. (C) 40:60 $\text{CH}_3\text{OH}:\text{H}_2\text{O}$ in 30 min. Flow = 1 mL min^{-1} ; $\lambda = 254$ nm.

The best separation was afforded by isocratic elution with 55% of CH_3OH in water (Figure 3.75, B), which was applied to the separation of the **30a** mixture via Biotage Isolera One through a SNAP Ultra 12 g cartridge. Due to the higher loading capacity of this improved cartridge (24% w/w), separation up to 150 mg of mixture with high efficiency was possible.

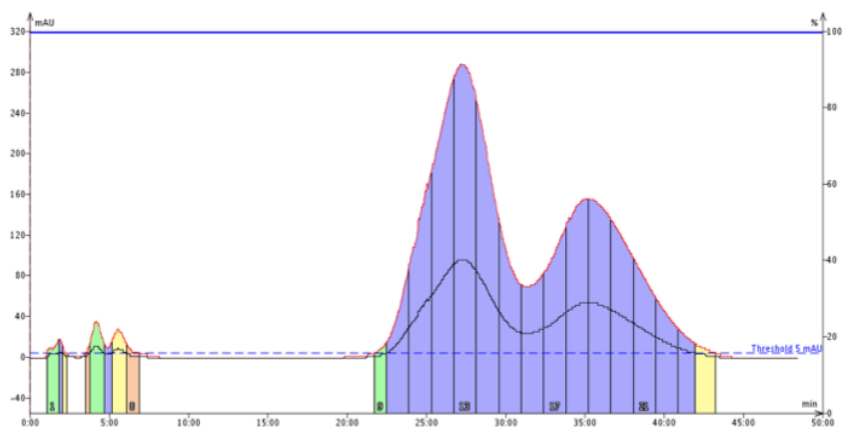


Figure 3.75 Biotage Isolera One chromatogram of the elution of **30a**. Run conditions: cartridge SNAP-Ultra 12g. Flow: 12 ml/min, isocratic eluent system: CH₃OH / H₂O 55/45, 100 mg sample. $\lambda = 280$ nm (black), 254 nm (red).

An amount of 76 mg of the FE isomer was collected with purity higher than 98%, along with 61 mg of SE isomer with similar purity.

With this methodology in hand to separate Protide **30a** isomers, separation of ProTide **49b** diastereoisomeric mixture via reverse phase preparative HPLC method was carried out, in order to have few mg of each isomer for *in vitro* cytotoxicity screening.

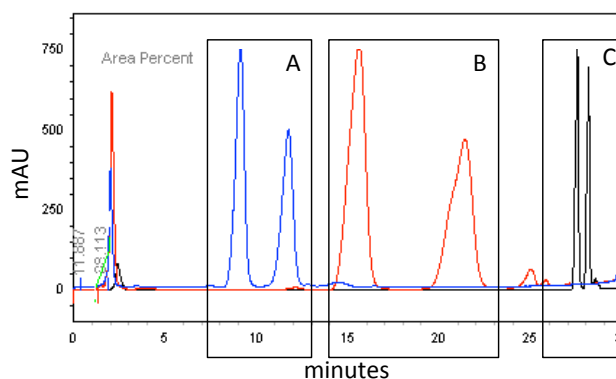


Figure 3.76: Analytical HPLC trace of **49b** diastereomeric mixture. HPLC isocratic conditions: (A) 60:40 CH₃OH:H₂O in 30 min. (B) 55:45 CH₃OH:H₂O in 30 min. (C) 40:60 CH₃OH:H₂O in 30 min. Flow = 1 mL min⁻¹; $\lambda = 254$ nm.

The different eluent system mixtures used for the separation of **30a** mixture were evaluated, and the isocratic elution with 55% of CH₃OH in water was selected (Figure 3.76, B). This method gave the best isomer separation, and allowed purification of 10 mg of mixture yielding pure fast eluting and slow eluting **49b** separated isomers.

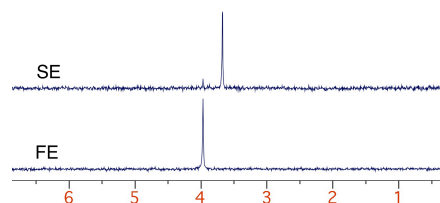


Figure 3.77: ^{31}P NMR spectra (CD_3OD , 202 MHz) of fast eluting (FE) and slow eluting (SE) isomers of ProTide **49b**.

Attempts to form crystals of each isomer are ongoing, with the aim of identifying the stereochemistry at the phosphorus center.

3.3.2 *In vitro* testing of separated isomers

The evaluation of parent nucleosides 3'dA and 2F3'dA, along with the mixtures of ProTides **30a** and **49b** and the separated fast eluting (FE) and slow eluting (SE) isomers was carried out on hematologic and solid tumour cell lines, already selected for previous *in vitro* screening of 3'dA and 2F3'dA ProTides (Table 3.30, Table 3.31, Table 3.32) by WuXi AppTech.

Cpnd	CCRF-CEM		MOLT-4		K562		HEL92.1.7		KG-1		MV4-11		HL-60	
	IC ₅₀	MI%	IC ₅₀	MI%	IC ₅₀	MI%	IC ₅₀	MI%	IC ₅₀	MI%	IC ₅₀	MI%	IC ₅₀	MI%
3'dA	>198	35	124.0	57	47.0	98	54.0	83	67.0	70	>198	32	82.0	74
30a(FE)	1.86	97	0.57	98	3.70	99	13.0	101	21.0	92	1.43	99	8.7	100
30a(SE)	2.04	97	0.43	98	2.60	95	11.0	98	14.0	90	0.98	100	11.0	92
30a(mix)	1.90	97	0.48	98	3.0	96	11.0	100	18.0	90	1.03	100	9.10	100
2F3'dA	14.0	99	12.0	102	13.0	98	9.69	97	6.50	93	2.79	100	8.80	98
49b(FE)	0.93	98	0.74	97	2.20	99	5.63	102	4.20	93	0.62	100	3.70	98
49b(SE)	1.06	98	0.82	97	2.50	99	5.98	99	6.20	92	0.69	100	3.70	98
49b(mix)	1.77	99	1.19	95	8.10	97	18.0	104	6.60	92	1.60	100	14.0	103
PTX	0.004	93	0.002	94	0.004	80	0.065	72	0.08	89	0.03	98	0.003	93

Table 3.30 *In vitro* cytotoxicity screening of 3'dA, 2F3'dA and diastereoisomeric mixture and separated diastereoisomers of **30a** and **49b**. Cytotoxicity data reported as μM IC₅₀ values (concentration of drug causing 50% of cell viability inhibition) and MI% (maximum inhibitory effect of the drug at the range of concentration considered). PTX: paclitaxel (control). Assays performed by WuXi AppTech.

Cpnd	Thp-1		RL		Jurkat		Hs-445		RPMI-8226		NCI-H929	
	IC ₅₀	MI%	IC ₅₀	MI%	IC ₅₀	MI%	IC ₅₀	MI%	IC ₅₀	MI%	IC ₅₀	MI%
3'dA	>198	1	>198	14.2	>198	19	>198	<50	>198	0.6	>198	-0.2
32a(FE)	35.0	91	4.0	96.8	2.82	97	42.0	99	25.0	90.8	19.0	97
32a(SE)	66.0	69	2.64	92.6	2.29	90	67.0	75	19.0	86.8	16.0	94
32a(mix)	38.0	89	3.21	95.7	3.37	94	41.0	93	21.0	89.8	14.0	98
2F3'dA	71.0	88	30.0	96.7	62.0	96	25.0	102	35.0	97.4	18.0	99
51b(FE)	8.48	102	3.11	98.3	4.21	93	30.0	106	11.0	94.7	5.63	100
51b(SE)	8.01	101	4.04	96.1	4.57	93	25.0	103	11.0	95.6	6.19	100
51b(mix)	29.0	96	4.33	96.3	11.0	91	74.0	88	31.0	93.5	12.0	99
PTX	0.02	30	0.005	64.9	0.003	82	0.05	84	0.003	95.6	0.03	95

Table 3.31 *In vitro* cytotoxicity screening of 3'dA, 2F3'dA and diastereoisomeric mixture and separated diastereoisomers of **30a** and **49b**. Cytotoxicity data reported as μM IC₅₀ values (concentration of drug causing 50% of cell viability inhibition) and MI% (maximum inhibitory effect of the drug at the range of concentration considered). PTX: paclitaxel (control). Assays performed by WuXi AppTech.

Cpnd	MIA PaCa-2		BxPC-3-Luc		HT29		SW620		HepG2		MCF-7		Cal 27	
	IC ₅₀	MI%	IC ₅₀	MI%	IC ₅₀	MI%	IC ₅₀	MI%	IC ₅₀	MI%	IC ₅₀	MI%	IC ₅₀	MI%
3'dA	>198	16	>198	4	132.0	63	>198	22	>198	11	76	79	>198	20
32a(FE)	18.0	94	99.0	73	25.0	95	35.0	87	57.0	73	5.87	94	24.0	101
32a(SE)	14.0	96	74.0	71	16.0	97	29.0	82	32.0	78	2.94	97	32.0	82
32a(mix)	15.0	97	73.0	76	18.0	97	29.0	91	47.0	86	3.59	96	25.0	108
2F3'dA	45.0	100	63.0	70	74.0	74	25.0	95	44.0	85	61.0	92	34.0	99
51b(FE)	6.35	98	52.0	78	25.0	86	17.0	97	17.0	71	4.06	91	12.0	95
51b(SE)	8.78	94	66.0	73	31.0	86	18.0	98	18.0	66	6.27	90	12.0	93
51b(mix)	18.0	92	114.0	63	56.0	87	41.0	89	28.0	70	4.90	92	26.0	95
PTX	0.004	85	>0.5	51	0.004	79	0.014	84	0.1	51	0.004	80	0.003	92

Table 3.32 *In vitro* cytotoxicity screening of 3'dA, 2F3'dA and diastereoisomeric mixture and separated diastereoisomers of **30a** and **49b**. Cytotoxicity data reported as μM IC₅₀ values (concentration of drug causing 50% of cell viability inhibition) and MI% (maximum inhibitory effect of the drug at the range of concentration considered). PTX: paclitaxel (control). Assays performed by WuXi AppTech.

The data obtained are consistent with the previous results on the same cell lines and there was no significant difference between the activity of ProTide **30a** mixture and separated isomers, the same was observed for ProTide **49b** mixture and separated isomers.

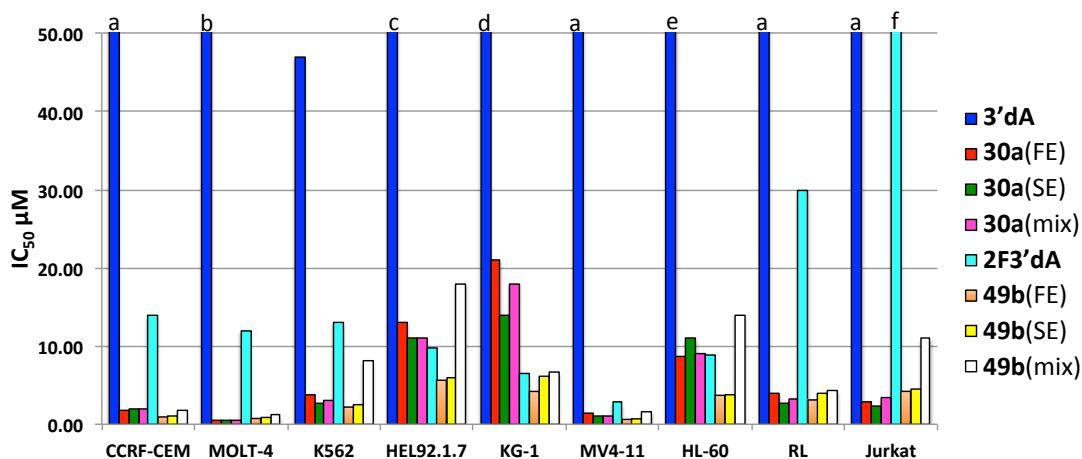


Figure 3.78 Activity of 3'dA, 2F3'dA and diastereoisomeric mixture and separated diastereoisomers of derivatives **30a** and **49b** on tumour cell lines. ^aIC₅₀ >198 μM; ^bIC₅₀ = 124 μM; ^cIC₅₀ = 54 μM. ^dIC₅₀ = 67 μM. ^eIC₅₀ = 82 μM. ^fIC₅₀ = 62 μM.

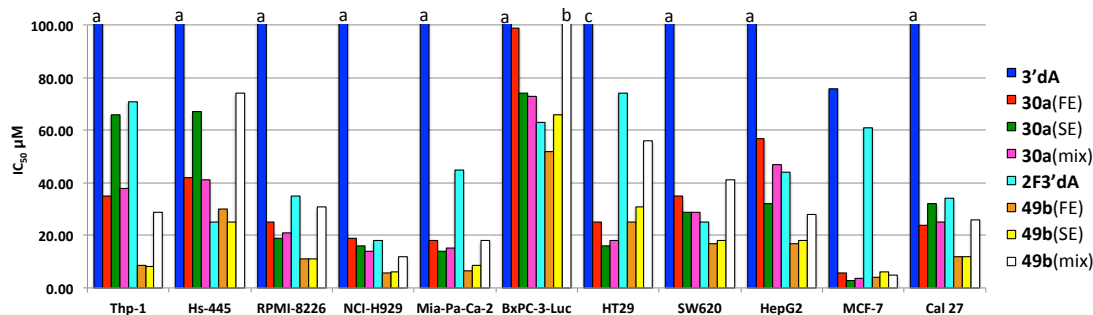


Figure 3.79: Activity of 3'dA, 2F3'dA and diastereoisomeric mixture and separated diastereoisomers of derivatives **30a** and **49b** on tumour cell lines. ^aIC₅₀ >198 μM; ^bIC₅₀ = 114 μM; ^cIC₅₀ = 132 μM.

Considering the promising *in vitro* cytotoxicity data relative to **30a** and **49b**, and the lack of noticeable difference between the activities of each isomer of both ProTides, *in vivo* evaluation of the activity of both diastereoisomeric mixtures of ProTides along with 3'dA were performed by WuXi AppTech on a mouse model of non-Hodgkin B lymphoma.

3.3.3 *In vivo* evaluation of ProTides **30a** and **49b** in a lymphoma mouse xenograft

Considering that 3'dA has already been the object of study in different *in vivo* anticancer evaluation plans, it was of interest to test the activity of both 3'dA and the most promising ProTide **30a** in a mouse tumour model. In this evaluation ProTide **49b** from the family of 2F3'dA derivatives was also included as it was endowed with intriguing *in vitro* anticancer activity (Figure 3.80).

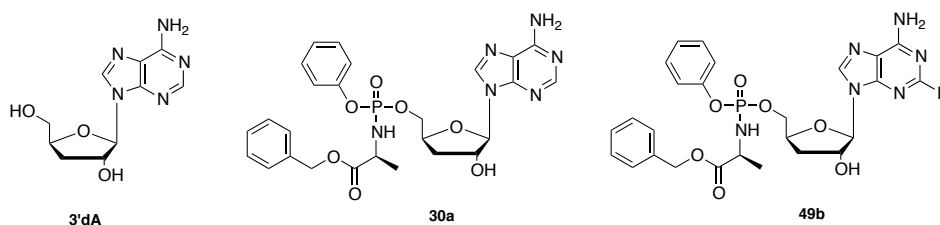


Figure 3.80: Structures of compounds assayed *in vivo* on mouse xenograft by WuXi AppTech.

The *in vivo* studies were performed on female nude mice (Balb/c). An initial tolerability study with ProTide **30a** (45 mg/kg) was carried out on 4 mice not inoculated with the tumour and resulted in no change in mobility and alimentary consumption. These positive results allowed the continuation of the study.

Therefore mice were inoculated subcutaneously with human RL (non-Hodgkin's B-lymphoma) cells. At two weeks from the cell inoculation, the enlarged tumour lump was weighed and afterwards the treatment was started. Three groups of 10 mice each were treated separately with equimolar amounts of drug (respectively 20 mg/kg of 3'dA, 45 mg/kg of ProTide **30a** or 47 mg/kg of ProTide **49b**) dissolved in a mixture of 20% dimethylacetamide (DMA), 15% Solutol and 65% water. One group was administered vehicle (20% DMA + 15% Solutol +65% water, control group). Treatments were administered *via* intraperitoneal injection per 5 days a week, over 14 days. The body weight was also recorded to assess the animal's tolerance to the compound.

A treatment-free period of 7 days at the end of the two-weeks of treatment was further carried out and 2 tumour assessments were performed during this period.

Notably, when examining **30a**, **49b** and 3'dA anticancer activities, both 3'dA and ProTide **30a** did not alter the tumour growth compared to mice injected with vehicle (Figure 3.81). On the other hand, mice treated with ProTide **49b** showed a decrease in tumour growth compared to control (vehicle). This effect was visible after day 10 from starting of the treatment and continued after the dosing was stopped (days 14-21).

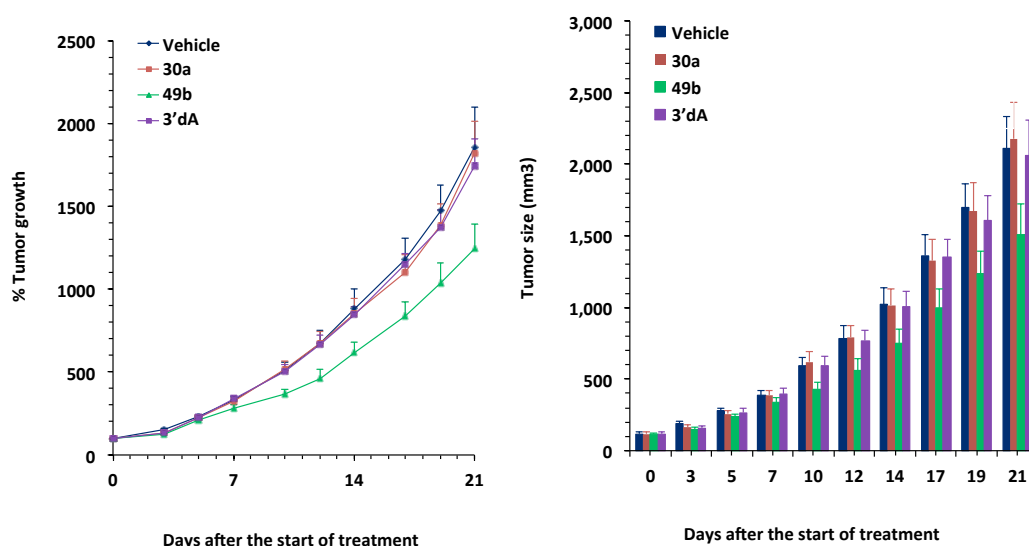


Figure 3.81: Antitumour effect of 3'dA, **30a** and **49b** against RL lymphoma tumours in nude mice, compared to administration of vehicle. **30a** (45 mpk, I.P., 5x/week *2 weeks), **49b** (47 mpk, I.P., 5x/week *2 weeks) and 3'dA (20 mpk, I.P., 5x/week *2 weeks). (A) Percentage of tumour growth. (B) Variation of tumour size (mm³). Assays performed by WuXi AppTech.

Over the course of the study, the observed change in body weight for the mice treated with 3'dA, **30a** and **49b** was stable and similar to mice treated with vehicle (Figure 3.82), and this was consistent after the treatment was stopped (days 14-21).

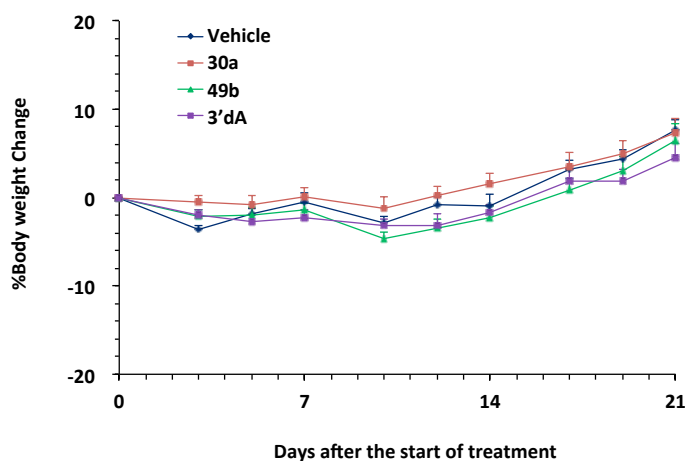


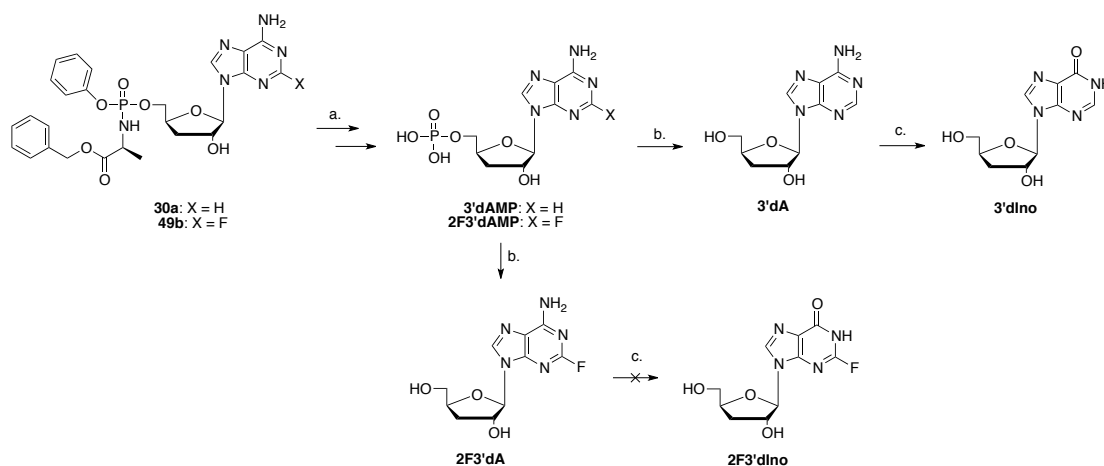
Figure 3.82: Mean body weight change (%) of RL bearing nude mice following administration of vehicle, **30a** (45 mpk), **49b** (47 mpk) and 3'dA (20 mpk). Assays performed by WuXi AppTech.

The lack of effect of 3'dA on the growth of RL tumour could be due to an ineffective targeting of the mass after intraperitoneal injection, possibly due to quick inactivation of the nucleoside analogue by ADA. The *in vitro* activity of 3'dA on RL tumour cell lines was similarly poor, suggesting that the lack of activity of the drug may also derive from intrinsic resistance mechanisms within the cell, such as ADA catabolism, lack of

phosphorylation or inefficient cell entering via nucleoside transporters. On the other hand, ProTide **30a** is immune to ADA mediated catabolism and should enhance the activity of the parent nucleoside at the intracellular level, as suggested by the more favourable activity profile. However, the complete lack in *in vivo* activity of such derivative could derive from the already reported instability of ProTides in rodent models, described as a limitation for the anticancer and anti-HCV activity of these prodrugs.^{151,268} In fact, the lack in potency exhibited by 3'dA ProTide **30a** could be the consequence of a quick breakdown in mouse plasma, with putative release of the parent nucleoside 3'dA, which could be in turn inactivated by ADA, hence the similar negative results for **30a** as for the parent nucleoside (Scheme 3.20).

On the other hand, the positive results shown by treatment of mice with 2F3'dA derived ProTide **49b** could either indicate an increased stability to esterase-mediated inactivation of this ProTide moiety due to the presence of a fluorine on the nucleobase, or more likely be due to the fact that even after breakdown of the ProTide moiety, 2F3'dA released could retain anticancer activity due to its stability towards ADA-mediated catabolism (Scheme 3.20).

Nevertheless, ProTides were reported to be more stable in other species, including humans, and this might translate into superior clinical efficacy of both ProTide analogues **30a** and **49b**.



Scheme 3.20: Putative *in vivo* metabolism of ProTides **30a** and **49b**: (a.) Conversion into 3'dAMP and 2F3'dAMP catalysed by the joint activity of carboxypeptidase and phosphoramidase enzymes; (b.) release of 3'dA and 2F3'dA due to activity of 5'-nucleotidase enzymes; (c.) conversion of 3'dA into 3'dIno catalysed by ADA.

3.3.4 Stability NMR assays

In order to investigate whether the stability of ProTides in rodent plasma could be responsible of the negative outcome of the mouse xenograft, the stability of ProTides **30a** and **49b** was compared in rodent serum and human serum.

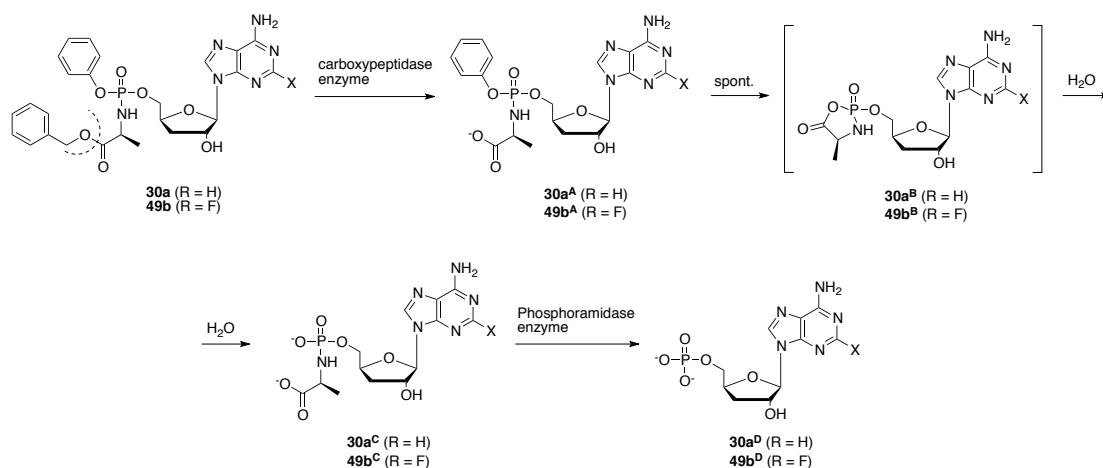


Figure 3.83: Putative metabolic processing of ProTides **30a** and **49b** in (rodent) serum.

Incubation of ProTide **30a** in rat plasma caused partial processing of the ProTide moiety with release of L-alanyl phosphate monoester intermediate **30a^C** and to a compound which could potentially be identified as nucleotide intermediate **30a^D**, as suggested by ES/MS analysis of the crude mixture and by previous literature report.

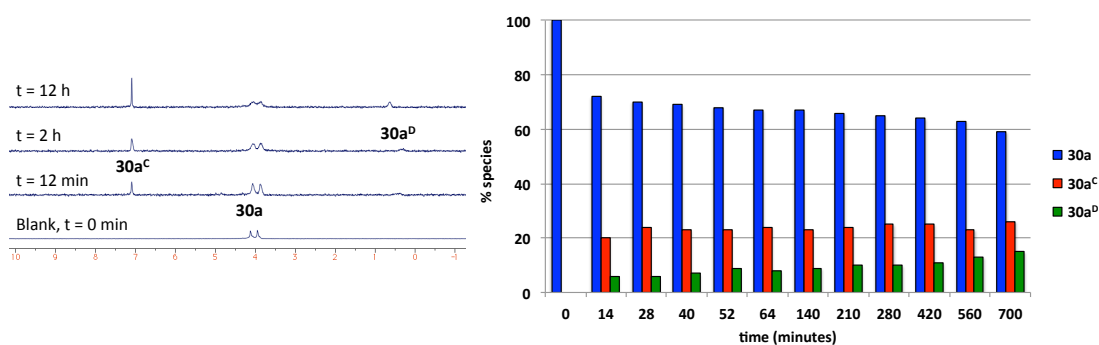


Figure 3.84 (A) Stacked ^{31}P NMR spectra (acetone- d_6 , 202 MHz) monitoring the stability of ProTide **30a** in rat serum. (B) Percentage of **30a** metabolites over time in rat serum (% determined from ^{31}P NMR integrals).

The presence of untouched compound **30a** is still prevalent after 12 h of incubation (Figure 3.84). On the other hand, treatment of ProTide **49b** in the same conditions led to complete conversion of the original structure into intermediate **49b^C** within 2 hours, paralleled by the formation of what potentially could be recognised as nucleotide **49b^D** (Figure 3.85).

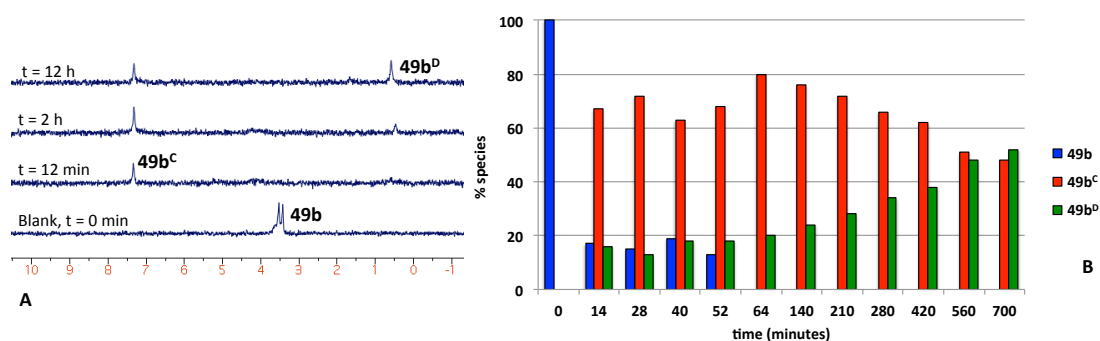


Figure 3.85 (A) Stacked ^{31}P NMR spectra (acetone- d_6 , 202 MHz) monitoring the stability of ProTide **49b** in rat serum. (B) Percentage of **49b** metabolites over time in rat serum (% determined from ^{31}P NMR integrals).

A very different picture could be noticed after incubation of both ProTides in human serum, with no detectable processing of both drugs after 12 h. The very different stability of **30a** in human and rat serum potentially gives an explanation for the lack of activity of ProTide **30a**, which could be processed partially or entirely in mouse plasma. This could lead to release of the parent nucleoside 3'dA, which could lose activity after ADA-catalysed deamination.

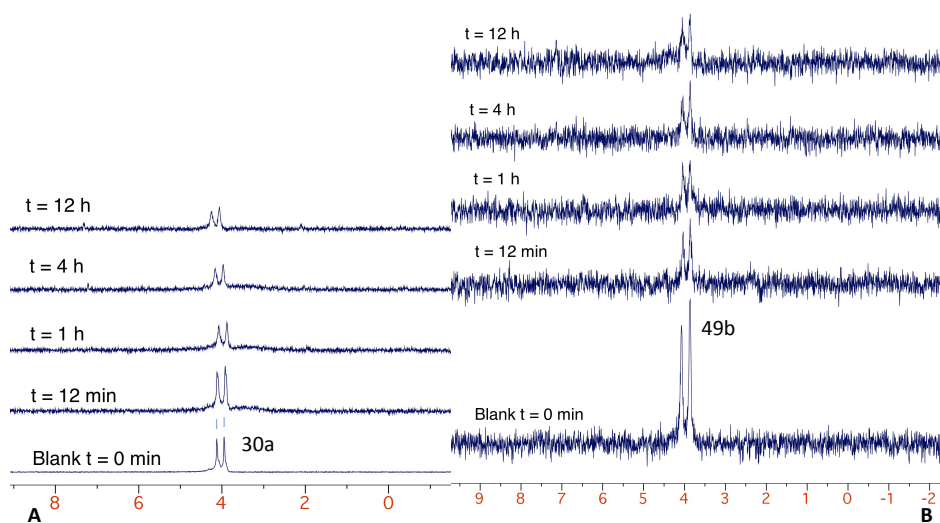


Figure 3.86: A. Stacked ^{31}P NMR spectra (acetone- d_6 , 202 MHz) monitoring the stability of ProTide **30a** in human serum. B. Stacked ^{31}P NMR spectra (acetone- d_6 , 202 MHz) monitoring the stability of ProTide **49b** in human serum.

On the other hand, the very quick metabolism of **49b** would not be associated with complete lack of activity, due to the stability of 2F3'dA to deamination, and this could explain the anticancer activity exerted by ProTide **49b**. The stability of both drugs in human serum suggests these drugs may have a different activity profile when tested in other species.

3.3.5 Conclusions

From anticancer evaluation of 3'dA derivatives, ProTide **30a** emerged as the one with the most intriguing activity, along with the 2-fluoro counterpart, ProTide **49b**, both deserving further preclinical investigations. Existing as mixtures of two diastereoisomers each, separation of the different isomers of **30a** and **49b** was performed, with the aim of testing the cytotoxic activity of each isomer separately. This was performed in order to understand whether any additional preclinical investigation would be performed on a single more active isomer of each drug or on the mixture. Reverse phase chromatography was successfully applied for the separation of the isomers, and anticancer evaluation showed no significant difference in activity of each isomer and the mixtures. Hence the diastereomeric mixtures of ProTides **30a** and **49b** were evaluated for efficacy and toxicity in a *in vivo* mouse model of non-Hodgkin's B lymphoma, along with the parent nucleoside 3'dA. ProTide **49b** succeeded in reducing the tumour growth over 14 days of treatment and up to 21 days of tumour observation. On the other hand, both ProTide **30a** and parent nucleoside failed to show any anticancer activity in this evaluation. NMR stability assays in rat and human serum suggested that the lack of activity of **30a** could derive from a quick catabolism in rodent plasma, with release of 3'dA, that could potentially be inactivated by ADA, leading to loss of anticancer potential. However, the noticed instability of ProTide **49b** in rat serum was not paralleled by a lack in activity in the *in vivo* mouse model. This was envisaged to be due to the potential release of 2F3'dA, an analogue of 3'dA endowed with improved stability towards ADA-mediated catabolism. Both ProTides **30a** and **49b** were moreover found to be stable in human serum up to 12 hours of incubation, promising a better anticancer outcome for the administration of both compounds in different tumour models.

3.4 5'-Modified 3'dA prodrugs

3.4.1 Introduction on rationale for 5'-modification

Introduction of a moiety in the 2-position on the adenine base led to an expected increased stability to ADA-mediated inactivation, and provided improved *in vitro* and *in vivo* anticancer activity (when using fluorine as a substituent). The exploration of alternative modifications in the structure of 3'dA ProTides was believed to offer an additional biological advantage, such as the alteration of position 5' on the sugar moiety. This moiety has already attracted attention, as groups in this position have been introduced to increase the metabolic stability *in vivo*, improving the pharmacokinetic drug profile when applied to anticancer and antiviral analogues.³⁰¹⁻³⁰⁴ Moreover, the 5'-modification on the nucleoside level was reported to increase the stability of the phosphodiester linkage once the nucleotide was incorporated into the DNA, reducing the recognition by nuclease enzyme.³⁰⁵ Introduction of a group in position 5' on the sugar moiety may improve stability of nucleoside analogues by reducing the recognition of substrates by intracellular and extracellular phosphatase enzymes, also known as 5'-nucleotidase enzymes (5'NT), which antagonise the activity of nucleoside kinase enzymes by catalysing the cleavage of the monophosphate group on nucleotides with release of the nucleoside structure. In this way they determine the sizes and turnover rates of the deoxyribonucleotide pools.^{30,306,307} These enzymes have been described as one of the resistance mechanisms to the activity of anticancer and antiviral nucleoside analogues.^{30,308-311}

One alternative method to improve the stability of nucleotide analogues is the replacement of the natural and labile phosphoester (phosphorus-oxygen) bond (5'-P-O-C) of the monophosphate group with a chemically and enzymatically stable phosphonate bond (5'-P-C-C).³¹² Phosphonates have been extensively explored especially as antiviral agents and on acyclic nucleoside analogues.^{53,65,313,314} Moreover, acyclic nucleoside phosphonates such as PMEAs have shown potent anticancer activity.³¹⁵⁻³¹⁷ To explore the potential benefits of a modification in position 5' on the sugar moiety of 3'dA that could improve stability of 3'dA ProTide structures, first the introduction of a 5'-alkyl moiety, and second the replacement of the phosphate with a phosphonate group were attempted (Figure 3.87).

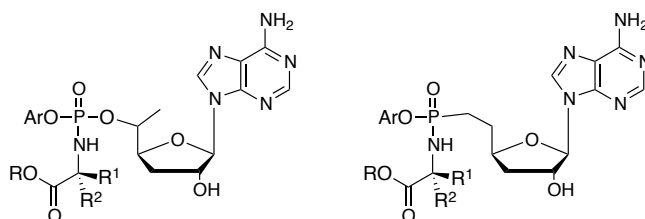


Figure 3.87 Plan of structural modifications on the scaffold of 3'dA ProTides. (A) Introduction of a 5'-alkyl moiety. (B) Replacement of the 5'-phosphate group with a phosphonate moiety.

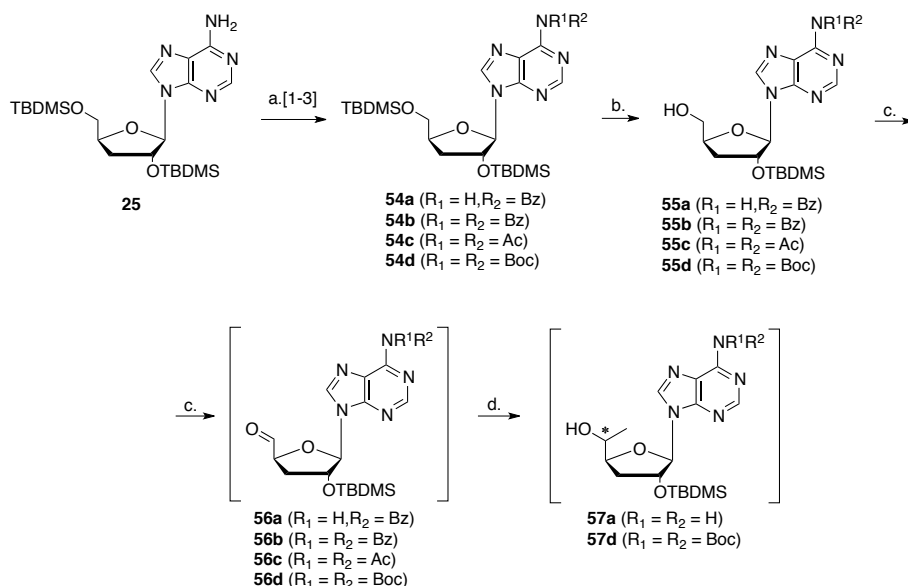
3.4.2 Synthesis of 5'-modified 3'dA ProTides

3.4.2.1 Attempts to introduce an alkyl group in the 5'-position.

Introduction of an alkyl moiety in position 5' of 3'dA, with the aim of synthesising 3'dA ProTides endowed with improved metabolic stability was attempted according to Scheme 3.21. The synthesis was reported to first go through oxidation of the 5' primary alcohol with subsequent alkylation *via* a Grignard reagent.

Alternatively, the modification is introduced first on the sugar moiety, which is only then coupled with the appropriate nucleobase.^{303,304,318-320}

With the nucleoside analogue 3'dA already available, the route reported in Scheme 3.21 was pursued.



Scheme 3.21: Synthesis of protected 5'-modified cordycepin. *Reagents and conditions*: (a.) [1] BzCl (3 eq), pyridine, 1.5 h, rt, **54a** (52%), **54b** (32%); [2] Ac₂O (6 eq), Et₃N (6 eq), DMAP (0.4 eq), CH₃CN, rt, 16h, **54c** (55%); [3] Boc₂O (4 eq), DMAP (0.4 eq), THF, rt, 16h, **54d** (100%); (b.) THF:H₂O:THF (1:1:4 v/v/v), 5h, 0 °C, **55a** (98%), **55b** (62%), **55c** (74%), **55d** (66%); (c.) Table 3.33; (d.) Table 3.34.

2',5'-TBDMS protected 3'dA (**25**), synthesised according to Scheme 3.19, was protected on the amino group of the adenine base with benzoyl group(s) by treatment with benzoyl chloride (BzCl) in pyridine, and conversion into both *N*-benzoyl (**54a**) and bis *N*-benzoyl (**54b**) derivatives, respectively in 52% and 32% yields. Derivative **54a** was subject to selective 5'-deprotection of the silyl group after treatment with a 1:1:4 mixture of trifluoroacetic acid (TFA) in water and THF,³⁰⁰ yielding 98% of desired product **55a**.

Entry	Scheme 3.21 (step c.)						
	Substrate	<i>N</i> -protecting group	Oxidising agent	Solvent	T	Time	Result
1	55a	NHBz	DMP (1.5 eq)	CH ₂ Cl ₂	0 °C	1 h	Traces ^a
2	55b	NBz ₂	DMP (2 eq)	CH ₂ Cl ₂	0 °C	2 h	- ^b
3	55c	NAc ₂	IBX (1 eq)	CH ₃ CN	80 °C	1.5 h	- ^b
4	55d	NBoc ₂	IBX (1 eq)	CH ₃ CN	80 °C	1.5 h	- ^a

Table 3.33 Substrates involved, reagents, conditions and results of Scheme 3.21 (step c.).^aCrude used directly for step d. Scheme 3.21. ^bMixture of species.

The first attempt of oxidation of the 5'-hydroxyl group was performed by treatment of intermediate **55a** with 1.5 equivalents of 1,1,1-triacetoxy-1,1-dihydro-1,2-benziodoxol-3(1*H*)-one (Dess-Martin periodinane, DMP) at 0 °C for 1 hour (Scheme 3.21, Table 3.33, entry 1).²⁰⁸ The mixture was then subject to the next step without purification, and the crude **56a** was treated with methyl magnesium bromide (MeMgBr, 1M solution) in THF at -20 °C. After 6 hours, TLC analysis of the reaction showed a mixture of spots. Chromatography separation of the components yielded one fraction containing traces of product lacking the benzoyl group on the amino function (**57a**), which was detected by ES/MS (calculated mass: $m/z = 483.23$ [M], found: $m/z = 506.2$ [M + Na⁺], 989.5 [2M + Na⁺]). However the yield was too low and the reaction needed to be optimised.

These side products were believed to derive from side reaction caused by partially protected amino group,²⁹⁹ therefore the fully benzoyl protected intermediate **54b** was used for the following attempt. Compound **54b** was selectively deprotected in position 5', affording **55b** in 62% yield. Oxidation was tried on product **55b** with 2 equivalents of DMP in CH₂Cl₂ for 2 hours at -20 °C (Table 3.33, entry 2).

Entry	Substrate	<i>N</i> -protecting group	Scheme 3.21 (step c.)				
			MeMgBr ^a	Solvent	T	Time	Result
1	56a (crude)	NHBz	1.5eq	CH ₂ Cl ₂	-20 °C	1 h	Traces ^b
2	56d (crude)	NBoc ₂	1.5eq	CH ₂ Cl ₂	-78 °C	1h	- ^c

Table 3.34 Substrates involved, reagents, conditions and results of Scheme 3.21 (step c.). ^aSol. 1M in THF. ^bDetected by ES/MS. ^cComplex mixture of products.

TLC analysis of the mixture at this step, revealed the presence a mixture of inseparable products, therefore the oxidation step was thought to limit the outcome of the reaction.

Modification of the protecting group on the amino moiety was attempted in order to stabilise the structure of the starting material, and improve the outcome of the reaction. Hence, acetyl moieties were introduced on the amino group. Fully silylated 3'dA (**25**) was therefore treated with acetic anhydride, DMAP and triethylamine in CH₃CN, yielding 55% of *bis-N*-acetyl derivative **54c** (Scheme 3.21). This intermediate was selectively deprotected in the 5' position, yielding compound **55c** in 74% yield.

For the following step, the oxidising conditions were changed by using 2-iodoxybenzoic acid (IBX) in place of DMP, which was reported to yield better outcomes in this step.²⁹⁹ Therefore **55c** was treated with IBX in CH₃CN at 80 °C for 1.5 hours. Unfortunately, after work up the crude was again a mixture of spots (Table 3.33. entry 3).

For the last attempt, the procedure reported by Schinazi *et al.* was followed, to yield 5'-oxidised derivatives.²⁹⁹ Hence, fully silylated 3'dA (**25**) was protected with di-*tert*-butyl dicarbonate (Boc₂O) and DMAP in THF for 16 hours (Scheme 3.21).³²¹ Product **54d** was then selectively deprotected on the 5' position yielding 66% of intermediate **55d** (Scheme 3.21. step c.). Oxidation of the free hydroxyl was attempted again by treatment with IBX (1.2 eq) at 80 °C for 1.5 hours. The mixture was then cooled down to 0 °C, insoluble IBX was filtered off and the solvent evaporated. This procedure does not involve isolation of the intermediate aldehyde, therefore the crude was directly dissolved in THF, cooled down to -78 °C and 1.5 equivalents of MeMgBr were added (Table 3.34. entry 2). After 1.5 hours stirring, the mixture appeared as a combination of spots on TLC. The mixture of spots potentially derived from degradation of the material, removal of protecting groups and possibly cleavage of the glycosidic bond.

Since the treatment with the Grignard reagents was not successful, the second route leading to modification in the 5' position involving introduction of a phosphonate bond was pursued.

3.4.2.2 *Synthesis of phosphonate bond containing analogue of ProTide 32a*

The synthesis of 5'-methylene nucleoside phosphonates prodrugs was already reported as a low yielding process, due to the requirement of different steps: (1) introduction of the phosphonate moiety (2) trimethylsilyl bromide driven cleavage of the phosphonate esters (3), purification of highly polar phosphonic acids, and (4) variable yields when coupling phosphonic acids with the prodrug portion (Scheme 3.22).²⁹⁹

The method used in this work involved the procedure reported by Schinazi *et al.* for the synthesis of bis-POM prodrugs of D-2'-deoxy-2'- α -fluoro-2'- β -C-methylphosphonate.²⁹⁹

However, for the introduction of the ProTide moiety, a methodology already established in the group for the synthesis of PMPA and PMEA ProTide and bis-diamidate prodrugs,²⁸⁹ was applied, adapted from already reported procedures by Holy *et al.*³²²

The synthesis of the 5'-phosphonate intermediate **61** involved the reaction of Wadsworth-Emmons (HWE) olefination by addition of dialkyl bisphosphonate salt **60** (Figure 3.88) on the 5'-aldehyde group in **58d** (Scheme 3.22).

Intermediate **58d** was treated with 2 equivalents of IBX for 1 hour at 80 °C in CH₃CN. Then, the crude was directly dissolved in THF and a mixture of tetraethyl methylene-bisphosphonate (**60**, Figure 3.88) and NaH in THF was added at 0 °C and then stirred for 12 hours at room temperature.

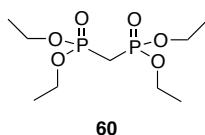
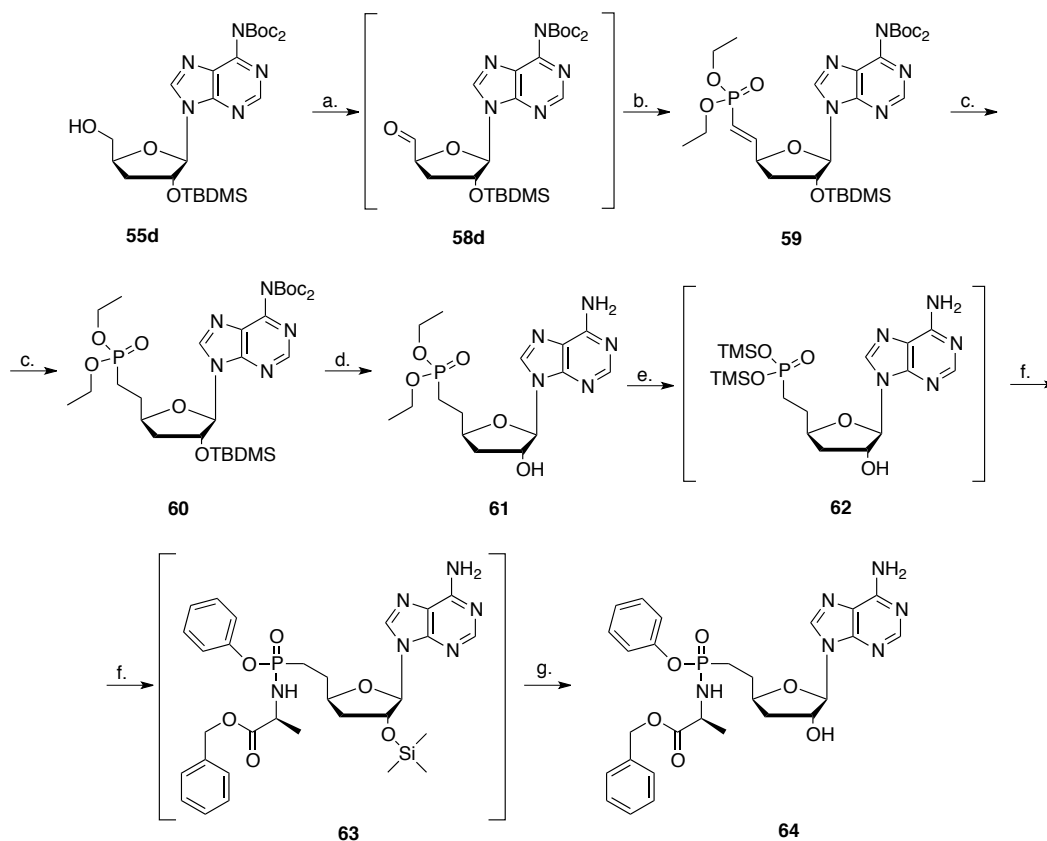


Figure 3.88 Structure of tetraethyl methylene-bisphosphonate (**60**).

The reaction yielded olefin **61** in 43% yield, and the recovered starting material was unreacted alcohol **55d**. The recovery of un-oxidised starting material suggested that the reaction could benefit from the use of either more equivalents of the oxidising agent (IBX) or by stirring for a longer period.



Scheme 3.22: Synthesis of 5'-phosphonate 3'dA analogue of ProTide **30a**. *Reagents and conditions*: (a.) IBX (2eq), CH₃CN, 80°C, 4h; (b.) **60** (1.6eq), NaH (2.5eq), THF, 0 °C to rt, 12h, 58% two steps; (c.) Pd/C (10%), H₂, EtOH/EtOAc (1:1), rt, 5h, 97%; (d.) HCOOH/H₂O (1/1), rt, 72h, 75%; (e.) TMSBr (3eq), 2,6-lutidine (3 eq), CH₃CN, 5h, 0 °C; (f.) L-AlaOBn pTSA (1eq), phenol (6 eq), aldrithiol-2 (6eq), Ph₃P (6eq), pyridine, TEA, 50 °C, 3h; (g.) HCl (0.5 N), 2% three steps.

However, the positive result confirmed that the oxidation process took place in these conditions, therefore the previous negative results for the 5'-alkylation of the nucleoside analogue potentially resulted from attempts to isolate the aldehyde intermediate, leading to degradation of the product.

In order to push the phosphonate synthesis to higher yields, the equivalents of IBX used were raised to 2 and the mixture was stirred at 80 °C for 4 hours with improvement in the yield to 58%.

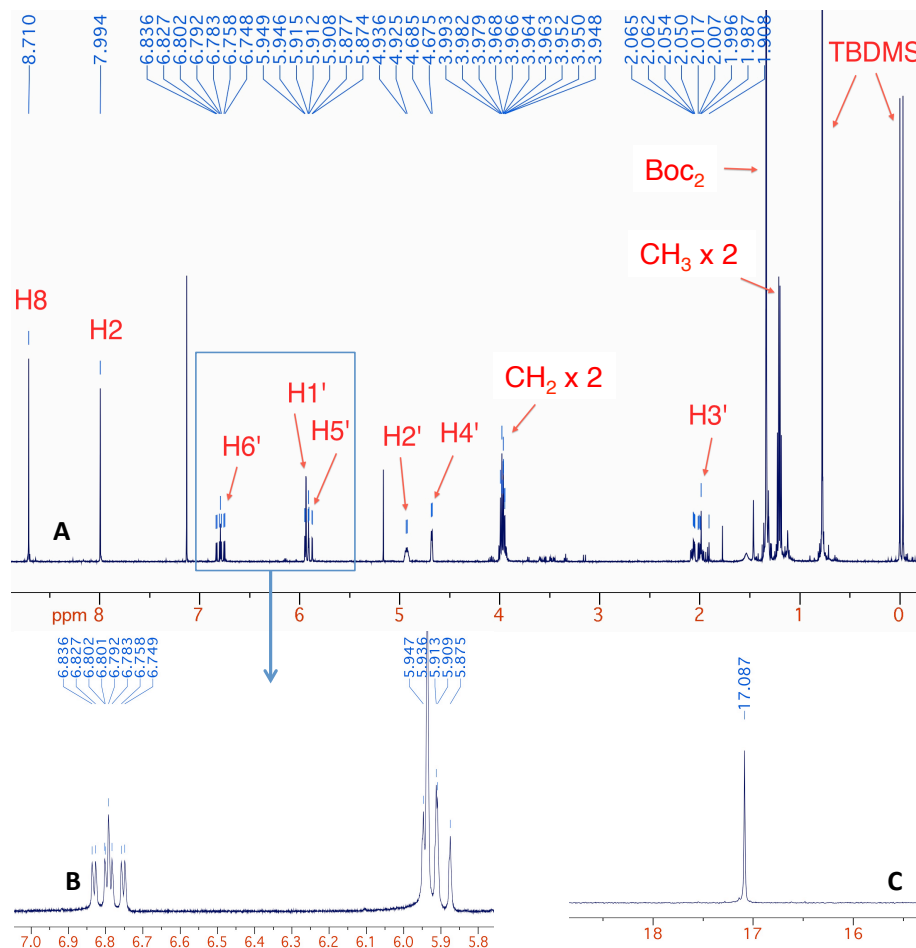


Figure 3.89 **A** ^1H NMR spectrum of intermediate **59** (500 MHz, CDCl_3). **B** H5', H1' and H6' signals of compound **59**. **C** ^{31}P NMR spectrum of compound **59** (CDCl_3 , 202 MHz).

The vinylidene phosphonate **59** was obtained as the *E*-isomer with no trace of the *Z*-isomer (Figure 3.89), as expected from a HWE reaction mechanism. The structure of compound **59** was confirmed by ^1H NMR analysis (Figure 3.89, **A**). Particularly informative is the presence of two signals corresponding to the two olefinic proton H5' and H6' integrating for one proton (H5' signals overlap with the H1' signal). The H6' signal resonates at 6.80 ppm and presents as a triplet of doublets with coupling with phosphorus defined by a $^1J_{\text{H-P}} = 22.1$ Hz, coupling with H5' with $^1J_{\text{H-H}} = 17.0$ Hz and coupling with H4' with $^2J_{\text{H-H}} = 4.6$ Hz (Figure 3.89, **B**). The presence of the phosphonate moiety is moreover confirmed by ^{31}P NMR analysis (Figure 3.89, **C**).

Intermediate **59** was then reduced by catalytic hydrogenation conditions by treatment with palladium activated on carbon (Pd/C 10%) in H_2 atmosphere in a solution 1:1 (v/v) of EtOAc and EtOH, yielding compound **60** in 97% yield (Scheme 3.22, step c.).

The deprotection of intermediate **60** was initially attempted in TFA, water and THF (1:1:4 v/v/v) at room temperature. However, only the TBDMS groups were cleaved with this

method, as confirmed by ES/MS. The mixture was therefore dissolved in CH₂Cl₂ and TFA was added (to yield a final mixture 2:3 TFA in CH₂Cl₂). This method proved to be too harsh for this substrate, leading to total glycosidic bond cleavage. The deprotection was finally achieved using a mixture of formic acid in water (2:3 v/v), yielding desired product **61** in 75% yield (Scheme 3.22), after 72 hours.

The first attempt for the synthesis of ProTide **64** involved treatment of deprotected intermediate **61** with TMSBr (5 equivalents) in CH₃CN at room temperature over 16 hours in order to obtain bis(trimethylsilyl) phosphonate ester **62**. The volatiles were then carefully removed to avoid contact with air. The crude ester, under an argon atmosphere, was dissolved in pyridine and triethylamine (TEA), then 1 equivalent of L-alanine benzyl ester *para*-toluene sulfonic salt (*p*TSA) and 6 equivalents of phenol were added, which were previously mixed in pyridine. In a separate flask aldrithiol-2 and triphenylphosphine (Ph₃P) were dissolved in pyridine and added to the initial mixture, which was stirred at 50 °C for 3 hours. The final mixture contained multiple products, which attempts to separate via column chromatography and analysis by NMR and ES/MS, did not identify.

Afterwards, 2,6-lutidine was used as a buffer against hydrobromic acid (HBr) that could develop after addition of TMSBr, leading to undesired side reactions such as glycosidic bond cleavage.³²³ Thus, the equivalents of TMSBr were reduced to 3.5 and an equimolar amount of 2,6-lutidine was added. The reaction was then treated with the same procedure as before (Scheme 3.22, step e.).

The product obtained was recognised as the 2'-trimethylsilyl derivative **63** by ES/MS analysis of the reaction mixture. The silyl ether bond was easily cleaved by stirring with a 0.5 N solution of HCl in water, and then extracted with EtOAc.

Tedious purification by column chromatography and reverse phase HPLC were further required, and yielded desired compound **64** in 2% yield.

Although very poor, the yield was not further optimised at this stage, but the synthesised compound was tested for anticancer activity, with the aim of improving the synthetic procedures and preparing an enlarged family of prodrugs at a later stage.

3.4.3 Biological evaluation

Compound **64** was evaluated for anticancer activity on a broad selection of cell lines, previously used for the evaluation of 3'dA prodrugs by WuXi AppTech.

A comparison between the activity of phosphonate **64** and the phosphate counterpart ProTide **30a**, along with the activity of 3'dA is given in Table 3.35, Table 3.36 and Table 3.37.

The activity of **64** is consistently higher than the parent nucleoside, with IC₅₀ reaching values as low as 4.28 and 6.83 μM respectively on Z-138 and MOLT-4 cell lines, and maximum inhibition percentage always close to 100%. On the other hand, 3'dA rarely reached MI% higher than 50%, as already noticed in previous *in vitro* evaluations.

Cpnd	CCRF-CEM		MOLT-4		K562		HEL92.1.7		KG-1		MV4-11		HL-60	
	IC ₅₀	MI%	IC ₅₀	MI%	IC ₅₀	MI%	IC ₅₀	MI%	IC ₅₀	MI%	IC ₅₀	MI%	IC ₅₀	MI%
3'dA	>198	35	124.0	57	47.0	98	54.0	83	67.0	70	>198	32	82.0	74
30a	1.90	97	0.48	98	3.0	96	11.0	100	18.0	90	1.03	100	9.10	100
64	17.0	99	6.83	102	9.50	103	28.0	104	72.0	94	4.73	100	27.0	99
PTX	0.004	93	0.002	94	0.003	80	0.03	72	0.08	89	0.003	98	0.003	93

Table 3.35 *In vitro* cytotoxicity screening of compounds 3'dA, **30a** and **64**. Cytotoxicity data reported μM IC₅₀ values (concentration of drug causing 50% of cell viability inhibition) and MI% (maximum inhibitory effect of the drug at the range of concentration considered). PTX: paclitaxel (control). Assays performed by WuXi AppTech.

The activity of **64** was generally lower than ProTide **30a**, as it could be expected due to a less effective recognition of the prodrug moiety by metabolising enzymes and of the free phosphonate by kinase enzymes responsible for the second and third phosphorylating steps, required for intracellular activity.

Cpnd	Thp-1		Z-138		RL		Jurkat		Hs-445		RPMI-8226		NCI-H929	
	IC ₅₀	MI%	IC ₅₀	MI%	IC ₅₀	MI%	IC ₅₀	MI%	IC ₅₀	MI%	IC ₅₀	MI%	IC ₅₀	MI%
3'dA	>198	1	>198	25	>198	14	>198	19	>198	<50	>198	0.6	>198	-0.2
30a	38.0	89	1.35	96	3.21	96	3.37	94	41.0	93	21.0	90	14.0	98
64	13.0	99	4.28	100	12.0	104	24.0	103	43.0	108	16.0	105	12.0	100
PTX	0.01	60	0.003	97	0.003	65	0.003	82	0.004	84	0.003	96	0.003	95

Table 3.36 *In vitro* cytotoxicity screening of compounds 3'dA, **30a** and **64**. Cytotoxicity data reported μM IC₅₀ values (concentration of drug causing 50% of cell viability inhibition) and MI% (maximum inhibitory effect of the drug at the range of concentration considered). PTX: paclitaxel (control). Assays performed by WuXi AppTech.

However, on many cell lines the activity of the two prodrugs was very similar, as in Hs-445 and SW620 cells (IC₅₀ ranging between 28 and 43 μM). In some examples, as on cells Thp-1 and HepG2, the activity of the phosphonate analogue (**64**) was better than ProTide **30a**. These positive results potentially indicate that after intracellular activation and release of 3'dAMP from ProTides, this moiety might undergo catabolism by phosphatase

enzymes, with release of 3'dA, which in turn could be converted to the inosine counterpart by ADA.

Cpnd	MIA PaCa-2		BxPC-3-Luc		HT29		SW620		HepG2		MCF-7		Cal 27	
	IC ₅₀	MI%	IC ₅₀	MI%	IC ₅₀	MI%	IC ₅₀	MI%	IC ₅₀	MI%	IC ₅₀	MI%	IC ₅₀	MI%
3'dA	>198	16	>198	4	132	63	>198	22	>198	11	76	79	>198	20.3
30a	15	97	73	76	18	97	29	91	47	86	3.59	95.7	25	108.2
64	30	105	81	88	38	96.	28	98	18	101	23	100.7	45	99.2
PTX	0.004	85	0.016	51	0.004	79	0.01	84	0.008	51	0.003	79.7	0.002	92.1

Table 3.37 *In vitro* cytotoxicity screening of compounds 3'dA, **30a** and **64**. Cytotoxicity data reported μM IC₅₀ values (concentration of drug causing 50% of cell viability inhibition) and MI% (maximum inhibitory effect of the drug at the range of concentration considered). PTX: paclitaxel (control). Assays performed by WuXi AppTech.

The phosphonate analogue **64**, on the other hand, would not undergo the same process, therefore might retain activity due to the increased stability.

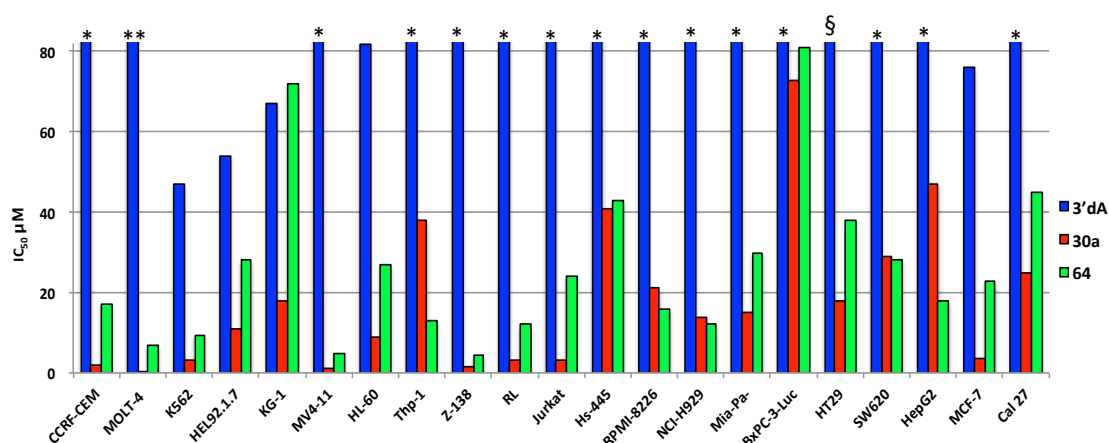


Figure 3.90 Bar chart representing the IC₅₀ values for 3'dA, and prodrugs **30a** and **64**. *IC₅₀ > 198 μM . **IC₅₀ = 124 μM . §IC₅₀ = 132 μM

Therefore the activity of 3'dA prodrugs could be considered as deriving from a balance between catabolic (catalysed by nucleotidase and deaminase enzymes) and anabolic processes (catalysed by kinase enzymes), which can lead to an advantage of one or the other prodrug analogue depending on the enzymatic expression of each cell line.

3.4.4 Mechanistic studies

A potential drawback in the activity of phosphonate prodrugs of nucleosides such as compound **64** might be the lack in recognition by enzymes responsible for the cleavage of

the prodrug moieties, such as CPY and Hint enzyme, due to the replacement of a natural phosphate group with the alternative phosphonate moiety.

The intracellular activation of compound **64** (Figure 3.91) was investigated by simulating the interaction with CPY and Hint enzyme through docking studies.

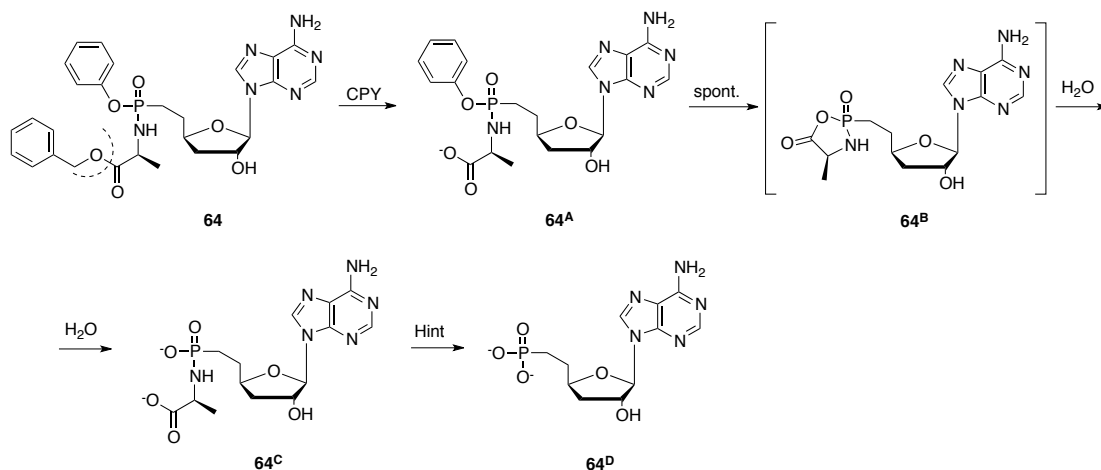


Figure 3.91: Putative intracellular metabolic activation of prodrug **64**.

Initially, docking of both diastereoisomers (*Sp* and *Rp*) was performed within the active pocket of CPY enzyme.

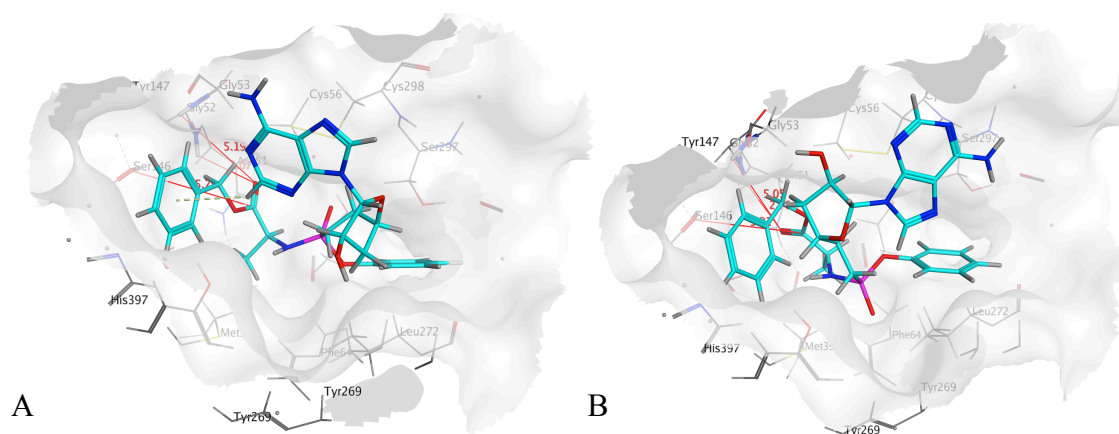


Figure 3.92 (A) Docking of *Rp* isomer of **64** in CPY active site. (B) Docking of *Sp* isomer of **64** in CPY active site. (Distances: [A] $\text{H}^{\text{Gly52}}-\text{O}=\text{C}$: 5.19 Å; $\text{O}^{\text{Ser146}}-\text{C}=\text{O}$: 5.79 Å; $\text{H}^{\text{Gly53}}-\text{O}$: 3.07 Å; [B] $\text{H}^{\text{Gly52}}-\text{O}$: 5.05 Å; $\text{O}^{\text{Ser146}}-\text{C}$: 3.97 Å; $\text{H}^{\text{Gly53}}-\text{O}=\text{C}$: 2.76 Å)

Both isomers seemed to interact similarly inside the enzyme, positioning the amino acid ester moiety close to the pocket containing catalytic residues, although no clear interactions of the adenine ring with additional residues inside the pocket could be noticed.

This might suggest a slower processing by CPY compared to the phosphate counterpart **30a**.

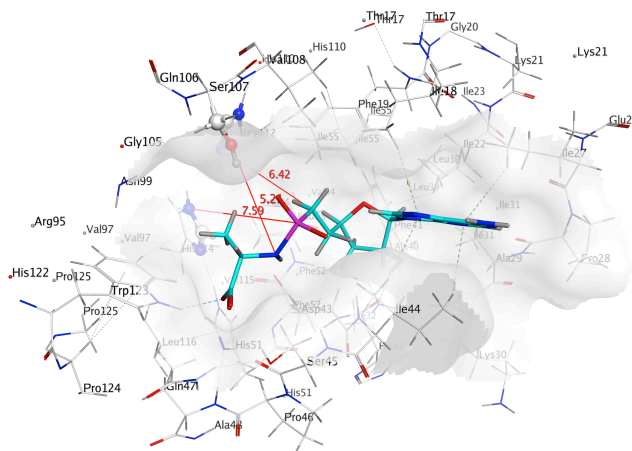


Figure 3.93 Docking of **64^C** in Hint active site. (Distances: O^{Ser107}-N: 7.59 Å; N^{His112}-C6': 6.42 Å; N^{His114}-P: 5.24 Å).

L-alaninyl phosphonate monoester intermediate **64^C** was further docked into the Hint enzyme, and the results are shown in Figure 3.93. The positioning of the phosphoramidate group is close to the key residues responsible for the cleavage of the P-N bond, although at a bigger distance (5.24 - 7.59 Å) compared to the phosphate analogue **30a^C** (3.99 - 6 Å) (Figure 3.34, **A**).

3.4.5 Conclusions

During the explorations of different structural variations to apply to 3'dA prodrugs in order to enhance the biological properties, a 5' modification was introduced in the form of replacement of the phosphate group (P-O bond) with a phosphonate (P-C) bond and insertion of an alkyl moiety. The latter modification was attempted by oxidation of the 5'-primary alcohol of 3'dA followed by alkylation by different Grignard reagents, however with no success. Therefore the application of the phosphonate technology was carried out, and the analogue of ProTide **30a** was synthesised via a 7 step synthetic procedure. Evaluation of phosphonate **64** in comparison with ProTide **30a** and 3'dA showed that phosphonate **64** had a superior anticancer profile compared to 3'dA, with IC₅₀ values in the same range as **30a** although generally lower. These results may derive from lower recognition of the molecule by prodrug-activating enzymes such as CPY and Hint by kinase enzymes responsible for the second and third phosphorylation steps. Due to the potential of this kind of modification in terms of significant improvement of the activity of

the parent nucleoside, further investigations should be aimed at altering the phosphonate structure in order to mimic more efficiently the phosphate counterpart, in order to improve the recognition by key enzymes. This could be accomplished by introducing a double bond in the portion linking sugar and phosphonate (Figure 3.94, **a.** and **b.**), or by introducing a fluorine in the same position (Figure 3.94, **c.** and **d.**), which was already reported to mimic the hydrogen bonding capacity of the phosphate group.³²⁴

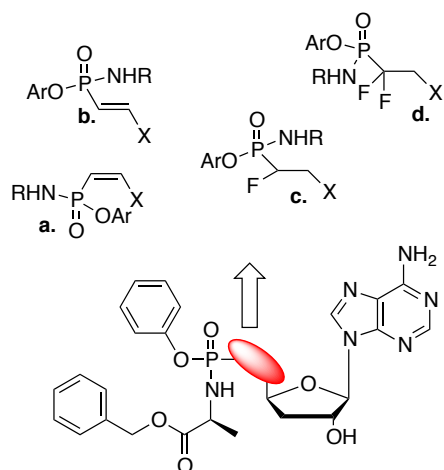


Figure 3.94 Possible modification of the phosphonate moiety in **64** aimed at improving the biological properties.

4 8-Chloroadenine nucleoside derivatives

4.1 8-Chloroadenosine

4.1.1 Background

Cyclic adenosine monophosphate (cAMP, **65**, Figure 4.1) is a second messenger that plays an important role in cell growth and differentiation.³²⁵

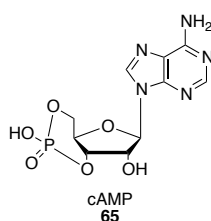
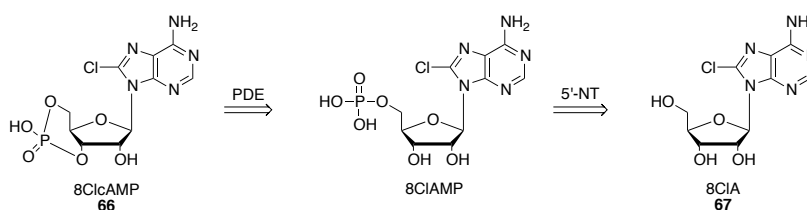


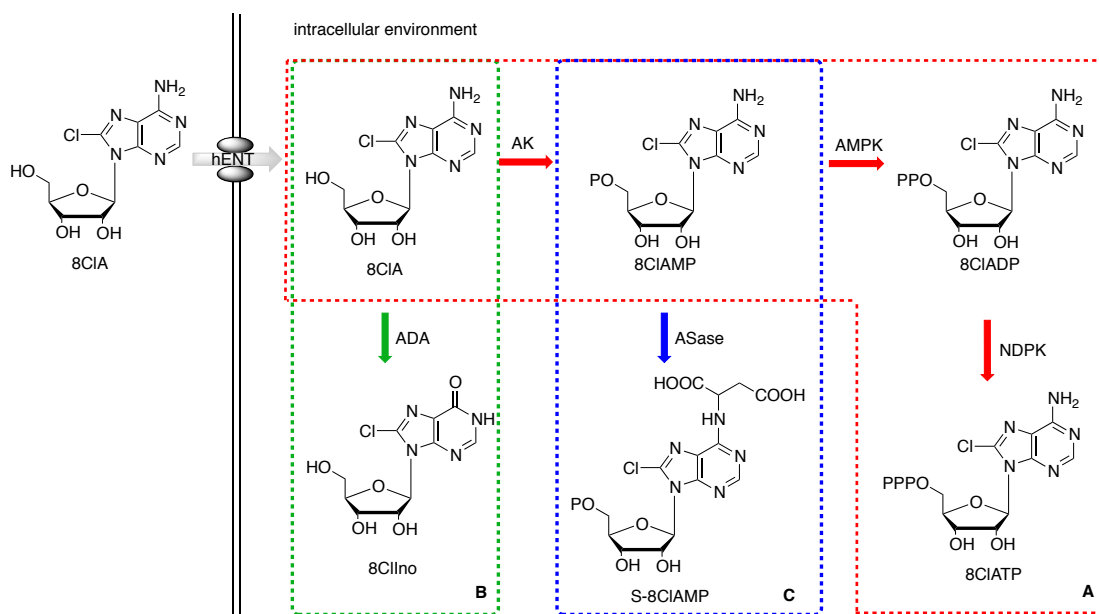
Figure 4.1 Structure of cAMP (**65**).

As such, the cAMP signalling pathway has been used as a target in the development of new anticancer drugs.³²⁶ The most promising cAMP analogue, tested for its anticancer activity, is 8-chloro cyclic adenosine monophosphate (8ClcAMP, **66**), also known as tocladesine (Scheme 4.1). Toccladesine was involved in a Phase II clinical trial study in patients with recurrent or refractory multiple myeloma (MM), a fatal B-cell malignancy with a median three years survival.³²⁷ Although reported as completed in 1999, the full clinical results of this study have not been published to date. Several studies confirmed that tocladesine acts after extracellular activation to its metabolite 8-chloroadenosine (8ClA, **67**), *via* two enzymatic steps, involving the first conversion to 8-chloroadenosine-5'-monophosphate (8ClAMP) by a serum phosphodiesterase (PDE), followed by dephosphorylation to 8ClA by an extracellular 5'-nucleotidase (5'-NT, Scheme 4.1).³²⁸



Scheme 4.1 Extracellular enzymatic conversion of 8ClcAMP (**66**) to 8ClA (**67**).

8ClA is currently involved in a Phase I clinical trial on patients with chronic lymphocytic leukaemia which is planned to end in 2016.^{329,330} As described in Scheme 4.2, 8ClA enters the cell exploiting a nucleoside transporter belonging to the ENT (equilibrative nucleoside transporter) family, also involved in the active transport of adenosine.³³¹ Once inside the cell, the intracellular concentration of 8ClA depends on the activity of adenosine kinase (AK), responsible for the phosphorylation to 8ClAMP (Scheme 4.2, **B**). Moreover, 8ClA was reported to be a poor substrate of the ADA enzyme, and the metabolite 8-chloroinosine (8ClIno) generated after deamination of 8ClA was recognised as an inactive metabolite.^{332,333} The phosphorylation is considered more efficient than deamination in many cells,³³² 8ClAMP is subsequently converted into the di- (8ClADP) and triphosphate (8ClATP) metabolites respectively by adenylate kinase (AMPK) and nucleoside diphosphate kinase (NDPK).^{5,6} The accumulation of 8ClATP inside the neoplastic cell increases the incorporation of the analogue in the RNA growing chain, leading to premature transcript termination.³²⁹ Moreover, 8ClA was found to inhibit mRNA processing inside neoplastic cells, by inhibiting polyadenylation of the mRNA by poly(A) polymerase, which is one of the key steps in the post-transcriptional processing of mRNA precursors.³³⁴



Scheme 4.2 Intracellular mechanism of action of 8ClA.

The poly(A) tail length has been shown to have a crucial role in mRNA stability, regulation of mRNA degradation and transport of mRNA from the nucleus to the cytoplasm where it promotes efficient translation. The enzyme poly(A) polymerase

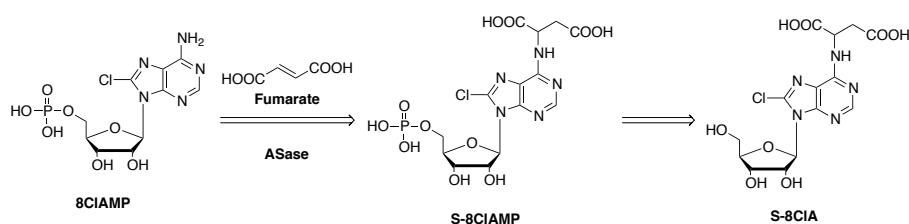
belongs to the superfamily of the nucleotidyl transferases and incorporates ATP onto the 3' ends of RNA substrates in a template-dependent manner.³³⁵

Cleavage of the RNA and polyadenylation inhibition may contribute to the decreased RNA levels observed upon treatment of cells with 8ClA. In addition to increased RNA degradation, the consequences of polyadenylation inhibition included impaired mRNA transport from the nucleus and altered translation efficiency.³³⁵

Furthermore, intracellular 8ClADP was reported to be a potential competitor of adenosine diphosphate (ADP) as a substrate of the ATP-synthase enzyme. This enzyme was involved in the oxidative phosphorylation process and it catalyses the synthesis of ATP from recycling ADP. The putative inhibition of this metabolic step may consequently explain the decrease of the ATP cellular pool that was noticed in the cells treated with 8ClA.^{336,337}

8ClA was also reported to cause indirect DNA damage by inhibition of the topoisomerase II enzyme.³³⁸ This enzyme resolves topological problems in DNA replication, transcription, recombination and chromosome condensation and segregation, by means of DNA double strand breakage and religation.³³⁹ To perform its activity, topoisomerase II needs energy derived from the hydrolysis of ATP, therefore 8ClATP could compete with the natural substrate and inhibit the activity of this enzyme leading to DNA double-stranded breaks.³³⁸

The intracellular energetic metabolism is additionally altered by 8ClAMP through the reversible succinylation of the amino group at the nucleobase level, presumably catalysed by the adenylosuccinase enzyme (ASase), with the synthesis of succinyl-8ClA monophosphate (S-8ClAMP) (Scheme 4.2C, Scheme 4.3).³²⁹



Scheme 4.3 Succinylation 8ClAMP by ASase and dephosphorylation to S-8ClA.

S-8ClAMP is then quickly dephosphorylated to succinyl-8ClA (S-8ClA). This reaction consumes fumarate, involved in the citric acid cycle, therefore causes perturbation of cellular metabolism and energetic pools inside the cell. Accumulation of 8ClA succinyl metabolites may also afford a pharmacokinetic advantage, as these metabolites can constitute deposit forms of the nucleoside inside the neoplastic cells, due to the much

longer half-life of S-8CIA compared to 8CIATP, the putative active metabolite (12 h vs 6 h). Thus, S-8CIA may preserve intracellular 8CIAMP levels as 8CIA concentrations fall in the plasma, and consequently prolong 8CIA therapeutic effects.³²⁹

4.1.2 Preliminary biological evaluation of 8CIA ProTides

The application of the ProTide technology to 8CIA was previously explored within the McGuigan group,³⁴⁰ with the aim of delivering the key metabolite, 8CIAMP, from which the two main causes of anticancer activity branch out: phosphorylation leading to accumulation of 8CIATP and succinylation leading to accumulation of S-8CIA. Moreover the application of this prodrug approach would reduce the already low intracellular conversion of 8CIA into inactive 8CIIno by ADA³⁴¹ and bypass other potential resistance mechanisms such as the dependency on nucleoside transporters to enter the cell and on AK for the first phosphorylation step.³⁴¹⁻³⁴³ The structures of 8CIA ProTides previously synthesised are reported in Table 4.1.

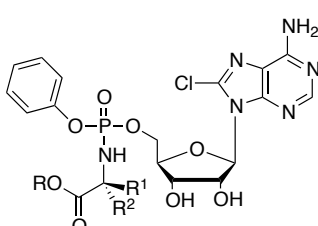
Common structure	Cpn	R	R ¹	R ²	AA
	68a	<i>i</i> Pr	Me	H	L-Ala
	68b	cHx	Me	H	L-Ala
	68c	Bn	Me	H	L-Ala
	68d	Neop	Me	Me	DMG
	68e	cHx	H	H	Gly
	68f	Bn	H	H	Gly
	68g	Bn	H	Me	D-Ala
	68h	Me	(CH ₂) ₂ SCH ₃	H	L-Met
	68i	Bn	<i>i</i> Pr	H	L-Val
	68j	Bn	<i>i</i> Bu	H	L-Leu
	68k	Bn	Bn	H	L-Phe

Table 4.1 Previously synthesised 8CIA ProTides (**68a-k**).

These compounds were tested vs different human and murine cancer cell lines (Table 4.2) by Tenovus (Cardiff University) and the Rega Institute (Leuven, Belgium), mainly derived from solid tumours, with the exception of L1210 and CEM leukaemic cell lines.

Cell line	Malignancy
MCF7	Human Breast adenocarcinoma
Lovo	Human Colorectal adenocarcinoma
PC3	Human Prostatic adenocarcinoma
A549	Human Lung carcinoma
L1210	Murine lymphocitic leukaemia
FM3A	Murine mammary carcinoma
CEM	Human acute lymphoblastic leukaemia
HeLa	Human cervical adenocarcinoma

Table 4.2 Set of cell lines used for the biological investigation of the first family of 8CIA ProTides.

The cytotoxic activities of compounds **68a-k** in relation to the parent nucleoside 8CIA are reported in Table 4.3. None of the ProTides in this series were more active than 8CIA *in vitro*, although several were equipotent.

Cpd	Lovo	MCF7	PC3	A549	L1210	FM3A	CEM	HeLa
8CIA (67)	0.5	0.5	0.5	5	7	3	4	2
68a	5	40	5	100	73	59	41	17
68b	0.5	5	5	50	-	-	-	-
68c	5	50	5	50	33	28	16	7
68d	5	50	5	>100	53	43	50	23
68e	5	50	50	50	58	>100	64	27
68f	0.5	50	0.5	10	6	4	8	2
68g	5	50	5	50	23	24	21	6
68h	50	100	50	>100	94	>100	84	36
68i	0.5	5	50	50	46	58	47	14
68j	0.5	0.5	0.5	0.5	28	22	14	3
68k	5	5	5	5	19	23	9	3

Table 4.3 Cytotoxic evaluation of previously synthesised 8CIA ProTides **68a-k**. Activity reported as μM IC_{50} values (compound concentration inhibiting the growth of 50% of cells). Data generated Cardiff University, Tenovus (Lovo, MCF7, PC3, A549 cell lines) and Rega Institute (L1210, FM3A, CEM, HeLa cell lines).

Glycine benzyl ester derivative (**68f**) showed submicromolar activity ($\text{IC}_{50} = 0.5 \mu\text{M}$) in PC3, MCF7 and Lovo cells, and it also stood out with low micromolar activity in the other cell lines tested. This derivative was therefore included among the lead compounds in this series, along with **68j** (L-leucine benzyl ester ProTide) and **68k** (L-phenylalanine). In fact these compounds, although less potent than 8CIA, still show the best overall activities in this series of prodrugs.

Considering this first set of data, the aim of the present work was to broaden the 8CIA ProTides structures by synthesising additional L-leucine, L-phenylalanine and glycine containing ProTides (Figure 4.2).

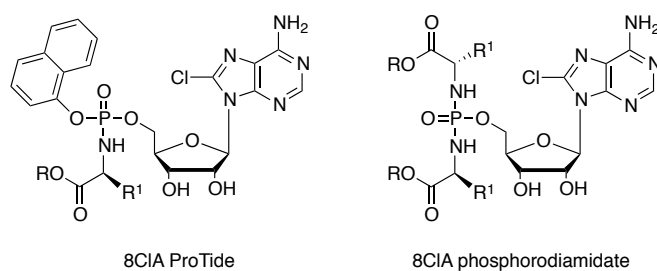
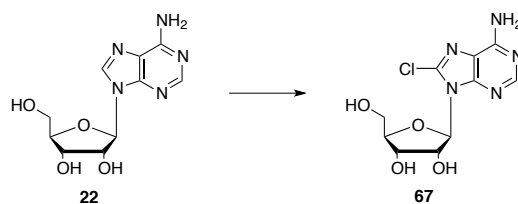


Figure 4.2 Structure of the new family of 8CIA ProTides.

Amino acid ester moieties varied among ethyl, *n*-pentyl, benzyl and cyclohexyl esters. L-Alanine was also considered, as a generally promising moiety in terms of biological activity.¹⁵² The aryl moiety was modified to 1-naphthyl, a moiety that was already reported to yield compounds with good activity,¹⁵² and was not used in previously synthesised 8CIA ProTides. Moreover modification of the monophosphate prodrug structure were performed, including the diamidate symmetrical approach, which was reported as promising both in the antiviral and anticancer fields.^{67,143,144,322}

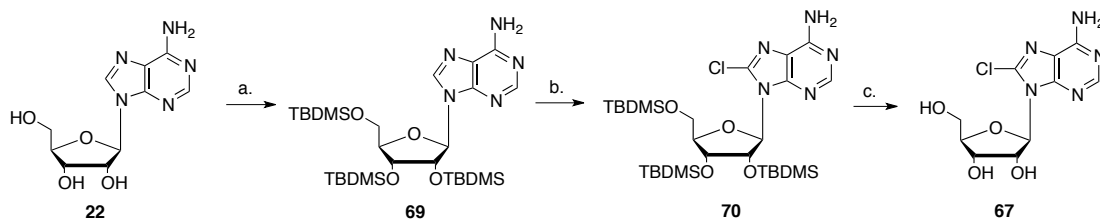
4.1.3 Synthesis of 8CIA

8CIA was first synthesised in 1972 by chlorination of adenosine (Ado) using tetrabutylammonium iodotetrachloride, although in low yield.³⁴⁴ Since then different methods have been developed.³⁴⁵ The methodology developed by Ryu and McCoss required the treatment of Ado with HCl followed by *meta*-chloroperbenzoic acid (*m*CPBA) oxidation,³⁴⁶ and was more recently improved by replacing HCl with benzoyl chloride.³⁴⁷ The latter methodology was already used in the McGuigan group and was initially reproduced in this work, leading to a low 20% yield of the desired 8CIA (Scheme 4.4, [1]). In an attempt to improve both the yield and the tedious purification of this first method, an alternative procedure was applied, involving the treatment of Ado (**22**) with an excess of *N*-chlorosuccinimide (NCS) in a mixture of DMF and acetic acid (AcOH) as solvents for the reaction, affording the desired product in 50% yield (Scheme 4.4, [2]).³⁴⁸



Scheme 4.4 Synthesis of 8CIA (**67**). *Reagents and Conditions*: [1] BzCl (1 eq), *m*CPBA (1.1 eq), DMF, rt, 20 min, 20%. [2] NCS (3.5 eq), AcOH, DMF, rt, 48 h, 50%.

A final optimisation of 8ClA synthesis was investigated at a later stage, and involved a 3-step process starting from Ado (**22**), firstly protected in quantitative yield on the hydroxyl groups of the sugar by treatment with *tert*-butyl dimethylsilyl chloride (TBDMSCl) and imidazole in DMF.³⁴⁹ Protected Ado (**69**) was then selectively lithiated in position 8 on the nucleobase with lithium diisopropyl amide (LDA) and subsequently chlorinated on the C-8 via tosyl chloride (TsCl) as an electrophilic chlorinating agent in a one pot reaction, yielding protected 8ClA (**70**) in 74% yield.^{350,351}



Scheme 4.5 Synthesis of 8ClA (**67**). *Reagents and Conditions*: (a.) TBDMSCl (4 eq), imidazole (8 eq), DMF, 16h, rt; (b.) LDA (5 eq), TsCl (4 eq), THF, -78 °C to rt, 2h, 74%; (c.) TFA:H₂O:THF (1:1:4 v/v/v), rt, 36h (67%).

Compound **70** was deprotected by treatment with TFA:H₂O:THF (1:1:4) at room temperature over 36 hours, yielding 8ClA (**67**) in 64% yield (Scheme 4.5, step c.). Although requiring 3 steps, and with an overall yield of 50%, this latter synthetic strategy was preferred due to the easier purification steps required.

NMR analysis confirmed the structure of the product, and Figure 4.3 shows the ¹H NMR spectrum of the final product, which lacks the H8, confirming the 8ClA structure. Moreover, characteristic splitting pattern due to chlorine isotopes could be observed via ES-MS analysis.

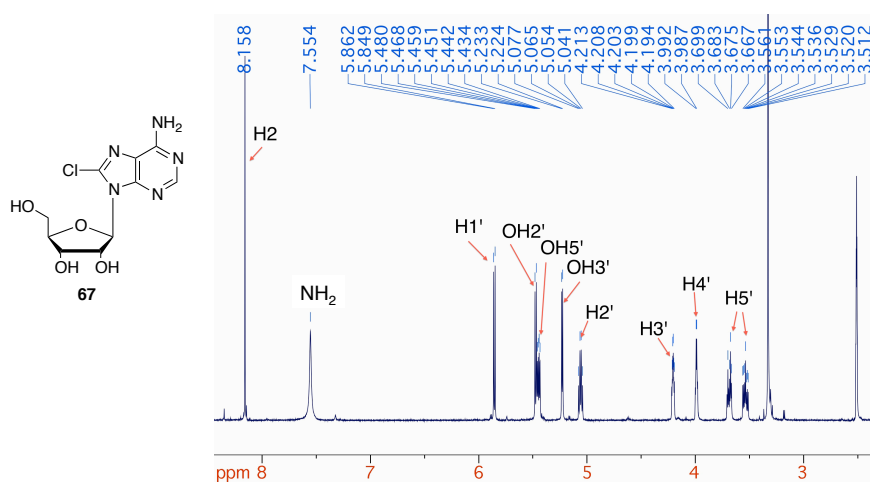


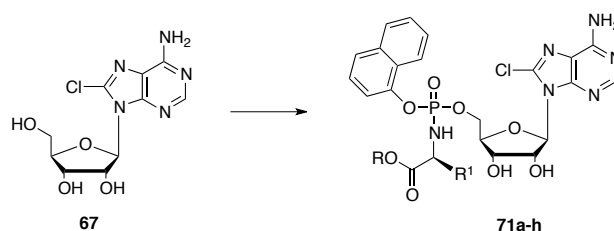
Figure 4.3 ¹H NMR spectrum of 8ClA **67** (DMSO-*d*₆, 500 MHz).

4.1.4 Synthesis of 8CIA prodrugs

4.1.4.1 8CIA phosphoramidates

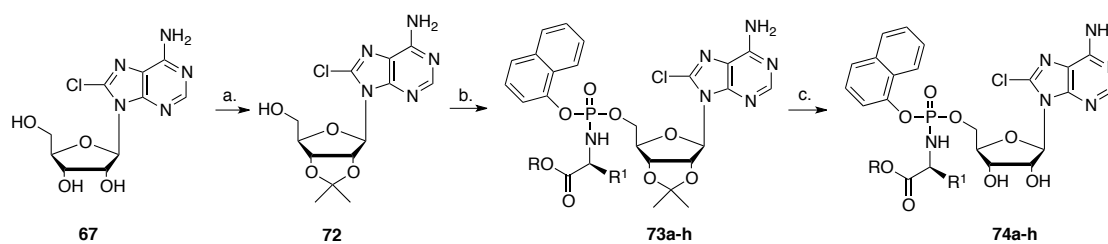
Two strategies for the synthesis of 8CIA ProTides were previously developed.^{105,152,154,340} Direct coupling between the nucleoside (**67**) and phosphorochloridates bearing non-bulky amino acids (such as glycine and L-alanine) was performed using 1.1 equivalents of *t*BuMgCl in THF. Alternatively, for the synthesis of ProTides bearing bulky amino acids (such as L-phenylalanine or L-leucine), the nucleoside was first protected on the 2' and 3'-hydroxyl groups and then coupled with the appropriate phosphorochloridate in the presence of up to 3 equivalents of *t*BuMgCl. This method allowed the use of more equivalents of the Grignard reagent, hence to facilitate the reaction between the 5'-hydroxyl group and the phosphorochloridate without regioisomerism.

For the first series of L-alanine and glycine bearing ProTides, the synthetic procedure is reported in Scheme 4.6.



Scheme 4.6 Synthesis of 8CIA ProTides **71a-h** from unprotected 8CIA (**67**). *Reagents and Conditions:* *t*BuMgCl (1.1 eq), appropriate phosphorochloridate (3 eq), anhydrous THF, rt, 16h, 4-17% (see Table 4.4).

The second series of naphthyl-bearing 8CIA ProTides was synthesised according to Scheme 4.7. The isopropylidene protection of 8CIA was performed using acetone in the presence of perchloric acid with 79% yield of intermediate **72**.³⁵² This intermediate was then reacted with the appropriate phosphorochloridate and 2-3 equivalents of *t*BuMgCl, yielding protected ProTides **73a-h**.



Scheme 4.7 Synthesis of 8CIA ProTides (**74a-h**) in a 3-step process requiring protection of 8CIA (**67**), coupling and final deprotection procedures. *Reagents and Conditions*: (a.) acetone, perchloric acid 70%, rt, 30 min, 79%; (b.) *t*BuMgCl, appropriate phosphorochloridate, anhydrous THF, rt, overnight; (c.) formic acid, water, rt, 16h, 6-35% (two steps, see Table 4.4).

Final deprotection was performed by treatment of protected ProTides (**73a-h**) with a solution of aqueous formic acid in water overnight,³⁵³ affording ProTides **74a-h** in low to moderate yields, as reported in Table 1.4.

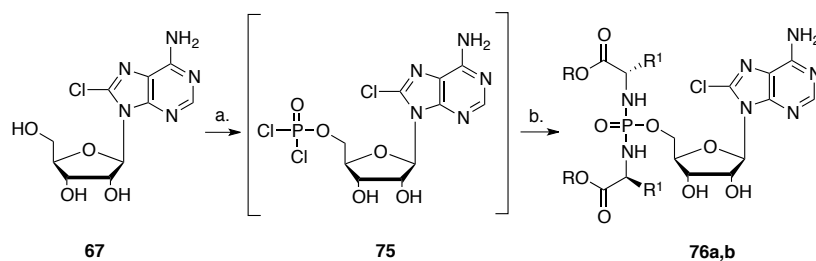
Common structure	Compound	R	R ¹	AA	Yield %
	71a	Bn	Me	L-Ala	17 %
	71b	Et	“	“	7 %
	71c	cHex	“	“	9 %
	71d	<i>n</i> -Pe	“	“	4 %
	71e	Et	H	Gly	4 %
	71f	Bn	“	“	4 %
	71g	<i>n</i> -Pe	“	“	15 %
	71h	cHex	“	“	4 %
	74a	Bn	<i>i</i> Bu	L-Leu	26 %
	74b	<i>n</i> -Pe	“	“	36 %
74c	cHex	“	“	8 %	
74d	Et	“	“	35 %	
74e	Bn	Bn	L-Phe	6 %	
74f	<i>n</i> -Pe	“	“	10 %	
74g	cHex	“	“	21 %	
74h	Et	“	“	26 %	

Table 4.4 Structures and % yields of 8CIA ProTides synthesised via one step (**71a-h**), or three steps (**74a-h**) method.

4.1.4.2 8CIA phosphorodiamidates

The phosphorodiamidate approach was the second nucleotide prodrug system applied to 8CIA. In the present work, the Yoshikawa¹⁵⁶ procedure was adopted to obtain 5'-phosphorylated nucleoside analogues using unprotected 8CIA. According to the cited study, in a one pot reaction the unprotected nucleoside is suspended in trialkyl phosphate, and phosphorus oxychloride is added in order to obtain the 5'-phosphorodichloridate (**75**,

Scheme 4.8) *in situ*.¹⁵⁵ In the first attempt, triethyl phosphate (TEP) was used, but no product could be observed and the starting material was recovered. For this reason trimethyl phosphate (TMP) was successfully used as a solvent in the second attempt, possibly due to better solubility of the 8ClA. Analysis of the reaction mixture by ³¹P NMR (CDCl₃, 202 MHz) revealed the formation of a species with a signal at ~7 ppm, which corresponded to **75**. This intermediate was not isolated but immediately coupled with the appropriate amino acid ester salt in the presence of diisopropyl ethyl amine (DIPEA). The progression of the reaction was monitored again by ³¹P-NMR: the appearance of a single peak in the range of 13-17 ppm, depending on the amino acid used for the synthesis, indicated the formation of the product. The overnight reaction, followed by purification on silica gel, resulted in achieving the final phosphorodiamidates **76a,b** (Scheme 4.8, Table 4.5).



Scheme 4.8 General synthesis of 8ClA phosphorodiamidates. *Reagents and Conditions*: (a.) POCl₃ (1 eq), TMP, -78 °C, 4h (b.) amino acid ester *p*-TSA or HCl salt (5 eq), DIPEA (10 eq), CH₂Cl₂, 27-45%, (see Table 4.5).

Cpnd	Common structure	R ¹	R	AA	Yield
76a		Bn	Me	L-Ala	45%
76b		Bn	H	Gly	27%

Table 4.5: Structures and yields (%) of 8ClA phosphorodiamidates **76a,b**.

4.1.5 Biological evaluation of 8ClA prodrugs

The new 8ClA ProTides (**71a-h**, **74a-h**) and the two diamidates (**76a,b**) were screened first on a small panel of cell lines including two leukemic cell lines (L1210 and CEM) and a solid tumour cell line (HeLa) by the Rega Institute (Leuven, Belgium) in order to compare the anticancer activity to the parent nucleoside 8ClA. The activity of some of the naphthyl-bearing new compounds could be directly compared to their phenyl-bearing counterparts, and the diamidates synthesised were compared to the corresponding ProTide analogues.

The compounds that emerged as the most promising in this initial screening and some interesting phenyl bearing analogues belonging to the first family of ProTides were further tested by WuXi AppTech on a broader number of cell lines in order to confirm the activity and potentially select candidates for additional biological evaluations.

4.1.5.1 Cytotoxic screening of the newly synthesised 8CIA prodrugs

The new 8CIA ProTides **71a-h**, **74a-h** and phosphorodiamidates **76a,b** were tested for cytotoxicity and Table 4.6 shows the activities as IC₅₀ μM values (compound concentration required to inhibit tumour cell proliferation by 50%).

None of the synthesised ProTides or phosphorodiamidates of 8CIA was found to be more active than the parent nucleoside. Most of the compounds, however, were reported to have similar activities compared to 8CIA. ProTides bearing benzyl as an ester moiety (**71a**, **71f**, **74a** and **74e**) had the lowest IC₅₀ values, typically in the low micromolar range. The *n*-pentyl group is an alternative ester moiety found in some of the most active compounds of all the families (**71d**, **71g**, **74b** and **74f**). On the other hand, ethyl and cyclohexyl ester groups were found to be the least active compounds of each series, with activities 10 to 20 fold lower than the parent nucleoside (respectively compounds **71b**, **71e**, **74d**, **74h** and compounds **71c**, **71h**, **74c**, **74g**). The two phosphorodiamidates (**76a** and **76b**) showed similar activities, with IC₅₀ values in the low micromolar range although higher than the parent nucleoside.

	Cpd	Ar	AA	Ester	L1210	CEM	HeLa	cLogP
	8CIA (67)	-	-	-	3.2 ± 0.7	1.1 ± 0.6	0.89 ± 0.50	-1.44
	71a	1-	L-Ala	Bn	10 ± 1	2.2 ± 0.3	1.6 ± 0.8	2.37
	71b	1-	“	Et	44 ± 8	8.4 ± 2.4	4.0 ± 2.2	1.19
	71c	1-		cHex	24 ± 3	10 ± 2	2.5 ± 1.8	2.69
	71d	1-	“	<i>n</i> -Pen	6.5 ± 1.1	2.5 ± 1.5	1.4 ± 1.1	2.77
	71e	1-	Gly	Et	48 ± 20	22 ± 13	4.2 ± 3.8	1.07
	71f	1-	“	Bn	5.3 ± 1.8	2.5 ± 1.7	1.4 ± 0.6	2.25
	71i	1-	“	<i>n</i> -Pen	4.6 ± 1.5	1.8 ± 1.2	1.1 ± 0.4	2.66
ProTides	71h	1-	“	cHex	39 ± 12	26 ± 1	19 ± 11	2.57
	74a	1-	L-Leu	Bn	7.8 ± 0.3	3.5 ± 1.4	1.7 ± 0.7	3.82
	74b	1-	“	<i>n</i> -Pen	9.4 ± 0.6	6.2 ± 1.6	2.4 ± 0.6	4.23
	74c	1-	“	cHex	12 ± 5	9.0 ± 1.1	5.7 ± 1.4	4.15
	74d	1-	“	Et	37 ± 5	12 ± 4	3.8 ± 2.4	2.65
	74e	1-	L-Phe	Bn	9.2 ± 2.6	3.2 ± 0.7	1.8 ± 0.5	3.79
	74f	1-	“	<i>n</i> -Pen	9.1 ± 1.0	3.6 ± 1.2	1.5 ± 0.7	4.19
	74g	1-	“	cHex	12 ± 5	5.5 ± 1.1	2.5 ± 0.5	4.11
	74h	1-	“	Et	29 ± 3	5.5 ± 3.6	2.0 ± 1.1	2.61
Diamidates	76a	-	L-Ala	Bn	10 ± 4	3.8 ± 0.2	2.3 ± 1.0	3.17
	76b	-	Gly	Bn	4.6 ± 0.0	3.4 ± 0.4	1.8 ± 0.4	2.55

Table 4.6 Biological evaluation of 8CIA, naphthyl-bearing ProTides (**71a-h**, **74a-h**) and phosphorodiamidates (**76a,b**) of 8CIA by the Rega Institute in Leuven, Belgium. Cytotoxicity is reported as IC₅₀ μM values (50% inhibitory concentration of cell viability).

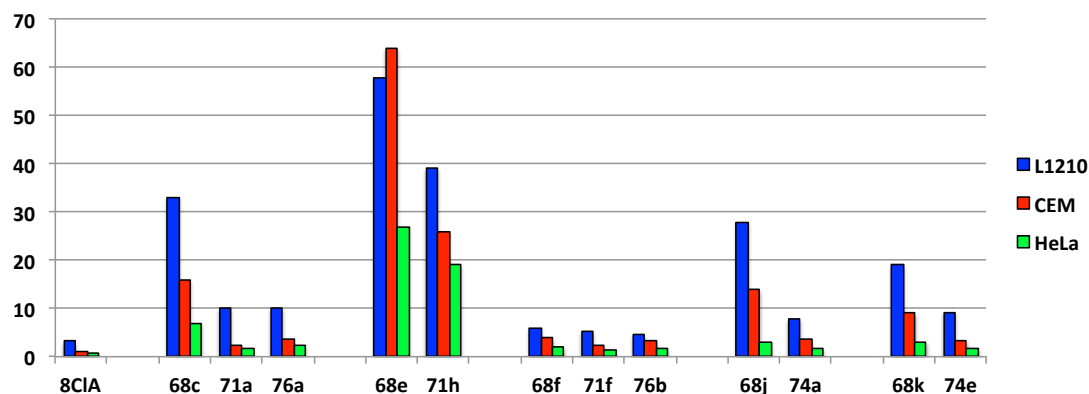


Figure 4.4: Activities of 8CIA and selected 8CIA prodrugs (phenyl ProTides **68c,e,f,j,k**; naphthyl ProTides **71a,h**, **74a,e**; phosphorodiamidates **76a,b**). IC₅₀ μM values are reported on the Y axis.

Figure 4.4 shows a comparison between the activities of some of the new naphthyl-bearing ProTides with the phenyl containing counterparts, which were previously tested on a number of cell lines including the ones considered in this screening. Similarly, the two phosphorodiamidates were compared to their ProTide counterparts.

The phosphorodiamidate **76a** and the naphthyl containing 5'-ProTide analogue **71a** emerged as similarly active on the three cell lines considered and 3 to 7-fold more potent

than the initially synthesised phenyloxy L-alanine benzyl ester ProTide **68c**. A similar pattern resulted from the comparison between the two glycinyloxy cyclohexyl-containing ProTides, with the naphthyl derivative **71h** being more potent than the phenyl analogue **68e**. Within the series of glycinyloxy compounds, a similar low micromolar activity profile emerged both for the phenyl (**68f**) and naphthyl (**71f**) ProTides and for the phosphorodiamidate (**76b**). The naphthyl analogues of ProTides containing both L-leucine and L-phenylalanine benzyl ester emerged as more active than the phenyl counterparts, confirming the superior activity profile of naphthyl ProTides compared to the phenyl analogues. This could be due to an increase in lipophilicity that may be responsible for a more efficient cell entering *via* passive diffusion. As an example, the phenyl L-alanine benzyloxy ProTide **68c** has a cLogP of 1.20, while the naphthyl counterpart has a cLogP of 2.37, and this difference could affect cell penetration. Moreover, the recognition by enzymes responsible for the processing of the ProTide moiety (catA and Hint) could also differ, and was further explored. In conclusion, the synthesis of ProTides bearing a naphthyl moiety and phosphorodiamidates as new 8ClA phosphate prodrugs generated a series of compounds endowed with intriguing cytotoxic activity and this prompted further biological evaluation of the most active compounds on a broader selection of cell lines.

4.1.5.2 Cytotoxic screening of 8ClA prodrugs on a broader panel of malignant cell lines.

The new set of cell lines selected for *in vitro* testing of 8ClA prodrugs derived from both haematological malignancies and solid tumours (Table 4.7).

Cell line	Malignancy	Cell line	Malignancy
MOLT-4	Acute lymphoblastic leukaemia	HEL92.1.7	Erythroleukaemia
CCRFCE	Acute lymphoblastic leukaemia	HL-60	Promyelocytic leukaemia
RL	Non-Hodgkin's lymphoma	MV4-11	Biphenotypic B myelomonocytic
HS445	Hodgkin lymphoma	HepG2	Hepatocellular carcinoma
RPMI8226	Human multiple myeloma	HT29	Colon adenocarcinoma
K562	Chronic myelogenous	BxPC-3	Pancreatic cancer
KG-1	Acute myelogenous leukaemia	MCF-7	Breast adenocarcinoma
THP-1	Acute monocytic leukaemia	MIA PaCa-2	Pancreatic adenocarcinoma
Z-138	Mantle cell lymphoma	MDAMB23	Human breast adenocarcinoma
NCI-H929	Plasmacytoma	SW620	Colon adenocarcinoma
Jurkat	Acute T cell leukaemia		

Table 4.7: New set of cell lines for biological evaluation of 8ClA most active ProTides by WuXi AppTech.

As previously mentioned, this second screening of 8CIA prodrugs aimed at broadening the spectra of cell lines used in order to have a more complete evaluation of the most promising candidates from the initial phenyl family, and the new naphthyl and phosphorodiamidate families (Table 4.8).

Structure	Cpnd	Ar	R	R ¹	AA	cLogP	
	68c	Ph	Bn	Me	L-Ala	1.20	
	68e	Ph	cHx	H	Gly	1.40	
	68f	Ph	Bn	H	Gly	1.08	
	68j	Ph	Bn	<i>i</i> Bu	L-Leu	2.65	
	71a	Nap	Bn	Me	L-Ala	2.37	
	71d	Nap	<i>n</i> -Pen	Me	L-Ala	2.77	
	71f	Nap	Bn	H	Gly	2.25	
	71g	Nap	<i>n</i> -Pen	H	Gly	2.66	
	74a	Nap	Bn	<i>i</i> Bu	L-Leu	3.82	
	74e	Nap	Bn	Bn	L-Phe	3.79	
	74f	Nap	<i>n</i> -Pen	Bn	L-Phe	4.19	
		76b	-	Bn	H	Gly	2.55

Table 4.8: Selected compounds from first and second families of 8CIA prodrugs (phenyl-bearing ProTides **68c,e,f,j**, naphthyl-bearing ProTides **71a,d,f,g**, **74a,e,f** and phosphorodiamidate **76b**), screened for cytotoxic activity of cell lines reported in Table 4.7. cLogP values calculated with ChemDraw 2010 software.

Cpnd	CCRFCEM		HEL92.1.7		HS445		KG-1		Jurkat		K562		THP-1	
	IC ₅₀	MI _%	IC ₅₀	MI _%	IC ₅₀	MI _%	IC ₅₀	MI _%	IC ₅₀	MI _%	IC ₅₀	MI _%	IC ₅₀	MI _%
8CIA	0.92	83	1.63	95	5.79	74	1.05	99	0.99	91	1.76	85	2.91	94
68c	5.22	91	32.43	90	>198	49	>198	38	24.0	91	15.16	92	59.67	77
68e	11.03	109	14.23	86	>198	55	>198	43	43.0	87	10.1	92	40.29	85
68f	0.59	85	0.87	99	10.99	78	1.14	99	1.35	94	0.85	97	4.51	86
68j	5.43	100	3.73	100	17.62	99	10.83	99	7.69	108	2.05	100	4.4	100
71a	2.84	100	4.35	100	11.36	99	6.7	99	1.36	98	2.47	100	3.11	99
71d	2.24	100	2.59	100	15.73	99	4.17	99	2.43	97	1.92	99	3.69	97
71f	6.32	90	4.81	92	ND	ND	13.07	88	ND	ND	5.41	87	ND	ND
71g	26.03	100	21.12	100	ND	ND	41.77	99	ND	ND	13.5	100	ND	ND
74a	6.53	100	3.07	100	ND	ND	13.88	99	ND	ND	1.84	100	ND	ND
74e	5.77	100	3.70	100	ND	ND	14.92	99	ND	ND	2.28	100	ND	ND
74f	5.14	100	2.48	100	ND	ND	13.66	99	ND	ND	1.70	100	ND	ND
76b	0.41	93	0.35	96	9.31	78	3.36	102	1.25	95	0.85	96	3.22	94
PTX	0.003	98	0.02	83	0.01	74	0.08	88	0.005	97	0.01	91	0.03	72

Table 4.9: Biological evaluation of 8CIA and relative prodrugs (phenyl-bearing ProTides **68c,e,f,j**, naphthyl-bearing ProTides **71a,d,f,g**, **74a,e,f** and phosphorodiamidate **76b**) by WuXi app. Tech. Cytotoxicity is reported as IC₅₀ μM values (50% inhibitory concentration of cell viability). MI_% is the maximum percentage of inhibition exerted by compounds up to the top dose (198 μM). PTX: paclitaxel, positive control. Assays performed by WuXi AppTech.

The anticancer activity of 8CIA was confirmed in this set of data, with IC₅₀ values in the low micromolar range on all cell lines and reaching sub-micromolar values in the leukaemic cell lines CCRFCEM, Jurkat, MV4-11, MOLT4, on the myeloma cell line RPMI-8226 and on the mantle cell lymphoma Z138 cell line (Table 4.9, Table 4.10).

Similar ranges of values were also gathered on the pancreatic tumour cell line MIA PaCa-2, on the colorectal cancer cell lines HT29 and SW620 and on the hepatocellular carcinoma cell line HepG2 (Table 4.11).

Cpnd	NCI-H929		MV4-11		RL		RPMI-8226		MOLT-4		HL-60		Z138	
	IC ₅₀	MI%	IC ₅₀	MI%	IC ₅₀	MI%	IC ₅₀	MI%	IC ₅₀	MI%	IC ₅₀	MI%	IC ₅₀	MI%
8ClA	4.35	98	0.25	100	6.64	85	0.43	98	0.53	99	1.62	99	0.17	100
68c	8.82	101	2.18	92	31.95	94	7.7	91	4.15	95	8.67	84	4.32	86
68e	38.92	103	4.14	100	14.94	98	10.29	96	15.72	110	11.77	94	0.41	99
68f	10.58	98	0.24	99	7.15	73	0.47	99	0.82	99	1.29	99	0.34	100
68j	4.04	99	0.64	99	>19.8	51	1.65	100	3.12	100	6.16	100	1.5	102
71a	0.51	98	0.76	100	11.27	74	1.81	100	0.99	99	5.07	100	0.19	100
71d	1.2	98	0.76	100	10.14	77	1.42	100	1.24	99	3.66	100	0.33	100
71f	53.62	98	0.79	97	6.57	74	3.54	98	ND	ND	10.0	94	ND	ND
71g	38.05	99	3.64	96	>19.8	27	7.52	100	ND	ND	18.21	100	ND	ND
74a	4.28	98	0.85	100	>19.8	28	1.09	100	ND	ND	6.36	100	ND	ND
74e	4.8	99	1.47	100	10.86	66	1.57	100	ND	ND	4.79	100	ND	ND
74f	5.9	99	0.72	100	7.47	79	2.78	100	ND	ND	5.92	100	ND	ND
76b	4.97	103	0.39	100	1.74	94	0.70	98	0.50	100	0.39	100	0.20	98
PTX	0.003	82	0.01	99	0.003	83	0.003	91	0.003	95	0.003	85	0.002	99

Table 4.10 Biological evaluation of 8ClA and relative prodrugs (phenyl-bearing ProTides **68c,e,f,j**, naphthyl-bearing ProTides **71a,d,f,g**, **74a,e,f** and phosphorodiamidate **76b**) by WuXi app. tech. Cytotoxicity is reported as IC₅₀ μM values (50% inhibitory concentration of cell viability). MI% is the maximum percentage of inhibition exerted by compounds up to the top dose (198 μM). PTX: paclitaxel, positive control. Assays performed by WuXi AppTech.

Some of the screened compounds were consistently less active than 8ClA, as in the case of the phenyl derivatives **68c**, **68e** and the naphthyl-containing derivatives **71g**, **74e** and **74f**. Some compound gave generally poor results apart from some sporadic cases, such as the phenyl L-leucine benzyl ester derivative **68j**, more active than 8ClA only on the leukaemic cell line NCI-H929 cell line, and on the breast and pancreatic cell lines MCF7 and BcPC-3. The naphthyl counterpart **74a**, was generally less active than 8ClA, although in some cases generated submicromolar IC₅₀ values. Similarly to compound **68j**, the glycyl derivative **71f** had activity in the same range as 8ClA on the RL cell line, although with an IC₅₀ value of 6.57 μM.

Cpnd	MiaPaCa-2		SW620		HepG2		HT29		MCF7		BxPC-3		MDAMB231	
	IC ₅₀	MI	IC ₅₀	MI	IC ₅₀	MI	IC ₅₀	MI	IC ₅₀	MI	IC ₅₀	MI	IC ₅₀	MI%
8CI	0.50	93	0.83	88	0.79	82	0.87	79	2.15	75	12.8	67	3.08	74
68c	7.77	98	23.5	97	20.6	84	14.6	98	16.1	100	26.4	80	ND	ND
68e	9.53	106	35.4	85	13.8	85	24.3	86	30.8	94	39.0	66	ND	ND
68f	0.78	96	1.44	87	1.03	86	2.05	86	3.51	92	13.8	68	7.78	76
68j	1.77	99	2.47	100	1.51	100	2.53	92	1.48	97	9.72	99	15.31	99
71a	0.95	99	2.01	99	1.53	102	1.6	92	2.63	99	6.92	99	ND	ND
71d	1.28	100	2.47	99	2.57	101	3.28	91	1.91	98	11.8	92	ND	ND
71f	ND	ND	ND	ND	ND	ND	ND	ND	ND	ND	ND	ND	ND	ND
71g	ND	ND	ND	ND	ND	ND	ND	ND	ND	ND	ND	ND	ND	ND
74a	ND	ND	ND	ND	ND	ND	ND	ND	1.09	99	ND	ND	13.45	99
74e	ND	ND	ND	ND	ND	ND	ND	ND	ND	ND	ND	ND	ND	ND
74f	ND	ND	ND	ND	ND	ND	ND	ND	ND	ND	ND	ND	ND	ND
76b	0.52	94	1.23	94	1.24	87	1.64	87	1.08	87	8.59	68	ND	ND
PTX	0.00	87	0.02	96	0.04	50	0.00	75	0.01	65	>0.5	42	0.008	69

Table 4.11 Biological evaluation of 8CIA and relative prodrugs (phenyl-bearing ProTides **68c,e,f,j**, naphthyl-bearing ProTides **71a,d,f,g**, **74a,e,f** and phosphorodiamidate **76b**) by WuXi app. tech. Cytotoxicity is reported as IC₅₀ μM values (50% inhibitory concentration of cell viability). MI% is the maximum percentage of inhibition exerted by compounds up to the top dose (198 μM). Assays performed by WuXi AppTech.

On the other hand, compound phenyl glycine benzyloxy ProTide **68f**, already mentioned as a promising derivative, confirmed its potency with generally low IC₅₀ values and better potency than the parent nucleoside on CCRFCM, HEL92.1.7, K562 and HL60 cell lines, belonging to hematologic malignancies. The naphthyl L-alanine benzyloxy ProTide **71a** was 1 to 6-fold less active than the parent nucleoside, with the exception of cell lines NCI-H929 where it demonstrated an improvement in activity by ca. ten-fold, with an IC₅₀ value of 0.51 μM, in contrast with the poor results obtained with the phenyl analogue **68c**, on all cell lines. On the pancreatic cell line BxPC-3, compound **71a** was slightly more active than 8CIA, although at relatively high concentration (6.92 μM).

The phosphorodiamidate **76b** was one of the most active 8CIA phosphate prodrugs, with better potency compared to the parent nucleoside in the leukaemic cell lines CCRFCM, HEL92.1.7, K562, MOLT-4 and HL-60 and on the lymphoma cell line RL. This compound was also more active than 8CIA on the pancreatic and breast cancer cell lines BxPC-3 and MCF7, at low μM concentrations.

In conclusion, this second set of data helped identify compounds with improved activity compared to 8CIA on many of the considered cell lines, such as the phosphorodiamidate **76b**, the glycine derivative **68f**, belonging to the initial family of 8CIA prodrugs, and the L-alanine-bearing naphthyl analogue **71a**, all containing the benzyl ester moiety.

4.1.5.3 Biological evaluation of selected ProTides on resistant cell lines

The cytotoxic activity of 8ClA and the ProTides **68e**, **68f** and **71a** was evaluated on a set of leukaemic cell lines by Barts Institute (London), both under normal conditions and under induced resistance conditions, by inhibiting adenosine kinase and equilibrative nucleoside transporter (hENT1), essential for the activity of 8ClA. Moreover adenosine deaminase deficiency was induced in cells, in order to evaluate the extent of ADA-mediated inactivation of 8ClA and the putative stability of ProTides in these conditions. Compounds **68f** and **71a** were selected due to the favourable cytotoxicity profile in the previous screenings, while **68e** was chosen as a weakly performing ProTide in order to have a negative control that could validate the data (Table 4.12).

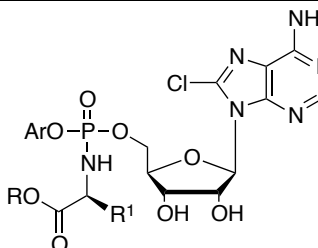
Common structure	Cpnd	Ar	R	R ¹	AA	cLogP
	8ClA	-	-	-	-	-1.44
	68e	Ph	cHx	H	Gly	1.40
	68f	Ph	Bn	H	Gly	1.08
	71a	Nap	Bn	Me	L-Ala	2.37

Table 4.12 Selected compounds for *in vitro* cytotoxicity evaluation on resistant cell lines. cLogP calculated with Chem Draw 2010 software. Assays performed by Barts Institute.

These assays were conducted on the leukaemic cell lines HL60 (human acute promyelocytic leukaemia), CTS (human acute myeloid leukaemia) and K562 (chronic myelogenous leukaemia). Resistance conditions were generated by the pre-treatment of the same cells with one of the following inhibitors: the ADA inhibitor erythro-9-(2-hydroxy-3-nonyl) adenine (EHNA) or the AK inhibitor N⁷-[(1'*R*,2'*S*,3'*R*,4'*S*)-2',3'-dihydroxy-4'-aminocyclopentyl]-4-amino-5-iodopyrrolopyrimidine dihydrochloride hydrate (A-134974) or the hENT1 inhibitor S-(4-nitrobenzyl)-6-thioinosine (NBTI), reported in Figure 4.5.

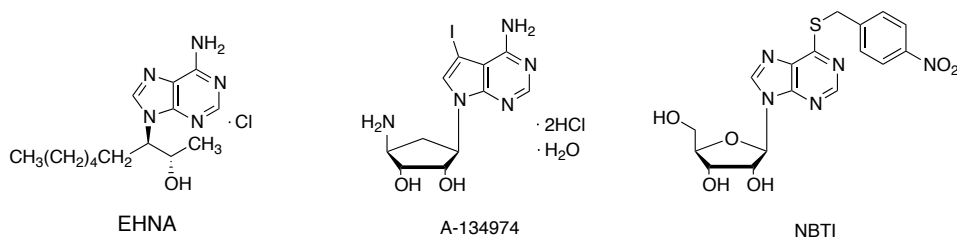


Figure 4.5 Structures of the ADA inhibitor EHNA, AK inhibitor A-134974 and hENT1 inhibitor NBTI.

When tested on cell lines not previously treated with inhibitor (Figure 4.6, Table 4.13-column **A**), 8CIA had EC₅₀ values in the submicromolar range, ranging from 0.32 to 0.64 μM on the three cell lines considered. When the cells were pre-treated with hENT1 nucleoside transporter inhibitor (Figure 4.6, Table 4.13-column **B**), the activity of 8CIA was roughly retained in the HL60 cell line, while it decreased considerably in CTS and K562 cells, respectively by 8 and 7-fold. This data confirmed the dependency of the nucleoside on the hENT-1 nucleoside transporter in CTS and K562 cell lines, and may suggest that it uses a different transport mechanism in HL60 cells. On the other hand, when cells were treated with an adenosine kinase inhibitor (Figure 4.6, Table 4.13, column-**C**), 8CIA was inactive up to the highest concentration considered (20 μM) in all cell lines, confirming that the activity of 8CIA is highly dependent on the first phosphorylation step catalysed by AK. The inhibition of adenosine deaminase (Figure 4.6, Table 4.13, columns-**D**), did not visibly affect 8CIA activity, in agreement with the already reported low substrate recognition of this nucleoside by ADA.³³²

Comp.	HL60				CTS				K562			
	A	B	C	D	A	B	C	D	A	B	C	D
8CIA	0.64	0.96	>20	0.04	0.32	5.48	>20	0.54	0.64	4.69	>20	0.32
68e	12.4	>20	>20	>20	>20	>20	>20	>20	>20	>20	>20	>20
68f	0.49	8.76	14.62	0.93	16.3	>20	>20	1.54	2.86	12.8	>20	7.94
71a	0.33	1.23	21.3	1.07	2.64	1.46	10.3	2.63	6.63	1.73	19.7	12

Table 4.13 Biological evaluation of 8CIA and ProTides **68e**, **68f** and **71a** by Barts Institute. Cytotoxicity reported as EC₅₀ μM values (50% effective concentration on inhibition of cell viability). **A**: control. **B**: cells pretreated with NBTI (ENT inhibitor). **C**: cells were pretreated with A-134974 (AK inhibitor). **D**: cells were pretreated with EHNA (ADA inhibitor). Assays performed by Barts Institute, London.

ProTide **68e** (GlyOchHex phenyl), chosen as a poorly cytotoxic ProTide in order to have a negative control, confirmed its cytotoxic profile as it was found to be inactive in all cell lines considered, up to the top concentration used (20 μM) apart from a 12.4 μM EC₅₀ value on the HL60 cell line. Likewise, the EC₅₀ values of **68e** were consistently higher than 20 μM also in resistance conditions, and when ADA was inhibited. These results reflect the previously reported IC₅₀ data regarding compound **68e**, which were generally higher than 15 μM.

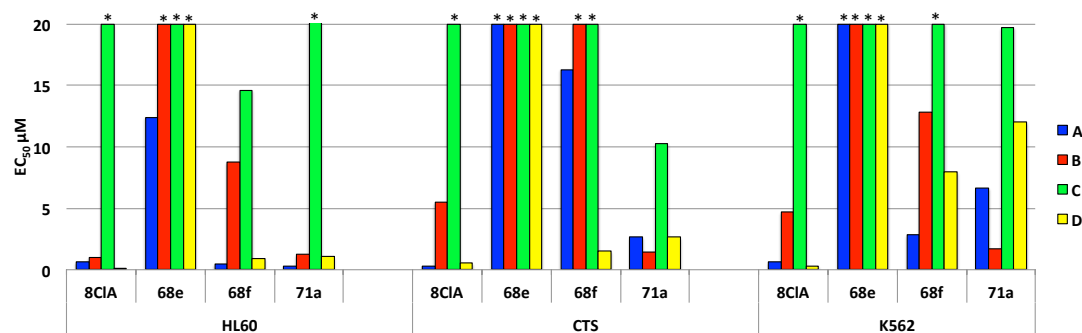


Figure 4.6: Biological evaluation of 8ClA and ProTides **68e**, **68f** and **71a**. Cytotoxicity reported as EC₅₀ µM values (50% effective concentration on inhibition of cell viability). **A**: control. **B**: cells pretreated with NBTI (ENT inhibitor). **C**: cells were pretreated with A-134974 (AK inhibitor). **D**: cells were pretreated with EHNA (ADA inhibitor). Assays performed by Barts Institute, London.

ProTide **68f** was approximately as active as 8ClA on the HL60 cell line but respectively 51 and 5-fold less active in the CTS and K562 cell lines. When cells were pre-treated with a hENT-1 inhibitor, the activity of this compound dropped by 18 and 4.5-fold in HL60 and K562 and was completely lost in CTS cell line. This surprising data may suggest a relation between the activity of this compound and this nucleoside transporter. In fact, **68f** could penetrate the cell through passive diffusion and once within the cell it could be enzymatically and/or chemically processed to release 8ClA (Figure 4.7). The nucleoside could be a substrate of an efflux pump.^{354,355} In the eventuality of 8ClA being expelled from the cell, and hENT1 being inhibited, the penetration inside the cell would be halted, hence potentially the reduced activity of **68f** is due to hENT1 inhibition.

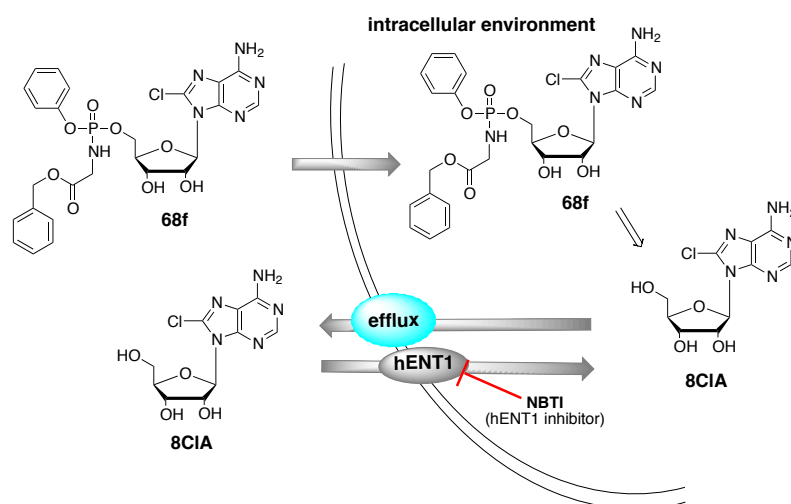


Figure 4.7: Putative explanation for compound **68f** reduced activity after hENT1 inhibition.

Similarly, **68f** activity decreased when the cells were treated with an AK inhibitor, becoming completely inactive up to 20 µM concentration in CTS and K562 cell lines, and

losing 30-fold potency in HL60 cell line. This result, compared to the drop in potency of 8CIA in the same conditions, may again confirm the conversion of **68f** into 8CIA within the cell, therefore the dependency on AK for intracellular activation to 8CIAMP. The prodrug **68f** was also affected by ADA inhibition on CTS cell line, in fact pre-treatment with ENHA caused an increase in the activity by 10-fold. On the other hand, the activity on the other cell lines treated in the same conditions did not differ from the untreated settings.

Compound **71a** was 8 to 10-fold less active than 8CIA on CTS and K562 cells, and approximately as active as 8CIA on the HL60 cell line. When the hENT1 inhibitor NBTI was used, the activity of this prodrug was generally retained in all the cell lines tested. Although the activity of **71a** decreased in parallel to the inhibition of AK, the compound still maintained a considerable cytotoxic activity in the micromolar range (EC_{50} values ranging from 10.3 to 21.3 μ M). On the other hand, the cytotoxicity of **71a** remained constant after ADA inhibition. Considering these data, compound **71a** emerged as the only ProTide able to generally overcome the mechanisms of resistance to 8CIA, by maintaining the cytotoxic activity even after inhibition of hENT1 and AK and being unaffected by ADA inhibition.

4.1.5.4 ATP assay on 8CIA ProTides

The cytotoxic activity of 8CIA and the prodrugs **68e**, **68f** and **71a** was also monitored through ATP assay by Dr. E. Ghazaly at the Barts Institute (London), by measuring the intracellular ratio between 8CIATP and ATP after cell treatment. In fact, one of the mechanisms of action of 8CIA is the decrease in this ratio, due to the competition between 8CIADP and ADP for the ATP-synthase enzyme, which leads to an increase in intracellular 8CIATP at the expense of ATP.³³⁶ As visible from the results reported in Figure 4.8, the ratio of 8CIATP/ATP was close to 1 when HL60, CTS and K562 cells were treated with 8CIA. The inhibition of hENT1 halved this ratio to 0.5, while AK inhibition seemed to totally abolish the level of 8CIATP inside the cells, lowering the ratio down to 0. On the other hand, treatment of cells with the ADA inhibitor EHNA did not significantly affect 8CIATP levels after treatment with 8CIA, generating a 8CIATP/ATP ratio close to unity.

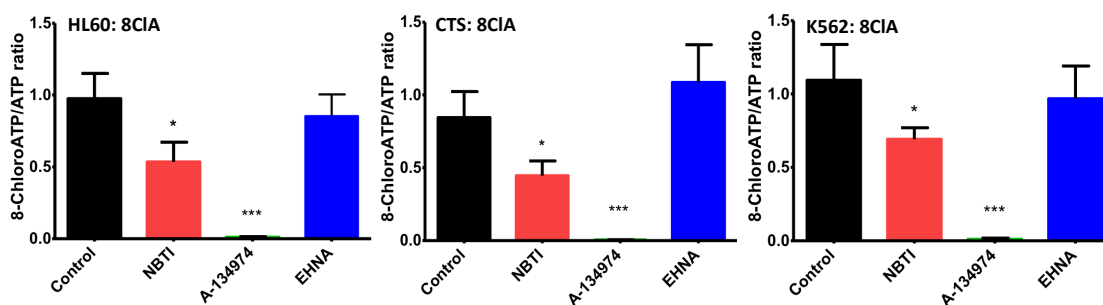


Figure 4.8: 8ClATP/ATP ratio after treatment of the cells with 8CIA (control), 8CIA and hENT1 inhibitor (NBTI), 8CIA and AK inhibitor (A-134974), 8CIA and ADA inhibitor (EHNA). Assays performed at Barts Institute, London.

The treatment of the cells with compound **68e** generated 8ClATP levels much lower than after treatment with 8CIA, inducing a ratio of 8ClATP/ATP ranging from 0.02 and 0.05 in all cell lines considered (Figure 4.8). Both pre-treatments of the cells with hENT1 and AK inhibitors did not significantly affect the ratio of 8ClATP/ATP generated by treatment with compound **68e**.

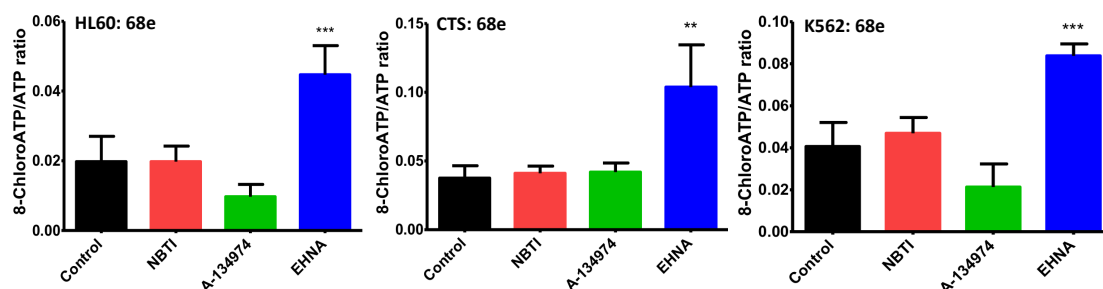


Figure 4.9: 8ClATP/ATP ratio after treatment of the cells with **68e** (control), **68e** and hENT1 inhibitor (NBTI), **68e** and AK inhibitor (A-134974), **68e** and ADA inhibitor (EHNA). Assays performed at Barts Institute, London.

However, ADA inhibition increased the ratio of 8ClATP/ATP, an explanation could be that the levels of 8ClATP released upon treatment with **68e** would be low and therefore ADA inhibition would mainly affect the levels of ATP. When these level decrease the ratio inevitably increases. When cells are treated with compound **68f**, as expected from the poor cytotoxic profile in the previously described assays, the levels of 8ClATP recorded are low, therefore the ratio of 8ClATP/ATP is close to 0.1, one-tenth of the levels generated by treatment with 8CIA (Figure 4.10).

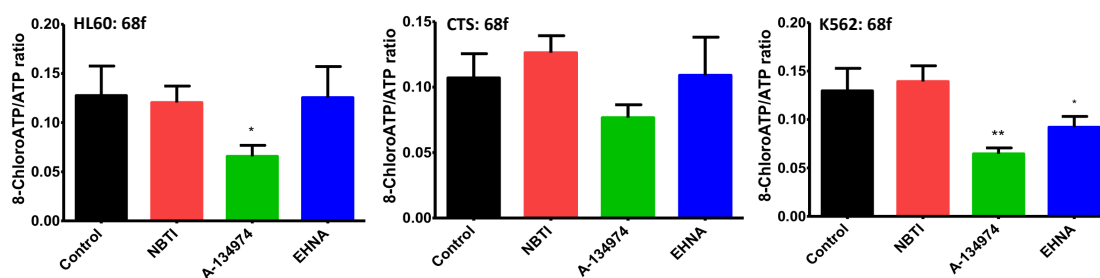


Figure 4.10: 8ClATP/ATP ratio after treatment of the cells with **68f** (control), **68f** and hENT1 inhibitor (NBTI), **68f** and AK inhibitor (A-134974), **68f** and ADA inhibitor (EHNA). Assays performed at Barts Institute, London.

The 8ClATP released by treatment with compound **68f** are generally unaffected by treatment with hENT1, AK or ADA inhibitors. In contrast, upon treatment with compound **71a**, the intracellular levels of 8ClATP were raised compared to the treatment with other ProTides, reaching a ratio of 8ClATP/ATP ranging from 0.6 and 0.8, similar to the 8ClA related ratios (Figure 4.10).

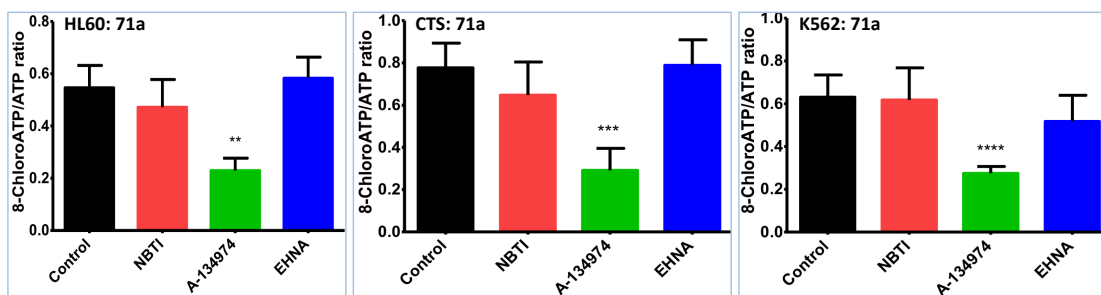


Figure 4.11: 8ClATP/ATP ratio after treatment of the cells with **71a** (control), **71a** and hENT1 inhibitor (NBTI), **71a** and AK inhibitor (A-134974), **71a** and ADA inhibitor (EHNA). Assays performed at Barts Institute, London.

The 8ClATP/ATP ratio was not significantly affected by hENT1 and ADA inhibition and only marginally by AK inhibition. These data suggested that compound **71a**, although not as active as 8ClA in normal conditions, is many-fold more potent than compounds **68e** and **68f** both in terms of cytotoxic activity and considering the 8ClATP levels generated in the intracellular compartment. Moreover, when tested in conditions of AK-deficiency, both cytotoxicity and release of 8ClATP after treatment with **71a** were retained, conversely to the complete drop in potency of 8ClA under the same conditions. This suggests that ProTide **71a** could potentially behave as an efficient prodrug of 8ClAMP especially in resistance conditions, and that it may represent a significant new lead.

4.1.6 8CIA and prodrug stability

4.1.6.1 8CIA ProTides stability in plasma

The optimal metabolism of ProTides depends on their chemical and enzymatic stability. Upon administration, the circulating ProTides are exposed to challenging conditions, such as catabolic enzymes in the liver, and they should resist long enough to enter tumour cells before being degraded. Conversely, ProTides unaffected by enzymatic digestion might not be efficiently converted into active compounds inside the cancer cells. Drug stability in human plasma was assayed by Barts Institute (London), both in the presence and in absence of the ADA inhibitor EHNA. Plasma contains ADA, therefore the concentration of substrates of this catabolic enzyme should decrease in plasma over time. 10 $\mu\text{g/mL}$ concentrations of 8CIA and ProTides **68e**, **68f** and **71a** were incubated in untreated plasma at 37 °C for 2 hours and their concentration was later analysed in the sample to monitor the stability of compounds to ADA-mediated catabolism. The same assay was repeated after treatment of plasma with EHNA (Figure 4.12).

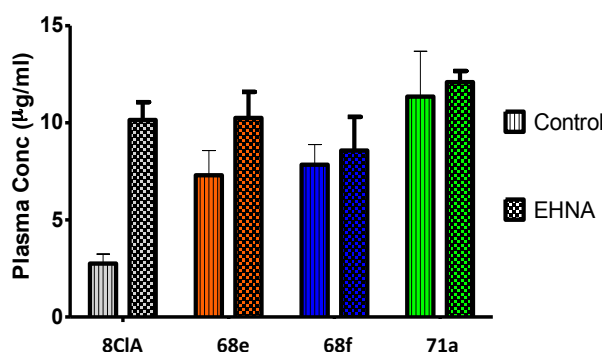


Figure 4.12 Concentration of compounds left after incubation in untreated plasma (control) and plasma treated with ADA-inhibitor (EHNA). Assays performed at Barts Institute, London.

8CIA is less stable than ProTides **68e**, **68f** and **71a** in plasma, in fact after 2 hours incubation the concentration of the parent nucleoside is significantly lower compared to ProTide concentrations, indicating a higher susceptibility to ADA-mediated catabolism. Moreover, inhibiting ADA by EHNA the stability of 8CIA increases, while the residual concentrations of ProTides **68e**, **68f** and **71a** are not significantly affected by ADA inhibition. These results suggest that 8CIA is a substrate of ADA, as previously reported,³⁴¹ while this enzyme does not affect ProTides stability, in human plasma.

4.1.6.2 8CIA ProTide stability in human hepatocytes

The stability of 8CIA and ProTides **68e**, **68f** and **71a** was further assayed by Eurofins CEREP laboratories (USA) in cryopreserved human hepatocytes.

Compound	$t_{1/2}$	Cl_{int}
8CIA	>120	<8.2
68e	39	25.70
68f	57	17.60
71a	53	18.70

Table 4.14 Stability of 8CIA (**1**) and ProTides **68e**, **68f** and **71a** in human hepatocytes, defined as $t_{1/2}$ (half life reported in minutes) and intrinsic clearance (Cl_{int} expressed in $\mu\text{L}/\text{min}/10^6$ cells). Assays performed by Eurofins CEREP laboratories, USA.

The parent nucleoside is very stable in the assay conditions, with a half-life higher than 120 minutes. This would suggest that the molecule is not a substrate of catabolic enzymes although this would be in contrast with the previously reported data, which underline increased stability of the nucleoside in the presence of the ADA inhibitor EHNA. On the other hand, the half-lives of 8CIA ProTides **68f** and **71a** are very similar and just under 1 hour, representing an appropriate stability compared to other ProTides in the clinic.¹⁵¹ Compound **68e** is slightly less stable, with a half-life under 40 minutes.

4.1.7 Evaluation of 8CIA ProTides on the CSC compartment of the KG1a cell line

A pilot unpublished study of the gemcitabine ProTide NUC-1031 currently in Phase III clinical trial and developed by the McGuigan group indicated some selectivity for the leukaemic stem cell compartment when compared to gemcitabine. This interesting result prompted the McGuigan group to study the effect of the most promising nucleoside prodrugs on the stem-like cell compartment of KG-1a cell line.

Similarly to the studies performed on 3'dA and relative ProTides, this study was performed on the KG-1a cell line, which is an acute myeloid leukaemia cell line manifesting a minor stem cell-like compartment with a distinct immunophenotype ($CD34^+/CD38^-/CD123^+$). 8CIA and ProTides **71a**, **68f** and **71d** (Table 4.15) were tested on the KG1a cell line and LD_{50} values (the concentration required to kill 50 % of the cells) were determined by Prof. C. Pepper (School of Medicine, Cardiff University).

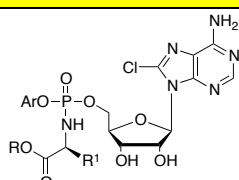
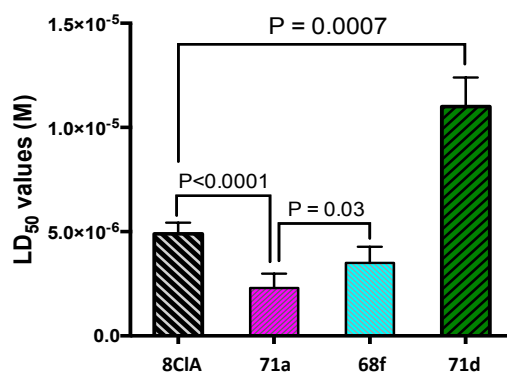
Cpnd	Common structure	Ar	R	R ¹	AA
8CIA		-	-	-	
68f		Ph	Bn	H	Gly
71a		Nap	Bn	CH ₃	L-Ala
71d		Nap	<i>n</i> -Pen	CH ₃	L-Ala

Table 4.15: 8CIA ProTides selected for evaluation of potential CSC selective cytotoxicity.

The cells were then treated with the calculated LD₅₀ concentration and the effect generated on the KG1a sub-population expressing the immunophenotype (CD34⁺/CD38⁻/CD123⁺) was subsequently identified via immunophenotypic identification of the leukaemic stem cell compartment, as percentage of all viable cells left in the culture. The percentages of stem cells remaining were then plotted on a dose-response graph and the effects of the ProTides were compared with the parent nucleosides.

Figure 4.13: Cytotoxic evaluation of 8CIA and relative ProTides **71a,d** and **68f** on KG1a cell line. LD₅₀: concentration required to kill 50 % of the cells. Data are presented as mean (±SD) of five independent experiments Assays performed by Prof. C. Pepper, Cardiff University.

Cpnd	LD ₅₀ values (μM)	KG-1a (CD34 ⁺ /CD38 ⁻ /CD123 ⁺) %
Control	-	3.3
8CIA	9.7	3.7
68f	7.1	2.7
71a	3.8	2.5
71d	20	3.5

Table 4.16: LD₅₀ cytotoxicity (μM) values for 8CIA and relative ProTides **71a,d** and **68f**. Percentage of CSCs left after treatment with the LD₅₀ dose of each compound. All assays were carried out using KG1a cells. Assays performed by Prof. C. pepper, Cardiff University.

Table 4.16 shows that ProTides **68f** and **71a** are more potent than 8CIA on the KG1a cell line, while **71d** has a much higher LD₅₀ value. The percentage of CSCs in the untreated sample (control) was 3.3%. When cells were treated at the LD₅₀ concentration of 8CIA and

compound **71d**, the percentage of stem cell population increased to respectively 3.7 and 3.5%. On the other hand this population decreased to 2.7% and 2.5% respectively after treatment with **68f** and **71a** at their respective LD₅₀s. These results suggested that some ProTide structures may offer an advantage over the parent nucleoside in terms of CSCs selectivity which could be linked to an increased cytotoxicity (as in the case of compound **71a**).

A further study was designed to extend these investigations and generate a more complete dose-response curve for ProTides **68f**, **71a** and **71d** and 8CIA, in order to evaluate the effect on the LSC compartment not only at the LD₅₀ values of each compound, but at a range of concentrations reaching 1mM. Compounds **68f** and **71a** demonstrated again a preferential LSC targeting when compared to 8CIA. These effects were observed at concentrations up to 1μM. There was no significant difference in the ability of **68f** and **71a** to deplete LSCs at this range of concentrations.

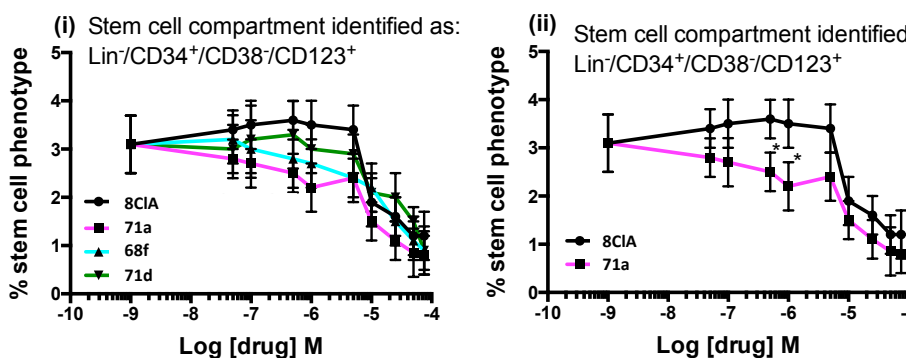


Figure 4.14: Analysis of the LSC targeting capacity of 8CIA and proTides **71a**, **68f** and **71d**. All data are the mean (\pm SD) of three independent experiments. Assays performed by Prof. C. pepper, Cardiff University.

The effect of ProTide **71a** to decrease the CSCs percentage in a KG1a cells sample might derive from a selective killing of these cells. Alternatively, the drug might induce a differentiation of these stem-like cells into bulk tumour cells. This would similarly lead to a reduction in % of CSCs in the sample. Further studies are ongoing to understand these results.

4.1.8 Mechanistic investigations

In order to suggest an explanation for the better *in vitro* activity of some of the 8CIA ProTides over others, enzymatic studies of the ester hydrolysis and molecular modelling studies of the Hint-1 processing of the phosphoramidate monoesters were carried out.

4.1.8.1 CPY NMR assays

CPY enzymatic experiments were carried out on three 8ClA prodrugs, bearing the same L-alanine benzyl ester motif: the ProTides **71a** and **68c**, respectively bearing naphthyl and phenyl aryloxy groups, and the diamidate **76a**. The aim of these experiments was to understand whether the higher activity of both **71a** and **76a** over **68c** on the cell lines L1210, CEM and HeLa could derive from a better intracellular processing to the same intermediate 5'-L-alaninyl-8-chloroadenosine. Moreover, ProTide **71a** showed consistently better activity on a broader selection of cell lines, compared to the phenyl-containing counterpart (**68c**).

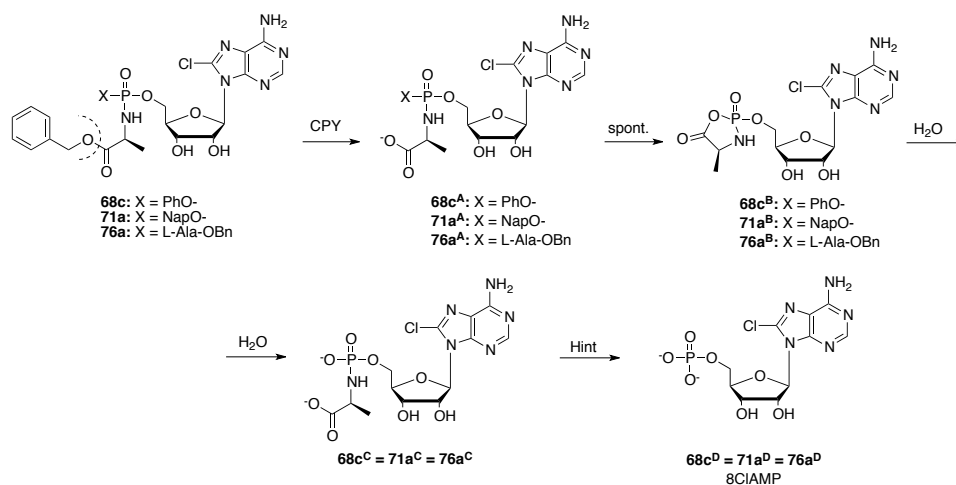


Figure 4.15: Putative enzymatic activation of ProTides **68c**, **71a** and diamidate **76a** by CPY. (a.) carboxypeptidase-catalysed ester cleavage. (b.) intramolecular cyclisation with release of the aryloxy/amino acid ester moiety. (c.) ring opening *via* hydrolysis.

The conversion of **71a** into intermediate **71a^A** (Figure 4.15) after benzyl ester cleavage by CPY enzyme was complete in 35 minutes as suggested by the formation of two additional signals at a more downfield chemical shift (Figure 4.16). The conversion into derivative **71a^C** was confirmed by the appearance of a peak at 7 ppm and by mass analysis of the crude sample after 12 hours.

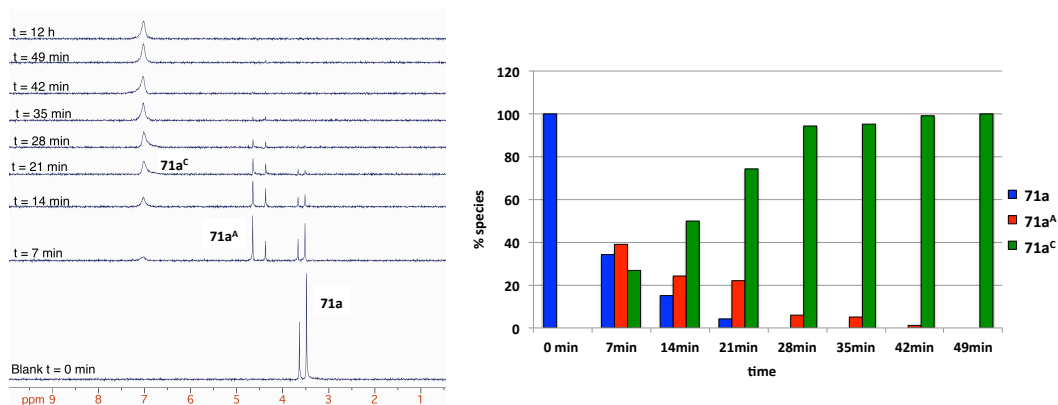


Figure 4.16: ^{31}P NMR monitoring of **71a** metabolism by CPY enzyme (Acetone- d_6 , 202 MHz).

A similar picture appeared after treatment of ProTide **68c** in the same conditions, yielding complete conversion to intermediate **68c^C** within 37 minutes.

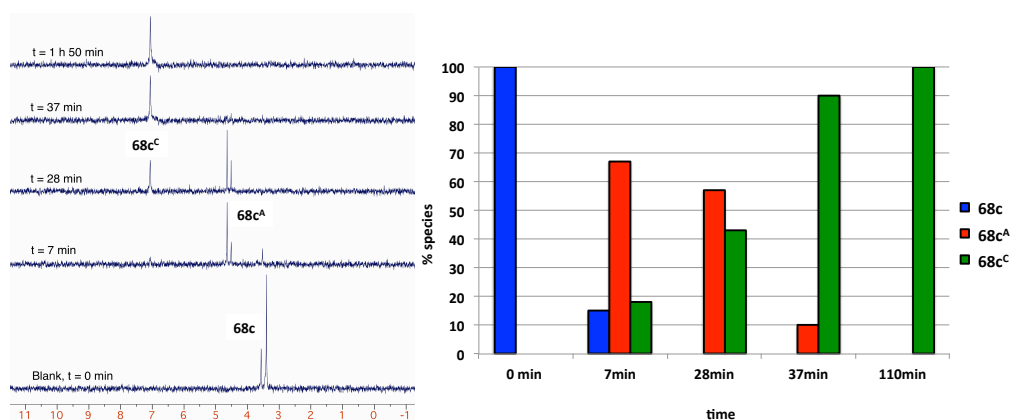


Figure 4.17: ^{31}P NMR monitoring of **68c** metabolism by CPY enzyme. (Acetone- d_6 , 202 MHz).

The same assay was performed on phosphorodiamidate **76a** and the conversion of the initial signal belonging to the prodrug at 13.6 ppm into a more downfield peak corresponding to intermediate **76a^A** was complete along with the formation of the final metabolite **76a^C**, within 57 minutes. Notably all of the compounds assayed gave an identical final peak in the ^{31}P NMR, consistent with the proposed metabolic route.

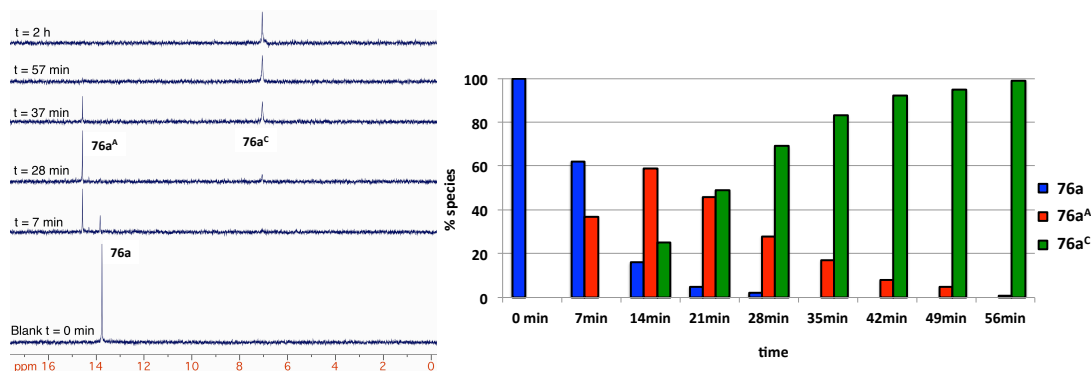


Figure 4.18: ^{31}P NMR monitoring of **76a** metabolism by CPY enzyme. (Acetone- d_6 , 202 MHz).

ProTides **71a** and **68c** were efficiently converted into the final common intermediate **71a^C** = **68a^C** within 37 minutes, while the phosphorodiamidate **76a** required twenty more minutes for complete conversion into **71a^C** = **68a^C**. This result might explain the relatively lower activity of **76a** compared to **71a** but not the improved activity of **76a** over **68c**. Moreover the very similar processing of **68c** and **71a** cannot explain the significantly improved activity of the naphthyl analogue (**71a**) over the phenyl derivative (**68c**). However, considering the differences in lipophilicity of the three considered compounds, in terms of cLogP corresponding to 1.19, 2.37 and 3.17 respectively for compounds **68c**, **71a** and **76a**, it could be suggested that a higher cLogP could cause an increase in activity of the compound. This could be a consequence of more efficient cell entering *via* passive diffusion. Therefore, this could explain the low activity of **68c** due to low lipophilicity compared to **71a**, and the better activity of **76a** over **68c**, in spite of the slower processing by CPY.

4.1.8.2 Molecular modelling studies

4.1.8.2.1 Docking of ProTides in the active site of CPY

As noticeable from *in vitro* cytotoxicity data, some ProTide moieties showed significantly better activity than others on most of the cell line considered. Some clear examples within the naphthyl-bearing family of ProTides are the superior activity of the L-alanine benzyl ester derivative **71a**, compared to compounds bearing glycine cyclohexyl ester (**71h**) and the L-leucine ethyl ester **74d**. An explanation for the substantial loss in activity of the latter compounds could be an inefficient intracellular processing. In order to understand whether this could be a consequence of inadequate recognition by the carboxypeptidase enzyme

responsible for the cleavage of the ester moiety, docking studies within the active site of CPY were carried out. The crystal structure of CPY was downloaded from the protein data bank (PDB 1YSC),³⁵⁶ interactions between each selected ProTide diastereoisomer and the crucial residues within the active pocket (Ser146, Gly53, Gly54) were analysed with MOE software. The residue Ser146 is responsible for the nucleophilic attack at the carbonyl group of the ester, and the glycine residues facilitate the right positioning of the ester moiety by forming H-bonds with the carbonyl group. The likelihood of correct interaction of each structure with the crucial residues was predicted by measuring the distances between the carbonyl group and the hydroxyl (Ser146) and amido (Gly53 and 54) groups.

As shown in Figure 4.19, the close positioning (a distance within 4.68 Å) of the carbonyl moiety of both isomers of compound **71a** from the specific residues could potentially predict a more efficient ester cleavage by CPY, while the increased distance of compounds **71h** and **74d** (respectively within 6.88 and 6.02 Å) could suggest that the low activity derives from a less efficient processing. This could be caused by the hindrance and rigidity of the cyclohexyl ester for compound **71h** and the presence of the bulky L-leucine amino acid for **74d**, causing a mispositioning of the carbonyl portion of the relative ProTides.

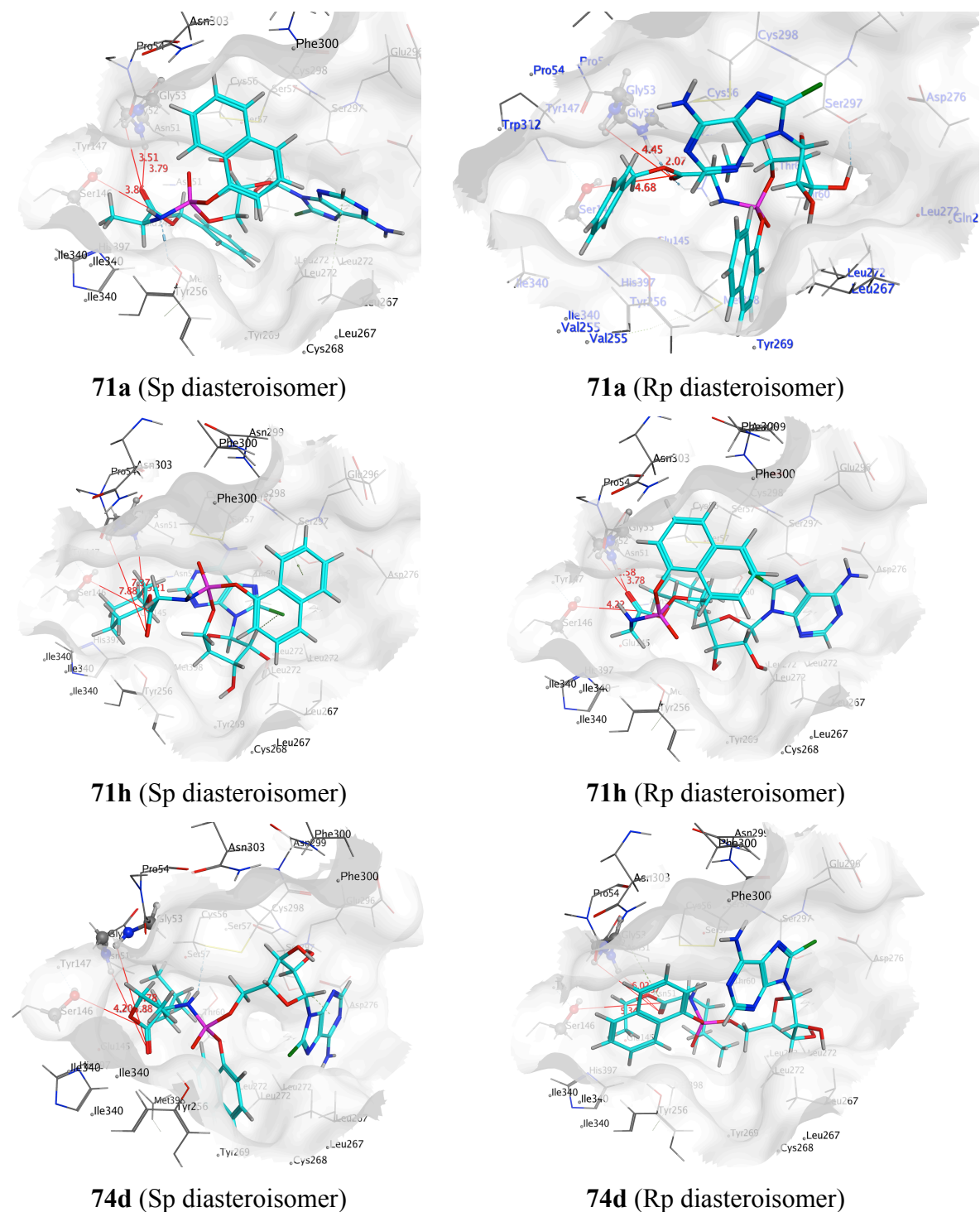


Figure 4.19: Docking of ProTides **71a**, **71h** and **74d** (each diastereoisomer) within the active site of CPY.

4.1.8.2.2 Docking of compounds in the active site of Hint-1

The second enzymatic step required for the activation of ProTides is the phosphoramidate bond cleavage, and the enzyme responsible for this step was reported to belong to the human histidine triad nucleotide-binding proteins (Hint).^{135,261} Adenosine monophosphate-bound amines are natural substrates of Hint, and the residues of Ser107, His 112 and

His114 are implicated in the P-N bond cleavage, therefore the distances between these residues and the phosphoramidate portion of substrates is crucially involved in the processing.

Dockings of the glycinyll and L-alaninyll monoester 8ClA intermediates (respectively **68c^C**, **71a^C**, **76a^C** and **77**) were carried out within the binding site of Hint enzyme.

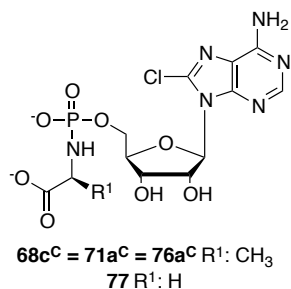


Figure 4.20: Structures of L-alaninyll (**68c^C**, **71a^C**, **76a^C**) and glycinyll (**77**) phosphate monoester derivatives of 8ClA docked within the active site of Hint enzyme.

These structures represent intermediates in the activation process of the families of glycine and L-alanine-bearing ProTides and phosphorodiamidates, which yielded some of the most active derivatives such as **71a**, **68f**, **76a** and **76b**. The very similar and close distances between both structures and the crucial residues of Hint suggest that a correct positioning within the binding site is the cause of the good activity of these analogues, as a consequence of efficient processing to 8ClAMP by Hint.

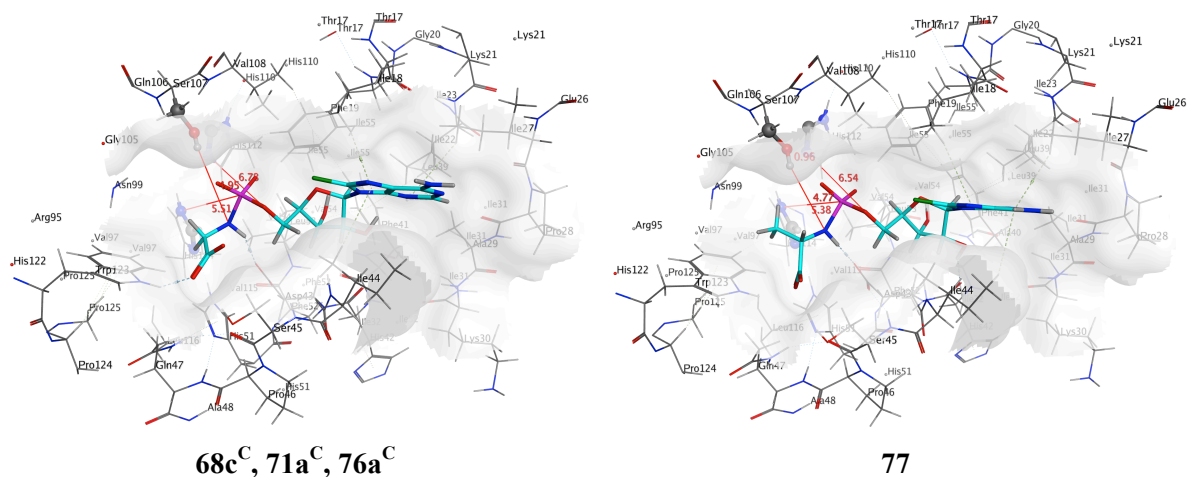


Figure 4.21: Docking of L-alaninyll (**68c^C**, **71a^C**, **76a^C**) and glycinyll (**77**) phosphate monoester derivatives of 8ClA within the active site of Hint.

4.1.9 Conclusions

The nucleoside analogue 8CIA, currently involved in phase III clinical studies against CML, was already considered by the McGuigan group as an interesting target for the application of a prodrug approach. In a previous programme, phenyl-bearing 8CIA ProTides were synthesised and tested *in vitro*, showing an interesting cytotoxic profile, although no improvement over the already active parent nucleoside. In this work, expansion of the 8CIA prodrug family was carried by synthesising naphthyl-bearing ProTides and phosphorodiamidates of 8CIA. Cytotoxic *in vitro* evaluation of these prodrugs on an extensive selection of cancer cell lines helped the identification of prodrugs with improved anticancer activity over the parent nucleoside, such as the naphthyl-bearing derivative **71a**, the phenyl-bearing compound **68f** and the phosphorodiamidate **76b**. A selection of derivatives was selected for cytotoxic evaluation in resistance conditions caused by inhibition of AK and hENT1 and ProTide **71a** proved to be the only derivative able to consistently retain cytotoxicity. Moreover, the activity of this compound correlated with intracellular levels of 8CIATP in the cell, which were retained in resistance conditions, unlike the parent nucleoside. In addition, **71a** was the most stable analogue to ADA-catalysed breakdown, both in cell culture and in plasma. The same analogue demonstrated stability to hepatocellular metabolism, showing a half-life comparable to ProTides currently in the clinic. A selection of compounds was also evaluated on the KG1a cell line and the effect on the CSC compartment was assayed. ProTides **71a** and **68f** showed the most significant reduction in the CSC population, suggesting a preferential targeting for this compartment.

Finally, mechanistic investigations performed both via CPY enzymatic metabolism and by docking within the active pocket of both CPY and Hint helped to reach the conclusion that the superior activity of L-alanine and glycine benzyl ester derivatives could be a consequence of efficient ester cleavage due to correct positioning in the active pocket of the carboxypeptidase enzyme. Moreover both glycinylnyl and L-alaninylnyl monoester intermediates fit correctly in the active site of Hint, suggesting an additional quick P-N bond cleavage with release of 8CIAMP.

The identification of **71a** as an active 8CIA derivative, capable of bypassing resistance mechanisms related to 8CIA activity is promising for pursuing this prodrug in further pre-clinical investigations.

Moreover, the promising *in vitro* activity of phosphorodiamidate **76b** should be investigated more thoroughly, also in resistance conditions, and a broader family of 8CIA

phosphorodiamidates should be prepared, carefully considering a balance between good enzymatic processing and lipophilicity of the prodrug.

4.2 5'-Modified 8-chloroadenosine analogues

4.2.1 Rationale behind the 5'-modification on 8ClA ProTides

In an attempt to improve the activity of 8ClA ProTides, the modification of the phosphate structure into a phosphonate was carried out.

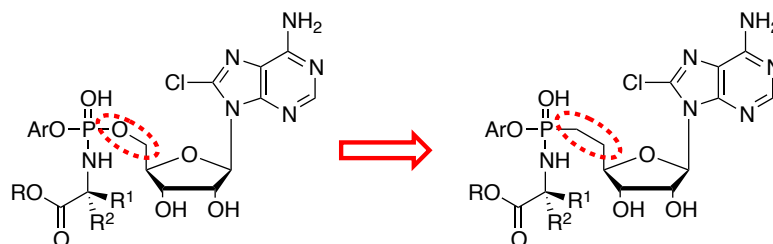


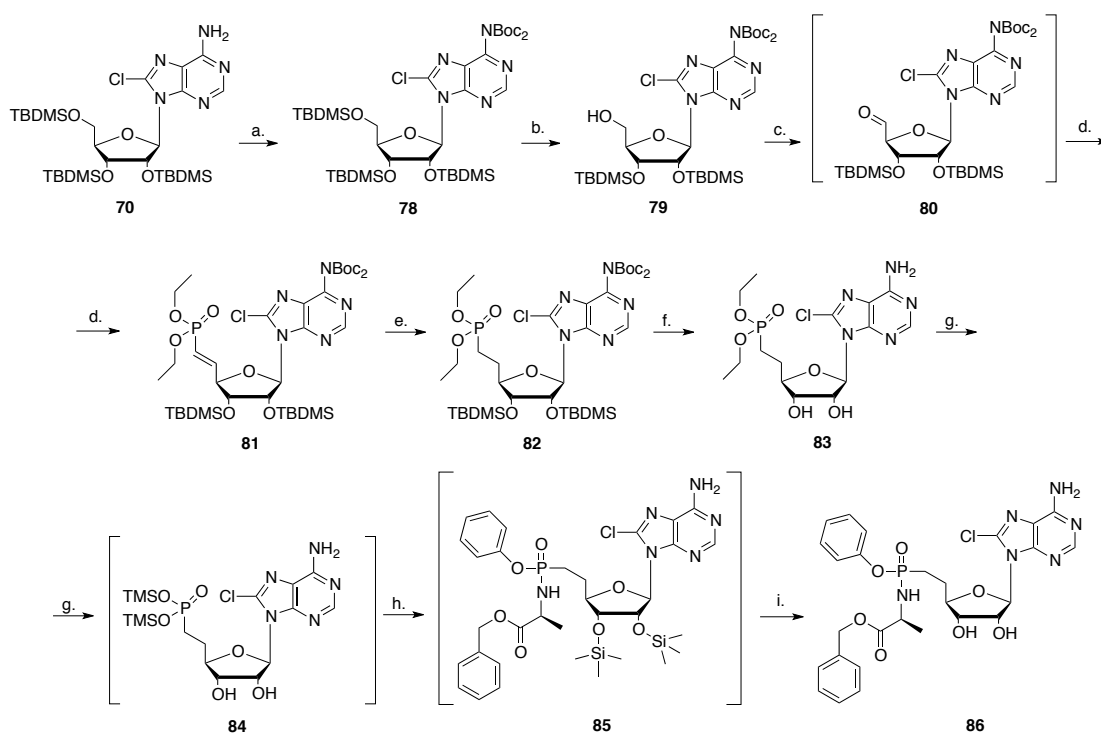
Figure 4.22: Modification of the phosphate moiety of 8ClA ProTides into a phosphonate group.

After a thorough investigation of the cytotoxic activity of a broad selection of differently modified 8ClA ProTides, most of the derivatives did not improve the biological potential of the parent nucleoside. Some analogues, such as the ProTide **71a** and phosphorodiamidate **76b**, were found to be more potent than the parent nucleoside by 1 to 3 fold. However, evaluation of some 8ClA ProTides in resistance conditions revealed that the inhibition of both the nucleoside transporter hENT1 and adenosine kinase enzyme led to a decrease in cytotoxicity of some of the tested derivatives. Hence, this could be a consequence of the lability of the phosphate bond of 8ClAMP, released after intracellular processing of 8ClA ProTides. In order to investigate the validity of this hypothesis, and the potential benefit of stabilising the phosphate bond in terms of cytotoxic activity,³¹² phosphonate derivatives of 8ClA ProTides were synthesised.

This methodology has already been applied in this work to the family of 3'dA ProTides, with the synthesis and biological evaluation of phosphonate prodrug **64**, which was found to be endowed with a 10-fold improved cytotoxic activity compared to the parent nucleoside. Although this derivative was not as potent as the phosphate ProTide counterpart **30a**, the promising anticancer activity of this compound prompted the application of this method to other promising families of ProTides, such as 8ClA derivatives.

4.2.2 Synthesis of 8ClA phosphonate ProTides

The synthetic strategy applied for the synthesis of 8ClA phosphonate ProTides was similar to the one used for the synthesis of phosphonate prodrugs of 3'dA. The starting material was the silyl protected derivative **70**, synthesised according to Scheme 4.5. As previously mentioned, the synthetic pathway to prepare phosphonoamidate prodrugs requires initial protection of amino and hydroxyl groups in the starting material.²⁹⁹ The adenine amino group was therefore protected with *tert*-butoxycarbonyl after treatment with Boc₂O and DMAP in THF (Scheme 4.9), yielding intermediate **78** in 87% yield.



Scheme 4.9 Synthesis of 5'-phosphonate 8ClA ProTide **86**. *Reagents and conditions*: (a.) Boc₂O (4 eq), DMAP (0.4 eq), THF, rt, 16h, 87% (b.) TFA, H₂O, THF (1:1:4), 0 °C, 5h, 68% (c.) IBX (2eq), CH₃CN, 80°C, 4h; (d.) tetraethyl methylenediphosphonate (1.6eq), NaH (2.5eq), THF, 0 °C to rt, 12h, 68% (two steps); (e.) Pd/C (10%), H₂, EtOH/EtOAc (1/1), rt, 5h, 81%; (f.) HCOOH/H₂O (1/1), rt, 72h, 75%; (g.) TMSBr (3eq), 2,6-lutidine (3 eq), CH₃CN, 5h, 0 °C; (h.) L-AlaOBn pTSA (1eq), phenol (6 eq), aldrithiol-2 (6eq), Ph₃P (6eq), pyridine, Et₃N, 50 °C, 3h; (i.) HCl 0.5N, 5% (three steps).

Selective deprotection of the primary hydroxyl function of intermediate **78** was performed by treatment with a mixture of TFA in water and THF (1:1:4 v/v/v) at 0 °C, affording intermediate **79** in 68% yield. Refluxing this intermediate with 2 equivalents of IBX in CH₃CN for 4 hours then resulted in oxidation of **79** into **80**, which was not isolated but immediately subject to Wadsworth-Emmons (HWE) olefination by addition of tetraethyl methylenediphosphonate sodium salt. These two steps yielded olefinic intermediate **81** in 68% yield. Saturation of the double bond in intermediate **81** was carried out by treatment

with Pd/C in a mixture of EtOH and EtOAc under hydrogen atmosphere for 5 hours, yielding **82** in 81% yield. Deprotection of the amino and hydroxyl groups of intermediate **82** was afforded in 75% yield by the use of a mixture of formic acid in water for 72 hours, similar to the procedure set up for the synthesis of 3'dA phosphonate ProTide **66**. Despite the long reaction time required for this deprotection step, the use of any harsher conditions was avoided. This was decided in order to prevent the cleavage of the glycosidic bond that had happened before after treatment of the 3'dA intermediate with TFA in water at room temperature. The final step for the synthesis of 8ClA phosphonate ProTide required at first the deprotection of the phosphonate bond by treatment with 3 equivalents of trimethylsilyl bromide (TMSBr) in CH₃CN for 5 hours at 0 °C. The presence of 3 equivalents of 2,6-lutidine was necessary to prevent the complete degradation caused by the release of hydrobromic acid during the reaction, as was already noticed for the synthesis of the 3'dA phosphonate ProTide **66**.¹²⁷ The reaction conditions were carefully kept anhydrous and after evaporation of the volatiles, the crude containing intermediate **85** was dissolved in pyridine and triethylamine (TEA), then 1 equivalent of L-alanine benzyl ester *para*-toluene sulfonic salt (*p*TSA) and 6 equivalents of phenol were added, which were previously mixed in pyridine. In a separate flask aldrithiol-2 and triphenylphosphine (Ph₃P) were dissolved in pyridine and added to the initial mixture, which was stirred at 50 °C for 3 hours. Evaporation of the mixture and extraction with CH₂Cl₂ afforded a mixture of compounds containing the 2',3'-bis-*O*-trimethyl silyl protected intermediate **85**, which was converted into desired **86** by quick treatment with a solution of HCl 0.5 N that cleaved the silyl ether bonds. Purification by column chromatography and reverse phase HPLC were required, and yielded desired compound **86** in 5% yield. Although very poor, the yield was not further optimised at this stage, but the synthesised compound was tested for anticancer activity, with the aim of improving the synthetic procedures and preparing an enlarged family of prodrugs at a later stage.

4.2.3 Biological evaluation

Compound **86** was evaluated for anticancer activity on a broad selection of malignant cell lines by WuXi AppTech, previously used for the evaluation of 3'dA prodrugs.

A comparison between the activity of phosphonate **86** and the phosphate counterpart ProTide **68c**, along with the activity of 8ClA is given in Table 4.17, Table 4.18, Table 4.19 and Figure 4.23.

Cpnd	CCRF-CEM		MOLT-4		K562		Hel92.1.7		KG1		MV4-11		HL-60	
	IC ₅₀	MI%	IC ₅₀	MI%	IC ₅₀	MI%	IC ₅₀	MI%	IC ₅₀	MI%	IC ₅₀	MI%	IC ₅₀	MI%
8CIA	1.47	91	1.08	100	0.64	95	0.66	94	1.72	100	0.19	100	1.29	100
68c	9.48	96	1.85	95	1.41	96	4.46	96	6.3	98	0.52	100	2.83	98
86	28.0	98	25.0	104.2	47.0	103	74.0	91	156.0	29	31.0	100	73.0	93
PTX	0.004	93	0.002	9	0.003	80	0.03	72	0.08	89	0.003	99	0.003	93

Table 4.17 *In vitro* cytotoxicity screening of 8CIA, ProTide **68c** and phosphonate ProTide **86**. Cytotoxicity data reported μM IC₅₀ values (concentration of drug causing 50% of cell viability inhibition) and MI% (maximum inhibitory effect of the drug at the range of concentration considered). PTX: paclitaxel (control). Assays performed by WuXi AppTech.

Cpnd	THP-1		Z138		RL		Jurkat		Hs-445		RPMI-8226		NCI-H929	
	IC ₅₀	MI%	IC ₅₀	MI%	IC ₅₀	MI%	IC ₅₀	MI%	IC ₅₀	MI%	IC ₅₀	MI%	IC ₅₀	MI%
8CIA	1.86	96	1.06	94	1.83	92	2.85	79	3.42	83	2.86	96	5.55	100
68c	2.58	99	0.11	95	9.66	94	3.46	86	0.11	79	3.40	97	5.89	98
86	48.0	86	28.0	99	73.0	81	40.16	99	76.0	78	52.0	79	52.0	86
PTX	0.01	60	0.003	99	0.003	65	0.003	82	0.004	84	0.003	96	0.003	95

Table 4.18 *In vitro* cytotoxicity screening of 8CIA, ProTide **68c** and phosphonate ProTide **86**. Cytotoxicity data reported μM IC₅₀ values (concentration of drug causing 50% of cell viability inhibition) and MI% (maximum inhibitory effect of the drug at the range of concentration considered). PTX: paclitaxel (control). Assays performed by WuXi AppTech.

Cpnd	MiaPaCa-2		BxPC-3-Luc		HT29		SW620		HepG2		MCF-7		Cal 27	
	IC ₅₀	MI%	IC ₅₀	MI%	IC ₅₀	MI%	IC ₅₀	MI%	IC ₅₀	MI%	IC ₅₀	MI%	IC ₅₀	MI%
8CIA	0.79	81	12	62	2.17	70	2.32	94	1.18	69	1.67	83	2.12	75
68c	2.28	93	15	74	3.62	88	3.06	87	3.09	82	4.29	100	13	88
86	86.0	91	73	11	81	43	88	58	91	43	103	59	116	28
PTX	0.004	85	0.016	51	0.004	79	0.01	84	0.008	51	0.003	80	0.002	92

Table 4.19 *In vitro* cytotoxicity screening of 8CIA, ProTide **68c** and phosphonate ProTide **86**. Cytotoxicity data reported μM IC₅₀ values (concentration of drug causing 50% of cell viability inhibition) and MI% (maximum inhibitory effect of the drug at the range of concentration considered). PTX: paclitaxel (control). Assays performed by WuXi AppTech.

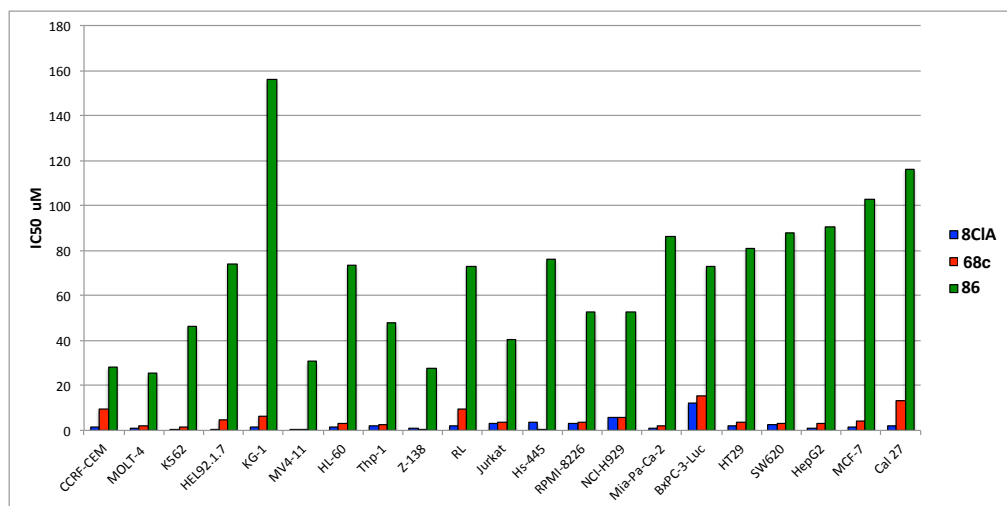


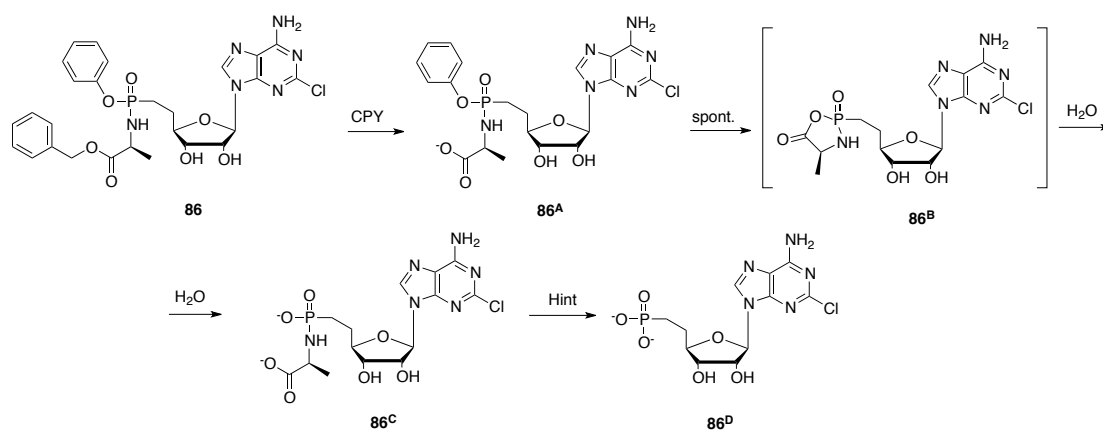
Figure 4.23: Comparison of the cytotoxic activity of 8ClA, ProTide **68c** and phosphonate ProTide **86**.

The phosphonate derivative **86** is consistently less active than both the parent nucleoside and the phosphate analogue **68c**. This might derive from an inefficient processing of the ProTide moiety with release of 8ClA phosphonate, which should in turn mimic 8ClAMP. Alternatively, the released 8ClA phosphonic acid might be poorly recognised by the kinase enzymes that would catalyse the next phosphorylation steps, required for intracellular activity. Despite being less active than 8ClA, compound **86** is still endowed with poor anticancer activity in the range between 30 and 80 μM on most cell lines, with a preference for cells deriving from haematologic malignancies, such as MOLT-4 and CCRF-CEM.

4.2.4 Mechanistic studies

As previously mentioned in the case of phosphoramidate ProTide of 3'dA **64**, a potential cause of the lack in activity of such prodrugs might be due to inefficient processing of the prodrug moiety by carboxypeptidase and phosphoramidase enzymes. This would negatively affect the release of nucleoside phosphonic acid, which should mimic the nucleoside monophosphate.

The investigation of the intracellular activation of 8ClA phosphonate prodrug **86** (Scheme 4.10) was carried out through docking studies, by simulation of the interaction with CPY and Hint enzymes.



Scheme 4.10: Putative intracellular metabolic activation of prodrug **86** by CPY/Hint enzymes.

Initially, docking of both diastereoisomers (*Sp* and *Rp*) was performed within the active pocket of the CPY enzyme. Both isomers seemed to interact similarly inside the enzyme, positioning the amino acid ester moiety close to the pocket containing catalytic residues.

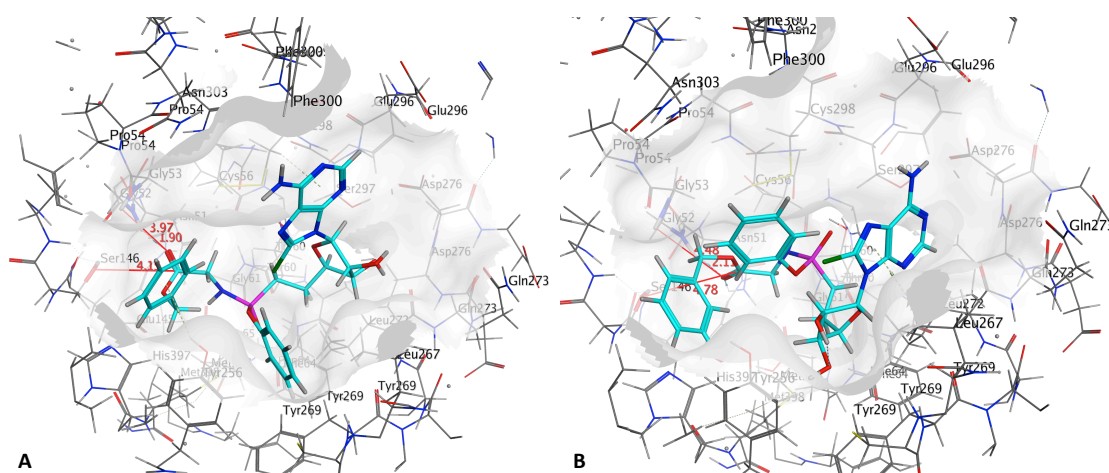


Figure 4.24 (A) Docking of *Rp* isomer of **86** in CPY active site. (B) Docking of *Sp* isomer of **86** in CPY active site.

These results suggest that the cleavage of the ester moiety might not be a limiting step in the intracellular activation of prodrug **86**.

The metabolite that is potentially formed after cleavage of the benzyl moiety and intramolecular rearrangements is **86^C** (Scheme 4.10). This L-alanyl phosphonate monoester intermediate was then docked inside the active site of Hint enzyme, which is thought to be responsible for the cleavage of the phosphoramidate bond. The results are shown in Figure 3.93. The positioning of the phosphoramidate group is close to the key residues responsible for the cleavage of the P-N bond, although the phosphonate moiety might lack crucial interactions owing to the missing oxygen from the phosphate group.

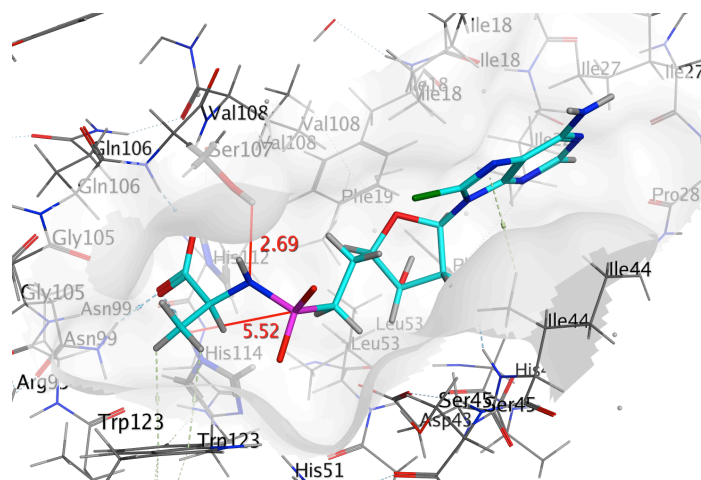


Figure 4.25 Docking of **86^C** in Hint active site.

However, the docking studies suggest that compound **86** would interact efficiently with carboxypeptidase and phosphoramidase processing enzymes. Hence the lack in improved activity of this prodrug compared to the phosphate counterpart **68c** might derive from an inefficient processing to diphosphonate and triphosphonate metabolites, by respectively nucleoside monophosphate and diphosphate kinase enzymes.

4.2.5 Conclusions

In an attempt to improve the activity of 8CIA ProTides, the modification of the phosphate group into more stable moieties such as phosphoramidate prodrugs was carried out. The synthetic route applied had already been determined for the synthesis of 3'dA phosphoramidate prodrugs, and yielded one example of an 8CIA derivative via a 7 step synthetic procedure, in low yield. Evaluation of this compound showed a poor anticancer profile, both in comparison with ProTide **68c** and 8CIA. Dockings of derivate **86** within the active pocked of CPY and Hint enzymes predict a correct interaction with the active pockets. This does not provide an explanation for the lack in activity of derivative **86**. However, provided compound **86** is effectively processed in the intracellular environment, with release of the metabolite 8CIA phosphonic acid, this compound might not mimic efficiently 8CIAMP. Therefore lack of recognition by kinase enzymes responsible for the conversion into active nucleoside triphosphate could be responsible for the low anticancer profile of this molecule.

4.3 8-Chloro-2'-deoxyadenosine

4.3.1 Background

8-Chloro-2'-deoxyadenosine (8CldA, **87**) is the 2'-deoxyribose analogue of 8ClA. This deoxyadenosine analogue was synthesised by Chen *et al.*³⁵¹ in order to investigate the effect of its incorporation into DNA growing chains. In fact, 8CldA was suggested to assume a preferential *syn* conformation instead of the *anti* conformation of natural nucleosides.

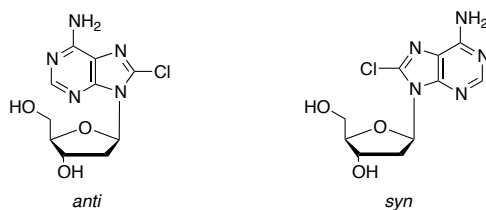


Figure 4.26: *Syn* and *anti* conformations of 8CldA caused by rotation around the glycosidic bond.

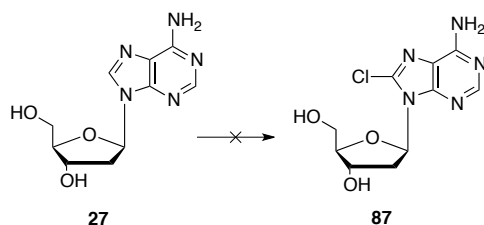
This preference was confirmed for purine nucleoside analogues modified at the C8 position with hindered groups, which frequently adopt *syn* glycosidic torsion angles instead of the preferred *anti* conformation found in unmodified nucleosides³⁵⁷ and was proven for 8-bromoadenosine and 8-methoxy-2'-deoxyadenosine,³⁵⁸⁻³⁶⁰ and suggested for 8ClA.^{351,361} The presence of such modification within the DNA growing chain was suggested to lead to base mispairing effects.

8CldA was inserted into a DNA template and although pairing with thymidine, the nucleotide exhibited decreased nucleotide incorporation efficiencies compared to the natural substrate 2'-deoxyadenosine 5'-triphosphate and induced DNA polymerase pausing during DNA synthesis, possibly caused by its altered conformation.³⁵¹

A study to explore the potential correlation between the reported data and the anticancer activity of this 8ClA derivative was of interest, especially concerning the application of the ProTide approach to this nucleoside analogue with the aim of potentially bypassing limiting steps in the phosphorylation and cell penetration, that could decrease the efficiency of intracellular release of the potential active metabolite 8-chloro-2'-deoxyadenosine-5'-triphosphate (8CldATP).

4.3.2 Synthesis of 8-chloro-2'-deoxyadenosine

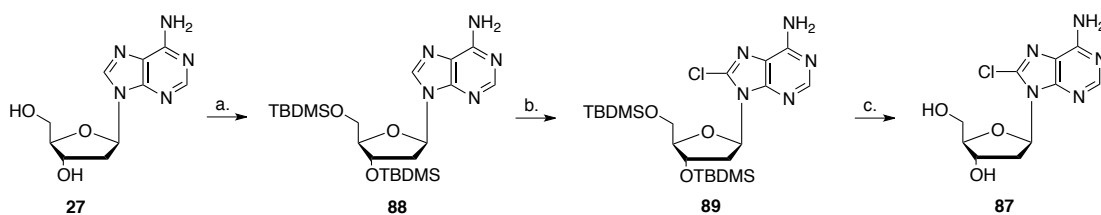
The first attempt to synthesise 8-chloro-2'-deoxyadenosine involved the treatment of commercially available 2'-deoxyadenosine (**29**) with *N*-chlorosuccinimide (NCS) in a solution of DMF and acetic acid, as successfully adopted for the synthesis of 8ClA (**87**).³⁴⁸



Scheme 4.11: Attempted synthesis of 8ClAdo using the NCS method. *Reagents and Conditions*: a) NCS (3.5 eq), acetic acid, DMF, rt, 48 hours.

Unfortunately, due to the increased instability and acid lability of the glycosidic bond in the 2'-deoxyadenosine nucleoside structure,^{362,363} this methodology caused degradation of the starting material with adenine detection *via* ¹H NMR.²⁷

This unsuccessful result prompted the use of a methodology involving first a *tert*-butyldimethyl protection of 2'-deoxyadenosine (**29**), followed by chlorination via one-pot treatment with LDA and tosyl chloride (TsCl) and final deprotection to yield desired 8ClAdo (**87**). This methodology was already applied to the synthesis of 8ClA and was used by Chen *et al.* for the synthesis of 8ClAdo.³⁵¹



Scheme 4.12 Synthesis of 8ClAdo. *Reagents and Conditions*: (a.) TBDMSCl (4 eq), imidazole (8 eq), DMF, rt, 15 hours (94%); (b.) LDA (5 eq), TsCl (10 eq), THF, -78 °C, 2 hours (75%, two steps); (c.) TBAF (3.5 eq), THF, rt, 1 hour (33%).

The initial protection of **29** was performed with TBDMSCl and imidazole in DMF, yielding desired **88** in 94% yield.³⁴⁹ This intermediate was then lithiated on the C-8 position of adenine using LDA. This makes the C-8 position available for an electrophilic substitution using tosyl chloride as a chlorine cation donor, yielding protected 8ClAdo (**89**) in 75 % yield.³⁵⁰ The final deprotection step was accomplished using a solution of TBAF (1 M) in THF.²⁶ This procedure, has the drawback of a challenging purification of the

product from hydrolysed TBAF residues, that were still present after column chromatography. In an attempt to remove the TBAF residues, a small portion of the impure compound was stirred with DOWEX sulfonic acid resin, and CaCO_3 in anhydrous CH_3OH .³⁶⁴ Unfortunately, through this procedure, it was impossible to recover the compound that appeared to have been degraded, likely due to the strong acidic nature of the resin. However, washing the residue with abundant Et_2O finally yielded clean product, as reported in the ^1H NMR spectrum in Figure 4.27.

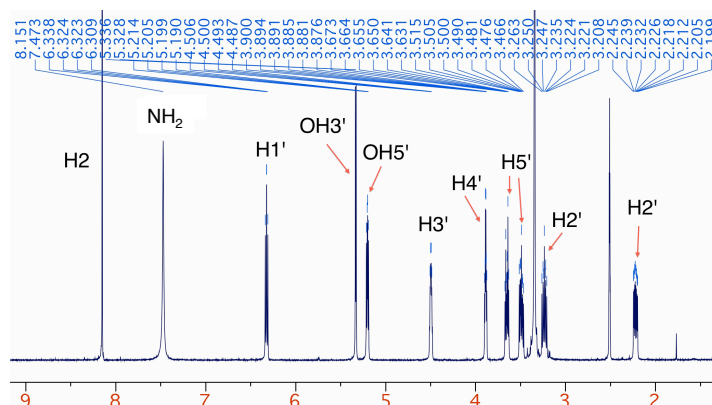
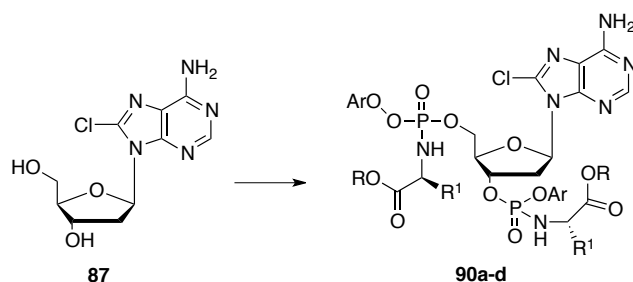


Figure 4.27: ^1H NMR spectrum of 8CldA ($\text{DMSO}-d_6$, 500 MHz).

4.3.3 Synthesis of 8CldA prodrugs

In the first attempt of the synthesis of 8CldA ProTides, 8CldA was treated with *t*BuMgCl (2.5 eq) and 1-naphthyl-(pentyloxy-L-leucinyloxy) phosphorochloridate (3 eq) in THF (Table 4.20, entry 1). This procedure failed to yield the desired 5'-phosphoramidate derivative but afforded the 3',5'-difunctionalised analogue **90a** (Scheme 4.13) in 8% yield.

A similar result was obtained when lowering the amount of Grignard reagent used and modifying (1.5 eq) the phosphorochloridate structure (Table 4.20, entry 2), yielding compound **90b** in 28% yield. Reducing the phosphorochloridate and *t*BuMgCl equivalents used (respectively 2 and 1.1 eq) (Table 4.20, entry 2), and further lowering the amount of phosphorochloridate used (to 1.1 eq) (Table 4.20, entry 3), yielded similar results.

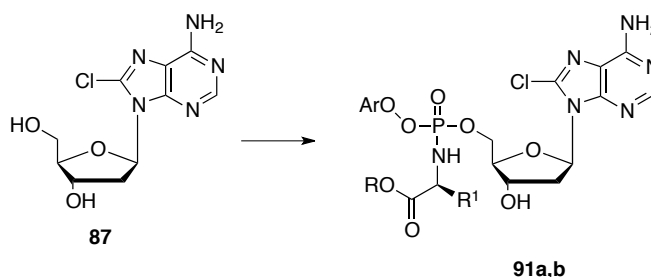


Scheme 4.13 Synthesis of 8CldA phosphoramidates (**90a-d**) from unprotected 8CldA. *Reagents and conditions*: *t*BuMgCl, appropriate phosphorochloridate, THF, rt, 16 h (Table 4.20).

Entry	Phosphorochloridate					<i>t</i> BuMgCl* eq.	3',5'-bisProTide (yield)
	Ar	R	R ¹	AA	Eq.		
1	Nap	<i>n</i> Pen	<i>i</i> Bu	L-Leu	3	2.5	90a (8%)
2	Ph	<i>n</i> Hex	Me	L-Ala	3	1.5	90b (28%)
3	Ph	Bn	Me	L-Ala	2	1.1	90c (25%)
4	Nap	Bn	H	Gly	1.1	1.1	90d (16%)

Table 4.20: Structures and number of equivalent of phosphorochloridate used, amount of *t*BuMgCl used and relative yields for the synthesis of derivatives **90a-d**. *1M solution in THF.

Replacing the Grignard reagent with NMI (5 equivalents), yielded the desired 5'-phosphoramidates, in low yield (2%) without trace of 3',5'-bisProTide (Scheme 4.14, Table 4.21, entry 1).



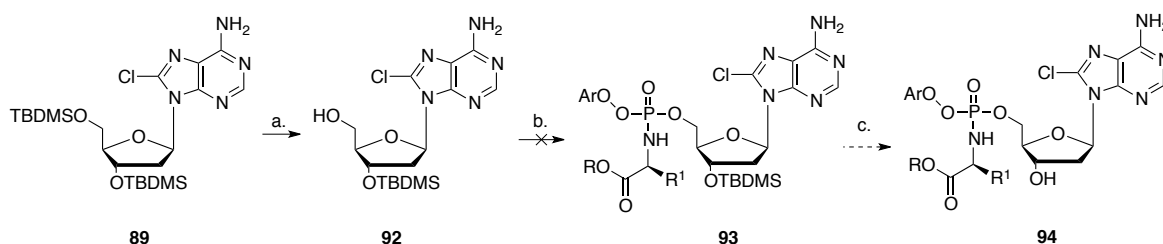
Scheme 4.14: Synthesis of 8CldA phosphoramidates (**91a-b**) from unprotected 8CldA. *Reagents and conditions*: NMI, appropriate phosphorochloridate, THF, rt, 16 h (Table 4.21).

A similar yield resulted using this same method and an alternative phosphorochloridate (Table 4.21, entry 2).

Entry	Phosphorochloridate					NMI eq.	5'-ProTide (yield)
	Ar	R	R ¹	AA	Eq.		
1	Nap	<i>c</i> Hex	<i>i</i> Bu	L-Leu	3	5	91a (2%)
2	Ph	Bn	H	Gly	3	5	91b (4%)

Table 4.21: Structures and number of equivalent of phosphorochloridate used, amount of NMI used and relative yields for the synthesis of derivatives **91a,b**.

In an attempt to improve the yield of 8-chloro-2'-deoxyadenosine ProTides, an alternative method was envisaged, involving selective deprotection of the 5'-position of the fully protected nucleoside (**89**) followed by *t*BuMgCl-mediated coupling reaction with the appropriate phosphorochloridate and final 3'-deprotection via TFA in CH₂Cl₂ to yield the desired 5'-ProTide. Compound **89**, was selectively deprotected on the 5'-hydroxyl position by treatment with a 1:1:4 mixture of TFA and water in THF in an ice-cold bath for 5 hours, affording **92** in 51% yield.³⁰⁰



Scheme 4.15: Attempted synthesis of 8CldA ProTides from 5'-protected 8CldA. *Reagents and conditions:* (a.) TFA, water, THF, (1:1:4 v/v/v), 0 °C, 5h, 51%; (b.) conditions reported in Table; (c.) TFA, CH₂Cl₂.

The 3'-silyl protected nucleoside (**92**) was then reacted with 3 equivalents of 1-phenyl-(benzyloxy-glycyl)] phosphorochloridate and 3 equivalents of *t*BuMgCl (1M in THF) in anhydrous THF (Table 4.22, entry 1). The mixture turned cloudy after 5 hours and after TLC analysis of the crude it was clear that the starting material had decomposed with no trace of product.

Entry	Phosphorochloridate					time	T	<i>t</i> BuMgCl eq.	NMI eq.	5'-ProTide yield
	Ar	R	R ¹	AA	Eq.					
1	Ph	Bn	H	Gly	3	5h	rt	3	-	-
2	Nap	nPen	<i>t</i> Bu	L-	3	16h	-10 °C to	1	-	-
3	Nap	nPen	<i>t</i> Bu	L-	3	16h	rt	-	5	-

Table 4.22: Structures and number of equivalent of phosphorochloridates, number of equivalents of *t*BuMgCl or NMI used in the attempt of synthesising derivatives **93a-c**.

The same reaction was attempted again using 3 equivalents of 1-naphthyl-(pentyloxy-L-leucyl)] phosphorochloridate and only one equivalent of *t*BuMgCl and adding the reagents to the 3'-protected starting material in THF at -10 °C in order to slow down any decomposition process, possibly due to the harsh alkaline conditions caused by the Grignard base. TLC analysis of the mixture revealed no conversion of the starting material after 2 hours at low temperature, therefore the reaction temperature was allowed to reach

room temperature. After overnight stirring, however, starting material was decomposed and no product could be detected (Table 4.22, entry 2).

When the 3'-protected starting material was reacted with 3 equivalents of 1-naphthyl-(pentyloxy-L-leucynyl)] phosphorochloridate and 5 equivalent of *N*-methylimidazole in THF overnight, TLC analysis of the crude mixture revealed complete lack of reactivity of the starting material, which was recovered (Table 4.22, entry 3).

In conclusion, attempts to synthesise 5'-ProTides of 8CIdA using the *t*BuMgCl methodology failed on both the unprotected nucleoside and the 3'-silyl protected one. Although in low yields, the NMI method afforded two desired products.

4.3.3.1 Schwartz's reagent as dephosphorylating agent

The Schwartz's reagent is an organometallic compound corresponding to the structure of chlorobis(cyclopentadienyl)hydrido-zirconium also known as zirconocene hydrochloride.

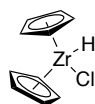
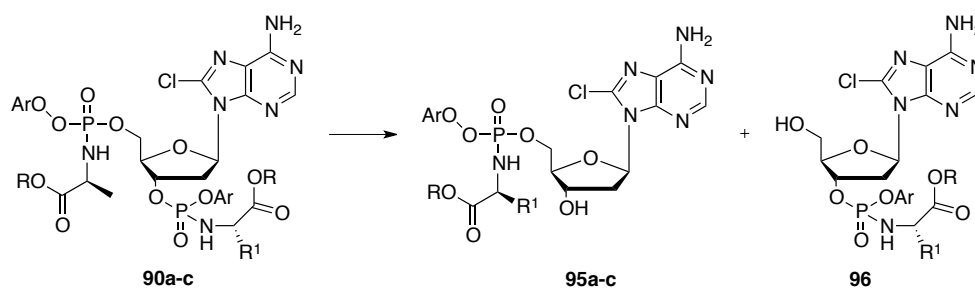


Figure 4.28: Structure of the Schwartz's reagent.

Among the many applications of this reagent there is the chemoselective reduction of tertiary and secondary amidic bonds,³⁶⁵⁻³⁶⁷ which was investigated on a broad selection of differently protected *N*-acetylated nucleosides,³⁶⁸ confirming that this reagent is selective for the cleavage of *N*-acetyl groups with no effect on other protecting moieties. During these investigations, this methodology was also applied to one example of *N*-acetyl-3',5'-bis-ProTide (*N*-acetyl-2'-deoxycytidine-3',5'-[1-naphthyl-(cyclohexyloxy-L-alaninyl)] diphosphate) and the main product of this reaction was the *N*-deacetylated 2'-deoxycytidine-5'-[1-naphthyl-(cyclohexyloxy-L-alaninyl)] phosphate. This serendipitous discovery suggested that the Schwartz's reagent could cleave preferentially the phosphoramidate group on the secondary hydroxyl moiety of 2'-deoxycytidine and not the primary one.

Intrigued by these results and considering the previously synthesised 3',5'-bisProTides, obtained as undesired products *via* application of the *t*BuMgCl method on unprotected 8CIdA, attempt to use of the Schwartz's reagent on such substrates as selective dephosphorylating agent was carried out.



Scheme 4.16: Synthesis of 8CldA 5'-phosphoramidates (**95a-c**) and 8CldA 3'-phosphoramidate (**96**) by dephosphorylation of 3',5'-bisProTides **95a,b,d**. *Reagents and conditions*: Schwartz reagent (3 eq), THF, 16h, rt.

Entry	Starting material					Product(s)	
	3',5'-BisProTide					5'-regioisomer	3'-regioisomer
	Cpnd	Ar	R	R ¹	AA	(yield)	(yield)
1	90a	Nap	<i>n</i> Pen	<i>i</i> Bu	L-Leu	95a (3%)	traces
2	90b	Ph	<i>n</i> Hex	Me	L-Ala	95c (15%)	traces
3	90c	Ph	Bn	Me	L-Ala	95b (15%)	96 (5%)

Table 4.23: Structures of starting material 3',5'-bisProTides **90a-c** and yields of 5' and/or 3' ProTides obtained.

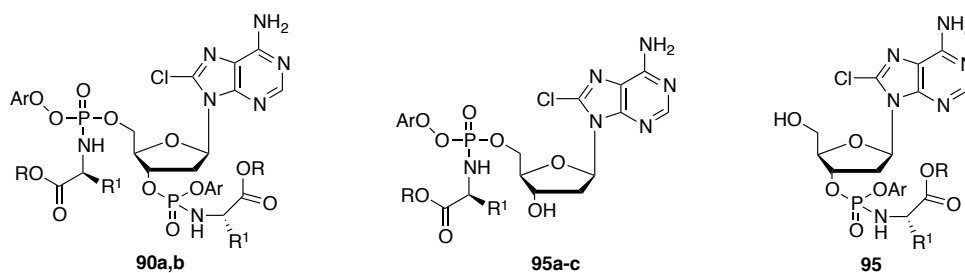
For this purpose, previously synthesised compound **90a** was treated with 3 equivalents of Schwartz's reagent in THF for 3 hours at room temperature, yielding only 3% of 5'-ProTide **95a** and traces of 3'-phosphoramidate, due to the low amount of starting material used (Table 4.23, entry 1). A similar yield was obtained when repeating the strategy on substrate **90b**, although due to the low amount of material available, only 5'-phosphoramidate **95b** could be isolated (Table 4.23, entry 2).

On the other hand, when a larger amount of starting material **90c** was treated in the same conditions, the reaction yielded 15% of 3'-dephosphorylated derivative **95c** and 5% of 5'-dephosphorylated derivative **96** (Table 4.23, entry 2).

In conclusion, the Schwartz's reagent proved to be a useful reagent for the dephosphorylation of bis-ProTides of both 2'-deoxycytidine and 8CldA and investigations to understand the mechanism of such reaction and to potentially improve this methodology are ongoing.

4.3.4 Cytotoxic *in vitro* screening of 8CldA prodrugs

The 8CldA derivatives selected for cytotoxic evaluation by WuXi AppTech were the 3',5'-bisProTides **90a** and **90b**, the 5'-ProTides **95a-c** and the 3'-regioisomer **96** (Table 4.24).



Cpnd	regioisomer	Ar	R	R ₁	AA	cLogP
95a	5'	Nap	<i>n</i> Pen	<i>i</i> Bu	L-Leu	4.76
95b	5'	Ph	<i>n</i> Hex	Me	L-Ala	2.13
95c	5'	Ph	Bn	Me	L-Ala	1.73
90a	3',5'	Nap	<i>n</i> Pen	<i>i</i> Bu	L-Leu	11.09
90c	3',5'	Ph	Bn	Me	L-Ala	6.09
96	3'	Ph	Bn	Me	L-Ala	1.91

Table 4.24: Structures and cLogP of 8CldA derivatives evaluated for their cytotoxic activity. cLogP calculated with ChemDraw 2010 software.

These derivatives were tested on a small selection of cell lines deriving from haematological malignancies and breast adenocarcinoma (Table 4.25).

Cell line	Malignancy
HEL92.1.7	Erythroleukaemia
HL-60	Promyelocytic leukaemia
RPMI8226	Human multiple myeloma
Z-138	Mantle cell lymphoma
MCF-7	Breast adenocarcinoma
MIA PaCa-2	Pancreatic adenocarcinoma

Table 4.25: Selection of cell lines used for cytotoxic evaluation of 8CldA derivatives.

8CldA was poorly active on most of the cell lines, reaching maximum inhibitions of cell viability (MI%) ranging between 11.6 and 22.6% at the highest concentration considered (198 μ M). However, on the pancreatic adenocarcinoma cell line MIA PaCa-2, it reached a maximum inhibitory effect of 86.1% and the IC₅₀ was 1.16 μ M (Table 4.26, Figure 4.29). This result suggests that the cytotoxic activity of this nucleoside analogue should be evaluated on a broader selection of solid tumour cell lines.

Cpnd	HEL92.1.7		HL-60		RPMI-8226		Z138		MCF-7		MIA PaCa-2	
	IC ₅₀	MI%	IC ₅₀	MI%	IC ₅₀	MI%	IC ₅₀	MI%	IC ₅₀	MI%	IC ₅₀	MI%
8ClIdA	>198	16	>198	23	>198	12	>198	22	>198	12	1.16	86
95c	>198	34	>198	20	105	63	>198	-8	>198	53	5.22	90
96	78	99	63	100	49	107	>198	33	46	106	14	100
90c	>198	19	>198	53	129	54	>198	48	>198	45	14	88
95a	9.08	99	6.85	99	7.36	100	22	104	9.67	99	2.6	95
90a	>198	47	29	51	11	79	>198	61	18	66	4.65	100
95b	109	70	92	86	80	91	>198	33	102	68	16	84
PTX	0.02	83	0.003	85	0.003	91	0.002	99	0.01	65	0.002	87

Table 4.26: Biological evaluation of 8ClIdA and relative prodrugs by WuXi app. tech. Cytotoxicity is reported as IC₅₀ μM values (50% inhibitory concentration of cell viability). MI% is the maximum percentage of inhibition exerted by compounds up to the top dose (198 μM).

Within the family of L-alanine benzyl ester phenyl phosphoramidates, the 3'-regioisomer (**96**) was generally the most active derivative, although not a very potent agent (Table 4.26, Figure 4.29). Although reaching complete inhibition of almost all the cell lines considered, the IC₅₀ values ranged between 14 and >198 μM. On the other hand, the 5'-analogue (**95c**) was less active on all cell lines apart from MIA PaCa-2 cell line, where it reached IC₅₀ value of 5.22 μM. The 3',5'-bisProTide **90c** was generally poorly active, although reaching better cell viability inhibition percentages compared to the parent nucleoside. The 3',5'- and 5'-phosphoramidates bearing L-leucine pentyl naphthyl moieties (respectively compounds **90a** and **95a**), were more active than the previously considered ones. ProTide **95a** reached complete inhibition of cell viability on all cells and IC₅₀ values ranging between 2.6 and 22 μM.

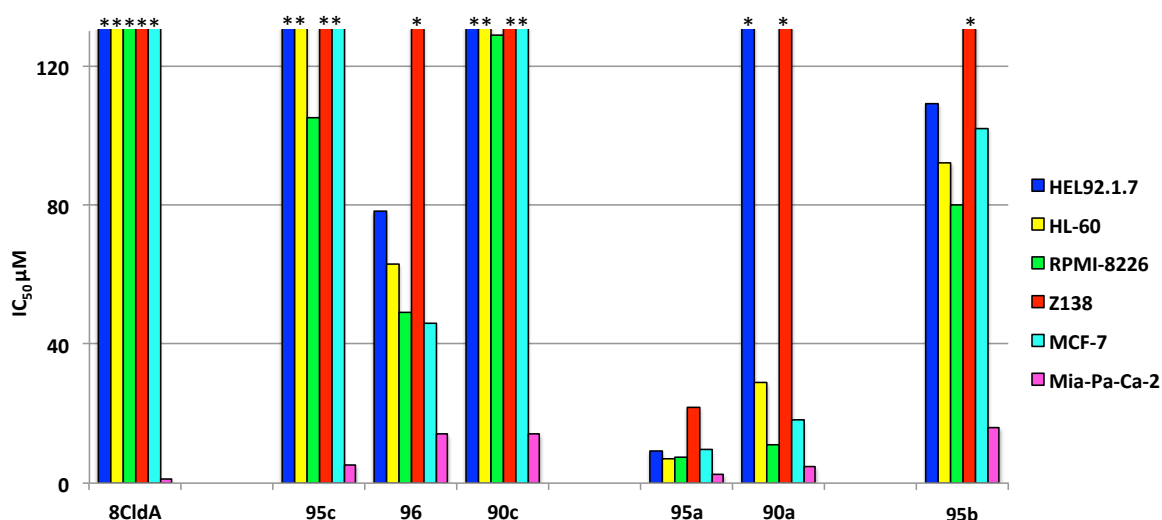


Figure 4.29: Comparison between cytotoxic data of 8ClIdA and relative prodrugs (phenyl L-alanine benzyl ester derivatives **95c**, **96** and **90c**, naphthyl L-leucine *n*-pentyl derivatives **95a** and **90a** and phenyl L-alanine *n*-hexyl analogue **95b**).

The 3',5'-bisProTide derivative **90a** was less active than **95a** but still more active than the parent nucleoside, reaching IC₅₀ values as low as 11 μM on cell lines where the parent nucleoside was only partially active. The L-alanine pentyl phenyl derivative **95c** was not as active as the other 5'-ProTides but still reached better results than the parent nucleoside on all cell lines but MIA PaCa-2 (Table 4.26, Figure 4.29).

Rationalising these data was easier when considering the calculated LogP, describing the lipophilicity of these compounds. Within the 5'-ProTides (**95a-c**), the most lipophilic derivative **95a** was the most active, followed by **95b** and **95c**, whose activity decreased with the lipophilic character. Similar results were also obtained in the 3',5'-series, with the very lipophilic analogue **90a** being more active than **90b**. The superior activity of the 3'-phosphoramidate (**96**) over the 5' analogue (**95b**) could also be linked to a slightly higher lipophilicity. These results suggest that a main reason for improved activity of the 8CIdA prodrug over the parent nucleoside may be the potential to cross the membrane by passive diffusion due to increased lipophilicity, therefore bypassing transport through nucleoside transporter. On the other hand, the higher activity of the 3'-ProTide (**96**) over the 5'-Protide (**95b**) suggest that these compounds act as a prodrug of 8CIdA more than 8CIdAMP, therefore they all tend to release 8CIA in the intracellular compartment and the better results are obtained only due to improved penetration in the cell.

4.3.5 Mechanistic investigations

4.3.5.1 Docking in CPY active site

The three most active 8CldA derivatives, 3'-phosphoramidate **96**, and the two ProTides **95a** and **95b** were docked within the binding site of CPY in order to predict the likelihood of intracellular ester cleavage. The puzzling higher cytotoxicity of compound **96** compared to the 5'-regioisomer **95b** on most of the cell lines prompted us to investigate whether it could be related to an enzymatic mechanism. Compound **96** could release 3'-8CldAMP which could act with an unknown mechanism of action. Otherwise, thus released 3'-8CldAMP could be finally hydrolysed to 8CldA, and be more active than the parent nucleoside because of an easier intracellular uptake by passive diffusion.

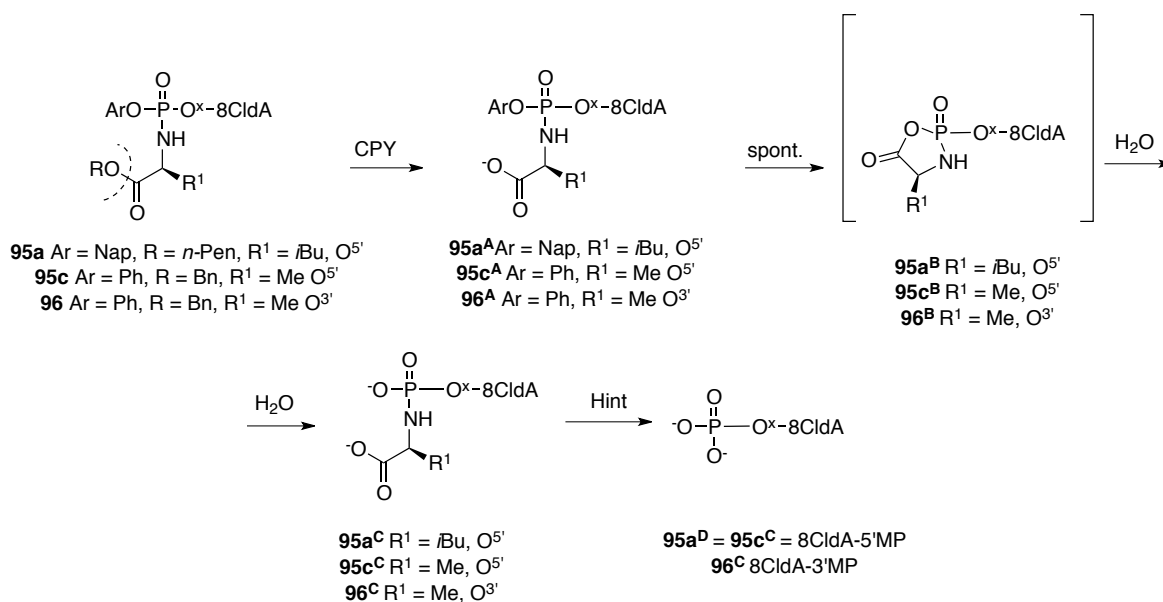
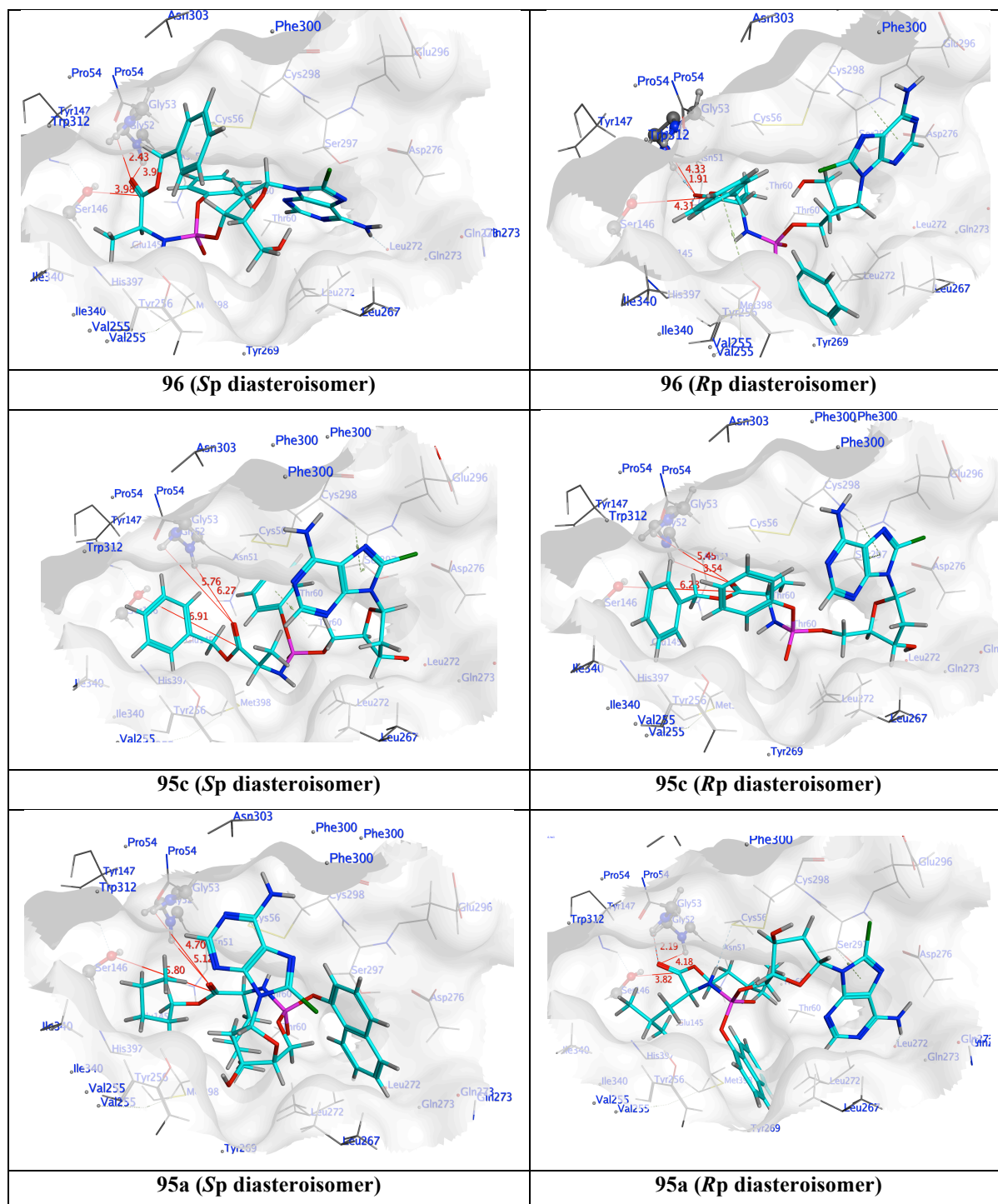


Figure 4.30: Putative intracellular metabolic activation of 8CldA prodrugs **95a**, **95c** and **96** by CPY/Hint enzymes.

In comparison to both diastereoisomers of **95c** (Figure 4.30), the positioning of the regioisomer **96** in the binding site of CPY (Table 4.27) is significantly closer to the crucial residues represented by Gly52, Gly53 and Ser146, for both diastereoisomer. This suggests that **96** may be processed quicker to the 8CldA-3'-L-alaninyl monoester phosphate (**96^A**, Figure 4.30), and this could potentially be due to a greater flexibility of the molecule, responsible for the better accommodation of the amino acid ester moiety inside the pocket.

Table 4.27: Docking interactions of compounds **95a**, **95b** and **96** in the active site of CPY enzyme.

Similarly, compound **95a**, seems to position the amino acid ester moiety close to the crucial residues, and this suggests a very quick processing, despite the very hindered structure.

4.3.5.2 Docking in Hint active site

The amino acid phosphate monoester intermediates resulting from the first enzymatic processing of compounds **95a**, **95c** and **96** (shown in Figure 4.30) were docked in the active pocket of the Hint enzyme (Table 4.28). Intermediates **95c^C** and **96^C** were characterised by a very similar arrangement within the enzyme, **96^C** accommodating the phosphoramidate moiety slightly further from the catalytic residues. Very close positioning to the key residues was also observed for intermediate **95a^C**.

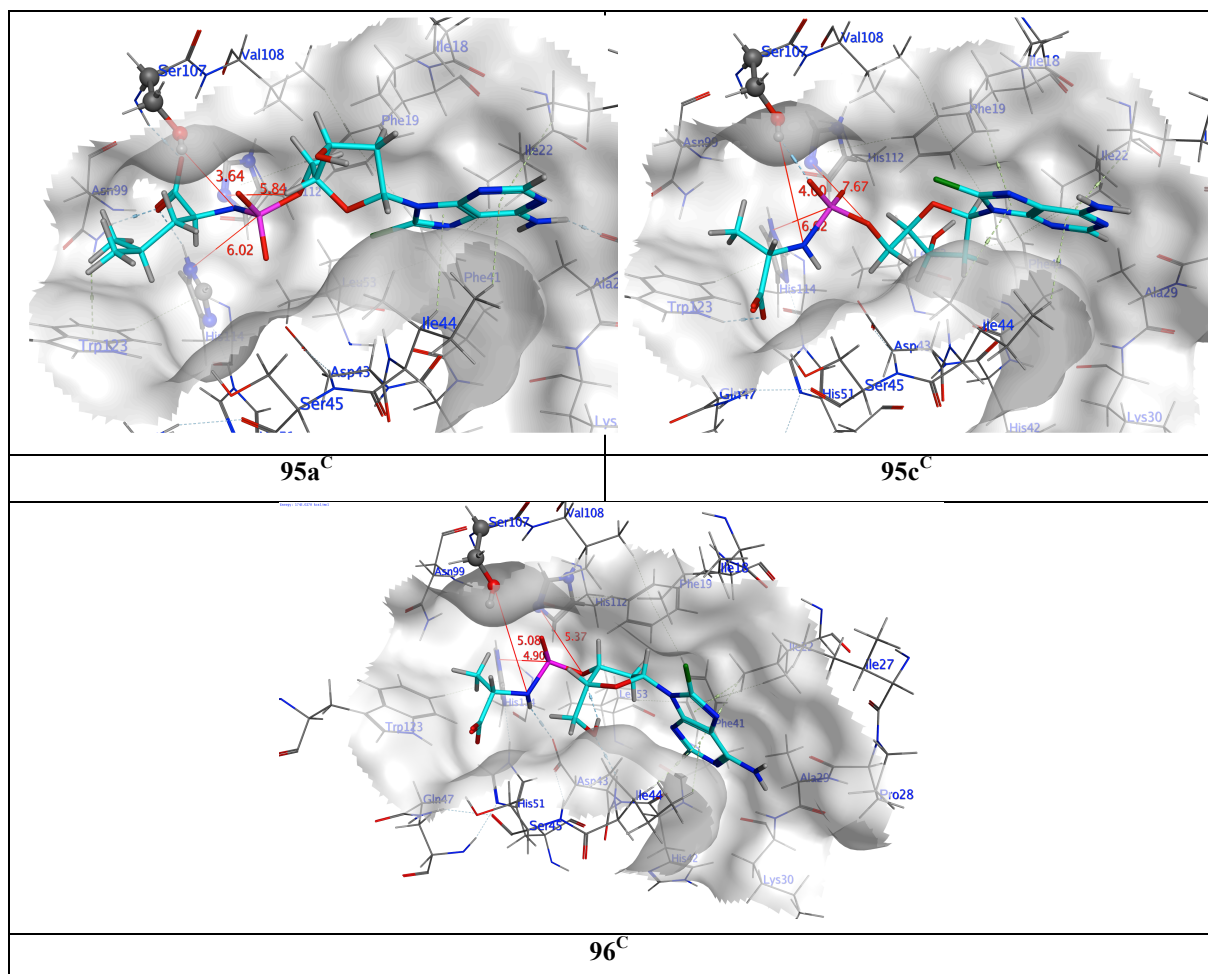


Table 4.28: Docking interactions of compounds **95a^C**, **95c^C** and **96^C** in the active site of Hint enzyme.

Molecular modelling studies suggest that the higher activity of the 3'-regioisomer **96^C** over **95c^C** could derive from a better processing by CPY. Moreover, slightly higher lipophilicity of **96^C** (Table 4.28) could account for better cell penetration by passive diffusion, in comparison to **95c^C**, hence improved activity. On the other hand, the better cytotoxic profile of compound **95a^C** over the other 8CIdA derivatives could derive from both high lipophilicity and good intracellular processing.

4.3.6 Conclusions

8CIdA was synthesised in order to explore *in vitro* the reported disrupting potential on DNA chain growth, potentially leading to cell death. ProTides of 8CIdA were synthesised in low yields either by the NMI coupling method or by first synthesis of 3',5'-bisProTides followed by 3'-dephosphorylation by the Schwartz's reagent. Investigations are currently underway to explain the mechanism of this previously unreported reaction. Biological evaluation of 8CIdA derivatives and parent nucleoside on a small selection of cancer cell lines showed a generally poor cytotoxic profile in relation to 8CIdA. The nucleoside analogue was active at low micromolar concentration only on the MIA PaCa-2 cell line. Tested 3',5'-bisProTides were generally poorly active, while the L-leucine 5'-ProTide **95a** was the most potent compound within the family, with consistently low micromolar activity on all cell lines, bringing a substantial advantage over the parent nucleoside in terms of anticancer potency. Surprisingly, L-alanine ProTide **95c** was poorly active, while the 3'-regioisomer **96** showed improved activity. Molecular modelling studies suggested that this could derive from a quicker intracellular processing by carboxypeptidase enzyme, coupled with an efficient phosphoramidase step.

More derivatives bearing linear amino acid esters and lipophilic amino acids could be synthesised in order to broaden the structure activity relationships (SAR) relative to this family of compounds, with the aim of identifying more active compounds. Moreover, 3'-regioisomers should be synthesised and investigated further, based on the improvement in activity yielded by compound **96** over **95c**. The enhanced activity of these unusual 3'-regioisomers merits further study.

5 CNDAC

5.1 Background

2'-C-cyano-2'-deoxy-1-β-D-*arabino*-pentofuranosylcytosine (CNDAC, **97**, Figure 5.1) is an analogue of the endogenous nucleoside 2'-deoxycytidine. The deoxyribose moiety has been replaced by an arabinoside group, bearing a cyano (CN) group in the 2' position.³⁶⁹

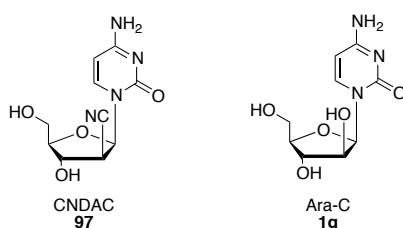
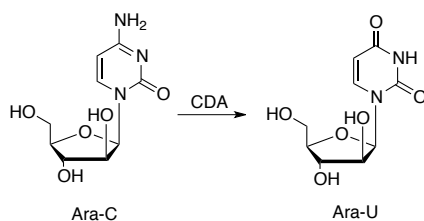


Figure 5.1 Structures of CNDAC (**97**) and Ara-C (**1g**).

CNDAC is therefore the 2'-cyano derivative of the anti-leukaemic agent Ara-C (**1g**, Figure 5.1), and it was developed in 1991 by Matsuda *et al.* as an analogue of Ara-C that could, in principle, offer advantage over the parent nucleoside.³⁶⁹ Ara-C was the first anticancer nucleoside approved by the FDA, in 1969, for the treatment of acute myelogenous leukaemia.¹⁸ Despite its potent activity on haematological malignancies, Ara-C lacks activity towards solid cancers. Moreover, it is a good substrate for cytidine deaminase (CDA), an enzyme that converts it to its inactive uracil derivative Ara-U,³⁷⁰ decreasing the plasma half-life of Ara-C and its activity (Scheme 5.1).³⁷¹

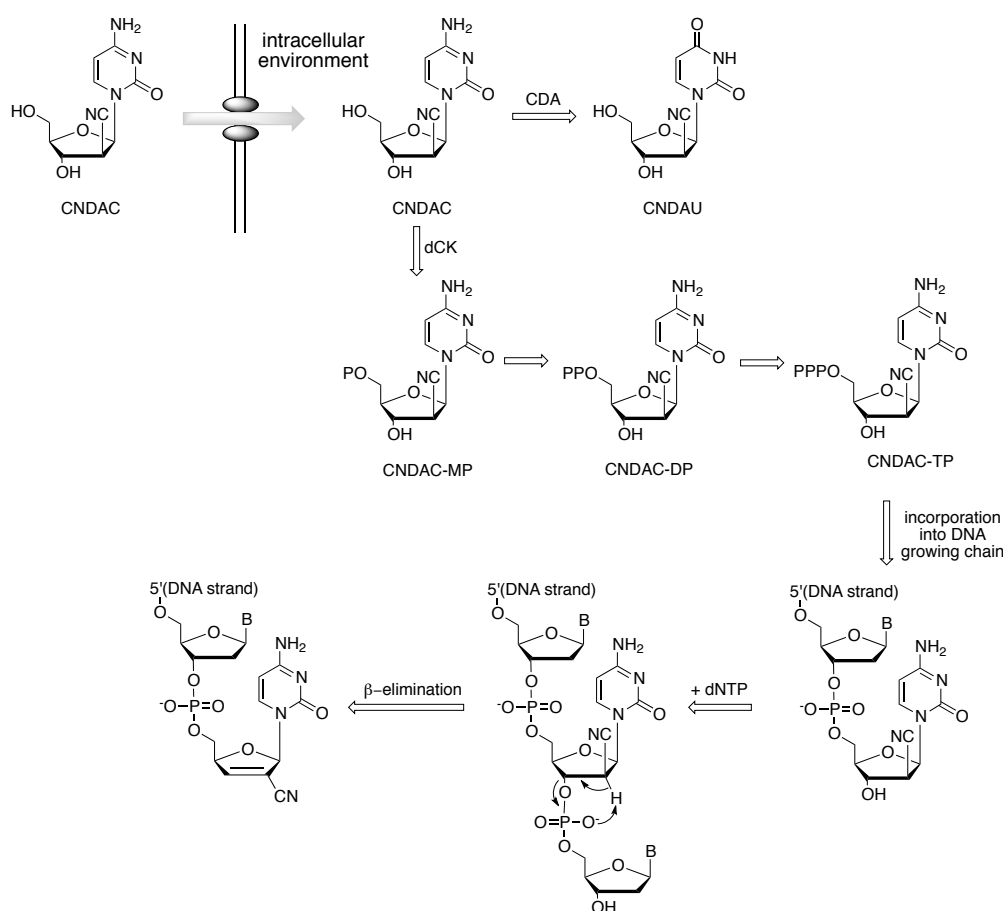


Scheme 5.1: Deactivation of Ara-C to Ara-U catalysed by CDA.

CNDAC was synthesised by Matsuda *et al.* along with other 2'-modified Ara-C analogues, in an attempt to induce resistance to CDA-mediated inactivation and to broaden the spectra of anticancer activity to solid tumours.^{369,372}

This nucleoside analogue resulted as one of the most promising analogues, improving both *in vitro* and *in vivo* activity compared to Ara-C.

After entering the cell through a nucleoside transporter recognised as the human equilibrative nucleoside transporter 1 (hENT1),³⁷³ this nucleoside is phosphorylated by deoxycytidine kinase (dCK) to CNDAC-monophosphate (CNDAC-MP) and finally to CNDAC-triphosphate (CNDAC-TP) by two sequential phosphorylation steps (Scheme 5.2).³⁷⁴ Although being a poorer substrate for cytidine deaminase, compared to Ara-C, CNDAC activity is still partially affected by CDA levels, causing the conversion into 2'-C-cyano-2'-deoxy-1- β -D-*arabino*-pentofuranosyluracil (CNDAU).³⁷¹



Scheme 5.2: CNDAC intracellular metabolism and mode of action. P: phosphate group.

Once in the triphosphate form, CNDAC is incorporated into the DNA growing chain by DNA polymerase α , which catalyses the addition of an additional endogenous nucleotide (Scheme 5.2) to the DNA growing chain.^{375,376} This process causes chemical instability of DNA. In fact, once CNDAC is integrated into the DNA in the 3'-5' phosphodiester linkage, upon the addition of a subsequent nucleotide (dNTP), the electron-withdrawing effect of the CN group at the arabinose 2'- β position increases the acidity of the 2'- α

proton. This in turn facilitates a β -elimination reaction, leading to single strand breakage.^{375,376}

Sapacitabine (CYC-682, Figure 5.2) is a CNDAC derivative, bearing a N^4 -palmitoyl chain on the amino group of the base.³⁷⁷ This compound was developed as a prodrug that could bypass plasma deamination by CDA due to the presence of a bulky alkyl chain on the amino group of its structure.

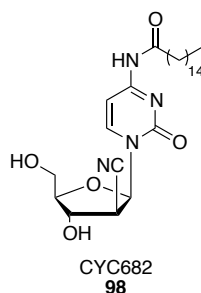


Figure 5.2: Structure of sapacitabine (CYC682, **98**).

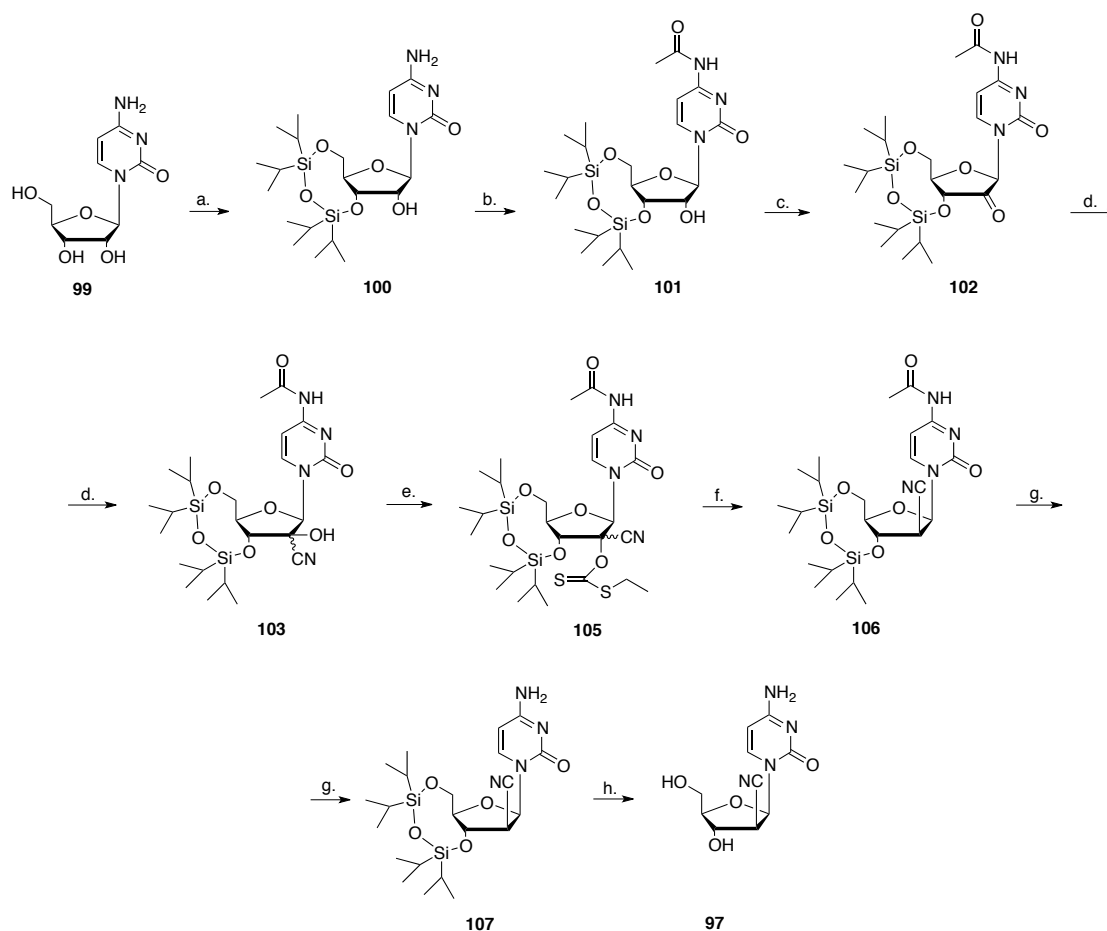
Moreover, the increased lipophilicity of the molecule enhances intestinal permeability of the drug, allowing oral administration. Once in the blood stream, sapacitabine is activated by plasma and liver amidase enzymes, releasing CNDAC. Oral administration of sapacitabine showed increased activity and lower toxicity compared to CNDAC in a mouse model implanted with reticulum cell sarcoma.³⁷⁶ Several Phase I and II clinical trials of sapacitabine alone or in combination with other anticancer drugs are underway in patients with chronic lymphocytic leukaemia, acute myeloid leukaemia (AML), non-small-cell lung cancer and other advanced solid tumours, and a Phase III study of sapacitabine has been initiated in elderly patients with newly diagnosed AML.³⁷⁸

In this work, the application of the ProTide approach to CNDAC was carried out in order to analyse a different prodrug moiety that could potentially increase the activity of this nucleoside, and offer advantage over sapacitabine. In fact, sapacitabine is a prodrug that increases lipophilicity and deaminase stability of CNDAC, but does not bypass other important limiting steps, such as the first phosphorylation step by deoxycytidine kinase. In fact, CNDAC was reported to be a worse substrate of dCK compared to the natural substrate dCyd.^{374,376} On the other hand, ProTides of CNDAC could potentially bypass the dependency on dCK for the first phosphorylation step and release CNDAC-MP inside the cell, along with increasing the lipophilicity of CNDAC and the stability towards deamination,¹⁵¹ therefore representing a potential advantage over sapacitabine. The synthesis of a family of CNDAC ProTides was therefore performed, along with the

required 8-step synthesis of the parent nucleoside, which is not commercially available. Moreover, to have a comparison with the prodrug in clinical development, sapacitabine was synthesised and tested *in vitro* along with CNDAC and CNDAC ProTides.

5.2 Synthesis of CNDAC

The CNDAC synthetic strategy was performed as reported in the literature,^{369,370,379} with some optimisation steps (Scheme 5.3).



Scheme 5.3: Synthesis of CNDAC. *Reagents and conditions:* (a.) TIPDSCl (1.1 eq), pyridine, rt, 16h, 57%; (b.) Ac₂O (1.2 eq), EtOH, reflux, 3.5h, 100%; (c.) DMP (1 eq), CH₂Cl₂, 150 °C to rt, 16h; (d.) TMSCN (3 eq), AlCl₃ (1.5 eq), CH₂Cl₂, 0 °C to rt, 1.5h; (e.) EtS₂CCl (1.2 eq), DMAP (0.4 eq), Et₃N (1.5 eq), CH₂Cl₂, 0 °C to rt, 2h; (f.) 2,4,6-collidine (1.2 eq), IPA, DLP (0.7 eq), 100 °C, 2h, 60% (4 steps); (g.) Schwartz reagent (3 eq), THF, rt, 3h, 75%; (h.) [1] HF-pyr (70%, 4 eq), pyr, EtOAc, 0 °C, 2 hours, 45%; [2] TFA:H₂O:THF (1:1:4 v/v/v), 0 °C to rt, 48h, 75%.

Commercially available cytidine (**99**) was protected in the first step by treatment with 1,3-dichloro-1,1,4,4-tetraisopropylidisiloxane (TIPDSCl, Markiewicz reagent) in pyridine (pyr) at room temperature overnight, to afford intermediate **100** in 57% yield.³⁸⁰⁻³⁸² Compound **100** was then protected by *N*-acetylation of the amino group on the base by treatment with

acetic anhydride (Ac_2O) in ethanol (EtOH) under reflux over a period of 3.5 hours. Ac_2O was added in two portions to push the reaction to completion, affording compound **101** in quantitative yield.³⁷⁹

The free 2'-hydroxyl group in intermediate **101** was oxidised to a ketone by treatment with Dess-Martin periodinane (DMP) in CH_2Cl_2 . The reagent (2 eq) was added at 10 °C and the mixture was stirred at room temperature overnight and finally quenched with a solution of sodium bicarbonate (NaHCO_3) and sodium thiosulfate ($\text{Na}_2\text{S}_2\text{O}_3 \cdot 5\text{H}_2\text{O}$); extraction of the mixture with diethyl ether yielded a crude mixture containing only desired compound **102** as confirmed by ES-MS and $^1\text{H-NMR}$ analysis of the crude, without any trace of starting material **101**. This crude was not purified further but used directly for the next step.^{379,383,384} The ketone group in **102** was converted into a cyanohydrin moiety by treatment with aluminium chloride (AlCl_3) and trimethylsilyl cyanide (TMSCN) that were added carefully to a solution of **102** in CH_2Cl_2 in an ice-cold bath under anhydrous conditions. The mixture was stirred in ice for 45 minutes and then at room temperature for another 45 minutes, and was then quenched with ammonium chloride (NH_4Cl) and extracted with CH_2Cl_2 . All publications describing the product of this reaction state that it yields a mixture of 2'-cyanohydrins (**103a** and **103b**) as reported in Figure 9.3.^{369,370,379}

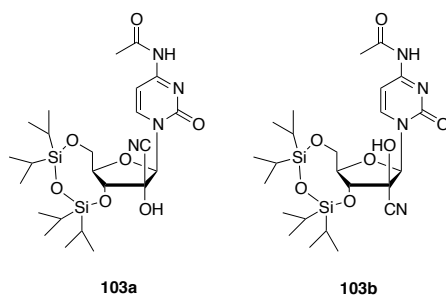


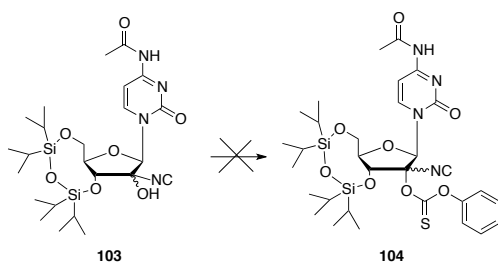
Figure 5.3 Structure of the two 2'-cyanohydrins **103a** and **b**.

However the ratio between the two diastereoisomers is never clearly specified. In our hands, the product of this reaction was not purified by chromatography, due to the well known instability of the 2'-cyanohydrin moiety, that easily reverts into the original ketone functionality (starting material **102**).³⁸⁵ Analysis of the crude mixture by $^1\text{H-NMR}$ suggested the presence of only one species, which could potentially be represented by isomer **103b**. In fact the steric hindrance on the β -face would interfere with the attack of the cyano anion from the β -face, leading to the synthesis of **103b** as a main product. This

would be in accordance with the reported synthesis of 3'-cyanohydrins of different pyrimidine and purine nucleosides via similar oxidation and cyano addition reaction.³⁸⁵

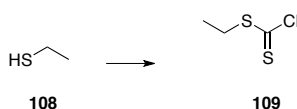
Different substituents could be used to protect the 2'-hydroxyl group of the 2'-cyanohydrin **103a,b** in order to generate a good leaving group for the following elimination reaction.³⁷⁹

The initial attempt involved the use of commercially available phenyl chlorothionocarbonate (PhOCSCl)²⁰⁶ in acetonitrile (CH₃CN) in the presence of DMAP as a catalyst and triethylamine (TEA) as a base.^{369,379} This reaction led to decomposition of the starting material without isolation of the desired product **104** (Scheme 9.4).



Scheme 5.4: Attempted synthesis of thiocarbonate derivatives **104**. Reagents and conditions: PhOCSCl (1.5 eq), Et₃N (1.5 eq), DMAP (0.5 eq), CH₃CN, 0 °C, 2h.

A second strategy was attempted, involving the use of ethyl chlorodithioformate (EtSCSCl, **109**),³⁷⁹ a less hindered reagent which is not commercially available and was synthesised according to Godt *et al.* as reported in Scheme 5.5.³⁸⁶

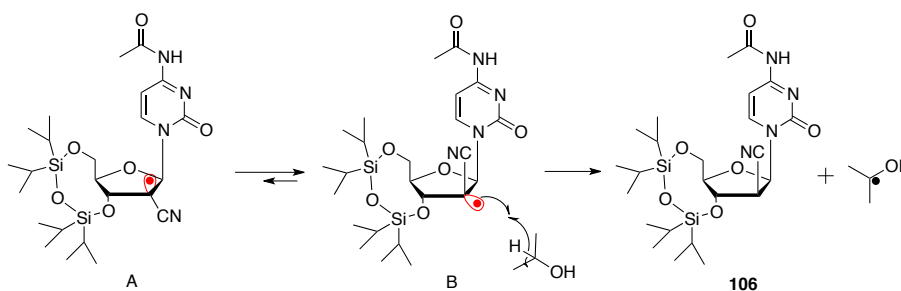


Scheme 5.5: Synthesis of ethyl chlorodithioformate (EtSCSCl, **109**). Reagents and conditions: thiophosgene (0.0015 eq), toluene, 10 °C, 16h.

Ethanethiol (EtSH) was dissolved in toluene (a less toxic alternative solvent to the reported benzene) and added to a solution of thiophosgene (CSCl₂) in toluene at 10 °C. the mixture was stirred overnight at low temperature, then the solvent and side-products were removed under reduced pressure and desired EtSCSCl was isolated by distillation as a dark orange oil.³⁸⁶

Freshly prepared **109** was then reacted with **103** to yield the thiocarbonyl intermediate **104**. The crude was not purified further but used directly in the next step, involving deoxygenation with 2,4,6-collidine and dilauroyl peroxide (DLP) in isopropanol (IPA) at 100 °C for 2 hours.^{387,388} This radical step afforded 2'-cyano arabinosyl derivative **106** as

the only product. According to previous reports on similar reactions, the 2'-*tert* radical formed from the deoxygenation reaction are in equilibrium between α (**A**) and β (**B**) face, as shown in Scheme 5.6.^{369,370,372,389-391}



Scheme 5.6: Equilibrium between position α (**A**) and β (**B**) for the *tert*-radical formed after deoxygenation of **105** and reaction of α -radical with isopropanol with formation of β -cyano derivative **106**.

Since the β face is more hindered than the α -face, the radical **B** would react more favorably with isopropanol, affording **105** as 2'-cyano arabinonucleoside. (Scheme 5.6).^{369,370,372,389-391}

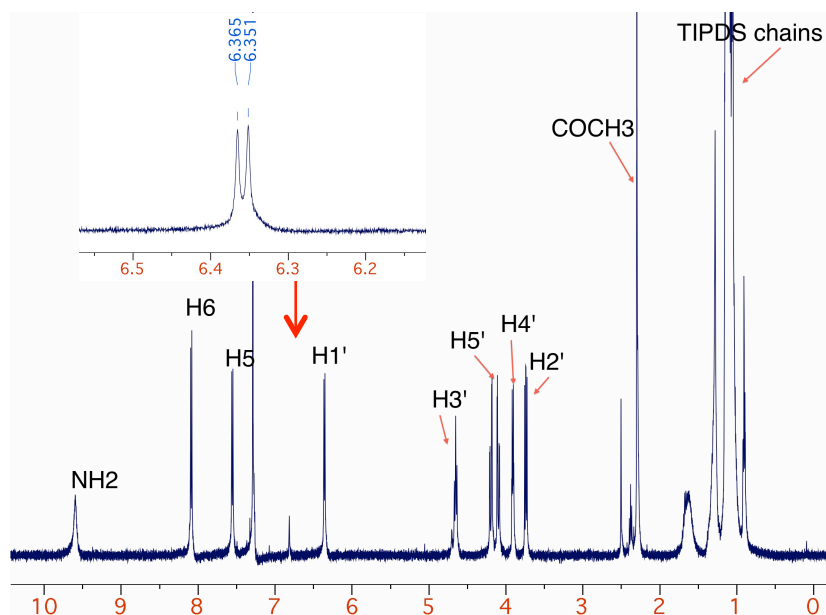


Figure 5.4: ¹H NMR spectrum of deoxygenated intermediate **106**.

The ¹H NMR spectra of intermediate **106** reported in Figure 5.4 confirms the success of the deoxygenation, due to the presence of a doublet signal corresponding to the H_{1'} in the sugar moiety, due to coupling with H_{2'} ($^1J = 7.0$ Hz). The signal corresponding to this same proton is a singlet in the previous intermediates **102**, **103** and **105** due to the lack of a proton in position 2'. The presence of only one product and the extensively documented

selectivity of the radical deoxygenation reaction strongly support that this product corresponds to the 2'-cyano arabino nucleoside **106**.

The selective removal of the acetyl group on the base in compound **106** was performed in 75% yield by treatment with zirconocene hydrochloride (Schwartz's reagent) in tetrahydrofuran (THF) for 3 hours, according to methodology by Bhat *et al.*³⁹² that had been previously applied with good results by our team on a broad selection of *N*-acetylated nucleoside analogues.³⁶⁸ This procedure was applied as an innovative and better yielding alternative to the reported treatment of intermediate **106** with a 3% solution of HCl in CH₃OH, which was described to afford desired **107** in 53% yield.³⁶⁹

The final step of the synthesis of CNDAC was the removal of the TIPDS protecting group. The reported procedure described the use of a 1N solution of TBAF in THF in the presence of acetic acid, yielding deprotected **107** in 84% yield. In order to avoid possible problems related to the removal of hydrolysed TBAF residues, and to the known instability of CNDAC in basic conditions,^{369,393} different deprotective strategies were attempted. Consequently, the deprotection was tested first on a small amount of the substrate (**106**), by treatment with HF-pyridine (HF-pyr, 70%) in pyridine and ethyl acetate (EtOAc) at 0 °C for 2 hours (Scheme 5.3).³⁹⁴ This method yielded free CNDAC in 45% yield.

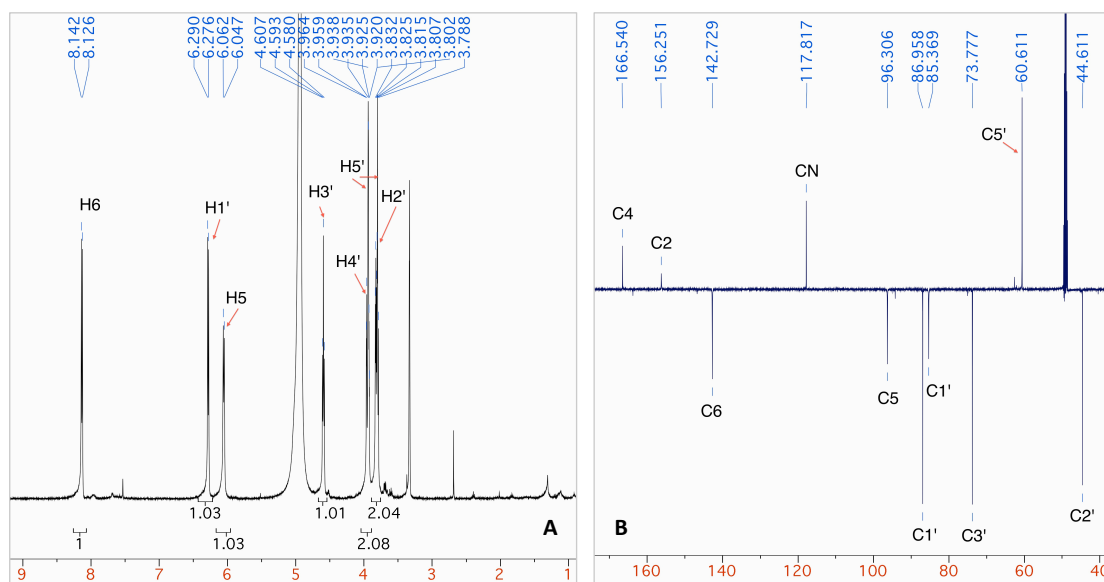
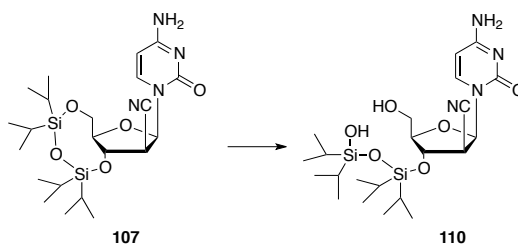


Figure 5.5: ¹H NMR (A, 500 MHz) and ¹³C NMR (B, 125 MHz) spectra of CNDAC (**97**) in CD₃OD.

The characteristic upfield signal corresponding to H2' in the ¹H NMR (Figure 9.5) and the presence of a CN signal (142.73 ppm) in the ¹³C NMR (Figure 9.6) confirm the structure of the synthesised nucleoside. A different procedure that afforded CNDAC in better yield was carried out by treating protected **106** in a 1:1:4 mixture of trifluoroacetic acid (TFA),

water and tetrahydrofuran (THF) at 0 °C and then stirring the mixture at rt (Scheme 5.3). The reaction was very slow but yielded 75% of fully deprotected CNDAC after 48 hours.³⁰⁰

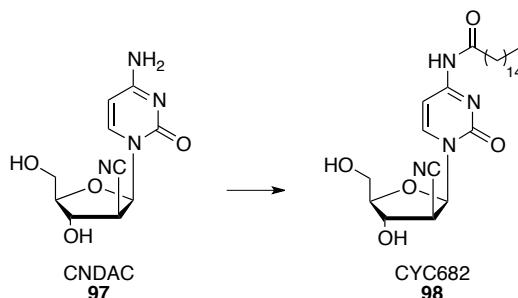
A similar method was used to synthesise selectively deprotected intermediate **110** in position 5' in order to have a suitable precursor for the synthesis of CNDAC ProTides. This intermediate was allowed to react with the appropriate phosphorochloridate and *t*BuMgCl to yield 5'-phosphoramidate silylated intermediates. These structures finally underwent a deprotection step in order to afford the desired CNDAC ProTides and the steps to the synthesis of CNDAC ProTides briefly outlined here will be thoroughly explained in the next paragraphs. The selective deprotection of **107** was carried out by treatment with a 1:1:4 mixture of TFA:H₂O:THF at 0 °C. The mixture was stirred for 2 hours and then stopped through evaporation of the volatiles to avoid complete deprotection of the nucleoside, yielding intermediate **110** in 62% yield, as confirmed by ¹H-NMR and bidimensional COSY experiment.³⁰⁰



Scheme 5.7: Synthesis of 5'-deprotected intermediate **110**. Reagents and conditions: TFA:H₂O:THF (1:1:4 v/v/v), 0 °C, 2h, 62%.

5.3 Synthesis of sapacitabine (CYC682)

CNDAC was used as a starting material for the synthesis of sapacitabine, *N*⁴-pamitoyl derivative involved in clinical studies.

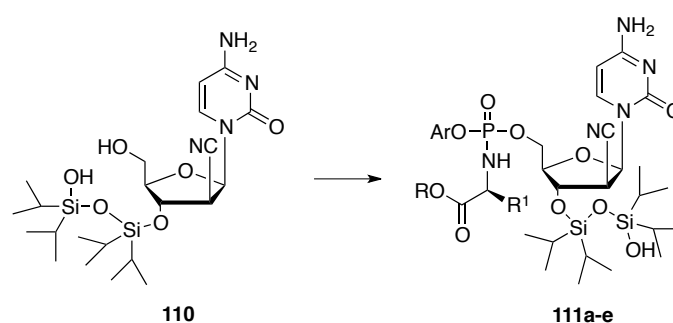


Scheme 5.8: Synthesis of sapacitabine. Reagents and conditions: palmitic anhydride (1.7 eq), 1,4-dioxane:H₂O (20:1), 85 °C, 4h, 45%.

The nucleoside was refluxed in a mixture of 1,4-dioxane and water (20:1) at 85 °C in the presence of palmitic anhydride heating the mixture for 4 hours, and was converted into the desired N^4 -protected nucleoside in 45% yield.³⁷⁹

5.4 Synthesis of CNDAC ProTides

As anticipated, 3'-TIPDS protected CNDAC (**110**) was selectively functionalised of the 5'-hydroxyl group *via* treatment with an appropriate phosphorochloridate and *t*BuMgCl in THF,¹⁰⁵ to afford the desired CNDAC ProTides (Scheme 5.9).



Scheme 5.9: Synthesis of CNDAC 3'-protected ProTides. Reagents and conditions: appropriate phosphorochloridate (3 eq), *t*BuMgCl (1.5 eq), anh. THF, rt, 16h.

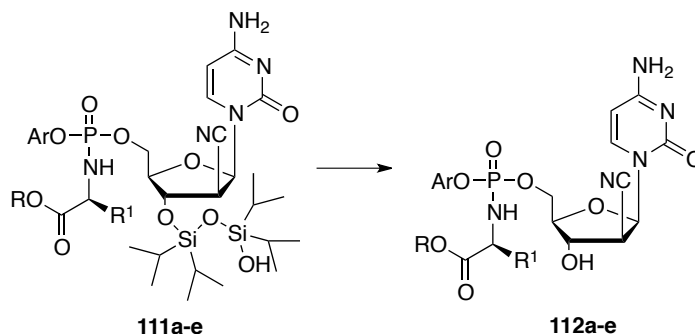
The coupling step between 3'-protected nucleoside **110** and the appropriate phosphorochloridate afforded moderate to good yields (38-70%) of the 3'-protected ProTides (**111a-e**, Table 5.1).

Cpnd	Ar	R	R ¹	AA	Yield
111a	Nap	<i>n</i> -Pen	<i>i</i> Bu	L-Leu	60%
111b	Ph	Bn	CH ₃	L-Ala	63%
111c		Bn	CH ₃	(L-Ala)	70%
111d	Nap	Bn	CH ₃	L-Ala	38%
111e	Ph	<i>n</i> -Hex	CH ₃	L-Ala	44%

Table 5.1: Structures and synthetic yield of 3'-TIPDS protected CNDAC ProTides (**111a-e**).

The first attempt of deprotection was carried out by treatment with TFA:H₂O:THF (1:1:4) at room temperature (Scheme 5.10, **[1]**). The reaction was monitored over 6 hours and then stopped because only small traces of potential product **112a** presented on TLC, along with degradation of the material into a baseline spot (Table 5.2, entry 1). This method was

therefore not considered suitable to our aims. Due to the small amount of starting material on which the reaction was attempted, the isolation of pure product was not successful.



Scheme 5.10: [1] TFA:H₂O:THF (1:1:4), rt, 6h. [2] TFA: CH₂Cl₂ (1:1) 0 °C to rt, 8h. [3] KF (6 eq), 18-crown-6 (0.3 eq), THF, rt, 48h. [4] HF-pyr (9.2 eq), pyr (9.2 eq), EtOAc, 0 °C, 16h.

Entry	Starting material	Procedure	Yield
1	111a	[1]	Traces
2	111a	[2]	Traces
3	111b	[3]	17%
4	111b	[4]	30%
5	111c	[4]	11%
6	111d	[4]	7%
7	111e	[4]	5%

Table 5.2: Structures of products from Scheme 5.10 and relative yields.

A different attempt of deprotection of **111a** was tried by stirring the material in a 1:1 mixture of TFA in CH₂Cl₂ at 0 °C for 2 hours and then allowing the reaction mixture to reach room temperature (Scheme 5.10, [2]).³⁹⁵ After 8 hours the mixture was evaporated and the unreacted material recovered (Table 5.2, entry 2); however due to the small amount it could not be subjected to any other deprotecting step.

Alternative deprotecting steps were further applied on the phenoxy L-alanine benzyl ester **111b**. One portion was treated with potassium fluoride (KF) and a catalytic amount of 18-crown-6 ether in THF, at room temperature (Scheme 5.10, [3]).³⁹⁶ The reaction proved to be very slow with only traces of product detected by TLC and HPLC after 16 hours. However the reaction was stirred for an additional 32 hours, until HPLC analysis of the crude showed 59% conversion. Purification of the crude was tedious, due to the close retention factor (R_f) on silica gel chromatography between starting material **111b** and product **112b** and especially because of the low amount of starting material used for the

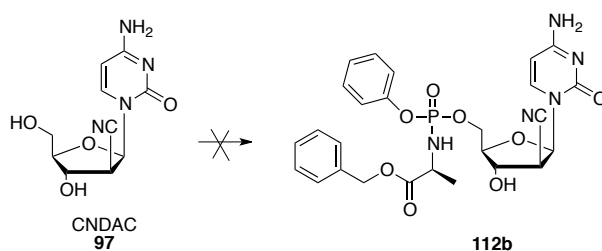
reaction, and finally the desired deprotected product was obtained in only 17% yield (Table 5.2, entry 3).

The other portion of **111b** was submitted to an alternative deprotecting strategy, involving the treatment with HF-pyridine (HF-pyr) in ethyl acetate (EtOAc) at 0 °C, in the presence of an additional amount of pyridine (Scheme 5.10, [4]).³⁹⁴ The reaction was monitored over time by HPLC and after 24 hours the conversion to desired product **112b** was 63%. The mixture was quenched by the addition of trimethylmethoxysilane (TMSOMe), evaporated and purified by column chromatography affording the desired product (**112b**) in 30% isolated yield (Table 5.2, entry 4).

Due to the higher yield obtained, this latter methodology was considered the most suitable to afford deprotected CNDAC ProTides, and was adopted in all other examples shown in Table 5.2 (entries 5-7).

Despite the moderate to good yields deriving from the coupling reaction between 3'-protected CNDAC (**110**) and the appropriate phosphorochloridates, final yield of desired compounds (**112a-e**) was greatly affected by the deprotection step that was unusually difficult. This was believed to be due to the steric hindrance of the cyano group in the α -position, as similar deprotecting attempts on different Ara-nucleosides were reported to lead to poor results.³⁹⁷ However an additional factor affecting the yield was the amount of starting material used, as the purification of small amounts of product was very low yielding when starting with amounts of **110** lower than 50 mg.

One attempt for the synthesis of phenyl (benzyloxy-L-alanyl) CNDAC ProTide (**112b**) was also performed by treatment of the unprotected parent nucleoside (**97**) with phenyl (benzyloxy-L-alanyl) phosphorochloridate and NMI in anhydrous THF.¹⁰⁵ However after 16 hours, analysis of the crude reaction by TLC did not show any trace of product but only evident decomposition of the nucleoside, possibly due to the already known instability of CNDAC in basic conditions.^{369,393}



Scheme 5.11: Attempted synthesis of CNDAC ProTide **112b** via the NMI method on unprotected CNDAC (**97**). Reagents and conditions: phenyl (benzyloxy-L-alanyl) phosphorochloridate (3 eq), NMI (5 eq), anh. THF, rt, 16h.

5.5 *In vitro* anticancer screening of CNDAC ProTides

CNDAC ProTides (**112b-e**) were tested by WuXi AppTech against a panel of cell lines and their cytotoxic activity was compared to the activity of the prepared parent nucleoside CNDAC (**97**) and synthesised sapacitabine (CYC682, **98**), a CNDAC prodrug currently in clinical development. The selection of cell lines (Table 5.3) depended on the clinical development of sapacitabine against haematologic malignancies.³⁹⁸

Cell line	Malignancy
CCRF-CEM	Acute lymphoblastic leukaemia
HEL92.1.7	Erythroleukaemia
HS445	Hodgkin's lymphoma
MOLT-4	Acute T lymphoblastic leukaemia
RL	Non Hodgkin's B-lymphoma
Z-138	Mantle cell lymphoma
HL-60	Acute promyelocytic leukaemia
K562	Chronic myelogenous leukaemia
MCF7	Breast adenocarcinoma
KG-1	Acute myelogenous leukaemia

Table 5.3: Selected cell lines for *in vitro* cytotoxic screening of CNDAC derivatives by WuXi AppTech.

In these *in vitro* evaluations, CNDAC was very potent, especially on leukaemic cells CCRF-CEM, HEL92.1.7 and on the lymphoma cell lines Z138, with IC₅₀ values often lower than the minimum concentration considered. CNDAC was also active at the submicromolar range on the solid cell line MCF7. On the other cells, the parent nucleoside did not perform as effectively, but with IC₅₀ still in the low micromolar range. However, a complete lack in activity was observed on the acute myeloid leukaemia cell line MOLT-4, which was paralleled by similar results for sapacitabine (CYC682) and CNDAC proTides **112b-e**.

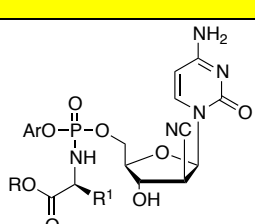
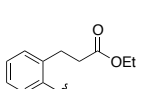
Common structure	Cpnd	Ar	R	R ₁	AA
	112b	Ph	Bn	CH ₃	L-Ala
	112c		Bn	CH ₃	L-Ala
	112d	Nap	Bn	CH ₃	L-Ala
	112e	Ph	<i>n</i> -Hex	CH ₃	L-Ala

Table 5.4: CNDAC ProTides tested for *in vitro* cytotoxicity on selected cell lines by WuXi AppTech.

Despite being 2 to 10 fold more active than CNDAC ProTides, sapacitabine (**CYC686**) was less active than the parent nucleoside on all considered cell lines. CNDAC ProTides **112b-e** were often more than ten fold less active than CNDAC.

Cpnd	CCRFCEM		HEL92.1.7		HS445		MOLT-4		RL	
	IC ₅₀	MI%	IC ₅₀	MI%	IC ₅₀	MI%	IC ₅₀	MI%	IC ₅₀	MI%
CNDAC	<0.02	100	0.05	91	4.59	88	>198	-1	0.97	72
CYC686	0.11	98	0.43	93	3.83	98	>198	-5	6.9	81
112b	1.47	98	1.36	89	25.95	90	>198	0	30.89	85
112c	3.26	102	6.05	93	81.52	83	>198	-1	55.34	82
112d	3.45	103	4.37	93	49.95	75	>198	-4	189.52	62
112e	0.63	99	0.64	92	9.84	93	>198	-2	17.81	81
PTX	0.003	98	0.02	83	0.01	74	0.003	95	0.003	83

Table 5.5: *In vitro* cell viability screening of CNDAC, sapacitabine (CYC686) and CNDAC ProTides (**112a-e**). Cytotoxicity data reported as μM IC₅₀ values (concentration of drug causing 50% of cell viability inhibition) and MI% (maximum inhibitory effect of the drug at the range of concentration considered). PTX: paclitaxel (control). Assays performed by WuXi AppTech.

The phenyl (hexyloxy-L-alaninyl) CNDAC ProTide **112e**, although never as potent as the parent nucleoside, showed the best activity among this family of prodrugs, with IC₅₀ values close to the clinically developed prodrug sapacitabine on cell lines CCRF-CEM, HEL92.1.7, Z138, and in the submicromolar range (0.63-0.78 μM).

Cpnd	K562		KG-1		MCF7		Z138	
	IC ₅₀	MI%	IC ₅₀	MI%	IC ₅₀	MI%	IC ₅₀	MI%
CNDAC	3.59	63	6.84	90	0.15	92	<0.02	100
CYC686	16.71	66	35.45	97	0.72	84	0.64	100
112b	39.8	82	86.95	87	14.29	94	2.39	100
112c	78.3	66	70.02	78	17.45	95	3.36	101
112d	83.28	59	67.65	76	8.9	70	2.01	100
112e	26.82	91	92.51	68	7.1	93	0.78	100
PTX	0.01	91	0.08	88	0.01	65	0.002	99

Table 5.6 *In vitro* cell viability screening of CNDAC, sapacitabine (CYC686) and CNDAC ProTides (**112a-e**). Cytotoxicity data reported as μM IC₅₀ values (concentration of drug causing 50% of cell viability inhibition) and MI% (maximum inhibitory effect of the drug at the range of concentration considered). PTX: paclitaxel (control). Assays performed by WuXi AppTech.

This result suggests that modification in the ProTides scaffold could be introduced, enlarging the number of ProTide bearing linear ester chains and also modifying the amino acid moiety, with the aim of identifying a suitable active alternative to sapacitabine.

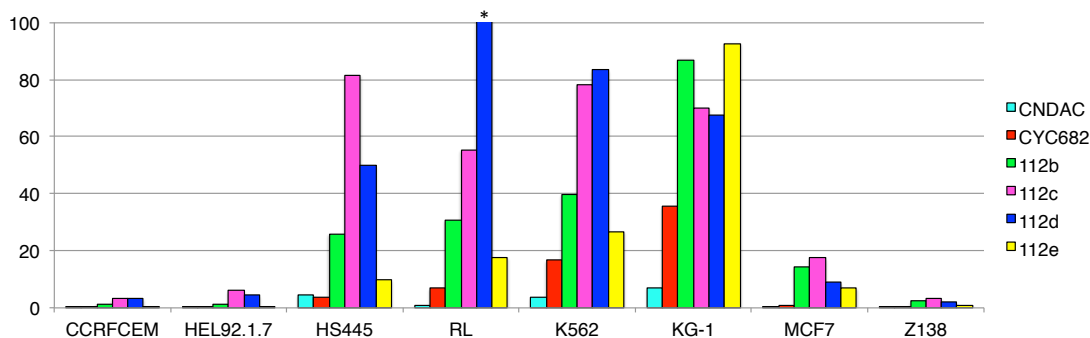
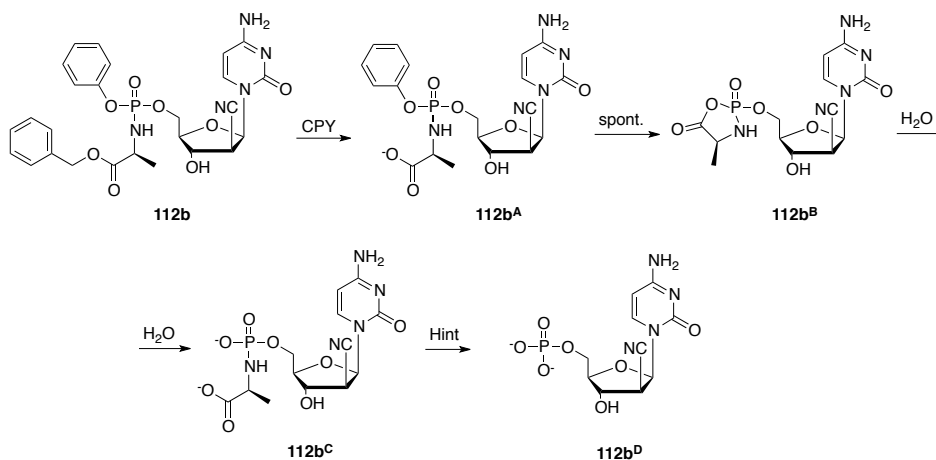


Figure 5.6: Cytotoxic evaluation of CNDAC proTides **112b-e**, compared to parent nucleoside and sapacitabine (**CYC682**). Molt4 cell line was not included as all compounds had $IC_{50} > 198 \mu\text{M}$. * $IC_{50} > 198 \mu\text{M}$.

Moreover, investigations on the lack of activity of some of the least active prodrugs could explain whether this is due to an ineffective processing of the ProTide moiety and therefore a lack of release of CNDAC-MP inside the cell.

5.6 Mechanistic investigations

Investigations on the enzymatic steps required for ProTides activation were performed in order to evaluate whether the reduced activity of CNDAC ProTides in comparison to the parent nucleoside could derive from inefficient intracellular processing. An enzymatic NMR assay was performed treating CNDAC ProTide **112b** with carboxypeptidase Y (CPY). Moreover, the final product of CPY-catalysed activation, **112b^C**, was docked into the active site of Hint enzyme, responsible for the final phosphoramidate bond cleavage, with release of CNDAC-monophosphate (**112b^D**).¹²⁸



Scheme 5.12 Putative intracellular activation of CNDAC ProTide **112b** catalysed by CPY/Hint enzymes.

5.6.1 CPY enzymatic assay

CNDAC ProTide **112b** was treated with CPY, and Figure 5.7 shows the spectra obtained after the overnight enzymatic processing. After 7 minutes from the enzyme addition, one more downfield peak corresponding to intermediate **112b^A** appears, and after 14 minutes one broad peak at 7.3 ppm shows the conversion to intermediate **112b^C**, which is complete after 42 minutes from addition of the enzyme, and is confirmed by ES-MS analysis of the crude after 12 hours (calculated m/z: 401.09 [M], found m/z: 403.1 [M + 2H⁺]).

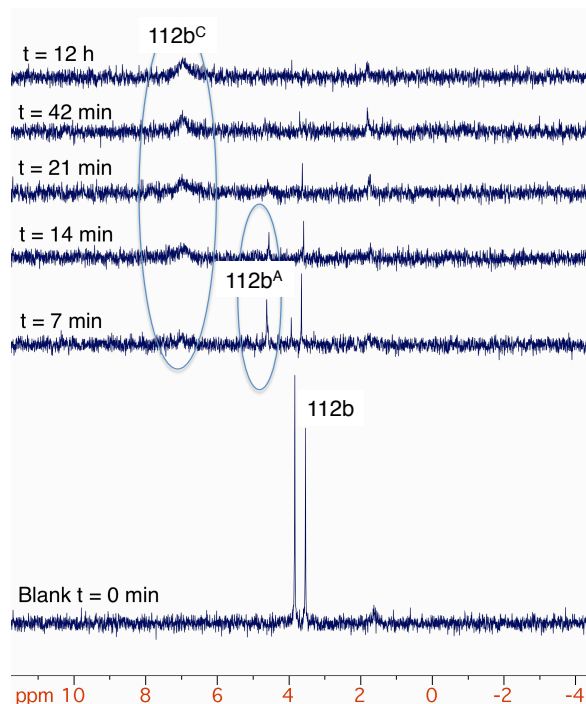


Figure 5.7: ³¹P NMR spectra showing conversion of ProTide **112b** to intermediate **112b^C** by CPY enzyme.

These results suggest that lower cytotoxic activity of CNDAC ProTide **112b** is not a consequence of inefficient processing to intermediate **112b^C**, therefore might derive from low recognition by the phosphoramidase enzyme Hint.

5.6.2 Docking in the active site of Hint1

In order to investigate whether the low activity of CNDAC ProTides such as **112b** could derive from inefficient intracellular processing to CNDAC-MP, docking of the L-alaninyl-phosphate intermediate (**112b^C**) was performed within the active site of Hint. Figure 5.8 shows an overlap between the co-crystallised substrate AMS-Lys and **112b^C** in the active pocket of Hint.³⁹⁹ Although fitting in the binding pocket, intermediate **112b^C** interacts differently from AMS-Lys. The nucleobase moiety is positioned outside the pocket,

potentially due to the presence of the cyano group in position 2', which would otherwise clash with the pocket residues. This leads to an incorrect positioning of the phosphoramidate moiety, which does not interact with the crucial residues involved in the phosphoramidase activity (His-51, His-112 and His-114).⁴⁰⁰

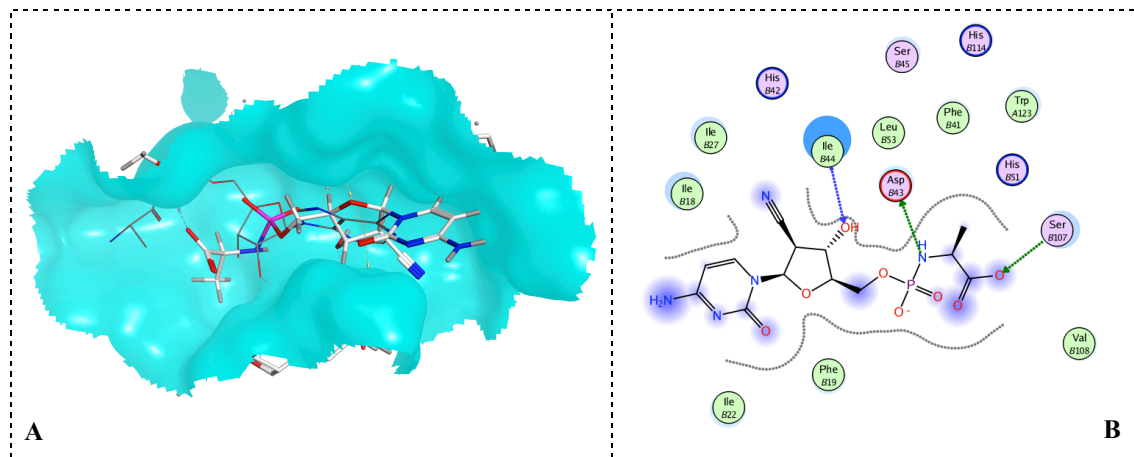


Figure 5.8: (A) Docking of the L-alanyl phosphoramidate monoester of CNDAC (**112b^C**) in the active site of Hint1. (B) 2D interactions between **112b^C** and Hint1 binding pocket.

In conclusion the docking simulation in Hint1 active pocket suggests that the poor activity of CNDAC ProTides could be a consequence of an inefficient processing by this enzyme.

5.7 Conclusions

The promising anticancer potential of sapacitabine (CYC686), a CNDAC prodrug, prompted the investigation of the cytotoxic activity of CNDAC ProTides, as an alternative prodrug strategy that could overcome potentially limiting steps in CNDAC activity, such as the cytidine deaminase-mediated catabolism or the dependency on dCK for the first phosphorylation step or on nucleoside transporters for the cell penetration. Synthesis of CNDAC, sapacitabine and a family of CNDAC ProTides was performed. Cytotoxic screening of these compounds showed that CNDAC ProTides represent less potent derivatives of the parent nucleoside *in vitro* and do not bring an advantage in terms of cytotoxic activity over sapacitabine. Investigations on the intracellular processing of CNDAC ProTides suggested that these results could be due to an inefficient recognition by the phosphoramidase enzyme Hint-1, involved in the last step of ProTides activation. However, interest should be given to the evaluation of CNDAC ProTides in resistance conditions, such as dCK deficiency, because as CNDAC-MP prodrugs, ProTides could

afford an advantage over both CNDAC and sapacitabine. This could lead to a clinical advantage of ProTides over sapacitabine.

6 Trifluorothymidine ProTides

6.1 Background

Trifluorothymidine (trifluridine, trifluoromethyl-2'-deoxyuridine, TFT, **113**), is a nucleoside analogue closely related to thymidine, bearing a trifluoromethyl (CF₃) functionality in position 5 on the pyrimidine ring (Figure 6.1).

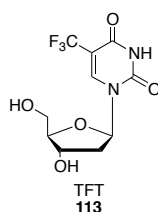
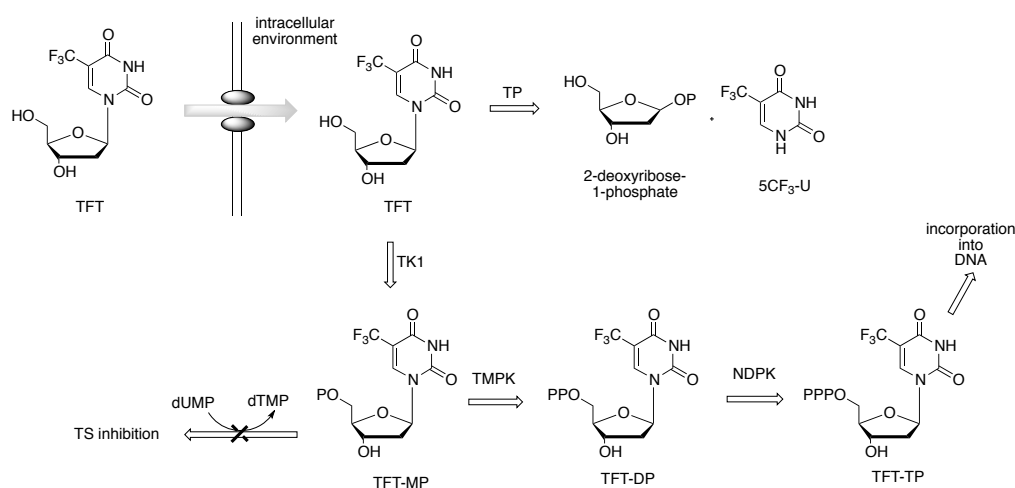


Figure 6.1: Structure of trifluorothymidine (TFT, **113**).

TFT was first synthesised by Heidelberger *et al.* in 1962 in the quest for new fluoropyrimidine analogues of 5-fluorouracil (5-FU) that could avoid the insurgence of resistance to the anticancer treatment.⁴⁰¹⁻⁴⁰⁴ TFT enters the cell via a nucleoside transporter identified as equilibrative transporters 1 and/or 2 (hENT1, hENT2). A recent study reports the involvement of the concentrative nucleoside transporter 1 (hCNT1) in the intestinal absorption of TFT.⁴⁰⁵ TFT is phosphorylated to TFT-monophosphate (TFT-MP) within the cell by the thymidine kinase 1 (TK1) enzyme (Scheme 6.1),⁴⁰³ involved in the salvage pathway.⁴⁰⁶ The efficacy of this nucleoside analogue was reported to derive from inhibition of thymidylate synthase (TS) by TFT-MP,^{404,407,408} similar to 5-fluoro-2'-deoxyuridine monophosphate (FUdR-MP). TS is a rate-limiting enzyme in the pyrimidine *de novo* deoxynucleotide synthesis which catalyses the methylation of 2'-deoxyuridine monophosphate (dUMP) to thymidine monophosphate (TMP) using 5,10-methylenetetrahydrofolate (5,10-CH₂THF) as the methyl-donor. An important difference between the activity of TFT and the other fluorinated pyrimidine analogues on TS is that TFT forms a non-covalent complex between with the enzyme and the cofactor 5,10-CH₂THF, in contrast with the covalent bond formed by FUdR-MP. TFT-MP is then phosphorylated to TFT-triphosphate (TFT-TP), which can be incorporated into the DNA of the cell with subsequent induction of fragmentation (Scheme 6.1).⁴⁰⁹⁻⁴¹²

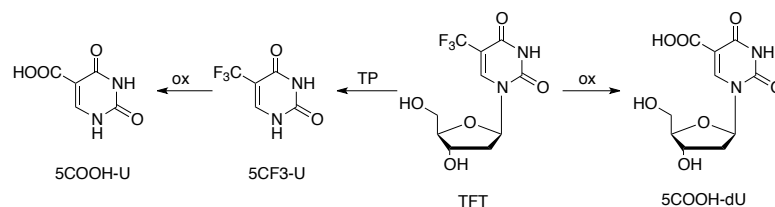


Scheme 6.1: Intracellular metabolism of TFT. P = monophosphate group.

Studies on the administration of TFT to cancer patients led to promising initial results, with responses in 8 of 23 patients with breast cancer, and in 1 out of 6 patients with colon cancer.^{413,414} Unfortunately, rapid recurrence seen after initial regression was evident. Moreover, attempts at using maintenance therapy were hindered by an unacceptable level of bone marrow toxicity. Therefore, the progression of TFT in the clinics as a single agent was halted.^{15,16}

TFT was also investigated as an antiviral agent against herpes simplex virus (HSV)⁴¹⁴ infections and was approved in 1980 by the Food and Drug Administration (FDA) for use in the topical treatment of primary keratoconjunctivitis and epithelial keratitis (Viroptic).^{46,415,416}

Metabolic studies after administrations of TFT reveal that the major metabolites found in the urine are 5-carboxy-2'-deoxyuridine (5COOH-dU), 5-trifluorouracil (5CF₃-U) and 5-carboxyuracil (5COOH-U)^{403,413,414}.



Scheme 6.2 Principal metabolites of TFT in urine, generated by TP de-phosphorylation and oxidation mechanisms.

5COOH-dU is formed in the liver due to the lability of the CF₃ group, which is oxidised in alkaline conditions.^{406,407} 5CF₃-U is formed after cleavage of the glycosidic moiety by thymidine phosphorylase (TP) and is then oxidised into 5COOH-U. A thorough

description of all the metabolites of TFT was documented by Wyrwicz *et al.*⁴⁰⁶ When given orally, TFT is well absorbed, although quickly degraded by thymidine phosphorylase (TP) in the liver.⁴¹¹ Recently, the interest in TFT as an anticancer agent has arisen as a combined therapy as TAS-102 (molar ratio TFT:TPI = 1:0.5) with the TP-inhibitor tipiracil hydrochloride (TPI, Figure 6.2).^{417,418}

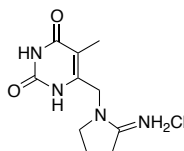
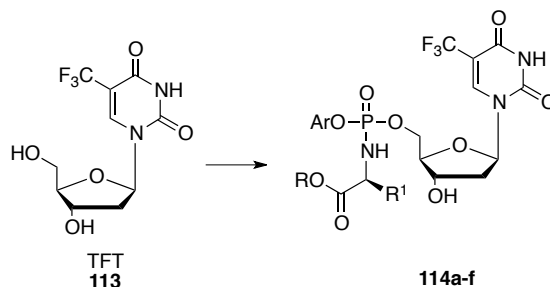


Figure 6.2 Structure of Tipiracil hydrochloride (TPI).

The increase stability of TAS-102 has led to an increase in antitumour activity,⁴¹⁶ therefore this combination has been involved in Phase I, II and III clinical studies showing prolonged survival in patients with metastatic colorectal cancer that were refractory or intolerant to standard chemotherapy often including 5FU.^{419,420} Based on the results of the phase II clinical study, TAS-102 was approved in 2012 in Japan for the treatment of unresectable advanced and recurrent colon cancers.⁴¹⁶ A phase III clinical study confirmed the efficacy of TAS102 with median overall survival improved from 5.3 months with placebo to 7.1 months with treatment.⁴²¹ Temmink *et al.* have conducted a study aimed at understanding the potential resistance mechanisms that can arise from TFT treatment.⁴²² In this study, resistance to TFT was induced in H630 colorectal cell line by intermittent short exposure to high concentrations of the drug. The results indicate the principal resistance mechanisms are the down-regulation of TK and a reduced expression of hENT transporters.⁴²² These findings prompted us to investigate the potential of applying the ProTide approach to TFT, with the aim of bypassing these two resistance mechanisms. Moreover, ProTides were already reported to be stable to TP deactivation,^{152,423} and this advantage could avoid the co-administration of TPI. A family of TFT ProTides was therefore synthesised and the cytotoxic potential of these prodrugs was analysed on colorectal, breast and pancreatic cell lines. Moreover, additional screening of these prodrugs was also performed on HSV infected cells, due to the well-known activity of TFT on DNA-viruses.

6.2 Synthesis of TFT ProTides

ProTides of TFT were synthesised from commercially available TFT that was treated with *N*-methylimidazole (NMI) and the appropriate phosphorochloridate in THF,¹⁰⁵ affording ProTides **114a-f** in 11-45 % yields.



Scheme 6.3: Synthesis of TFT ProTides **114a-f**. *Reagents and conditions*: NMI (5eq), appropriate phosphorochloridate (3 eq), anhydrous THF, 16h, rt.

Common structure	Cpnd	Aryl	R	R ₁	AA	¹⁹ F (ppm)	³¹ P (ppm)	Yield %
	114a		Bn	Me	L-Ala	-64.34, -64.35	3.95, 3.54	11
	114b	1-Naph	Bn	Me	L-Ala	-64.30, -64.33	4.47, 4.03	31
	114c	Ph	Bn	Me	L-Ala	-64.11, -64.15	4.12, 3.55	45
	114d	1-Naph	cHex	Me	L-Ala	-64.32, -64.24	4.06, 3.71	41
	114e	Ph	Neop	Me	L-Ala	-64.23, -64.30	4.40, 4.10	27
	114f	1-Naph	<i>n</i> -Pen	<i>i</i> Bu	L-Leu	-64.32, -64.23	4.79, 4.23	26

Table 6.1: Structures, ¹⁹F-NMR and ³¹P-NMR peaks corresponding to the two diastereoisomers of each ProTide, and yields of synthesised compounds (**114a-f**), ¹⁹F-NMR spectra performed in CD₃OD (470 MHz), ³¹P-NMR spectra performed in CD₃OD (202 MHz).

The structures of synthesised ProTides included mainly L-alanine as the amino acid moiety, with the exception of compound **114f** bearing L-Leucine. The aryl moiety varied between phenyl (**114c** and **114e**) and naphthyl (**114b**, **114d**, **114f**) with one example of a compound bearing the ethyl-3-phenyl propanoate group (**114a**). The ester group on the synthesised ProTides varied between the benzyl, cyclohexyl, the linear *n*-pentyl and the branched neopentyl (Table 6.1).

The identity of compounds **114a-f** was confirmed by NMR analyses. The distinctive splitting pattern in ³¹P NMR and ¹⁹F NMR spectra due to the presence of an approximately 1:1 ratio of two diastereoisomers is reported in Table 6.1. ¹⁹F NMR and ³¹P NMR spectra of compound **114c** are reported in Figure 6.3.

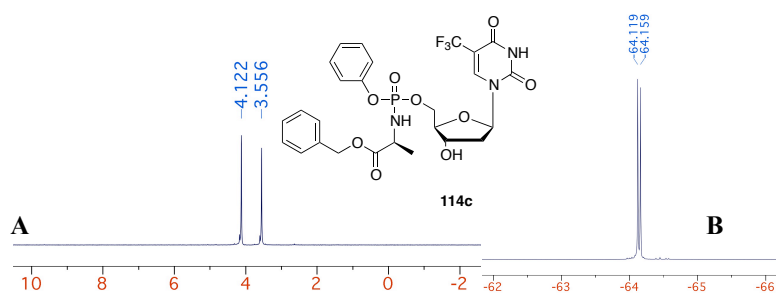


Figure 6.3: ^{31}P NMR (CD_3OD , 202 MHz, **A**) and ^{19}F NMR (CD_3OD , 470 MHz, **B**) spectra of compound **114c**.

The presence of a CF_3 group in position 5 on the pyrimidine ring is confirmed by the presence of a quadruplet at 123.87 ppm corresponding to the CF_3 carbon, whose coupling constant with fluorine is $^1J_{\text{FC}} = 267.5$ Hz (Figure 6.4, **A**). Moreover, two overlapping quadruplets at 105.5 ppm correspond to the C5 carbon of the two diastereoisomers, with $^2J_{\text{FCC}}$ coupling constant of 32.5 Hz (Figure 6.4, **B**).

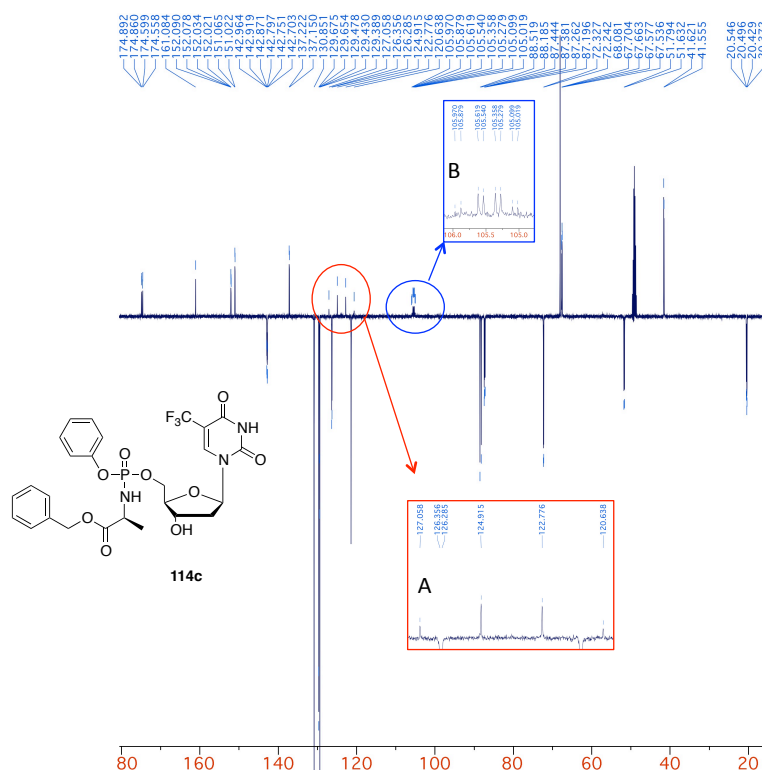


Figure 6.4 ^{13}C -NMR spectrum (CD_3OD , 125 MHz) of compound **114c**, and expansions of selected regions of ^{13}C -NMR. **A**: CF_3 (q, 123.87 ppm, $^1J_{\text{FC}} = 267.5$ Hz), **B**: C5 (2 x q, 105.5 ppm, $^2J_{\text{FCC}} = 32.5$ Hz).

6.3 Biological evaluation

TFT ProTides **114a-f** were screened for their anticancer potential by WuXi AppTech on the cell lines reported, belonging to colon adenocarcinoma, pancreas and breast tumours (Table 6.2, Figure 6.5). The activity of TFT was, in fact, extensively documented *in vitro* and *in vivo* on colon carcinoma models, prior to the clinical trials in patients affected by this malignancy.^{416,424,425} However, TFT was also tested on breast^{426,427} and pancreatic cancer models,⁴²⁸ hence the decision to broaden the set of solid tumours cell lines for this screening.

Cell line	Malignancy
SW620	colon adenocarcinoma
BxPC-3-Luc	pancreatic cancer
HT29	colon adenocarcinoma
MIA PaCa-2	pancreatic carcinoma
MCF-7	breast carcinoma

Table 6.2: Selection of cell lines for the *in vitro* screening of TFT ProTides by WuXi AppTech.

The activity of TFT on the two colorectal cell lines was dissimilar, with submicromolar IC₅₀ on SW620 cell line (0.7 μM) and lower cytotoxicity on HT29 cells (IC₅₀ = 31.7 μM) (Table 6.3). However the MI% was similarly low, and corresponded to approximately 60%, meaning that TFT exerts cytotoxic activity only on this percentage of cells.

Cpnd	SW620		HT29		BxPC-3		MiaPaCa-2		MCF7	
	IC ₅₀	MI%	IC ₅₀	MI%	AbIC ₅₀	MI%	AbIC ₅₀	MI%	AbIC ₅₀	MI%
TFT	0.7	62	31.7	65	>198	45	1.84	86	23.22	57
114a	23.05	100	16.72	99	49.65	98	5.6	90	14.74	100
114b	8.77	100	9.86	110	22.18	98	2.92	95	7.44	100
114c	25.18	60	49.71	92	>198	31	18.74	84	45.37	83
114d	39.59	69	31.75	92	>198	44	16.66	89	33.52	88
114e	11.79	100	10.01	110	32.75	99	4.68	100	8.78	100
114f	17	100	15.33	103	32.69	99	14.03	100	17.81	100
PTX	0.02	96	0.004	75	>0.5	42	0.002	87	0.01	65

Table 6.3: Cytotoxic evaluation of TFT (**113**) and ProTides **114a-c**. Cytotoxicity data reported as IC₅₀ values (concentration of drug causing 50% of cell viability inhibition) and MI% (maximum inhibitory effect of the drug at the range of concentrations considered). PTX: paclitaxel (control). Assays performed by WuXi AppTech.

This could be due to resistance to TFT on the other 40% of cells. Treatment of the two pancreatic cell lines BxPC-3 and MIA PaCa-2 with TFT led again to contrasting results: the nucleoside reached 45% of maximum inhibition of viability on the former cell line therefore an IC_{50} value could not be calculated (reported as $> 198 \mu\text{M}$).

Although TFT ProTides **114a-f** were characterised by higher IC_{50} values on these two cell lines, 4 out of 6 of the compounds reached a complete inhibition of cell viability at moderate μM values. On HT29 cell line, some of the compounds (**114a**, **114b**, **114e** and **114f**) were also 1 to 2-fold more active than TFT, in terms of IC_{50} values. These data may suggest that TFT ProTides could overcome resistance mechanisms associated with the treatment with TFT, due to the ability to exert cytotoxic activity on the total cell population. On this cell line, similarly to the results obtained on SW620, ProTides **114a**, **114b**, **114e** and **114f** reached, instead, the complete inhibition of cell viability and moderate micromolar IC_{50} values. On the other hand, TFT had good cytotoxicity on the latter cell line, with IC_{50} of $1.84 \mu\text{M}$ and $MI_{\%}$ of 86%, while ProTides were all less active than the parent nucleoside in terms of IC_{50} values. TFT was a weak cytotoxic agent on the breast cancer cell line MCF7, while some of the ProTides (**114a** and **114e**) were approximately 3-fold more potent than TFT with complete inhibition of cell viability.

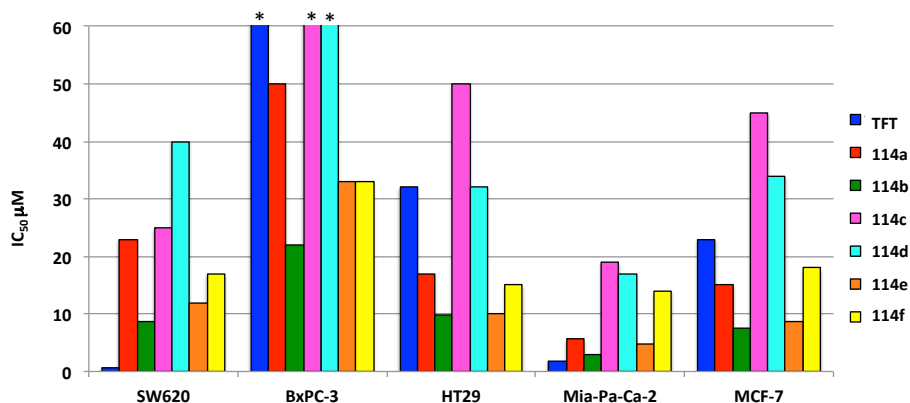


Figure 6.5: Cytotoxic activity of TFT and ProTides **114a-f** on selected cell lines. * $IC_{50} > 198 \mu\text{M}$.

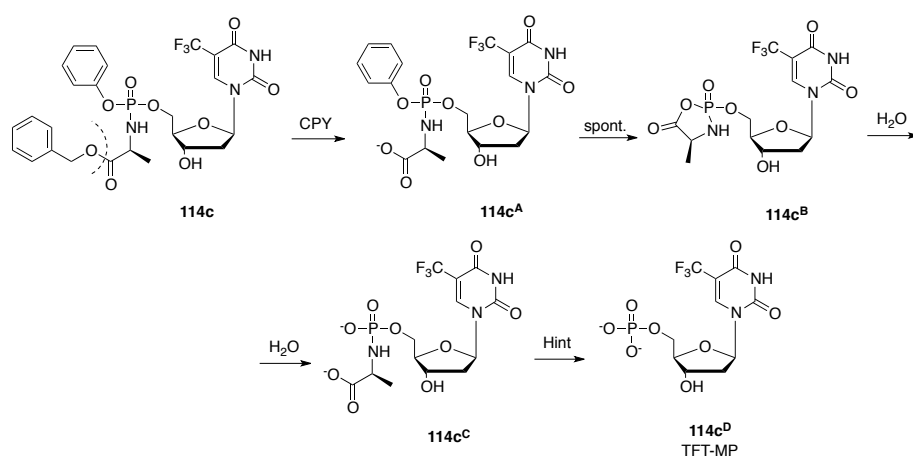
These data show that some TFT ProTides appear to be more active than TFT itself on some of the cell lines considered, both in terms of IC_{50} values and $MI_{\%}$. However high concentrations of compound are required to exert the cell viability inhibition. This could be due to a slow intracellular processing of the ProTide moiety which affects the rate of release of TFT-MP, the active species within the cell. In order to investigate whether the ProTide processing could be the limiting step in the activity of TFT ProTides, mechanistic investigations were performed.

6.4 Mechanistic investigations on TFT ProTides

As previously described, an NMR enzymatic assay with CPY and docking within the active site of Hint were performed.

6.4.1 CPY enzymatic assay

CPY is putatively involved in the cleavage of the amino acid ester, which triggers the metabolic activation of ProTide **114c** with spontaneous cyclisation and release of the phenoxy moiety (**114c^B**), followed by hydrolysis to L-alanyl intermediate **114c^C** (Scheme 6.4).



Scheme 6.4 Putative intracellular conversion of ProTide **114c** into TFT-MP (**114c^D**) catalysed by CPY/Hint enzymes.

^{31}P NMR spectra were recorded over 12 hours to monitor the processing by CPY and Figure 6.6 shows that the peaks corresponding to the diastereomeric mixture of **114c** were quickly converted into two more downfield peaks corresponding to intermediate **114c^A**, lacking the ester group on the amino acid moiety (Scheme 6.4).

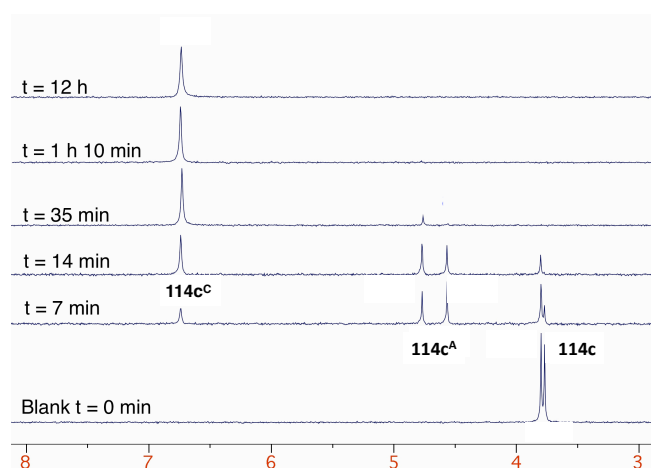


Figure 6.6: ^{31}P NMR spectra showing conversion of ProTide **1.12** to intermediate **1.12^C** in 1h 10 minutes.

Subsequent, the conversion into a peak at 6.80 ppm potentially corresponding to final compound **114c^C**, was confirmed by ES/MS analysis of the solution.

The activation catalysed by CPY is complete in 1 hour and 10 minutes, therefore the first enzymatic step does not appear to be rate-limiting for the initial activation towards TFT-MP.

The CF₃ group in position 5 on the pyrimidine ring of TFT also represents a probe that can be used to monitor the metabolism of TFT ProTides through ¹⁹F NMR, in parallel to ³¹P NMR. In fact comparison between the ¹⁹F NMR spectrum of **114c** at time 0 and after treatment with CPY shows a shift from -63.07 and -63.09 ppm (peaks corresponding to the diastereomeric mixture of **114c**) to one peak at -62.89 ppm, after 12 hours, corresponding to the final structure **114c^C**.

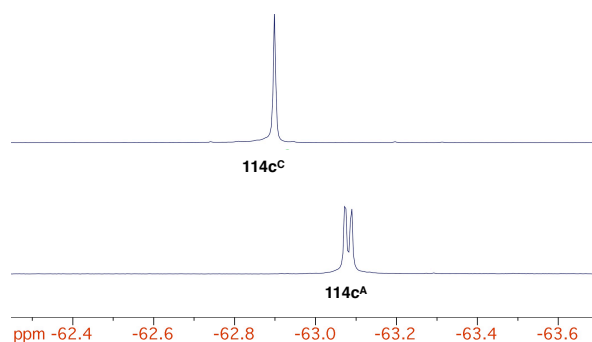


Figure 6.7: ¹⁹F NMR spectra showing conversion of ProTide **114c** to intermediate **114c^C**.

6.5 Docking in the Hint enzyme

The efficient processing by CPY of the ProTide **114c** suggests the first step in the ProTide activation is not a limiting one, and therefore a reason for lack in potent activity of ProTides could depend on the effectiveness of the phosphoramidase-mediated second enzymatic step, responsible for the cleavage of the phosphoramidate moiety with release of the active metabolite TFT-MP. Docking of the L-alaninyl-phosphate intermediate (**114c^C**) was performed within the active site of Hint.

invasion) measured.²²⁴ The activity of TFT was compared both to TFT ProTides and to acyclovir (ACV), a well-known anti-HSV agent.⁴³¹

CPF	% CPE inhibition	CC ₅₀
ACV	50	>10
TFT	-	>10
114a	-	>10
114b	-	>10
114c	-	>10
114d	-	>10
114e	-	>10
114f	50	>10

Table 6.4: Anti-HSV activity of TFT and ProTide **114a-f**. Activity expressed as % reduction of viral CPE at 10 μ M concentration. Assays performed by Dr. J. Bugert, Cardiff University.

Compounds were tested at 10 μ M concentrations. ACV could reach 50% of protection at this dose, while both TFT and ProTides **114a-e** were not effective. Only **114f**, bearing L-leucine pentyloxy naphthyl phosphoramidate moiety, could reach 50% effect at the given dose. This could be due to bypass of resistance mechanisms and could deserve further investigations.

6.7 Conclusions

TFT is a very promising nucleoside analogue used as an antiviral in the topical treatment of HSV infections and has recently also shown intriguing anticancer activity both *in vitro* and *in vivo*. The combination of TFT and TPI, a TP inhibitor, is currently undergoing phase III clinical studies in the USA and has already been approved for the treatment of unresectable advanced and recurrent colon cancers in Japan. Due to the interesting anticancer profile of this agent and the documented resistance mechanisms due to TP inactivation and TK1 and hENT1 down regulation, causing a decrease in intracellular concentrations of the two active metabolites TFT-MP and TFT-TP, the ProTide prodrug approach was applied to TFT with the aim of bypassing all the aforementioned limiting steps in its anticancer activity. A series of TFT ProTides was synthesised in moderate yields and was evaluated *in vitro* on solid cancer cells. These studies revealed that although being a moderate to potent anticancer agent, TFT does not lead to complete inhibition of cell viability at the highest concentration considered. On the other hand, although often reported as less potent than the parent nucleoside, TFT ProTides tend to reach the complete

inhibition of cell viability. This finding could be linked to the bypassing by ProTides of the resistance mechanisms that potentially lead to lack in activity of TFT on some cells, and deserve some further investigations. Moreover, when tested on HSV infected cells, TFT resulted in a weak antiviral agent while one of the pro-drugs (the L-leucinyll derivative **114f**) was effective at a concentration of 10 μ M. In light of these results, the family of TFT ProTides could be expanded in order to include more lipophilic prodrugs such as the L-Leucinyll derivative **114f**.

7 2'-SCF₃ deoxyuridine and 2'-SH deoxyuridine

7.1 Background

The introduction of a trifluoromethylthio (SCF₃) functionality on the sugar moiety of nucleosides was reported to serve as a probe for RNA-ligand interactions and to monitor RNA structure at secondary and tertiary level, through ¹⁹F NMR spectroscopy.⁴³²⁻⁴³⁷ Moreover, the insertion of 2'-SCF₃-bearing nucleoside analogues in double helical regions of the RNA was related to disrupting effects on base-pairing interactions.^{435,436,438}

To date, 2'-deoxy-2'-SCF₃ modified uridine (**115**),⁴³⁷ cytidine (**116**)⁴³⁶ and, more recently, adenosine (**117**) and guanosine (**118**)⁴³⁵ (Figure 7.1) were synthesised and incorporated into oligonucleotides to study their physicochemical properties, however no cell-based *in vitro* data were reported.

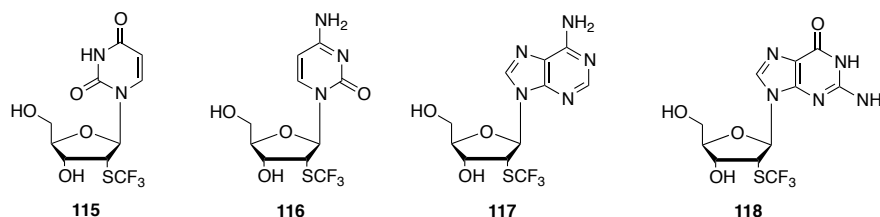


Figure 7.1: Structures of 2'-SCF₃-2'-deoxynucleosides (**115-118**) synthesised to date.

The destabilising properties of these nucleoside analogues on RNA structure were considered as an interesting starting point for the investigation of the potential anticancer properties of 2'-SCF₃-2'-deoxyuridine (2'-SCF₃-2'-dU, **115**), an easily chemically accessible nucleoside analogue within the family of structurally related nucleosides depicted in Figure 7.1. No data regarding the recognition of this nucleoside by kinase enzymes required for the first phosphorylation step or nucleoside transporters responsible for cell penetration was reported. However, a bulky modification such as the 2'-SCF₃ group may cause inefficient recognition of the structure by nucleoside transporters or kinase enzymes.⁴³⁹ ProTide 5'-monophosphate prodrugs could therefore offer an advantage in terms of bypassing the first monophosphorylation step or the dependency on a nucleoside transporter for cell entry, due to increased lipophilicity of the ProTide, enabling passive diffusion. Therefore, the ProTide approach was applied to this nucleoside analogue, for the synthesis of a family of 2'-SCF₃-2'-dU ProTides (Figure 7.2) to be tested

on a selection of malignant cell lines along with the parent nucleoside and investigate the potential anticancer activity of these derivatives.

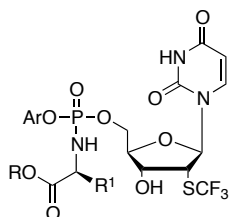


Figure 7.2: Common structure of 2'-SCF₃-2'-dU ProTides.

Since the synthetic strategy described by Fauster *et al.*⁴³⁷ for the preparation of compound **115** consisted of four steps (Scheme 7.1) including the synthesis of the 2'-mercapto-2'-deoxyuridine intermediate (2'-SH-2'-dU, **119**, Figure 7.3), the anticancer activity of this nucleoside analogue was also investigated.

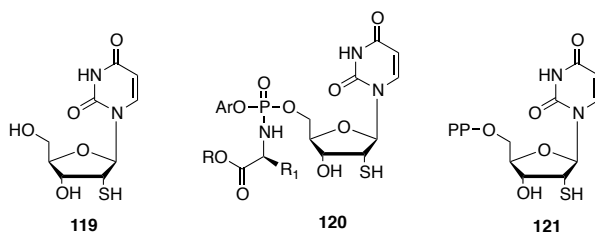


Figure 7.3: Structure of 2'-SH-2'-dU (**119**), relative ProTides (**120**) and intracellular active metabolite 2'-SH-2'-dUDP (**121**). PP: diphosphate group.

In fact, 2'-mercapto-2'-deoxyuridine 5'-diphosphate (2'-SH-2'-dUDP, **121**, Figure 7.3) was found to be a potent inhibitor of ribonucleotide reductase (RNR).⁴⁴⁰ This enzyme has a crucial function in DNA biosynthesis and repair, as it is involved in the synthesis of deoxynucleotides.⁴⁴¹ As such, this enzyme has already been a target for the design of antitumour and antiviral agents such as cytarabine.^{442,443} The *in vitro* activity of the mercapto nucleoside **119** has not been reported to date. However, Roy *et al.* investigated both the cytotoxic activity of the disulphide dimer form of this nucleoside (**122**) and some disulphide prodrugs of **119** (**123**, Figure 7.4), assuming that these disulphide-containing molecules would release the 2'-mercapto analogue **119** after intracellular reduction.⁴⁴⁴

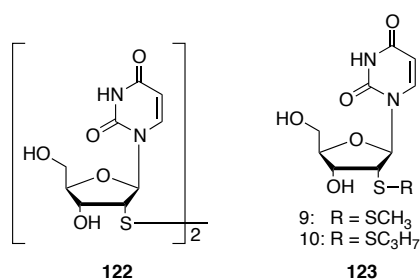
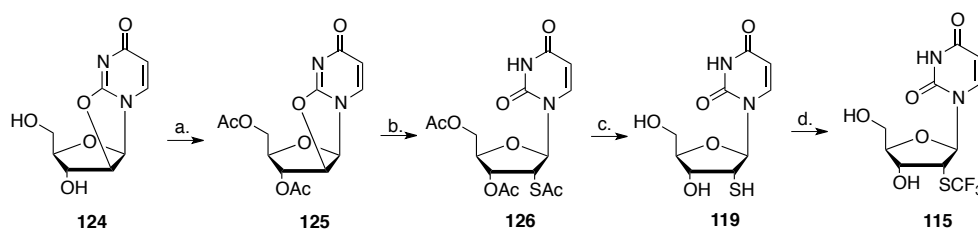


Figure 7.4: Structures of 2'-deoxyuridine 2'-thio derivatives, which were previously reported in the literature.

However, they observed neither intracellular inhibition of the RNR enzyme nor cytotoxic activity on malignant cell lines. They hypothesised that these negative results could be a result of poor intracellular phosphorylation to the active 5'-diphosphate metabolite.⁴⁴⁴ As a consequence of these results, the ProTide approach was applied on this nucleoside analogue, in order to potentially release the 5'-monophosphate analogue in the intracellular environment bypassing the potentially limiting step of first phosphorylation. The *in vitro* cytotoxic screening of this family of prodrugs and the parent nucleoside **119** was then performed, in order to investigate the potential anticancer properties of these structures.

7.2 Synthesis of nucleosides 2'-SH-2'-dU and 2'-SCF₃-2'-dU

Parent nucleosides 2'-SH-2'-dU (**119**) and 2'-SCF₃-2'-dU (**115**) were synthesised following Scheme 7.1.^{437,445,446}



Scheme 7.1: Synthesis of 2'-SH-2'-dU (**119**) and 2'-SCF₃-2'-dU (**115**). *Reagents and conditions:* (a.) Ac₂O (4 eq), DMAP (0.4 eq), TEA (4 eq) CH₃CN, rt, 16h, 97%; (b.) [1] AcSH, DMF, 110 °C, 6 hours, 25% [2] AcSH (25 eq), 1,4-dioxane, 110 °C, 6 hours, 73%; (c.) 1 N KOH, H₂O:EtOH (1:1, v/v), 0 °C, 30 min, 87%; (d.) Togni's reagent (**123**, 2.5 eq), CH₃OH, -78 °C, 1h, 76%.

Commercially available 2'-deoxy-2'-anhydrouridine (**124**) was first acetylated in position 3' and 5' on the sugar moiety by treatment with acetic anhydride, triethylamine and DMAP in acetonitrile at room temperature for 16 hours, affording the desired protected compound (**125**) in 97% yield (Scheme 7.1, a.).^{447,448}

Intermediate **125** was treated with thioacetic acid (AcSH) in DMF at 110 °C for 6 hours to afford the 2'-thioacetylated product (**126**) (Scheme 7.1b.[1]).⁴⁴⁵ The cleavage of the 2,2'-

anhydro linkage with the introduction of the thioacetic moiety in 2'-position proceeded with only 25% yield, similar to the yield reported in the literature (30%) due to unreacted starting material and possibly the already reported reactivity of DMF with thioacetic acid.⁴⁴⁶ However, the product formation was confirmed by the presence of a new singlet integrating for 3 protons corresponding to the thioacetyl group (SAc), at 2.37 ppm in the ¹H NMR (CDCl₃, 500 MHz), slightly downfield by comparison to the OAc groups (δ 2.14 and 2.19 ppm) and comparable to the reported spectroscopic data.⁴⁴⁶ An improvement in the reaction yield up to 73% was reached by using 1,4-dioxane instead of DMF as a solvent (Scheme 7.1, b.[2]).⁴⁴⁶ Complete deprotection of the acetylated precursor **126** was accomplished by treatment with KOH in a mixture of water and methanol at 0 °C (Scheme 7.1, c.),⁴⁴⁶ affording deprotected 2'-mercapto-2'-deoxyuridine (**119**) in 87% yield.

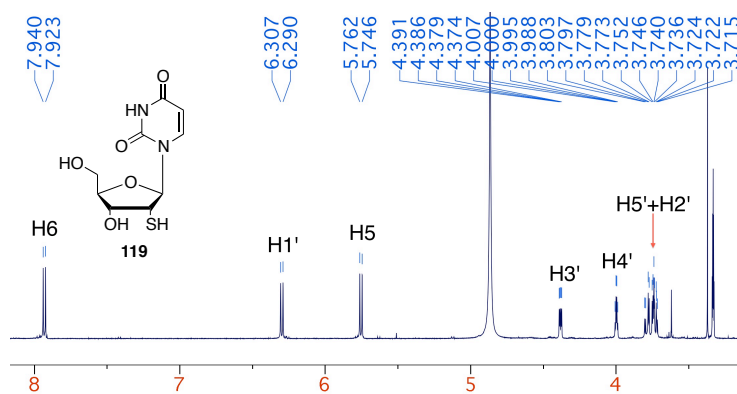


Figure 7.5: ¹H NMR spectrum of 2'-SH-2'-dU (**119**) in CD₃OD (500 MHz).

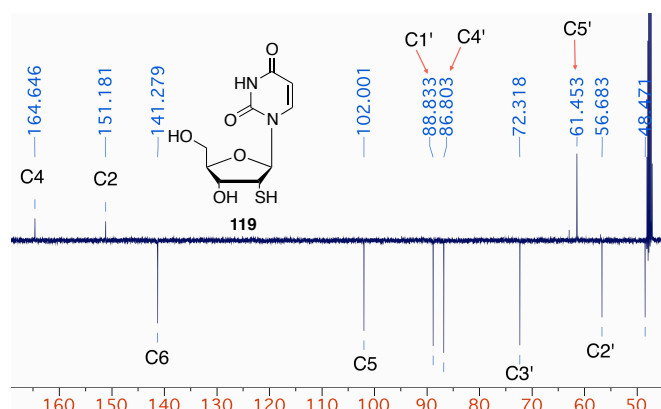


Figure 7.6: ¹³C NMR (pendant) spectrum of 2'-SH-2'-dU (**119**) in CD₃OD (125 MHz).

The structure of **119** was confirmed by ¹H NMR and ¹³C NMR and ES/MS analysis, and by comparison with the reported spectroscopic data.⁴⁴⁶ The most characteristic features of these spectra is the presence of very upfield H2' and C2' signals due to the presence of the 2'-SH group. This group has a lower electronegativity compared to the 2'-OH group,

therefore has a lower de-shielding effect, hence the resonance of both H2' and C2' at lower ppm values.

The final step for the synthesis of **115** consisted of the trifluoromethylation of the 2'-SH group of derivative **119**. This step was accomplished by treatment with 3,3-dimethyl-1-(trifluoromethyl)-1,2-benzodioxole (Togni's reagent, **127**, Figure 7.7)^{449,450} in methanol at -78 °C, yielding the desired product **115** in 76% yield (Scheme 7.1, d).⁴³⁷

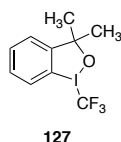


Figure 7.7: Structure of 3,3-dimethyl-1-(trifluoromethyl)-1,2-benzodioxole (Togni's reagent, **127**).

This electrophilic trifluoromethylation is totally selective for the thiol group over the hydroxyl group, because the soft nucleophiles (with high lying HOMO) such as the SH group are preferred over harder nucleophiles such as OH groups at low temperature.⁴⁵⁰

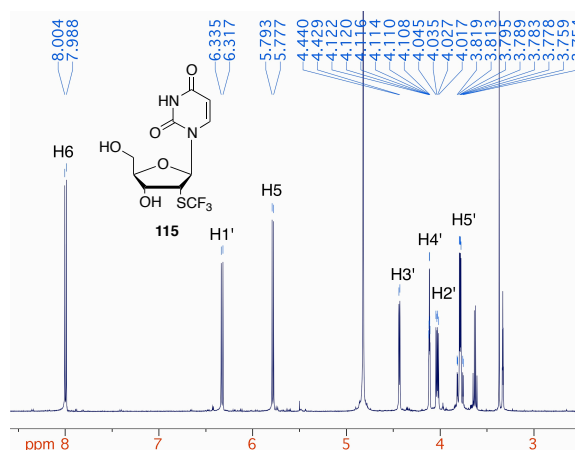


Figure 7.8: ¹H NMR spectrum of 2'-SCF₃-2'-dU (**115**) in CD₃OD (500 MHz).

The presence of the CF₃ moiety exclusively on the thiol group was suggested by the shift in the ¹H NMR signal of the proton in 2'-position higher ppm values, while all the other signals were in a similar range as precursor **119**, in CD₃OD (Figure 7.8). Moreover, the ¹⁹F NMR spectrum showed one signal corresponding to one SCF₃ group at -41.60 ppm (in CD₃OD), in accordance with the value reported in the literature (δ -38.94 ppm in DMSO-*d*6).

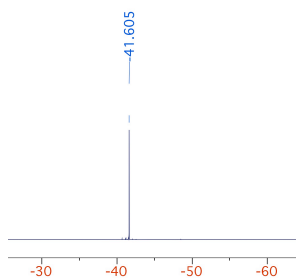


Figure 7.9: ^{19}F -NMR spectrum of 2'-SCF₃-2'-dU (**115**) in CD₃OD (470 MHz).

Very characteristic is also the splitting pattern related to the CF₃ group in the ^{13}C NMR spectrum (Figure 7.10), showing a quadruplet with a $^1J_{\text{C-F}}$ value of 303.5 Hz. Moreover, the SCF₃ group represents an isolated spin system,⁴³⁷ hence the lack of coupling between fluorine and the carbon in the 2'-position.

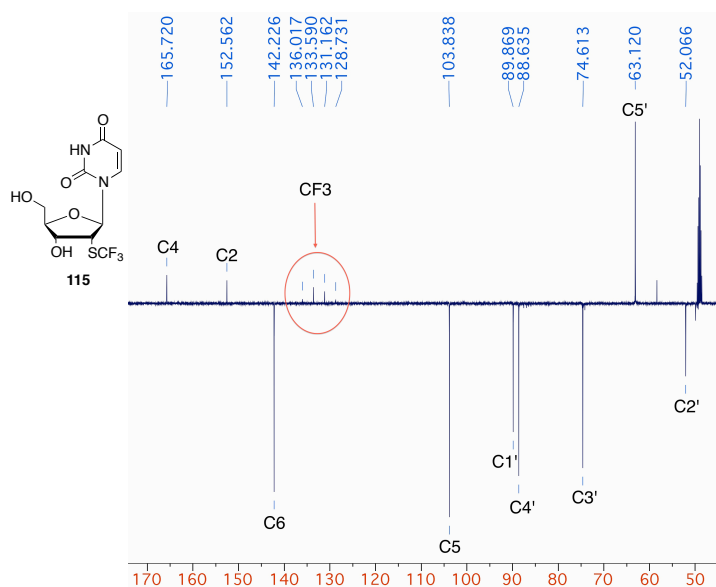
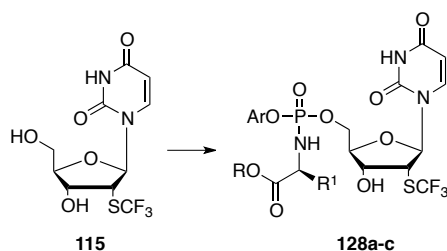


Figure 7.10: ^{13}C NMR spectrum of 2'-SCF₃-2'-dU (**115**) in CD₃OD (125 MHz).

7.3 Synthesis of 2'-SCF₃-2'-dU and 2'-SH-2'-dU ProTides

7.3.1 Synthesis of 2'-SCF₃-2'-dU ProTides

The synthetic strategy applied to the synthesis of 2'-SCF₃-2'-dU ProTides involved the treatment of the nucleoside with NMI and the appropriate phosphorochloridate in THF at room temperature overnight (Scheme 7.2).¹⁰⁵



Scheme 7.2: Synthesis of 2'-SCF₃-2'-dU ProTides **128a-c**. *Reagents and conditions*: appropriate phosphorochloridate (3 eq), NMI (5 eq), THF, rt, 16h.

Common structure	Compound	Ar	R	R ₁	AA	Yield %
	128a	Ph	Bn	Me	L-Ala	87
	128b	Ph	Hex	“	“	56
	128c	Nap	Bn	“	“	42

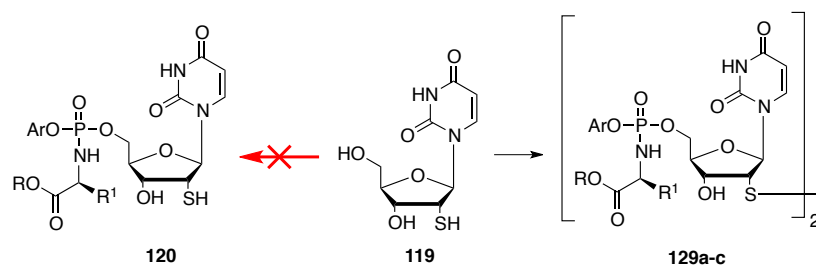
Table 7.1: Structures and synthetic yields for ProTides **128a-c**.

Three examples of ProTides were synthesised in moderate to good yields (Table 7.1), with no traces of 3'-phosphoramidate regioisomer or 3',5'-bisphosphoramidate. These analogues were then evaluated for anticancer activity as approximate 1/1 mixtures of two diastereoisomers.

7.3.2 Synthesis of 2'-SH-2'-dU prodrugs

The attempted synthesis of 2'-mercapto-2'-deoxyuridine ProTides (**129**) by treatment of the parent nucleoside **120** with the appropriate phosphorochloridate and NMI in THF yielded prodrugs characterised by dimeric disulphide structure (**129a-c**, Scheme 7.3).

This result might be connected to the reaction environment created by NMI, as a consequence of the tendency of the thiol groups to form disulphide bonds, as was specifically reported also on nucleosides bearing the thiol functionality on the sugar moiety.⁴⁵¹⁻⁴⁵³



Scheme 7.3: Synthesis of of 2'-SH-2'-dU derivatives **129a-c**. *Reagents and conditions*: appropriate phosphorochloridate (3 eq), NMI (5 eq), THF, rt, 16h.

Common structure	Cpnd	Ar	(R ₁)	R	AA	Yield %
	129a	Ph	Me	Bn	L-Ala	21%
	129b	Nap	“	Bn	“	11%
	129c	Ph	“	Hex	“	5%

Table 7.2: Structures and synthetic yields of disulfide dimers **129a-c**.

An example of the symmetric disulphide structures yielding from the coupling reaction reported in Scheme 7.3 is given in Figure 7.13, with compound **129a**. The dimeric structure of the product was firstly suggested by mass, (m/z $[M + Na^+] = 1175.2$, $C_{50}H_{54}N_6O_{18}P_2S_2$, calculated m/z $[M] = 1152.24$). The ^{31}P NMR spectrum (Figure 7.11), nevertheless, shows only three peaks, presumably due to overlapping of two species.

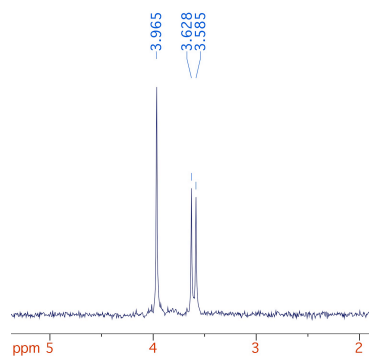


Figure 7.11: ^{31}P NMR spectrum of compound **129a**. (CD_3OD , 202 MHz)

However, the 1H NMR analysis of the product is shown in Figure 7.12 and the enlarged area of the spectra corresponding to protons H6 and H2' showed characteristic signal pattern of the structures depicted in Figure 7.13. The presence of 4 doublets for the H6 signal and 8 doublets corresponding to H2' confirmed the presence of a disulphide bond, giving rise to three different species depending on the phosphorus chirality.

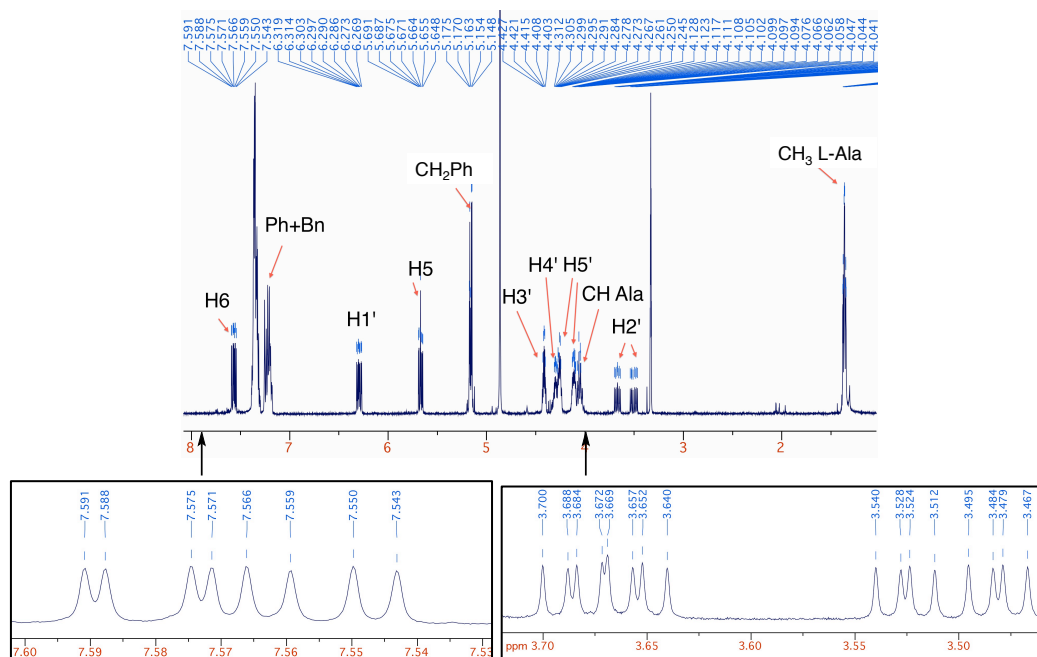


Figure 7.12: ^1H NMR spectrum of compound **129a** in CD_3OD (500 MHz), enlarged portions of the spectra with signals corresponding to H6 and H2'.

As shown in Figure 7.13, in fact, the coupling of 5'-hydroxyl groups with either a S_p or a R_p phosphorochloridate (respectively yielding structures **A** and **B**), would generate two different isomers, while the coupling of the two 5'-OH groups with two different phosphorochloridate diastereoisomers (S_p and R_p) would generate a single meso structure (**C**).

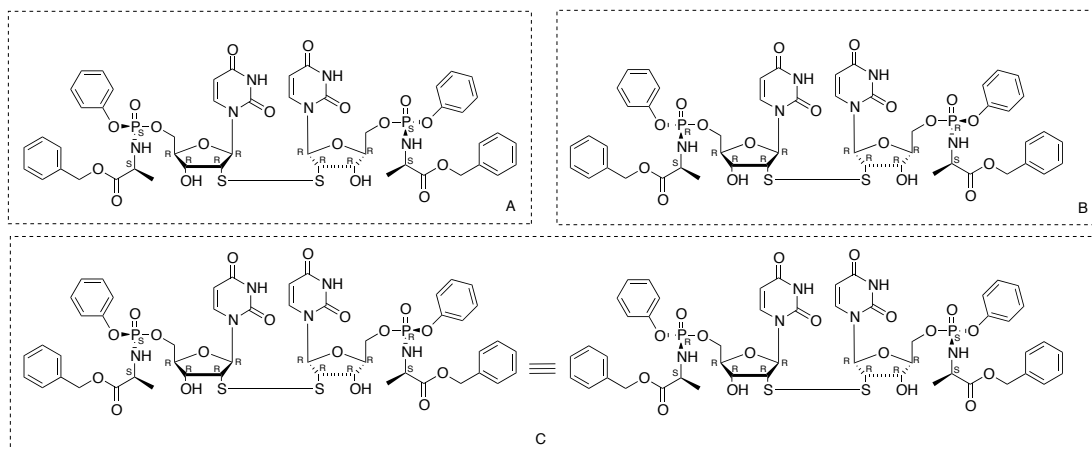


Figure 7.13: Structures (**A**, **B** and **C**) corresponding to compound **129a**.

Therefore, the ^1H NMR spectrum of compound **129a** shows the presence of 4 doublets (δ 7.58 $^2J = 8.0$ Hz; δ 7.57 $^2J = 8.5$ Hz; 7.56 $^2J = 8.0$ Hz; 7.55 $^2J = 8.0$ Hz), corresponding to the H6 signal. In fact, the symmetric species **A** and **B** give one doublet each respectively

corresponding to the two overlapping H6 protons of each species (Figure 7.12). In addition, the isomer **C** will give two doublets of the two non-overlapping signals of the H6 protons, due to the different chemical environments around the two protons generated by the different chirality of the two phosphoramidate groups.

The synthesised derivatives **129a-c** were tested on malignant cell lines. In fact, the disulphide bond was thought to be cleaved in the reducing intracellular environment, similarly to both disulphide containing bioconjugates⁴⁵⁴ and other prodrugs in clinical development.⁴⁵⁵⁻⁴⁵⁷ These compounds (**129a-c**) would therefore be double prodrugs, requiring both intracellular reduction of the disulphide bridge and the enzymatic activation of the ProTide moiety.

7.4 Biological evaluation of 2'-SCF₃-2'-dU ProTides

7.4.1 *In vitro* cytotoxicity assay

The synthesised prodrugs of 2'-SCF₃-2'-dU (**128a-c**) were tested by WuXi AppTech on a small selection of malignant cell lines, described in Table 7.3.

Cell line	Malignancy
MOLT-4	Acute T lymphoblastic leukaemia
K562	chronic myelogenous leukaemia
HL-60	Acute promyelocytic leukaemia
MCF-7	breast adenocarcinoma
Mia-Pa-Ca	breast adenocarcinoma

Table 7.3: Malignant cell lines selected for testing of prodrugs of 2'-SCF₃-2'-dU (**128a-c**) and 2'-SH-2'-dU (**129a-c**) by WuXi AppTech.

The cytotoxic screening of the parent nucleoside (**115**) on both leukaemic cell lines and breast cancer cell lines revealed very poor to negligible anticancer activity on all cell lines, with cell viability inhibition reaching a maximum of 16.5% on HL60 cell line at the highest concentration considered (198 μM).

Cpnd	MOLT4		K562		HL60		Mia-Pa-Ca		MCF7	
	IC ₅₀	MI%	IC ₅₀	MI%	IC ₅₀	MI%	IC ₅₀	MI%	IC ₅₀	MI%
2'-SCF₃-2'-dU (115)	>198	-2	>198	4.2	>198	16.5	>198	4.6	>198	11
128a	33.0	100	52.0	106	45.0	101	61.0	99	80.0	94
128b	104.0	66	139.0	50	86.0	71	>198	35	>198	34
128c	18.0	102	23.0	100	23.0	102	38.0	99	58.0	99

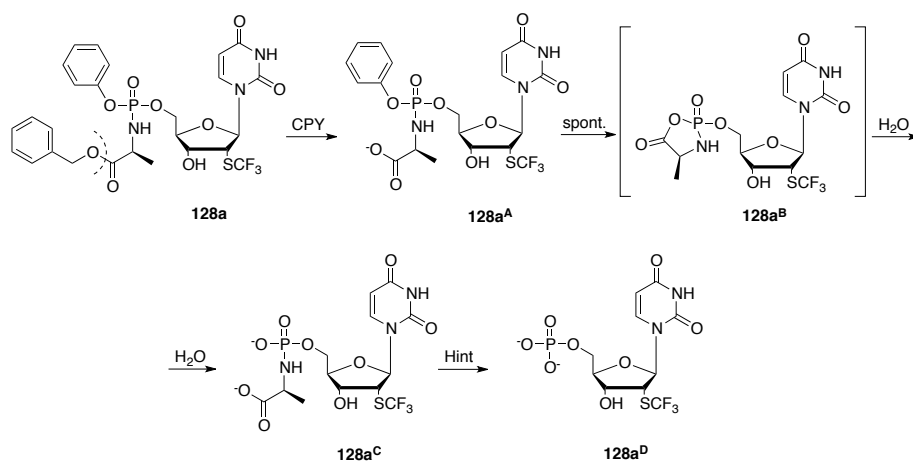
Table 7.4: *In vitro* cytotoxicity screening of parent nucleoside **115** and ProTides (**128a-c**). Cytotoxicity data reported as IC₅₀ values (concentration of drug causing 50% of cell viability inhibition) and MI% (maximum inhibitory effect of the drug at the range of concentration considered). PTX: paclitaxel (control). Assays performed by WuXi AppTech.

ProTides **128a-c** were generally more active than the parent nucleoside, especially compounds **128a** and **128c**, respectively the phenyl and naphthyl-L-alanine benzyl ester ProTides, which reached complete inhibition of cell viability within the range of concentrations considered (19 μ M to 198 μ M). Moreover, the IC₅₀ value of compound **128c** was as low as 18 and 23 μ M respectively on MOLT4 and HL60 cell lines. The significantly improved anticancer activities of ProTides **128a-c** over the parent nucleoside suggested that the lack of activity of **115** could potentially derive from a poor phosphorylation to 2'-SCF₃-2'-dUMP, causing inefficient intracellular activation to the supposedly active 5'-triphosphate species, or improved cell permeation. On the other hand, ProTides **128a-c** should release 2'-SCF₃-2'-dUMP efficiently and therefore facilitate the intracellular metabolism to the active metabolite 5'-triphosphate.

7.4.2 Mechanistic investigations

7.4.2.1 Enzymatic CPY experiment

Enzymatic carboxypeptidase-Y (CPY) experiment was performed on compound **128a** in order to predict the likelihood of intracellular processing of this ProTide to L-alaninyl phosphate intermediate **128a^C** (Scheme 7.4).



Scheme 7.4: Intracellular conversion of **128a** to **128a^D** catalysed by CPY/Hint enzymes.

From Figure 7.14, showing the ³¹P NMR monitoring of this conversion, it is clear that ProTide **128a** was quickly and completely converted to intermediate **128a^A** within 4 minutes from enzyme addition, and the total conversion into 5'-L-alaninyl phosphate monoester **128a^C** was complete after 32 minutes.

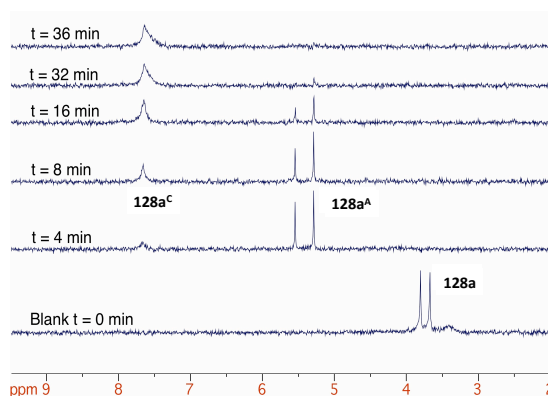


Figure 7.14: ³¹P NMR spectra monitoring the conversion of **128a** to **128a^C** recorded in acetone-*d*₆ (202 MHz).

The presence of the SCF₃ functionality allows the additional use of ¹⁹F NMR spectroscopy to evaluate the enzymatic conversion catalysed by CPY, and Figure 7.15 depicts the signals corresponding to starting material **128a** (δ_F -39.43 ppm, -40.01 ppm) being converted into a more downfield single signal (δ_F -39.60 ppm), corresponding to **128a^C**.

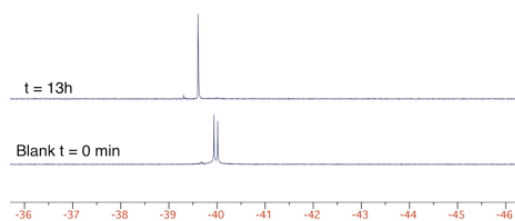


Figure 7.15: ^{19}F NMR spectra corresponding to **128a** (at time 0) and **128^c** (at time = 13h) recorded in acetone-*d*6 (407 MHz).

7.4.2.2 Docking into Hint active site

Prediction of the effective conversion of 2'-SCF₃-2'-dU ProTides into the desired 2'-SCF₃-2'-dUMP intracellular metabolite was performed by docking the L-alanyl monophosphate intermediate **128a^c** into the active site of Hint. As shown in Figure 7.16 the intermediate appears to correctly position the phosphoramidate moiety close to the residues recognised to have a crucial role in the cleavage of such portion (Ser107, His112 and His114), and this suggests the intracellular release of the desired metabolite 2'-SCF₃-2'-dUMP.

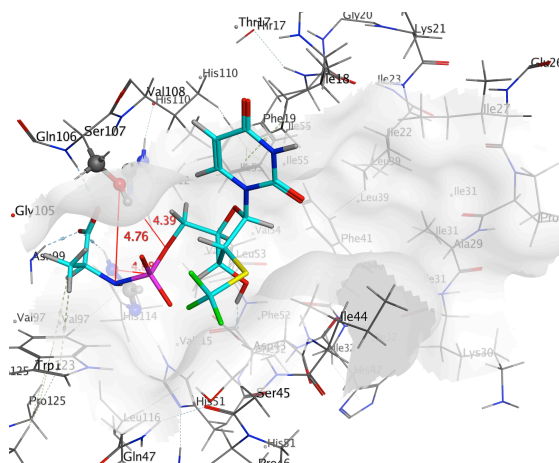


Figure 7.16: Docking of intermediate **128a^c** into the active site of Hint enzyme.

However, as noted also for the docking of other pyrimidine nucleoside derivatives within the same pocket (e.g. TFT), the rest of the molecule is exposed outside the active site, and this could potentially cause a less efficient interaction with the enzyme that may cause a slower processing of such prodrugs.

7.5 Biological evaluation of 2'-SH-2'-dU ProTides

7.5.1 *In vitro* cytotoxicity evaluation

The biological evaluation of 2'-SH-2'-dU (**119**) and relative disulphide-bond bearing ProTide dimers (**129a-c**) was performed by WuXi AppTech on the cell lines reported in Table 7.3. Parent nucleoside **119** was completely inactive in the assay conditions, causing no significant cell viability inhibition up to the highest concentration used (198 μ M). ProTides **129a-c** had very poor activity, despite causing a more effective inhibition of cell viability compared to the parent nucleoside, up to 49% at the highest concentrations used (such as MI% = 49.5 recorded for compound **129c** on HL60 cell line).

Cpnd	MOLT4		K562		HL60		Mia-Pa-Ca		MCF7	
	IC ₅₀	MI%	IC ₅₀	MI%	IC ₅₀	MI%	IC ₅₀	MI%	IC ₅₀	MI%
2'-SH-2'-dU (119)	>198	1	>198	3	>198	-0.5	>198	1	>198	0.1
129a	>198	40	>198	45	>198	48	>198	22	>198	7
129b	>198	49	>198	34	>198	35	>198	16	>198	3
129c	>198	38	>198	49	>198	49	>198	4	>198	5

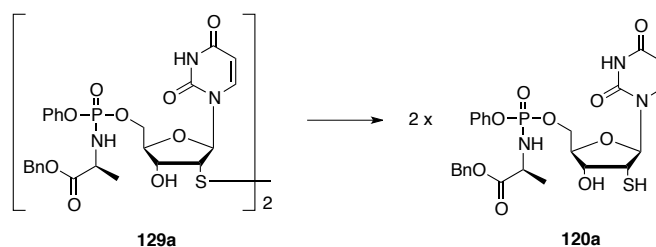
Table 7.5: *In vitro* cytotoxicity screening of parent nucleoside **119** and derivatives **129a-c**. Cytotoxicity data reported as IC₅₀ values (concentration of drug causing 50% of cell viability inhibition) and MI% (maximum inhibitory effect of the drug at the range of concentration considered). PTX: paclitaxel (control). Assays performed by WuXi AppTech.

The low activity of parent **119** potentially derives from different factors, such as inefficient cell penetration due to lack of recognition by a nucleoside transporter or poor phosphorylation by nucleoside and nucleotide kinases to active diphosphate **121**. Moreover, **119** was already reported to be unstable at a range of pH,⁴⁵⁸ including pH = 7, close to physiological conditions, and this would decrease the percentage of nucleoside being phosphorylated to active species once inside the cell. At this pH, the prevalent species detected were dimer **122** and uracil, respectively in 44 and 27 %.⁴⁵⁸

Regarding compounds **129a-c**, it is important to specify that these potential 'bis-prodrugs' should undergo a double activation process inside the cell: disulphide bridge reduction to 2'-thiol functionality and ProTide activation to 2'-mercapto-2'-deoxyuridine 5'-monophosphate (2'-SH-2'-dUMP). However, 2'-SH-2'-dUMP must also be recognised by a nucleotide kinase enzyme and be phosphorylated to diphosphate **121**, the active species that could interact and inhibit RNR enzyme.

Cleavage of disulphide bonds as a way of activating prodrugs inside cancer cells has been extensively exploited,^{454-456,459,460} considering the higher amount of reducing agent

glutathione inside neoplastic cells compared to normal cells,⁴⁶¹ which cleaves these bonds by disulphide exchange.^{459,462} Chemical cleavage of the disulphide bond in different nucleoside based compounds was performed by treatment with a reducing agent such as dithiothreitol (DTT).^{440,463-466} An NMR assay was set up by Gerland *et al.*,⁴⁶⁵ in order to monitor the reduction of alkyl and aryl disulphide bonds in position 3' on the uridine sugar ring by treatment with an excess (5 equivalents) of DTT at 20 °C.⁴⁶⁵ This group noted that the reduction was complete within 10 minutes from the DTT addition in the case of alkyl disulfides, while the presence of an aromatic moiety linked to the disulphide group caused increase in the half-life of these compounds up to 8 hours. The susceptibility of the disulphide bond cleavage in compound **129a** was assayed in the same conditions.



Scheme 7.5: Disulfide bond cleavage of compound **129a** yielding ProTide **120a**. Reagents and conditions: DTT (5 eq), CD₃OD, rt, 12 h, 50% (analysed by ¹H NMR).

¹H NMR evaluation of this reaction was performed over 12 hours, and key spectra are reported in Figure 7.17 (this conversion was also monitored by ³¹P NMR, although not reported because overlapping of the signals corresponding to **129a** (δ_p 3.97 ppm, 3.63 ppm, 3.59 ppm) and **120a** (δ_p 4.14 ppm, 3.73 ppm) caused unclear spectra.

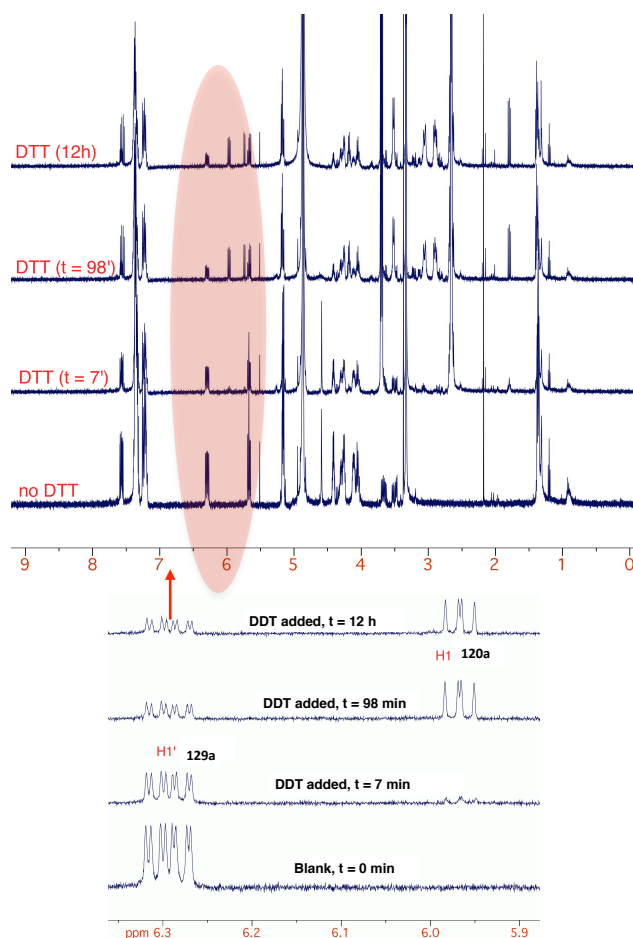


Figure 7.17: Stacked ^1H NMR spectra (CD_3OD , 500 MHz) showing the partial conversion of dimer **129a** into ProTide **120a**.

The disulfide bond cleavage reaches approximately 50% within 12 hours as calculated from the ratio of starting material over product, whose structure was confirmed by analysis of the ^1H NMR new peaks that were formed (Figure 7.17), which matched with the structure of ProTide **120a**. As an example, the enlarged portion (between 6.35–5.9 ppm) of Figure 7.17, shows the H1' doublets corresponding to compound **120a** (δ_{H} 6.31 ppm, $^2J = 8.5$ Hz; 6.30 ppm, $^2J = 8.2$ Hz; 6.28 ppm, $^2J = 8.2$ Hz, 6.27 ppm, $^2J = 8.5$ Hz) slowly converting into new doublets corresponding to the H1' signals of the two diastereoisomers of ProTide **120a** (δ_{H} 5.97 ppm, $^2J = 9.0$ Hz; δ 5.95 ppm, $^2J = 9.5$ Hz).

Comparison between this reaction and the half-life of compounds reported by Gerland *et al.*⁴⁶⁴ seems to suggest a relatively slow activation process for compound **129a**. The low activity of compounds **129a-c** could therefore derive from either an ineffective reduction of the disulphide bond or by a slow processing of the ProTide moiety to 2'-SH-2'-dUMP.

In addition, there could be a lack of recognition of 2'-SH-2'-dUMP by a nucleotide kinase, with poor conversion to active metabolite 2'-SH-2'-dUDP.

7.5.2 Mechanistic investigations on the processing of 2'-SH-2'-dU derivatives

As previously mentioned, 2'-SH-2'-dU derivatives, prior to having an effect on cell viability, need to be processed to 2'-SH-2'-dUMP, which should then in turn undergo phosphorylation to 2'-SH-2'-dUDP. The intracellular prodrug processing requires both cleavage of the disulphide bond, which was simulated by treatment of derivative **129a** with DTT (Figure 7.17), and cleavage of the ProTide moieties with release of the monophosphate group(s). The order in which these two processes would happen in the intracellular environment is not clear, therefore we decided to simulate the interaction of derivative **129a** within the active site of CPY in order to understand whether the phosphoramidate moiety processing could happen first. Figure 7.18 shows the results obtained for the structure with R_p / R_p stereochemistry (Figure 7.13, **B**), as an example of what resulted from the docking also of the other two isomers S_p / S_p and R_p / S_p (Figure 7.13, **A** and **C**), which gave similar results.

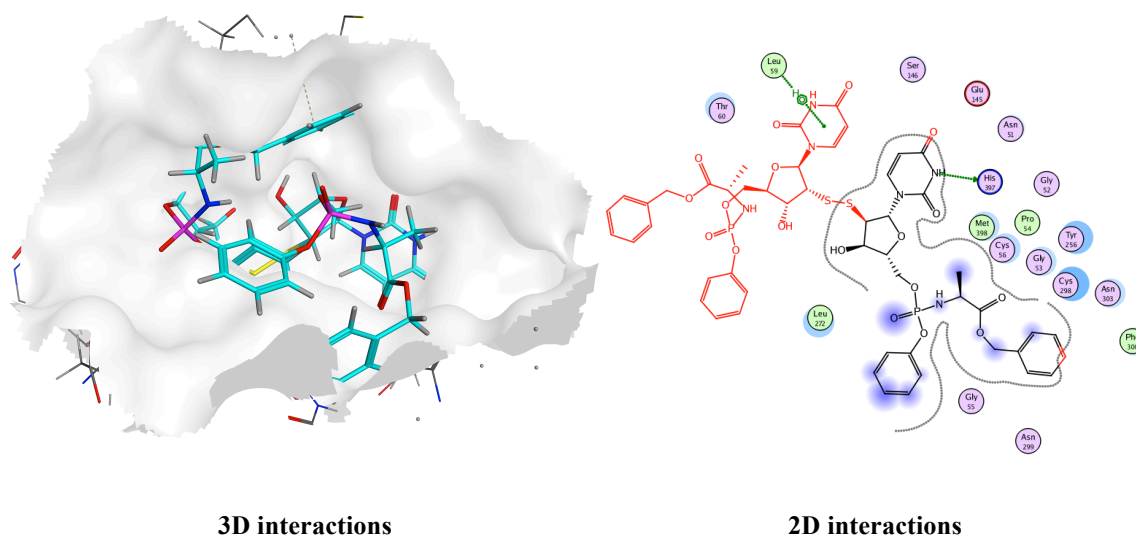
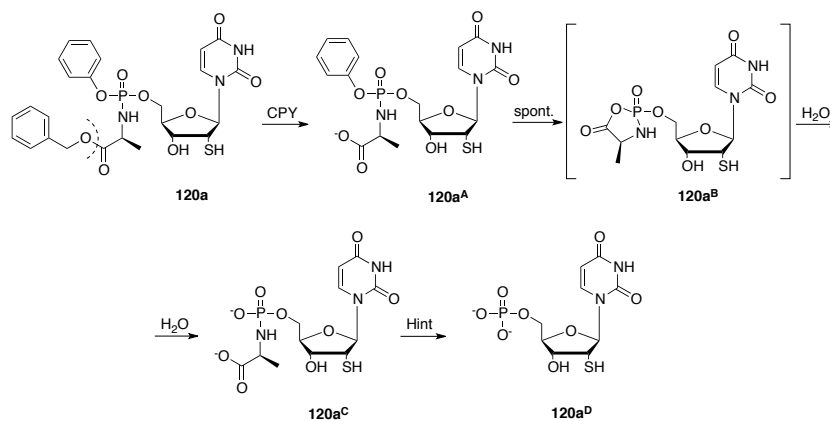


Figure 7.18: Docking of dimer **129a** (R_p / R_p stereochemistry), within the active pocket of CPY enzyme.

Dimer **129a** does not appear to fit appropriately within the CPY active site, as a result of the very bulky structure, as evident from the 2D ligand interactions, showing clashing of a portion of the molecule with amino acid residues in the pocket (red portion, Figure 7.18). These results suggest that a first ProTide activation would be unlikely to occur and dimer **129a** should first undergo disulphide bond cleavage.

7.5.2.1 CPY docking of ProTide **120a** in CPY

One possible mechanism of intracellular activation of 2'-SH-2'-dU derivatives **129a-c** involves first cleavage of the disulphide bond, followed by processing of the ProTide moiety with final release of 2'-SH-2'-dUMP.



Scheme 7.6: Intracellular conversion of **120a** to **120a^D** catalysed by CPY/Hint enzymes.

In order to predict the likelihood of processing of 2'-SH-2'-dU ProTides by carboxypeptidase and phosphoramidase enzymes, docking of compound **120a** was performed within the active pocket of CPY enzyme, which should cleave the benzyl ester moiety and trigger the conversion into metabolite **120a^C** (Scheme 7.6, Figure 7.19). The activation process was then finally investigated with the docking of the L-alaninyl intermediate **120a^C** within the Hint active pocket, in order to predict the likelihood of P-N bond cleavage with release of 2'-SH-2'-dUMP **120a^D**.

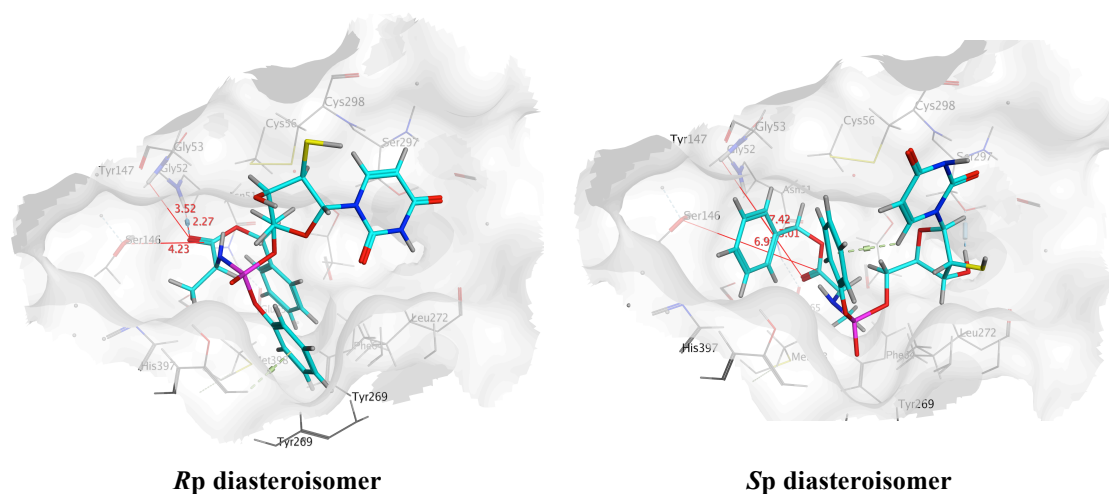


Figure 7.19: Docking of isomers of ProTide **120a** within the active site of CPY.

Both isomers interact with the pocket with the amino acid ester moiety close to the key residues responsible for ester cleavage (Ser146, Gly52 and Gly53), however, the Sp isomer seems to position such moiety in closer proximity.

7.5.2.2 CPY docking of 2'-SH-2'-dU intermediate **120a^C** in Hint

Docking of intermediate **120a^C** in the active site of Hint (Figure 7.20) are predictive of a relatively efficient processing of the phosphoramidate group with release of 2'-SH-2'-dUMP. In fact, such groups are positioned in proximity with the catalytic residues, and would thus be processed by the enzyme.

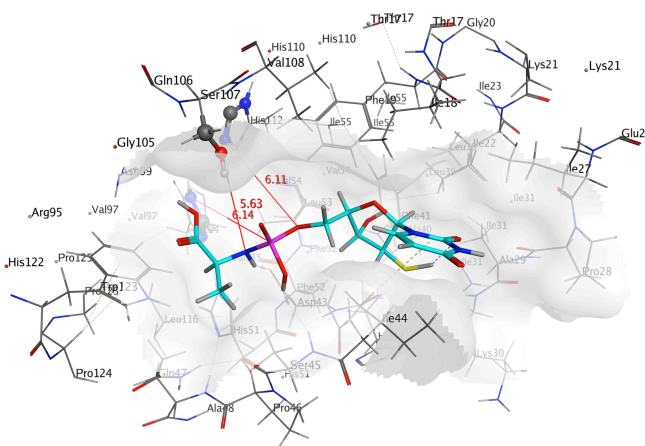


Figure 7.20 Docking of intermediate **120a^C** in the active site of Hint enzyme.

The outcome of docking of ProTide **120a** within CPY and intermediate **120a^C** within Hint active sites, in parallel with the docking results obtained for dimer **129a**, suggest that the ProTide moiety is more likely to be processed after cleavage of the disulphide bond.

7.6 Conclusions

In the present work the anticancer potential of 2'-SCF₃-2'-dU, already reported to be endowed with RNA-base pairing disrupting effects, was assessed *in vitro* for the first time. Moreover the cytotoxic properties of the 2'-SH-2'-dU were evaluated, as the diphosphate analogue of such molecule was reported to be an efficient inhibitor of the RNR enzyme, with potential anticancer activity. In addition, the ProTide approach was applied to both nucleoside analogues, with the aim of enhancing their properties by potentially bypassing limiting steps in the intracellular activation. ProTides of 2'-SCF₃-2'-dU were synthesised in moderate to good yields, while the NMI-mediated coupling reaction, applied to 2'-SH-2'-dU, led to the synthesis of dimeric ProTide analogues, linked via a 2',2'-SS disulphide

bond, as the 2'-thiol moiety is prone to oxidation. All derivatives were tested and 2'-SCF₃-2'-dU ProTides were found to enhance the very poor anticancer profile of the parent nucleoside, leading to 100% cell viability inhibition at concentrations as low as 18 μM, potentially a consequence of the very quick processing noted by CPY and the correct positioning within the active site of Hint. With regard to 2'-SH-2'-dU disulphide dimers, these compounds were poor anticancer compounds, leading to inhibition of cell viability up to 50% at the highest concentration considered (198 μM). However, these derivatives improved the activity of the parent nucleoside, which was completely inactive up to 198 μM. The poor activity of 2'-SH-2'-dU disulphide derivatives was proposed to derive from slow disulphide bond cleavage, as simulated *via* the DTT assay, leading to a delay in the processing of the ProTide moiety.

The promising results obtained after cytotoxic evaluation of proTides of 2'-SCF₃-2'-dU should direct future investigations at applying the ProTide approach to other 2'-SCF₃ bearing nucleosides such as compounds **128a-c**.

Moreover, the synthesis and biological evaluation of prodrugs of 2'-SH-2'-dUDP should be included in a future project, since the low activity of monophosphate prodrugs could also be a consequence of defective processing to diphosphate by nucleotide kinase. In addition, any 2'-SH nucleoside prodrug should be treated prior to cytotoxic screening with DTT, as disulphide bond cleavage might potentially be an issue for such hindered molecules.

Alternatively, exploration of structures such as **132** (Figure 7.21) could lead to potential double prodrugs of 2'-SH-2'-dU.

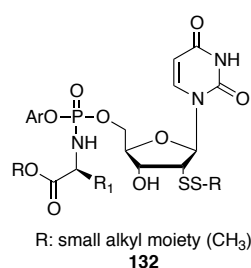


Figure 7.21: Potential new prodrugs of 2'-SH-2'-dU.

The small disulphide moiety in the 2'-position should be easily cleaved intracellularly, as already suggested by previous studies.⁴⁶⁴ This would allow the synthesis of prodrugs of 2'-SH-2'-dU endowed with improved chemical stability and potentially better cytotoxicity.

8 Conclusions

Herein is reported the design, synthesis and biological evaluation of different families of ProTides as potential therapeutic agents. All synthesised compounds were tested on a broad selection of cell lines, and in some cases as antiviral agents.

The mechanism of activation of the ProTides was supported by studying their bioactivation to the corresponding monophosphate forms, through enzymatic NMR studies and molecular modeling simulations.

The most active analogues were tested on resistant cancer cell lines, and their stability was assayed in serum, plasma and liver microsomes. Furthermore, the investigation of the selective targeting of the most promising ProTides on the stem cell population of the KG1a leukaemic cell line was carried out.

8-Chloroadenosine prodrugs were found to be endowed with higher cytotoxic activity compared to the parent nucleoside in conditions of AK of hENT1 deficiency, such as the 1-naphthyl-L-alanine benzyl ester ProTide **71a**. The 8-ClA phosphorodiamidate **76b** also emerged as one of the most potent derivatives.

Regarding the families of ProTides of TFT, CNDAC, 2'-SCF3-2'-dU and 2'-SH-2'-dU, many compounds were found to be more potent than the parent nucleosides, validating the potential of applying the ProTide approach as a way to improve the activity of nucleoside analogues.

Moreover, within the 3'-deoxyadenosine family of prodrugs, compounds with nearly 300 fold improved activity compared to their parent nucleoside were synthesised, with the two most potent derivatives, the phenyl L-alanine benzyl ester ProTide **30a** and the 2-fluoro counterpart **49b**, with low to sub micromolar activity. These analogues were evaluated in a mouse model of human non-Hodgkin's lymphoma, leading to promising results. These compounds represent potential new anticancer agents and will be further investigated in alternative tumour *in vivo* models.

Alteration of the phosphate structure of **30a** using the phosphonoamidate prodrug approach generated a compound, **64**, with improved anticancer activity in comparison to 3'dA.

9 Experimental part

9.1 General experimental details

All solvents used were anhydrous and used as supplied by Sigma-Aldrich. All commercially available reagents were supplied by Sigma-Aldrich, Fisher, Carbosynth or TCI chemicals and used without further purification. All nucleosides and solid reagents were dried for several hours under high vacuum prior to use.

All glassware was oven-dried at 130 °C for several hours or overnight and allowed to cool in a desiccator or under a stream of dry nitrogen.

For analytical thin-layer chromatography (TLC), precoated aluminium-backed plates (60 F-54, 0.2 mm thickness; supplied by E. Merck AG, Darmstadt, Germany) were used and developed by an ascending elution method. For preparative thin-layer chromatography (prepTLC), preparative TLC plates (20 cm × 20 cm, 500-2000 μm) were purchased from Merck. After solvent evaporation, compounds were detected by quenching of the fluorescence, at 254 nm upon irradiation with a UV lamp.

Column chromatography purifications were carried out by means of normal or reverse phase silica gel flash chromatography or automatic Biotage Isolera One. Fractions containing the product were identified by TLC and pooled, and the solvent was removed under *vacuum*.

^1H , ^{31}P , ^{13}C and ^{19}F NMR spectra were recorded on a Bruker Avance 500 spectrometer operating at 500 MHz, 202 MHz and 125 MHz and 407 MHz respectively and auto-calibrated to the deuterated solvent reference peak. All ^{31}P and ^{13}C NMR spectra were proton-decoupled.

Chemical shifts are given in parts per million (ppm) and coupling constants (J) are measured in Hertz. The following abbreviations are used in the assignment of NMR signals: s (singlet), d (doublet), t (triplet), q (quartet), m (multiplet), br s (broad singlet), dd (doublet of doublet), ddd (doublet of doublet of doublet), dt (doublet of triplet). The assignment of the signals in ^1H NMR and ^{13}C NMR was done based on the analysis of coupling constants and additional two-dimensional experiments (COSY, HSQC).

All analytical high-performance liquid chromatography (HPLC) experiments were done on a Thermo Fisher Scientific Spectra System SCM1000 provided with a System Controller SN4000, a pump Spectra System P4000 and a Spectra UV2000 detector set or a Varian Prostar (LC Workstation-Varian Prostar 335 LC detector) using a C18-Varian Pursuit (150 × 4.6 mm, 5 µm) reverse phase column. All final compounds were isolated with purity ≥ 95%

Low resolution mass spectrometry was performed on a Bruker Daltonics microTof-LC system (atmospheric pressure ionization, electron spray mass spectroscopy) in positive mode.

UV experiments were conducted using a Varian 50 Bio UV-visible spectrophotometer.

9.2 Molecular modelling studies

All molecular modelling studies were performed on a MacPro dual 2.66 GHz Xeon running Ubuntu 9.10, using molecular operating environment (MOE) 2008.10.⁴⁶⁷

The structures of adenosine deaminase (ADA, PDB 3IAR), carboxypeptidase Y (CPY, PDB 1YSC),⁴⁶⁸ human Hint1 (Hint, PDB 1RZY)²⁶⁶ enzymes were downloaded from the PDB website (<http://www.rcsb.org/>).

Hydrogen atoms were added to the protein and all minimisations were performed with MOE keeping all heavy atoms fixed until RMSD gradient of 0.05 kcal mol⁻¹ was reached with MMFF94x force field and partial charges were automatically calculated. Ligands in mol2 format, prepared using MOE, were minimised using the default settings and used as input for the docking. Ligand docking was performed using the default values configured, using PLANTS 1.1.⁴⁶⁹ The binding site center and radius corresponding to each enzyme considered were as follows:

- [ADA] binding site center: 9.386, -1.572, 0.772; binding site radius: 9 Å.
- [Hint] binding site center: 30.48, 4.591, 32.494; binding site radius: 10 Å.
- [CPY] binding site center: 54.903, -1.594, 31.704; binding site radius: 9 Å.

Docking parameters: aco_ants 20; aco_evap 1; aco_sigma 1; flip_amide_bonds 0; flip_planar_n 0; force_flipped_bonds_planarity 0; force_planar_bond_rotation 1; rescore_mode simplex
scoring_function chemplp; outside_binding_site_penalty 50; enable_sulphur_acceptors 0;


```
ligand_intra_score clash2; chemplp_clash_include_14 0.25; chemplp_clash_include_HH
0; chemplp_weak_cho 1; chemplp_charged_hb_weight 2; chemplp_charged_metal_weight
2; chemplp_hbond_weight -3; chemplp_hbond_cho_weight -3; chemplp_metal_weight -3;
chemplp_plp_weight 1; chemplp_plp_steric_e -0.4; chemplp_plp_burpolar_e -0.1;
chemplp_plp_hbond_e -1; chemplp_plp_metal_e -1; chemplp_plp_repulsive_weight 1;
chemplp_tors_weight 2; chemplp_lipo_weight 0; chemplp_intercept_weight -20;
write_protein_conformations 0; write_protein_bindingsite 0; write_protein splitted 0;
write_rescored_structures 0; write_multi_mol2 1; write_ranking_links 0;
write_ranking_multi_mol2 0; write_per_atom_scores 0; write_merged_ligand 0;
write_merged_protein 0; write_merged_water 0; keep_original_mol2_description 1;
merge_multi_conf_output 0; merge_multi_conf_character _;
merge_multi_conf_after_characters 1; rigid_ligand 0; rigid_all 0.
```

Twenty-five output configurations were obtained from each input compound and a visual inspection, in MOE, was used to identify interaction types between ligand and protein (discussed in each chapter).

9.3 Enzymatic and stability assays

9.3.1 Carboxypeptidase Y assay

The appropriate substrate (5 mg, \pm 0.008 mmol) was dissolved in 150 μ L of acetone-*d*6 and 300 μ L of TRIZMA buffer (pH 7.6) was added. A 31 P NMR (202 MHz, 64-128 scans) was conducted at this stage as a reference (blank, $t = 0$). To this mixture, 130 μ L of a stock solution of carboxypeptidase enzyme (Purchased from Sigma Aldrich, > 50 unit/mg, dissolved in TRIZMA buffer 7.6 pH to a concentration of 50 units/mL, EC 3.4.16.1) was added. 31 P NMR (128 scans) were carried out with 1 minute of delay between experiments for 14 hours at 25 °C.

9.3.2 Adenosine deaminase UV assay

Bovine recombinant adenosine deaminase (ADA, EC:3.5.4.4) was purchased from Sigma (Sigma-Aldrich, product number 59722). The ADA suspension (containing > 2 U/mL), was aliquoted into 55 μ L portions and kept at -20 °C. Before use, a 55 μ L sample was thawed and 1 mL of phosphate buffer (0.1 N, pH 7.6) was added. The suspension was filtered through a 0.2 μ m filter to remove precipitates that could interfere with the absorbance measurements. The clear supernatant was used for the degradation

experiments. The experiments were conducted in UV transparent cuvettes (Sigma Aldrich, code: Z637092) using an Envision microplate reader (PerkinElmer). Samples contained 62.5 μM of substrate, which were added to 17 μL of the ADA solution. Scans of the absorption spectrum were taken between 220 and 350 nm with 2 nm resolution every 0.1 min over a period of 10 minutes to 12 hours. One sample containing only ADA was also prepared, and this was subtracted to obtain the spectrum over time for substrates.

9.3.3 Serum stability assay

The appropriate substrate (5 mg, \pm 0.008 mmol) was dissolved in 100 μL of DMSO-*d*6 and 300 μL of D₂O. A ³¹P NMR (202 MHz, 256 scans) was conducted at this stage as a reference (blank, t = 0). To this mixture, 300 μL of a stock solution of rat/human serum (Purchased from Sigma Aldrich, codes R9759 and H4522) was added. ³¹P NMR (256 scans) were carried out with 1 minute of delay between experiments for 14 hours at 37 °C.

9.3.4 KG1a cell culture conditions

The acute myeloid leukaemia (AML) KG1a cell line was maintained in RPMI medium (Invitrogen, Paisley, UK) supplemented with 100 units/mL penicillin, 100 $\mu\text{g}/\text{mL}$ streptomycin and 20% foetal calf serum. Cells were subsequently aliquoted (10^5 cells/100 μL) into 96-well plates and were incubated at 37 °C in a humidified 5% carbon dioxide atmosphere for 72 hours in the presence of nucleoside analogues and their respective ProTides at concentrations that were experimentally determined for each series of compounds. In addition, control cultures were carried out to which no drug was added. Cells were subsequently harvested by centrifugation and were analysed by flow cytometry using the Annexin V assay.

9.3.5 Measurement of *in vitro* apoptosis

Cultured cells were harvested by centrifugation and then resuspended in 195 μL of calcium-rich buffer. Subsequently, 5 μL of Annexin V (Caltag Medsystems, Botolph Claydon, UK) was added to the cell suspension and cells were incubated in the dark for 10 min prior to washing. Cells were finally resuspended in 190 μL of calcium-rich buffer together with 10 μL of propidium iodide. Apoptosis was assessed by dual-colour immunofluorescent flow cytometry. Subsequently LD₅₀ values (the dose required to kill 50% of the cells in a culture) were calculated for each nucleoside analogue and ProTide.

9.3.6 Immunophenotypic identification of the leukaemic stem cell compartment

Once the LD₅₀ value for each compound was established, KG1a cells were cultured with the LD₅₀ concentration of each compound for 72h. Cells were then harvested and labelled with 5 µL each of CD34-FITC, CD38-PE and CD123 PERCP-cy5 antibodies. The CD34⁺/CD38⁻/CD123⁺ sub-population in each culture was quantified and expressed as a proportion of the total culture. The effect of each compound on the stem cell compartment was compared with untreated cultures labelled with the same antibodies.

9.3.7 Identification of β-catenin levels in the leukaemic stem cell compartment

KG1a cells were cultured with the LD₅₀ concentration of each compound for 72h. Cells were then harvested and labelled with 5 µL each of CD34-FITC, CD38-PE and CD123 PERCP-cy5 antibodies and with anti-β-catenin-FITC. Before adding the last β-catenin specific antibody, cell permeability was increased by incubation with PBS-Tween. The levels of β-catenin were quantified and compared in CD34⁺/CD38⁻/CD123⁺ sub-population in each culture and in the total culture.

9.4 Standard synthetic procedures

9.4.1 Standard procedure A₁ for the synthesis of amino acid ester hydrochloride salt

The appropriate alcohol (15 eq) was cooled to 0 °C and SOCl₂ (2 eq) was added dropwise. After stirring for 30 minutes at 0 °C the solution was allowed to reach rt. The appropriate amino acid (1 eq) was added and the reaction mixture was stirred at reflux overnight. The solvent was then removed under *vacuum* and co-evaporation with increasingly volatile solvents yielded the hydrochloride salt as a white solid.¹⁰⁵

9.4.2 Standard procedure A₂ for the synthesis of amino acid ester *p*-toluene sulfonate salts

A mixture of the appropriate amino acid (1 eq), the appropriate alcohol (5eq), and *p*-toluene sulfonic acid (*p*-TSA) monohydrate (1.1 eq), in toluene (20 mL/mmol) was heated at reflux overnight, using a Dean-Stark apparatus. The solvent was removed under reduced pressure and co-evaporation with increasingly volatile solvents yielded the solid *p*-toluene sulfonate salt as a white solid.¹⁰⁵

9.4.3 Standard procedure B for the synthesis of aryl phosphorodichloridate

Phosphorus oxychloride (1 eq) and the appropriate substituted aryl alcohol (1 eq) were stirred in Et₂O (5 mL per 1 mmol of POCl₃). The solution was cooled to -78 °C and Et₃N (1 eq) was added. After 30 minutes the solution was allowed to reach rt and stirred for 1.5 hours. The triethylamine hydrochloride salt was filtered off through a sintered funnel and the solvent removed under *vacuum* to afford the crude product as a clear oil.¹⁰⁵

9.4.4 Standard procedure C for the synthesis of aryl amino acid ester phosphorochloridates from amino acid hydrochloride or *p*-toluene sulfonate salts

The appropriate amino acid ester salt (1 eq) was dissolved in CH₂Cl₂ (4 mL per mmol of amino acid ester) under Argon atmosphere. A solution of the appropriate phosphorodichloridate (1 eq) in CH₂Cl₂ (1 mL per mmol of amino acid ester) was added and the mixture cooled to -78 °C. Et₃N (2 eq) was added dropwise and the reaction mixture was stirred at -78 °C for 20 minutes and thereafter at rt for 2.5 hours.

In the case of amino acid ester hydrochloride salt as starting material, the solvent was evaporated under reduced pressure and the resulting oil was triturated with anh. Et₂O and the filtrate reduced to give the crude product as an oil.

In the case of amino acid ester *p*-toluene sulfonate salt as starting material, the solvent was evaporated under vacuum and the crude was purified by silica gel column chromatography (50% EtOAc/hexane), to yield the title compound as a white solid.¹⁰⁵

9.4.5 Standard procedure D for the synthesis of 2',3'-anhydrous adenosine analogues

To a stirring suspension of the appropriate adenosine analogue (1 eq) in CH₃CN (7 mL per mmol of adenosine analogue), α-AIBBr (4 eq) and H₂O (0.001 eq) were added, and stirring was continued at room temperature. After 1 hour, the mixture was neutralised by addition of a saturated solution of NaHCO₃ (a change in colour from dark orange to clear-white could be noticed) and the solution was extracted with EtOAc (2 x 5 mL per mmol of adenosine analogue). The combined organic phase was washed with brine (1 mL x mmol of adenosine analogue). The aqueous phase was extracted with EtOAc (1 x 5 mL per mmol of adenosine analogue) and the combined organic phase was dried over Na₂SO₄, filtered and evaporated to give a white gum. The crude mixture was dissolved in the appropriate

solvent (CH₃OH, EtOH, or THF/H₂O (4/1), 7 mL per mmol of adenosine analogue initially used) and stirred for 1 to 16 hours with Amberlite (2 x OH⁻) resin (4 mL per mmol of initial adenosine analogue used, ≥ 1.1 meq/mL by wetted bed volume), previously washed well with the appropriate solvent (CH₃OH, EtOH or THF). The solution was then filtered and the resin carefully washed with CH₃OH until no spot of the product by TLC could be detected in the filtrate. Evaporation of the combined filtrate and crystallisation of the residue from EtOH gave the appropriate 2',3'-anhydrous adenosine analogue as a white powder.

9.4.6 Standard procedure E for the synthesis of 3'-deoxyadenosine analogues

The appropriate 2',3'-anhydrous adenosine analogue (1 eq) was dissolved in DMSO (1.5 mL per mmol of starting material) and diluted with THF (15 mL per mmol of starting material), under Argon atmosphere. The solution was cooled down in an ice-cold bath and a solution of LiEt₃BH (1M in THF, 3 eq) was added dropwise.

Stirring was continued at ~ 4 °C for 1 h and at rt for 16 h. The mixture was cooled down to 0 °C and an additional portion of LiEt₃BH (1M in THF, 3 eq) was added dropwise. The mixture was stirred at 0 °C for 1 hour and then at rt for one additional hour. The reaction mixture was carefully acidified (5% AcOH/H₂O), purged with N₂ for 1 h (under the fume hood) to remove *pyrophoric* triethylborane, and evaporated. The residue was chromatographed on silica gel (see specifications for each nucleoside) to give the title compound as a white powder.

9.4.7 Standard procedure F₁ for the synthesis of ProTides

Nucleoside (1 eq) was dissolved in THF (20 mL per 1 mmol of nucleoside) under Argon atmosphere. *t*BuMgCl (1.0 M in THF, 1.1-3 eq) was added dropwise. The appropriate phosphorochloridate (3-4 eq) was dissolved in THF (4 mL per 1 mmol of phosphorochloridate) and added to the initial mixture. The mixture was stirred overnight and the solvent evaporated under vacuum. The obtained crude was purified by silica gel CC or Biotage Isolera One. In some cases further purification by prep. TLC and prep. HPLC was necessary. The title compound was obtained as a white solid.

9.4.8 Standard procedure F₂ for the synthesis of ProTides

Nucleoside (1 eq) was dissolved in THF (7 ml per 0.1 mmol of nucleoside) under Argon atmosphere. The appropriate phosphorochloridate (3-4 eq) was dissolved in THF (4 mL per 1 mmol of phosphorochloridate) and added to the initial mixture, followed by NMI (5 eq). The mixture was stirred for 12-16 hours and the solvent evaporated under vacuum. The obtained crude was purified by silica gel CC or Biotage Isolera One. In some cases further purification by prep. TLC and/or prep. HPLC was necessary. The title compound was obtained as a white solid.

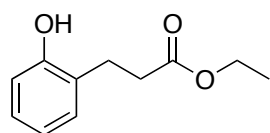
9.4.9 Standard procedure G for the synthesis of phosphorodiamidates.

To a solution of nucleoside (1 eq) in trimethyl phosphate (20 mL per 1 mmol of nucleoside), phosphoryl chloride (1 eq) was added dropwise at -5 °C and the reaction mixture was left stirring for 4 hours. The formation of the intermediate was monitored by ³¹P-NMR. A suspension of the appropriate amino acid ester (5 eq) in dichloromethane (4 mL per 1 mmol of amino acid ester) was added followed by diisopropyl ethyl amine (10 eq) at -78 °C. After stirring at room temperature for 20 hours, water (10 mL per mmol of nucleoside) was added and the layers were separated. The aqueous phase was extracted with CH₂Cl₂ (10 mL per mmol of nucleoside) and the organic phase washed with brine (10 mL per mmol of nucleoside). The combined organic layers were dried over Na₂SO₄ and concentrated. The residue was purified by column chromatography or Biotage Isolera One to give the title compound as a white solid.

9.5 Experimental details

9.5.1 Synthesis of aryl alcohol

[13c] Ethyl 3-(2-hydroxyphenyl)propanoate

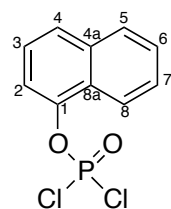


2,3-Dichloro-5,6-dicyano-1,4-benzoquinone (771 mg, 3.4 mmol) was added to a solution of 3,4-dihydrocoumarin (7.63 g, 51.5 mmol) in EtOH (40 mL) and the resulting orange solution was stirred at room temperature for 8 hours. The crude was purified by flash column chromatography (eluent: CH₂Cl₂) to afford **13c** as a yellow solid (9.6 g, 96%). Lit. mp = 36-36.5 °C.¹⁵⁰

¹H NMR (500 MHz, CDCl₃) δ_H 7.29-7.20 (m, 1H, Ar), 7.19-7.16 (m, 1H, Ar), 7.10-7.05 (m, 2H, Ar), 4.12 (q, *J* = 7.2 Hz, 2H, CH₂CH₂CO₂CH₂CH₃), 3.00 (t, *J* = 7.7 Hz, 2H, CH₂CH₂CO₂CH₂CH₃), 2.61 (t, *J* = 7.7 Hz, 2H, CH₂CH₂CO₂CH₂CH₃), 1.22 (t, *J* = 7.2 Hz, 3H, CH₂CH₂CO₂CH₂CH₃).

9.5.2 Synthesis of aryl phosphorodichloridates

[14b] Naphth-1-yl dichlorophosphate



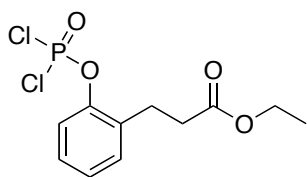
Prepared according to the general procedure **B** using POCl₃ (3.9 mL, 41.8 mmol), 1-naphthol (6.06 g, 42.03 mmol) and Et₃N (5.9 mL, 42.3 mmol).

The product was obtained as a clear oil (9.98 g, 91%).¹⁰⁵

³¹P NMR (202 MHz, CDCl₃) δ_P 3.69 [lit. ³¹P NMR (202 MHz, CDCl₃) δ_P 3.72].¹⁴⁷

¹H NMR (500 MHz, CDCl₃) δ_H 8.14 (d, *J* = 8.3 Hz, 1H, H8), 7.90 (d, *J* = 8.1 Hz, 1H, H5), 7.81 (d, *J* = 8.3 Hz, 1H, H4), 7.68-7.54 (m, 3H, H2, H6, H7), 7.46 (d, *J* = 8.0 Hz, 1H, H3).

[14c] Ethyl 3-(2-hydroxyphenyl)propanoyl dichlorophosphate



Prepared according to the general procedure **B** using ethyl 3-(2-hydroxyphenyl)propanoate [**13c**] (5.17 g, 26.62 mmol), POCl₃ (2.48 mL g, 26.62 mmol) and Et₃N (3.71 mL, 26.62 mmol). The product was obtained as a clear oil (7.45 g, 90%).¹⁵⁰

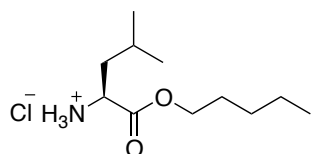
³¹P NMR (202 MHz, CDCl₃) δ_P 3.22.

¹H NMR (500 MHz, CDCl₃) δ_H 7.43-7.40 (m, 1H, Ar), 7.36-7.33 (m, 1H, Ar), 7.31-7.23 (m, 2H, Ar), 4.15 (q, *J* = 7.2 Hz, 2H, CH₂CH₂CO₂CH₂CH₃), 3.06 (t, *J* = 7.7 Hz, 2H,

$\text{CH}_2\text{CH}_2\text{CO}_2\text{CH}_2\text{CH}_3$), 2.67 (t, $J = 7.7$ Hz, 2H, $\text{CH}_2\text{CH}_2\text{CO}_2\text{CH}_2\text{CH}_3$), 1.25 (t, $J = 7.2$ Hz, 3H, $\text{CH}_2\text{CH}_2\text{CO}_2\text{CH}_2\text{CH}_3$).

9.5.3 Synthesis of amino acid ester salts

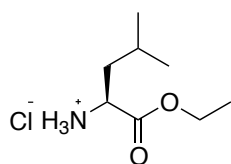
[16a] L-Leucine pent-1-yl ester hydrochloride salt



Prepared according to the general procedure **A₁** using SOCl_2 (6.10 mL, 84.12 mmol), *n*-pentanol (68.57 mL) and L-leucine (5.52 g, 42.06 mmol). The product was obtained as a white solid (9.80 g, 98%).¹⁰⁵

$^1\text{H NMR}$ (500 MHz, CDCl_3) δ_{H} 8.72 (br s, 3H, NH_3), 4.18-4.09 (m, 2H, $\text{CH}_2\text{CH}_2\text{CH}_2\text{CH}_2\text{CH}_3$ *n*-Pen), 3.88 (t, $J = 7.1$ Hz, 1H, $\text{CHCH}_2\text{CH}(\text{CH}_3)_2$ L-Leu), 1.82-1.73 (m, 1H, $\text{CHCH}_2\text{CH}(\text{CH}_3)_2$ L-Leu), 1.74-1.64 (m, 2H, $\text{CHCH}_2\text{CH}(\text{CH}_3)_2$ L-Leu), 1.64-1.57 (m, 2H, $\text{CH}_2\text{CH}_2\text{CH}_2\text{CH}_2\text{CH}_3$ *n*-Pen), 1.35-1.27 (m, 4H, $\text{CH}_2\text{CH}_2\text{CH}_2\text{CH}_2\text{CH}_3$ *n*-Pen), 0.93-0.85 (m, 9H, $\text{CH}_2\text{CH}_2\text{CH}_2\text{CH}_2\text{CH}_3$ *n*-Pen, $\text{CHCH}_2\text{CH}(\text{CH}_3)_2$ L-Leu).

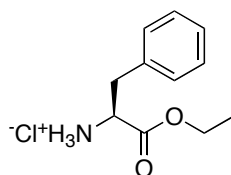
[16b] L-Leucine ethyl ester hydrochloride salt



Prepared according to the general procedure **A₁** using SOCl_2 (5.53 mL, 76.24 mmol), ethanol (33.39 mL) and L-leucine (5.0 g, 38.12 mmol). The product was obtained as a white solid (7.01 g, 94 %).

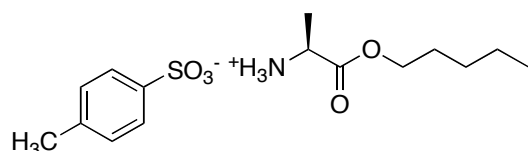
$^1\text{H NMR}$ (500 MHz, CDCl_3) δ_{H} 8.85 (br s, 3H, NH_3), 4.32-4.21 (m, 2H, CH_2CH_3 Et), 4.06 (t, $J = 7.0$ Hz, 1H, $\text{CHCH}_2\text{CH}(\text{CH}_3)_2$ L-Leu), 2.05-1.94 (m, 2H, $\text{CHCH}_2\text{CH}(\text{CH}_3)_2$ L-Leu) 1.89-1.80 (m, 1H, $\text{CHCH}_2\text{CH}(\text{CH}_3)_2$ L-Leu), 1.32 (t, $J = 7.12$ Hz, 3H, CH_2CH_3 Et), 0.99 (d, $J = 5.4$ Hz, 6H, $\text{CHCH}_2\text{CH}(\text{CH}_3)_2$ L-Leu).

[16c] L-Phenylalanine ethyl ester hydrochloride salt



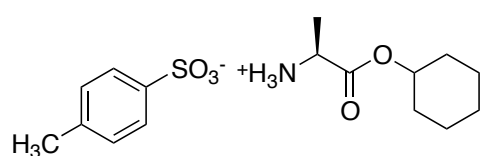
Prepared according to the general procedure **A₁** using SOCl_2 (3.16 mL, 43.54 mmol), ethanol (19.07 mL) and L-phenylalanine (3.60 g, 21.77 mmol). The product was obtained as a white solid (4.20 g, 84 %).

$^1\text{H NMR}$ (500 MHz, CDCl_3) δ_{H} 8.72 (br s, 3H, NH_3), 7.34-7.25 (m, 5H, Ar L-Phe), 4.43-4.36 (m, 1H, CHCH_2Ph L-Phe), 4.18-4.10 (m, 2H, CH_2CH_3 Et), 3.41-3.31 (m, 2H, CHCH_2Ph L-Phe), 1.20-1.12 (m, 3H, CH_2CH_3 Et).⁴⁶⁷

[16d] L-Alanine pent-1-yl ester tosylate salt

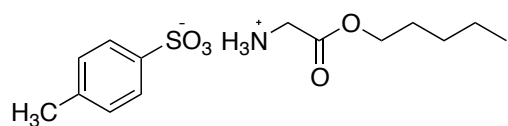
Prepared according to the general procedure **A₂** using *n*-pentanol (16.4 mL), L-alanine (2.7 g, 30.3 mmol) and *p*-TSA (6.3 g, 33.3 mmol) and toluene (109 mL). The product was obtained as a white solid (8.03 g, 80 %).¹⁵¹

¹H NMR (500 MHz, CDCl₃) δ_H 8.17 (br s, 3H, NH₃), 7.77 (d, *J* = 8.0 Hz, 2H, Ar *p*-TSA), 7.15 (d, *J* = 8.0 Hz, 2H, Ar *p*-TSA), 4.10-3.97 (m, 3H, CHCH₃ L-Ala, CH₂CH₂CH₂CH₂CH₃ *n*-Pen), 2.36 (s, 3H, CH₃ *p*-TSA), 1.59-1.51 (m, 2H, CH₂CH₂CH₂CH₂CH₃ *n*-Pen), 1.46 (d, *J* = 7.4 Hz, 3H, CHCH₃ L-Ala), 1.32-1.20 (m, 4H, CH₂CH₂CH₂CH₂CH₃ *n*-Pen), 0.88 (t, *J* = 7.0 Hz, 3H, CH₂CH₂CH₂CH₂CH₃ *n*-Pen).

[16e] L-Alanine cyclohex-1-yl ester tosylate salt

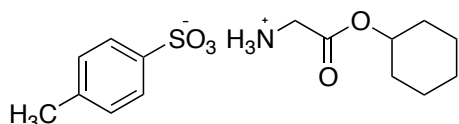
Prepared according to the general procedure **A₂** using cyclohexanol (23.4 mL), L-alanine (4.0 g, 44.9 mmol), *p*-TSA (9.39 g, 49.39 mmol) and toluene (102 mL). The product was obtained as a white solid (13.57 g, 88%).¹⁵¹

¹H NMR (500 MHz, CDCl₃) δ_H 8.52 (br s, 3H, NH₃), 7.79 (d, *J* = 8.0 Hz, 2H, Ar *p*-TSA), 7.25 (d, *J* = 8.0 Hz, 2H, Ar *p*-TSA), 4.90-3.87 (m, 1H, CHCH₃ L-Ala), 4.24-4.10 (m, 1H, CH(CH₂)₅ cHex), 2.31 (s, 3H, CH₃ *p*-TSA), 1.89-1.61 (m, 2H, CH(CH₂)₅ cHex), 1.66-1.52 (m, 3H, CHCH₃ L-Ala), 1.59-1.11 (m, 8H, CH(CH₂)₅ cHex).

[16f] Glycine pent-1-yl ester tosylate salt

Prepared according to the general procedure **A₂**, using 1-pentanol (11.87 mL), glycine (1.64 g, 21.85 mmol), *p*-TSA (4.57 g, 24.03 mmol) and toluene (113 mL). The product was obtained as a white solid (6.66 g, 96%).

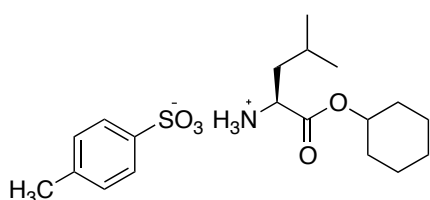
¹H NMR (500 MHz, CDCl₃) δ_H 8.01 (br s, 3H, NH₃), 7.73 (d, *J* = 8.1 Hz, 2H, Ar *p*-TSA), 7.12 (d, *J* = 8.1 Hz, 2H, Ar *p*-TSA), 4.01 (t, *J* = 6.87 Hz, 2H, CH₂CH₂CH₂CH₂CH₃ *n*-Pen), 3.72-3.67 (m, 2H, CH₂ Gly), 2.35 (s, 3H, CH₃ *p*-TSA), 1.55-1.48 (m, 2H, CH₂CH₂CH₂CH₂CH₃ *n*-Pen), 1.32-1.19 (m, 4H, CH₂CH₂CH₂CH₂CH₃ *n*-Pen), 0.90-0.86 (m, 3H, CH₂CH₂CH₂CH₂CH₃ *n*-Pen).

[16g] Glycine cyclohexyl ester tosylate salt

Prepared according to the general procedure **A₂** using cyclohexanol (11.06 mL), glycine (1.60 g, 21.25 mmol) and *p*-TSA (4.45 g, 23.37 mmol) and toluene

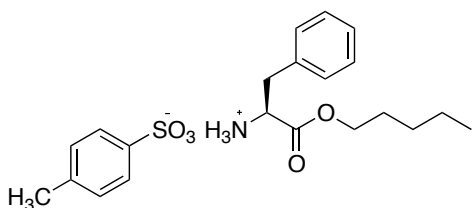
(110 mL). The product was obtained as a white solid (6.15 g, 88 %).

¹H NMR (500 MHz, CDCl₃) δ_H 8.01 (br s, 3H, NH₃), 7.74 (d, *J* = 8.0 Hz, 2H, Ar *p*-TSA), 7.12 (d, *J* = 8.0 Hz, 2H, Ar *p*-TSA), 4.77-4.69 (m, 1H, CH(CH₂)₅ cHex), 3.70-3.64 (m, 2H, CH₂ Gly), 2.35 (s, 3H, CH₃ *p*-TSA), 1.76-1.20 (m, 10H, CH(CH₂)₅ cHex).

[16h] L-Leucine cyclohexyl ester tosylate salt

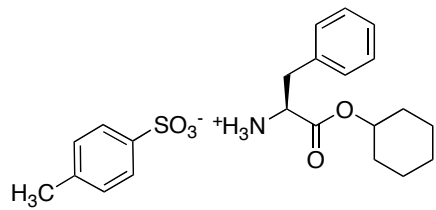
Prepared according to the general procedure **A₂** using cyclohexanol (20.82 mL), L-leucine (6.61 g, 40.0 mmol), *p*-TSA (8.37 g, 44.0 mmol) and toluene (104 mL). The product was obtained as a white solid (6.17 g, 40%).

¹H NMR (500 MHz, CDCl₃) δ_H 8.08 (br s, 3H, NH₃), 7.78 (d, *J* = 8.0 Hz, 2H, Ar *p*-TSA), 7.15 (d, *J* = 8.0 Hz, 2H, Ar *p*-TSA), 4.77-4.68 (m, 1H, CH(CH₂)₅ cHex), 3.96-3.88 (m, 1H, CHCH₂CH(CH₃)₂ L-Leu), 2.37 (s, 3H, CH₃ *p*-TSA), 1.81-1.14 (m, 13H, CHCH₂CH(CH₃)₂ L-Leu, CH(CH₂)₅ cHex), 0.81 (t, *J* = 7.2 Hz, 6H, CHCH₂CH(CH₃)₂ L-Leu).

[16i] L-Phenylalanine pent-1-yl ester tosylate salt

Prepared according to the general procedure **A₂** using 1-pentanol (10.83 mL), L-phenylalanine (3.30 g, 20.0 mmol), *p*-TSA (4.18 g, 22 mmol) and toluene (114 mL). The product was obtained as a white solid (7.74 g, 95%).¹⁵²

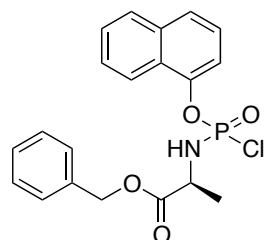
¹H NMR (500 MHz, CDCl₃) δ_H 8.25 (br s, 3H, NH₃), 7.77 (d, *J* = 8.0 Hz, 2H, Ar *p*-TSA), 7.21-7.09 (m, 7H, Ar *p*-TSA, CHCH₂Ph L-Phe), 4.31-4.24 (m, 1H, CHCH₂Ph L-Phe), 3.96-3.86 (m, 2H, CH₂CH₂CH₂CH₂CH₃ *n*-Pen), 3.32-3.23 (m, 1H, CHCH₂Ph L-Phe), 3.13-3.05 (m, 1H, CHCH₂Ph L-Phe), 2.35 (s, 3H, CH₃ *p*-TSA), 1.42-1.34 (m, 2H, CH₂CH₂CH₂CH₂CH₃ *n*-Pen), 1.25-1.16 (m, 2H, CH₂CH₂CH₂CH₂CH₃ *n*-Pen), 1.11-1.02 (m, 2H, CH₂CH₂CH₂CH₂CH₃ *n*-Pen), 0.87-0.81 (m, 3H, CH₂CH₂CH₂CH₂CH₃ *n*-Pen).

[16j] L-Phenylalanine cyclohexyl ester tosylate salt

(6.76 g, 83%).

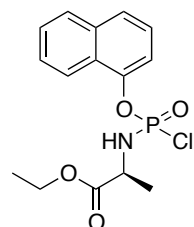
Prepared according to the general procedure **A₂** using cyclohexanol (10.41 mL), L-phenylalanine (3.30 g, 20.0 mmol), *p*-TSA (4.18 g, 22 mmol) and toluene (100 mL). The product was obtained as a white solid

¹H NMR (500 MHz, CDCl₃) δ_H 8.22 (br s, 3H, NH₃), 7.76, 7.12 (d, *J* = 7.2 Hz, 2H, Ar *p*-TSA), 7.21-7.11 (m, 7H, Ar *p*-TSA, CHCH₂Ph L-Phe), 4.67-4.59 (m, 1H, CH(CH₂)₅ cHex), 4.30-4.22 (m, 1H, CHCH₂Ph L-Phe), 3.32-3.24 (m, 1H, CHCH₂Ph L-Phe), 3.14-3.05 (m, 1H, CHCH₂Ph L-Phe), 2.35 (s, 3H, CH₃ *p*-TSA), 1.64-1.49 (m, 4H, CH(CH₂)₅ cHex), 1.47-1.39 (m, 1H, CH(CH₂)₅ cHex), 1.25-1.08 (m, 5H, CH(CH₂)₅ cHex).

9.5.4 Synthesis of aryl amino acid phosphorochloridates**[17a] Naphth-1-yl-(benzoxy-L-alaninyl) dichlorophosphate**

Prepared according to the general procedure **C** using L-alanine benzyl ester hydrochloride salt (430 mg, 1.99 mmol), naphth-1-yl dichlorophosphate [**14b**] (0.52 g, 1.99 mmol) and Et₃N (0.55 mL, 3.98 mmol) in CH₂Cl₂ (8 ml). The product was obtained as a clear oil (87%, 0.70 g).

³¹P NMR (202 MHz, CDCl₃) δ_P 8.23, 8.02 [**³¹P NMR (202 MHz, CDCl₃)** δ_P 8.14, 7.88].¹⁴⁷
¹H NMR (500 MHz, CDCl₃) δ_H 8.10-7.30 (m, 12H, Ar), 5.12 (s, 1H, CH₂Ph), 5.19 (s, 1H, CH₂Ph), 4.70-4.64 (m, 1H, NH), 4.42-4.33 (m, 1H, CHCH₃ L-Ala), 1.59-1.57 (m, 3H, CHCH₃ L-Ala).

[17b] Naphth-1-yl-(ethoxy-L-alaninyl)dichlorophosphate

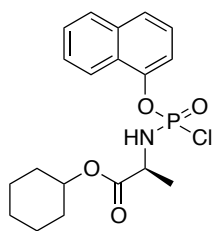
Prepared according to the general procedure **C** using L-alanine ethyl ester hydrochloride salt (0.77 g, 3.57 mmol), naphth-1-yl dichlorophosphate [**14b**] (0.93 g, 3.57 mmol) and Et₃N (0.99 mL, 7.14 mmol) in CH₂Cl₂ (15 mL). The product was obtained as a clear oil (1.20 g, 99 %).

³¹P NMR (202 MHz, CDCl₃) δ_P 8.30, 8.05. [**³¹P NMR (202 MHz, CDCl₃)** δ_P 8.23, 7.91].¹⁴⁷

¹H NMR (500 MHz, CDCl₃) δ_H 8.13-8.08 (m, 1H, Nap, H8), 7.92-7.87 (m, 1H, Nap, H5), 7.78-7.72 (m, 1H, H4 Nap), 7.63-7.56 (m, 3H, H2, H6, H7, Nap) 7.46 (t, *J* = 7.78 Hz, 1H,

H3, Nap), 4.61-4.37 (m, 1H, NH), 4.32-4.22 (m, 2H, CH_2CH_3 Et), 4.18-3.96 (m, 1H, $CHCH_3$ L-Ala), 1.62-1.52 (m, 3H, CH_2CH_3 Et), 1.36-1.27 (m, 3H, $CHCH_3$ L-Ala).

[17c] Naphth-1-yl-(cyclohexyloxy-L-alaninyl)dichlorophosphate

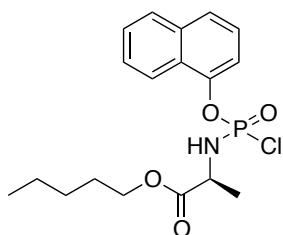


Prepared according to the general procedure **C** using L-alanine cyclohexyl ester tosylate salt **[16e]** (8.24 g, 24.0 mmol), naphth-1-yl dichlorophosphate **[14b]** (6.26 g, 24.0 mmol) and Et_3N (6.69 ml, 48 mmol) in CH_2Cl_2 (100 mL). The product was obtained as clear oil (7.58 g, 92%).¹⁵¹

^{31}P NMR (202 MHz, $CDCl_3$) δ_P 8.33, 7.99.

1H NMR (500 MHz, $CDCl_3$) δ_H 8.24-7.40 (m, 7H, Ar), 4.92-4.84 (m, 1H, $CH(CH_2)_5$ cHex) 4.55-4.39 (m, 1H, NH), 4.34-4.25 (m, 1H, $CHCH_3$ L-Ala), 1.88-1.75 (m, 4H, $CHCH_3$ L-Ala, $CH(CH_2)_5$ cHex), 1.58-1.55 (m, 3H, $CH(CH_2)_5$ cHex), 1.54-1.35 (m, 6H, $CH(CH_2)_5$ cHex).

[17d] Naphth-1-yl-(pent-1-yloxy-L-alaninyl)dichlorophosphate

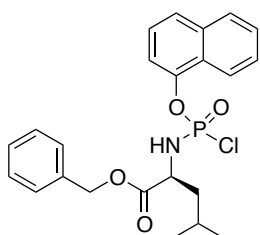


Prepared according to the general procedure **C** using L-alanine pent-1-yl ester tosylate salt **[16d]** (7.95 g, 24.0 mmol), naphth-1-yl dichlorophosphate **[14b]** (6.26 g, 24.0 mmol) and Et_3N (6.69 ml, 48.0 mmol) in CH_2Cl_2 (100 mL). The product was obtained as a clear oil (7.83 g, 85%).¹⁵¹

^{31}P NMR (202 MHz, $CDCl_3$) δ_P 8.74, 8.63.

1H NMR (500 MHz, $CDCl_3$) δ_H 8.16 (d, $J = 8.0$ Hz, 1H, Nap, H8), 7.98-7.89 (m, 1H, Nap, H5), 7.72, 7.67 (m, 1H, Nap, H4), 7.65-7.52 (m, 3H, H2, H6, H7) 7.49-7.43 (m, 1H, H3), 4.36-4.18 (m, 1H, NH), 4.25-4.18 (m, 3H, $CH_2CH_2CH_2CH_2CH_3$ *n*-Pen, $CHCH_3$ L-Ala), 1.92-1.76 (m, 3H, $CHCH_3$ L-Ala), 1.77-1.58 (m, 2H, $CH_2CH_2CH_2CH_2CH_3$ *n*-Pen), 1.41-1.30 (m, 4H, $CH_2CH_2CH_2CH_2CH_3$ *n*-Pen), 0.99-0.82 (m, 3H, $CH_2CH_2CH_2CH_2CH_3$ *n*-Pen).

[17e] Naphth-1-yl-(benzyloxy-L-leucinyl)dichlorophosphate

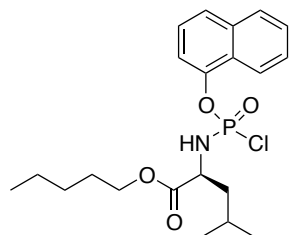


Prepared according to the general procedure **C** using L-leucine benzyl ester tosylate salt (2.00 g, 5.08 mmol), naphth-1-yl dichlorophosphate **[14b]** (1.33 g, 5.08 mmol) and Et_3N (1.42 mL, 10.16 mmol) in CH_2Cl_2 (20 mL). The product was obtained as a clear oil (2.01 g, 89 %).¹⁵²

^{31}P NMR (202 MHz, CDCl_3) δ_{P} 8.32, 8.07.

^1H NMR (500 MHz, CDCl_3) δ_{H} 8.12-8.04 (m, 1H, Nap, H8), 7.91-7.86 (m, 1H, Nap, H5), 7.78-7.71 (m, 1H, H4 Nap), 7.63-7.53 (m, 3H, H2, H6, H7, Nap) 7.44 (t, $J = 7.97$ Hz, 1H, H3, Nap), 7.40-7.31 (m, 5H, Ph), 5.27-4.93 (m, 2H, CH_2Ph), 4.31-4.21 (m, 2H, NH, $\text{CHCH}_2\text{CH}(\text{CH}_3)_2$ L-Leu), 1.74-1.61 (m, 2H, $\text{CHCH}_2\text{CH}(\text{CH}_3)_2$ L-Leu), 1.36-1.31 (m, 1H, $\text{CHCH}_2\text{CH}(\text{CH}_3)_2$ L-Leu), 0.98-0.92 (m, 6H, $\text{CHCH}_2\text{CH}(\text{CH}_3)_2$ L-Leu).

[17f] Naphth-1-yl-(pentyl-1-oxy-L-leucinyl)dichlorophosphate

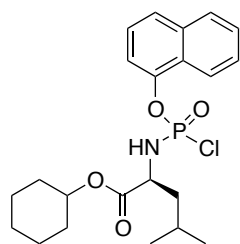


Prepared according to the general procedure **C** using L-leucine pent-1-yl ester hydrochloride salt [**16a**] (2.00 g, 8.41 mmol), naphth-1-yl dichlorophosphate [**14b**] (2.19 g, 8.41 mmol) and Et_3N (2.34 mL, 16.82 mmol) in CH_2Cl_2 (35 mL). The product was obtained as a clear oil (3.19 g, 89%).¹⁵²

^{31}P NMR (202 MHz, CDCl_3) δ_{P} 8.78, 8.52.

^1H NMR (500 MHz, CDCl_3) δ_{H} 8.12 (d, $J = 8.0$ Hz, 1H, Nap, H8), 7.91-7.87 (m, 1H, Nap, H5), 7.77, 7.73 (m, 1H, Nap, H4), 7.65-7.54 (m, 3H, H2, H6, H7) 7.47-7.42 (m, 1H, H3), 4.48-4.36 (m, 1H, NH), 4.28-4.21 (m, 1H, $\text{CHCH}_2\text{CH}(\text{CH}_3)_2$ L-Leu), 4.21-4.12 (m, 2H, $\text{CH}_2\text{CH}_2\text{CH}_2\text{CH}_2\text{CH}_3$ *n*-Pen), 1.91-1.76 (m, 2H, $\text{CHCH}_2\text{CH}(\text{CH}_3)_2$ L-Leu), 1.76-1.60 (m, 3H, $\text{CHCH}_2\text{CH}(\text{CH}_3)_2$ L-Leu, $\text{CH}_2\text{CH}_2\text{CH}_2\text{CH}_2\text{CH}_3$ *n*-Pen), 1.41-1.30 (m, 4H, $\text{CH}_2\text{CH}_2\text{CH}_2\text{CH}_2\text{CH}_3$ *n*-Pen), 1.01-0.94 (m, 6H, $\text{CHCH}_2\text{CH}(\text{CH}_3)_2$ L-Leu), 0.94-0.86 (m, 3H, $\text{CH}_2\text{CH}_2\text{CH}_2\text{CH}_2\text{CH}_3$ *n*-Pen).

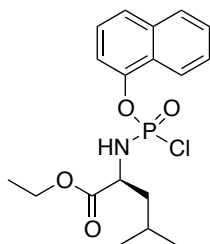
[17g] Naphth-1-yl-(cyclohexyloxy-L-leucinyl)dichlorophosphate



Prepared according to the general procedure **C** using L-leucine cyclohexyl ester tosylate salt [**16h**] (1.80 g, 4.67 mmol), naphth-1-yl dichlorophosphate [**14b**] (1.22 g, 4.67 mmol) and Et_3N (1.30 mL, 9.34 mmol) in CH_2Cl_2 (20 mL). The product was obtained as a clear oil (1.84 g, 90%).

^{31}P NMR (202 MHz, CDCl_3) δ_{P} 8.82, 8.55.

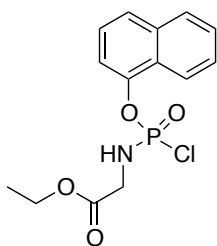
^1H NMR (500 MHz, CDCl_3) δ_{H} 8.12 (d, $J = 8.0$ Hz, 1H, Nap, H8), 7.91-7.86 (m, 1H, H5 Nap), 7.74 (d, $J = 8.2$ Hz, 1H, H4 Nap), 7.64-7.54 (m, 3H, H2, H6, H7, Nap) 7.47-7.42 (m, 1H, H3, Nap), 4.92-4.82 (m, 1H, $\text{CH}(\text{CH}_2)_5$ cHex), 4.42-4.31 (m, 1H, NH), 4.25-4.16 (m, 1H, $\text{CHCH}_2\text{CH}(\text{CH}_3)_2$ L-Leu), 1.93-1.26 (m, 13H, $\text{CHCH}_2\text{CH}(\text{CH}_3)_2$ L-Leu, $\text{CH}(\text{CH}_2)_5$ cHex), 1.00-0.94 (m, 6H, $\text{CHCH}_2\text{CH}(\text{CH}_3)_2$ L-Leu).

[17h] Naphth-1-yl-(ethyloxy-L-leucinyl)dichlorophosphate

Prepared according to the general procedure **C** using L-leucine ethyl ester hydrochloride salt [**16b**] (1.06 g, 5.42 mmol), naphth-1-yl dichlorophosphate [**14b**] (1.41 g, 5.42 mmol) and Et₃N (1.51 mL, 10.84 mmol) in CH₂Cl₂ (20 mL). The product was obtained as a clear oil (1.77 g, 85%).

³¹P NMR (202 MHz, CDCl₃) δ_P 8.72, 8.49.

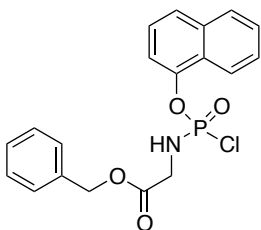
¹H NMR (500 MHz, CDCl₃) δ_H 8.12 (d, *J* = 7.9 Hz, 1H, Nap, H8), 7.89 (d, *J* = 7.6 Hz, 1H, Nap, H5), 7.75 (d, *J* = 8.4 Hz, 1H, H4 Nap), 7.65-7.53 (m, 3H, H2, H6, H7, Nap) 7.45 (t, *J* = 7.9 Hz, 1H, H3, Nap), 4.52-3.91 (m, 4H, NH, CHCH₂CH(CH₃)₂ L-Leu, CH₂CH₃ Et), 1.95-1.75 (m, 2H, CHCH₂CH(CH₃)₂ L-Leu), 1.74-1.59 (m, 1H, CHCH₂CH(CH₃)₂ L-Leu), 1.35-1.27 (m, 3H, CH₂CH₃ Et), 1.00-0.93 (m, 6H, CHCH₂CH(CH₃)₂ L-Leu).

[17i] Naphth-1-yl-(ethoxy-glycinyl)dichlorophosphate

Prepared according to the general procedure **C** using glycine ethyl ester hydrochloric salt (0.85 g, 6.10 mmol), naphth-1-yl dichlorophosphate [**14b**] (1.59 g, 6.10 mmol) and Et₃N (1.70 mL, 12.21 mmol) in CH₂Cl₂ (24 mL). The product was obtained as a clear oil (1.90 g, 95%).

³¹P NMR (202 MHz, CDCl₃) δ_P 9.29.

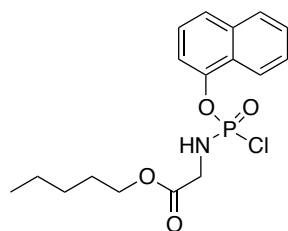
¹H NMR (500 MHz, CDCl₃) δ_H 8.12-8.08 (m, 1H, Nap, H8), 7.98-7.87 (m, 1H, Nap, H5), 7.77-7.72 (m, 1H, H4 Nap), 7.64-7.55 (m, 3H, H2, H6, H7, Nap) 7.45 (t, *J* = 8.0 Hz, 1H, H3, Nap), 4.28 (q, *J* = 7.1 Hz, 2H, CH₂CH₃ Et), 4.03-3.98 (m, 2H, CH₂ Gly), 1.32 (t, *J* = 7.1 Hz, 3H, CH₂CH₃ Et).

[17j] Naphth-1-yl(benzyloxy-glycinyl)dichlorophosphate

Prepared according to the general procedure **C** using glycine benzyl ester hydrochloric salt (1.03 g, 5.13 mmol), naphth-1-yl dichlorophosphate [**14b**] (1.34 g, 5.13 mmol) and Et₃N (1.43 mL, 10.26 mmol) in CH₂Cl₂ (20 mL). The product was obtained as a clear oil (1.60 g, 80%).

³¹P NMR (202 MHz, CDCl₃) δ_P 8.87. [Lit. ³¹P NMR (202 MHz, CDCl₃) δ_P 8.90].¹⁴⁸

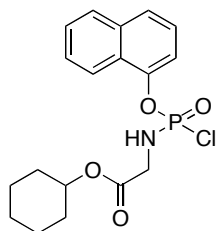
¹H NMR (500 MHz, CDCl₃) δ_H 8.10-8.06 (m, 1H, Nap, H8), 7.92-7.88 (m, 1H, Nap, H5), 7.76 (d, *J* = 8.2 Hz, 1H, H4 Nap), 7.63-7.56 (m, 3H, H2, H6, H7, Nap) 7.46 (t, *J* = 8.0 Hz, 1H, H3, Nap), 7.42-7.38 (m, 5H, Ph), 5.27 (s, 2H, CH₂Ph), 4.41-4.26 (m, 1H, NH), 4.10-4.05 (m, 2H, CH₂ Gly).

[17k] Naphth-1-yl(pentyl-1-oxy-glyciny)dichlorophosphate

Prepared according to the general procedure **C** using glycine pent-1-yl ester tosylate salt **[16f]** (2.57 g, 8.11 mmol), naphth-1-yl dichlorophosphate **[14b]** (2.12 g, 8.11 mmol) and Et₃N (2.26 mL, 16.22 mmol) in CH₂Cl₂ (32 mL). The product was obtained as a clear oil (2.64 g, 88%).

³¹P NMR (202 MHz, CDCl₃) δ_P 9.10.

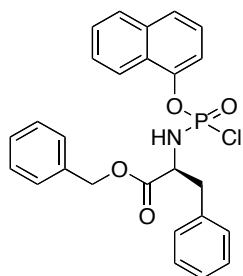
¹H NMR (500 MHz, CDCl₃) δ 8.10 (d, *J* = 8.1 Hz, 1H, Nap, H8), 7.92-7.88 (m, 1H, Nap, H5), 7.75 (d, *J* = 8.1 Hz, 1H, H4 Nap), 7.64-7.54 (m, 3H, H2, H6, H7, Nap) 7.46 (t, *J* = 8.0 Hz, 1H, H3, Nap), 4.48-4.41 (m, 1H, NH), 4.23 (t, *J* = 6.8 Hz, 2H, CH₂CH₂CH₂CH₂CH₃ *n*-Pen), 4.05-3.99 (m, 2H, CH₂ Gly), 1.75-1.65 (m, 2H, CH₂CH₂CH₂CH₂CH₃ *n*-Pen), 1.39-1.34 (m, 4H, CH₂CH₂CH₂CH₂CH₃ *n*-Pen), 0.93 (t, *J* = 6.9 Hz, 3H, CH₂CH₂CH₂CH₂CH₃ *n*-Pen).

[17l] Naphth-1-yl(cyclohexyloxy-glyciny)dichlorophosphate

Prepared according to the general procedure **C** using glycine cyclohexyl ester tosylate salt **[16g]** (2.59 g, 7.86 mmol), naphth-1-yl dichlorophosphate **[14b]** (2.05 g, 7.86 mmol) and Et₃N (2.19 mL, 15.72 mmol) in CH₂Cl₂ (30 mL). The product was obtained as a clear oil (2.31 g, 77%).

³¹P NMR (202 MHz, CDCl₃) δ_P 9.04.

¹H NMR (500 MHz, CDCl₃) δ_H 8.10 (d, *J* = 8.1 Hz, 1H, H8 Nap), 7.90 (d, *J* = 8.0 Hz, 1H, H5 Nap), 7.76 (d, *J* = 8.1 Hz, 1H, H4 Nap), 7.64-7.57 (m, 3H, H2, H6, H7 Nap), 7.46 (t, *J* = 8.1 Hz, 1H, H3 Nap), 4.95-4.88 (m, 1H, CH(CH₂)₅ cHex), 4.43-4.30 (m, 1H, NH), 4.04-3.98 (m, 2H, CH₂ Gly), 1.96-1.37 (m, 10H, CH(CH₂)₅ cHex).

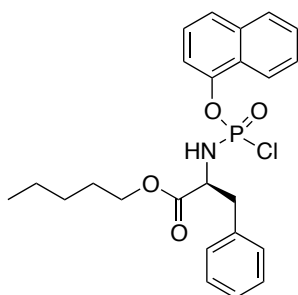
[17m] Naphth-1-yl-(benzoxy-L-phenylalaniny)dichlorophosphate

Prepared according to the general procedure **C** using L-phenylalanine benzyl ester tosylate salt (3.42 g, 8.00 mmol), naphth-1-yl dichlorophosphate **[14b]** (2.09 g, 8.00 mmol) and Et₃N (2.23 mL, 16.00 mmol) in CH₂Cl₂ (30 mL). The product was obtained as clear oil (3.34 g, 87%).

³¹P NMR (202 MHz, CDCl₃) δ_P 8.29, 8.17. [Lit. ³¹P NMR (202 MHz, CDCl₃) δ_P 8.32, 8.19].¹⁴⁸

$^1\text{H NMR}$ (500 MHz, CDCl_3) δ_{H} 7.93-6.96 (m, 17H, Nap, Ph L-Phe, CH_2Ph), 5.20-4.95 (m, 2H, CH_2Ph), 4.66-4.51 (m, 1H, CHCH_2Ph L-Phe), 4.32-4.11 (m, 1H, NH), 3.27-3.07 (m, 2H, CHCH_2Ph L-Phe).

[17n] Naphth-1-yl-(pentyloxy-L-phenylalaninyl)dichlorophosphate

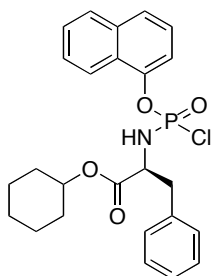


Prepared according to the general procedure **C** using L-phenylalanine pent-1-yl ester tosylate salt [**16i**] (3.26 g, 8.00 mmol), naphth-1-yl dichlorophosphate [**14b**] (2.09 g, 8.00 mmol) and Et_3N (2.23 mL, 16.00 mmol) in CH_2Cl_2 (30 mL). The product was obtained as a clear oil (3.02 g, 82%).¹⁵²

$^{31}\text{P NMR}$ (202 MHz, CDCl_3) δ_{P} 8.35, 8.25.

$^1\text{H NMR}$ (500 MHz, CDCl_3) δ_{H} 8.13-7.07 (m, 12H, Nap, CHCH_2Ph L-Phe), 4.56-4.46 (m, 1H, CHCH_2Ph L-Phe), 4.36-4.21 (m, 1H, NH), 4.13-4.07 (m, 1H, $\text{CH}_2\text{CH}_2\text{CH}_2\text{CH}_2\text{CH}_3$ *n*-Pen), 4.03-3.94 (m, 1H, $\text{CH}_2\text{CH}_2\text{CH}_2\text{CH}_2\text{CH}_3$ *n*-Pen), 3.25-3.10 (m, 2H, CHCH_2Ph L-Phe), 1.66-1.56 (m, 2H, $\text{CH}_2\text{CH}_2\text{CH}_2\text{CH}_2\text{CH}_3$ *n*-Pen), 1.37-1.31 (m, 4H, $\text{CH}_2\text{CH}_2\text{CH}_2\text{CH}_2\text{CH}_3$ *n*-Pen), 0.94-0.87 (m, 3H, $\text{CH}_2\text{CH}_2\text{CH}_2\text{CH}_2\text{CH}_3$ *n*-Pen).

[17o] Naphth-1-yl-(cyclohexyloxy-L-phenylalaninyl)dichlorophosphate

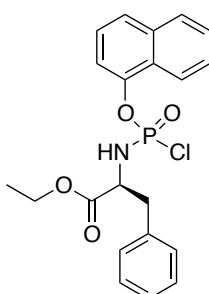


Prepared according to the general procedure **C** using L-phenylalanine cyclohexyl ester tosylate salt [**16j**] (3.36 g, 8.00 mmol), naphth-1-yl dichlorophosphate [**14b**] (2.09 g, 8.00 mmol) and Et_3N (2.23 mL, 16.00 mmol) in CH_2Cl_2 (32 mL). The product was obtained as a clear oil (3.25 g, 86%).

$^{31}\text{P NMR}$ (202 MHz, CDCl_3) δ_{P} 8.45, 8.35.

$^1\text{H NMR}$ (500 MHz, CDCl_3) δ_{H} 8.12-7.10 (m, 12H, Nap, CHCH_2Ph L-Phe), 4.86-4.78 (m, 1H, $\text{CH}(\text{CH}_2)_5$ *c*Hex), 4.57-4.42 (m, 1H, CHCH_2Ph L-Phe), 4.39-4.33 (m, 0.5H, NH), 4.29-4.23 (m, 0.5H, NH), 3.24-3.06 (m, 2H, CHCH_2Ph L-Phe), 1.85-1.31 (m, 10H, $\text{CH}(\text{CH}_2)_5$ *c*Hex).

[17p] Naphth-1-yl-(ethyloxy-L-phenylalaninyl)dichlorophosphate

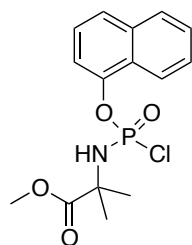


Prepared according to the general procedure **C** using L-phenylalanine ethyl ester hydrochloride salt [**16c**] (1.84 g, 8.00 mmol), naphth-1-yl dichlorophosphate [**14b**] (2.09 g, 8.00 mmol) and Et_3N (2.23 mL, 16.00 mmol) in CH_2Cl_2 (32 mL). The product was obtained as a clear oil (3.01 g, 90%).

^{31}P NMR (202 MHz, CDCl_3) δ_{P} 8.36, 8.23.

^1H NMR (500 MHz, CDCl_3) δ_{H} 8.12-7.10 (m, 12H, Nap, CHCH_2Ph L-Phe), 4.84-4.71 (m, 2H, CH_2CH_3 Et), 4.57-4.42 (m, 1H, CHCH_2Ph L-Phe), 4.35-4.31 (m, 0.5H, NH), 4.28-4.19 (m, 0.5H, NH), 3.29-3.16 (m, 2H, CHCH_2Ph L-Phe), 1.95-1.73 (m, 3H, CH_2CH_3 Et).

[17q] Naphth-1-yl-(methoxy-dimethylglyciny)dichlorophosphate

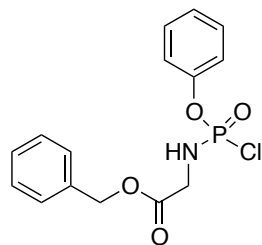


Prepared according to the general procedure C using dimethyl glycine methyl ester hydrochloride salt (1.0 g, 6.50 mmol), naphth-1-yl dichlorophosphate [**14b**] (1.70 g, 6.50 mmol) and Et_3N (1.81 mL, 13.00 mmol) in CH_2Cl_2 (26 mL). The product was obtained as a clear oil (1.66 g, 75%).¹⁵³

^{31}P NMR (202 MHz, CDCl_3) δ_{P} 6.02.

^1H NMR (500 MHz, CDCl_3) δ_{H} 8.15 (d, $J = 8.1$ Hz, 1H, H8 Nap), 7.87 (d, $J = 8.1$ Hz, 1H, H5 Nap), 7.73 (d, $J = 8.1$ Hz, 1H, H4 Nap), 7.64-7.61 (m, 1H, H2 Nap), 7.60-7.52 (m, 2H, H6, H7 Nap), 7.44 (t, $J = 7.7$ Hz, 1H, H3 Nap), 4.97 (br s, 1H, NH), 3.81 (s, 3H, CH_3), 1.77 (s, 3H, CH_3 DMG), 1.73 (s, 3H, CH_3 DMG).

[17r] Phenyl-(benzyloxy-glyciny)dichlorophosphate

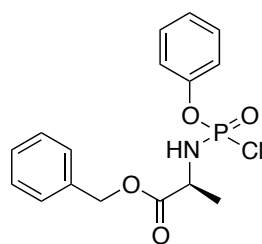


Prepared according to the general procedure C using glycine benzyl ester hydrochloride salt (1.78 g, 8.83 mmol), phenyl dichlorophosphate (1.32 mL, 8.83 mmol) and Et_3N (2.50 mL, 17.66 mmol) in CH_2Cl_2 (35 mL). The product was obtained as a clear oil (2.40 g, 80%).

^{31}P NMR (202 MHz, CDCl_3) δ_{P} 9.04. [Lit. ^{31}P NMR (202 MHz, CDCl_3) δ_{P} 8.75].¹⁴⁷

^1H NMR (500 MHz, CDCl_3) δ_{H} 7.42-7.34 (m, 7H, Ar), 7.31-7.22 (m, 3H, Ar), 5.25 (s, 2H, CH_2Ph), 4.62-4.48 (m, 1H, NH), 4.01-3.94 (m, 2H, CH_2 Gly).

[17s] Phenyl-(benzyloxy-L-alaniny)dichlorophosphate

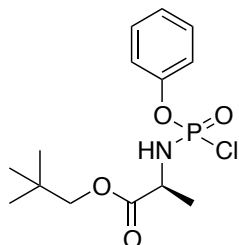


Prepared according to the general procedure C using L-alanine benzyl ester hydrochloride salt (1.12 g, 5.20 mmol), phenyl dichlorophosphate (1.10 g, 5.20 mmol) and Et_3N (1.45 mL, 10.40 mmol) in CH_2Cl_2 (20 mL). The product was obtained as a clear oil (1.51 g, 82%).

^{31}P NMR (202 MHz, CDCl_3) δ_{P} 7.51, 7.85. [Lit. ^{31}P NMR (202 MHz, CDCl_3) δ_{P} 7.86, 7.52].¹⁴⁷

^1H NMR (500 MHz, CDCl_3) δ_{H} 7.36-7.25 (m, 10 H, Ar), 5.15 (s, 1H, CH_2Ph), 5.11 (s, 1H, CH_2Ph), 4.25-4.14 (m, 2H, NH, CHCH_3 L-Ala), 1.59-1.57 (m, 3H, CHCH_3 L-Ala).

[17t] Phenyl-(neopentyloxy-L-alaninyl)dichlorophosphate

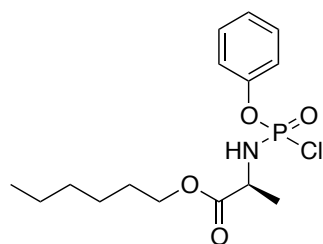


Prepared according to the general procedure C using L-alanine neopentyl ester hydrochloride salt (1.20 g, 6.12 mmol), phenyl dichlorophosphate (1.29 mL, 6.12 mmol) and Et_3N (1.71 mL, 12.24 mmol) in CH_2Cl_2 (25 mL). The product was obtained as a clear oil (1.61 g, 79%).

^{31}P NMR (202 MHz, CDCl_3) δ_{P} 7.51, 7.85.

^1H NMR (500 MHz, CDCl_3) δ_{H} 7.16-7.22 (m, 5H, Ar), 4.26-4.21 (m, 1H, NH), 4.20-4.15 (m, 1H, CHCH_3 L-Ala), 3.90-3.93 (m, 2H, $\text{CH}_2\text{C}(\text{CH}_3)_3$ Neop), 1.59-1.52 (m, 3H, CHCH_3 L-Ala), 1.34-1.01 (m, 9H, $\text{CH}_2\text{C}(\text{CH}_3)_3$ Neop).

[17u] Phenyl-(hexyl-1-oxy-L-alaninyl)dichlorophosphate

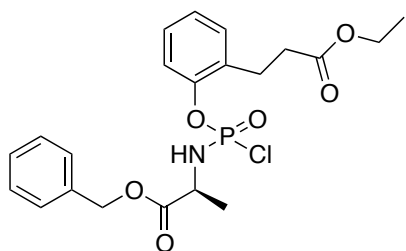


Prepared according to the general procedure C using L-alanine hex-1-yl ester hydrochloride salt (1.55 g, 7.40 mmol), phenyl dichlorophosphate (1.93 g, 7.40 mmol) and Et_3N (2.06 mL, 14.80 mmol) in CH_2Cl_2 (30 mL). The product was obtained as a clear oil (2.11 g, 82%).¹⁵¹

^{31}P NMR (202 MHz, CDCl_3) δ_{P} 7.96, 7.64.

^1H NMR (500 MHz, CDCl_3) δ_{H} 7.24-7.18 (m, 5H, Ar), 4.34-4.20 (m, 1H, NH), 4.20-4.05 (m, 3H, CHCH_3 L-Ala, $\text{CH}_2\text{CH}_2\text{CH}_2\text{CH}_2\text{CH}_2\text{CH}_3$ n-Hex), 4.03-3.94 (m, 2H, $\text{CH}_2\text{CH}_2\text{CH}_2\text{CH}_2\text{CH}_2\text{CH}_3$ n-Hex), 1.66-1.56 (m, 2H, m, $\text{CH}_2\text{CH}_2\text{CH}_2\text{CH}_2\text{CH}_2\text{CH}_3$ n-Hex), 1.59-1.53 (m, 3H, CHCH_3 L-Ala), 1.37-1.31 (m, 4H, m, $\text{CH}_2\text{CH}_2\text{CH}_2\text{CH}_2\text{CH}_2\text{CH}_3$ n-Hex), 0.94-0.87 (m, 3H, m, 1H, $\text{CH}_2\text{CH}_2\text{CH}_2\text{CH}_2\text{CH}_2\text{CH}_3$ n-Hex).

[17v] Ethyl 3-(2-hydroxyphenyl)propanoyl-(benzyloxy-L-alaninyl)dichlorophosphate



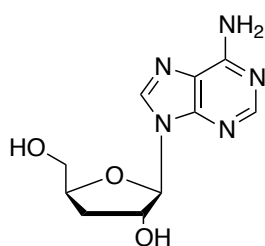
Prepared according to the general procedure C using L-alanine-O-benzyl ester hydrochloric salt (1.70 g, 7.88 mmol), ethyl 3-(2-hydroxyphenyl)propanoyl dichlorophosphate [14c] (2.45 g, 7.88 mmol) and Et_3N (2.20 mL, 15.76 mmol) in CH_2Cl_2 (35 mL). The product was obtained as a clear oil (3.29 g, 92%).¹⁵⁰

^{31}P NMR (202 MHz, CDCl_3) δ_{P} 7.53, 7.70.

¹H NMR (500 MHz, CDCl₃) δ_{H} 7.50-7.44 (m, 1H, Ar), 7.41-7.32 (m, 5H, Ar), 7.28-7.14 (m, 3H, Ar), 5.26-5.17 (m, 2H, CH₂Ph), 4.67-4.56 (m, 1H, NH), 4.34-4.22 (m, 1H, CHCH₃ L-Ala), 4.15-4.09 (m, 2H, CH₂CH₂CO₂CH₂CH₃), 3.15-2.93 (m, 2H, CH₂CH₂CO₂CH₂CH₃), 2.66-2.59 (m, 2H, CH₂CH₂CO₂CH₂CH₃), 1.58-1.52 (m, 3H, CHCH₃ L-Ala), 1.24-1.20 (m, 3H, CH₂CH₂CO₂CH₂CH₃).

9.5.5 Synthesis of 3'-deoxyadenosine

[21] 3'-Deoxyadenosine



3'-Deoxyadenosine was synthesised according to standard procedure **E** using 9-(2,3-anhydro- β -D-ribofuranosyl) adenine [26] (9.12 g, 36.59 mmol), LiEt₃BH (1M in THF, 109.77 mmol followed by a second addition of 36.59 mmol) in DMSO (55 mL) and THF (550 mL). The title compound was obtained as a white solid (9.01 g, 98%).

Melting point: 188-190 °C (Lit. mp: 191-192 °C).²¹²

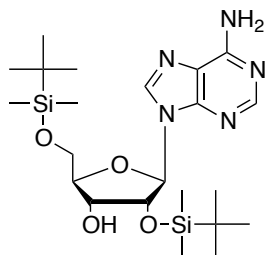
¹H NMR (500 MHz, DMSO-*d*₆) δ_{H} 8.37 (s, 1H, H8), 8.17 (s, 1H, H2), 7.29 (br s, 2H, NH₂), 5.89 (d, *J* = 2.5 Hz, 1H, H1'), 5.68 (d, *J* = 4.5 Hz, 1H, OH-2'), 5.19 (t, *J* = 6.0 Hz, 1H, OH-5'), 4.63-4.58 (m, 1H, H2'), 4.40-4.34 (m, 1H, H4'), 3.71 (ddd, *J* = 12.0, 6.0, 3.0 Hz, 1H, H5'), 3.53-3.49 (ddd, *J* = 12.0, 6.0, 4.0 Hz, 1H, H5').

¹³C NMR (125 MHz, DMSO-*d*₆) δ_{C} 156.00 (C6), 152.41 (C2), 148.82 (C4), 139.09 (C8), 119.06 (C5), 90.79 (C1'), 80.66 (C4'), 74.56 (C2'), 62.61 (C5'), 34.02 (C3').

MS (ES⁺) *m/z* found 258.12 [M+Li⁺], 274.09 [M+Na⁺], 252.11 [M+H⁺] C₁₀H₁₃N₅O₃ required *m/z* 251.24 [M].

HPLC Reverse-phase HPLC eluting with H₂O/CH₃CN from 100/0 to 75/25 in 30 minutes, 1ml/min, λ = 254 nm, showed one peak with tR 11.22 min.

[23] 2',5'-(Bis-*O*-*tert*-butyldimethylsilyl)adenosine

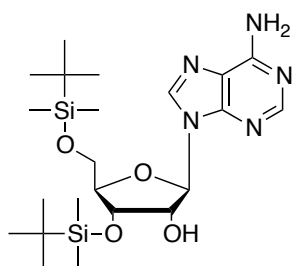


Adenosine (1 g, 3.74 mmol) was dissolved in a mixture of THF and DMF (1:1, 100 mL) and pyridine was added (1.51 mL, 18.71 mmol), followed by AgNO₃ (1.90 g, 11.22 mmol). After 15 minutes, TBDMSCl (1.24 g, 8.23 mmol) was finally added to the reaction mixture and the solution was stirred at 30 °C for 2 hours. The solvent was evaporated *in vacuo* and the residue was dissolved in

CH₂Cl₂ (50 mL) and washed with brine (50 mL). The organic phase was dried over NaSO₄, filtered and evaporated. The crude was purified by column chromatography nHex/EtOac=5/5 to 2/8 to give the title compound as a white foam (0.28 g, 15%).²⁰⁸

¹H NMR (500 MHz, DMSO-*d*6) δ_H 8.28 (s, 1H, H8), 8.14 (s, 1H, H2), 7.30 (br s, 2H, NH₂), 5.94 (d, *J* = 5.5 Hz, 1H, H1'), 5.15 (br s, 1H, OH-3'), 4.62 (t, *J* = 5.0 Hz, H2'), 4.17-4.13 (m, 1H, H4'), 3.92 (dd, *J* = 11.5, 4.0 Hz, 1H, H5'), 3.79 (dd, *J* = 11.5, 4.0 Hz, 1H, H5'), 0.90 (s, 9H, (CH₃)₃ *t*Bu), 0.74 (s, 9H, (CH₃)₃ *t*Bu), 0.09 (s, 3H, CH₃), 0.08 (s, 3H, CH₃), 0.06 (s, 3H, CH₃), -0.15 (s, 3H, CH₃).

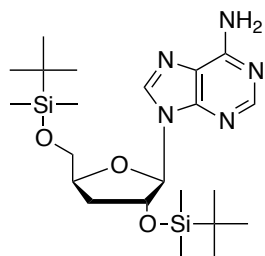
(ES⁺) m/z found 518.27 [M+Na⁺], 496.29 [M+H⁺] C₂₂H₄₁N₅NaO₄Si₂ required m/z 495.76 [M].



3',5'-*O*-*tert*-butyldimethylsilyladenine was isolated through the same reaction procedure (0.06 g, 3%), as a more hydrophilic regioisomer.

¹H NMR (500 MHz, DMSO-*d*6) δ_H 8.31 (s, 1H, H8), 8.14 (s, 1H, H2), 7.27 (br s, 2H, NH₂), 5.90 (d, *J* = 6.0 Hz, 1H, H1'), 5.41 (d, *J* = 6.5 Hz, 1H, OH-2'), 4.80-4.74 (m, 1H, H2'), 4.36 (dd, *J* = 5.0 Hz, 3.5 Hz, 1H, H3'), 3.98-3.94 (m, 1H, H4'), 3.88 (dd, *J* = 11.5, 6.0 Hz, 1H, H5'), 3.69 (dd, *J* = 11.0, 4.0 Hz, 1H, H5'), 0.92 (s, 9H, *t*Bu), 0.87 (s, 9H, *t*Bu), 0.134 (s, 3H, CH₃), 0.131 (s, 3H, CH₃), 0.05 (s, 3H, CH₃), 0.04 (s, 3H, CH₃).

[25] 2',5'-(Bis-*O*-*tert*-butyldimethylsilyl)3'-deoxyadenosine

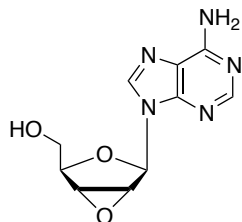


3'-Deoxyadenosine (1.00 g, 3.98 mmol) was dissolved in anhydrous pyridine (10 mL) and TBDMSCl (1.2 g, 7.96 mmol) was added to the flask. The reaction was stirred under argon atmosphere at room temperature for 16 hours. The reaction mixture was diluted with CHCl₃ (20 mL) and the organics were washed with NH₄Cl (saturated solution, 20 mL x 3). The organics were dried over Na₂SO₄, filtered, evaporated and the crude was purified by flash column chromatography to afford the product as a sticky solid (0.89 g, 50 %).²⁰⁸

[Alternative procedure] 3'-Deoxyadenosine (1.13 g, 4.5 mmol), was dissolved in DMF (50 mL) and TBDMSCl (2.03 g, 13.5 mmol) and imidazole (1.84 g, 27 mmol) were added to the flask. The mixture was stirred for 16 hours at rt. The reaction mixture was diluted with CHCl₃ (20 mL) and the organics were washed with NH₄Cl (saturated solution, 20 mL x 3). The organics were dried over Na₂SO₄, filtered and evaporated to afford the product as a sticky solid (1.56 g, 72%).

¹H NMR (500 MHz, CDCl₃) δ_{H} 8.36 (s, 1H, H8), 8.34 (s, 1H, H2), 6.03 (d, $J = 1.2$ Hz, 1H, H1'), 5.54 (br s, 2H, NH₂), 4.66-4.63 (m, 1H, H2'), 4.61-4.55 (m, 1H, H4'), 4.14 (dd, $J = 11.7, 2.7$ Hz, 1H, H5'), 3.80 (dd, $J = 11.7, 2.7$ Hz, 1H, H5'), 2.32-2.25 (m, 1H, H3'), 1.91-1.85 (m, 1H, H3'), 0.97 (s, 9H, *t*Bu), 0.92 (s, 9H, *t*Bu), 0.17 (s, 3H, CH₃), 0.16 (s, 3H, CH₃), 0.15 (s, 3H, CH₃), 0.10 (s, 3H, CH₃).

[26] 9-(2,3-Anhydro- β -D-ribofuranosyl) adenine



The title compound was synthesised according to standard procedure **D** using adenosine (10.00 g, 37.42 mmol), α -AIBr (22.03 mL, 149.68 mmol) and H₂O (0.67 mL, 0.037 mmol), in CH₃CN (250 mL). The crude was then dissolved in CH₃OH (260 mL) and stirred with Amberlite (2 x OH⁻, 150 mL) for 16 hours. The title compound was obtained as a white powder (8.86 g, 95%).

Melting point 178-180 °C (Lit. mp: 180-181 °C).²¹²

¹H NMR (500 MHz, DMSO-*d*6) δ_{H} 8.33 (s, 1H, H2), 8.18 (s, 1H, H8), 7.29 (br s, 2H, NH₂), 6.21 (s, 1H, H1'), 5.05 (br s, 1H, OH-5'), 4.46 (d, $J = 2.6$ Hz, 1H, H2'), 4.22 (d, $J = 2.6$ Hz, 1H, H3'), 4.18 (t, $J = 5.2$ Hz, 1H, H4'), 3.60-3.55 (m, 1H, H5'), 3.53-3.49 (m, 1H, H5').

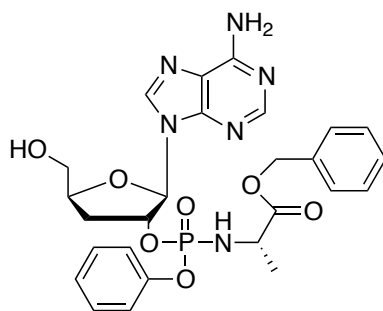
¹³C NMR (125 MHz, DMSO-*d*6) δ_{C} 156.01 (C6), 152.61 (C2), 149.11 (C4), 139.55 (C8), 119.52 (C5), 91.25 (C1'), 81.15 (C4'), 75.06 (C2'), 58.75 (C3'), 57.70 (C5').

HPLC Reverse-phase HPLC eluting with H₂O/CH₃CN from 100/0 to 75/25 in 30 minutes, F = 1ml/min, $\lambda = 254$ nm, showed one peak with t_R 13.20 min.

(ES⁺) m/z found 272.09 [M+Na⁺], 250.09 [M+H⁺] C₁₀H₁₃N₅O₃ required m/z 249.23 [M].

9.5.6 Synthesis of 3'-deoxyadenosine prodrugs

[28a] 3'-Deoxyadenosine-2'-*O*-phenyl-(benzyloxy-L-alaninyl)-phosphate



Prepared according to general procedure **F₁** using 3'-deoxyadenosine (0.05 g, 0.20 mmol) in THF (4 mL), *t*BuMgCl (1.0 M solution in THF, 0.22 mL, 0.22 mmol), phenyl(benzyloxy-L-alaninyl) phosphorochloridate [**17s**] (0.21 g, 0.60 mmol) in THF (2.4 mL). Purification by column chromatography (eluent system CH₃OH/CH₂Cl₂

0/100 to 8/92) and preparative TLC (500 μ M, eluent system CH₃OH/CH₂Cl₂ = 5/95) afforded the compound as a white solid (0.006 g, 5%).

³¹P NMR (202 MHz, CD₃OD) δ_P 2.44, 2.92.

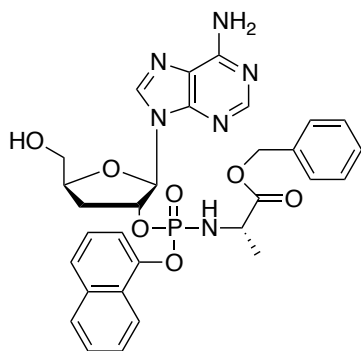
¹H NMR (500 MHz, CD₃OD): δ_H 8.41 (s, 0.5 H, H8), 8.28 (s, 0.5 H, H8), 8.19 (s, 0.5H, H2), 8.18 (s, 0.5H, H2), 7.39-7.30 (m, 4H, Ar), 7.28-7.18 (m, 4H, Ar), 7.17-7.11 (m, 1H, Ar), 7.08-7.03 (m, 1H, Ar), 6.23 (d, J = 2.0 Hz, 0.5H, H1'), 6.08 (d, J = 3.4 Hz, 0.5H, H1'), 5.52-5.43 (m, 1H, H2'), 5.19-5.12 (m, 1H, CH₂Ph), 5.07-4.95 (m, 1H, CH₂Ph), 4.48-4.42 (m, 1H, H4'), 4.05-3.97 (m, 1H, CHCH₃ L-Ala), 3.95-3.87 (m, 1H, H5'), 3.69-3.61 (m, 1H, H5'), 2.59-2.45 (m, 1H, H3'), 2.31-2.23 (m, 1H, H3'), 1.36-1.27 (m, 3H, CHCH₃ L-Ala).

¹³C NMR (125 MHz, CD₃OH) δ_C 174.76 (d, ³ J_{C-P} = 5.0 Hz, C=O), 174.52 (d, ³ J_{C-P} = 5.0 Hz, C=O), 157.44 (C6), 153.76 (C2), 151.93 (C4), 150.06 (C-Ar), 149.93 (C-Ar), 141.38 (C8), 141.18 (C8), 137.33 (C-Ar), 137.10 (C-Ar), 130.69 (CH-Ar), 130.79 (CH-Ar), 129.61 (CH-Ar), 129.51 (CH-Ar), 129.40 (CH-Ar), 129.30 (CH-Ar), 129.23 (CH-Ar), 126.33 (CH-Ar), 126.16 (CH-Ar), 121.53 (d, ³ J_{C-P} = 4.5 Hz, CH-Ar), 121.20 (d, ³ J_{C-P} = 4.5 Hz, CH-Ar), 120.76 (C5), 91.56 (d, ³ J_{C-P} = 7.7 Hz, C1'), 91.45 (d, ³ J_{C-P} = 7.7 Hz, C1'), 82.78 (C4'), 82.28 (C4'), 80.98 (d, ² J_{C-P} = 4.7 Hz, C2'), 80.95 (d, ² J_{C-P} = 4.7 Hz, C2'), 67.95 (CH₂Ph), 67.92 (CH₂Ph), 64.13 (C5'), 63.59 (C5'), 51.88 (CHCH₃ L-Ala), 51.75 (CHCH₃ L-Ala), 33.75 (d, ³ J_{C-P} = 3.0 Hz, C3'), 33.59 (d, ³ J_{C-P} = 3.0 Hz, C3'), 20.33 (d, ³ J_{C-P} = 7.1, CHCH₃ L-Ala), 20.18 (d, ³ J_{C-P} = 7.1, CHCH₃ L-Ala).

HPLC Reverse-phase HPLC eluting with H₂O/CH₃OH from 90/10 to 0/100 in 30 minutes, F = 1 mL/min, λ = 254 nm, showed two peaks of the diastereoisomers with tR 22.16 min and tR 22.43 min.

(ES+) m/z found: 569.2 [M+H⁺], 591.2 [M+Na⁺], 1159.4 [2M+Na⁺] C₂₆H₂₉N₆O₇P required m/z 568.2 [M].

[28b] 3'-Deoxyadenosine 2'-O-naphth-1-yl-(benzyloxy-L-alaninyl)-phosphate



Prepared according to general procedure F₁ using 3'-deoxyadenosine (0.05 g, 0.20 mmol) in THF (4 mL), *t*BuMgCl (1.0 M solution in THF, 0.22 mL, 0.22 mmol), 1-naphth-1-yl(benzyloxy-L-alaninyl) phosphorochloridate [17a] (0.32 g, 0.80 mmol) in THF (3.2 mL). Purification by column chromatography (eluent system CH₃OH/CH₂Cl₂ 0/100 to 6/94) and preparative TLC (500 μ M, eluent system

CH₃OH/CH₂Cl₂ 5/95) afforded the compound as a white solid (0.014 g, 11 %).

^{31}P NMR (202 MHz, CD_3OD) δ_{P} 3.27, 2.75.

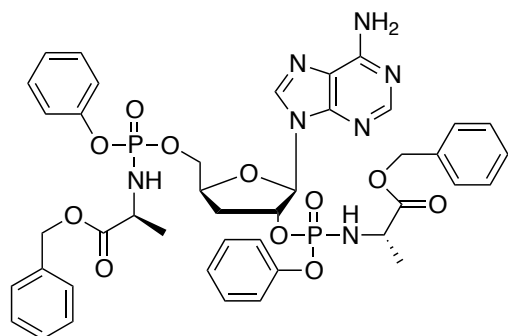
^1H NMR (500 MHz, CD_3OD) δ_{H} 8.37 (s, 0.5H, H8), 8.18 (s, 0.5H, H8), 8.14 (s, 0.5H, H2), 8.13-8.11 (m, 0.5H, Ar) 8.11 (s, 0.5H, H2), 7.94-7.90 (m, 0.5H, Ar), 7.90-7.87 (m, 0.5H, Ar), 7.86-7.82 (m, 0.5H, Ar), 7.74-7.70 (m, 0.5H, Ar), 7.66-7.61 (m, 0.5H, Ar), 7.57-7.47 (m, 1.5H, Ar), 7.46-7.37 (m, 2.5H, Ar), 7.34-7.27 (m, 4H, Ar), 7.25-7.17 (m, 1H, Ar), 6.19 (d, $J = 2.4$ Hz, 0.5H, H1'), 6.04 (d, $J = 2.4$ Hz, 0.5H, H1'), 5.60-5.54 (m, 0.5H, H2'), 5.50-5.42 (m, 0.5H, H2'), 5.16-4.99 (m, 2H, CH_2Ph), 4.46-4.40 (m, 0.5H, H4'), 4.36-4.30 (m, 0.5H, H4'), 4.13-4.04 (m, 1H, CHCH_3 L-Ala), 3.90-3.83 (m, 1H, H5'), 3.64-3.56 (m, 1H, H5'), 2.61-2.54 (m, 0.5H, H3'), 2.49-2.41 (m, 0.5H, H3'), 2.35-2.27 (m, 0.5H, H3'), 2.22-2.16 (m, 0.5H, H3'), 1.35-1.24 (m, 3H, CHCH_3 L-Ala).

^{13}C NMR (125 MHz, CD_3OD) δ_{C} 174.52 (C=O), 174.49 (C=O), 157.27 (C6), 153.58 (C2), 149.97 (C4), 149.93 (C-4), 147.70 (d, $^3J_{\text{C-P}} = 7.5$ Hz, C-Ar), 147.48 (d, $^3J_{\text{C-P}} = 7.5$ Hz, C-Ar), 141.36 (C8), 141.19 (C8), 137.25 (C-Ar), 137.05 (C-Ar), 136.31 (C-Ar), 136.20 (C-Ar), 129.58 (CH-Ar), 129.48 (CH-Ar), 129.37 (CH-Ar), 129.26 (CH-Ar), 129.22 (CH-Ar), 128.88 (CH-Ar), 127.84 (CH-Ar), 127.75 (CH-Ar), 127.49 (CH-Ar), 127.44 (CH-Ar), 126.48 (CH-Ar), 126.39 (CH-Ar), 126.26 (CH-Ar), 126.05 (CH-Ar), 122.76 (CH-Ar), 122.38 (CH-Ar), 120.68 (C5), 120.61 (C5), 116.64 (d, $^3J_{\text{C-P}} = 3.75$ Hz, CH-Ar), 116.13 (d, $^3J_{\text{C-P}} = 3.75$, CH-Ar), 91.60 (d, $^3J_{\text{C-P}} = 7.5$ Hz, C1'), 91.43 (d, $^3J_{\text{C-P}} = 7.5$ Hz, C1'), 82.74 (C4'), 82.27 (C4'), 81.99 (d, $^2J_{\text{C-P}} = 5.5$ Hz, C2'), 81.12 (d, $^2J_{\text{C-P}} = 5.5$ Hz, C2'), 67.97 (CH_2Ph), 67.94 (CH_2Ph), 64.16 (C5'), 63.51 (C5'), 51.96 (CHCH_3 L-Ala), 51.89 (CHCH_3 L-Ala), 33.89 (d, $^3J_{\text{C-P}} = 7.5$ Hz, CHCH_3 L-Ala), 33.63 (d, $^3J_{\text{C-P}} = 7.5$ Hz, CHCH_3 L-Ala).

HPLC Reverse-phase HPLC eluting with $\text{H}_2\text{O}/\text{CH}_3\text{OH}$ from 100/10 to 0/100 in 30 minutes, $F = 1\text{ml}/\text{min}$, $\lambda = 200\text{ nm}$, showed two peaks of the diastereoisomers with $t_{\text{R}} 24.84\text{ min}$ and $t_{\text{R}} 25.43\text{ min}$.

(ES^+) m/z , found 619.2 [$\text{M}+\text{H}^+$], 641.2 [$\text{M}+\text{Na}^+$], 1259.4 [$2\text{M}+\text{Na}^+$], $\text{C}_{30}\text{H}_{31}\text{N}_6\text{O}_7\text{P}$ required $m/z 618.20$ [M].

[29a] 3'-Deoxyadenosine 2',5'-bis-*O*-phenyl-(benzyloxy-L-alaninyl)-phosphate



Isolated from reaction used for the synthesis of 3'-deoxyadenosine-2'-*O*-phenyl-(benzyloxy-L-alaninyl)-phosphate [28a] (0.019 g, 11%).

^{31}P NMR (202 MHz, CD_3OD) δ_{P} 3.98, 3.88, 3.59, 3.12, 3.05, 2.45, 2.32.

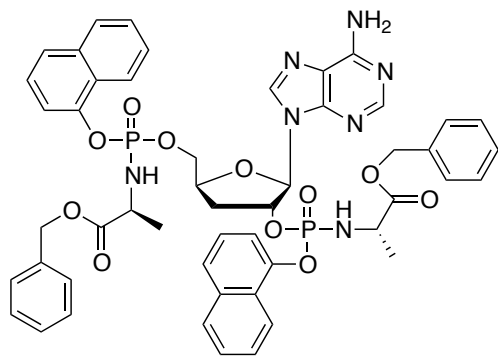
^1H NMR (500 MHz, CD_3OD) δ_{H} 8.24-8.13 (m,

2H, H8, H2), 7.39-7.08 (m, 20H, Ph), 6.27-6.23 (m, 0.5H, H1'), 6.16-6.13 (m, 0.5H, H1'), 5.61-5.48 (m, 1H, H2'), 5.17-4.91 (m, 4H, CH₂Ph x 2), 4.57-4.49 (m, 1H, H4'), 4.41-4.29 (m, 1H, H5'), 4.25-4.15 (m, 1H, H5'), 4.10-4.01 (m, 1H, CHCH₃ L-Ala), 3.99-3.89 (m, 1H, CHCH₃ L-Ala), 2.57-2.41 (m, 1H, H3'), 2.28-2.17 (m, 1H, H3'), 1.38-1.23 (m, 6H, CHCH₃ L-Ala x 2).

¹³C NMR (125 MHz, CD₃OD) δ_C 174.88 (C=O), 174.83 (C=O), 174.79 (C=O), 174.73 (C=O), 174.61 (C=O), 174.57 (C=O), 174.53 (C=O), 157.36 (C6), 157.34 (C6), 157.32(C6), 157.29 (C6), 154.04 (C2), 154.01 (C2), 153.97 (C2), 153.94 (C2), 152.09 (C4), 152.04 (C4), 152.02 (C4), 151.97 (C4), 150.31 (C-Ar), 150.29 (C-Ar), 150.16 (C-Ar), 140.98 (C8), 140.91 (C8), 140.81 (C8), 137.31 (C-Ar), 137.28 (C-Ar), 137.22 (C-Ar), 137.09 (C-Ar), 130.86 (CH-Ar), 130.78 (CH-Ar), 130.77 (CH-Ar), 129.65 (CH-Ar), 129.61 (CH-Ar), 129.58 (CH-Ar), 129.55 (CH-Ar), 129.44 (CH-Ar), 129.42 (CH-Ar), 129.38 (CH-Ar), 129.34 (CH-Ar), 129.32 (CH-Ar), 129.30 (CH-Ar), 129.28 (CH-Ar), 129.23 (CH-Ar), 129.21 (CH-Ar), 12.42 (CH-Ar), 126.23 (CH-Ar), 126.20 (CH-Ar), 126.17 (CH-Ar), 121.65 (CH-Ar), 121.63 (CH-Ar), 121.61 (CH-Ar), 121.59 (CH-Ar), 121.52 (CH-Ar), 121.50 (CH-Ar), 121.47 (CH-Ar), 121.46 (CH-Ar), 121.40 (CH-Ar), 121.39 (CH-Ar), 121.36 (CH-Ar), 121.35 (CH-Ar), 121.30 (CH-Ar), 121.28 (CH-Ar), 121.26 (CH-Ar), 121.24 (CH-Ar), 120.61 (C5), 120.57 (C5), 120.56 (C5), 120.54 (C5), 91.56 (C1'), 91.51 (C1'), 91.45 (C1'), 91.25 (C1'), 91.20 (C1'), 81.84 (C2'), 81.82 (C2'), 81.79 (C2'), 81.27 (C2'), 81.22 (C2'), 81.18 (C2'), 80.49 (C4'), 80.43 (C4'), 80.06 (C4'), 79.99 (C4'), 68.29 (C5', CH₂Ph), 68.25 (C5', CH₂Ph), 68.00 (C5', CH₂Ph), 67.96 (C5', CH₂Ph), 67.94 (C5', CH₂Ph), 67.90 (C5', CH₂Ph), 67.71 (C5', CH₂Ph), 67.67 (C5', CH₂Ph), 51.91 (CHCH₃ L-Ala), 51.74 (CHCH₃ L-Ala), 51.70 (CHCH₃ L-Ala), 51.59 (CHCH₃ L-Ala), 34.22 (C3'), 34.20 (C3'), 34.16 (C3'), 33.97 (C3'), 33.94 (C3'), 33.91 (C3'), 20.44 (CHCH₃ L-Ala), 20.43 (CHCH₃ L-Ala), 20.39 (CHCH₃ L-Ala), 20.29 (CHCH₃ L-Ala), 20.27 (CHCH₃ L-Ala), 20.24 (CHCH₃ L-Ala), 20.21 (CHCH₃ L-Ala), 20.19 (CHCH₃ L-Ala).

HPLC Reverse-phase HPLC eluting with H₂O/CH₃CN from 100/10 to 0/100 in 30 minutes, F = 1ml/min, λ = 254 nm, showed one broad peak with tR 15.97 min.

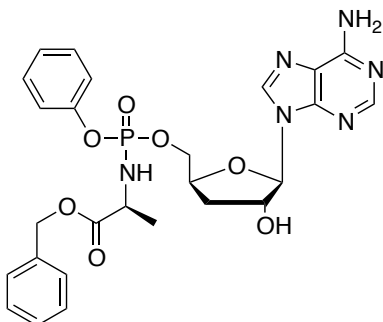
(ES⁺) m/z, found 886.3 [M+H⁺], 1771.6 [2M+H⁺] C₄₂H₄₅N₇O₁₁P₂ required m/z 885.3 [M].

[29b] 3'-Deoxyadenosine 2',5'-bis-O-naphth-1-yl-(benzyloxy-L-alaninyl)-phosphate

Isolated from reaction used for the synthesis of 3'-deoxyadenosine-2'-*O*-naphth-1-yl-(benzyloxy-L-alaninyl)-phosphate [28b] as a white solid (0.069 g, 35%).

^{31}P NMR (202 MHz, CD_3OD) δ_{P} 4.23, 4.18, 3.97, 3.94, 3.48, 3.39, 2.78, 2.77.

^1H NMR (500 MHz, CD_3OD) δ_{H} 8.18-8.05 (m, 3H, H8, H2, Ar), 8.03-7.81 (m, 3H, Ar), 7.74-7.62 (m, 2H, Ar), 7.54-7.39 (m, 7H, Ar), 7.37-7.16 (m, 11H, Ar), 6.22-6.18 (m, 0.5H, H1'), 6.05-6.02 (m, 0.5H, H1'), 5.67-5.54 (m, 1H, H2'), 5.15-4.96 (m, 4H, CH_2Ph x 2), 4.50-4.42 (m, 1H, H4'), 4.39-4.31 (m, 1H, H5'), 4.24-4.16 (m, 1H, H5'), 4.15-4.08 (m, 1H, CHCH_3 L-Ala), 4.04-3.91 (m, 1H, CHCH_3 L-Ala), 3.60-2.41 (m, 1H, H3'), 2.29-2.09 (m, 1H, H3'), 1.37-1.27 (m, 6H, CHCH_3 L-Ala x 2).

[30a] 3'-Deoxyadenosine 5'-*O*-phenyl-(benzyloxy-L-alaninyl)-phosphate

Prepared according to general procedure **F**₂ using 3'-deoxyadenosine (0.05 g, 0.20 mmol) in anhydrous THF (4 mL), *N*-methylimidazole (80 μL , 1.0 mmol), phenyl(benzyloxy-L-alaninyl) phosphorochloridate [17s] (0.021 g, 0.6 mmol) in THF (2.4 mL) Purification by Biotage Isolera One (cartridge SNAP 25g, 25 mL/min, $\text{CH}_3\text{OH}/\text{CH}_2\text{Cl}_2$ 1-8% 10 CV, 8% 5 CV) and preparative

TLC (1000 μM , eluent system $\text{CH}_3\text{OH}/\text{CH}_2\text{Cl}_2$ 5/95) afforded the title compound as a white solid (0.032 g, 28%).

^{31}P NMR (202 MHz, CD_3OD) δ_{P} 3.91, 3.73.

^1H NMR (500 MHz, CDCl_3) δ_{H} 8.26 (s, 0.5H, H8), 8.24 (s, 0.5H, H8), 8.22 (s, 0.5H, H2), 8.21 (s, 0.5H, H2), 7.34-7.25 (m, 7H, Ar), 7.21-7.13 (m, 3H, Ar), 6.01 (d, $J = 1.5$ Hz, 0.5H, H1'), 6.00 (d, $J = 1.5$ Hz, 0.5H, H1'), 5.15-5.04 (m, 2H, CH_2Ph), 4.73-4.63 (m, 2H, H2', H4'), 4.43-4.35 (m, 1H, H5'), 4.27-4.20 (m, 1H, H5'), 4.03-3.91 (m, 1H, CHCH_3 L-Ala), 2.35-2.28 (m, 1H, H3'), 2.09-2.02 (m, 1H, H3'), 1.32 (d, $J = 7.4$ Hz, 1.5 H, CHCH_3 L-Ala), 1.28 (d, $J = 7.4$ Hz, 1.5 H, CHCH_3 L-Ala).

^{13}C NMR (125 MHz, CD_3OD) δ_{C} 174.84 (d, $^3J_{\text{C-P}} = 4.5$ Hz, C=O), 174.63 (d, $^3J_{\text{C-P}} = 4.5$ Hz, C=O), 157.32 (C6), 157.31 (C6), 153.86 (C2), 153.84 (C2), 152.13 (C4), 152.07 (C4), 150.20 (C-Ar), 150.18 (C-Ar), 140.47 (C8), 137.26 (C-Ar), 137.19 (C-Ar), 130.76 (CH-

Ar), 130.74 (CH-Ar), 129.57 (CH-Ar), 129.32 (CH-Ar), 129.31 (CH-Ar), 129.29 (CH-Ar), 129.26 (CH-Ar), 126.16 (CH-Ar), 126.14 (CH-Ar), 121.46 (d, $^3J_{C-P} = 4.7$ Hz, CH-Ar), 121.38 (d, $^3J_{C-P} = 4.7$ Hz, CH-Ar) 120.54 (C5), 120.53 (C5), 93.24 (C1'), 93.18 (C1'), 80.43 (d, $^3J_{C-P} = 3.6$ Hz, C4'), 80.36 (d, $^3J_{C-P} = 3.6$ Hz, C4'), 76.62 (C2'), 68.62 (d, $^2J_{C-P} = 5.3$ Hz, C5'), 68.30 (d, $^2J_{C-P} = 5.3$ Hz, C5'), 67.95 (CH₂Ph), 67.92 (CH₂Ph), 51.74 (CHCH₃ L-Ala), 51.60 (CHCH₃ L-Ala), 34.91 (C3'), 34.70 (C3'), 20.45 (d, $^3J_{C-P} = 7.0$ Hz, CHCH₃ L-Ala), 20.28 (d, $^3J_{C-P} = 7.0$ Hz, CHCH₃ L-Ala).

HPLC Reverse-phase HPLC eluting with H₂O/CH₃CN from 100/10 to 0/100 in 30 minutes, F = 1 mL/min, $\lambda = 200$ nm, showed two peaks of the diastereoisomers with tR 14.02 min. and tR 14.26 min.

MS (ES⁺) m/z found 569.2 [M+H⁺], 591.2 [M+Na⁺], 1159.4 [2M+Na⁺] C₂₆H₂₉N₆O₇P required m/z 568.2 [M].

The two diastereoisomers were separated via Biotage Isolera One (cartridge SNAP-Ultra C18 12 g, F: 12 mL/min, isocratic eluent system: H₂O/CH₃OH 45% in 30 min, 50 mg sample).

Fast eluting isomer:

³¹P NMR (202 MHz, CD₃OD) δ_P 3.91.

¹H NMR (500 MHz, CDCl₃) δ_H 8.26 (s, 1H, H8), 8.22 (s, 1H, H2), 7.37-7.25 (m, 7H, Ar), 7.22-7.12 (m, 3H, Ar), 6.01 (d, $J = 1.5$ Hz, 1H, H1'), 5.12 (AB q, $J_{AB} = 12.0$ Hz, $\Delta\delta_{AB} = 0.04$, 2H, CH₂Ph), 4.74-4.70 (m, 1H, H2'), 4.69-4.62 (m, 1H, H4'), 4.44-4.38 (m, 1H, H5'), 4.28-4.21 (m, 1H, H5'), 3.99-3.90 (m, 1H, CHCH₃ L-Ala), 2.35-2.27 (m, 1H, H3'), 2.09-2.02 (m, 1H, H3'), 1.29 (d, $J = 7.0$ Hz, 3H, CHCH₃ L-Ala).

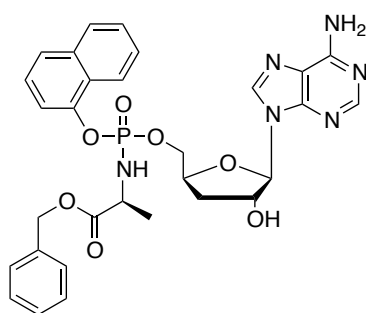
HPLC Reverse-phase HPLC eluting with H₂O/CH₃CN from 100/10 to 0/100 in 30 minutes, F: 1 mL/min, $\lambda = 200$ nm, showed one peak with tR 14.02 min.

Slow eluting isomer:

³¹P NMR (202 MHz, CD₃OD) δ_P 3.73.

¹H NMR (500 MHz, CDCl₃) δ_H 8.24 (s, 1H, H8), 8.22 (s, 1H, H2), 7.36-7.26 (m, 7H, Ar), 7.22-7.13 (m, 3H, Ar), 6.01 (d, $J = 1.5$ Hz, 1H, H1'), 5.08 (AB q, $J_{AB} = 12.0$ Hz, $\Delta\delta_{AB} = 0.01$, 2H, CH₂Ph), 4.70-4.67 (m, 1H, H2'), 4.66-4.60 (m, 1H, H4'), 4.41-4.35 (m, 1H, H5'), 4.26-4.19 (m, 1H, H5'), 4.02-3.94 (m, 1H, CHCH₃ L-Ala), 2.36-2.27 (m, 1H, H3'), 2.08-2.01 (m, 1H, H3'), 1.34-1.30 (m, 3H, CHCH₃ L-Ala).

HPLC Reverse-phase HPLC eluting with H₂O/CH₃CN from 100/10 to 0/100 in 30 minutes, F: 1 mL/min, $\lambda = 200$ nm, showed one peak with tR 14.26 min.

[30b] 3'-Deoxyadenosine 5'-O-naphth-1-yl(benzyloxy-L-alaninyl)-phosphate

Prepared according to general procedure **F₂** using 3'-deoxyadenosine (0.15 g, 0.6 mmol) in THF (12 mL), *N*-methylimidazole (240 μ L, 3.0 mmol), naphth-1-yl-(benzyloxy-L-alaninyl) phosphorochloridate [**17a**] (727 mg, 1.8 mmol) in THF (7 mL). Purification by Biotage Isolera One (cartridge SNAP KP-SIL 50g, 100 mL/min, CH₃OH/CH₂Cl₂ 1-10% 10 CV, 10% 5 CV) and preparative TLC (2000 μ M, eluent system CH₃OH/CH₂Cl₂ 5/95) afforded compound as white solid (0.045 g, 12%).

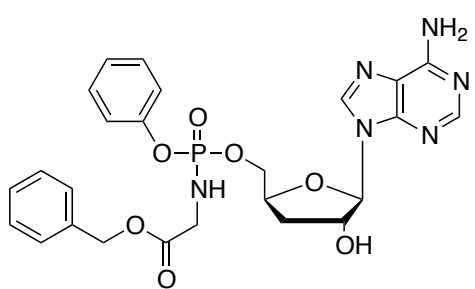
³¹P NMR (202 MHz, CD₃OD) δ_P 4.32, 4.14.

¹H NMR (500 MHz, CD₃OD) δ_H 8.24 (s, 0.5H, H8), 8.22 (s, 0.5H, H8), 8.20 (s, 0.5H, H2), 8.19 (s, 0.5H, H2), 8.14-8.09 (m, 1H, Ar), 7.89-7.85 (m, 1H, Ar), 7.70-7.67 (m, 1H, Ar), 7.53-7.42 (m, 3H, Ar), 7.39-7.34 (m, 1H, Ar), 7.31-7.25 (m, 5H, Ar), 5.99 (d, $J = 2.0$ Hz, 0.5H, H1'), 5.98 (d, $J = 2.0$ Hz, 0.5H, H1'), 5.10-5.01 (m, 2H, CH₂Ph), 4.72-4.61 (m, 2H, H2', H4'), 4.47-4.40 (m, 1H, H5'), 4.33-4.24 (m, 1H, H5'), 4.09-3.98 (m, 1H, CHCH₃ L-Ala) 2.35-2.26 (m, 1H, H3'), 2.07-1.98 (m, 1H, H3'), 1.30-1.24 (m, 3H, CHCH₃ L-Ala).

¹³C NMR (125 MHz, CD₃OD) δ_C 174.85 (d, $^3J_{C-P} = 3.7$ Hz, C=O), 174.56 (d, $^3J_{C-P} = 3.7$ Hz, C=O), 157.33 (C6), 157.31 (C6), 153.87 (C2), 153.85 (C2), 150.24 (C4), 150.23 (C4), 147.91 (d, $^3J_{C-P} = 7.5$ Hz, C-Ar), 147.95, (d, $^3J_{C-P} = 7.5$ Hz, C-Ar), 140.56 (C8), 140.50 (C8), 137.22 (C-Ar), 137.17 (C-Ar), 136.28 (C-Ar), 129.55 (CH-Ar), 129.53 (CH-Ar), 129.30 (CH-Ar), 129.25 (CH-Ar), 128.88 (CH-Ar), 128.82 (CH-Ar), 127.91 (d, $^2J_{C-P} = 6.2$ Hz, C-Ar), 127.83 (d, $^2J_{C-P} = 6.2$ Hz, C-Ar), 127.77 (CH-Ar), 127.75 (CH-Ar), 127.49 (CH-Ar), 127.45 (CH-Ar), 126.48 (CH-Ar), 126.47 (CH-Ar), 126.02 (CH-Ar), 125.97 (CH-Ar), 122.77 (CH-Ar), 122.63 (CH-Ar), 120.58 (C5), 120.53 (C5), 116.35 (d, $^3J_{C-P} = 3.7$ Hz, CH-Ar), 116.15 (d, $^3J_{C-P} = 3.7$ Hz, CH-Ar), 93.22 (C1'), 93.20 (C1'), 80.30 (d, $^3J_{C-P} = 2.7$ Hz, C4'), 80.24 (d, $^3J_{C-P} = 2.7$ Hz, C4'), 76.51 (C2'), 76.44 (C2'), 68.87 (d, $^2J_{C-P} = 5.2$ Hz, C5'), 68.64 (d, $^2J_{C-P} = 5.2$ Hz, C5'), 67.93 (CH₂Ph), 51.82 (CHCH₃ L-Ala), 51.73 (CHCH₃ L-Ala), 35.01 (C3'), 34.76 (C3'), 20.41 (d, $^3J_{C-P} = 6.7$ Hz, CHCH₃ L-Ala), 20.22 (d, $^3J_{C-P} = 6.7$ Hz, CHCH₃ L-Ala).

HPLC Reverse-phase HPLC eluting with H₂O/CH₃CN from 100/10 to 0/100 in 30 minutes, F = 1ml/min, $\lambda = 200$ nm, showed two peaks of the diastereoisomers with tR 16.36 min. and tR 16.60 min.

(ES⁺) m/z found 619.2 [M+H⁺], 641.2 [M+Na⁺], 1259.4 [2M+Na⁺] C₃₀H₃₁N₆O₇P required m/z 618.58 [M].

[30c] 3'-Deoxyadenosine 5'-O-(benzyloxy-glyciny)-phosphate

Prepared according to general procedure **F₂** using 3'-deoxyadenosine (0.05 g, 0.20 mmol) in THF (4 mL), *N*-methylimidazole (80 μ L, 1.0 mmol), phenyl (benzyloxy-glyciny) phosphorochloridate [**17r**] (204 mg, 0.6 mmol) in THF (2.4 mL). Purification

by column chromatography (eluent system CH₃OH/CH₂Cl₂ 0/100 to 6/94) and preparative TLC (500 μ M, eluent system CH₃OH/CH₂Cl₂ 5/95) afforded the compound as a white solid (0.021 g, 19%).

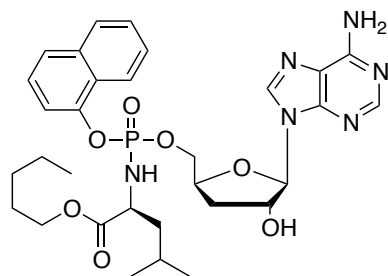
³¹P NMR (202 MHz, CD₃OD) δ_P 5.12, 4.91.

¹H NMR (500 MHz, CD₃OD) δ_H 8.27 (s, 0.5H, H8), 8.24 (s, 0.5H, H8), 8.22 (s, 0.5H, H2), 8.21 (s, 0.5H, H2), 7.37-7.26 (m, 7H, Ph), 7.22-7.13 (m, 3H, Ph), 6.02 (d, $J = 1.8$ Hz, 0.5H, H1'), 6.00 (d, $J = 1.8$ Hz, 0.5H, H1'), 5.15-5.12 (m, 2H, CH₂Ph), 4.73-4.64 (m, 2H, H2', H4'), 4.50-4.39 (m, 1H, H5'), 4.36-4.24 (m, 1H, H5'), 3.53-3.71 (m, 2H, CH₂ Gly), 2.39-2.25 (m, 1H, H3'), 2.13-2.02 (m, 1H, H3').

¹³C NMR (125 MHz, CD₃OD) δ_C 172.30 (d, $^3J_{C-P} = 5.0$ Hz, C=O), 172.27 (d, $^3J_{C-P} = 5.0$ Hz, C=O), 157.34 (C6), 157.32 (C6), 153.88 (C2), 153.87 (C2), 152.08 (d, $^2J_{C-P} = 7.5$ Hz, C-Ar), 152.05 (d, $^2J_{C-P} = 7.5$ Hz, C-Ar), 150.20 (C4), 150.19 (C4), 140.52 (C8), 140.42 (C8), 137.15 (C-Ar), 130.79 (CH-Ar), 129.57 (CH-Ar), 129.55 (CH-Ar), 129.35 (CH-Ar), 129.34 (CH-Ar), 129.33 (CH-Ar), 126.22 (CH-Ar), 121.44 (d, $^3J_{C-P} = 3.7$ Hz, CH-Ar), 121.40 (d, $^3J_{C-P} = 3.7$ Hz, CH-Ar), 120.51 (C5), 120.49 (C5), 93.19, 93.14 (C1'), 80.46 (d, $^3J_{C-P} = 4.6$ Hz, C4'), 80.39 (d, $^3J_{C-P} = 4.6$ Hz, C4'), 76.66 (C2'), 68.68 (d, $^2J_{C-P} = 5.4$ Hz, C5'), 68.24 (d, $^2J_{C-P} = 5.4$ Hz, C5'), 67.95 (CH₂Ph), 67.93 (CH₂Ph), 43.90 (CH₂ Gly), 43.83 (CH₂ Gly), 34.83 (C3'), 34.54 (C3').

HPLC Reverse-phase HPLC eluting with H₂O/CH₃CN from 100/10 to 0/100 in 30 minutes, F = 1mL/min, $\lambda = 200$ nm, showed two peaks of the diastereoisomers with tR 13.63 min. and tR 13.41 min.

(ES⁺) m/z found: 555.2 [M+H⁺], 577.2 [M+Na⁺], 1131.4 [2M+Na⁺] C₂₅H₂₇N₆O₇P required m/z 554.2 [M].

[30d] 3'-Deoxyadenosine 5'-O-naphth-1-yl-(pentyl-1-oxy-L-leucinyl)-phosphate

Prepared according to general procedure **F**₂ using 3'-deoxyadenosine (0.048 g, 0.19 mmol) in THF (4 mL), *N*-methylimidazole (76 μ L, 0.95 mmol), naphth-1-yl(pentyl-1-oxy-L-leucinyl) phosphorochloridate [**17f**] (0.25 g, 0.6 mmol) in THF (2.4 mL).

Purification by Biotage Isolera One, cartridge SNAP 25 g, 25 mL/min, CH₃OH/CH₂Cl₂ 20% (15 CV), 20% (5 CV) and preparative TLC (1000 μ M, eluent system CH₃OH/CH₂Cl₂ 4/96) afforded the compound as white solid (0.027 g, 22%).

³¹P NMR (202 MHz, CD₃OD) δ_{P} 4.64, 4.37.

¹H NMR (500 MHz, CD₃OD) δ_{H} 8.28 (s, 0.5H, H8), 8.25 (s, 0.5H, H8), 8.21 (s, 0.5H, H2), 8.20 (s, 0.5H, H2), 8.17-8.12 (m, 1H, H8 Nap), 7.88-7.83 (m, 1H, H5 Nap), 7.69-7.66 (m, 1H, H4 Nap), 7.54-7.42 (m, 3H, H2, H6, H7 Nap), 7.40-7.35 (m, 1H, H3 Nap), 6.01 (d, $J = 2.1$ Hz, 0.5H, H1'), 6.00 (d, $J = 2.1$ Hz, 0.5H, H1'), 4.47-4.67 (m, 2H, H2', H4'), 4.55-4.44 (m, 1H, H5'), 4.43-4.31 (m, 1H, H5'), 4.00-3.87 (m, 3H, CHCH₂CH(CH₃)₂ L-Leu, CH₂CH₂CH₂CH₂CH₃ *n*-Pen), 2.44-2.30 (m, 1H, H3'), 2.14-2.04 (m, 1H, H3'), 1.66-1.39 (m, 5H, CHCH₂CH(CH₃)₂ L-Leu, CH₂CH₂CH₂CH₂CH₃ *n*-Pen), 1.1.28-1.21 (m, 4H, CH₂CH₂CH₂CH₂CH₃ *n*-Pen), 0.86-0.81 (m, 3H, CH₂CH₂CH₂CH₂CH₃ *n*-Pen), 0.81-0.68 (m, 6H, CHCH₂CH(CH₃)₂ L-Leu).

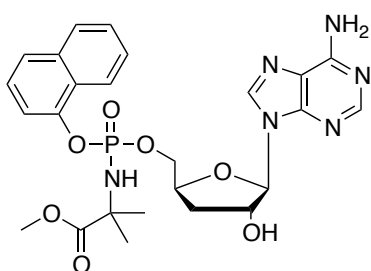
¹³C NMR (125 MHz, CD₃OD) δ_{C} 175.42 (d, $^3J_{\text{C-P}} = 2.5$ Hz, C=O), 175.04 (d, $^3J_{\text{C-P}} = 2.5$ Hz, C=O), 157.32 (C6), 153.87 (C2), 153.86 (C2), 150.23 (C4), 147.97 (d, $^3J_{\text{C-P}} = 6.2$ Hz, C-Ar), 140.55 (C8), 136.30 (C-Ar), 136.29 (C-Ar), 128.89 (CH-Ar), 128.84 (CH-Ar), 127.95 (C-Ar), 127.91 (C-Ar), 127.84 (C-Ar), 127.78 (CH-Ar), 127.76 (CH-Ar), 127.46 (CH-Ar), 126.50 (C-Ar), 126.48 (C-Ar), 126.46 (C-Ar), 126.01 (CH-Ar), 125.91 (CH-Ar), 122.80 (CH-Ar), 122.70 (CH-Ar), 120.58 (C5), 120.56 (C5), 116.40 (d, $^3J_{\text{C-P}} = 3.7$ Hz, CH-Ar), 116.01 (d, $^3J_{\text{C-P}} = 3.7$ Hz, CH-Ar), 93.31 (C1'), 93.27 (C1'), 80.35 (d, $^3J_{\text{C-P}} = 3.5$ Hz, C4'), 80.29 (d, $^3J_{\text{C-P}} = 3.5$ Hz, C4'), 76.54 (C2'), 76.50 (C2'), 69.07 (d, $^2J_{\text{C-P}} = 5.5$ Hz, C5'), 68.85 (d, $^2J_{\text{C-P}} = 5.5$ Hz, C5'), 66.33 (CH₂CH₂CH₂CH₂CH₃ *n*-Pen), 66.32 (CH₂CH₂CH₂CH₂CH₃ *n*-Pen), 54.81 (CHCH₂CH(CH₃)₂ L-Leu), 54.71 (CHCH₂CH(CH₃)₂ L-Leu), 44.22 (d, $^3J_{\text{C-P}} = 7.6$ Hz, CHCH₂CH(CH₃)₂ L-Leu), 43.93 (d, $^3J_{\text{C-P}} = 7.6$ Hz, CHCH₂CH(CH₃)₂ L-Leu), 35.15 (C3'), 34.86 (C3'), 29.32 (CH₂CH₂CH₂CH₂CH₃ *n*-Pen), 29.30 (CH₂CH₂CH₂CH₂CH₃ *n*-Pen), 29.11 (CH₂CH₂CH₂CH₂CH₃ *n*-Pen), 25.67 (CHCH₂CH(CH₃)₂ L-Leu), 25.45 (CHCH₂CH(CH₃)₂ L-Leu), 23.30 (CH₂CH₂CH₂CH₂CH₃ *n*-Pen), 23.12 (CHCH₂CH(CH₃)₂ L-Leu), 23.02 (CHCH₂CH(CH₃)₂ L-Leu), 22.04

(CHCH₂CH(CH₃)₂ L-Leu), 21.78 (CHCH₂CH(CH₃)₂ L-Leu), 14.28 (CH₂CH₂CH₂CH₂CH₃ *n*-Pen).

(ES⁺) *m/z* found 641.3 [M+H⁺], 663.3 [M+Na⁺], 1303.6 [2M+Na⁺] C₃₁H₄₁N₆O₇P required *m/z* 640.3 [M].

HPLC Reverse-phase HPLC eluting with H₂O/CH₃CN from 100/10 to 0/100 in 30 minutes, F = 1 mL/min, λ = 200 nm, showed one peak of the two overlapping diastereoisomers with tR 20.84 min.

[30e] 3'-Deoxyadenosine 5'-*O*-naphth-1-yl(methoxy-2,2-dimethylglycyl)-phosphate



Prepared according to general procedure F₂ using 3'-deoxyadenosine (0.15 g, 0.6 mmol) in THF (4 mL), *N*-methylimidazole (240 μL, 3.0 mmol), naphth-1-yl(methoxy-2,2-dimethylglycyl) phosphorochloridate [17q] (0.61 g, 1.8 mmol) in THF (2.4 mL). Purification by

Biotage Isolera One, cartridge SNAP KP-SIL 50 g, 100 mL/min, CH₃OH/CH₂Cl₂ 2-20% (10 CV), 20% (5 CV) and preparative TLC (1000 μM, eluent system CH₃OH/CH₂Cl₂ 4/96) afforded the compound as a white solid (0.02 g, 6%).

³¹P NMR (202 MHz, CD₃OD) δ_P 2.73.

¹H NMR (500 MHz, CD₃OD) δ_H 8.28 (s, 0.5H, H8), 8.25 (s, 0.5H, H8), 8.21 (s, 0.5H, H2), 8.19 (s, 0.5H, H2), 8.18-8.14 (m, 1H, H8 Nap), 7.90-7.84 (m, 1H, H5 Nap), 7.71-7.66 (m, 1H, H4 Nap), 7.53-7.47 (m, 3H, H2, H6, H7 Nap), 7.41-7.35 (m, 1H, H3 Nap), 6.03 (d, *J* = 2.1 Hz, 0.5H, H1'), 5.99 (d, *J* = 2.1 Hz, 0.5H, H1'), 4.76-4.67 (m, 2H, H2', H4'), 4.52-4.44 (m, 1H, H5'), 4.42-4.33 (m, 1H, H5'), 3.65 (s, 1.5H, OCH₃), 3.64 (s, 1.5H, OCH₃), 2.48-2.41 (m, 0.5H, H3'), 2.37-2.30 (m, 0.5H, H3'), 2.15-2.09 (m, 0.5H, H3'), 2.08-2.02 (m, 0.5H, H3'), 1.47-1.44 (m, 6H, (CH₃)₂ DMG).

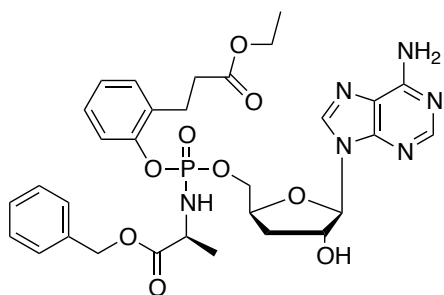
¹³C NMR (125 MHz, CD₃OD) δ_C 177.25 (d, ³*J*_{C-P} = 3.7 Hz, C=O), 157.53 (C6), 157.51 (C6), 153.86 (C2), 150.28 (C4), 150.25 (C4), 148.06 (d, ³*J*_{C-P} = 7.5 Hz, C-Ar), 148.04 (d, ³*J*_{C-P} = 7.5 Hz, C-Ar), 140.67 (C8), 140.60 (C8), 136.28 (C-Ar), 136.27 (C-Ar), 128.82 (CH-Ar), 128.80 (CH-Ar), 127.93 (d, ²*J*_{C-P} = 6.25 Hz, C-Ar), 127.92 (d, ²*J*_{C-P} = 6.25 Hz, C-Ar), 127.71 (CH-Ar), 127.69 (CH-Ar), 127.32 (CH-Ar), 126.44 (CH-Ar), 125.84 (CH-Ar), 122.93 (CH-Ar), 120.56 (C5), 120.50 (C5), 116.38 (d, ³*J*_{C-P} = 3.75 Hz, CH-Ar), 116.36 (d, ³*J*_{C-P} = 3.7 Hz, CH-Ar), 93.25 (C1'), 80.40 (d, ³*J*_{C-P} = 8.0 Hz, C4'), 80.33 (d, ³*J*_{C-P} = 8.0 Hz, C4'), 76.57 (C2'), 76.43 (C2'), 68.99 (d, ²*J*_{C-P} = 5.5 Hz, C5'), 68.84 (d, ²*J*_{C-P} = 5.5 Hz, C5'), 53.01 (OCH₃), 35.22 (C3'), 34.90 (C3'), 27.85 (d, ³*J*_{C-P} = 6.0 Hz, (CH₃)₂)

DMG), 27.80 (d, $^3J_{C-P} = 6.0$ Hz, $(CH_3)_2$ DMG), 27.60 (d, $^3J_{C-P} = 6.0$ Hz, $(CH_3)_2$ DMG), 27.56 (d, $^3J_{C-P} = 6.0$ Hz, $(CH_3)_2$ DMG).

HPLC Reverse-phase HPLC eluting with H_2O/CH_3CN from 100/10 to 0/100 in 30 minutes, $F = 1$ mL/min, $\lambda = 254$ nm, showed two peaks with tR 16.51 min, tR 16.75 min.

(ES+) m/z found 557.2 $[M+H^+]$, 579.2 $[M+Na^+]$, 1135.4 $[2M+Na^+]$ $C_{25}H_{29}N_6O_7P$ required m/z $[M]$ 556.51.

[30f] 3'-Deoxyadenosine 5'-O-ethyl-3-(2-hydroxyphenyl)propanoyl-(benzyloxy-L-alaninyl)-phosphate



Prepared according to general procedure **F₂** using 3'-deoxyadenosine (0.021 g, 0.84 mmol) in THF (4 mL), *N*-methylimidazole (320 μ L, 4.2 mmol), ethyl 3-(2-hydroxyphenyl)propanoyl-L-alanine benzyl ester phosphorochloridate [**17v**] (1.14 g, 2.5 mmol) in THF (2.4 mL). Purification by Biotage Isolera One,

cartridge ZIP Sphere 80 g, 100 mL/min, CH_3OH/CH_2Cl_2 1-8% (10 CV), 8% (5 CV) and preparative TLC (1000 μ M, eluent system CH_3OH/CH_2Cl_2 5/95) afforded the title compound as a white solid (0.032 g, 18%).

^{31}P NMR (202 MHz, CD_3OD) δ_P 3.95, 3.65.

1H NMR (500 MHz, CD_3OD) δ_H 8.25 (s, 0.5H, H8), 8.21 (s, 1H, H8, H2), 8.20 (s, 0.5H, H2), 7.35-7.29 (m, 6H, Ar), 7.25-7.21 (m, 1H, Ar), 7.16-7.07 (m, 2H, Ar), 6.00 (d, $J = 1.9$ Hz, 0.5H, H1'), 5.98 (d, $J = 1.9$ Hz, 0.5H, H1'), 5.17-5.05 (m, 2H, CH_2Ph), 4.76-4.73 (m, 0.5H, H2'), 4.70-4.59 (m, 1.5H, H2', H4'), 4.45-4.34 (m, 1H, H5'), 4.30-4.22 (m, 1H, H5'), 4.08-3.96 (m, 3H, $CH_2CH_2OCH_2CH_3$, $CHCH_3$ L-Ala), 2.98-2.92 (m, 2H, $CH_2CH_2OCH_2CH_3$), 2.62-2.56 (m, 2H, $CH_2CH_2OCH_2CH_3$), 2.40-2.29 (m, 1H, H3'), 2.11-2.03 (m, 1H, H3'), 1.36 (d, $J = 6.9$ Hz, 1.5 H, $CHCH_3$ L-Ala), 1.33 (d, $J = 6.9$ Hz, 1.5 H, $CHCH_3$ L-Ala), 1.17 (t, $J = 7.0$ Hz, 1.5 H, $CH_2CH_2OCH_2CH_3$), 1.16 (t, $J = 7.0$ Hz, 1.5 H, $CH_2CH_2OCH_2CH_3$).

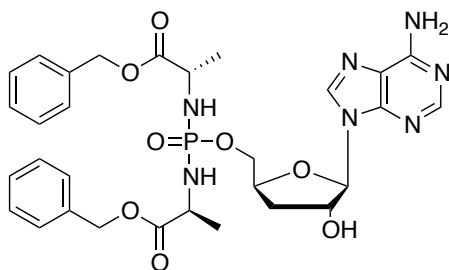
^{13}C NMR (125 MHz, CD_3OD) δ_C 174.82 (d, $^3J_{C-P} = 3.7$ Hz, C=O), 174.62 (C=O), 174.58 (C=O), 174.55 (d, $^3J_{C-P} = 3.7$ Hz, C=O), 157.34 (C6), 157.32 (C6), 153.86 (C2), 153.84 (C2), 150.48 (d, $^3J_{C-P} = 2.5$ Hz, C-Ar), 150.44 (C4), 150.22 (d, $^3J_{C-P} = 2.5$ Hz, C-Ar), 140.49 (C8), 137.29 (C-Ar), 137.21 (C-Ar), 133.09 (d, $^2J_{C-P} = 7.5$ Hz, C-Ar), 132.94 (d, $^2J_{C-P} = 7.5$ Hz, C-Ar), 131.62 (CH-Ar), 131.59 (CH-Ar), 129.58 (CH-Ar), 129.34 (CH-Ar), 129.31 (CH-Ar), 129.28 (CH-Ar), 128.70 (d, $^3J_{C-P} = 5.0$ Hz, CH-Ar), 128.69 (d, $^3J_{C-P} = 5.0$ Hz, CH-Ar), 126.18 (CH-Ar), 121.02 (d, $^3J = 2.5$ Hz, CH-Ar), 120.49 (d, $^3J = 2.5$ Hz, CH-

Ar), 120.58 (C5), 93.28 (C1'), 93.24 (C1'), 80.32 (d, $^3J_{C-P} = 8.7$ Hz, C4'), 76.57 (C2'), 68.86 (d, $^2J_{C-P} = 5.0$ Hz, C5'), 68.53 (d, $^2J_{C-P} = 5.0$ Hz, C5'), 67.98 (CH₂Ph), 67.95 (CH₂Ph), 61.57 (CH₂CH₂OCH₂CH₃), 51.76 (CHCH₃ L-Ala), 51.65 (CHCH₃ L-Ala), 35.37 (CH₂CH₂OCH₂CH₃), 35.30 (CH₂CH₂OCH₂CH₃), 35.08 (C3'), 34.85 (C3'), 26.77 (CH₂CH₂OCH₂CH₃), 26.72 (CH₂CH₂OCH₂CH₃), 20.55 (d, $^3J_{C-P} = 6.2$ Hz, CHCH₃ L-Ala), 20.33 (d, $^3J_{C-P} = 6.2$ Hz, CHCH₃ L-Ala), 14.53 (CH₂CH₂OCH₂CH₃).

HPLC Reverse-phase HPLC eluting with H₂O/CH₃CN from 100/10 to 0/100 in 30 minutes, F = 1 mL/min, $\lambda = 245$ nm, showed one peak with tR 15.99 min.

(ES⁺) m/z found 669.3 [M+H⁺], 691.3 [M+Na⁺], C₃₁H₃₇N₆O₉P required m/z 668.63 [M].

[32] 3'-Deoxyadenosine 5'-O-bis(benzyloxy-L-alaninyl) phosphate



Prepared according to general procedure **G** using 3'-deoxyadenosine (0.20 g, 0.80 mmol), (OCH₃)₃PO (5 mL), POCl₃ (75 μ L, 0.80 mmol), L-alanine O-benzyl ester tosylate salt (1.4 g, 4.0 mmol), CH₂Cl₂ (5 mL) and diisopropyl ethyl amine (1.4 mL, 8.0 mmol). The residue was purified by column chromatography

(gradient elution of CH₂Cl₂/CH₃OH = 100/0 to 93/7) to give white foam (0.26 g, 49%).

³¹P NMR (202 MHz, CD₃OD) δ_P 13.9.

¹H NMR (500 MHz, CD₃OD) δ_H 8.28 (s, 1H, H8), 8.22 (s, 1H, H2), 7.37-7.26 (m, 10H, Ph), 6.00 (d, $J = 1.9$ Hz, 1H, H1'), 5.15-5.05 (m, 4H, CH₂Ph), 4.74-4.70 (m, 1H, H2'), 4.63-4.56 (m, 1H, H4'), 4.24-4.18 (m, 1H, H5'), 4.11-4.05 (m, 1H, H5'), 3.97-3.87 (m, 2H, CHCH₃ L-Ala x 2), 2.35-2.27 (m, 1H, H3'), 2.07-2.01 (m, 1H, H3'), 1.34-1.27 (m, 6H, CHCH₃ L-Ala x 2).

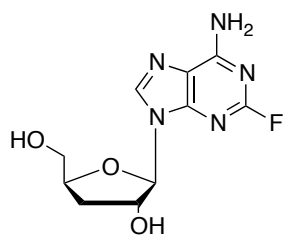
¹³C NMR (125 MHz, CD₃OD) δ_C 175.40 (d, $^3J_{C-P} = 5.0$ Hz, C=O), 175.36 (d, $^3J_{C-P} = 5.0$ Hz, C=O), 157.36 (C6), 153.91 (C2), 150.25 (C4), 140.64 (C8), 137.33 (C-Ar), 137.29 (C-Ar), 129.58 (CH-Ar), 129.57 (CH-Ar), 129.33 (CH-Ar), 129.31 (CH-Ar), 129.29 (CH-Ar), 120.55 (C5), 93.18 (C1'), 80.67 (d, $^3J_{C-P} = 8.4$ Hz, C4'), 76.59 (C2'), 67.90 (CH₂Ph), 67.47 (d, $^2J_{C-P} = 5.2$ Hz, C5'), 51.14 (d, $^2J_{C-P} = 1.7$ Hz, CHCH₃ L-Ala), 51.11 (d, $^2J_{C-P} = 1.7$ Hz, CHCH₃ L-Ala), 35.08 (C3'), 20.77 (d, $^3J_{C-P} = 6.5$ Hz, CHCH₃ L-Ala), 20.59 (d, $^3J_{C-P} = 6.5$ Hz, CHCH₃ L-Ala).

(ES⁺) m/z found 654.2 [M+H⁺], 676.2 [M+Na⁺], 1329.5 [2M+Na⁺] C₃₀H₃₆N₇O₈P required m/z 653.62 [M].

HPLC Reverse-phase HPLC eluting with H₂O/CH₃CN from 90/10 to 0/100 in 30 minutes, F = 1 mL/min, $\lambda = 254$ nm, showed one peak with tR 13.87 min.

9.5.7 Synthesis of 2-modified 3'-deoxyadenosine analogues

[33] 2-Fluoro-3'-deoxyadenosine



2-Fluoro-3'-deoxyadenosine was synthesised according to standard procedure **E** using 2-fluoro-9-(2,3-anhydro- β -D-ribofuranosyl) adenine [**41b**] (1.13 g, 4.18 mmol), LiEt_3BH (1M in THF, 12.54 mmol, 12.54 mL) followed by a second addition of 4.18 mmol, 4.18 mL) in DMSO (6.5 mL) and THF (64 mL). The title compound was obtained as a white solid (0.87 g, 77%).²²⁵ (Lit. mp: 259-260 °C).²⁷⁰

¹H NMR (500 MHz, DMSO-*d*6) δ_{H} 8.34 (s, 1H, H8), 7.80 (br s, 2H, NH₂), 5.78 (d, $J = 2.2$ Hz, 1H, H1'), 5.68 (br s, 1H, OH-2'), 5.01 (br s, 1H, OH-5'), 4.55-4.51 (m, 1H, H2'), 4.39-4.32 (m, 1H, H4'), 3.73-3.76 (m, 1H, H5'), 3.56-3.50 (m, 1H, H5'), 2.26-2.18 (m, 1H, H3'), 1.94-1.85 (m, 1H, H3').

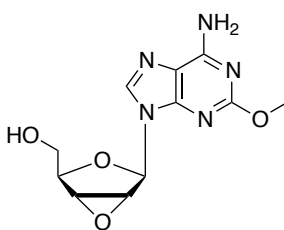
¹³C NMR (125 MHz, DMSO-*d*6) δ_{C} 158.51 (d, $^1J_{\text{C-F}} = 202.7$ Hz, C2), 157.55 (d, $^3J_{\text{C-F}} = 21.2$ Hz, C6), 150.11 (d, $^3J_{\text{C-F}} = 20.3$ Hz, C4), 139.22 (d, $^6J_{\text{C-F}} = 2.2$ Hz, C8), 117.37 (d, $^4J_{\text{C-F}} = 4.1$ Hz, C5), 90.67 (C1'), 80.90 (C4'), 74.73 (C2'), 62.35 (C5'), 33.89 (C3').

¹⁹F NMR (470 MHz, DMSO-*d*6) δ_{F} -52.19.

(ES+) m/z found 276.11 [$\text{M}+\text{Li}^+$], 292.08 [$\text{M}+\text{Na}^+$], 270.10 [$\text{M}+\text{H}^+$] $\text{C}_{10}\text{H}_{13}\text{N}_5\text{O}_3$ required m/z 269.23 [M].

HPLC Reverse-phase HPLC eluting with $\text{H}_2\text{O}/\text{CH}_3\text{CN}$ from 100/0 to 75/25 in 30 minutes, $F = 1$ mL/min, $\lambda = 280$ nm, showed one peak with t_{R} 11.86 min.

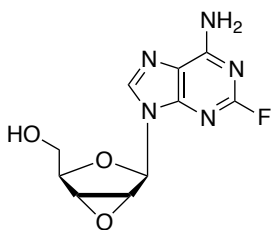
[41a] 2-Methoxy-9-(2,3-anhydro- β -D-ribofuranosyl) adenine



The title compound was synthesised according to standard procedure **D** using 2-fluoroadenosine (2.0 g, 7.01 mmol), α -AIBBr (4.10 mL, 28.05 mmol) and H_2O (0.14 mL, 0.008 mmol) in CH_3CN (50 mL). The crude was then dissolved in CH_3OH (50 mL) and stirred with Amberlite (2 x OH⁻, 28 mL) for 16 hours. The title compound was obtained as a white powder (1.57 g, 84%).

Melting point 175-176 °C.

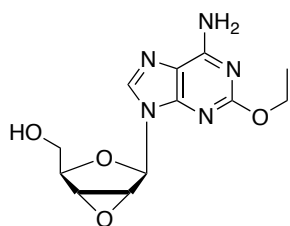
¹H NMR (500 MHz, DMSO-*d*6) δ_{H} 8.12 (s, 1H, H8), 7.28 (br s, 2H, NH₂), 6.12 (s, 1H, H1'), 4.99 (br s, 1H, OH-5'), 4.43 (d, $J = 3$ Hz, 1H, H2'), 4.21 (d, $J = 2.5$ Hz, 1H, H3'), 4.16 (t, $J = 6$ Hz, 1H, H4'), 3.82 (s, 3H, CH₃O), 3.60 (dd, $J = 11.5, 6.5$ Hz, 1H, H5'), 3.50 (dd, $J = 11.5, 5$ Hz, 1H, H5').

[41b] 2-Fluoro-9-(2,3-anhydro-β-D-ribofuranosyl) adenine

The title compound was synthesised according to standard procedure **D** using 2-fluoroadenosine (2.0 g, 7.01 mmol), α-AIBr (4.10 mL, 28.05 mmol) and H₂O (0.14 mL, 0.008 mmol) in CH₃CN (50 mL). The crude was then dissolved in CH₃OH (50 mL) and stirred with Amberlite (2 x OH⁻, 28 mL) for 1.5 hours. Purification by Biotage Isolera One, cartridge SNAP Ultra 50 g, 100 mL/min, CH₃OH/EtOAc 1-10% (10 CV), 10% (2 CV) afforded the title compound as a white solid (1.01 g, 54%).

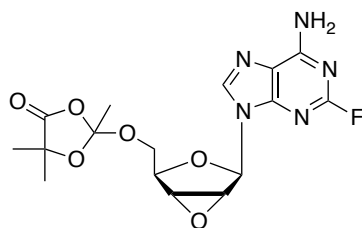
¹H NMR (500 MHz, DMSO-*d*₆) δ_H 8.30 (s, 1H, H8), 7.84 (br s, 2H, NH₂), 6.11 (s, 1H, H1'), 5.02 (t, *J* = 5.0 Hz, 1H, OH-5'), 4.44 (d, *J* = 2.5 Hz, 1H, H2'), 4.20 (d, *J* = 3.0 Hz, 1H, H3'), 4.18 (t, *J* = 5.5 Hz, 1H, H4'), 3.59-3.48 (m, 2H, H5').

¹⁹F NMR (470 MHz, DMSO-*d*₆) δ_F -51.57.

[41c] 2-Ethoxy-9-(2,3-anhydro-β-D-ribofuranosyl) adenine

The title compound was synthesised according to standard procedure **D** using 2-fluoroadenosine (0.50 g, 1.75 mmol), α-AIBr (1.0 mL, 7.01 mmol) and H₂O (0.03 mL, 0.002 mmol) in CH₃CN (12 mL). The crude was then dissolved in CH₃CH₂OH (12 mL) and stirred with Amberlite (2 x OH⁻, 7 mL) for 16 hours. The title compound was obtained as a white solid (0.43 g, 83%).

¹H NMR (500 MHz, DMSO-*d*₆) δ_H 8.16 (s, 1H, H8), 7.28 (br s, 2H, NH₂), 6.16 (s, 1H, H1'), 5.06 (br s, 1H, OH-5'), 4.48 (d, *J* = 2.5 Hz, 1H, H2'), 4.35-4.28 (m, 2H, OCH₂CH₃), 4.25 (d, *J* = 2.5 Hz, 1H, H3'), 4.21 (t, *J* = 5.5 Hz, 1H, H4'), 3.63 (dd, *J* = 11.5, 6 Hz, 1H, H5'), 3.54 (dd, *J* = 11.5, 6.0 Hz, 1H, H5'), 1.35 (t, *J* = 7.0 Hz, 1H, OCH₂CH₃).

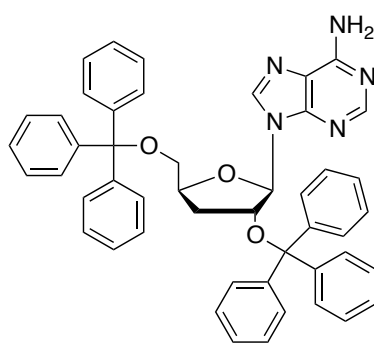
[41e] 2-Fluoro-9-[2,3-anhydro-5-(2,5,5-trimethyl-1,3-dioxolan-4-on-2-yl)-β-D-ribofuranosyl] adenine

Compound **40e** was synthesised according to standard procedure **D** using 2-fluoroadenosine (2.0 g, 7.01 mmol), α-AIBr (4.10 mL, 28.05 mmol) and H₂O (0.14 mL, 0.008 mmol) in CH₃CN (50 mL). The crude was then dissolved in THF (40 mL) and water (10 mL) was added and stirred with Amberlite (2 x OH⁻, 28 mL) for 96 h, affording 2-fluoro-2',3'-anhydroadenosine **40b** (0.58 g, 31%) and the title compound **40e** (0.47 g, 17%) as a white foam.

^1H NMR (500 MHz, DMSO-*d*6) δ_{H} 8.26 (s, 1H, H8), 7.89 (br s, 2H, NH₂), 6.18 (s, 1H, H1'), 4.52 (d, J = 2.5 Hz, 1H, H2'), 4.36 (dd, J = 7.0, 5.5 Hz, 1H, H4'), 4.30 (dd, J = 12.0, 5.5 Hz, 1H, H5'), 4.21 (d, J = 2.5 Hz, 1H, H3'), 4.15 (dd, J = 11.5, 7.0 Hz, 1H, H5'), 1.95 (s, 3H, CH₃), 1.40 (s, 3H, CH₃), 1.38 (s, 3H, CH₃).

^{19}F NMR (470 MHz, DMSO-*d*6) δ_{F} -51.57.

[42] 2',5'-Bis-*O*-trityloxy-3'-deoxyadenosine



3'-Deoxyadenosine (0.20 g, 0.80 mmol) was coevaporated twice with dry pyridine and dissolved in dry pyridine (3.6 mL). Triphenylmethyl chloride (0.62 g, 2.24 mmol) was added and the solution was heated to 80 °C overnight under argon. The reaction was quenched by adding CH₃OH (3 mL) at room temperature, and stirred for 30 min. The solution was then co-evaporated with toluene and diluted in

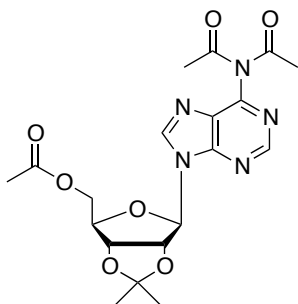
CH₂Cl₂ (30 mL). The organic solution was washed with a solution of saturated NaHCO₃ (3 x 15 mL) and the combined aqueous layers were extracted with CH₂Cl₂ (50 mL). Combined organic layers were dried over Na₂SO₄, filtered and concentrated under vacuum. The residue was purified by flash column chromatography on silica (eluent system nHex/EtOAc = 1/1 containing 0.5% triethylamine), and afforded the title compound as a white foam (0.22 g, 38%).

^1H NMR (500 MHz, CDCl₃) δ_{H} 8.06 (s, 1H, H8), 8.00 (s, 1H, H2), 7.44-7.37 (m, 12H, Ar), 7.32-7.25 (m, 18H, Ar), 5.88 (d, J = 2.9 Hz, 1H, H1'), 5.73 (br s, 1H, NH₂), 4.80-4.76 (m, 1H, H2'), 4.72-4.66 (m, 1H, H4'), 3.44 (dd, J = 10.5, 3.2 Hz, 1H, H5'), 3.28 (dd, J = 10.5, 4.5 Hz, 1H, H5'), 2.26-2.12 (m, 2H, H3').

^{13}C NMR (125 MHz, CDCl₃) δ_{C} 154.21 (C6), 151.75 (C2), 147.64 (C4), 144.95 (C-Ar), 143.71 (C-Ar), 137.97 (C8), 129.13 (CH-Ar), 128.75 (CH-Ar), 128.01 (CH-Ar), 127.95 (CH-Ar), 127.28 (CH-Ar), 127.00 (CH-Ar), 121.39 (C5), 93.24 (C1'), 87.06 (C-Tr), 80.55 (C4'), 76.05 (C2'), 71.60 (C-Tr), 65.17 (C5'), 33.92 (C3').

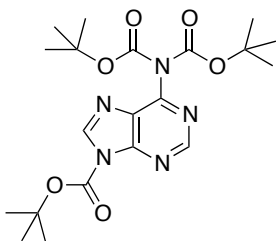
HPLC Reverse-phase HPLC eluting with H₂O/CH₃CN from 80/20 to 0/100 in 50 min, F = 1 mL/min, λ = 245 nm, showed one peak with t_R 30.27 min.

(ES⁺) m/z found 736.3 [M+H⁺], 758.3 [M+Na⁺], C₄₈H₄₁N₅O₃ required m/z 735.87 [M].

[44] 5'-*O*-Acetyl-2',3'-*O*-isopropylidene-adenosine

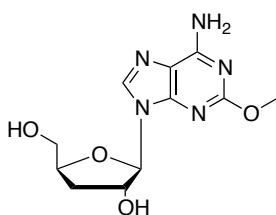
2',3'-*O*-Isopropylidene-adenosine (0.20 g, 0.65 mmol) was dissolved in CH₃CN (15 mL). To this stirring solution, DMAP (0.032 g, 0.26 mmol), acetic anhydride (0.36 mL, 3.9 mmol) and triethylamine (0.54 mL, 3.9 mmol) were added, and the reaction was stirred at 70 °C for 4 hours. The mixture was evaporated, re-dissolved in CH₂Cl₂ (30 mL) and washed with aqueous HCl (0.5 N, 15 mL), aqueous NaHCO₃ saturated solution (15 mL) and brine (15 mL). The organic layers were combined, dried over MgSO₄ and evaporated. The crude was purified by silica gel column chromatography (eluent system EtOAc/*n*Hex = 50-100%) to yield the title compound as a sticky solid (0.038 g, 15%).³⁶⁸

¹H-NMR (CDCl₃, 500 MHz) δ_H 8.91 (s, 1H, H2), 8.16 (s, 1H, H8), 6.14 (d, *J* = 2.3 Hz, 1H, H1'), 5.41 (dd, *J* = 2.3 Hz, 6.3 Hz, 1H, H2'), 4.96 (dd, *J* = 3.4 Hz, 6.3 Hz, 1H, H3'), 4.50-4.46 (m, 1H, H4'), 4.29 (dd, *J* = 4.8 Hz, 12.1 Hz, 1H, H5'), 4.22 (dd, *J* = 6.5 Hz, 12.1 Hz, 1H, H5'), 2.29 (s, 6H, N(COCH₃)₂), 1.91 (s, 3H, OCOCH₃), 1.58 (s, 3H, CH₃), 1.35 (s, 3H, CH₃).

[46] *N*⁹-*tert*-butylcarbonate-[bis-*N*⁴,*N*⁴-(*tert*-butylcarbonate)]-adenine

Adenine (0.30 g, 2.22 mmol) was dissolved in anhydrous THF (10 mL) and DMAP (0.027 mg, 0.22 mmol) and Boc₂O (1.94 g, 8.88 mmol) were added. The mixture was stirred at rt for 8 h and evaporated. The mixture was extracted with *n*Hex/water to yield the title compound as a clear oil (0.97 g, 81%).⁴⁷⁰

¹H-NMR (CDCl₃, 500 MHz) δ_H 8.94 (s, 1H, H8), 8.43 (s, 1H, H2), 1.64 (s, 9H, *t*Bu), 1.37 (s, 18h, *t*Bu x 2).

[48] 2-Methoxy-3'-deoxyadenosine

The title compound was synthesised according to standard procedure **E** using 2-methoxy-9-(2,3-anhydro-β-D-ribofuranosyl) adenine [**41a**] (0.76 g, 2.84 mmol), LiEt₃BH (1M in THF, 8.53 mL, 8.53 mmol, followed by a second addition of 2.84 mL, 2.84 mmol) in DMSO (4.3 mL) and THF (43 mL). The residue was chromatographed on silica gel (3-17% CH₃OH in CH₂Cl₂) to give 3'-deoxy-2-methoxy-adenosine as a white powder (0.65 g, 81%).

Melting point 179-180 °C.

¹H NMR (500 MHz, CD₃OD) δ_{H} 8.20 (s, 1H, H8), 5.90 (d, $J = 2.4$ Hz, 1H, H1'), 4.75-4.71 (m, 1H, H2'), 4.54-4.48 (m, 1H, H4'), 3.91 (dd, $J = 12.3, 2.5$ Hz, 1H, H5'), 3.69 (dd, $J = 12.3, 4.0$ Hz, 1H, H5'), 3.37 (s, 3H, OCH₃), 2.43-2.35 (m, 1H, H3'), 2.08-2.02 (m, 1H, H3').

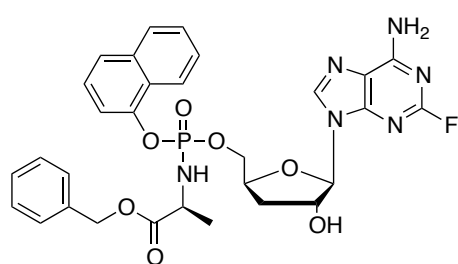
¹³C NMR (125 MHz, CD₃OD) δ_{C} 163.68 (C2), 158.12 (C6), 151.94 (C4), 139.71 (C8), 116.64 (C5), 93.36 (C1'), 82.53 (C4'), 76.59 (C2'), 64.24 (C5'), 55.29 (OCH₃), 34.81 (C3').

HPLC Reverse-phase HPLC eluting with H₂O/CH₃CN from 100/0 to 75/25 in 30 minutes, F = 1 mL/min, $\lambda = 280$ nm, showed one peak with t_R 8.84 min.

(ES⁺) m/z found 282.3 [M+H⁺] C₁₁H₁₅N₅O₄ required m/z 281.27 [M].

9.5.8 Synthesis of 2-fluoro-3'-deoxyadenosine ProTides

[49a] 2-Fluoro-3'-deoxyadenosine-5'-O-naphth-1-yl-(benzyloxy-L-alaninyl) phosphate



Prepared according to general procedure F₂ using 2-fluoro-3'-deoxyadenosine [33] (0.05 g, 0.18 mmol), *N*-methylimidazole (74 μ L, 0.93 mmol) and 1-naphth-1-yl(benzyloxy-L-alaninyl) phosphorochloridate [17a] (0.20 g, 0.56 mmol) in

THF (2.4 mL). Purification by Biotage Isolera One, cartridge SNAP KP-Sil 50g, 100 mL/min, CH₃OH/CH₂Cl₂ 1-10% (10 CV), 10% (5 CV) and preparative TLC (1000 μ M, eluent system CH₃OH/CH₂Cl₂ 5/95) afforded the title compound as a white solid (0.017 g, 15%).

³¹P NMR (202 MHz, CD₃OD) δ_{P} 4.33, 4.08.

¹H NMR (500 MHz, CD₃OD) δ_{H} 8.17 (s, 0.5H, H8), 8.14 (s, 0.5H, H8), 8.14-8.09 (m, 1H, Ar), 7.89-7.85 (m, 1H, Ar), 7.70-7.66 (m, 1H, Ar), 7.54-7.42 (m, 4H, Ar), 7.40-7.24 (m, 5H, Ar), 5.89 (d, $J = 2.3$ Hz, 0.5H, H1'), 5.88 (d, $J = 2.3$ Hz, 0.5H, H1'), 5.08-5.01 (m, 2H, CH₂Ph), 4.70-4.60 (m, 2H, H2', C4'), 4.46-4.39 (m, 1H, C5'), 4.32-4.24 (m, 1H, C5'), 4.09-3.97 (m, 1H, CHCH₃ L-Ala), 2.36-2.25 (m, 1H, H3'), 2.06-1.98 (m, 1H, H3'), 1.32-1.25 (m, 3H, CHCH₃ L-Ala).

¹³C NMR (125 MHz, CD₃OD) δ_{C} 175.54 (CO), 175.22 (CO), 161.02 (d, $^1J_{\text{C-F}} = 207.3$ Hz, C2), 160.89 (d, $^1J_{\text{C-F}} = 207.3$ Hz, C2), 158.45 (d, $^3J_{\text{C-F}} = 18.2$ Hz, C6), 158.23 (d, $^3J_{\text{C-F}} = 18.2$ Hz, C6), 150.63 (d, $^3J_{\text{C-F}} = 18.4$ Hz, C4), 140.67 (C8), 136.26 (C-Ar), 131.62, 131.54,

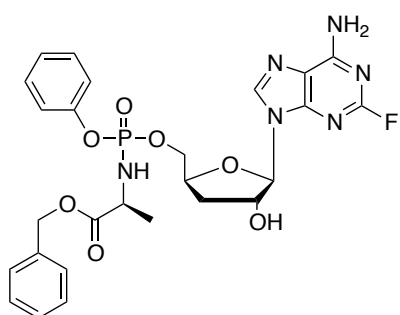
129.56 (CH-Ar), 129.52 (CH-Ar), 129.37 (CH-Ar), 129.31 (CH-Ar), 129.26 (CH-Ar), 128.87 (CH-Ar), 128.81 (CH-Ar), 128.29 (CH-Ar), 128.02 (CH-Ar), 127.79 (CH-Ar), 127.76 (CH-Ar), 127.51 (CH-Ar), 127.49 (CH-Ar), 127.47 (CH-Ar), 126.47 (CH-Ar), 126.33 (C-Ar), 126.27 (C-Ar), 125.97 (CH-Ar), 122.78 (CH-Ar), 122.74 (CH-Ar), 122.64 (CH-Ar), 122.62 (CH-Ar), 116.35 (d, $^4J_{C-F} = 3.0$ Hz, C5), 116.15 (d, $^4J_{C-F} = 3.0$ Hz, C5), 93.25 (C1'), 93.20 (C1'), 80.41 (d, $^3J_{C-P} = 7.5$ Hz, C4'), 80.33 (d, $^3J_{C-P} = 7.5$ Hz, C4'), 76.43 (C2'), 76.35 (C2'), 68.84 (d, $^2J_{C-P} = 5.5$ Hz, C5'), 68.45 (d, $^2J_{C-P} = 5.5$ Hz, C5'), 67.92 (CH₂Ph), 67.92 (CH₂Ph), 51.75 (CHCH₃ L-Ala), 51.52 (CHCH₃ L-Ala), 34.97 (C3'), 34.74 (C3'), 20.42 (d, $^3J_{C-P} = 6.7$ Hz, CHCH₃ L-Ala), 20.20 (d, $^3J_{C-P} = 6.7$ Hz, CHCH₃ L-Ala).

¹⁹F NMR (470 MHz, CD₃OD) δ_F -53.14, -53.22.

HPLC Reverse-phase HPLC eluting with H₂O/CH₃CN from 100/10 to 0/100 in 30 minutes, F = 1 mL/min, $\lambda = 254$ nm, showed two peaks of the diastereoisomers with tR 17.09 min. and tR 17.34 min.

(ES+) m/z found 637.2 [M+H⁺], C₃₀H₃₀FN₆O₇P required m/z 636.57 [M].

[49b] 2-Fluoro-3'-deoxyadenosine-5'-O-phenyl-(benzyloxy-L-alaninyl) phosphate



Prepared according to general procedure F₂ using 2-fluoro-3'-deoxyadenosine [33] (0.05 g, 0.18 mmol), N-methylimidazole (74 μ L, 0.93 mmol) and phenyl(benzyloxy-L-alaninyl) phosphorochloridate [17s] (0.20 g, 0.56 mmol) in THF (2.4 mL). Purification by Biotage Isolera One (cartridge SNAP Ultra 50g, 100 mL/min, CH₃OH/CH₂Cl₂ 1-10% 10 CV, 10% 3 CV) and preparative TLC (1000 μ M, eluent system CH₃OH/CH₂Cl₂ 5/95) afforded the title compound as a white solid (0.005 g, 7%).

³¹P NMR (202 MHz, CD₃OD) δ_P 3.95, 3.67.

¹H NMR (500 MHz, CD₃OD) δ_H 8.19 (s, 0.5H, H8), 8.16 (s, 0.5H, H8), 7.36-7.27 (m, 7H, Ar), 7.22-7.13 (m, 3H, Ar), 5.91 (d, $J = 1.5$ Hz, 0.5H, H1'), 5.89 (d, $J = 1.7$ Hz, 0.5H, H1'), 5.15-5.06 (m, 2H, CH₂Ph), 4.73-4.58 (m, 2H, H2', H4'), 4.42-4.34 (m, 1H, H5'), 4.02-3.90 (m, 1H, H5'), 3.89-3.77 (m, 1H, CHCH₃ L-Ala), 3.27-3.24 (m, 1H, H3'), 2.08-2.00 (m, 1H, H3'), 1.33 (d, $J = 7.1$ Hz, 1.5H, CHCH₃ L-Ala), 1.29 (d, $J = 7.1$ Hz, 1.5H, CHCH₃ L-Ala).

¹³C NMR (125 MHz, CD₃OD) δ_C 175.85 (d, $^3J_{C-P} = 3.7$ Hz, C=O), 174.63 (d, $^3J_{C-P} = 5.0$ Hz, C=O), 160.58 (d, $^1J_{C-F} = 207.5$ Hz, C2), 160.53 (d, $^1J_{C-F} = 207.5$ Hz, C2), 159.06 (d,

$^3J_{C-F} = 18.7$ Hz, C6), 159.05 (d, $^3J_{C-F} = 17.5$ Hz, C6), 152.11 (d, $^2J_{C-P} = 8.7$ Hz, C-Ar), 152.08 (d, $^2J_{C-P} = 8.7$ Hz, C-Ar), 151.58 (d, $^3J_{C-F} = 19.7$ Hz, C4), 151.56 (d, $^3J_{C-F} = 19.5$ Hz, C4), 140.63 (C8), 137.28 (C-Ar), 137.21 (C-Ar), 130.78 (CH-Ar), 130.75 (CH-Ar), 129.58 (CH-Ar), 129.38 (CH-Ar), 129.34 (CH-Ar), 129.32 (CH-Ar), 129.28 (CH-Ar), 128.3 (CH-Ar), 128.02 (CH-Ar), 121.16 (CH-Ar), 121.18 (CH-Ar), 121.47 (CH-Ar), 121.51 (CH-Ar), 121.42 (CH-Ar), 121.39 (CH-Ar), 121.36 (CH-Ar), 118.75 (d, $^4J_{C-F} = 3.7$ Hz, C5), 118.72 (d, $^4J_{C-F} = 3.7$ Hz, C5), 93.25 (C1'), 93.18 (C1'), 80.48 (d, $^3J_{C-P} = 8.3$ Hz, C4'), 80.46 (d, $^3J_{C-P} = 8.1$ Hz, C4'), 76.51 (C2'), 76.49 (C2'), 68.54 (d, $^2J_{C-P} = 5.2$ Hz, C5'), 68.18 (d, $^2J_{C-P} = 5.6$ Hz, C5'), 67.94 (CH₂Ph), 67.91 (CH₂Ph), 51.71 (CHCH₃ L-Ala), 51.56 (CHCH₃ L-Ala), 34.85 (C3'), 34.64 (C3'), 20.42 (d, $^3J_{C-P} = 7.1$ Hz, CHCH₃ L-Ala), 20.25 (d, $^3J_{C-P} = 7.5$ Hz, CHCH₃ L-Ala).

^{19}F NMR (470 MHz, CD₃OD) δ_{F} -53.17, -53.23.

HPLC Reverse-phase HPLC eluting with H₂O/CH₃CN from 100/10 to 0/100 in 30 minutes, F = 1 mL/min, l = 280 nm, showed two peaks of the diastereoisomers with t_{R} 14.98 min. and t_{R} 15.12 min.

(ES⁺) m/z found 587.1 [M+H⁺], C₂₆H₂₈FN₆O₇P required m/z 586.17 [M].

The two diastereoisomers were separated via preparative HPLC (isocratic eluent system: H₂O/CH₃OH 45% in 30 min, 10 mg sample).

Slow eluting isomer (SE)

^{31}P NMR (202 MHz, CD₃OD) δ_{P} 3.67.

^1H NMR (500 MHz, CD₃OD) δ_{H} 8.19 (s, 1H, H8), 7.36-7.27 (m, 7H, Ar), 7.22-7.13 (m, 3H, Ar), 5.91 (d, $J = 1.5$ Hz, 1H, H1'), 5.09 (AB q, $J_{\text{AB}} = 12.5$ Hz, $\Delta\delta_{\text{AB}} = 0.01$, 2H, CH₂Ph), 4.73-4.70 (m, 1H, H2'), 4.66-4.61 (m, 1H, H4'), 4.42-4.37 (m, 1H, H5'), 4.26-4.20 (m, 1H, H5'), 3.97-3.89 (m, 1H, CHCH₃ L-Ala), 2.34-2.27 (m, 1H, H3'), 2.07-2.02 (m, 1H, H3'), 1.30-1.27 (m, 3H, CHCH₃ L-Ala).

^{19}F NMR (470 MHz, CD₃OD) δ_{F} -53.23.

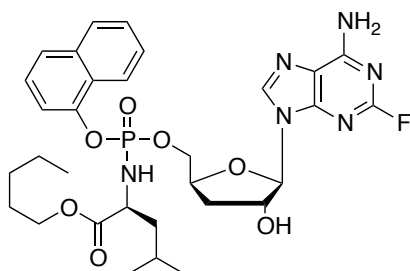
Fast eluting isomer (FE)

^{31}P NMR (202 MHz, CD₃OD) δ_{P} 3.95.

^1H NMR (500 MHz, CD₃OD) δ_{H} 8.17 (s, 1H, H8), 7.36-7.27 (m, 7H, Ar), 7.24-7.12 (m, 3H, Ar), 5.89 (d, $J = 1.5$ Hz, 1H, H1'), 4.95 (AB q, $J = 12.0$ Hz, $\Delta\delta_{\text{AB}} = 0.02$, 2H, CH₂Ph), 4.69-4.66 (m, 1H, H2'), 4.64-4.59 (m, 1H, H4'), 4.39-4.34 (m, 1H, H5'), 4.25-4.19 (m, 1H, H5'), 4.02-3.95 (m, 1H, CHCH₃ L-Ala), 2.34-2.27 (m, 1H, H3'), 2.05-2.00 (m, 1H, H3'), 1.34-1.31 (m, 3H, CHCH₃ L-Ala).

^{19}F NMR (470 MHz, CD₃OD) δ_{F} -53.17.

[49c] 2-Fluoro-3'-deoxyadenosine-5'-O-naphth-1-yl-(pentyl-1-oxy-L-leucinyl)-phosphate



Prepared according to general procedure **F₂** using 2-fluoro-3'-deoxyadenosine [**33**] (0.05 g, 0.18 mmol), N-methylimidazole (74 μ L, 0.93 mmol) and naphth-1-yl(pentyl-1-oxy-L-leucinyl) phosphorochloridate [**17f**] (0.25 mg, 0.56 mmol) in THF (2.2 mL). Purification by Biotage Isolera One, cartridge SNAP Ultra 50g, 100 mL/min, CH₃OH/CH₂Cl₂ 1-10% (10 CV), 10% (3 CV) and preparative TLC (1000 μ M, eluent system CH₃OH/CH₂Cl₂ 5/95) afforded the title compound as a white solid (0.018 g, 16%).

³¹P NMR (202 MHz, CD₃OD) δ_P 4.60, 4.35.

¹H NMR (500 MHz, CD₃OD) δ_H 8.23 (s, 0.5H, H8), 8.20 (s, 0.5H, H8), 8.18-8.12 (m, 1H, H8 Nap), 7.92-7.86 (m, 1H, H5 Nap), 7.73-7.68 (m, 1H, H4 Nap), 7.57-7.46 (m, 3H, H2, H6, H7 Nap), 7.42-7.36 (m, 1H, H3 Nap), 5.93-5.91 (m, 1H, H1'), 4.74-4.62 (m, 2H, H2', H4'), 4.55-4.50 (m, 0.5H, H5'), 4.49-4.44 (m, 0.5H, H5'), 4.43-4.37 (m, 0.5H, H5'), 4.36-4.31 (m, 0.5H, H5'), 4.02-3.86 (m, 3H, CHCH₂CH(CH₃)₂ L-Leu, CH₂CH₂CH₂CH₂CH₃ *n*-Pen), 2.43-2.29 (m, 1H, H3'), 2.12-2.04 (m, 1H, H3'), 1.67-1.20 (m, 9H, CH₂CH₂CH₂CH₂CH₃ *n*-Pen, CHCH₂CH(CH₃)₂ L-Leu), 0.89-0.67 (m, 9H, CH₂CH₂CH₂CH₂CH₃ *n*-Pen, CHCH₂CH(CH₃)₂ L-Leu).

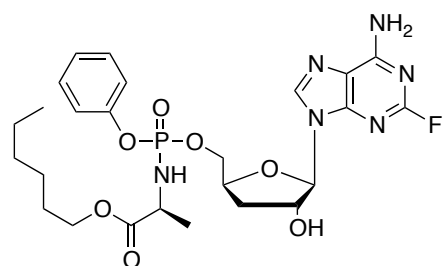
¹³C NMR (125 MHz, CD₃OD) δ_C 175.03 (d, ³*J*_{C-P} = 2.5 Hz, C=O), 174.93 (d, ³*J*_{C-P} = 2.5 Hz, C=O), 161.45 (d, ¹*J*_{C-F} = 205.5 Hz, C2), 160.39 (d, ¹*J*_{C-F} = 205.5 Hz, C2), 158.33 (C6), 151.60 (C4), 147.92 (C-Ar), 140.69 (C8), 136.30 (C-Ar), 128.88 (CH-Ar), 128.83 (CH-Ar), 127.80 (CH-Ar), 127.76 (CH-Ar), 127.49 (CH-Ar), 127.46 (CH-Ar), 126.48 (CH-Ar), 126.45 (CH-Ar), 126.02 (CH-Ar), 125.91 (CH-Ar), 123.03 (C-Ar), 122.81 (CH-Ar), 122.69 (CH-Ar), 116.39 (d, ³*J*_{C-P} = 2.9 Hz, CH-Ar), 116.28 (C5), 116.26 (C5), 115.97 (d, ³*J*_{C-P} = 2.9 Hz, CH-Ar), 93.29 (C1'), 93.23 (C1'), 80.45 (d, ³*J*_{C-P} = 6.0 Hz, C4'), 80.38 (d, ³*J*_{C-P} = 6.0 Hz, C4'), 76.45 (C2'), 76.41 (C2'), 68.99 (d, ²*J*_{C-P} = 5.4 Hz, C5'), 68.78 (d, ²*J*_{C-P} = 5.4 Hz, C5'), 66.31 (CH₂CH₂CH₂CH₂CH₃ *n*-Pen), 66.29 (CH₂CH₂CH₂CH₂CH₃ *n*-Pen), 54.78 (CHCH₂CH(CH₃)₂ L-Leu), 54.66 (CHCH₂CH(CH₃)₂ L-Leu), 44.16 (d, ³*J*_{C-P} = 7.25 Hz, CHCH₂CH(CH₃)₂ L-Leu), 43.84 (d, ³*J*_{C-P} = 7.3 Hz, CHCH₂CH(CH₃)₂ L-Leu), 35.09 (C3'), 34.79 (C3'), 29.31 (CH₂CH₂CH₂CH₂CH₃ *n*-Pen), 29.12 (CH₂CH₂CH₂CH₂CH₃ *n*-Pen), 25.65 (CHCH₂CH(CH₃)₂ L-Leu), 25.41 (CHCH₂CH(CH₃)₂ L-Leu), 23.33 (H₂CH₂CH₂CH₂CH₃ *n*-Pen), 23.11 (CHCH₂CH(CH₃)₂ L-Leu), 23.00 (CHCH₂CH(CH₃)₂ L-Leu), 21.95 (CHCH₂CH(CH₃)₂ L-Leu), 21.68 (CHCH₂CH(CH₃)₂ L-Leu), 14.29 (CH₂CH₂CH₂CH₂CH₃ *n*-Pen).

^{19}F NMR (470 MHz, CD_3OD) δ_{F} -53.15, -53.20.

HPLC Reverse-phase HPLC eluting with $\text{H}_2\text{O}/\text{CH}_3\text{CN}$ from 100/10 to 0/100 in 30 minutes, $F = 1 \text{ mL/min}$, $l = 254 \text{ nm}$, showed one peak of the overlapping diastereoisomers with $t_{\text{R}} 21.95 \text{ min}$.

(ES⁺) m/z found 659.3 [$\text{M}+\text{H}^+$], $\text{C}_{31}\text{H}_{40}\text{FN}_6\text{O}_7\text{P}$ required m/z 658.66 [M].

[49d] 2-Fluoro-3'-deoxyadenosine-5'-*O*-phenyl-(hexyl-1-oxy-L-alaninyl) phosphate



Prepared according to the general procedure **F2** using 2-fluoro-3'-deoxyadenosine [**33**] (0.05 g, 0.18 mmol), *N*-methylimidazole (74 μL , 0.93 mmol) and phenyl(hex-1-yloxy-L-alaninyl) phosphorochloridate [**17u**] (0.19 g, 0.56 mmol). Purification by column chromatography (eluent system $\text{CH}_3\text{OH}/\text{CHCl}_3$ 0/100 to 6/94) and preparative TLC (500 μM , eluent system $\text{CH}_3\text{OH}/\text{CH}_2\text{Cl}_2$ 5/95) afforded the title compound as a white solid (0.03 g, 28%).

^{31}P NMR (202 MHz, CD_3OD) δ_{P} 3.91, 3.73.

^1H NMR (500 MHz, CD_3OD) δ_{H} 8.21 (s, 0.5H, H8), 8.20 (s, 0.5H, H8), 7.37-7.29 (m, 2H, Ar), 7.26-7.13 (m, 3H, Ar), 5.94-5.91 (m, 1H, H1'), 4.76-4.64 (m, 2H, H2', H4'), 4.49-4.44 (m, 0.5H, H5'), 4.43-4.37 (m, 0.5H, H5'), 4.33-4.26 (m, 1H, H5'), 4.11-3.99 (m, 2H, $\text{CH}_2\text{CH}_2\text{CH}_2\text{CH}_2\text{CH}_2\text{CH}_3$ *n*-Hex), 3.97-3.83 (m, 1H, CHCH_3 L-Ala), 2.41-2.32 (m, 1H, H3'), 2.13-2.06 (m, 1H, H3'), 1.62-1.52 (m, 2H, $\text{CH}_2\text{CH}_2\text{CH}_2\text{CH}_2\text{CH}_2\text{CH}_3$ *n*-Hex), 1.37-1.23 (m, 9H, CHCH_3 L-Ala, $\text{CH}_2\text{CH}_2\text{CH}_2\text{CH}_2\text{CH}_2\text{CH}_3$ *n*-Hex), 0.92-0.85 (m, 3H, $\text{CH}_2\text{CH}_2\text{CH}_2\text{CH}_2\text{CH}_2\text{CH}_3$ *n*-Hex).

^{13}C NMR (125 MHz, CD_3OD) δ_{C} 175.15 (d, $^3J_{\text{C-P}} = 3.7 \text{ Hz}$, C=O), 174.96 (d, $^3J_{\text{C-P}} = 5.0 \text{ Hz}$, C=O), 160.59 (d, $^1J_{\text{C-F}} = 207.5 \text{ Hz}$, C2), 160.56 (d, $^1J_{\text{C-F}} = 207.5 \text{ Hz}$, C2), 159.09 (d, $^3J_{\text{C-F}} = 21.2 \text{ Hz}$, C6), 159.08 (d, $^3J_{\text{C-F}} = 20.0 \text{ Hz}$, C6), 152.16 (d, $^2J_{\text{C-P}} = 7.5 \text{ Hz}$, C-Ar), 152.14 (d, $^2J_{\text{C-P}} = 6.3 \text{ Hz}$, C-Ar), 151.71 (d, $^3J_{\text{C-F}} = 20.0 \text{ Hz}$, C4), 151.67 (d, $^3J_{\text{C-F}} = 20.0 \text{ Hz}$, C4), 140.70 (d, $^5J_{\text{C-F}} = 2.5 \text{ Hz}$, C8), 140.68 (d, $^5J_{\text{C-F}} = 2.5 \text{ Hz}$, C8), 130.77 (CH-Ar), 130.74 (CH-Ar), 126.16 (CH-Ar), 126.24 (CH-Ar), 121.48 (CH-Ar), 121.44 (CH-Ar), 121.41 (CH-Ar), 121.37 (CH-Ar), 118.80 (d, $^4J_{\text{C-F}} = 3.7 \text{ Hz}$, C5), 118.77 (d, $^4J_{\text{C-F}} = 3.7 \text{ Hz}$, C5), 93.37 (C1'), 93.25 (C1'), 80.52 (d, $^3J_{\text{C-P}} = 3.7 \text{ Hz}$, C4'), 80.45 (d, $^3J_{\text{C-P}} = 4.1 \text{ Hz}$, C4'), 76.52 (C2'), 76.49 (C2'), 68.69 (d, $^2J_{\text{C-P}} = 5.4 \text{ Hz}$, C5'), 68.30 (d, $^2J_{\text{C-P}} = 4.9 \text{ Hz}$, C5'), 66.46 ($\text{CH}_2\text{CH}_2\text{CH}_2\text{CH}_2\text{CH}_2\text{CH}_3$ *n*-Hex), 51.68 (CHCH_3 L-Ala), 51.57 (CHCH_3 L-Ala), 35.02 (C3'), 34.80 (C3'), 32.58 ($\text{CH}_2\text{CH}_2\text{CH}_2\text{CH}_2\text{CH}_2\text{CH}_3$ *n*-Hex), 29.65 ($\text{CH}_2\text{CH}_2\text{CH}_2\text{CH}_2\text{CH}_2\text{CH}_3$ *n*-Hex), 26.61 ($\text{CH}_2\text{CH}_2\text{CH}_2\text{CH}_2\text{CH}_2\text{CH}_3$ *n*-Hex), 23.59

(CH₂CH₂CH₂CH₂CH₂CH₃ *n*-Hex), 20.60 (d, ³J_{C-P} = 7.1 Hz, CHCH₃ L-Ala), 20.43 (d, ³J_{C-P} = 7.5 Hz, CHCH₃ L-Ala), 14.35 (CH₂CH₂CH₂CH₂CH₂CH₃ *n*-Hex).

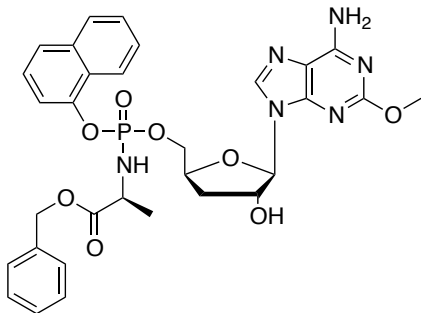
¹⁹F NMR (470 MHz, CD₃OD) δ_F -53.15, -53.20.

(ES⁺) m/z, found: 581.2 (M + H⁺), C₂₅H₃₄FN₆O₇P required m/z 580.55 (M).

HPLC Reverse-phase HPLC eluting with H₂O/CH₃CN from 100/10 to 0/100 in 30 minutes, F = 1 mL/min, l = 254 nm, showed two peaks of the diastereoisomers with tR 17.83 min. and tR 18.02 min.

9.5.9 Synthesis of 2-methoxy-3'-deoxyadenosine ProTides

[50a] 2-Methoxy-3'-deoxyadenosine-5'-O-naphth-1-yl(benzyloxy-L-alaninyl)-phosphate



Prepared according to the general procedure A using 2-methoxy-3'-deoxyadenosine [48] (0.07 g, 0.25 mmol), *N*-methylimidazole (99 μL, 1.24 mmol) and naphthyl(benzyloxy-L-alaninyl) phosphorochloridate [17a] (0.30 g, 0.75 mmol). Purification by column chromatography (eluent system CH₃OH/CHCl₃ 0/100 to

6/94) and preparative TLC (2000 μM, eluent system CH₃OH/CH₂Cl₂ 5/95) afforded the title compound as a white solid (0.096 g, 60%).

³¹P NMR (202 MHz, CD₃OD) δ_P 4.38, 4.08.

¹H NMR (500 MHz, CD₃OD) δ_H 8.31-8.23 (m, 1H, Ar), 8.14-8.06 (m, 1H, Ar), 8.05 (s, 0.5H, H8), 8.02 (s, 0.5H, H8), 7.90-7.78 (m, 3H, Ar), 7.70-7.20 (m, 6H, Ar), 5.91-5.88 (m, 1H, H1'), 5.10-4.99 (m, 2H, CH₂Ph), 4.75-4.68 (m, 1H, H4'), 4.66-4.57 (m, 1H, H2'), 4.46-4.37 (m, 1H, H5'), 4.33-4.25 (m, 1H, H5'), 4.16-3.98 (m, 1H, CHCH₃ L-Ala), 3.92 (s, 1.5H, OCH₃), 3.91 (s, 1.5H, OCH₃), 2.43-2.34 (m, 1H, H3'), 2.06-1.99 (m, 1H, H3'), 1.30-1.21 (m, 3H, CHCH₃ L-Ala).

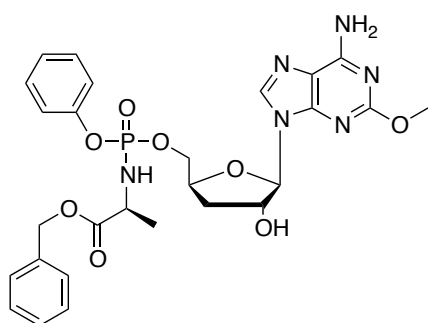
¹³C NMR (125 MHz, CH₃OD) δ_C 174.83 (d, ³J_{C-P} = 3.7 Hz, C=O), 174.60 (d, ³J_{C-P} = 3.7 Hz, C=O), 163.70 (C2), 158.10 (C6), 151.95 (C4), 147.95 (d, ³J_{C-P} = 7.5, C-Ar), 147.91, (d, ³J_{C-P} = 7.5, C-Ar), 139.39 (C8), 139.37 (C8), 137.12 (C-Ar), 137.17 (C-Ar), 136.22 (C-Ar), 129.57 (CH-Ar), 129.54 (CH-Ar), 129.48 (CH-Ar), 129.32 (CH-Ar), 129.27 (CH-Ar), 129.12 (CH-Ar), 129.24 (CH-Ar), 128.89 (CH-Ar), 128.83 (CH-Ar), 127.85 (d, ²J_{C-P} = 6.2 Hz, C-Ar), 127.86 (CH-Ar), 127.76 (CH-Ar), 127.51 (CH-Ar), 127.48 (CH-Ar), 126.49 (CH-Ar), 126.00 (CH-Ar), 125.97 (CH-Ar), 122.73 (CH-Ar), 122.63 (CH-Ar), 116.86

(C5), 116.72 (C5), 116.29 (d, $^3J_{C-P} = 3.7$ Hz, CH-Ar), 116.22 (d, $^3J_{C-P} = 3.7$ Hz, CH-Ar), 93.33 (C1'), 93.31 (C1'), 80.24 (d, $^3J_{C-P} = 2.7$ Hz, C4'), 76.29 (C2'), 76.26 (C2'), 69.09 (d, $^2J_{C-P} = 5.0$ Hz, C5'), 68.16 (d, $^2J_{C-P} = 8.2$ Hz, C5'), 67.95 (CH₂Ph), 55.28 (OCH₃), 55.32 (OCH₃), 51.79 (CHCH₃ L-Ala), 51.71 (CHCH₃ L-Ala), 35.40 (C-3'), 35.12 (C3'), 20.49 (d, $^3J_{C-P} = 6.7$ Hz, CHCH₃ L-Ala), 20.35 (d, $^3J_{C-P} = 6.7$ Hz, CHCH₃ L-Ala).

MS (ES+) m/z found 649.2 [M+H⁺] C₃₁H₃₃N₆O₈P required m/z 648.21 [M].

HPLC Reverse-phase HPLC eluting with H₂O/CH₃CN from 100/10 to 0/100 in 30 minutes, F = 1 mL/min, λ = 254 nm, showed two peaks with t_R 16.22 min and t_R 16.48 min.

[50b] 2-Methoxy-3'-deoxyadenosine-5'-O-phenyl-(benzyloxy-L-alaninyl)- phosphate



Prepared according to the general procedure **F2** using 2-methoxy-3'-deoxyadenosine [**48**] (0.07 g, 0.25 mmol), *N*-methylimidazole (99 μL, 1.24 mmol) and phenyl(benzyloxy-L-alaninyl) phosphorochloridate [**17s**] (0.26 g, 0.75 mmol). Purification by column chromatography (eluent system CH₃OH/CHCl₃ 0/100 to 6/94) and preparative TLC (2000 μM, eluent system

CH₃OH/CH₂Cl₂ 5/95) afforded the title compound as a white solid (0.013 mg, 10%).

³¹P NMR (202 MHz, CD₃OD) δ_P 3.97, 3.64.

¹H NMR (500 MHz, CD₃OD) δ_H 8.06 (s, 0.5H, H8), 8.04 (s, 0.5H, H8), 7.33-7.28 (m, 7H, Ph), 7.20-7.14 (m, 3H, Ph), 5.92 (d, *J* = 1.5 Hz, 0.5H, H1'), 5.90 (d, *J* = 1.5 Hz, 0.5H, H1'), 5.14-5.04 (m, 2H, OCH₂Ph), 4.78-4.76 (m, 0.5H, H4'), 4.74-4.72 (m, 0.5H, H4'), 4.63-4.59 (m, 1H, H2'), 4.10-4.34 (m, 1H, H5'), 4.25-4.20 (m, 1H, H5'), 3.94 (s, 1.5H, OCH₃), 3.95 (s, 1.5H, OCH₃), 3.99-3.90 (m, 1H, CHCH₃ L-Ala), 2.40-2.37 (m, 1H, H3'), 2.07-2.04 (m, 1H, H3'), 1.31 (d, *J* = 7.0 Hz, 1.5H, CHCH₃ L-Ala), 1.26 (d, *J* = 7.0 Hz, 1.5H, CHCH₃ L-Ala).

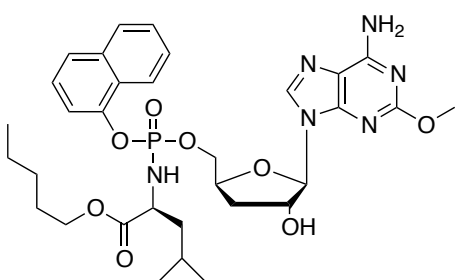
¹³C NMR (125 MHz, CD₃OD) δ_C 174.82 (d, $^3J_{C-P} = 3.7$ Hz, C=O), 174.62 (d, $^3J_{C-P} = 3.7$ Hz, C=O), 163.80 (C2), 158.16, 158.13 (C6), 152.15 (C4), 152.05 (d, $^3J_{C-P} = 4.8$ Hz, C-Ar), 152.00 (d, $^3J_{C-P} = 4.8$ Hz, C-Ar), 139.39 (C8), 137.30 (C-Ar), 137.21 (C-Ar), 130.72 (CH-Ar), 129.57 (CH-Ar), 129.31 (CH-Ar), 129.27 (CH-Ar), 126.122 (CH-Ar), 121.42 (d, $^3J_{C-P} = 4.5$ Hz, CH-Ar), 121.37 (d, $^3J_{C-P} = 4.5$ Hz, CH-Ar), 116.72 (C5), 116.69 (C5), 93.33, 93.24 (C1'), 80.26 (d, $^3J_{C-P} = 8.9$, C4'), 80.19 (d, $^3J_{C-P} = 8.9$, C4'), 76.35 (C2'), 68.78 (d, $^2J_{C-P} = 5.0$ Hz, C5'), 68.35 (d, $^2J_{C-P} = 5.0$ Hz, C5'), 67.94 (CH₂Ph), 67.92 (CH₂Ph), 55.25 (OCH₃), 55.28 (OCH₃), 51.69 (CHCH₃ L-Ala), 51.57 (CHCH₃ L-Ala),

35.23 (C3'), 34.96 (C3'), 20.38 (d, $^3J_{C-P} = 6.7$ Hz, CHCH₃ L-Ala), 20.26 (d, $^3J_{C-P} = 6.7$ Hz, CHCH₃ L-Ala).

(ES+) m/z found 599.2 [M+H⁺], C₂₇H₃₁N₆O₈P required m/z 598.19 [M].

HPLC Reverse-phase HPLC eluting with H₂O/CH₃CN from 100/10 to 0/100 in 30 minutes, F = 1 mL/min, λ = 254 nm, showed two peaks of the diastereoisomers with t_R 14.22 min and t_R 14.51 min.

[50c] 2-Methoxy-3'-deoxyadenosine-5'-O-naphth-1-yl-(pentyl-1-oxy-L-leucinyl)-phosphate



Prepared according to the general procedure **F2** using 2-methoxy-3'-deoxyadenosine **[48]** (0.07 g, 0.25 mmol), *N*-methylimidazole (99 μL, 1.24 mmol) and naphthyl(pentyl-1-oxy-L-leucinyl) phosphorochloridate **[17f]** (0.33 g, 0.75 mmol). Purification by column chromatography (eluent

system gradient CH₃OH/CH₂Cl₂ 0/100 to 6/94) and preparative TLC (2000 μM, eluent system CH₃OH/CH₂Cl₂ 7/93) afforded the title compound as a white solid (0.05 mg, 30%).

³¹P NMR (202 MHz, CD₃OD) δ_P 4.53, 4.28.

¹H NMR (500 MHz, CD₃OD) δ_H 8.04-7.96 (m, 1H, H8), 7.77-7.71 (m, 1H, Nap), 7.58-7.53 (m, 1H, Nap), 7.45-7.17 (m, 5H, Nap), 5.83-5.75 (m, 1H, H1'), 4.64-4.51 (m, 2H, H2', H4'), 4.40-4.16 (m, 2H, H5'), 3.88-3.75 (m, 6H, OCH₃, CH₂CH₂CH₂CH₂CH₃ *n*-Pen, CHCH₂CH(CH₃)₂ L-Leu), 2.38-2.24 (m, 1H, H3'), 2.00-1.91 (m, 1H, H3'), 1.53-1.05 (m, 9H, CH₂CH₂CH₂CH₂CH₃ *n*-Pen, CHCH₂CH(CH₃)₂ L-Leu), 0.77-0.55 (m, 9H, CH₂CH₂CH₂CH₂CH₃ *n*-Pen, CHCH₂CH(CH₃)₂ L-Leu).

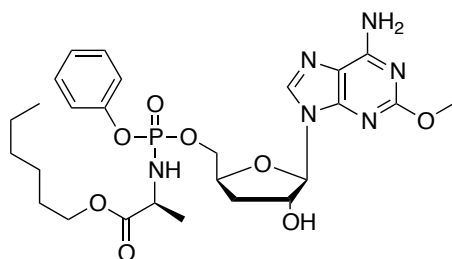
¹³C NMR (125 MHz, CD₃OD) δ_C 175.02 (d, $^3J_{C-P} = 2.5$ Hz, C=O), 174.78 (d, $^3J_{C-P} = 2.5$ Hz, C=O), 163.76 (C2), 158.14 (C6), 151.03 (C4), 147.96 (d, $^3J_{C-P} = 7.2$ Hz, C-Ar), 138.96 (C8), 136.30 (C-Ar), 136.28 (C-Ar), 136.22 (C-Ar), 128.93 (CH-Ar), 128.88 (CH-Ar), 128.81 (CH-Ar), 128.48 (CH-Ar), 127.77 (CH-Ar), 127.73 (CH-Ar), 127.44 (CH-Ar), 127.42 (CH-Ar), 127.06 (CH-Ar), 126.86 (CH-Ar), 126.45 (CH-Ar), 126.44 (CH-Ar), 126.31 (CH-Ar), 125.98 (CH-Ar), 125.88 (CH-Ar), 123.83 (CH-Ar), 123.43 (CH-Ar), 123.24 (CH-Ar), 122.81 (CH-Ar), 122.77 (CH-Ar), 122.69 (CH-Ar), 116.34 (d, $^3J_{C-P} = 3.7$ Hz, CH-Ar), 116.02 (d, $^3J_{C-P} = 3.7$ Hz, CH-Ar), 115.71 (C5), 93.42 (C1'), 93.32 (C1'), 80.22 (d, $^3J_{C-P} = 5.3$ Hz, C4'), 80.15 (d, $^3J_{C-P} = 5.3$ Hz, C4'), 76.29 (C2'), 76.27 (C2'), 69.22 (d, $^2J_{C-P} = 5.2$ Hz, C5'), 69.028 (d, $^2J_{C-P} = 5.2$ Hz, C5'), 66.31 (CH₂CH₂CH₂CH₂CH₃ *n*-Pen), 66.30 (CH₂CH₂CH₂CH₂CH₃ *n*-Pen), 55.29 (OCH₃), 55.24 (OCH₃), 54.79

(CHCH₂CH(CH₃)₂ L-Leu), 54.68 (CHCH₂CH(CH₃)₂ L-Leu), 44.20 (d, ³J_{C-P} = 7.2 Hz, CHCH₂CH(CH₃)₂ L-Leu), 43.93 (d, ³J_{C-P} = 7.2 Hz, CHCH₂CH(CH₃)₂ L-Leu), 35.49 (C3'), 35.17 (C3'), 29.31 (CH₂CH₂CH₂CH₂CH₃ *n*-Pen), 29.11 (CH₂CH₂CH₂CH₂CH₃ *n*-Pen), 25.67 (CHCH₂CH(CH₃)₂ L-Leu), 25.44 (CHCH₂CH(CH₃)₂ L-Leu), 23.30 (CH₂CH₂CH₂CH₂CH₃ *n*-Pen), 23.10 (CHCH₂CH(CH₃)₂ L-Leu), 23.00 (CHCH₂CH(CH₃)₂ L-Leu), 22.94 (CHCH₂CH(CH₃)₂ L-Leu), 22.81 (CHCH₂CH(CH₃)₂ L-Leu), 14.27 (CH₂CH₂CH₂CH₂CH₃ *n*-Pen).

(ES⁺) *m/z*, found: 671.3 [M+H⁺], C₃₂H₄₃N₆O₈P required *m/z* 670.69 [M].

HPLC Reverse-phase HPLC eluting with H₂O/CH₃CN from 100/10 to 0/100 in 30 minutes, F = 1 mL/min, λ = 254 nm, showed two peaks with t_R 20.83 min and t_R 20.93 min.

[50d] 2-Methoxy-3'-deoxyadenosine-5'-*O*-phenyl-(hex-1-yloxy-L-alaninyl)-phosphate



Prepared according to the general procedure F2 using 2-methoxy-3'-deoxyadenosine [48] (0.07 g, 0.25 mmol), *N*-methylimidazole (99 μL, 1.24 mmol) and phenyl(hex-1-yloxy-L-alaninyl) phosphorochloridate [17u] (0.26 g, 0.75 mmol). Purification by column

chromatography (eluent system gradient CH₃OH/CH₂Cl₂ 0/100 to 6/94) and preparative TLC (1000 μM, eluent system CH₃OH/CH₂Cl₂ 7/93) afforded the title compound as a white solid (0.026 g, 18%).

³¹P NMR (202 MHz, CD₃OD) δ_P 3.87, 3.65.

¹H NMR (500 MHz, CD₃OD) δ_H 8.08 (s, 0.5H, H8), 8.07 (s, 0.5H, H8), 7.36-7.29 (m, 2H, Ph), 7.24-7.14 (m, 3H, Ph), 5.94 (d, *J* = 2.0 Hz, 0.5H, H1'), 5.92 (d, *J* = 2.0 Hz, 0.5H, H1'), 4.81-4.76 (m, 1H, H2'), 4.71-4.62 (m, 1H, H4'), 4.48-4.43 (m, 0.5H, H5'), 4.42-4.36 (m, 0.5H, H5'), 4.33-4.25 (m, 1H, H5'), 4.10-3.83 (m, 6H, OCH₃, CH₂CH₂CH₂CH₂CH₂CH₃ *n*-Hex, CHCH₃ L-Ala), 2.48-2.40 (m, 1H, H3'), 2.13-2.07 (m, 1H, H3'), 1.61-1.51 (m, 2H, CH₂CH₂CH₂CH₂CH₂CH₃ *n*-Hex), 1.33-1.24 (m, 9H, CH₂CH₂CH₂CH₂CH₂CH₃ *n*-Hex, CHCH₃ L-Ala), 0.89 (m, 3H, CH₂CH₂CH₂CH₂CH₂CH₃ *n*-Hex).

¹³C NMR (125 MHz, CD₃OD) δ_C 175.13 (d, ³J_{C-P} = 4.3 Hz, C=O), 174.94 (d, ³J_{C-P} = 4.3 Hz, C=O), 163.80 (C2), 163.78 (C2), 158.17 (C6), 158.15 (C6), 152.17 (d, ²J_{C-P} = 6.3 Hz, C-Ar), 152.15 (d, ²J_{C-P} = 6.3 Hz, C-Ar), 152.03 (C4), 151.99 (C4), 139.42 (C8), 139.39 (C8), 130.75 (CH-Ar), 130.74 (CH-Ar), 126.13 (CH-Ar), 121.43 (CH-Ar), 121.41 (CH-Ar), 121.39 (CH-Ar), 121.37 (CH-Ar), 116.74 (C5), 116.69 (C5), 93.40 (C1'), 93.27 (C1'),

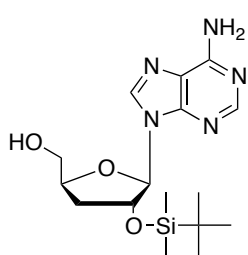
80.26 (d, $^3J_{C-P} = 8.7$ Hz, C4'), 76.40 (C2'), 68.85 (d, $^2J_{C-P} = 5.2$ Hz, C5'), 68.42 (d, $^2J_{C-P} = 5.2$ Hz, C5'), 66.43 (CH₂CH₂CH₂CH₂CH₂CH₃ *n*-Hex), 55.30 (OCH₃), 55.26 (OCH₃), 51.64 (CHCH₃ L-Ala), 51.54 (CHCH₃ L-Ala), 35.30 (C3'), 35.04 (C3'), 32.58 (CH₂CH₂CH₂CH₂CH₂CH₃ *n*-Hex), 29.67 (CH₂CH₂CH₂CH₂CH₂CH₃ *n*-Hex), 29.64 (CH₂CH₂CH₂CH₂CH₂CH₃ *n*-Hex), 26.61 (CH₂CH₂CH₂CH₂CH₂CH₃ *n*-Hex), 23.59 (CH₂CH₂CH₂CH₂CH₂CH₃ *n*-Hex), 20.56 (d, $^3J_{C-P} = 6.4$ Hz, CHCH₃ L-Ala), 20.41 (d, $^3J_{C-P} = 6.4$ Hz, CHCH₃), 14.36 (CH₂CH₂CH₂CH₂CH₂CH₃ *n*-Hex).

(ES+) *m/z*, found: 593.3 [M+H⁺], C₃₂H₄₃N₆O₈P required *m/z* 592.58 [M].

HPLC Reverse-phase HPLC eluting with H₂O/CH₃CN from 100/10 to 0/100 in 30 minutes, F = 1 mL/min, λ = 254 nm, showed two peaks with t_R 17.02 min and t_R 17.23 min.

9.5.10 Synthesis of 5'-modified 3'-deoxyadenosine analogues

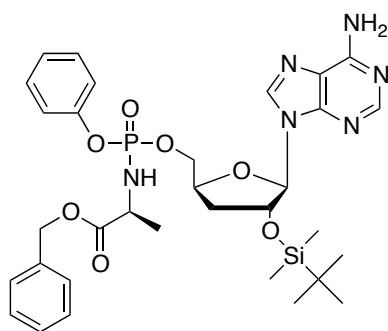
[51] 2'-*O*-*tert*-butyldimethylsilyl-3'-deoxyadenosine



2',5'-*O*-Bis-*tert*-butyldimethylsilyl-3'-deoxyadenosine [25] (1.56 g, 3.25 mmol) was dissolved in THF (2 mL) and cooled down to 0 °C. A solution of TFA in water (1 mL, 1/1 v/v) was added dropwise and the mixture was stirred for 5 hours at 0 °C. The solution was evaporated under *vacuum* and the crude purified via Biotage Isolera One (30g ZIP cartridge KP SIL, 60 mL/min, gradient eluent system 2-20% CH₃OH/CH₂Cl₂ 10CV, 20% 5CV) to yield the title compound as a white foam (1.16 g, 98%).²⁰⁸

¹H NMR (500 MHz, CDCl₃) δ_H 8.45 (s, 1H, H8), 7.97 (s, 1H, H2), 6.29 (br s, 2H, NH₂), 5.74 (d, *J* = 6.0 Hz, 1H, H1'), 5.19-5.12 (m, 1H, H2'), 4.65-4.60 (m, 1H, H4'), 4.11 (dd, *J* = 13.0, 1.5 Hz, 1H, H5'), 3.67 (dd, *J* = 12.5, 1.5 Hz, 1H, H5'), 2.72-2.62 (m, 1H, H3'), 2.37-2.26 (m, 1H, H3'), 1.48 (d, *J* = 7.0 Hz, 1H, OH-5'), 0.91 (s, 9H, *t*Bu), 0.00 (s, 3H, CH₃), -0.12 (s, 3H, CH₃).

[52] 3'-Deoxyadenosine-2'-O-[tert-butyl dimethylsilyl-5'-phenyl-(benzyloxy-L-alaninyl)]-phosphate



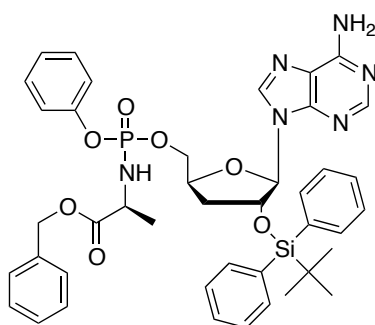
Prepared according to general procedure **F₂** using 2'-*O*-*tert*-butyldimethylsilyl-3'-deoxyadenosine [**51**] (0.05 g, 0.14 mmol) in THF (2 mL), phenyl-(benzyloxy-L-alaninyl) phosphorochloridate [**17s**] (0.14 g, 0.41 mmol) in THF (0.5 mL) and *N*-methylimidazole (56 μ L, 0.7 mmol). The crude was purified via Biotage Isolera One (10g SNAP cartridge KP SIL, 10 mL/min, gradient eluent

system 1-10% CH₃OH/CH₂Cl₂ 12CV, 10% 2CV) to afford the title compound as a white solid (0.06 g, 62%).

³¹P NMR (202 MHz, CH₃OD) δ_P 2.89, 2.98.

¹H NMR (500 MHz, CDCl₃) δ_H 8.436 (s, 0.5H, H8), 8.431 (s, 0.5H, H8), 8.20 (s, 0.5H, H2), 8.19 (s, 0.5H, H2), 7.49-7.20 (m, 10H, Ar), 6.23 (br s, 2H, NH₂), 6.05 (d, *J* = 9.0 Hz, 0.5H, H1'), 6.03 (d, *J* = 9.0 Hz, 0.5H, H1'), 4.98-4.89 (m, 1H, H2'), 4.81-4.72 (m, 1H, H3'), 4.56-4.32 (m, 2H, H5'), 4.26-4.16 (m, 1H, CHCH₃ L-Ala), 2.32-1.99 (m, 2H, H3'), 1.01 (s, 4.5H, *t*Bu), 1.00 (s, 4.5H, *t*Bu), 0.23 (s, 1.5H, CHCH₃ L-Ala), 0.21 (s, 1.5H, CHCH₃ L-Ala), 0.20 (s, 1.5H, CH₃), 0.19 (s, 1.5H, CH₃).

[53] 3'-Deoxyadenosine-2'-O-[tert-butyl diphenylsilyl-5'-O-phenyl(benzyloxy-L-alaninyl)] phosphate



3'-Deoxyadenosine 5'-*O*-phenyl-(benzyloxy-L-alaninyl)-phosphate [**30a**] (0.025 g, 0.04 mmol) was dissolved in DMF (0.5 mL). TBDPSCl (0.036 g, 0.13 mmol), imidazole (16 mg, 0.24 mmol) and DMAP (0.003 g) were added to the mixture, which was stirred at rt for 16 hours. The mixture was evaporated, and the crude purified via Biotage Isolera One (10g ZIP cartridge KP SIL 10 mL/min,

gradient eluent system 1-10% CH₃OH/CH₂Cl₂ 10CV, 10% 2CV), to yield the title compound as a white solid (0.024 g, 76%).

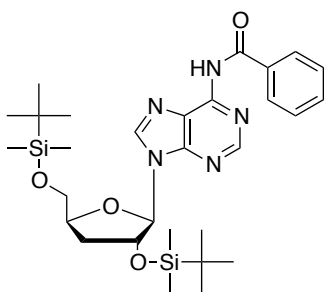
³¹P NMR (202 MHz, CH₃OD) δ_P 2.71, 2.80.

¹H NMR (500 MHz, CDCl₃) δ_H 8.146 (s, 0.5H, H8), 8.142 (s, 0.5H, H8), 7.94-7.92 (m, 1H, H2), 7.51-7.43 (m, 4H, Ar), 7.34-6.95 (m, 16H, Ar), 5.94-5.81 (m, 3H, H1', NH₂), 5.02-4.88 (m, 2H, CH₂Ph), 4.78-4.73 (m, 1H, H2'), 4.63-4.56 (m, 1H, H4'), 4.33-4.22 (m, 1H, H5'), 4.16-4.09 (m, 1H, H5'), 4.04-3.86 (m, 2H, NH, CHCH₃ L-Ala), 2.20-2.11 (m,

1H, H3'), 1.95-1.86 (m, 1H, H3'), 1.21-1.14 (m, 3H, CHCH₃ L-Ala), 1.00 (s, 3H, CH₃ *t*Bu), 0.99 (s, 6H, 2 x CH₃ *t*Bu).

(ES⁺) *m/z* found 807.3 [M+H⁺], 829.3 [M+Na⁺], C₄₂H₄₇N₆O₇PSi required *m/z* 806.3 [M].

[54a] 2',5'-Bis-*O*-*tert*-butyldimethylsilyl-*N*⁶-benzoyl-3'-deoxyadenosine

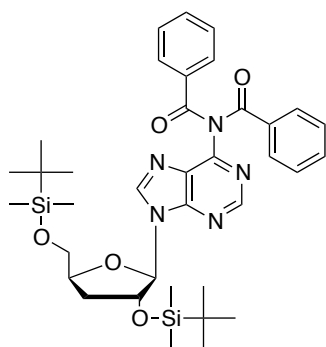


2',5'-Bis-*O*-(*tert*-butyldimethylsilyl)-3'-deoxyadenosine [25]

(0.89 g, 1.85 mmol) was dissolved in anhydrous pyridine (15 mL) and benzoyl chloride (0.65 mL, 5.56 mmol) was added dropwise. The reaction was stirred at room temperature for 1.5 hours, then the flask was lowered in an ice-cold bath and water (5 mL) was added. After 10 minutes 28 % NH₃ in water (10 mL) was added and the mixture stirred for 30 minutes. The reaction was allowed to reach room temperature, the solvent evaporated *in vacuo*, the residue dissolved in EtOAc (150 mL) and washed with water (70 mL) and NaHCO₃ (saturated solution). The organics were dried over Na₂SO₄, filtered and evaporated to yield the product as a clear oil (0.56 g, 52%).²⁰⁸

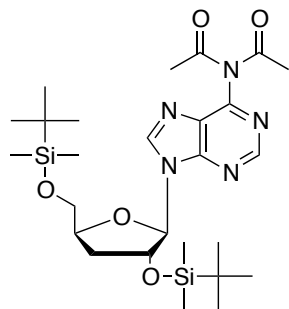
¹H NMR (500 MHz, CDCl₃) δ_H 10.11 (br s, 1H, NH), 8.54 (s, 1H, H8), 8.36 (s, 1H, H2), 7.83 (d, *J* = 7.3 Hz, 2H, Ar), 7.28 (t, *J* = 7.3 Hz, 1H, Ar), 7.18 (t, *J* = 7.3 Hz, 2H, Ar), 5.90 (s, 1H, H1'), 4.49-4.46 (m, 1H, H2'), 4.45-4.39 (m, 1H, H4'), 3.97-3.92 (m, 1H, H5'), 3.64-3.58 (m, 1H, H5'), 2.11-2.03 (m 1H, H3'), 1.75-1.68 (m, 1H, H3'), 0.74 (s, 9H, ^tBu), 0.72 (s, 9H, ^tBu), 0.00 (s, 3H, CH₃), -0.05 (s, 3H, CH₃), -0.06 (s, 3H, CH₃), -0.07 (s, 3H, CH₃).

[54b] (2',5'-*O*-bis-*tert*-butyldimethylsilyl-*N*-benzoyl)cordycepin



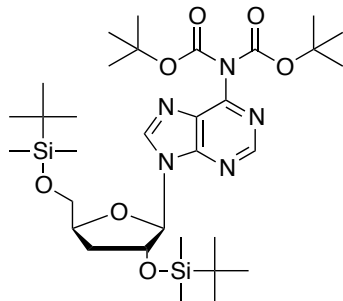
Isolated from the same procedure to obtain [54a]. Product obtained as a clear oil (0.41 g, 32%).

¹H NMR (500 MHz, CDCl₃) δ_H 8.67 (s, 1H, H8), 8.54 (s, 1H, H2), 7.88 (d, *J* = 8.1 Hz, 2H, Ar), 7.87 (d, *J* = 8.4 Hz, 2H, Ar), 7.50-7.45 (m, 2H, Ar), 7.38-7.32 (m, 4H, Ar), 6.07 (d, *J* = 1.4 Hz, 1H, H1'), 4.74-4.70 (m, 1H, H2'), 4.63-4.57 (m, 1H, H4'), 4.09 (dd, *J* = 11.5 Hz, 2.9 Hz, 1H, H5'), 3.80 (dd, *J* = 11.5 Hz, 2.9 Hz, 1H, H5'), 2.28-2.20 (m 1H, H3'), 1.97-1.90 (m, 1H, H3'), 0.94 (s, 9H, ^tBu), 0.92 (s, 9H, ^tBu), 0.13 (s, 6H, CH₃), 0.12 (s, 3H, CH₃), 0.10 (s, 3H, CH₃).

[54c] 2',5'-Bis-*O*-*tert*-butyldimethylsilyl-bis-*N*⁶,*N*⁶-acetyl-3'-deoxyadenosine

2',5'-Bis-*O*-(*tert*-butyldimethylsilyl)-3'-deoxyadenosine [25] (0.38 g, 0.79 mmol) was dissolved in CH₃CN (15 mL) and acetic anhydride was added dropwise (0.45 mL, 4.74 mmol), followed by DMAP (0.04 g, 0.31 mmol), and Et₃N (0.66 mL, 4.74 mmol). The mixture was diluted with aqueous NH₄Cl (saturated solution, 10 mL) and extracted with *n*-Hex (3 x 20 mL). The collected organics were dried over Na₂SO₄, filtered and evaporated. The crude was purified by flash column chromatography (eluent system: EtOAc/*n*-Hex 5-15%) to yield the title compound as a clear oil (0.24 mg 55%).

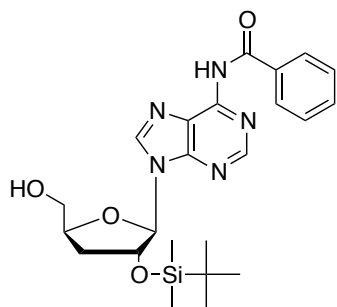
¹H NMR (500 MHz, CDCl₃) δ_H 8.80 (s, 1H, H8), 8.56 (s, 1H, H2), 5.98 (d, *J* = 1.0 Hz, 1H, H1'), 5.62-4.58 (m, 1H, H2'), 4.52-4.46 (m, 1H, H4'), 4.03 (dd, *J* = 11.7 Hz, 2.3 Hz, H5'), 3.67 (dd, *J* = 11.7 Hz, 2.3 Hz, H5), 2.21 (s, 6H, 2 x COCH₃), 2.18-2.11 (m, 1H, H3'), 1.77 (ddd, *J* = 13.05 Hz, 5.55 Hz, 1.90 Hz, 1H, H3'), 0.81 (s, 9H, *t*Bu), 0.79 (s, 9H, *t*Bu), 0.04 (s, 3H, CH₃), 0.01 (s, 3H, CH₃), 0.00 (s, 6H, CH₃).

[52d] 2',5'-Bis-*O*-*tert*-butyldimethylsilyl-bis-*N*⁶,*N*⁶-*tert*-butylcarbonyl-3'-deoxyadenosine

2',5'-Bis-*O*-(*tert*-butyldimethylsilyl)-3'-deoxyadenosine [25] (1.56 g, 3.25 mmol) was dissolved in THF (20 mL) and Boc₂O was added (2.83 g, 13.0 mmol), followed by DMAP (0.16 mg, 1.3 mmol). The mixture was stirred at room temperature overnight and was then diluted with *n*-Hex (20 mL) and washed with brine (3 x 15 mL). The collected

organics were dried over Na₂SO₄, filtered and evaporated. The title compound was obtained as a clear oil (2.21 g, 100%).

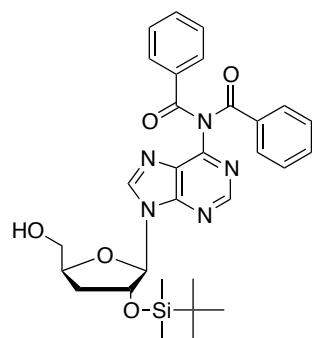
¹H NMR (500 MHz, CDCl₃) δ_H 8.68 (s, 1H, H8), 8.49 (s, 1H, H2), 5.95 (d, *J* = 1.4 Hz, 1H, H1'), 4.49-4.42 (m, 2H, H2', H4'), 4.00 (dd, *J* = 11.6 Hz, 2.5 Hz, H5'), 3.65 (dd, *J* = 11.6 Hz, 2.5 Hz, H5'), 2.15-2.08 (m, 1H, H3'), 1.74 (ddd, *J* = 13.0 Hz, 5.6 Hz, 2.1 Hz, 1H, H3'), 1.30 (s, 18H, Boc₂), 0.80 (s, 9H, *t*Bu), 0.76 (s, 9H, *t*Bu), 0.00 (s, 6H, CH₃), -0.01 (s, 3H, CH₃), -0.04 (s, 3H, CH₃).

[55a] 2'-*O*-*tert*-butyldimethylsilyl-*N*⁶-benzoyl-3'-deoxyadenosine

(2',5'-*O*-bis-*tert*-butyldimethylsilyl-*N*-benzoyl)cordycepin

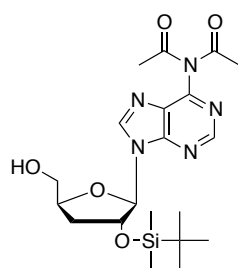
[54a] (0.56 g, 0.96 mmol) was stirred in a solution of trifluoroacetic acid, water and THF (0.5 mL:0.5 mL:2mL) for 5 hours in an ice-cold bath. The solution was carefully neutralised by dropwise addition of NaHCO₃ (saturated aqueous solution), the mixture was diluted with *n*-Hex (20 mL), washed with brine (2 x 20 mL); the organics were dried over Na₂SO₄, filtered and evaporated to give the product as a sticky solid (0.46 mg, 100%).²⁰⁸

¹H NMR (500 MHz, CDCl₃) δ_H 9.24 (br s, 1H, NH), 8.83 (s, 1H, H8), 8.13 (s, 1H, H2), 8.05 (d, *J* = 7.4 Hz, 2H, Ar), 7.63 (t, *J* = 8.9 Hz, 1H, Ar), 7.54 (t, *J* = 7.4 Hz, 2H, Ar), 5.74 (d, *J* = 5.5 Hz, 1H, H1'), 5.42 (d, *J* = 10.1 Hz, 1H, OH-5'), 5.03 (dd, *J* = 14.3, 6.5 Hz, 1H, H2'), 4.59-4.54 (m, 1H, H4'), 4.06-4.03 (m, 1H, H5'), 3.64-3.59 (m, 1H, H5'), 2.60-2.53 (m 1H, H3'), 2.55-2.16 (m, 1H, H3'), 0.81 (s, 9H, *t*Bu), -0.07(s, 3H, CH₃), -0.20 (s, 3H, CH₃).

[55b] 2'-*O*-*tert*-butyldimethylsilyl-bis-*N*⁶,*N*⁶-benzoyl-3'-deoxyadenosine

(2',5'-*O*-bis-*tert*-butyldimethylsilyl-bis-*N*⁶,*N*⁶-benzoyl) 3'-deoxyadenosine **[54b]** (1.22 g, 1.77 mmol) was stirred in a solution of trifluoroacetic acid, water and THF (1 mL:1 mL:4 mL) for 5 hours in an ice-cold bath. The solution was carefully neutralised by dropwise addition of aqueous NaHCO₃ (saturated solution), the mixture was diluted with *n*-Hex (20 mL), washed with brine (2 x 20 mL); the organics were dried over Na₂SO₄, filtered and evaporated to give the product as a sticky solid (0.88 g, 87%).

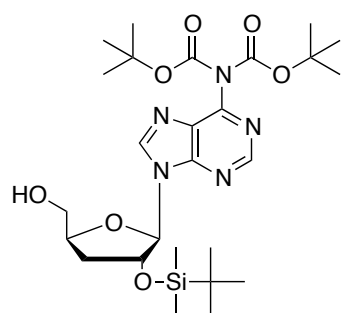
¹H NMR (500 MHz, CDCl₃) δ_H 8.68 (s, 1H, H8), 8.19 (s, 1H, H2), 7.88-7.86 (m, 4H, Ar), 7.52-7.50 (m, 2H, Ar), 7.40-7.36 (m, 4H, Ar), 5.73 (d, *J* = 5.5 Hz, 1H, H1'), 5.01-4.96 (m, 1H, H2'), 4.93-4.90 (m, 1H, OH-5'), 4.59-4.56 (m, 1H, H4'), 4.05-4.02 (m, 1H, H5'), 3.64-3.58 (m, 1H, H5'), 2.57-2.52 (m 1H, H3'), 2.24-2.18 (m, 1H, H3'), 0.82 (s, 9H, *t*Bu), -0.10 (s, 3H, CH₃), -0.23 (s, 3H, CH₃).

[55c] 2'-*O*-*tert*-butyldimethylsilyl-bis-*N*⁶,*N*⁶-acetyl-- 3'-deoxyadenosine

(2',5'-*O*-bis-*tert*-butyldimethylsilyl-bis-*N*⁶,*N*⁶-acetyl) 3'-deoxyadenosine **[54c]** (0.20 g, 0.35 mmol) was stirred in a solution of trifluoroacetic acid, water and THF (0.25 mL : 0.25 mL : 1 mL) for 5 hours in an ice-cold bath. The solution was carefully neutralised by dropwise addition of NaHCO₃ (saturated aqueous solution), the mixture was diluted with *n*-Hex (20 mL), washed with brine (2 x 20

mL); the organics were dried over Na₂SO₄, filtered and evaporated to give the product as a sticky solid (0.12 g, 75%).

¹H NMR (500 MHz, CDCl₃) δ_H 8.89 (s, 1H, H8), 8.61 (s, 1H, H2), 5.84 (d, *J* = 3.0 Hz, 1H, H1'), 4.80-4.76 (m, 1H, H2'), 4.58-4.49 (m, 1H, H4'), 4.06-4.02 (m, 1H, H5'), 3.77-3.68 (m, 1H, H5'), 2.38-2.31 (m, 1H, H3'), 2.23 (s, 6H, 2 x COCH₃), 2.08-2.01 (m, 1H, H3'), 0.81 (s, 9H, *t*Bu), 0.00 (s, 3H, CH₃), -0.09 (s, 3H, CH₃), -0.13 (s, 6H, CH₃).

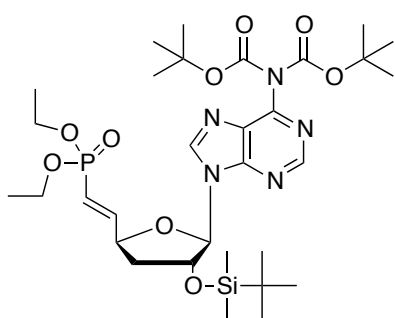
[55d] 2'-*O*-*tert*-butyldimethylsilyl-bis-*N*⁶,*N*⁶-*tert*-butylcarbonyl-3'-deoxyadenosine

2'-*O*-*tert*-butyldimethylsilyl-(bis-*N*⁶,*N*⁶-*tert*-butylcarbonate)-3'-deoxyadenosine **[54d]** (1.26 g, 1.85 mmol) was stirred in a mixture of TFA, H₂O and THF (1:1:4) at 0 °C for 5 hours. The mixture was then neutralised with solid NaHCO₃ and extracted with *n*-Hex (3 x 40 mL). The combined organic layers were dried over Na₂SO₄, filtered and the volatiles were

concentrated under *vacuum*. The residue was purified by silica gel column chromatography (EtOAc:*n*Hex = 1:1 v/v) to give the title compound as a sticky solid (0.70 g, 66%).

¹H NMR (500 MHz, CDCl₃) δ_H 8.80 (s, 1H, H8), 8.68 (s, 1H, H2), 5.77 (d, *J* = 4.0 Hz, 1H, H1'), 4.75-4.71 (m, 1H, OH-5'), 4.56-4.48 (m, 2H, H2', H4'), 4.01 (dd, *J* = 12.5 Hz, 2.0 Hz, 1H, H5'), 3.61 (dd, *J* = 12.5 Hz, 2.0 Hz, 1H, H5'), 2.04-1.97 (m 1H, H3'), 1.80-1.72 (m, 1H, H3'), 1.36 (s, 18H, 2 x *t*Bu Boc), 0.80 (s, 9H, *t*Bu), -0.09 (s, 3H, CH₃), -0.13 (s, 3H, CH₃).

[59] 9-[5',6'-Vinyl-6'-(bis-ethylphosphinyl)-2'-*O*-*tert*-butyldimethylsilyl-D-ribohexofuranosyl] bis-*N*⁶,*N*⁶-*tert*-butoxycarbonyl 3-deoxyadenosine

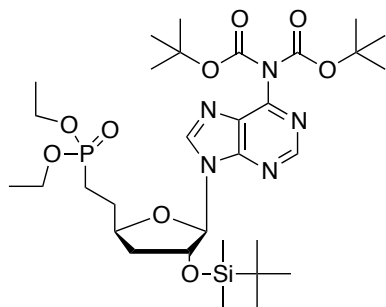


To a solution of 2'-*O*-*tert*-butyldimethylsilyl-(bis-*N*⁶,*N*⁶-*tert*-butoxycarbonyl)-3'-deoxyadenosine [**55d**] (0.50 g, 0.73 mmol) in CH₃CN (5 mL) was added 2-iodoxybenzoic acid (IBX) (1.2 g, 4.28 mmol). After stirring for 4 h at 80 °C, the reaction mixture was concentrated under reduced pressure and co-evaporated with THF. The residue was then dissolved in THF (10 mL) and filtered through a sintered funnel. The solution was concentrated under *vacuum* and dried under high vacuum for 1 h. Subsequently, the crude was dissolved in THF (10 mL) and a solution of tetraethyl methylenediphosphonate sodium salt (freshly prepared by addition, at 0 °C, of tetraethyl methylenediphosphonate (0.8 mL, 3.21 mmol) to a suspension of NaH (128 mg, 5.35 mmol) in THF (2 mL) and stirring for 10 min) was added dropwise at 0 °C. The reaction mixture was then stirred at room temperature for 12 h before addition of NH₄Cl (15 mL, saturated aqueous solution). The mixture was then extracted with EtOAc (3 x 10 mL). The combined organic layers were washed with water (2 x 10 mL) and brine (10 mL) and the resulting solution was dried over Na₂SO₄, filtered and concentrated under vacuum. The residue was purified by Biotage Isolera One (50g SNAP cartridge KP SIL 50 mL/min, gradient eluent system 16-100% EtOAc/nHex 7CV, 100% 5CV) to yield the title compound as a sticky solid (single *E* isomer, 0.29 g, 0.51 mmol).

³¹P NMR (202 MHz, CDCl₃) δ_P 17.15.

¹H NMR (500 MHz, CDCl₃) δ_H 8.71 (s, 1H, H8), 7.99 (s, 1H, H2), 6.90 (ddd, *J*_{HP} = 22.1 Hz, *J*_{HH} = 17.0, 4.6 Hz, 1H, H6'), 5.93 (d, *J* = 1.2 Hz, 1H, H1'), 5.91 (ddd, *J*_{HP} = 19.1 Hz, *J*_{HH} = 17.0, 1.4 Hz, 1H, H5'), 4.96-4.89 (m, 1H, H2'), 4.69-4.64 (m, 1H, H4'), 4.01-3.91 (m, 4H, 2 x CH₂CH₃), 2.09-2.03 (m, 1H, H3'), 2.02-1.95 (m, 1H, H3'), 1.33 (s, 18H, 2 x *t*Bu Boc₂), 1.22-1.17 (m, 6H, 2 x CH₂CH₃), 0.77 (s, 9H, *t*Bu), 0.00 (s, 3H, CH₃), -0.03 (s, 3H, CH₃).

[60] 9-[5',6'-Dideoxy-6'-(bis-ethylphosphinyl)-2'-*O*-*tert*-butyldimethylsilyl-D-ribo-hexofuranosyl] bis-*N*⁶,*N*⁶-*tert*-butoxycarbonyl 3'-deoxyadenosine



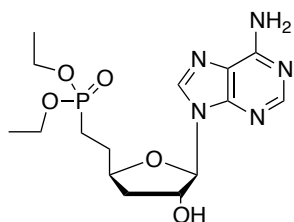
To a solution of 9-[5',6'-vinyl-6'-(bis-ethylphosphinyl)-2'-*O*-*tert*-butyldimethylsilyl-D-ribo-hexofuranosyl] bis-*N*⁶,*N*⁶-*tert*-butoxycarbonyl 3'-deoxyadenosine [**59**] (0.14 g, 0.20 mmol) was dissolved in a 1:1 mixture of EtOAc and EtOH (10 mL) under Argon atmosphere. To this solution, Pd/C (0.02 g, 10% Pd on activated carbon) was added, and the suspension was stirred under H₂ atmosphere for 1 hour

at room temperature. NaCl (0.02 g) was added and the mixture stirred for additional 15 minutes, and then filtered through a short pad of celite and washed with EtOH (10 mL x 3). The collected solution was concentrated under *vacuum* to yield the title compound as a sticky solid (107 mg, 93%).

³¹P NMR (202 MHz, CDCl₃) δ_P 31.03.

¹H NMR (500 MHz, CDCl₃) δ_H 8.75 (s, 1H, H8), 8.08 (s, 1H, H2), 5.88 (s, 1H, H1'), 4.76 (d, *J* = 4.5 Hz, 1H, H2'), 4.47-4.37 (m, 1H, H4'), 4.09-3.97 (m, 4H, 2 x CH₂CH₃), 2.03-1.71 (m, 6H, H3', H5', H6'), 1.38 (s, 18H, Boc₂), 1.25 (t, *J* = 7.0 Hz, 6H, 2 x CH₂CH₃), 0.81 (s, 9H, *t*Bu), 0.02 (s, 3H, CH₃), 0.00 (s, 3H, CH₃).

[61] 9-[5',6'-Dideoxy-6'-(bis-ethylphosphinyl)-3'-deoxy-D-ribo-hexofuranosyl] adenine



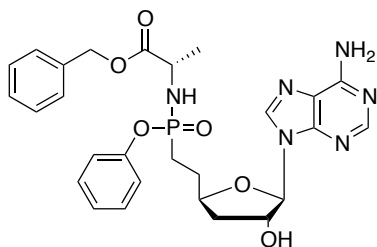
9-[5',6'-Dideoxy-6'-(bis-ethylphosphinyl)-2'-*O*-*tert*-butyldimethylsilyl-D-ribo-hexofuranosyl] bis-*N*⁶,*N*⁶-*tert*-butoxycarbonyl 3'-deoxyadenosine [**60**] (0.19 g, 0.27 mmol) was stirred in a solution of HCOOH and water (3/2 v/v, 5 mL) for 96 hours. The solution was evaporated under *vacuum* and the residue

purified via Biotage Isolera One (10 g ZIP cartridge KP-SIL, 36 mL/min, gradient eluent system 2-20% CH₃OH in CH₂Cl₂ 10CV, 20% 6CV) to yield the title compound as a white solid (0.10 g, 96%).

³¹P NMR (202 MHz, CDCl₃) δ_P 32.82.

¹H NMR (500 MHz, CDCl₃) δ_H 8.23 (s, 1H, H8), 8.20 (s, 1H, H2), 5.98 (d, *J* = 2.0 Hz, 1H, H1'), 4.82-4.79 (m, 1H, H2'), 4.52-4.46 (m, 1H, H4'), 4.14-4.04 (m, 4H, 2 x CH₂CH₃), 2.24-2.15 (m, 2H, H3'), 2.06-1.83 (m, 4H, H5', H6'), 1.31 (t, *J* = 7 Hz, 6H, 6H, 2 x CH₂CH₃).

[64] 9-[5',6'-Dideoxy-6'-(phenyloxy-(benzyloxy-L-alanin-N-yl-phosphinyl)-3'-deoxy)-D-ribo-hexofuranosyl] adenine



9-[5',6'-Dideoxy-6'-(bis-ethylphosphinyl)-3'-deoxy-D-ribo-hexofuranosyl] adenine [**61**] (0.06 g, 0.15 mmol) was dissolved in CH₃CN (6 mL) under Argon atmosphere, and 2,6-lutidine (55 μL, 0.47 mmol) was added to the solution, followed by TMSBr (62 μL, 0.47 mmol), and the mixture was stirred at 0 °C for 3 hours. The solvents were removed

under reduced pressure without any contact with air. The residue was dissolved in anhydrous Et₃N (0.31 mL) and pyridine (1.25 mL) and L-alanine benzyl ester HCl salt was added (0.05 g, 0.16 mmol) along with phenol (0.09 mg, 0.94 mmol). In a separated flask, aldrithiol-2 (0.21 g, 0.93 mmol) and Ph₃P (0.24 g, 0.93 mmol) were dissolved in pyridine (1.56 mL) and this solution was immediately added to the reaction. The resulting mixture was stirred at 50 °C for 16 h, then cooled to room temperature and the solvent evaporated. The residue was dissolved in CH₂Cl₂ (20 mL) and washed with HCl (aqueous solution, 0.5N, 5 mL x 3), the organics collected, dried over Na₂SO₄, filtered and evaporated. The crude was purified by Biotage Isolera One (10 g SNAP cartridge KP-SIL, 36 mL/min, gradient eluent system 2-16% CH₃OH in CH₂Cl₂ in 25 CV), and preparative HPLC (20 mL/min, isocratic eluent system 55% CH₃OH in water, 30 minutes), to afford the title compound as a white solid (0.002 g, 2%).

³¹P NMR (202 MHz, CDCl₃) δ_P 34.21, 33.56.

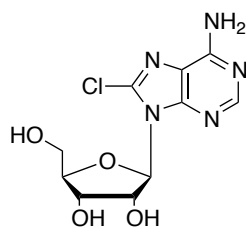
¹H NMR (500 MHz, CDCl₃) δ_H 8.13-8.09 (m, 2H, H8, H2), 7.26-7.17 (m, 7H, Ar), 7.11-7.03 (m, 3H, Ar), 5.89-5.87 (m, 1H, H1'), 5.02 (AB q, J_{AB} = 12.3 Hz, Δδ_{AB} = 0.03, 1H, CH₂Ph), 4.94 (s, 1H, CH₂Ph), 4.68-4.63 (m, 1H, H2'), 4.40-4.33 (m, 1H, H4'), 3.95-3.87 (m, 1H, CHCH₃ L-Ala), 2.11-1.84 (m, 6H, H3', H5', H6'), 1.19-1.08 (m, 3H, CHCH₃ L-Ala).

MS (ES+) m/z found 589.2 [M+Na⁺], 566.2 [M+H⁺], C₃₀H₃₀ClN₆O₈P required m/z 566.5 [M].

HPLC Reverse-phase HPLC eluting with CH₃CN/H₂O from 90/10 to 0/100 in 35 minutes, F = 1 mL/min, λ = 254 nm, two peaks with t_R 13.37 min, t_R 13.53 min.

9.5.11 Synthesis of 8-chloroadenosine

[67] 8-Chloroadenosine



Adenosine (1.97 g, 7.37 mmol) was suspended in DMF (20 mL) and BzCl (0.9 mL, 7.7 mmol) was added. *m*CPBA (70-75%, 2.03 g, 8.6 mmol) was dissolved in DMF (10 mL) and added dropwise. The reaction mixture was stirred at rt for 20 min before it was poured into ice-cold water (100 mL) and filtered. The filtrate was extracted with Et₂O (3 x 100 mL). The combined aqueous phases were evaporated under vacuum to give an oil. The oil was absorbed on silica and purified by silica gel CC (packed in 5% CH₃OH /CHCl₃, eluted with 7% CH₃OH /CHCl₃) to yield the title compound as a white solid (0.53 g, 24%).

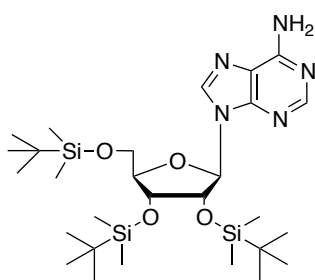
[Alternative procedure-1] Adenosine (1.09g, 4.08 mmol) was suspended in DMF (50 mL) and glacial acetic acid (10 mL) was added. A solution of *N*-chlorosuccinimide (2 g, 15 mmol) in DMF (15 mL) was added dropwise. The reaction mixture was stirred at rt for 48 hours and the volatiles were evaporated *in vacuo* to give a yellow gum. The crude was absorbed on silica and purified by silica gel CC (packed in 5% CH₃OH /CHCl₃, eluted with 7% CH₃OH/CHCl₃) to yield the title compound as a white powder (0.65 g, 52%).³⁴⁴

[Alternative procedure-2] 2'-3',5'-tri-*O*-*tert*-butyldimethylsilyl 8-chloroadenosine [70] (1.0 g, 1.55 mmol) was dissolved in THF (10 mL) and the solution was cooled down to 0 °C. TFA (2.5 mL) was diluted with water (2.5 mL) and the solution was added dropwise to the initial mixture. The reaction was stirred at rt for 36 hours. The solvent was evaporated and the crude was absorbed on silica and purified by silica gel CC (packed in 5% CH₃OH /CHCl₃, eluted with 7% CH₃OH /CHCl₃) to yield the title compound as a white powder (0.31 g, 64%).

Melting point: 188-189 °C (Lit. mp: 189-191 °C).⁴⁷¹

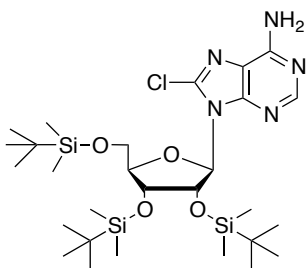
¹H NMR (500 MHz, DMSO-*d*6) δ_H 8.16 (s, 1H, H₂), 7.55 (br s, 2H, NH₂), 5.86 (d, *J* = 6.8 Hz, 1H, H1'), 5.48 (d, *J* = 6.2 Hz, 1H, 2'-OH), 5.45 (d, *J* = 4.0 Hz, 1H, 5'-OH), 5.23 (d, *J* = 4.6 Hz, 1H, 3'-OH), 5.08-5.06 (m, 1H, H2'), 4.23-4.18 (m, 1H, H3'), 4.01-3.96 (m, 1H, H4'), 3.72-3.65 (m, 1H, H5'), 3.57-3.50 (m, 1H, H5').

¹³C NMR (126 MHz, DMSO-*d*6) δ_C 156.2 (C6), 152.3 (C2), 149.6 (C4), 137.0 (C8) 117.9 (C5), 89.2 (C1'), 86.7 (C4'), 71.2 (C2'), 70.77 (C3'), 62.0 (C5').

[69] 2',3',5'-Tri-*O*-*tert*-butyldimethylsilyl-D-ribo-hexofuranosyl-adenosine

Adenosine (10.0 g, 37.42 mmol) was dissolved in DMF (60 mL) and TBDMSCl (24.8 g, 149.7 mmol), imidazole (22.4 g, 329.3 mmol) and DMAP (1.83 g, 14.97 mmol) were added. The mixture was stirred at rt for 16 hours, then the solution was evaporated under *vacuum* and the mixture was suspended in *n*-hexane (250 mL) and washed with aqueous NH₄Cl (saturated solution, 2 x 150 mL) and brine (1 x 150 mL). The organic were collected, dried over Na₂SO₄, filtered off and evaporated to yield the title compound as a sticky solid (22.83 g, 100%).⁴⁷¹

¹H NMR (CDCl₃, 500 MHz) δ_H 8.23 (s, 1H, H8), 8.03 (s, 1H, H2), 5.90 (d, *J* = 5.0 Hz, 1H, H1'), 5.46 (br s, 2H, NH₂), 4.59 (t, *J* = 4.5 Hz, 1H, H2'), 4.22 (t, *J* = 3.5 Hz, 1H, H3'), 4.03-3.99 (m, 1H, H4'), 3.92 (dd, *J* = 11.5, 4.5 Hz, 1H, H5'), 3.68 (dd, *J* = 11.0, 3.0 Hz, 1H, H5'), 0.846 (s, 9H, *t*Bu), 0.826 (s, 9H, *t*Bu), 0.68 (s, 9H, *t*Bu), 0.02 (s, 3H, CH₃), 0.02 (s, 3H, CH₃), 0.00 (s, 3H, CH₃), -0.05 (s, 3H, CH₃), -0.15 (s, 3H, CH₃), -0.33 (s, 3H, CH₃).

[70] 2',3',5'-tri-*O*-*tert*-butyldimethylsilyl-D-ribo-hexofuranosyl-8-chloroadenosine

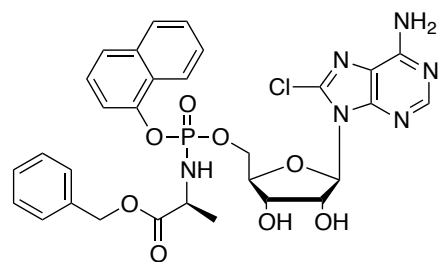
To a stirring solution of LDA (2M in THF, 93.55 mL, 187.1 mmol) in a -78 °C bath was added a solution of 2',3',5'-tri-*O*-*tert*-butyldimethylsilyl-D-ribo-hexofuranosyl-adenosine [69] (22.83 g, 37.42 mmol) in THF (15 mL) dropwise via a dropping funnel. The funnel was washed with THF (5 mL) and the reaction was stirred for 1 hour at -78 °C. A solution of TsCl (28.54 g, 149.68 mmol) in THF (20 mL) was added dropwise, then the funnel rinsed with THF (5 mL). The reaction was stirred for 1 hour and then quenched by dropwise addition of glacial AcOH (10 mL). The mixture was allowed to reach room temperature and evaporated. The crude was dissolved in *n*-hexane (50 mL) and washed with brine (3 x 50 mL). The organic phase was dried over Na₂SO₄, filtered and evaporated. The crude was purified by Biotage Isolera flash chromatography (100g SNAP cartridge KP SIL, eluent system 3-30% EtOAc/*n*Hex 10 CV, 30% AcOEt/*n*Hex 4 CV) to yield the title compound as a clear oil (17.84 g, 74%).³⁵⁰

¹H NMR (CDCl₃, 500 MHz) δ_H 8.11 (s, 1H, H2), 5.79 (d, *J* = 5.5 Hz, 1H, H1'), 5.34-5.28 (m, 2H, H4', H5'), 4.42-4.40 (dd, *J* = 4, 2.4 Hz, 1H, H3'), 3.94-3.87 (m, 2H, H4', H5'), 3.59-3.54 (m, 1H, H5'), 0.80 (s, 9H, *t*Bu), 0.68 (s, 9H, *t*Bu), 0.63 (s, 9H, *t*Bu), 0.003 (s, 3H, CH₃),

0.00 (s, 3H, CH₃), -0.13 (s, 3H, CH₃), -0.16 (s, 3H, CH₃), -0.21 (s, 3H, CH₃), -0.484 (s, 3H, CH₃).

9.5.12 Synthesis of 8-chloroadenosine ProTides

[71a] 8-chloroadenosine-5'-naphth-1-yl(benzyloxy-L-alaninyl) phosphate



Prepared according to the general procedure **F₁** using 8-chloroadenosine [**67**] (0.10 g, 0.33 mmol) in THF (7 mL), *t*BuMgCl (1.1 M in THF, 0.36 mL, 0.36 mmol), naphth-1-yl-(benzyloxy-L-alaninyl)phosphorochloridate [**17a**] (0.42 g, 1.04 mmol) in THF (3 mL). The crude was purified first by silica gel CC (0-6% CH₃OH/CH₂Cl₂) and secondly by prep. TLC (5% CH₃OH/CH₂Cl₂) to yield the title compound as a white solid (0.037 g, 17%).

³¹P NMR (202 MHz, CD₃OD) δ_P 3.82, 3.94.

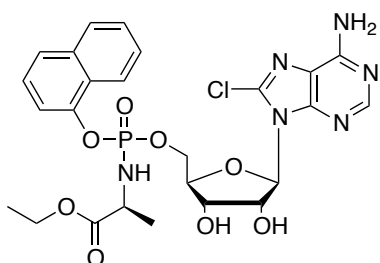
¹H NMR (500 MHz, CD₃OD) δ_H 8.12-8.03 (m, 3H, H₂, Ar), 7.81-7.83 (m, 1H, Ar), 7.66-7.61 (m, 1H, Ar), 7.52-7.18 (m, 8H, Ar) 6.05-6.01 (m, 1H, H1'), 5.35-5.31 (m, 0.5H, H2'), 5.30-5.26 (m, 0.5 H, H-2'), 5.05-4.91 (m, 2H, CH₂Ph), 4.69-4.63 (m, 1H, H3'), 4.53-4.45 (m, 1H, H5') 4.43-4.34 (m, 1H, H5'), 4.26-4.20 (m, 1H, H4'), 4.08-4.00 (m, 0.5H, CHCH₃ L-Ala), 3.97-3.89 (m, 0.5H, CHCH₃ L-Ala), 1.28-1.14 (m, 3H, CHCH₃ L-Ala).

¹³C NMR (125 MHz, CD₃OD) δ_C 174.70 (d, ³J_{C-P} = 5.0 Hz, C=O), 174.60 (d, ³J_{C-P} = 5.0 Hz, C=O), 156.24 (C6), 156.22 (C6), 154.11 (C2), 154.01 (C-2), 151.62 (C4), 151.58 (C4), 147.94 (C8), 147.88 (C8) 139.82 (C-Ar), 139.76 (C-Ar), 137.17 (C-Ar), 137.12 (C-Ar), 136.19 (C-Ar), 129.54 (CH-Ar), 129.46 (CH-Ar), 129.27 (CH-Ar), 129.22 (CH-Ar), 129.17 (CH-Ar), 129.14 (CH-Ar), 128.82 (CH-Ar), 128.78 (CH-Ar), 127.84 (d, ²J_{C-P} = 6.2 Hz, C-Ar), 127.78 (d, ²J_{C-P} = 6.2 Hz, C-Ar), 127.75 (CH-Ar), 127.71 (CH-Ar), 127.39 (CH-Ar), 127.36 (CH-Ar), 126.42 (CH-Ar), 125.88 (CH-Ar), 122.79 (CH-Ar), 122.62 (CH-Ar), 119.53 (C5), 116.23 (d, ³J_{C-P} = 2.5 Hz, CH-Ar), 116.08 (d, ³J_{C-P} = 2.5 Hz, CH-Ar), 91.40 (C1'), 91.31 (C1'), 84.34 (d, ³J_{C-P} = 8.0 Hz, C4'), 84.22 (d, ³J_{C-P} = 8.0 Hz, C4'), 72.78 (C2'), 72.65 (C2'), 71.66 (C3'), 71.14 (C3'), 67.96 (C5', CH₂Ph), 67.87 (C5', CH₂Ph), 67.80 (C5', CH₂Ph), 67.15 (C5', CH₂Ph), 67.11 (C5', CH₂Ph), 51.63 (CHCH₃ L-Ala), 51.56 (CHCH₃ L-Ala), 20.48 (d, ³J_{C-P} = 6.2 Hz, CHCH₃ L-Ala), 20.28 (d, ³J_{C-P} = 6.2 Hz, CHCH₃ L-Ala).

MS (ES⁺) m/z found 691.16 [M+Na⁺], 707.13 [M+K⁺], C₃₀H₃₀ClN₆O₈P required m/z 669.02 [M].

HPLC Reverse-phase HPLC eluting with CH₃CN/H₂O from 90/10 to 0/100 in 35 minutes, F = 1 mL/min, λ = 254 nm, two peaks with t_R 16.48 min, t_R 17.07 min.

[71b] 8-chloroadenosine-5'-naphth-1-yl(ethoxy-L-alaninyl) phosphate



Prepared according to the general procedure F₁ using 8-chloroadenosine [67] (0.10 g, 0.33 mmol) in THF (7 mL), *t*BuMgCl (1.1 M in THF, 0.36 mL, 0.36 mmol), naphth-1-yl-(ethoxy-L-alaninyl) phosphorochloridate [17b] (0.35 g, 1.04 mmol) in THF (3 mL). The crude was purified first by silica gel CC (0-5% CH₃OH/CH₂Cl₂) and secondly by prep. TLC (10% CH₃OH/CH₂Cl₂) to yield the title compound as a white solid (0.015 g, 7%).

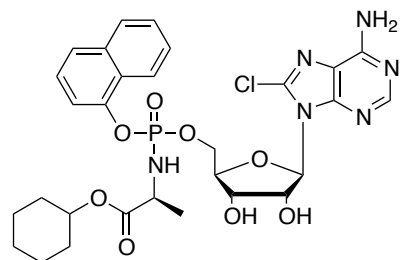
³¹P NMR (202 MHz, CD₃OD) δ_P 3.98, 3.80.

¹H NMR (500 MHz, CD₃OD) δ_H 8.12 (s, 0.5H, H2) 8.11-8.07 (m, 1H, Naph) 8.05 (s, 0.5 H, H2), 7.87-7.84 (m, 1H, Nap), 7.67 (d, *J* = 8.1 1H, Nap), 7.54-7.31 (m, 6H, Nap), 6.05-6.02 (m, 1H, H1'), 5.36-5.32 (m, 0.5H, H2'), 5.31-5.28 (m, 0.5H, H2'), 4.72-4.66 (m, 1H, H-3'), 4.55-4.49 (m, 1H, H5') 4.46-4.37 (m, 1H, H5'), 4.28-4.22 (m, 1H, H4'), 4.06-3.91 (m, 2.5H, CHCH₃ L-Ala, CH₂CH₃ Et), 3.87-3.79 (m, 0.5H, CHCH₃ L-Ala), 1.28-1.25 (m, 1H, CHCH₃ L-Ala), 1.19-1.08 (m, 5H, CHCH₃ L-Ala, CH₂CH₃ Et).

¹³C NMR (125 MHz, CD₃OD) δ_C 174.97 (d, ³*J*_{C-P} = 4.9 Hz, C=O), 174.80 (d, ³*J*_{C-P} = 4.9 Hz, C=O), 156.28 (C-6), 154.09 (C2), 154.01 (C2), 151.63 (C4), 151.60 (C4), 147.98 (C8), 147.92 (C8), 139.82 (C-Ar), 139.79 (C-Ar), 136.22 (C-Ar), 128.81 (C-Ar), 128.79 (C-Ar), 127.83 (C-Ar), 127.78 (C-Ar), 127.72 (CH-Ar), 127.36 (CH-Ar), 127.34 (CH-Ar), 126.43 (CH-Ar), 126.39 (CH-Ar), 125.82 (CH-Ar), 122.73 (CH-Ar), 122.62 (CH-Ar), 119.53 (C5), 116.06 (CH-Ar), 116.04 (CH-Ar), 91.42 (C1'), 91.35 (C1'), 84.34 (d, ³*J*_{C-P} = 8.1 Hz, C4'), 84.23 (d, ³*J*_{C-P} = 8.0 Hz, C4'), 72.76 (C2'), 72.67 (C2'), 71.64 (C3'), 71.14 (C3'), 67.80 (d, ²*J*_{C-P} = 5.2 Hz, C5'), 67.09 (d, ²*J*_{C-P} = 5.2 Hz, C5'), 62.36 (CH₂CH₃ Et), 62.23 (CH₂CH₃ Et), 51.55 (CHCH₃ L-Ala), 51.45 (CHCH₃ L-Ala), 20.54 (d, ³*J*_{C-P} = 7.0 Hz, CHCH₃ L-Ala), 20.33 (d, ³*J*_{C-P} = 7.0 Hz, CHCH₃ L-Ala), 14.39 (CH₂CH₃ Et).

MS (ES+) m/z found 629.14 [M+Na⁺], 645.11 [M+K⁺], C₂₅H₂₈ClN₆O₈P required m/z 606.95 [M].

HPLC Reverse-phase HPLC eluting with H₂O/CH₃CN from 90/10 to 0/100 in 35 minutes, F = 1 mL/min, λ = 254 nm, two peaks with t_R 14.43 min, t_R 13.73 min.

[71c] 8-chloroadenosine-5'-naphth-1-yl(cyclohexyloxy-L-alaninyl) phosphate

Prepared according to the general procedure **F₁** using 8-chloroadenosine [**67**] (0.10 g, 0.33 mmol) in THF (7 mL), *t*BuMgCl (1.1 M in THF, 0.36 mL, 0.36 mmol), naphth-1-yl-(cyclohexyloxy-L-alaninyl) phosphorochloridate [**17c**] (0.41 g, 1.04 mmol) in THF (3 mL). The crude was purified first by silica gel CC (0-5% CH₃OH/CH₂Cl₂) and secondly by prep. TLC (10% CH₃OH/CH₂Cl₂) to yield the title compound as a white solid (0.02 g, 9%).

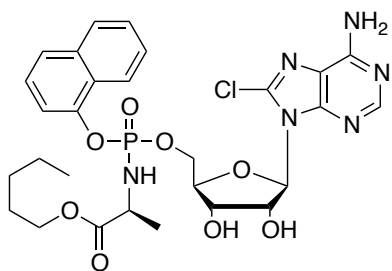
³¹P NMR (202 MHz, CD₃OD) δ_P 3.93, 3.90.

¹H NMR (500 MHz, CD₃OD) δ_H 8.13 (s, 0.5H, H2) 8.11-8.07 (m, 1H, Nap), 8.06 (s, 0.5 H, H2), 7.83 (d, *J* = 8.3 Hz, 1H, Nap), 7.64 (d, *J* = 8.3 Hz, 1H, Nap), 7.52–7.39 (m, 3H, Nap), 7.37–7.30 (m, 1H, Nap), 6.06–6.02 (m, 1H, H1'), 5.35-5.31 (m, 0.5H, H2'), 5.30-5.27 (m, 0.5 H, H2'), 4.70-4.65 (m, 1H, H3'), 4.65-4.38 (m, 3H, H5', CH(CH₂)₅ cHex), 4.29-4.23 (m, 1H, H4'), 4.00-3.92 (m, 0.5H, CHCH₃ L-Ala), 3.91-3.83 (m, 0.5H, CHCH₃ L-Ala), 1.79-1.13 (m, 13H, CHCH₃ L-Ala, CH(CH₂)₅ cHex).

¹³C NMR (125 MHz, CD₃OD) δ_C 174.44 (d, ³*J*_{C-P} = 5.1 Hz, C=O), 174.28 (d, ³*J*_{C-P} = 5.1 Hz, C=O), 156.24, (C6), 154.10 (C2), 154.03 (C2), 151.64 (C4), 151.59 (C4), 147.98 (C8), 147.93 (C8), 139.80 (C-Ar), 139.76 (C-Ar), 136.21 (C-Ar), 128.81 (C-Ar), 127.82 (CH-Ar), 127.77 (CH-Ar), 127.72 (CH-Ar), 127.36 (CH-Ar), 127.34 (CH-Ar), 126.44 (CH-Ar), 125.83 (CH-Ar), 122.76 (CH-Ar), 122.64 (CH-Ar), 119.51 (C5), 116.07 (d, ³*J*_{C-P} = 2.5 Hz, CH-Ar), 116.03 (d, ³*J*_{C-P} = 2.5 Hz, CH-Ar), 91.42 (C1'), 91.28 (C1'), 84.36 (d, ³*J*_{C-P} = 8.0 Hz, C4'), 84.30 (d, ³*J*_{C-P} = 8.0 Hz, C4'), 74.96 (CH(CH₂)₅ cHex), 74.93 (CH(CH₂)₅ cHex), 72.81 (C2'), 72.66 (C2'), 71.70 (C3'), 71.27 (C3'), 67.87 (d, ²*J*_{C-P} = 5.6 Hz, C5'), 67.27 (d, ²*J*_{C-P} = 5.6 Hz, C5'), 51.71 (CHCH₃ L-Ala), 51.69 (CHCH₃ L-Ala), 32.44 (CH(CH₂)₅ cHex), 32.41 (CH(CH₂)₅ cHex), 32.37 (CH(CH₂)₅ cHex), 32.32 (CH(CH₂)₅ cHex), 32.30 (CH(CH₂)₅ cHex), 26.37 (CH(CH₂)₅ cHex), 26.34 (CH(CH₂)₅ cHex), 24.63 (CH(CH₂)₅ cHex), 24.59 (CH(CH₂)₅ cHex) 20.73 (d, ³*J*_{C-P} = 6.3 Hz, CHCH₃ L-Ala), 20.53 (d, ³*J*_{C-P} = 6.3 Hz, CHCH₃ L-Ala).

MS (ES⁺) *m/z* found 683.19 [M+Na⁺], 699.17 [M+K⁺], C₂₉H₃₄ClN₆O₈P required *m/z* 660.19 [M].

HPLC Reverse-phase HPLC eluting with H₂O/CH₃CN from 90/10 to 0/100 in 35 minutes, F = 1 mL/min, λ = 254 nm, two peaks with t_R 17.36 min, t_R 17.93 min.

[71d] 8-chloroadenosine-5'-naphth-1-yl(pentyl-1-oxy-L-alanyl) phosphate

Prepared according to the general procedure **F₁** using 8-chloroadenosine [**67**] (0.10 g, 0.33 mmol) in THF (7 mL), *t*BuMgCl (1.1 M in THF, 0.36 mL, 0.36 mmol), naphth-1-yl-(pentyl-1-oxy-L-alanyl) phosphorochloridate [**17d**] (0.40 g, 1.04 mmol) in THF (3 mL). The crude was purified first by silica gel CC (0-5% CH₃OH/CH₂Cl₂) and

secondly by prep. TLC (10% CH₃OH/CH₂Cl₂) to yield the title compound as a white solid (0.009 g, 4%).

³¹P-NMR (202 MHz, CD₃OD) δ_P 3.88, 3.89.

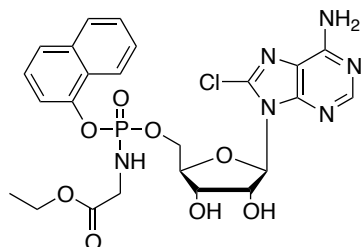
¹H-NMR (500 MHz, CD₃OD) δ_H 8.13 (s, 0.5H, H₂) 8.12-8.09 (m, 1H, Nap), 8.06 (s, 0.5 H, H₂), 7.88-7.85 (m, 1H, Nap), 7.68 (d, *J* = 8.2 Hz, 1H, Nap), 7.55-7.48 (m, 2H, Nap), 7.45-7.33 (m, 2H, Nap), 6.04 (d, *J* = 4.7 Hz, 0.5H, H₁'), 6.03 (d, *J* = 4.7 Hz, 0.5H, H₁'), 5.36-5.32 (m, 0.5H, H₂'), 5.30-5.27 (m, 0.5 H, H₂'), 4.69-4.64 (m, 1H, H₃'), 4.55-4.49 (m, 1H, H₅'), 4.45-4.36 (m, 1H, H₅'), 4.27-4.22 (m, 1H, H₄'), 4.02-3.83 (m, 3H, CHCH₃ L-Ala, CH₂CH₂CH₂CH₂CH₃ *n*-Pen), 1.55-1.46 (m, 2H, CHCH₃ L-Ala), 1.32-1.16 (m, 7H, CHCH₃ L-Ala, CH₂CH₂CH₂CH₂CH₃ *n*-Pen), 0.86 (t, *J* = 6.9 Hz, 1.5H, CH₂CH₂CH₂CH₂CH₃ *n*-Pen), 0.82 (t, *J* = 6.9 Hz, 1.5H, CH₂CH₂CH₂CH₂CH₃ *n*-Pen).

¹³C-NMR (125 MHz, CD₃OD) δ_C 175.04 (d, ³*J*_{C-P} = 5.0 Hz, C=O), 174.86 (d, ³*J*_{C-P} = 5.0 Hz, C=O), 156.29 (C₆), 154.09 (C₂), 154.01 (C₂), 151.65 (C₄), 151.61 (C₄), 147.98 (C₈), 147.92 (C₈), 139.82 (C-Ar), 139.77 (C-Ar), 136.23 (C-Ar), 128.82 (CH-Ar), 128.79 (CH-Ar), 127.85 (C-Ar), 127.80 (C-Ar), 127.71 (C-Ar), 127.36 (CH-Ar), 126.33 (CH-Ar), 126.43 (CH-Ar), 126.42 (CH-Ar), 126.40 (CH-Ar), 125.83 (CH-Ar), 122.77 (CH-Ar), 122.64 (CH-Ar), 119.54, (C₅), 116.11 (d, ³*J*_{C-P} = 2.5 Hz, CH-Ar), 116.03 (d, ³*J*_{C-P} = 2.5 Hz, CH-Ar), 91.42 (C₁'), 91.32 (C₁'), 84.36 (d, ³*J*_{C-P} = 8.2 Hz, C₄'), 84.27 (d, ³*J*_{C-P} = 8.2 Hz, C₄'), 72.75 (C₂'), 72.62 (C₂'), 71.66 (C₃'), 71.16 (C₃'), 67.81 (d, ²*J*_{C-P} = 4.8 Hz, C₅'), 67.11, (d, ²*J*_{C-P} = 4.8 Hz, C₅'), 66.43 (CH₂CH₂CH₂CH₂CH₃ *n*-Pen), 66.31 (CH₂CH₂CH₂CH₂CH₃ *n*-Pen), 51.58 (CHCH₃ L-Ala), 51.52 (CHCH₃ L-Ala), 30.76 (CH₂CH₂CH₂CH₂CH₃ *n*-Pen), 30.47 (CH₂CH₂CH₂CH₂CH₃ *n*-Pen), 29.29 (CH₂CH₂CH₂CH₂CH₃ *n*-Pen), 29.07 (CH₂CH₂CH₂CH₂CH₃ *n*-Pen), 23.73 (CH₂CH₂CH₂CH₂CH₃ *n*-Pen), 23.31 (CH₂CH₂CH₂CH₂CH₃ *n*-Pen), 20.56 (d, ³*J*_{C-P} = 7.2 Hz, CHCH₃ L-Ala), 20.37 (d, ³*J*_{C-P} = 7.2 Hz, CHCH₃ L-Ala), 14.25 (CH₂CH₂CH₂CH₂CH₃ *n*-Pen), 14.22 (CH₂CH₂CH₂CH₂CH₃ *n*-Pen).

MS (ES⁺) *m/z* found 671.19 [M+Na⁺], 687.16 [M+K⁺], C₂₈H₃₄ClN₆O₈P required *m/z* 649.03 [M].

HPLC Reverse-phase HPLC eluting with H₂O/CH₃CN from 90/10 to 0/100 in 35 minutes, F = 1 mL/min, λ = 254 nm, two peaks with tR 18.44 min, tR 17.79 min.

[71e] 8-chloroadenosine-5'-naphth-1-yl(ethoxyglycyl) phosphate



Prepared according to the general procedure **F₁** using 8-chloroadenosine [**67**] (0.10 mg, 0.33 mmol) in THF (7 mL), *t*BuMgCl (1.1 M in THF, 0.36 mL, 0.36 mmol), naphth-1-yl(ethoxyglycyl) phosphorochloridate [**17i**] (0.43 g, 1.33 mmol) in THF (3 mL). The crude was purified first by silica gel CC (0-6% CH₃OH/CH₂Cl₂) and secondly by prep. TLC (5% CH₃OH/CH₂Cl₂) to yield a white solid (0.007 g, 4 %).

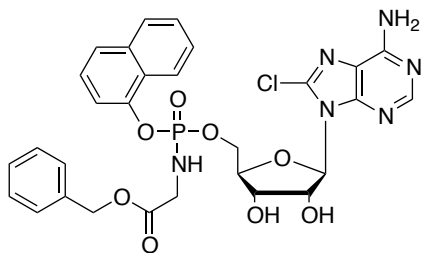
³¹P NMR (202 MHz, CD₃OD) δ_P 4.96, 4.94.

¹H NMR (500 MHz, CD₃OD) δ_H 8.15-8.07 (m, 1.5H, H₂, H₈ Nap) 8.05 (s, 0.5 H, H₂), 7.89-7.85 (m, 1H, H₅ Nap), 7.69-7.66 (m, 1H, H₄ Nap), 7.55-7.33 (m, 4H, H₂, H₆, H₇, H₃ Nap), 6.04 (d, *J* = 5.1 Hz, 0.5H, H_{1'}), 6.02 (d, *J* = 5.1 Hz, 0.5H, H_{1'}), 5.35-5.29 (m, 1H, H_{2'}), 4.69-4.66 (m, 0.5H, H_{3'}), 4.64-4.61 (m, 0.5H, H_{3'}), 4.56-4.50 (m, 1H, H_{5'}), 4.49-4.43 (m, 1H, H_{5'}), 4.27-4.22 (m, 1H, H_{4'}), 4.10-4.00 (m, 2H, CH₂CH₃ Et), 3.73-3.62 (m, 2H, CH₂ Gly), 1.21-1.13 (m, 3H, CH₂CH₃ Et).

¹³C NMR (125 MHz, CD₃OD) δ_C 175.02 (d, ³*J*_{C-P} = 3.7 Hz, C=O), 174.92 (d, ³*J*_{C-P} = 3.7 Hz, C=O), 156.99 (C₆), 154.02 (C₂), 153.99 (C₂), 151.30 (C₄), 151.22 (C₄), 147.42 (C₈), 147.36 (C₈), 139.82 (C-Ar), 139.75 (C-Ar), 136.19 (C-Ar), 128.44 (C-Ar), 128.36 (C-Ar), 127.80 (C-Ar), 127.75 (C-Ar), 127.67 (CH-Ar), 127.36 (CH-Ar), 127.32 (CH-Ar), 126.45 (CH-Ar), 126.32 (CH-Ar), 125.79 (CH-Ar), 122.71 (CH-Ar), 122.62 (CH-Ar), 119.51 (C₅), 116.05 (CH-Ar), 116.02 (CH-Ar), 91.40 (C_{1'}), 91.35 (C_{1'}), 84.25 (d, ³*J*_{C-P} = 7.6 Hz, C_{4'}), 84.22 (d, ³*J*_{C-P} = 7.6 Hz, C_{4'}), 72.72 (C_{2'}), 72.67 (C_{2'}), 71.64 (C_{3'}), 71.39 (C_{3'}), 67.78 (d, ²*J*_{C-P} = 5.0 Hz, C_{5'}), 67.09 (d, ²*J*_{C-P} = 5.0 Hz, C_{5'}), 62.35 (CH₂CH₃ Et), 62.29 (CH₂CH₃ Et), 44.02 (CHCH₃ L-Ala), 43.88 (CH₂ Gly), 14.22 (CH₂CH₃ Et).

MS (ES⁻) *m/z* found 591.10 [M-H⁺], 627.08 [M+Cl⁻], C₂₄H₂₆ClN₆O₈P required *m/z* 592.93 [M].

HPLC Reverse-phase HPLC eluting with H₂O/CH₃CN from 90/10 to 0/100 in 35 minutes, F = 1 ml/min, λ = 254 nm, two peaks with tR 13.88, tR 13.92.

[71f] 8-chloroadenosine-5'-naphth-1-yl(benzyloxy-glyciny) phosphate

Prepared according to the general procedure **F₁** using 8-chloroadenosine [67] (0.15 g, 0.50 mmol) in THF (10 mL), *t*BuMgCl (1.0 M in THF, 0.55 mL, 0.55 mmol), naphth-1-yl-(benzyloxy-glyciny) phosphorochloridate [17j] (0.78 g, 2 mmol) in THF (5 mL). The crude was purified first by silica gel CC (0-6% CH₃OH/CH₂Cl₂)

and secondly by prep. TLC (5% CH₃OH/CH₂Cl₂) to yield the title compound as a white powder (0.023 g, 7%).

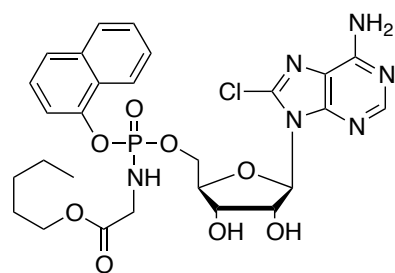
³¹P NMR (202 MHz, CD₃OD) δ_P 4.93.

¹H NMR (500 MHz, CD₃OD) δ_H 8.13-8.06 (m, 1.5H, H2, H8 Nap), 8.05 (s, 0.5H, H2), 7.87-7.84 (m, 1H, H5 Nap), 7.68-7.64 (m, 1H, H4 Nap), 7.53-7.26 (m, 9H, H2, H6, H7, H3 Nap, Ph), 6.04 (d, *J* = 5.1 Hz, 1H, H1'), 6.02 (d, *J* = 5.1 Hz, 1H, H1'), 5.33-5.28 (m, 1H, H2'), 5.10-5.01 (m, 2H, CH₂Ph), 4.67-4.63 (m, 0.5H, H3'), 4.63-4.59 (m, 0.5H, H3'), 4.55-4.48 (m, 1H, H5'), 4.48-4.40 (m, 1H, H5'), 4.26-4.20 (m, 1H, H4'), 3.79-3.71 (m, 2H, CH₂ Gly).

¹³C NMR (125 MHz, CD₃OD) δ_C 172.09 (d, ³*J*_{C-P} = 5.0 Hz, C=O), 156.25 (C6), 154.01 (C2), 151.66 (C4), 151.60 (C4), 147.91 (C8), 148.85 (C8), 139.79 (C-Ar), 137.12 (C-Ar), 137.11 (C-Ar), 136.22 (C-Ar)₂, 129.53 (CH-Ar), 129.30 (CH-Ar), 129.28 (CH-Ar), 129.26 (CH-Ar), 128.80 (CH-Ar), 128.79 (CH-Ar), 127.85 (d, ³*J*_{C-P} = 1.8 Hz, CH-Ar), 127.79 (d, ³*J*_{C-P} = 1.8 Hz, CH-Ar), 127.69 (CH-Ar), 127.38 (CH-Ar), 127.36 (CH-Ar), 126.44 (CH-Ar), 126.39 (CH-Ar), 125.89 (CH-Ar), 122.69 (CH-Ar), 122.65 (CH-Ar), 119.53 (C5), 119.52, (C5), 116.18 (d, ³*J*_{C-P} = 3.7 Hz, CH-Ar), 116.12 (d, ³*J*_{C-P} = 3.7 Hz, CH-Ar), 91.37 (C1'), 91.17 (C1'), 84.45 (d, ³*J*_{C-P} = 6.2 Hz, C4'), 84.39 (d, ³*J*_{C-P} = 6.2 Hz, C4'), 2.75 (C3'), 72.57 (C3'), 71.64 (C2'), 71.28 (C2'), 67.90 (C5'), 67.82 (C5'), 67.41 (CH₂Ph), 67.37 (CH₂Ph), 43.91 (CH₂ Gly), 43.85 (CH₂ Gly).

MS (ES-) *m/z* found 653.19 [M-H⁺], 688.64 [M+Cl⁻], C₂₉H₂₈ClN₆O₈P required *m/z* 654.99 [M].

HPLC Reverse-phase HPLC eluting with H₂O/CH₃CN from 90/10 to 0/100 in 35 minutes, F = 1 mL/min, λ = 254 nm, two peaks with t_R 15.84 min, t_R 15.35 min.

[71g] 8-chloroadenosine-5'-naphth-1-yl(pentyl-1-oxy-glycinyl) phosphate

Prepared according to the general procedure **F₁** using 8-chloroadenosine **[67]** (0.13 g, 0.43 mmol) in THF (10 mL), *t*BuMgCl (1.0 M in THF, 0.47 mL, 0.47 mmol), naphth-1-yl-(pentyl-1-oxy-glycinyl) phosphorochloridate **[17k]** (0.64 g, 1.72 mmol) in THF (5 mL). The crude was purified first by silica gel CC (0-6% CH₃OH /CH₂Cl₂) and secondly by prep. TLC (7% CH₃OH /CH₂Cl₂), to yield the product as a white solid (0.039 g, 15 %).

³¹P NMR (202 MHz, CD₃OD) δ_P 4.93.

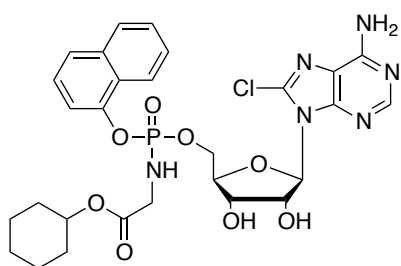
¹H NMR (500 MHz, CD₃OD) δ_H 8.15-8.07 (m, 1.5H, H₂, H₈ Nap), 8.05 (s, 0.5H, H₂), 7.87-7.82 (m, 1H, H₅ Nap), 7.68-7.64 (m, 1H, H₄ Nap), 7.54-7.42 (m, 3H, H₂, H₆, H₇ Nap), 7.35 (t, *J* = 8.0 Hz, 1H, H₃ Nap), 6.04 (d, *J* = 4.7 Hz, 1H, H₁'), 6.02 (d, *J* = 4.7 Hz, 1H, H₁'), 5.37-5.25 (m, 1H, H₂'), 4.69-4.65 (m, 0.5H, H₃'), 4.64-4.60 (m, 0.5H, H₃'), 4.58-4.50 (m, 1H, H₅'), 4.50-4.41 (m, 1H, H₅'), 4.29-4.22 (m, 1H, H₄'), 4.03-9.94 (m, 2H, CH₂CH₂CH₂CH₂CH₃ *n*-Pen), 3.75-3.64 (m, 2H, CH₂ Gly), 1.57-1.47 (m, 2H, CH₂CH₂CH₂CH₂CH₃ *n*-Pen), 1.31-1.22 (m, 4H, CH₂CH₂CH₂CH₂CH₃ *n*-Pen), 0.86 (t, *J* = 6.9 Hz, 3H, CH₂CH₂CH₂CH₂CH₃ *n*-Pen).

¹³C NMR (125 MHz, CD₃OD) δ_C 172.29 (d, ³*J*_{C-P} = 5.4 Hz, C=O), 172.30 (d, ³*J*_{C-P} = 5.4 Hz, C=O), 156.26 (C₆), 154.02 (C₂), 151.67 (C₄), 151.60 (C₄), 147.95 (C₈), 147.89 (C₈), 139.77 (C-Ar), 136.22 (C-Ar), 128.82 (CH-Ar), 128.80 (CH-Ar), 127.85 (C-Ar), 127.80 (C-Ar), 127.72 (C-Ar), 127.70 (C-Ar), 127.37 (CH-Ar), 127.36 (CH-Ar), 126.45 (CH-Ar), 126.41 (CH-Ar), 125.89 (CH-Ar), 122.70 (CH-Ar), 122.65 (CH-Ar), 116.15 (d, ³*J*_{C-P} = 3.0 Hz, CH-Ar), 116.17 (d, ³*J*_{C-P} = 3.0 Hz, CH-Ar), 91.38 (C₁'), 91.17 (C₁'), 84.47 (d, ³*J*_{C-P} = 7.5 Hz, C₄'), 84.40 (d, ³*J*_{C-P} = 7.5 Hz, C₄'), 72.78 (C₂'), 72.57 (C₂'), 71.66 (C₃'), 71.27 (C₃'), 67.81 (d, ²*J*_{C-P} = 5.1 Hz, C₅'), 67.37 (d, ²*J*_{C-P} = 5.1 Hz, C₅'), 67.41 (CH₂CH₂CH₂CH₂CH₃ *n*-Pen), 67.35 (CH₂CH₂CH₂CH₂CH₃ *n*-Pen), 43.83 (CH₂ Gly), 43.75 (CH₂ Gly), 29.32 (CH₂CH₂CH₂CH₂CH₃ *n*-Pen), 29.29 (CH₂CH₂CH₂CH₂CH₃ *n*-Pen), 29.07 (CH₂CH₂CH₂CH₂CH₃ *n*-Pen), 29.04 (CH₂CH₂CH₂CH₂CH₃ *n*-Pen), 23.33 (CH₂CH₂CH₂CH₂CH₃ *n*-Pen), 14.28 (CH₂CH₂CH₂CH₂CH₃ *n*-Pen).

MS (ES⁺) m/z found 657.19 [M+Na⁺], C₂₇H₃₂ClN₆O₈P required m/z 635.01 [M].

HPLC Reverse-phase HPLC eluting with H₂O/CH₃CN from 90/10 to 0/100 in 35 minutes, F = 1 mL/min, λ = 254 nm, two peaks with t_R 17.91min, t_R 17.39 min.

[71h] 8-chloroadenosine-5'-naphth-1-yl(cyclohexyloxy-L-alaninyl) phosphate



Prepared according to the general procedure **F**₁ using 8-chloroadenosine [**67**] (0.13 g, 0.43 mmol) in THF (10 mL), *t*BuMgCl (1.0 M in THF, 0.47 mL, 0.47 mmol), naphth-1-yl-(cyclohexyloxy-glycinyldichlorophosphate [**171**] (0.50 g, 1.29 mmol) in THF (5 mL). The crude was purified first by silica gel CC (0-6% CH₃OH/CH₂Cl₂) and

secondly by prep. TLC (7% CH₃OH/CH₂Cl₂), to yield the product as a white solid (0.012 g, 4%).

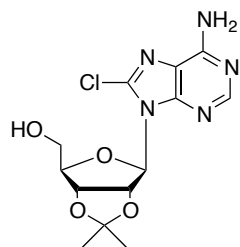
³¹P NMR (202 MHz, CD₃OD) δ_P 4.96, 4.94.

¹H NMR (500 MHz, CD₃OD) δ_H 8.15-8.04 (m, 2 H, H2, H8 Nap), 7.89-7.85 (m, 1H, H5 Nap), 7.70-7.65 (m, 1H, H4 Nap), 7.55-7.44 (m, 3H, H2, H6, H7 Nap), 7.42-7.33 (m, 1H, H3 Nap), 6.04 (d, *J* = 6.0 Hz, 0.5 H, H1'), 6.02 (d, *J* = 6.0 Hz, 0.5H, H1'), 5.32-5.28 (m, 1H, H2'), 4.70-4.63 (m, 1.5H, H3', CH(CH₂)₅ cHex), 4.61-4.58 (m, 0.5H, H3'), 4.57-4.50 (m, 1H, H5'), 4.49-4.42 (m, 1H, H5'), 4.27-4.23 (m, 1H, H4'), 3.72-3.62 (m, 2H, CH₂ Gly), 1.81-1.64 (m, 4H, CH(CH₂)₅ cHex), 1.56-1.49 (m, 1H, CH(CH₂)₅ cHex), 1.39-1.22 (m, 5H, CH(CH₂)₅ cHex).

¹³C NMR (125 MHz, CD₃OD) δ_C 172.67 (d, ³*J*_{C-P} = 5.0 Hz, C=O), 156.14 (C6), 153.82 (C2), 151.66 (C4), 151.59 (C4), 147.96 (C8), 147.87 (C8), 139.84 (C-Ar), 128.82 (C-Ar), 128.80 (C-Ar), 127.81 (d, ³*J*_{C-P} = 2.5 Hz, C-Ar), 127.71 (d, ³*J*_{C-P} = 2.5 Hz, C-Ar), 126.45 (CH-Ar), 126.41 (CH-Ar), 125.89 (CH-Ar), 122.70 (CH-Ar), 122.65 (CH-Ar), 116.16 (CH-Ar), 116.14 (CH-Ar), 91.38 (C1'), 91.14 (C1'), 84.53 (d, ³*J*_{C-P} = 8.2 Hz, C4'), 84.43 (d, ³*J*_{C-P} = 8.2 Hz, C4'), 75.08 (CH(CH₂)₅ cHex), 75.02 (CH(CH₂)₅ cHex), 72.76 (C2'), 72.55 (C2'), 71.64 (C3'), 71.27 (C3'), 67.79 (d, ²*J*_{C-P} = 5.0 Hz, C5'), 67.39 (d, ²*J*_{C-P} = 5.0 Hz, C5'), 44.05 (CH₂ Gly), 43.99 (CH₂ Gly), 32.48 (CH(CH₂)₅ cHex), 32.45 (CH(CH₂)₅ cHex), 26.36 (CH(CH₂)₅ cHex), 26.35 (CH(CH₂)₅ cHex), 24.69 (CH(CH₂)₅ cHex).

MS (ES+) *m/z* found 669.01 [M+Na⁺], 685.12 [M+K⁺], C₂₈H₃₂ClN₆O₈P required *m/z* 647.02 [M].

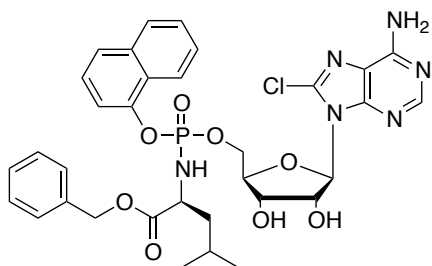
HPLC Reverse-phase HPLC eluting with H₂O/CH₃CN from 90/10 to 0/100 in 35 minutes, F = 1 mL/min, λ = 254 nm, two peaks with t_R 17.52 min, t_R 17.00 min.

[72] 2',3'-Isopropylidene-8-chloroadenosine

8-Chloroadenosine [67] (0.40 g, 1.33 mmol) was suspended in acetone (30 mL) and HClO₄ (70%, 0.2 mL) was added dropwise. The mixture was stirred at rt for 30 minutes and then neutralised by addition of NaHCO₃ (saturated aqueous solution). The mixture was extracted with CH₂Cl₂ (3 x 30 mL); the organics were collected and dried over

Na₂SO₄, filtered and evaporated. The crude was purified by flash silica gel chromatography (gradient eluent system 0-3% CH₃OH/CH₂Cl₂), to afford the title compound as a white foam (0.36 g, 79%).

¹H NMR (500 MHz, DMSO-*d*6) δ_H 8.18 (s, 1H, H2) 7.53 (br s, 2H, NH₂), 6.05 (d, *J* = 2.5 Hz, 1H, H1'), 5.68 (dd, *J* = 6.5 Hz, 2.5 Hz, 1H, H2'), 5.07 (t, *J* = 6.0 Hz, 1H, OH5'), 5.04 (dd, *J* = 6.5 Hz, 3.0 Hz, 1H, H3'), 4.17-4.14 (m, 1H, H4'), 3.53-3.48 (m, 1H, H5'), 3.45-3.41 (m, 1H, H5'), 1.55 (s, 3H, CH₃), 1.34 (s, 3H, CH₃).

[74a] 8-chloroadenosine-5'-naphth-1-yl(benzyloxy-L-leucinyl) phosphate

Prepared according to the general procedure F₁ using 2',3'-*O*-isopropylidene-8-chloroadenosine [72] (0.20 g, 0.59 mmol), in THF (5 mL), *t*BuMgCl (1.0 M in THF, 3eq, 1.76 mL, 1.76 eq) and naphth-1-yl-(benzyloxy-L-leucinyl)dichlorophosphate [17e] (0.80 g, 1.77 mmol) in THF (3 mL). Purification by silica gel CC (0-4%

CH₃OH/CH₂Cl₂) gave a residue that was stirred at rt in HCOOH/H₂O (3/2, 10 mL) overnight. The solvents were evaporated *in vacuo* and the crude purified first by silica gel CC (3-6% CH₃OH/CH₂Cl₂) and secondly by prep. TLC (10% CH₃OH/CH₂Cl₂) to yield the product as a white foam (0.118 g, 26% over two steps).

³¹P NMR (202 MHz, CD₃OD) δ_P 4.13, 3.95.

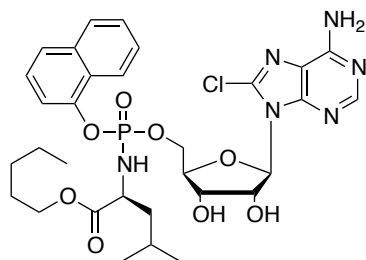
¹H NMR (500 MHz, CD₃OD) δ_H 8.10 (s, 0.5H, H2) 8.09-8.05 (m, 1H, H8 Nap), 8.04 (s, 0.5 H, H2), 7.83-7.79 (m, 1H, H5 Nap), 7.62 (d, *J* = 8.4 Hz, 1H, H4 Nap), 7.49- 7.38 (m, 3H, H2, H6, H7 Nap), 7.32-7.19 (m, 6H, H3 Nap, Ph), 6.07-6.02 (m, 1H, H1'), 5.36-5.32 (m, 0.5H, H2'), 5.29-5.25 (m, 0.5H, H2'), 5.02-4.91 (m, 2H, CH₂Ph), 4.67-4.60 (m, 1H, H3'), 4.55-4.41 (m, 2.5H, H5'), 4.40-4.33 (m, 0.5H, H5'), 4.29-4.22 (m, 1H, H4'), 3.99-3.86 (m, 1H, CHCH₂CH(CH₃)₂ L-Leu), 1.65-1.54 (m, 2.5H, CHCH₂CH(CH₃)₂ L-Leu), 1.51-1.31 (m, 0.5 H, CHCH₂CH(CH₃)₂ L-Leu), 0.80-0.62 (m, 6H, CHCH₂CH(CH₃)₂ L-Leu).

^{13}C NMR (125 MHz, CD_3OD) δ_{C} 174.96 (d, $^3J_{\text{C-P}} = 4.5$ Hz, C=O), 174.94 (d, $^3J_{\text{C-P}} = 4.5$ Hz, C=O), 156.19 (C6), 156.17 (C6), 154.05 (C2), 154.02 (C2), 151.64 (C4), 151.57 (C4), 147.95 (C8), 147.89 (C8), 139.79 (C-Ar), 139.71 (C-Ar), 137.07 (C-Ar), 137.03 (C-Ar), 136.20 (C-Ar), 136.18 (C-Ar), 129.52 (CH-Ar), 129.50 (CH-Ar), 129.35 (CH-Ar), 129.33 (CH-Ar), 129.32 (CH-Ar), 129.28 (CH-Ar), 128.83 (CH-Ar), 128.79 (CH-Ar), 127.81 (d, $^2J_{\text{C-P}} = 6.2$ Hz, C-Ar), 127.77 (d, $^2J_{\text{C-P}} = 6.2$ Hz, C-Ar), 127.71 (CH-Ar), 127.40 (CH-Ar), 127.35 (CH-Ar), 126.43 (CH-Ar), 125.88 (CH-Ar), 125.82 (CH-Ar), 122.79 (CH-Ar), 122.66 (CH-Ar), 119.51 (C5), 119.49 (C5), 116.24 (d, $^3J_{\text{C-P}} = 2.5$ Hz, CH-Ar), 115.92 (d, $^3J_{\text{C-P}} = 2.5$ Hz, CH-Ar), 91.40 (C1'), 91.23 (C1'), 84.53 (d, $^3J_{\text{C-P}} = 8.2$ Hz, C4'), 84.33 (d, $^3J_{\text{C-P}} = 8.2$ Hz, C4'), 72.83 (C2'), 72.65 (C2'), 71.75 (C3'), 71.48 (C3'), 68.05 (d, $^2J_{\text{C-P}} = 5.3$ Hz, C5'), 68.01 (d, $^2J_{\text{C-P}} = 5.3$ Hz, C5'), 67.91 (CH₂Ph), 67.83 (CH₂Ph), 67.62 (d, $^2J_{\text{C-P}} = 5.5$ Hz, C5'), 67.57 (d, $^2J_{\text{C-P}} = 5.5$ Hz, C5'), 54.68 (CHCH₂CH(CH₃)₂ L-Leu), 54.64 (CHCH₂CH(CH₃)₂ L-Leu), 44.09 (d, $^3J_{\text{C-P}} = 7.9$ Hz, CHCH₂CH(CH₃)₂ L-Leu), 43.09 (d, $^3J_{\text{C-P}} = 7.9$ Hz, CHCH₂CH(CH₃)₂ L-Leu), 25.57 (CHCH₂CH(CH₃)₂ L-Leu), 25.37 (CHCH₂CH(CH₃)₂ L-Leu), 23.09 (CHCH₂CH(CH₃)₂ L-Leu), 23.05 (CHCH₂CH(CH₃)₂ L-Leu), 22.04 (CHCH₂CH(CH₃)₂ L-Leu), 21.92 (CHCH₂CH(CH₃)₂ L-Leu).

MS (ES⁺) m/z found 733.20 [M+Na⁺], 749.19 [M+K⁺], C₃₃H₃₆ClN₆O₈P required m/z 711.10 [M].

HPLC Reverse-phase HPLC eluting with H₂O/CH₃CN from 90/10 to 0/100 in 35 minutes, F = 1 mL/min, λ = 254 nm, two peaks with tR 19.33 min, tR 18.93 min.

[74b] 8-chloroadenosine-5'-O-naphth-1-yl-(pentyl-1-oxy-L-leucinyl) phosphate



Prepared according to the general procedure **F₁** using 2',3'-*O*-isopropylidene-8-chloroadenosine [72] (0.18 g, 0.53 mmol), in THF (5 mL), *t*BuMgCl (1.0 M in THF, 1.59 mL, 1.59 eq) and naphth-1-yl-(pentyl-1-oxy-L-leucinyl) phosphorochloridate [17f] (0.68 g, 1.59 mmol) in THF (3 mL). Purification by silica gel CC (0-4% CH₃OH/CH₂Cl₂)

gave a residue that was stirred at rt in HCOOH/H₂O (3/2, 10 mL) overnight. The solvents were evaporated *in vacuo* and the crude purified first by silica gel CC (3-6% CH₃OH/CH₂Cl₂) and secondly by prep. TLC (10% CH₃OH/CH₂Cl₂) to yield the product as a white foam (0.13 g, 36% over two steps).

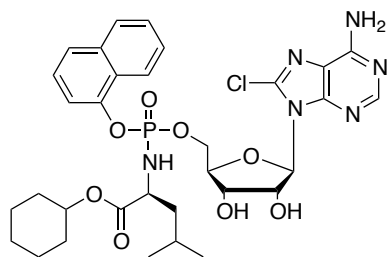
^{31}P NMR (202 MHz, CD_3OD) δ_{P} 4.06, 4.02.

¹H NMR (500 MHz, CD₃OD) δ_H 8.12 (s, 0.5H, H2) 8.11-8.06 (m, 1H, H8 Nap), 8.06 (s, 0.5H, H2), 7.84-7.79 (m, 1H, H5 Nap), 7.65-7.60 (m, 1H, H4 Nap), 7.51- .40 (m, 3H, H2, H6, H7 Nap), 7.32 (t, *J* = 8.0 Hz, 1H, H3 Nap), 6.07-6.03 (m, 1H, H1'), 5.37-5.33 (m, 0.5H, H2'), 5.30-5.26 (m, 0.5H, H2'), 4.69-4.62 (m, 1H, H-3'), 4.57-4.46 (m, 1.5H, H5'), 4.42-4.36 (m, 0.5H, H5'), 4.32-4.24 (m, 1H, H4'), 3.95-3.89 (m, 2H, CH₂CH₂CH₂CH₂CH₃ *n*-Pen), 3.89-3.83 (m, 0.5H, CHCH₂CH(CH₃)₂ L-Leu), 1.70-1.57 (m, 0.5H, CHCH₂CH(CH₃)₂ L-Leu), 1.52-1.35 (m, 5H, CHCH₂CH(CH₃)₂ L-Leu, CH₂CH₂CH₂CH₂CH₃ *n*-Pen, CHCH₂CH(CH₃)₂ L-Leu), 1.26-1.15 (m, 4H, CH₂CH₂CH₂CH₂CH₃ *n*-Pen), 0.85-0.80 (m, 3H, CH₂CH₂CH₂CH₂CH₃ *n*-Pen), 0.80-0.68 (m, 6H, CHCH₂CH(CH₃)₂ L-Leu).

¹³C NMR (125 MHz, CD₃OD) δ_C 175.27 (d, ³*J*_{C-P} = 4.0 Hz, C=O), 175.08 (d, ³*J*_{C-P} = 4.0 Hz, C=O), 156.21 (C6), 156.18 (C6), 154.04 (C2), 151.64 (C4), 151.58 (C4), 148.00 (C8), 147.94 (C8) 139.79 (C-Ar), 139.73 (C-Ar), 136.22 (C-Ar), 136.19 (C-Ar), 129.52 (CH-Ar), 129.35 (CH-Ar), 129.31 (CH-Ar), 128.84 (CH-Ar), 128.80 (CH-Ar), 127.84 (CH-Ar), 127.79 (CH-Ar), 127.73 (CH-Ar), 127.71 (CH-Ar), 127.36 (CH-Ar), 127.32 (CH-Ar), 125.84 (CH-Ar), 125.80 (CH-Ar), 122.77 (CH-Ar), 122.68 (CH-Ar), 119.50, (C5), 116.13 (d, ³*J*_{C-P} = 2.5 Hz, CH-Ar), 115.89 (d, ³*J*_{C-P} = 2.5 Hz, CH-Ar), 91.42 (C1'), 91.25 (C1'), 84.58 (d, ³*J*_{C-P} = 8.2 Hz, C4'), 84.34 (d, ³*J*_{C-P} = 8.2 Hz, C4'), 72.83 (C2'), 72.67 (C2'), 71.79 (C3'), 71.56 (C3'), 68.01 (d, ²*J*_{C-P} = 5.5 Hz, C5'), 67.63, (d, ²*J*_{C-P} = 5.5 Hz, C5'), 66.35 (CH₂CH₂CH₂CH₂CH₃ *n*-Pen), 66.29 (CH₂CH₂CH₂CH₂CH₃ *n*-Pen), 54.64 (CHCH₂CH(CH₃)₂ L-Leu), 44.30 (CH₂CH₂CH₂CH₂CH₃ *n*-Pen), 44.24 (CH₂CH₂CH₂CH₂CH₃ *n*-Pen), 44.15 (CH₂CH₂CH₂CH₂CH₃ *n*-Pen), 44.09 (CH₂CH₂CH₂CH₂CH₃ *n*-Pen), 29.27 (d, ³*J*_{C-P} = 7.0 Hz, CHCH₂CH(CH₃)₂ L-Leu), 29.11 (d, ³*J*_{C-P} = 7.0 Hz, CHCH₂CH(CH₃)₂ L-Leu), 25.65 (CHCH₂CH(CH₃)₂ L-Leu), 25.47 (CHCH₂CH(CH₃)₂ L-Leu), 23.31 (CH₂CH₂CH₂CH₂CH₃ *n*-Pen), 23.28 (CH₂CH₂CH₂CH₂CH₃ *n*-Pen), 23.11 (CHCH₂CH(CH₃)₂ L-Leu), 23.09 (CHCH₂CH(CH₃)₂ L-Leu), 22.13 (CHCH₂CH(CH₃)₂ L-Leu), 22.03 (CHCH₂CH(CH₃)₂ L-Leu), 14.33 (CH₂CH₂CH₂CH₂CH₃ *n*-Pen).

MS (ES⁺) m/z found 713.24 [M+Na⁺], 729.20 [M+K⁺], C₃₁H₄₀ClN₆O₈P required m/z 691.11 [M].

HPLC Reverse-phase HPLC eluting with H₂O/CH₃CN from 90/10 to 0/100 in 35 minutes, F = 1 mL/min, λ = 254 nm, two peaks with t_R 21.33 min, t_R 20.87 min.

[74c] 8-chloroadenosine 5'-O-naphth-1-yl-(cyclohexyloxy-L-leucyn) phosphate

Prepared according to the general procedure **F₁** using 2',3'-*O*-isopropylidene-8-chloroadenosine [**72**] (0.064 g, 0.19 mmol), in THF (2 mL), *t*BuMgCl (1.0 M in THF, 0.57 mL, 0.57 mmol) and naphth-1-yl-(cyclohexyloxy-L-leucynyl) phosphorochloridate [**17g**] (0.25 g, 0.57 mmol) in THF (1 mL). Purification by silica gel CC (0-3% CH₃OH/CH₂Cl₂) gave a residue that was stirred at rt in HCOOH/H₂O (3/2, 10 mL) overnight. The solvents were evaporated *in vacuo* and the crude purified first by silica gel CC (3-6% CH₃OH/CH₂Cl₂) and secondly by prep. TLC (10% CH₃OH/CH₂Cl₂) to yield the product as a white foam (0.01 g, 8% over two steps).

³¹P NMR (202 MHz, CD₃OD) δ_P 4.12, 4.02.

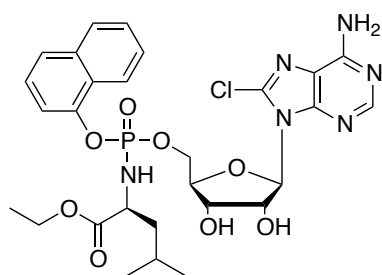
¹H NMR (500 MHz, CD₃OD) δ_H 8.13 (s, 0.5H, H2) 8.12-8.07 (m, 1H, H8 Nap), 8.07 (s, 0.5 H, H2), 7.89-7.84 (m, 1H, H5 Nap), 7.69-7.64 (m, 1H, H4 Nap), 7.54-7.40 (m, 3H, H2, H6, H7 Nap), 7.37-7.32 (m, 1H, H3 Nap), 6.06-6.02 (m, 1H, H1'), 5.36-5.32 (m, 0.5H, H2'), 5.29-5.25 (m, 0.5H, H2'), 4.67-4.45 (m, 3.5H, H3', H5', CH(CH₂)₅ cHex), 4.41-4.34 (m, 0.5H, H5'), 4.30-4.21 (m, 1H, H4'), 3.91-3.79 (m, 1H, CHCH₂CH(CH₃)₂ L-Leu), 1.74-1.22 (m, 13H, CHCH₂CH(CH₃)₂ L-Leu, CH(CH₂)₅ cHex), 0.85-0.70 (m, 6H, CHCH₂CH(CH₃)₂ L-Leu).

¹³C NMR (125 MHz, CD₃OD) δ_C 174.61 (d, ³J_{C-P} = 3.9 Hz, C=O), 174.43 (d, ³J_{C-P} = 3.9 Hz, C=O), 156.27 (C6), 156.25 (C6), 154.03 (C2), 151.67 (C4), 151.60 (C4), 147.95 (C8) 139.79 (C-Ar), 139.72 (C-Ar), 136.25 (C-Ar), 136.23 (C-Ar), 128.82 (C-Ar), 128.79 (C-Ar), 127.84 (d, ²J_{C-P} = 6.2 Hz, C-Ar), 127.70 (d, ²J_{C-P} = 6.2 Hz, C-Ar), 127.33 (CH-Ar), 127.29 (CH-Ar), 126.40 (CH-Ar), 125.81 (CH-Ar), 125.76 (CH-Ar), 122.79 (CH-Ar), 122.69 (CH-Ar), 119.53 (C5), 116.12 (d, ³J_{C-P} = 2.5 Hz, CH-Ar), 115.85 (d, ³J_{C-P} = 2.5 Hz, CH-Ar), 91.43 (C1'), 91.24 (C1'), 84.60 (d, ³J_{C-P} = 8.0 Hz, C4'), 84.37 (d, ³J_{C-P} = 8.0 Hz, C4'), 72.78 (C2'), 72.61 (C2'), 71.76 (C3'), 71.53 (C3'), 68.00 (d, ²J_{C-P} = 5.4 Hz, C5'), 67.61, (d, ²J_{C-P} = 5.4 Hz, C5'), 54.76 (CH(CH₂)₅ cHex), 54.71 (CHCH₂CH(CH₃)₂ L-Leu), 44.34 (d, ³J_{C-P} = 7.3 Hz, CHCH₂CH(CH₃)₂ L-Leu), 44.15 (d, ³J_{C-P} = 7.3 Hz, CHCH₂CH(CH₃)₂ L-Leu), 32.40 (CH(CH₂)₅ cHex), 32.35 (CH(CH₂)₅ cHex), 32.32 (CH(CH₂)₅ cHex), 26.37 (CH(CH₂)₅ cHex), 26.35 (CH(CH₂)₅ cHex), 25.66 (CH(CH₂)₅ cHex), 25.48 (CH(CH₂)₅ cHex), 24.62 (CHCH₂CH(CH₃)₂ L-Leu), 24.57 (CHCH₂CH(CH₃)₂ L-Leu), 23.02 (CHCH₂CH(CH₃)₂ L-Leu), 23.01 (CHCH₂CH(CH₃)₂ L-Leu), 22.11 (CHCH₂CH(CH₃)₂ L-Leu), 21.99 (CHCH₂CH(CH₃)₂ L-Leu).

MS (ES-VE) m/z found 701.21 [M-H⁺], 737.19 [M+Cl⁻], C₃₂H₄₀ClN₆O₈P required m/z 702.2 [M].

HPLC Reverse-phase HPLC eluting with H₂O/CH₃CN from 90/10 to 0/100 in 35 minutes, F = 1 mL/min, λ = 254 nm, two peaks with tR 20.53 min, tR 20.00 min.

[74d] 8-chloroadenosine-5'-O-naphth-1-yl-(ethyloxy-L-leucinyl) phosphate



Prepared according to the general procedure F₁ using 2',3'-*O*-isopropylidene-8-chloroadenosine [72] (0.08 g, 0.23 mmol) in THF (15 mL), *t*BuMgCl (1.0 M in THF, 0.69 mL, 0.69 mmol) and naphth-1-yl-(ethyloxy-L-leucinyl) phosphorochloridate [17h] (0.25 g, 0.69 mmol) in THF (1.5 mL). Purification by silica gel CC (0-3% CH₃OH /

CH₂Cl₂) gave a residue that was stirred at rt in HCOOH/H₂O (3/2, 10 mL) overnight. The solvents were evaporated *in vacuo* and the crude purified by prep. TLC (10% CH₃OH/CH₂Cl₂) to yield a white solid (0.03 g, 35 % over two steps).

³¹P NMR (202 MHz, CD₃OD) δ_P 4.11, 4.04.

¹H NMR (500 MHz, CD₃OD) δ_H 8.12 (s, 0.5H, H2) 8.10-8.06 (m, 1H, H8 Nap), 8.05 (s, 0.5H, H2), 7.86-7.82 (m, 1H, H5 Nap), 7.67-7.63 (m, 1H, H4 Nap), 7.53-7.39 (m, 3H, H2, H6, H7 Nap), 7.36-7.31 (m, 1H, H3 Nap), 6.06-6.03 (m, 1H, H1'), 5.36-5.33 (m, 0.5H, H2'), 5.30-5.27 (m, 0.5H, H2'), 4.68-4.62 (m, 1H, H3'), 4.57-4.46 (m, 1.5H, H5'), 4.41-4.35 (m, 0.5H, H5'), 4.30-4.23 (m, 1H, H4'), 4.02-3.92 (m, 2H, CH₂CH₃ Et), 3.91-3.81 (m, 1H, CHCH₂CH(CH₃)₂ L-Leu), 1.70-1.61 (m, 0.5H, CHCH₂CH(CH₃)₂ L-Leu), 1.50-1.35 (m, 2.5H, CHCH₂CH(CH₃)₂ L-Leu), 1.16-1.08 (m, 3H, CH₂CH₃ Et), 0.84-0.68 (m, 6H, CHCH₂CH(CH₃)₂ L-Leu).

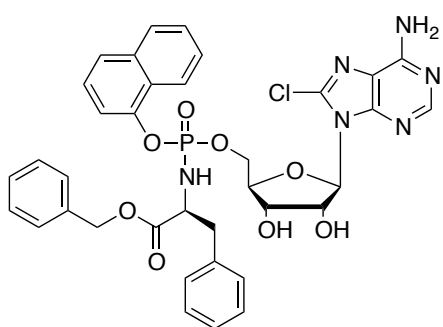
¹³C NMR (125 MHz, CD₃OD) δ_C 175.18 (d, ³J_{C-P} = 2.7 Hz, C=O), 174.97 (d, ³J_{C-P} = 2.7 Hz, C=O), 156.26 (C6), 156.22 (C6), 154.02 (C2), 151.66 (C4), 151.60 (C4), 147.98 (C8), 148.93 (C8), 139.77 (d, ²J_{C-P} = 6.2 Hz, C-Ar), 136.22 (d, ²J_{C-P} = 6.2 Hz, C-Ar), 128.81 (C-Ar), 128.78 (C-Ar), 127.84 (C-Ar), 127.79 (C-Ar), 127.72 (C-Ar), 127.69 (CH-Ar), 127.34 (CH-Ar), 127.30 (CH-Ar), 126.40 (CH-Ar), 125.81 (CH-Ar), 125.78 (CH-Ar), 122.75 (CH-Ar), 122.66 (CH-Ar), 119.52 (C5), 116.08 (d, ³J_{C-P} = 3.7 Hz, CH-Ar), 115.88 (d, ³J_{C-P} = 3.7 Hz, CH-Ar), 91.42 (C1'), 91.27 (C1'), 84.58 (d, ³J_{C-P} = 8.9 Hz, C4'), 84.33 (d, ³J_{C-P} = 8.9 Hz, C4'), 72.77 (C2'), 72.64 (C2'), 71.73 (C3'), 71.52 (C3'), 67.96 (d, ²J_{C-P} = 5.4 Hz, C5'), 67.58, (d, ²J_{C-P} = 5.4 Hz, C5'), 62.23 (CH₂CH₃ Et), 62.17 (CH₂CH₃ Et), 54.58

(CHCH₂CH(CH₃)₂ L-Leu), 44.17 (d, ³J_{C-P} = 7.3 Hz, CHCH₂CH(CH₃)₂ L-Leu), 43.97 (d, ³J_{C-P} = 7.3 Hz, CHCH₂CH(CH₃)₂ L-Leu), 25.60 (CHCH₂CH(CH₃)₂ L-Leu), 25.41 (CHCH₂CH(CH₃)₂ L-Leu), 23.09 (CHCH₂CH(CH₃)₂ L-Leu), 21.98 (CHCH₂CH(CH₃)₂ L-Leu), 21.87 (CHCH₂CH(CH₃)₂ L-Leu), 14.40 (CH₂CH₃ Et).

MS (ES -VE) m/z found 647.22 [M-H⁺], 683.14 [M+Cl⁻], C₂₈H₃₄ClN₆O₈P required m/z 649.03 [M].

HPLC Reverse-phase HPLC eluting with H₂O/CH₃CN from 90/10 to 0/100 in 35 minutes, F = 1 mL/min, λ = 254 nm, two peaks with tR 17.88 min, tR 17.43 min.

[74e] 8-chloroadenosine-5'-O-naphth-1-yl-(benzyloxy-L-phenylalaninyl)phosphate



Prepared according to the general procedure F₁ using 2',3'-O-isopropylidene-8-chloroadenosine [72] (0.10 g, 0.29 mmol) in THF (3 mL), *t*BuMgCl (1.0 M in THF, 0.88 mL, 0.88 mmol) and naphth-1-yl-(benzyloxy-L-phenylalaninyl)phosphorochloridate [17m] (0.42 g, 0.87 mmol) in THF (1.5 mL). Purification by silica gel CC (0-3% CH₃OH/CH₂Cl₂)

gave a residue that was stirred at rt in HCOOH/H₂O (3/2, 10 mL) overnight. The solvents were evaporated *in vacuo* and the crude purified by prep. TLC (10% CH₃OH/CH₂Cl₂) to yield the title compound as a white solid (0.012 g, 6% over two steps).

³¹P NMR (202 MHz, CD₃OD) δ_P 3.66, 3.46.

¹H NMR (500 MHz, CD₃OD) δ_H 8.08 (s, 0.5H, H2), 8.03 (s, 0.5H, H2), 8.00-7.97 (m, 1H, H8 Naph), 7.85-7.82 (m, 1H, H5 Nap), 7.64-7.61 (m, 1H, H4 Nap), 7.52-7.47 (m, 1H, H2 Nap), 7.44-7.38 (m, 1H, H6 Nap), 7.28-7.20 (m, 5H, Ph), 7.19-7.11 (m, 5H, Ph), 7.05-7.02 (m, 1H, H7 Nap), 7.00-6.96 (m, 1H, H3 Nap), 6.02-6.00 (m, 1 H, H1'), 5.32-5.25 (m, 1H, H2'), 4.98-4.88 (m, 2H, CH₂Ph), 4.58-4.54 (m, 0.5H, H3'), 4.52-4.49 (m, 0.5H, H3'), 4.34-4.10 (m, 4H, H4', H5', CHCH₂Ph L-Phe), 3.01-2.90 (m, 1H, CHCH₂Ph L-Phe), 2.83-2.76 (m, 1H, CHCH₂Ph L-Phe).

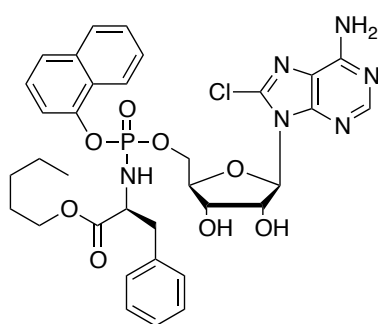
¹³C NMR (125 MHz, CD₃OD) δ_C 173.73 (d, ³J_{C-P} = 3.6 Hz, C=O), 173.65 (d, ³J_{C-P} = 3.6 Hz, C=O), 156.23 (C6), 154.08 (C2), 154.02 (C2), 151.68 (C4), 151.60 (C4), 147.90 (C8), 147.78 (C8), 139.79 (C-Ar), 139.79 (C-Ar), 137.75 (C-Ar), 136.90 (C-Ar), 136.87 (C-Ar), 136.18 (C-Ar), 136.15 (C-Ar), 130.48 (C-Ar), 129.49 (CH-Ar), 129.44 (CH-Ar), 129.42 (CH-Ar), 129.39 (CH-Ar), 129.28 (CH-Ar), 129.23 (CH-Ar), 128.77 (C-Ar), 128.73 (C-Ar), 127.91 (C-Ar), 127.87 (C-Ar), 127.78 (CH-Ar), 127.76 (CH-Ar), 127.73 (CH-Ar),

127.71 (CH-Ar), 128.77 (C-Ar), 128.73 (CH-Ar), 126.40 (CH-Ar), 125.80 (CH-Ar), 125.74 (CH-Ar), 122.78 (CH-Ar), 122.71 (CH-Ar), 119.54 (C5), 119.50 (C5), 115.98 (d, $^3J_{C-P} = 2.5$ Hz, CH-Ar), 115.95 (d, $^3J_{C-P} = 2.5$ Hz, CH-Ar), 91.33 (C1'), 91.13 (C1'), 84.38 (d, $^3J_{C-P} = 8.1$ Hz, C4'), 84.29 (d, $^3J_{C-P} = 8.1$ Hz, C4'), 72.63 (C2'), 72.51 (C2'), 71.66 (C3'), 71.33 (C3'), 67.96 (CH₂Ph), 67.88 (CH₂Ph), 67.71 (d, $^2J_{C-P} = 5.5$ Hz, C5'), 67.22 (d, $^2J_{C-P} = 5.5$ Hz, C5'), 57.77 (CHCH₂Ph L-Phe), 57.70 (CHCH₂Ph L-Phe), 41.05 (d, $^3J_{C-P} = 7.3$ Hz, CHCH₂Ph L-Phe), 40.96 (d, $^3J_{C-P} = 7.3$ Hz, CHCH₂Ph L-Phe).

MS (ES+) m/z found 767.21 [M+Na⁺], C₃₆H₃₄ClN₆O₈P required m/z 745.12 [M].

HPLC Reverse-phase HPLC eluting with H₂O/CH₃CN from 90/10 to 0/100 in 35 minutes, F = 1 mL/min, λ = 254 nm, two peaks with tR 20.48 min, tR 20.03 min.

[74f] 8-chloroadenosine-5'-O-naphth-1-yl-(pentyl-1-oxy-L-phenylalaninyl)phosphate



Prepared according to the general procedure **F**₁ using 2',3'-*O*-isopropylidene-8-chloroadenosine [72] (0.10 g, 0.29 mmol) in THF (3 mL), *t*BuMgCl (1.0 M in THF, 0.88 mL, 0.88 mmol) and naphth-1-yl-(pentyl-1-oxy-L-phenylalaninyl)phosphorochloridate [17n] (0.40 g, 0.87 mmol) in THF (1.5 mL). Purification by silica gel CC (0-3% CH₃OH /CH₂Cl₂) gave a residue that was stirred at rt in

HCOOH/H₂O (3/2, 10 mL) overnight. The solvents were evaporated *in vacuo* and the crude purified by prep. TLC (10% CH₃OH/CH₂Cl₂) to yield the title compound as a white solid (0.02 g, 10% over two steps).

³¹P NMR (202 MHz, CD₃OD) δ_P 3.72, 3.39.

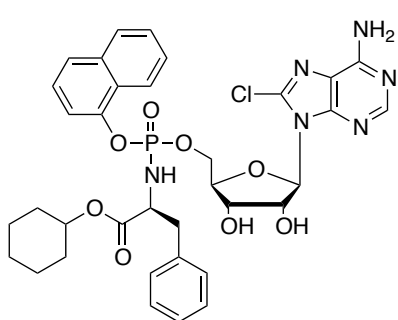
¹H NMR (500 MHz, CD₃OD) δ_H 8.11 (s, 0.5H, H2), 8.05 (s, 0.5H, H2), 8.04-8.00 (m, 1H, H8 Nap), 7.87-7.83 (m, 1H, H5 Nap), 7.67-7.61 (m, 1H, H4 Nap), 7.54-7.43 (m, 2H, H2, H6 Nap), 7.32-7.26 (m, 2H, Ph), 7.22-7.12 (m, 3H, Ph), 7.11-7.08 (m, 1H, H7 Nap), 7.07-7.04 (m, 1H, H3 Nap), 6.04-6.00 (m, 1H, H1'), 5.32-5.26 (m, 1H, H2'), 4.58-4.54 (m, 0.5H, H3'), 4.53-4.50 (m, 0.5H, H3'), 4.37-4.31 (m, 0.5H, H5'), 4.29-4.24 (m, 0.5H, H5'), 4.18-4.05 (m, 3H, H5', H4', CHCH₂Ph L-Phe), 3.90-3.79 (m, 2H, CH₂CH₂CH₂CH₂CH₃ *n*-Pen), 3.00-2.90 (m, 1H, CHCH₂Ph L-Phe), 2.85-2.78 (m, 1H, CHCH₂Ph L-Phe), 1.45-1.35 (m, 2H, CH₂CH₂CH₂CH₂CH₃ *n*-Pen), 1.25-1.09 (m, 4H, CH₂CH₂CH₂CH₂CH₃ *n*-Pen), 0.83 (t, *J* = 7.2 Hz, 1.5H, CH₂CH₂CH₂CH₂CH₃ *n*-Pen), 0.80 (t, *J* = 7.2 Hz, 1.5H, CH₂CH₂CH₂CH₂CH₃ *n*-Pen).

¹³C NMR (125 MHz, CD₃OD) δ_C 174.06 (d, ³J_{C-P} = 3.2 Hz, C=O), 173.95 (d, ³J_{C-P} = 3.2 Hz, C=O), 156.27 (C6), 156.25 (C6), 154.08 (C2), 154.02 (C2), 151.70 (C4), 151.62 (C4), 147.91 (C8), 147.85 (C8), 139.79 (C-Ar), 139.78 (C-Ar), 137.94 (C-Ar), 136.21 (C-Ar), 136.18 (C-Ar), 130.46 (C-Ar), 129.48 (C-Ar), 129.44 (C-Ar), 128.78 (C-Ar), 128.75 (C-Ar), 127.92 (C-Ar), 127.89 (C-Ar), 127.80 (CH-Ar), 127.75 (CH-Ar), 127.67 (CH-Ar), 127.32 (CH-Ar), 127.28 (CH-Ar), 126.40 (CH-Ar), 125.79 (CH-Ar), 125.70 (CH-Ar), 122.77 (CH-Ar), 122.73 (CH-Ar), 119.55 (C5), 119.52 (C5), 115.96 (d, ³J_{C-P} = 3.0 Hz, CH-Ar), 115.84 (d, ³J_{C-P} = 3.0 Hz, CH-Ar), 91.34 (C1'), 91.14 (C1'), 84.43 (d, ³J_{C-P} = 8.4 Hz, C4'), 84.31 (d, ³J_{C-P} = 8.4 Hz, C4'), 72.63 (C2'), 72.54 (C2'), 71.69 (C3'), 71.39 (C3'), 67.72 (d, ²J_{C-P} = 5.4 Hz, C5'), 67.23 (d, ²J_{C-P} = 5.4 Hz, C5'), 66.38 (CH₂CH₂CH₂CH₂CH₃ *n*-Pen), 66.33 (CH₂CH₂CH₂CH₂CH₃ *n*-Pen), 57.74 (CHCH₂Ph L-Phe), 57.70 (CHCH₂Ph L-Phe), 41.21 (d, ³J_{C-P} = 6.2 Hz, CHCH₂Ph L-Phe), 41.16 (d, ³J_{C-P} = 6.2 Hz, CHCH₂Ph L-Phe), 29.20 (CH₂CH₂CH₂CH₂CH₃ *n*-Pen), 29.03 (CH₂CH₂CH₂CH₂CH₃ *n*-Pen), 28.99 (CH₂CH₂CH₂CH₂CH₃ *n*-Pen), 23.30 (CH₂CH₂CH₂CH₂CH₃ *n*-Pen), 23.26 (CH₂CH₂CH₂CH₂CH₃ *n*-Pen), 14.24 (CH₂CH₂CH₂CH₂CH₃ *n*-Pen), 14.21 (CH₂CH₂CH₂CH₂CH₃ *n*-Pen).

MS (ES+) *m/z* found 747.23 [M+Na⁺], C₃₄H₃₈ClN₆O₈P required *m/z* 725.13 [M].

HPLC Reverse-phase HPLC eluting with H₂O/CH₃CN from 90/10 to 0/100 in 35 minutes, F = 1 mL/min, λ = 254 nm, two peaks with t_R 22.04 min, t_R 21.48 min.

[74g] 8-chloroadenosine-5'-*O*-naphth-1-yl-(cyclohexyloxy-L-alaninyl)phosphate



Prepared according to the general procedure **F₁** using 2',3'-*O*-isopropylidene-8-chloroadenosine [**72**] (0.12 mg, 0.36 mmol) in THF (3 mL), *t*BuMgCl (1.0 M in THF, 1.1 mL, 1.1 mmol) and naphth-1-yl-(cyclohex-1-yloxy-L-phenylalaninyl)phosphorochloridate [**17o**] (0.50 g, 1.1 mmol) in THF (1.5 mL). Purification by silica gel CC (0-3% CH₃OH /CH₂Cl₂) gave a residue that was stirred at rt in HCOOH/H₂O (3/2, 10 mL) overnight. The solvents were evaporated *in vacuo* and the crude purified by prep. TLC (10% CH₃OH/CH₂Cl₂) to yield the title compound as a white solid (0.053 g, 21% over two steps).

³¹P NMR (202 MHz, CD₃OD) δ_P 3.73, 3.74.

¹H NMR (500 MHz, CD₃OD) δ_H 8.10 (s, 0.5H, H2), 8.05 (s, 0.5H, H2), 8.04-8.00 (m, 1H, H8 Nap), 7.86-7.82 (m, 1H, H5 Nap), 7.65-7.61 (m, 1H, H4 Nap), 7.53-7.48 (m, 1H, H2

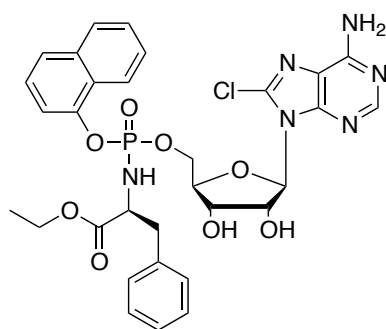
Nap), 7.47-7.42 (m, 1H, H6 Nap), 7.32-7.22 (m, 2H, Ph), 7.21-7.12 (m, 3H, Ph), 7.11-7.08 (m, 1H, H7 Nap), 7.07-7.04 (m, 1H, H3 Nap), 6.04-6.01 (m, 1H, H1'), 5.32-5.27 (m, 1H, H2'), 4.59-4.50 (m, 2H, H3', CH(CH₂)₅ cHex), 4.39-4.26 (m, 1H, H5'), 4.20-4.04 (m, 3H, H5', H4', CHCH₂Ph L-Phe), 2.99-2.90 (m, 1H, CHCH₂Ph L-Phe), 2.86-2.78 (m, 1H, CHCH₂Ph L-Phe), 1.69-1.52 (m, 4H, CH(CH₂)₅ cHex), 1.50-1.41 (m, 1H, CH(CH₂)₅ cHex), 1.32-1.12 (m, 5H, CH(CH₂)₅ cHex).

¹³C NMR (126 MHz, CD₃OD) δ_C 173.45 (d, ³J_{C-P} = 3.6 Hz, C=O), 173.34 (d, ³J_{C-P} = 3.6 Hz, C=O), 156.25 (C6), 154.09 (C2), 154.04 (C2), 151.70 (C4), 151.61 (C4), 147.91 (C8), 147.86 (C8), 139.79 (C-Ar), 139.77 (C-Ar), 137.94 (C-Ar), 137.89 (C-Ar), 136.21 (C-Ar), 136.19 (C-Ar), 130.52 (C-Ar), 130.51 (C-Ar), 129.46 (C-Ar), 129.42 (C-Ar), 128.79 (CH-Ar), 128.76 (CH-Ar), 127.90 (C-Ar), 127.87 (C-Ar), 127.80 (CH-Ar), 127.74 (CH-Ar), 127.67 (CH-Ar), 127.32 (CH-Ar), 127.27 (CH-Ar), 126.41 (CH-Ar), 125.78 (CH-Ar), 125.70 (CH-Ar), 122.78 (CH-Ar), 122.73 (CH-Ar), 119.54, (C5), 115.94 (d, ³J_{C-P} = 3.5 Hz, CH-Ar), 115.83 (d, ³J_{C-P} = 3.5 Hz, CH-Ar), 91.35 (C1'), 91.14 (C1'), 84.46 (d, ³J_{C-P} = 8.2 Hz, C4'), 84.33 (d, ³J_{C-P} = 8.2 Hz, C4'), 75.03 (C2'), 75.01 (C2'), 72.64 (C3'), 72.55 (C3'), 71.72 (CH(CH₂)₅ cHex), 71.40 (CH(CH₂)₅ cHex), 67.78 (d, ²J_{C-P} = 5.4 Hz, C5'), 67.28 (d, ²J_{C-P} = 5.4 Hz, C5'), 57.78 (CHCH₂Ph L-Phe), 41.33 (d, ³J_{C-P} = 7.5 Hz, CHCH₂Ph L-Phe), 41.25 (d, ³J_{C-P} = 7.5 Hz, CHCH₂Ph L-Phe), 32.36 (CH(CH₂)₅ cHex), 32.32 (CH(CH₂)₅ cHex), 26.32 (CH(CH₂)₅ cHex ex), 26.29 (CH(CH₂)₅ cHex), 24.56 (CH(CH₂)₅ cHex).

MS (ES+) m/z found 759.19 [M+Na⁺], C₃₅H₃₈ClN₆O₈P required m/z 737.14 [M].

HPLC Reverse-phase HPLC eluting with H₂O/CH₃CN from 90/10 to 0/100 in 35 minutes, F = 1 mL/min, λ = 254 nm, two peaks with t_R 21.81 min., t_R 21.27 min.

[74h] 8-chloroadenosine-5'-O-naphth-1-yl-(ethoxy-L-phenylalaninyl) phosphate



Prepared according to the general procedure F₁ using 2',3'-O-isopropylidene-8-chloroadenosine [72] (0.17 g, 0.50 mmol) in THF (3 mL), *t*BuMgCl (1.0 M in THF, 1.5 mL, 1.5 mmol) and naphth-1-yl-(ethoxy-L-phenylalaninyl) phosphorochloridate [17p] (1.05 g, 2.5 mmol) in THF (1.5 mL). Purification by silica gel CC (0-2% CH₃OH/CH₂Cl₂) gave a residue that was stirred at rt in HCOOH/H₂O (3/2,

10 mL) overnight. The solvents were evaporated *in vacuo* and the crude purified by prep. TLC (7% CH₃OH/CH₂Cl₂) to yield the title compound as a white solid (0.09 g, 26% over two steps).

³¹P NMR (202 MHz, CD₃OD) δ_P 3.73, 3.42.

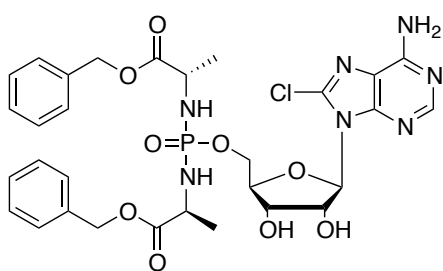
¹H NMR (500 MHz, CD₃OD) δ_H 8.09 (s, 0.5H, H2), 8.04 (s, 0.5H, H2), 8.00 (d, *J* = 8.4 Hz, 1H, H8 Nap), 7.80 (d, *J* = 8.2 Hz, 1H, H5 Nap), 7.62-7.58 (m, 1H, H4 Nap), 7.50-7.40 (m, 2H, H2, H6 Nap), 7.32-7.23 (m, 2H, Ph), 7.20-7.07 (m, 4H, Ar), 7.05-7.01 (m, 1H, H3 Nap), 6.05-6.01 (m, 1H, H1'), 5.33-5.28 (m, 1H, H2'), 4.60-4.53 (m, 1H, H3'), 4.38-4.31 (m, 0.5H, H5'), 4.30-4.24 (m, 0.5H, H5'), 4.20-4.10 (m, 4.5H, H5', H4', CHCH₂Ph L-Phe, CH₂CH₃ Et), 4.09-4.03 (m, 0.5H, H5'), 3.97-3.85 (m, 2H, CHCH₂Ph L-Phe), 1.07-0.98 (m, 3H, CH₂CH₃ Et).

¹³C NMR (125 MHz, CD₃OD) δ_C 174.00 (d, ³*J*_{C-P} = 3.6 Hz, C=O), 173.90 (d, ³*J*_{C-P} = 3.6 Hz, C=O), 156.20 (C6), 154.09 (C2), 154.04 (C2), 151.67 (C4), 151.59 (C4), 147.92, 147.86 (C8), 147.80 (C8), 139.82 (C-Ar), 139.79 (C-Ar), 137.90 (C-Ar), 136.17 (C-Ar), 136.15 (C-Ar), 130.51 (C-Ar), 129.48 (C-Ar), 129.43 (C-Ar), 128.76 (CH-Ar), 127.92 (CH-Ar), 127.89 (C-Ar), 127.79 (CH-Ar), 127.73 (CH-Ar), 127.69 (CH-Ar), 127.33 (CH-Ar), 127.30 (CH-Ar), 126.43 (CH-Ar), 125.80 (CH-Ar), 125.71 (CH-Ar), 122.73 (CH-Ar), 122.70 (CH-Ar), 119.52, (C5), 115.97 (d, ³*J*_{C-P} = 3.6 Hz CH-Ar), 115.81 (d, ³*J*_{C-P} = 3.6 Hz CH-Ar), 91.33 (C1'), 91.16 (C1'), 84.35 (d, ³*J*_{C-P} = 8.7 Hz, C-4'), 84.27 (d, ³*J*_{C-P} = 8.7 Hz, C-4'), 72.66 (C2'), 72.60 (C2'), 71.70 (C3'), 71.38 (C3'), 67.74 (d, ²*J*_{C-P} = 5.4 Hz, C5'), 67.23 (d, ²*J*_{C-P} = 5.4 Hz, C5'), 62.33 (CH₂CH₃ Et), 62.27 (CH₂CH₃ Et), 57.69 (CHCH₂Ph L-Phe), 57.62 (CHCH₂Ph L-Phe), 41.20 (d, ³*J*_{C-P} = 6.2 Hz, CHCH₂Ph L-Phe), 41.13 (d, ³*J*_{C-P} = 6.2 Hz, CHCH₂Ph L-Phe), 14.35 (CH₂CH₃ Et).

MS (ES+) *m/z* found 705.18 [M+Na⁺], C₃₁H₃₂ClN₆O₈P required *m/z* 683.05 [M].

HPLC Reverse-phase HPLC eluting with H₂O/CH₃CN from 90/10 to 0/100 in 35 minutes, F = 1 mL/min, λ = 254 nm, two peaks with t_R 17.00 min, t_R 16.53 min.

[76a] 8-chloroadenosine 5'-*O*-bis(benzyloxy-L-alaninyl)phosphate



Prepared according to the general procedure G, using 8-chloroadenosine [67] (0.25 g, 0.83 mmol), in (CH₃O)₃PO (5 mL), POCl₃ (77 μL, 0.83 mmol), L-alanine-*O*-benzyl ester tosylate salt (1.46 g, 4.15 mmol) in CH₂Cl₂ (5 mL) and DIPEA (1.45 mL, 8.3 mmol). The crude was purified by column

chromatography (gradient elution of 4-7% CH₃OH/CH₂Cl₂) to give the title compound as a white solid (0.24 g, 42%).

³¹P NMR (202 MHz, CD₃OD) δ_P 13.54.

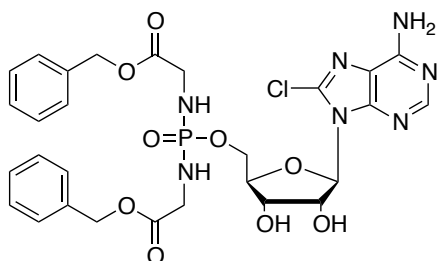
¹H NMR (500 MHz, CD₃OD) δ_H 8.21 (s, 1H, H₂), 7.36-7.26 (m, 10H, Ph), 6.02 (d, *J* = 4.8 Hz, 1H, H₁'), 5.30 (t, *J* = 5.5 Hz, 1H, H₂'), 5.14-5.02 (m, 4H, CH₂Ph), 4.62 (dd, *J* = 7.5, 5.0 Hz, 1H, H₃'), 4.31-4.24 (m, 1H, H₅'), 4.18-4.11 (m, 2H, H₅' , H₄'), 3.95-3.82 (m, 2H, CHCH₃ L-Ala), 1.28 (d, *J* = 7.2 Hz, 3H, CHCH₃ L-Ala), 1.23 (d, *J* = 7.2 Hz, 3H, CHCH₃ L-Ala).

¹³C NMR (125 MHz, CD₃OD) δ_C 175.34 (d, ³*J*_{C-P} = 5.0 Hz, C=O), 175.30 (d, ³*J*_{C-P} = 5.0 Hz, C=O), 156.35 (C₆), 154.22 (C₂), 151.71 (C₄), 139.83 (C-Ar), 137.32 (C-Ar), 137.27 (C-Ar), 129.58 (CH-Ar), 129.56 (CH-Ar), 129.32 (CH-Ar), 129.28 (CH-Ar), 119.55 (C₅), 91.28 (C₁'), 84.50 (d, ³*J*_{C-P} = 7.3 Hz, C₄'), 72.65 (C₂'), 71.47 (C₃'), 67.91 (CH₂Ph), 67.86 (CH₂Ph), 66.17 (d, ²*J*_{C-P} = 4.4 Hz, C₅'), 51.01 (CHCH₃ L-Ala), 50.98 (CHCH₃ L-Ala), 20.81 (d, ³*J*_{C-P} = 6.0 Hz, CHCH₃ L-Ala), 20.53 (d, ³*J*_{C-P} = 6.0 Hz, CHCH₃ L-Ala).

MS (ES+) *m/z* found 704.1 [M+H⁺], 726.1 [M+Na⁺], C₃₀H₃₅ClN₇O₉P required *m/z* 704.07 [M].

HPLC Reverse-phase HPLC eluting with H₂O/CH₃CN from 90/10 to 0/100 in 35 minutes, F = 1 mL/min, λ = 254, one peak with t_R 24.98 min.

[74b] 8-chloroadenosine 5'-*O*-bis(benzyloxy-glyciny)l phosphate



Prepared according to the general procedure G, using 8-chloroadenosine [67] (0.10 g, 0.33 mmol), in (CH₃O)₃PO (2.5 mL), POCl₃ (31 μL, 0.33 mmol), glycine-*O*-benzyl ester hydrochloride salt (0.33 g, 1.65 mmol), in CH₂Cl₂ (5 mL) and DIPEA (0.57 mL, 3.3 mmol). The crude was purified by column chromatography (gradient elution of 4-7% CH₃OH/CH₂Cl₂) to give the title compound as a white solid (0.06 g, 27 %).

³¹P NMR (202 MHz, CD₃OD) δ_P 15.96.

¹H NMR (500 MHz, CD₃OD) δ_H 8.23 (s, 1H, H₂), 7.35-7.26 (m, 10H, Ph), 6.03 (d, *J* = 5.1 Hz, 1H, H₁'), 5.31 (dd, *J* = 5.5, 5.1 Hz, 1H, H₂'), 5.11-5.08 (m, 4H, CH₂Ph), 4.59 (dd, 5.5 Hz, 5.1 Hz, 1H, H₃'), 4.34-4.28 (m, 1H, H₅'), 4.27-4.16 (m, 2H, H₅' , H₄'), 3.70-3.64 (m, 4H, CH₂ Gly).

¹³C NMR (125 MHz, CD₃OD) δ_C 172.91 (d, ³*J*_{C-P} = 4.7 Hz, C=O), 172.89 (d, ³*J*_{C-P} = 4.7 Hz, C=O), 156.24 (C₆), 154.08 (C₂), 151.69 (C₄), 139.88 (C-Ar), 137.22 (C-Ar), 129.57 (CH-Ar), 129.56 (CH-Ar), 129.33 (CH-Ar), 129.31 (CH-Ar), 119.56 (C₅), 91.16 (C₁'),

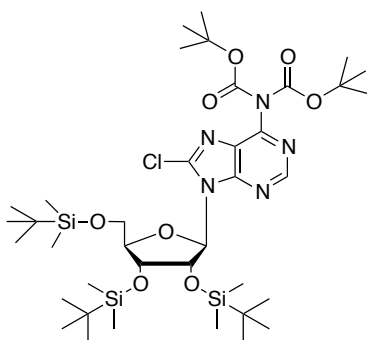
84.70 (d, $^3J_{C-P} = 7.2$ Hz, C4'), 72.62 (C2'), 71.58 (C3'), 67.86 (CH₂Ph), 67.84 (CH₂Ph), 66.17 (d, $^2J_{C-P} = 4.6$ Hz, C5'), 43.56 (CH₂ Gly), 43.47 (CH₂ Gly).

MS (ES+) *m/z* found 704.1 [M+H⁺], 726.1 [M+Na⁺], C₂₈H₃₁ClN₇O₉P required *m/z* 676.01 [M].

HPLC Reverse-phase HPLC eluting with H₂O/CH₃CN from 90/10 to 0/100 in 35 minutes, F = 1 mL/min, λ = 254, one peak with t_R 23.23 min.

9.5.13 Synthesis of 5'-modified 8-chloroadenosine analogues

[78] 2',3',5'-tri-*O*-*tert*-butyldimethylsilyl-(bis-*N*⁶,*N*⁶-*tert*-butylcarbonyl)-8-chloroadenosine

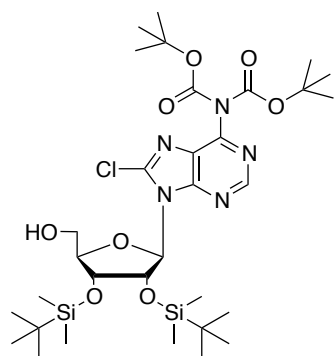


Procedure 2',3',5'-tri-*O*-*tert*-butyldimethylsilyl-8-chloroadenosine [70] (4.0 g, 6.2 mmol) was dissolved in anhydrous THF (50 mL) and DMAP (0.30 g, 2.48 mmol) was added in one portion to the stirring solution, followed by Boc₂O (5.41 g, 24.8 mmol). The reaction was stirred at rt for 18 h. The solvent was evaporated and the crude dissolved in *n*-Hex (30 mL) and washed with brine (20 mL

x 3). The organic phase was dried over Na₂SO₄, filtered and evaporated. The crude was purified by Biotage Isolera One (100g SNAP cartridge KP SIL, 100 mL/min, eluent system 1-20% EtOAc/*n*Hex 10CV, 20% 2CV) to yield the desired compound as syrup (5.24 g, 87%).

¹H NMR (500 MHz, CDCl₃) δ_H 8.76 (s, 1H, H2), 6.02 (d, *J* = 6.5 Hz, 1H, H1'), 5.42 (dd, *J* = 6.5 Hz, 4.5 Hz, 1H, H2'), 4.51 (dd, *J* = 4.5 Hz, 2.5 Hz, 1H, H3'), 4.08 (ddd, *J* = 7.5 Hz, 4.5 Hz, 2.5 Hz, 1H, H4'), 4.02 (dd, *J* = 11.0 Hz, 7.5 Hz, 1H, H5'), 3.74 (dd, *J* = 10.5 Hz, 4.5 Hz, 1H, H5'), 1.50 (s, 18H, Boc), 0.953 (s, 9H, *t*Bu), 0.864 (s, 9H, *t*Bu), 0.761 (s, 9H, *t*Bu), 0.150 (s, 3H, CH₃), 0.14 (s, 3H, CH₃), 0.02 (s, 3H, CH₃), 0.00 (s, 3H, CH₃), -0.09 (s, 3H, CH₃), -0.42 (s, 3H, CH₃).

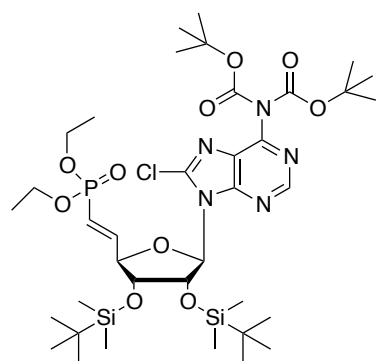
[79] 2',3'-bis-*O*-*tert*-butyldimethylsilyl-(bis-*N*⁶,*N*⁶-*tert*-butylcarbonyl)-8-chloroadenosine



2',3',5'-tri-*O*-*tert*-butyldimethylsilyl-(bis-*N*⁶,*N*⁶-*tert*-butylcarbonate)-8-chloroadenosine [78] (4.18 g, 5.04 mmol) was dissolved in a mixture of THF/water (5 mL, 4/1) and the solution was cooled to 0 °C in an ice bath. TFA (1 mL) was added dropwise and the reaction was stirred for 5h at 0 °C. The solution was then evaporated and the crude dissolved in CH₂Cl₂ (30 mL) and washed with NaHCO₃ (20 mL) and brine (20 mL x 2). The organic phase was dried over Na₂SO₄, filtered and evaporated. The crude was purified via Biotage Isolera One (120g ZIP cartridge KP SIL, 100 mL/min, eluent system 12-23% EtOAc/*n*Hex 5CV, 23% 5CV) to afford the desired product as a white foam (2.50 g, 68%).

¹H NMR (500 MHz, CDCl₃) δ_H 8.67 (s, 1H, H2), 5.96 (d, *J* = 8.0 Hz, 1H, H1'), 5.66 (dd, *J* = 12.1 Hz, 1.5 Hz, 1H, OH5'), 4.93 (dd, *J* = 8.0 Hz, 4.5 Hz, 1H, H2'), 4.20 (d, *J* = 4.5 Hz, 1H, H3'), 4.01-4.03 (m, 1H, H4'), 3.80 (d, *J* = 13.1, 1H, H5'), 3.58 (t, *J* = 12.7, 1H, H5'), 1.30 (s, 18H, 2 x Boc), 0.81 (s, 9H, *t*Bu), 0.63 (s, 9H, *t*Bu), 0.00 (s, 3H, CH₃), -0.01 (s, 3H, CH₃), -0.26 (s, 3H, CH₃), -0.78 (s, 3H, CH₃).

[81] 9-[5',6'-Vinyl-6'-(bis-*O*-ethylphosphinyl)-2',3'-bis-*O*-*tert*-butyldimethylsilyl-D-ribo-hexofuranosyl] bis-*N*⁶,*N*⁶-*tert*-butoxycarbonyl-8-chloroadenine



To a solution of 2',3'-bis-*O*-*tert*-butyldimethylsilyl-(bis-*N*⁶,*N*⁶-*tert*-butylcarbonate)-8-chloroadenosine [79] (1.25 g, 1.80 mmol) in CH₃CN (10 mL) was added 2-iodoxybenzoic acid (IBX) (1.00 g, 3.60 mmol). After stirring for 2 hours at 80 °C, the reaction mixture was cooled to 0 °C and filtered. The filtrate was washed with anhydrous THF (10 mL) and the solution was concentrated and co-evaporated with THF. Subsequently, to a solution of the resulting aldehyde [80] in THF (2 mL) was added dropwise, at 0 °C, a freshly prepared solution of tetraethyl-bisphosphonate sodium salt [prepared by addition, at 0 °C, of tetraethyl-bisphosphonate (0.71 mL, 2.88 mmol) to a suspension of NaH (0.11 g, 2.60 mmol) in THF (1.5 mL) and stirring for 10 min]. The reaction mixture was then stirred at room temperature for 16h before addition of NH₄Cl (10 mL, saturated aqueous solution). The mixture was then extracted with EtOAc (3 x 5 mL). The combined organic layers were washed with water (2 x 5 mL) and brine (5 mL)

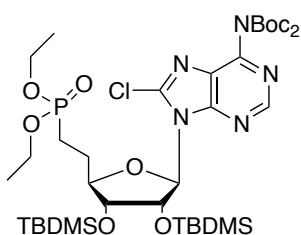
and the resulting solution was dried over Na₂SO₄. The collected solution was concentrated under reduced pressure and the residue was purified on Biotage Isolera One (50g SNAP cartridge KP SIL, 50 mL/min, eluent system 12-100% EtOAc/*n*Hex 10CV, 100% 5CV) to give the title compound as a white foam (single *E* isomer, 1.05 g, 68%).

³¹P NMR (202 MHz, CDCl₃) δ_P 17.55.

¹H NMR (500 MHz, CDCl₃) δ_H 8.64 (s, 1H, H₂), 6.83 (ddd, ¹J_{HP} = 22.4 Hz, ¹J_{HH} 17.0 Hz, ²J_{HH} 5.0 Hz, 1H, H_{6'}), 5.99-5.89 (m, 2H, H_{5'}, H_{1'}), 5.16 (dd, *J* = 6.0 Hz, 4.5 Hz, 1H, H_{2'}), 4.47-4.43 (m, 1H, H_{4'}), 4.33 (dd, *J* = 4.5 Hz, 3.5 Hz, H_{3'}), 3.98-3.85 (m, 4H, 2 x CH₂CH₃), 1.29 (s, 18H, Boc₂), 1.18 (t, *J* = 7.0 Hz, 3H, CH₂CH₃), 1.13 (t, *J* = 7.0 Hz, 3H, CH₂CH₃), 0.81 (s, 9H, *t*Bu), 0.62 (s, 9H, *t*Bu), 0.01 (s, 3H, CH₃), 0.00 (s, 3H, CH₃), -0.21 (s, 3H, CH₃), -0.55 (s, 3H, CH₃).

MS (ES+) *m/z* found 862.3 [M+H⁺], 884.3 [M+Na⁺], 762.3 [M(-Boc)+H⁺], 784.3 [M(-Boc)+Na⁺], required *m/z* C₃₇H₆₅ClN₅O₁₀PSi₂ 861.37 [M].

[82] 9-[5',6'-dideoxy-6'-(bis-ethylphosphinyl)-2',3'-bis-*O*-*tert*-butyldimethylsilyl-D-ribo-hexofuranosyl] bis-*N*⁶,*N*⁶-*tert*-butoxycarbonyl 8-chloroadenine

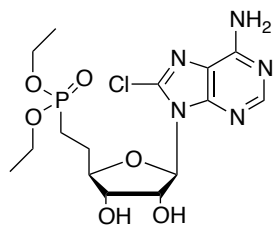


9-[5',6'-vinyl-6'-(bis-ethylphosphinyl)-2',3'-bis-*O*-*tert*-butyldimethylsilyl-D-ribo-hexofuranosyl]bis-*N*⁶,*N*⁶-*tert*-butoxycarbonyl-8-chloroadenine [**81**] (0.30 g, 0.35 mmol) was dissolved in EtOH/EtOAc (15 mL, 1/1) and Pd/C (0.03 g, 10% Pd on activated carbon) was added. The mixture was stirred for 5

hours under an atmosphere of H₂. NaCl (0.02 g) was added and the mixture stirred for 15 minutes and then filtered through a short pad of celite and washed with EtOH (10 mL x 3). The collected solution was concentrated under *vacuum* and the residue was purified via Biotage Isolera One (25g SNAP cartridge Ultra, 75 mL/min, eluent system 0-6% CH₃OH/CH₂Cl₂ 10CV, 6% 2CV) to give the title compound as a white foam (0.24 g, 81%)

³¹P NMR (202 MHz, CDCl₃) δ_P 31.81.

¹H NMR (500 MHz, CDCl₃) δ_H 8.67 (s, 1H, H₂), 5.88 (d, *J* = 6.0 Hz, 1H, H_{1'}), 5.17 (d, *J* = 4.0 Hz, 5.5 Hz, 1H, H_{2'}), 4.13 (d, *J* = 2.5 Hz, 4.5 Hz, 1H, H_{3'}), 4.00-3.86 (m, 5H, H_{4'}, 2 x CH₂CH₃), 2.12-2.00 (m, 1H, H_{5'}), 1.92-1.80 (m, 1H, H_{5'}), 1.78-1.68 (m, 1H, H_{6'}), 1.63-1.49 (m, 1H, H_{6'}), 1.30 (s, 18H, *t*Bu Boc₂), 1.18-1.12 (m, 6H, CH₂CH₃ x 2), 0.81 (s, 9H, *t*Bu), 0.64 (s, 9H, *t*Bu), 0.002 (s, 3H, CH₃), 0.00 (s, 3H, CH₃), -0.22 (s, 3H, CH₃), -0.56 (s, 3H, CH₃).

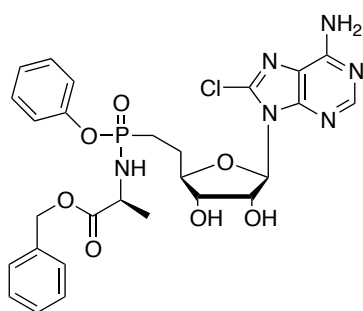
[83] 9-[5',6'-dideoxy-6'-(bis-ethylphosphinyl)-D-ribo-hexofuranosyl]-8-chloroadenine

A solution of 9-[5',6'-dideoxy-6'-(bis-ethylphosphinyl)-2',3'-bis-*O*-*tert*-butyldimethylsilyl-D-ribo-hexofuranosyl]bis-*N*⁶,*N*⁶-*tert*-butoxycarbonyl 8-chloroadenine [**82**] (0.24 g, 0.28 mmol) was stirred at room temperature for 72 hours in HCOOH/H₂O (10 mL, 1/1). The volatiles were evaporated and the crude purified via

Biotage Isolera One (25 g SNAP cartridge Ultra, 75 mL/min, eluent system 2-20% CH₃OH/CH₂Cl₂ 10 CV, 20% 7CV) to afford the title compound as a white solid (0.09 g, 75%).

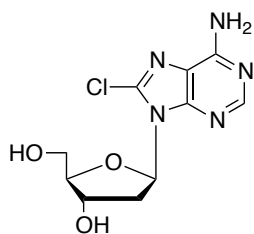
³¹P NMR (202 MHz, CDCl₃) δ_P 33.04.

¹H NMR (500 MHz, CD₃OD) δ_H 8.20 (s, 1H, H₂), 6.01 (d, *J* = 4.5 Hz, 1H, H₁'), 5.25 (t, *J* = 5.0 Hz, 1H, H₂'), 4.43 (d, *J* = 5.5 Hz, 1H, H₃'), 4.13-4.01 (m, 5H, H₄', CH₂CH₃ x 2), 2.14-1.84 (m, 4H, H₅', H₆'), 1.32 (t, *J* = 7.5 Hz, 1.5 Hz, 3H, CH₂CH₃), 1.30 (t, *J* = 7.5 Hz, 1.5 Hz, 3H, CH₂CH₃).

[86] 9-[5',6'-dideoxy-6'-(phenyloxy-(benzyloxy-L-alanine-*N*-yl-phosphinyl)-D-ribo-hexofuranosyl]-8-chloroadenine

A solution of 9-[5',6'-dideoxy-6'-(bis-ethylphosphinyl)-D-ribo-hexofuranosyl]-8-chloroadenine [**83**] (0.05 g, 0.12 mmol) in dry CH₃CN (2 mL) was cooled to 0 °C and 2,6-lutidine (0.04 mL, 0.36 mmol) was added, followed by TMSBr (0.05 mL, 0.36 mmol). The mixture was stirred under argon at 0 °C for 5 hours. Then the solvents were

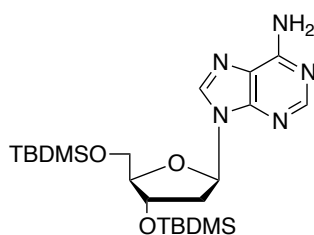
removed under reduced pressure without any contact with air. The residue was dissolved in anhydrous Et₃N (0.25 mL) and pyridine (1 mL) and L-alanine benzyl ester *p*TSA salt (0.042 g, 0.12 mmol) and phenol (0.068 g, 0.72 mmol) were added. In a separated flask, aldrithiol-2 (0.06 g, 0.72 mmol) and Ph₃P (0.188 g, 0.72 mmol) were dissolved in anhydrous pyridine (1.2 mL) and this solution was immediately added to the reaction. The resulting mixture (green solution) was stirred at 50 °C for 16 hours. The residue was taken up in CH₂Cl₂ (15 mL) and washed with HCl (0.5 N in water) (2 x 15 mL) and brine (15 mL). The organics were combined and dried over Na₂SO₄, filtered and evaporated to dryness. The crude was purified *via* Biotage Isolera One (10g SNAP cartridge Ultra, 12 mL/min, eluent system 2-100% CH₃OH/CH₂Cl₂ 10CV, 100% 7CV), prep. HPLC (isocratic eluent system CH₃OH/H₂O 55%, in 30 minutes, 20 mL/min, λ = 254) to afford the two separated diastereoisomers as white solids (0.004 g, 5%).

More polar isomer (fast eluting-FE)**³¹P NMR (202 MHz, CD₃OD) δ_P** 34.42.**¹H NMR (500 MHz, CD₃OD) δ_H** 8.00 (s, 1H, H₂), 7.20-7.10 (m, 7H, Ph), 7.02-6.92 (m, 3H, Ph), 5.84 (d, *J* = 5.0 Hz, 1H, H₁'), 5.09 (t, *J* = 5.0 Hz, 1H, H₂'), 4.93-4.84 (m, 2H, CH₂Ph), 4.24 (t, *J* = 5.4 Hz, 1H, H₃'), 3.86-3.76 (m, 2H, H₄', CHCH₃ L-Ala), 2.02-1.79 (m, 4H, H₅', H₆'), 0.99 (d, *J* = 7.0 Hz, 3H, CHCH₃ L-Ala).**Least polar isomer (slow eluting-SE)****³¹P NMR (202 MHz, CD₃OD) δ_P** 33.67.**¹H NMR (500 MHz, CD₃OD) δ_H** 8.18 (s, 1H, H₂), 7.34-7.26 (m, 7H, Ph), 7.18-7.11 (m, 3H, Ph), 6.00 (d, *J* = 4.5 Hz, 1H, H₁'), 5.19 (dd, *J* = 4.5, 5.5 Hz, 1H, H₂'), 5.02-4.98 (m, 2H, CH₂Ph), 4.47 (t, *J* = 5.5 Hz, 1H, H₃'), 4.04-3.94 (m, 2H, H₄', CHCH₃ L-Ala), 2.19-1.95 (m, 4H, H₅', H₆'), 1.26 (d, *J* = 7.0 Hz, 3H, CHCH₃ L-Ala).**HPLC** Reverse-phase HPLC eluting with H₂O/CH₃CN from 90/10 to 0/100 in 35 minutes, F = 1 mL/min, λ = 254, one peak of the overlapping diastereoisomers with t_R 23.23 min.**9.5.14 Synthesis of 8-chloro-2'-deoxyadenosine****[87] 8-Chloro-2'-deoxyadenosine**

3',5'-(Bis-*O-tert*-butyldimethylsilyl) 8-chloroadenosine [89] (0.81 g, 1.57 mmol) was dissolved in THF (10 mL) and the solution was cooled to 0 °C. TBAF (1M in THF, 5.51 mL, 5.51 mmol) was added dropwise and the mixture was stirred at room temperature for 1 hour.

The solvents were evaporated and the crude washed with *n*-hex (4 x 5 mL), The crude was packed as a silica slurry and purified via flash column chromatography (gradient eluent system 3-10% CH₃OH/CHCl₃) to afford the title compound as a white solid (0.094 g, 33%).³⁵¹

¹H NMR (500 MHz, CD₃OD) δ_H 8.16 (s, 1H, H₂), 6.39 (dd, *J* = 8.5, 6.0 Hz, 1H, H₁'), 5.67 (br s, 2H, NH₂), 4.67-4.65 (m, 1H, H₃'), 4.12-4.10 (m, 1H, H₄'), 3.89 (dd, *J* = 12.5, 2.5 Hz, 1H, H₅'), 3.75 (dd, *J* = 12.5, 3.5 Hz, 1H, H₅'), 3.16-3.10 (m, 1H, H₂'), 2.34-2.30 (m, 1H, H₂').**¹³C NMR (126 MHz, DMSO-*d*₆) δ_C** 156.15 (C₆), 152.03 (C₂), 149.52 (C₄), 136.92 (C₈), 116.54 (C₅), 88.95 (C₁'), 86.59 (C₄'), 72.05 (C₃'), 62.69 (C₅'), 38.39 (C₂').**[88] 3',5'-Bis-*O-tert*-butyldimethylsilyl-2'-deoxyadenosine**

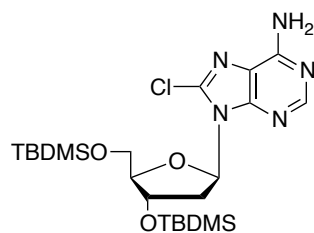


2'-Deoxyadenosine (6.0 g, 23.88 mmol) was dissolved in DMF (30 mL) and imidazole (7.15 g, 105.07 mmol) was added, followed by TBDMSCl (7.98 g, 52.53 mmol).

The mixture was stirred at rt for 16 hours, then the volatiles were evaporated and the crude taken up with *n*-hex (40 mL) and washed with aqueous NH₄Cl (saturated solution, 20 mL x 2) and brine (20 mL). The organics were collected, dried over Na₂SO₄, filtered and evaporated, to yield the title compound as a sticky solid (10.77 g, 94%).³⁵¹

¹H NMR (500 MHz, CDCl₃) δ_H 8.37 (s, 1H, H8), 8.15 (s, 1H, H2), 6.47 (t, *J* = 6.5 Hz, 1H, H1'), 5.78 (br s, 2H, NH₂), 4.63 (dt, *J* = 6.0, 3.5 Hz, 1H, H3'), 4.05-4.00 (m, 1H, H4'), 3.89 (dd, *J* = 11.0, 4.0 Hz, 1H, H5'), 3.79 (dd, *J* = 11.5, 3.5 Hz, 1H, H5'), 2.69-2.62 (m, 1H, H2'), 2.49-2.42 (m, 1H, H2'), 0.937 (s, 9H, *t*Bu), 0.935 (s, 9H, *t*Bu), 0.12 (s, 6H, CH₃ x 2), 0.11 (s, 3H, CH₃), 0.10 (s, 3H, CH₃).

[89] 3',5'-Bis-*O*-*tert*-butyldimethylsilyl-8-chloro-2'-deoxyadenosine

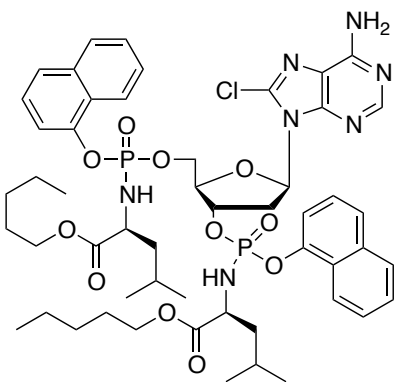


To a stirring solution of LDA (2M in THF, 130.25 mL, 260.5 mmol) in a -78 °C bath was added a solution of 3',5'-*O*-*tert*-butyldimethylsilyl-2'-deoxyadenosine [88] (10.0 g, 52.10 mmol) in THF (25 mL) dropwise *via* a dropping funnel. The funnel was washed with THF (5 mL) and the reaction was stirred for 1 hour

at -78 °C. A solution of TsCl (39.73 g, 208.4 mmol) in THF (30 mL) was added dropwise, and the funnel rinsed with THF (5 mL). The reaction was stirred for 1h and then quenched by dropwise addition of glacial AcOH (15 mL). The mixture was allowed to reach room temperature and evaporated. The crude was dissolved in *n*Hex (50 mL) and washed with brine (3 x 50 mL). The organic phase was dried over Na₂SO₄, filtered and evaporated. The crude was purified by Biotage Isolera flash chromatography (100g SNAP cartridge KP SIL, eluent system 3-30% EtOAc/*n*Hex 10 CV, 30% EtOAc/*n*Hex 4 CV) to yield the title compound as a white foam (20.09 g, 75%).³⁵¹

¹H NMR (500 MHz, CDCl₃) δ_H 8.30 (s, 1H, H2), 6.47 (t, *J* = 6.5 Hz, 1H, H1'), 5.67 (br s, 2H, NH₂), 4.89-4.86 (m, 1H, H3'), 3.99-3.96 (m, 1H, H4'), 3.91 (dd, *J* = 11.0, 6.5 Hz, 1H, H5'), 3.69 (dd, *J* = 11.0, 5.0 Hz, 1H, H5'), 3.65-3.60 (m, 1H, H2'), 2.28-2.23 (m, 1H, H2'), 0.96 (s, 9H, *t*Bu), 0.85 (s, 9H, *t*Bu), 0.17 (s, 6H, CH₃ x 2), 0.02 (s, 3H, CH₃), 0.01 (s, 3H, CH₃).

9.5.15 Synthesis of 8-chloro-2'-deoxyadenosine prodrugs

[90a] 8-Chloro-2'-deoxyadenosine-3',5'-bis-O-naphth-1-yl(pentyl-1-oxy-L-leucinyl) phosphate

Prepared according to general procedure **F₁** using 8-chloro-2'-deoxyadenosine [**87**], (0.10 g, 0.35 mmol) in THF (7 mL), *t*BuMgCl (1.0 M in THF, 0.87 mL, 0.87 mmol) and naphth-1-yl-(pentyl-1-oxy-L-leucinyl) phosphorochloridate [**17f**] (0.45 g, 1.05 mmol) in THF (3 mL). Purification by Biotage Isolera One (50g SNAP cartridge, 50 mL/min, gradient eluent system 1-10% CH₃OH/CH₂Cl₂ 10CV, 10% 5CV) and prep TLC (2000

μm, 5% CH₃OH/CH₂Cl₂) yielded the title compound as a white solid (0.03 g, 8%)

³¹P NMR (202 MHz, CD₃OD) δ_P 4.05, 3.97, 3.92, 3.84, 3.49, 2.46.

¹H NMR (500 MHz, CD₃OD) δ_H 8.26-8.22 (m, 1H, Nap), 8.10-8.01 (m, 2H, H₂, Nap), 7.93-7.87 (m, 1H, Nap), 7.85-7.89 (m, 1H, Nap), 7.76-7.69 (m, 1H, Nap), 7.65-7.60 (m, 1H, Nap), 7.60-7.35 (m, 7H, Nap), 7.33-7.23 (m, 1H, Nap), 6.49-6.45 (m, 0.5H, H1'), 6.35-6.29 (m, 0.5H, H1'), 5.78-5.60 (m, 1H, H3'), 4.62-4.35 (m, 3H, H5', H4'), 4.06-3.79 (m, 6H, CH₂CH₂CH₂CH₂CH₃ *n*-Pent, CHCH₂CH(CH₃)₂ L-Leu), 3.79-3.71 (m, 0.5H, H2'), 3.68-3.53 (m, 0.5H, H2'), 2.83-2.75 (m, 0.5H, H2'), 2.62-2.52 (m, 0.5H, H2'), 1.77-1.13 (m, 16H, CH₂CH₂CH₂CH₂CH₃ *n*-Pent, CHCH₂CH(CH₃)₂ L-Leu), 0.89-0.63 (m, 20H, CH₂CH₂CH₂CH₂CH₃ *n*-Pent, CHCH₂CH(CH₃)₂ L-Leu).

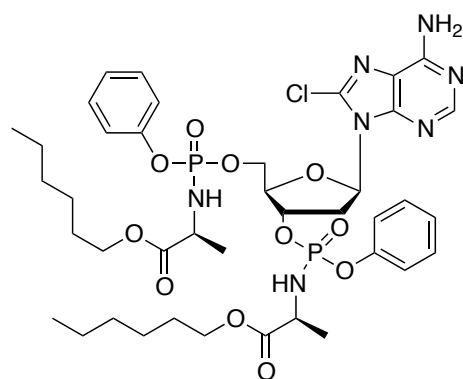
¹³C NMR (125 MHz, CD₃OD) δ_C 175.44 (d, ³J_{CP} = 2.5 Hz, CO), 175.37 (d, ³J_{CP} = 2.5 Hz, CO), 175.23 (d, ³J_{CP} = 2.5 Hz, CO), 175.03 (d, ³J_{CP} = 2.5 Hz, CO), 175.00 (d, ³J_{CP} = 2.5 Hz, CO), 174.89 (d, ³J_{CP} = 2.5 Hz, CO), 174.87 (d, ³J_{CP} = 2.5 Hz, CO), 156.22 (C6), 156.17 (C6), 156.12 (C6), 153.90 (C2), 153.88 (C2), 153.85 (C2), 151.52 (C4), 151.45 (C4), 151.43 (C4), 151.33 (C4), 148.93 (C8), 148.89 (C8), 148.88 (C8), 148.84 (C8), 139.43 (C-Ar), 139.42 (C-Ar), 136.40 (C-Ar), 136.23 (C-Ar), 136.21 (C-Ar), 136.14 (C-Ar), 128.99 (CH-Ar), 128.95 (CH-Ar), 128.93 (CH-Ar), 128.80 (CH-Ar), 128.74 (CH-Ar), 128.02 (C-Ar), 128.01 (C-Ar), 127.98 (C-Ar), 127.96 (C-Ar), 127.93 (C-Ar), 127.88 (CH-Ar), 127.84 (CH-Ar), 127.82 (CH-Ar), 127.80 (C-Ar), 127.78 (C-Ar), 127.75 (C-Ar), 127.73 (C-Ar), 127.68 (CH-Ar), 127.63 (CH-Ar), 127.61 (CH-Ar), 127.60 (CH-Ar), 127.34 (CH-Ar), 127.29 (CH-Ar), 126.61 (CH-Ar), 126.57 (CH-Ar), 126.56 (CH-Ar), 126.43 (CH-Ar), 126.39 (CH-Ar), 126.24 (CH-Ar), 126.21 (CH-Ar), 126.15 (CH-Ar), 126.13 (CH-Ar), 125.78 (CH-Ar), 125.72 (CH-Ar), 122.91 (CH-Ar), 122.80 (CH-Ar),

122.75 (CH-Ar), 119.69 (C5), 119.56 (C5), 116.73 (CH-Ar), 116.71 (CH-Ar), 116.47 (CH-Ar), 116.44 (CH-Ar), 116.41 (CH-Ar), 116.39 (CH-Ar), 116.19 (CH-Ar), 116.17 (CH-Ar), 115.91 (CH-Ar), 115.88 (CH-Ar), 86.32 (C1'), 86.20 (C1'), 86.17 (C1'), 86.03 (C1'), 85.43 (C4'), 85.38 (C4'), 85.36 (C4'), 85.29 (C4'), 85.24 (C4'), 85.23 (C4'), 85.20 (C4'), 85.18 (C4'), 85.13 (C4'), 85.07 (C4'), 78.55 (d, $^2J_{CP} = 5.4$ Hz, C3'), 78.52 (d, $^2J_{CP} = 5.2$ Hz, C3'), 78.20 (d, $^2J_{CP} = 5.3$ Hz, C3'), 78.16 (d, $^2J_{CP} = 5.2$ Hz, C3'), 67.34 (d, $^2J_{CP} = 5.4$ Hz, C5'), 67.23 (d, $^2J_{CP} = 5.4$ Hz, C5'), 67.18 (d, $^2J_{CP} = 5.2$ Hz, C5'), 67.08 (d, $^2J_{CP} = 5.2$ Hz, C5'), 66.43 (CH₂ Gly), 66.42 (CH₂ Gly), 66.41 (CH₂ Gly), 66.39 (CH₂ Gly), 66.25 (CH₂ Gly), 66.23 (CH₂ Gly), 54.94 (CHCH₂CH(CH₃)₂ L-Leu), 54.90 (CHCH₂CH(CH₃)₂ L-Leu), 54.66 (CHCH₂CH(CH₃)₂ L-Leu), 54.64 (CHCH₂CH(CH₃)₂ L-Leu), 54.62 (CHCH₂CH(CH₃)₂ L-Leu), 44.28 (CH₂), 44.26 (CH₂), 44.22 (CH₂), 44.20 (CH₂), 44.12 (CH₂), 44.09 (CH₂), 44.06 (CH₂), 44.04 (CH₂), 43.98 (CH₂), 43.86 (CH₂), 43.93 (CH₂), 43.90 (CH₂), 36.62 (C2'), 36.59 (C2'), 36.54 (C2'), 36.51 (C2'), 29.39 (CH₂), 29.34 (CH₂), 29.29 (CH₂), 29.25 (CH₂), 29.16 (CH₂), 29.10 (CH₃/CH), 29.08 (CH₂), 29.06 (CH₂), 25.76 (CH₃), 25.65 (CH₃), 25.62 (CH₃), 25.47 (CH₃), 25.38 (CH₃), 23.34 (CH₂), 23.29 (CH₂), 23.27 (CH₂), 23.23 (CH₃/CH), 23.22 (CH₃/CH), 23.15 (CH₃/CH), 23.11 (CH₃/CH), 23.08 (CH₃/CH), 23.05 (CH₃/CH), 23.03 (CH₃/CH), 22.13 (CH₃/CH), 22.06 (CH₃/CH), 21.87 (CH₃/CH), 21.85 (CH₃/CH), 21.79 (CH₃/CH), 21.75 (CH₃/CH), 14.30 (CHCH₂CH(CH₃)₂ L-Leu), 14.28 (CHCH₂CH(CH₃)₂ L-Leu), 14.26 (CHCH₂CH(CH₃)₂ L-Leu).

MS (ES⁺) *m/z* found 1064.21 [M+H⁺], C₅₂H₆₈ClN₇O₁₁P₂ required *m/z* 1064.54 [M].

HPLC Reverse-phase HPLC eluting with H₂O/CH₃CN from 80/20 to 1/90 in 15 minutes, then to 0/100 in 35 min, F = 1 mL/min, λ = 280 nm, broad peak with tR 21.98 min.

[90b] 8-Chloro-2'-deoxyadenosine-3',5'-bis-*O*-phenyl-(hex-1-yloxy-L-alaninyl)phosphate



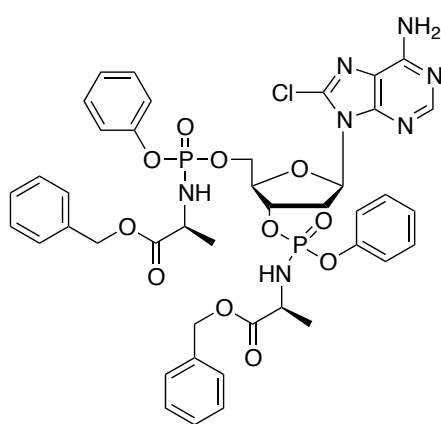
Prepared according to general procedure **F₁** using 8-chloro-2'-deoxyadenosine [**87**], (0.10 g, 0.35 mmol) in THF (10 mL), *t*BuMgCl (1.0 M in THF, 0.52 mL, 0.52 mmol) and phenyl-(hexyl-1-oxy-L-alaninyl)phosphorochloridate [**17u**] (0.36 g, 1.05 mmol) in THF (2 mL). Purification by Biotage Isolera One (50g SNAP cartridge, 50 mL/min,

gradient eluent system 1-10% CH₃OH/CH₂Cl₂ 10CV, 10% 5CV) and prep TLC (2000 μm, 5% CH₃OH/CH₂Cl₂) yielded the title compound as a white solid (0.089 g, 28%).

³¹P NMR (202 MHz, CD₃OD) δ_P 3.55, 3.52, 3.49, 3.26, 3.14, 2.89, 2.84.

¹H NMR (500 MHz, CD₃OD) δ_{H} 8.21-8.12 (m, 1H, H2), 7.42-7.07 (m, 10H, Ph), 6.53-6.45 (m, 0.5H, H1'), 6.42-6.36 (m, 0.5H, H1'), 5.69-5.53 (m, 1H, H3'), 4.53-4.43 (m, 1H, H5'), 4.41-4.26 (m, 2H, H4', H5'), 4.15-3.93 (m, 6H, CH₂CH₂CH₂CH₂CH₂CH₃ *n*-Hex, CHCH₃ L-Ala), 3.91-3.83 (m, 0.5H, H2'), 3.81-3.61 (m, 0.5H, H2'), 2.82-2.72 (m, 0.5H, H2'), 2.66-2.57 (m, 0.5H, H2'), 1.65-1.48 (m, 4H, 2 x CH₂CH₂CH₂CH₂CH₂CH₃ *n*-Hex), 1.43-1.18 (m, 18H, CH₂CH₂CH₂CH₂CH₂CH₃ *n*-Hex, CHCH₃ L-Ala), 0.91-0.82 (m, 6H, CH₂CH₂CH₂CH₂CH₂CH₃ *n*-Hex).

[90c] 8-Chloro-2'-deoxyadenosine-3',5'-bis-*O*-phenyl-(benzyloxy-L-alaninyl) phosphate



Prepared according to general procedure F₁ using 8-chloro-2'-deoxyadenosine [87], (0.10 g, 0.35 mmol) in THF (10 mL), *t*BuMgCl (1.0 M in THF, 0.38 mL, 0.38 mmol) and phenyl-(benzyloxy-L-alaninyl) phosphorochloridate [17s] (0.25 g, 0.7 mmol) in THF (1.5 mL). Purification by Biotage Isolera One (50g SNAP cartridge, 50 mL/min, gradient eluent system 1-10% CH₃OH/CH₂Cl₂ 10CV, 10% 5CV) and prep TLC

(2000 μm , 5% CH₃OH/CH₂Cl₂) yielded the title compound as a white solid (0.08 g, 25%).

³¹P NMR (202 MHz, CD₃OD) δ_{P} 3.49, 3.43, 3.42, 3.39, 3.30, 3.18.

¹H NMR (500 MHz, CD₃OD) δ_{H} 8.17 (s, 0.25H, H2), 8.158 (s, 0.25H, H2), 8.152 (s, 0.25H, H2), 8.13 (s, 0.25H, H2), 7.39-7.06 (m, 20H, Ar), 6.44-6.40 (m, 0.5H, H1'), 6.36-6.32 (m, 0.5H, H1'), 5.63-5.53 (m, 1H, H3'), 5.15-5.00 (m, 4H, CH₂Ph), 4.47-4.38 (m, 1H, H5'), 4.34-4.22 (m, 2H, H5', H4'), 4.14-4.04 (m, 1H, CHCH₃ L-Ala), 3.98-3.80 (m, 1H, CHCH₃ L-Ala), 3.69-3.53 (m, 1H, H2'), 2.68-2.60 (m, 0.5H, H2'), 2.57-2.50 (m, 0.5H, H2'), 1.44-1.17 (m, 6H, CHCH₃ L-Ala).

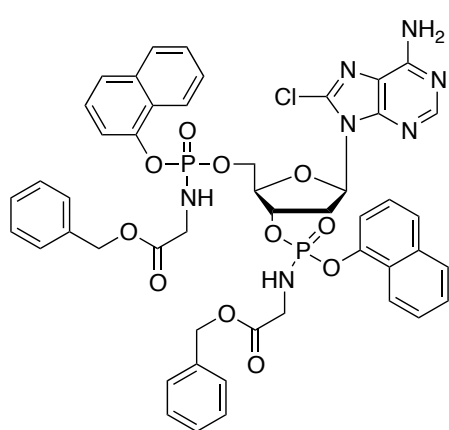
¹³C NMR (125 MHz, CD₃OD) δ_{C} 174.85 (CO), 174.84 (CO), 174.81 (CO), 174.72 (CO), 174.69 (CO), 174.67 (CO), 174.57 (CO), 174.53 (CO), 156.30 (C6), 156.28 (C6), 156.27 (C6), 154.00 (C2), 153.94 (C2), 153.92 (C2), 152.16 (C-Ar), 152.15 (C-Ar), 152.12 (C-Ar), 152.11 (C-Ar), 152.07 (C-Ar), 152.04 (C-Ar), 152.99 (C-Ar), 151.51 (C4), 151.49 (C4), 151.44 (C4), 151.41 (C4), 139.54(C-Ar), 139.53(C-Ar), 139.48(C-Ar), 139.45(C-Ar), 137.32(C-Ar), 137.26(C-Ar), 137.24(C-Ar), 137.22(C-Ar), 137.20(C-Ar), 130.91 (CH-Ar), 130.68 (CH-Ar), 129.65 (CH-Ar), 129.57 (CH-Ar), 129.39 (CH-Ar), 129.38 (CH-Ar), 129.32 (CH-Ar), 129.31 (CH-Ar), 129.26 (CH-Ar), 129.24 (CH-Ar), 126.37 (CH-Ar), 126.34 (CH-Ar), 126.07 (CH-Ar), 126.02 (CH-Ar), 121.67 (CH-Ar), 121.64

(CH-Ar), 121.60 (CH-Ar), 121.57 (CH-Ar), 121.56 (CH-Ar), 121.49 (CH-Ar), 121.46 (CH-Ar), 121.40 (CH-Ar), 121.37 (CH-Ar), 121.34 (CH-Ar), 119.68 (C5), 119.65 (C5), 119.62 (C5), 119.58 (C5), 86.16 (C1'), 86.12 (C1'), 86.08 (C1'), 86.05 (C1'), 85.12 (C4'), 85.07 (C4'), 85.00 (C4'), 84.92 (C4'), 84.85 (C4'), 84.78 (C4'), 84.72 (C4'), 78.01 (C3'), 77.96 (C3'), 77.94 (C3'), 77.90 (C3'), 77.86 (C3'), 67.94 (CH₂Ph), 67.93 (CH₂Ph), 67.88 (CH₂Ph), 67.86 (CH₂Ph), 66.99 (d, ²J_{CP} = 5.4 Hz, C5'), 66.94 (d, ²J_{CP} = 5.4 Hz, C5'), 66.57 (d, ²J_{CP} = 5.4 Hz, C5'), 66.53 (d, ²J_{CP} = 5.4 Hz, C5'), 51.92 (CHCH₃ L-Ala), 51.91 (CHCH₃ L-Ala), 51.83 (CHCH₃ L-Ala), 51.81 (CHCH₃ L-Ala), 36.41 (C2'), 36.39 (C2'), 36.37 (C2'), 36.35 (C2'), 36.33 (C2'), 36.30 (C2'), 36.27 (C2'), 20.58 (CHCH₃ L-Ala), 20.56 (CHCH₃ L-Ala), 20.52 (CHCH₃ L-Ala), 20.47 (CHCH₃ L-Ala), 20.45 (CHCH₃ L-Ala), 20.43 (CHCH₃ L-Ala), 20.39 (CHCH₃ L-Ala), 20.38 (CHCH₃ L-Ala).

MS (ES⁺) m/z found 920.2 [M+H⁺], C₄₂H₄₄ClN₇O₁₁P₂ required m/z 920.24 [M].

HPLC Reverse-phase HPLC eluting with H₂O/CH₃CN from 90/10 to 0/100 in 30 minutes, F = 1 mL/min, λ = 280 nm, three broad peaks with t_R 21.97 min, 22.26 min, 22.59 min.

[90d] 8-Chloro-2'-deoxyadenosine-3',5'-bis-O-naphth-1-yl-(benzyloxy-L-glyciny)phosphate



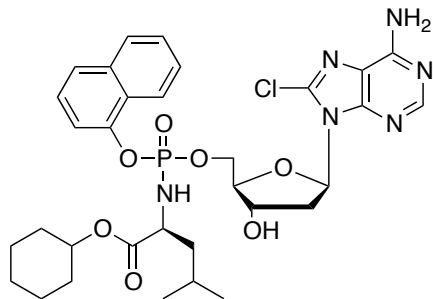
Prepared according to general procedure F₁ using 8-chloro-2'-deoxyadenosine [87], (0.10 g, 0.35 mmol) in THF (10 mL), *t*BuMgCl (1.0 M in THF, 0.38 mL, 0.38 mmol) and naphth-1-yl-(benzyloxy-L-alaninyl)phosphorochloridate [17a] (0.15 g, 0.38 mmol) in THF (1.5 mL). Purification by Biotage Isolera One (50g SNAP cartridge, 50 mL/min, gradient eluent system 1-10% CH₃OH/CH₂Cl₂ 10CV, 10% 5CV) and prep TLC (2000 μm, 5% CH₃OH/CH₂Cl₂) yielded the title compound as a

white solid (0.056 g, 16%).

³¹P NMR (202 MHz, CD₃OD) δ_P 4.96, 4.89, 4.80, 4.71, 4.68, 4.61, 4.59, 4.46.

¹H NMR (500 MHz, CD₃OD) δ_H 8.24-8.19 (m, 1H, Nap), 8.10-8.02 (m, 2H, H₂, Nap), 7.95-7.77 (m, 2H, Nap, Ph), 7.73-7.66 (m, 1H, Nap), 7.62-7.15 (m, 19H, Nap, Ph), 6.33-6.13 (m, 1H, H1'), 5.75-5.60 (m, 1H, H3'), 5.14-4.96 (m, 4H, CH₂Ph), 4.59-4.26 (m, 3H, H5', H4'), 3.95-3.83 (m, 2H, CH₂ Gly), 3.78-3.51 (m, 3H, CH₂ Gly, H2'), 2.60-2.41 (m, 1H, H2').

[91a] 8-Chloro-2'-deoxyadenosine-5'-O-naphth-1-yl-(cyclohexyloxy-L-leucinyl)phosphate

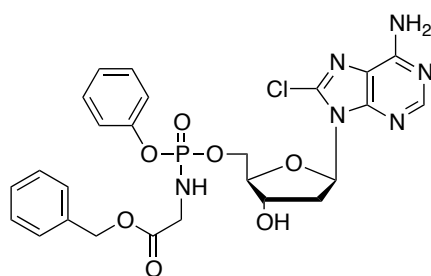


Prepared according to generale procedure **F₂** using 8-chloro-2'-deoxyadenosine [**87**], (0.05 g, 0.17 mmol) in THF (1.5 mL), *N*-methylimidazole (0.06 ml, 0.87 mmol) and naphth-1-yl-(cyclohexyloxy-L-leucinyl)phosphorochloridate (230 mg, 0.52 mmol) in THF (1 mL). Purification by Biotage Isolera One (10g SNAP cartridge, 10 mL/min, gradient eluent system 1-10% CH₃OH/CH₂Cl₂ 10CV, 10% 5CV) and prep TLC (500 μm, 5% CH₃OH/CH₂Cl₂) yielded the title compound as a white solid (0.002 g, 2%).

³¹P NMR (202 MHz, CD₃OD) δ_P 4.11, 4.04.

¹H NMR (500 MHz, CD₃OD) δ_H 8.14-8.06 (m, 2H, H₂, Nap), 7.89-7.84 (m, 1H, Nap), 7.70-7.65 (m, 1H, Nap), 7.55-7.45 (m, 2H, Nap), 7.44-7.40 (m, 1H, Nap), 7.39-7.31 (m, 1H, Nap), 6.499 (t, *J* = 7.0 Hz, 0.5H, H1'), 6.49 (t, *J* = 6.8 Hz, 0.5H, H1'), 4.81-4.75 (m, 1H, H3'), 4.65-4.56 (m, 1H, CH(CH₂)₅ cHex), 4.53-4.42 (m, 1.5H, H5'), 4.36-4.29 (m, 0.5H, H5'), 4.23-4.18 (m, 0.5H, H4'), 4.18-4.12 (m, 0.5H, H4'), 3.90-3.81 (m, 1H, CHCH₂CH(CH₃)₂ L-Leu), 3.54-3.43 (m, 1H, H2'), 2.24-2.32 (m, 1H, H2'), 1.76-1.59 (m, 4H, CH(CH₂)₅ cHex), 1.53-1.22 (m, 9H, CH(CH₂)₅ cHex, CHCH₂CH(CH₃)₂ L-Leu), 0.85-0.62 (m, 6H, CHCH₂CH(CH₃)₂ L-Leu).

[91b] 8-Chloro-2'-deoxyadenosine-5'-O-phenyl-(benzyloxy-glyciny)phosphate



Prepared according to generale procedure **F₂** using 8-chloro-2'-deoxyadenosine [**87**], (0.025 g, 0.08 mmol) in THF (1.0 mL), *N*-methylimidazole (0.03 ml, 0.46 mmol) and phenyl-(benzyloxy-glyciny)phosphorochloridate [**17r**] (0.085 g, 0.26 mmol) in THF (1 mL). Purification by Biotage Isolera One (10g SNAP cartridge, 10 mL/min, gradient eluent system 1-10% CH₃OH/CH₂Cl₂ 10CV, 10% 5CV) and prep TLC (500 μm, 5% CH₃OH/CH₂Cl₂) yielded the title compound as a white solid (0.002 g, 4%)

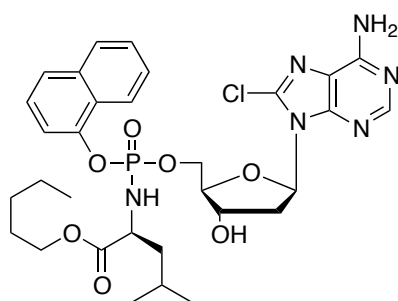
³¹P NMR (202 MHz, CD₃OD) δ_P 4.61, 4.52.

¹H NMR (500 MHz, CD₃OD) δ_H 8.19 (s, 0.5H, H₂), 8.16 (s, 0.5H, H₂), 7.37-7.26 (m, 7H, Ph), 7.18-7.10 (m, 3H, Ph), 6.50-6.45 (m, 1H, H1'), 5.15-5.08 (m, 2H, CH₂Ph), 4.82-4.78

(m, 1H, H3'), 4.46-4.39 (m, 1H, H5'), 4.37-4.28 (m, 1H, H5'), 4.15-4.10 (m, 1H, H4'), 3.76-3.67 (m, 2H, CH₂ Gly), 3.56-3.46 (m, 1H, H2'), 2.41-2.33 (m, 1H, H2').

¹³C NMR (125 MHz, CD₃OD) δ_C 156.32 (C6), 153.94 (C2), 151.60 (C4), 149.01 (C8), 139.62 (C-Ar), 137.22 (C-Ar), 134.64 (CH-Ar), 132.88 (CH-Ar), 130.68 (CH-Ar), 129.56 (CH-Ar), 129.36 (CH-Ar), 129.34 (CH-Ar), 129.31 (CH-Ar), 128.77 (C-Ar), 126.07 (CH-Ar), 121.42 (CH-Ar), 121.38 (CH-Ar), 121.36 (CH-Ar), 119.48 (C5), 86.81 (d, ³J_{CP} = 8.1 Hz, C4'), 86.67 (d, ³J_{CP} = 8.4 Hz, C4'), 86.53 (C1'), 86.50 (C1'), 72.51 (C3'), 72.33 (C3'), 67.90 (CH₂Ph), 67.87 (CH₂Ph), 67.77 (d, ²J_{CP} = 5.6 Hz, C5'), 67.35 (d, ²J_{CP} = 5.0 Hz, C5'), 43.78 (CH₂ Gly), 43.75 (CH₂ Gly), 37.80 (C2'), 37.77 (C2').

[95a] 8-Chloro-2'-deoxyadenosine-5'-O-naphth-1-yl-(pentyl-1-oxy-L-leucinyl)phosphate



8-Chloro-2'-deoxyadenosine-3',5'-bis-O-naphth-1-yl-(pentyl-1-oxy-L-leucinyl)phosphate [**90a**] (0.03 g, 0.03 mmol) was dissolved in THF (2.5 mL), and zirconocene hydrochloride (Schwartz reagent) was added (0.023 g, 0.09 mmol). The mixture was stirred at room temperature for 3 hours, quenched with water (0.2 mL) and

evaporated. The crude was purified via Biotage Isolera One (10g ZIP cartridge, 10 mL/min, gradient eluent system 1-12% CH₃OH/CH₂Cl₂ 10CV, 12% 2CV) to afford the title compound as a white solid (0.003 g, 14%).

³¹P NMR (202 MHz, CD₃OD) δ_P 4.03, 4.01.

¹H NMR (500 MHz, CD₃OD) δ_H 8.03-7.93 (m, 2H, Nap, H2), 7.77-7.72 (m, 1H, Nap), 7.58-7.53 (m, 1H, Nap), 7.43-7.19 (m, 4H, Nap), 6.39-6.34 (m, 1H, H1'), 4.70-4.64 (m, 1H, H3'), 4.40-4.30 (m, 1.5H, H5'), 4.23-4.16 (m, 0.5H, H5'), 4.10-4.06 (m, 0.5H, H4'), 4.05-4.01 (m, 0.5H, H4'), 3.84-3.68 (m, 3H, CH₂CH₂CH₂CH₂CH₃ *n*-Pen, CHCH₂CH(CH₃)₂ L-Leu), 3.42-3.30 (m, 1H, H2'), 2.29-2.20 (m, 1H, H2'), 1.55-1.06 (m, 9H, CH₂CH₂CH₂CH₂CH₃ *n*-Pen, CHCH₂CH(CH₃)₂ L-Leu), 0.77-0.56 (m, 9H, CH₂CH₂CH₂CH₂CH₃ *n*-Pen, CHCH₂CH(CH₃)₂ L-Leu).

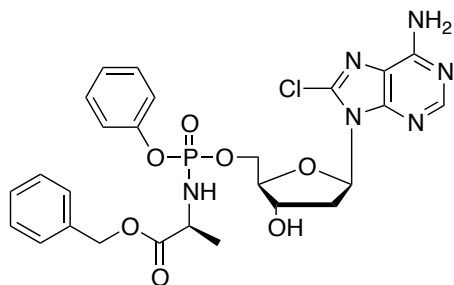
¹³C NMR (125 MHz, CD₃OD) δ_C 175.27 (CO), 175.17 (CO), 175.03 (CO), 174.87 (CO), 156.02 (C6), 155.88 (C6), 153.86 (C2), 153.85 (C2), 151.61 (C4), 151.50 (C4), 149.02 (C-Ar), 148.97 (C8), 148.88 (C8), 147.97 (C-Ar), 147.80 (C-Ar), 147.75 (C-Ar), 144.47 (C-Ar), 144.44 (C-Ar), 144.29 (C-Ar), 144.25 (C-Ar), 139.53 (C-Ar), 139.51 (C-Ar), 136.29 (C-Ar), 136.23 (C-Ar), 128.84 (CH-Ar), 128.79 (CH-Ar), 127.87 (C-Ar), 127.78 (C-Ar), 127.37 (CH-Ar), 127.31 (CH-Ar), 126.42 (d, ²J_{CP} = 8.5 Hz, 5.0 Hz, C-Ar), 126.40 (d, ²J_{CP}

= 8.5 Hz, 5.0 Hz, C-Ar), 125.81 (CH-Ar), 125.80 (CH-Ar), 122.76 (CH-Ar), 122.71 (CH-Ar), 119.59 (C5), 119.46 (C5), 116.09 (d, $^3J_{CP}$ = 3.75 Hz, CH-Ar), 115.02 (d, $^3J_{CP}$ = 3.7 Hz, CH-Ar), 86.91 (d, $^3J_{CP}$ = 8.4 Hz, C4'), 86.77 (d, $^3J_{CP}$ = 8.5 Hz, C4'), 86.57 (C1'), 86.44 (C1'), 72.57 (C3'), 72.46 (C3'), 68.11 (d, $^2J_{CP}$ = 5.4 Hz, C5'), 67.77 (d, $^2J_{CP}$ = 5.6 Hz, C5'), 66.29 (CH₂Ph), 66.25 (CH₂Ph), 54.65 (CHCH₂CH(CH₃)₂ L-Leu), 54.63 (CHCH₂CH(CH₃)₂ L-Leu), 44.23 (d, $^3J_{CP}$ = 7.4 Hz, CHCH₂CH(CH₃)₂ L-Leu), 44.06 (d, $^3J_{CP}$ = 8.2 Hz, CHCH₂CH(CH₃)₂ L-Leu), 37.81 (CH₂CH₂CH₂CH₂CH₃ *n*-Pen), 37.76 (CH₂CH₂CH₂CH₂CH₃ *n*-Pen), 29.29 (CH₂CH₂CH₂CH₂CH₃ *n*-Pen), 29.28 (CH₂CH₂CH₂CH₂CH₃ *n*-Pen), 29.12 (CH₂CH₂CH₂CH₂CH₃ *n*-Pen), 29.08 (CH₂CH₂CH₂CH₂CH₃ *n*-Pen), 25.56 (CHCH₂CH(CH₃)₂ L-Leu) 25.45 (CHCH₂CH(CH₃)₂ L-Leu), 23.31 (CH₂CH₂CH₂CH₂CH₃ *n*-Pen), 23.28 (CH₂CH₂CH₂CH₂CH₃ *n*-Pen), 23.06 (CH₃ L-Leu/*n*-Pen), 23.01 (CH₃ L-Leu/*n*-Pen), 22.03 (CH₃ L-Leu/*n*-Pen), 21.90 (CH₃ L-Leu/*n*-Pen), 14.25 (CH₃ L-Leu/*n*-Pen).

MS (ES⁺) *m/z* found 676.2 [M+H⁺], C₃₁H₄₀ClN₆O₇P required *m/z* 675.11 [M].

HPLC Reverse-phase HPLC eluting with H₂O/CH₃CN from 90/10 to 0/100 in 35 minutes, F = 1 mL/min, λ = 280 nm, two peaks with tR 21.50, tR 21.02 min.

[95b] 8-Chloro-2'-deoxyadenosine-5'-O-phenyl-(benzyloxy-L-alaninyl)phosphate



8-Chloro-2'-deoxyadenosine-3',5'-bis-O-phenyl(benzyloxy-L-alaninyl)phosphate **[90c]** (0.08 g, 0.09 mmol) was dissolved in THF (5 mL), and zirconocene hydrochloride (Schwartz reagent) was added (0.067 g, 0.26 mmol). The mixture was stirred at room temperature for 3 hours, quenched with

water (0.5 mL) and evaporated. The crude was purified via Biotage Isolera One (80g ZIP cartridge, 50 mL/min, gradient eluent system 1-12% CH₃OH/CH₂Cl₂ 10CV, 12% 2CV) to afford the title compound as a white solid (0.008 g, 15%).

³¹P NMR (202 MHz, CD₃OD) δ_P 3.53, 3.43.

¹H NMR (500 MHz, CD₃O) δ_H 8.18 (s, 0.5H, H2), 8.15 (s, 0.5H, H2), 7.37-7.25 (m, 7H, Ph), 7.18-7.07 (m, 3H, Ph), 6.50-6.045 (m, 1H, H1'), 5.13-5.03 (m, 2H, CH₂Ph), 4.94-4.86 (m, 1H, H3'), 4.42-4.36 (m, 1H, H5'), 4.31-4.22 (m, 1H, H5'), 4.14-4.08 (m, 1H, H4'), 3.98-3.91 (m, 0.5H, CHCH₃ L-Ala), 3.90-3.81 (m, 0.5H, CHCH₃ L-Ala), 3.57-3.44 (m, 1H, H2'), 2.41-2.34 (m, 1H, H2'), 1.32-1.22 (m, 3H, CHCH₃ L-Ala).

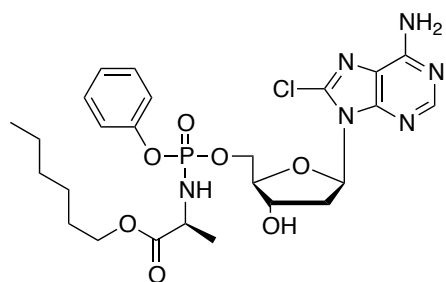
¹³C NMR (125 MHz, CD₃OD) δ_C 174.70 (C=O), 174.54 (C=O), 156.31 (C6), 156.26 (C6), 153.92 (C2), 153.88 (C2), 152.16 (C4), 152.10 (C4), 151.57 (C8), 151.52 (C8),

139.18 (C-Ar), 137.46 (C-Ar), 137.30 (C-Ar), 137.21 (C-Ar), 130.66 (CH-Ar), 130.64 (CH-Ar), 129.54 (CH-Ar), 129.29 (CH-Ar), 129.27 (CH-Ar), 129.25 (CH-Ar), 126.02 (CH-Ar), 121.42 (d, $^3J_{CP} = 4.9$ Hz, CH-Ar), 121.34 (d, $^3J_{CP} = 4.9$ Hz, CH-Ar), 86.65 (d, $^3J_{CP} = 8.4$ Hz, C4'), 86.60 (d, $^3J_{CP} = 8.4$ Hz, C4'), 86.45 (C1'), 72.50 (C3'), 72.19 (C3'), 67.93 (CH₂Ph), 67.86 (CH₂Ph), 67.78 (d, $^2J_{CP} = 5.4$ Hz, C5'), 67.20 (d, $^2J_{CP} = 5.4$ Hz, C5'), 51.55 (CHCH₃ L-Ala), 51.53 (CHCH₃ L-Ala), 37.80 (C2'), 37.71 (C2'), 20.39 (d, $^3J_{CP} = 6.4$ Hz, CHCH₃ L-Ala), 20.30 (d, $^3J_{CP} = 6.4$ Hz, CHCH₃ L-Ala).

MS (ES+) m/z found 625.1 [M+Na⁺], 603.1 [M+H⁺], C₂₄H₂₄ClN₆O₇P required m/z 588.13 [M].

HPLC Reverse-phase HPLC eluting with H₂O/CH₃CN from 90/10 to 0/100 in 35 minutes, F = 1 mL/min, λ = 280 nm, two peaks with tR 11.44, tR 11.10 min.

[95c] 8-Chloro-2'-deoxyadenosine-5'-O-phenyl-(hex-1-yloxy-L-alaninyl)phosphate



8-Chloro-2'-deoxyadenosine-3',5'-bis-*O*-phenyl(hex-1-yloxy-L-alaninyl)phosphate [**90b**] (0.089 g, 0.10 mmol) was dissolved in THF (5 mL), and zirconocene hydrochloride (Schwartz reagent) was added (0.077 g, 0.30 mmol). The mixture was stirred at room temperature for 3 hours, quenched with water (0.5

mL) and evaporated. The crude was purified via Biotage Isolera One (10g ZIP cartridge, 10 mL/min, gradient eluent system 1-12% CH₃OH/CH₂Cl₂ 10CV, 12% 2CV) to afford the title compound as a white solid (0.003 g, 5%).

³¹P NMR (202 MHz, CD₃OD) δ_P 3.54, 3.49.

¹H NMR (500 MHz, CD₃OD) δ_H 8.07 (s, 0.5H, H2), 8.04 (s, 0.5H, H2), 7.22-7.15 (m, 2H, Ph), 7.07-6.99 (m, 3H, Ph), 6.39-6.34 (m, 1H, H1'), 4.70-4.66 (m, 1H, H3'), 4.34-4.26 (m, 1H, H5'), 4.21-4.12 (m, 1H, H5'), 4.04-3.98 (m, 1H, H4'), 3.95-3.86 (m, 2H, CH₂CH₂CH₂CH₂CH₂CH₃ *n*-Hex), 3.81-3.65 (m, 1H, CHCH₃ L-Ala), 3.53-3.33 (m, 1H, H2'), 2.30-2.23 (m, 1H, H2'), 1.50-1.41 (m, 2H, CH₂CH₂CH₂CH₂CH₂CH₃ *n*-Hex), 1.26-1.10 (m, 9H, CH₂CH₂CH₂CH₂CH₂CH₃ *n*-Hex, CHCH₃ L-Ala), 0.83-0.74 (m, 3H, CH₂CH₂CH₂CH₂CH₂CH₃ *n*-Hex).

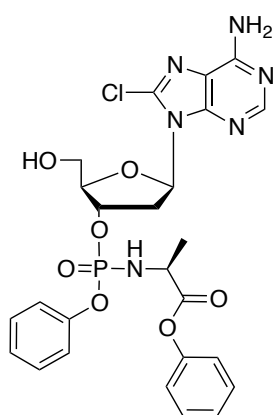
¹³C NMR (125 MHz, CD₃OD) δ_C 156.32 (C6), 153.92 (C2), 153.89 (C2), 151.37 (C4), 150.99 (C-Ar), 147.54 (C8), 130.67 (CH-Ar), 126.04 (CH-Ar), 121.44 (CH-Ar), 121.37 (CH-Ar), 121.33 (CH-Ar), 119.63 (C5), 86.77 (d, $^3J_{CP} = 8.25$ Hz, C4'), 86.49 (C1'), 72.53 (C3'), 72.25 (C3'), 67.75 (d, $^2J_{CP} = 5.5$ Hz, C5'), 67.22 (d, $^2J_{CP} = 5.5$ Hz, C5'), 66.43 (CH₂CH₂CH₂CH₂CH₂CH₃ *n*-Hex), 66.28 (CH₂CH₂CH₂CH₂CH₂CH₃ *n*-Hex), 51.54

(CHCH₃ L-Ala), 51.49 (CHCH₃ L-Ala), 37.79 (C2'), 37.70 (C2'), 29.67 (CH₂CH₂CH₂CH₂CH₂CH₃ *n*-Hex), 29.64 (CH₂CH₂CH₂CH₂CH₂CH₃ *n*-Hex), 26.63 (CH₂CH₂CH₂CH₂CH₂CH₃ *n*-Hex), 26.60 (CH₂CH₂CH₂CH₂CH₂CH₃ *n*-Hex), 23.57 (CH₂CH₂CH₂CH₂CH₂CH₃ *n*-Hex), 20.49 (d, ³J_{CP} = 7.2 Hz, CHCH₃ L-Ala), 20.40 (d, ³J_{CP} = 7.2 Hz, CHCH₃ L-Ala), 14.35 (CH₂CH₂CH₂CH₂CH₂CH₃ *n*-Hex).

MS (ES⁺) m/z found 597.2 [M+H⁺], C₂₅H₃₄ClN₆O₇P required m/z 597.00 [M].

HPLC Reverse-phase HPLC eluting with H₂O/CH₃CN from 90/10 to 0/100 in 35 minutes, F = 1 mL/min, λ = 280 nm, two peaks with tR 12.32, tR 12.39 min.

[96] 8-Chloro-2'-deoxyadenosine-3'-O-phenyl-(benzyloxy-L-alaninyl)phosphate



Isolated from reaction to afford 8-chloro-2'-deoxyadenosine-5'-O-phenyl-(benzyloxy-L-alaninyl)phosphate **[95b]** as a white solid (3 mg, 5%).

³¹P NMR (202 MHz, CD₃OD) δ_P 3.29, 2.58.

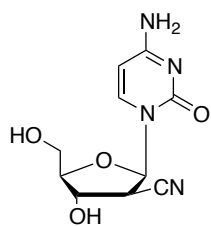
¹H NMR (500 MHz, CD₃OD) δ_H 8.05 (s, 0.5H, H2), 8.03 (s, 0.5H, H2), 7.31-7.21 (m, 5H, Ph), 7.20-7.08 (m, 5H, Ph), 6.29 (dd, *J* = 6.0 Hz, 8.5 Hz, 0.5H, H1'), 6.17 (dd, *J* = 6.0 Hz, 8.5 Hz, 0.5H, H1'), 5.31-5.26 (m, 0.5H, H3'), 5.23-5.19 (m, 0.5H, H3'), 5.10-5.01 (m, 2H, CH₂Ph), 4.16-4.13 (m, 0.5H, H4'), 4.11-4.07 (m, 0.5H, H4'), 4.00-3.92 (m, 1H, CHCH₃ L-Ala), 3.74-3.68 (m, 1H, H5'), 3.67-3.60 (m, 1H, H5'), 3.13-3.02 (m, 1H, H2'), 2.49-2.43 (m, 0.5H, H2'), 2.39-2.36 (m, 0.5H, H2'), 1.32-1.29 (m, 1.5H, CHCH₃ L-Ala), 1.26-1.23 (m, 1.5H, CHCH₃ L-Ala).

¹³C NMR (125 MHz, CD₃OD) δ_C 174.92 (d, ³J_{CP} = 4.5 Hz, CO), 174.69 (d, ³J_{CP} = 4.4 Hz, CO), 156.77 (C6), 156.76 (C6), 153.53 (C2), 153.51 (C2), 152.11 (C4), 152.06 (C4), 150.79 (C8), 150.76 (C8), 138.91 (C-Ar), 138.86 (C-Ar), 137.37 (C-Ar), 137.3 (C-Ar), 130.92 (CH-Ar), 130.88 (CH-Ar), 129.65 (CH-Ar), 129.54 (CH-Ar), 129.39 (CH-Ar), 129.28 (CH-Ar), 129.26 (CH-Ar), 126.37 (CH-Ar), 121.63 (d, ³J_{CP} = 4.7 Hz, CH-Ar), 121.55 (d, ³J_{CP} = 4.7 Hz, CH-Ar), 88.64 (d, ³J_{CP} = 5.3 Hz, C4'), 88.45 (d, ³J_{CP} = 5.3 Hz, C4'), 87.63 (C1'), 87.54 (C1'), 79.95 (d, ²J_{CP} = 5.2 Hz, C3'), 68.01 (CH₂Ph), 67.97 (CH₂Ph), 63.62 (C5'), 51.91 (d, ²J_{CP} = 1.9 Hz, CHCH₃ L-Ala), 51.72 (CHCH₃ L-Ala), 38.43 (d, ³J_{CP} = 4.4 Hz, C2'), 38.27 (d, ³J_{CP} = 4.4 Hz, C2'), 20.37 (d, ³J_{CP} = 7.4 Hz, CHCH₃ L-Ala), 20.28 (d, ³J_{CP} = 7.4 Hz, CHCH₃ L-Ala).

MS (ES⁺) m/z found 611.1 [M+Na⁺], C₂₄H₂₄ClN₆O₇P required m/z 588.13 [M].

HPLC Reverse-phase HPLC eluting with H₂O/CH₃CN from 90/10 to 0/100 in 35 minutes, F = 1 mL/min, λ = 280 nm, two peaks with tR 16.38, tR 16.80 min.

9.5.16 Synthesis of CNDAC and sapacitabine

[97] 2'-C-cyano-2'-deoxy-1-β-D-arabino-pentofuranosylcytosine (CNDAC)

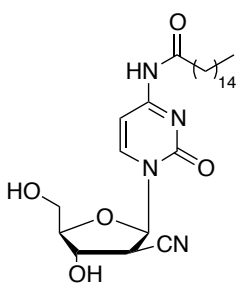
*N*⁴-Acetyl-1-[3,5-*O*-(tetraisopropylidisiloxanyl)-β-D-erythro-*N*-pentofuran-2-β-cyano]cytosine [**106**] (0.30 g, 0.6 mmol) was dissolved in THF (1 mL), and cooled to 0 °C in an ice-cold bath. Trifluoroacetic acid (0.25 mL) and water (0.25 mL) were added dropwise, and the mixture was stirred at rt for 48 hours. The volatiles were evaporated and the mixture was purified by column chromatography (eluent CH₃OH/CH₂Cl₂ 5-25%), affording the title compound as a white solid (0.11 g, 75%).

(Lit. mp = 175-176 °C).³⁶⁹

¹H NMR (500 MHz, CD₃OD) δ_H 8.13 (d, *J* = 7.5 Hz, 1H, H6), 6.28 (d, *J* = 6.3 Hz, 1H, H1'), 6.05 (d, *J* = 7.6 Hz, 1H, H5), 4.62-4.56 (m, 1H, H3'), 3.97-3.90 (m, 2H, H5', H4'), 3.84-3.77 (m, 2H, H5', H2').

¹³C (125 MHz, CD₃OD) δ_C 166.58 (C4), 156.28 (C2), 142.82 (C6), 117.86 (CN), 96.30 (C5), 86.96 (C4'), 85.37 (C1'), 73.81 (C3'), 60.61 (C5'), 44.62 (C2').

HPLC Reverse-phase HPLC eluting with H₂O/CH₃OH from 100/0 to 75/25 in 30 minutes, F = 1 mL/min, λ = 254 nm, showed one peak with tR 6.79 min.

[98] 2'-C-cyano-2'-deoxy-1-β-D-arabino-pentofuranosyl-*N*⁴-palmitoyl-cytosine (sapacitabine)

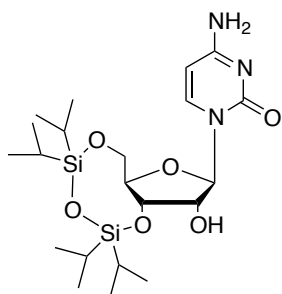
CNDAC [**97**] (0.04 g, 0.16 mmol) was suspended in 1,4-dioxane (1 mL). Water (0.04 mL) and palmitic anhydride (0.14 g, 0.28 mmol) were added and the mixture was brought to 90 °C for 3 hours. The solvent was evaporated, the mixture diluted with EtOAc (5 mL) and washed with brine (3 x 5 mL). The organic phase was collected, dried over Na₂SO₄, filtered and evaporated to yield the title compound as a white solid (0.035 mg, 45%).³⁷⁹

¹H NMR (500 MHz, CDCl₃) δ_H 9.73 (br s, 1H, NH), 8.27-8.03 (m, 1H, H6), 7.62-7.43 (m, 1H, H5), 6.26-6.06 (m, 1H, H1'), 4.79-4.62 (m, 1H, H2'), 4.13-3.66 (m, 4H, H3', H4', H5'), 2.32-2.20 (m, 2H, CH₂), 1.63-1.49 (m, 2H, CH₂), 1.28-1.07 (m, 24H, CH₂), 0.84-0.76 (m, 3H, CH₃).

MS (ES⁺) *m/z* found 491.3 [M+H⁺], C₂₆H₄₂N₄O₅ required *m/z* 490.64 [M].

HPLC Reverse-phase HPLC eluting with H₂O/CH₃CN from 90/10 to 0/100 in 45 minutes, F = 1 mL/min, λ = 254 nm, showed one peak with t_R 30.34 min.

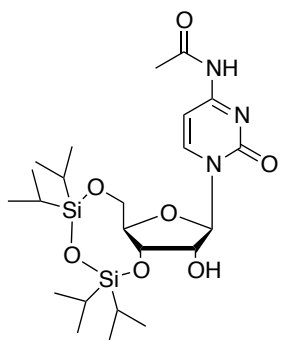
[100] 3',5'-O-(tetraisopropyldisiloxanyl)-cytidine



Cytidine (5.0 g, 20.56 mmol) was pre-dried by azeotroping with pyridine (2 x 10 mL), and suspended in anhydrous pyridine (15 mL) and the flask purged with Argon. 1,3-Dichloro-1,1,3,3-tetraisopropyldisiloxane (7.1 mL, 22.20 mmol) was added dropwise at room temperature. A heavy white precipitate gradually settled at the bottom of the flask, and it was broken up to a suspension, by vigorous stirring overnight. The mixture was poured into water (100 mL) and extracted with AcOEt (3 x 100 mL). The combined organics were washed with brine, dried over Na₂SO₄, filtered and finally evaporated to give the title compound as a white solid (5.70 g, 57%).³⁶⁹ (Lit. mp: 177 °C).⁴⁷¹

¹H NMR (500 MHz, CD₃OD) δ_{H} 8.14 (d, J = 7.7 Hz, 1H, H6), 6.03 (d, J = 7.7 Hz, 1H, H5), 5.70 (s, 1H, H1'), 4.33-4.16 (m, 4H, H3', H4', H2', H5'), 4.08 (dd, J = 13.6 Hz, 2.4 Hz, 1H, H5'), 1.25-0.94 (m, 28H, *i*Pr).

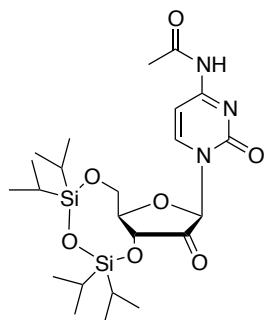
[101] N⁴-Acetyl-3',5'-O-(tetraisopropyldisiloxanyl)-cytidine



3',5'-O-(tetraisopropyldisiloxanyl)-cytidine [100] (5.70 g, 11.73 mmol) was dissolved in EtOH (40 mL) and Ac₂O (1.4 mL, 14.77 mmol) was added dropwise. The mixture was heated to reflux (T = 65 °C) for 3 hours and then cooled to room temperature, evaporated, neutralised with 5% NaHCO₃ solution. The mixture was then extracted with Et₂O/*n*Hex (1:1, 100 mL) and the organic phase washed with brine and dried over Na₂SO₄, filtered, and evaporated to give the title compound as a white solid (6.19 g, 100%).³⁶⁹ (Lit. mp: 157-159 °C).⁴⁷¹

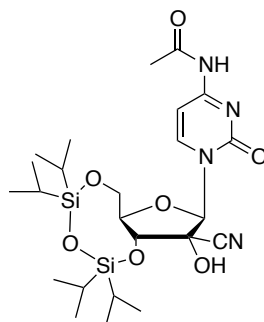
¹H NMR (500 MHz, CDCl₃) δ_{H} 10.07 (br s, 1H, NH), 8.21 (d, J = 7.5 Hz, 1H, H6), 7.46 (d, J = 7.5 Hz, 1H, H5), 5.84 (s, 1H, H1'), 4.32-4.26 (m, 2H, H3', H5'), 4.24-4.20 (m, 2H, H2', H4'), 4.03 (dd, J = 13.4, 2.6 Hz, 1H, H5'), 3.02 (br s, 1H OH2'), 2.31 (s, 3H, Ac), 1.15-0.97 (m, 28H, *i*Pr).

[102] *N*⁴-Acetyl-1-[3,5-*O*-(tetraisopropylidisiloxane-1,3-diyl)-β-*D*-erythro-*N*-pentofuran-2-ulosyl] cytosine



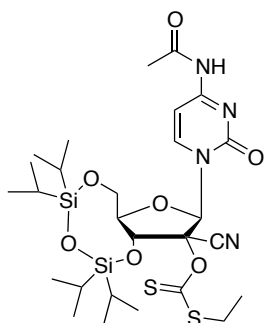
*N*⁴-Acetyl-3',5'-*O*-(tetraisopropylidisiloxanyl)-cytidine [101] (6.19 g, 11.73 mmol) was dissolved in anhydrous CH₂Cl₂ (50 mL) and cooled to 0 °C in an ice-cold bath. Dess-Martin periodinane (10.20 g, 24.05 mmol) was added in small portions, the resulting cloudy solution was stirred with cooling for 10 minutes and then at room temperature overnight. The mixture was cooled to 0 °C and a second portion of Dess-Martin periodinane (4.97 g, 11.73 mmol) was added. The reaction was stirred in the ice cold bath for 10 minutes and then at room temperature for 5 hours. The mixture was diluted with Et₂O (100 mL) and washed with NaHCO₃ saturated aqueous solution (100 mL) in which Na₂S₂O₄·5H₂O (5.70g) had been dissolved. The aqueous phase was extracted with Et₂O (100 mL). The combined organics were washed with NaHCO₃ saturated aqueous solution (100 mL), brine (100 mL), dried over Na₂SO₄ and evaporated to white foam, which was used without purification for the next step (crude 5.49 g, 10.44 mmol).³⁷⁹

[103] *N*⁴-Acetyl-1-[3,5-*O*-(tetraisopropylidisiloxanyl)-β-*D*-erythro-*n*-pentofuran-2-hydroxyl-2-cyano]cytosine



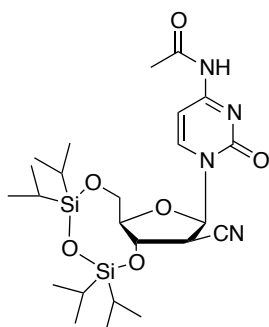
Crude [102] from previous synthetic step (5.49 g, 10.44 mol) was dissolved in anhydrous CH₂Cl₂ (60 mL) and cooled to 0 °C in an ice-cold bath. AlCl₃ (2.09 g, 15.66 mmol) was added in small portions, and the flask flushed with Argon. TMSCN (3.92 mL, 31.32 mmol) was added dropwise at 0 °C. The mixture was stirred with cooling for 45 minutes and then for further 45 minutes at room temperature. The mixture was cooled in an ice-cold bath and quenched by the addition of NH₄Cl saturated aqueous solution (30 mL) in a steady stream. The reaction was then transferred into a separating funnel, the organic phase separated from the aqueous phase, which was extracted with CH₂Cl₂ (2 x 30 mL). The combined organics were washed with brine (50 mL) and dried over Na₂SO₄, filtered and evaporated to give a crude (5.48 g, 9.92 mmol) that was used without further purification for the following step.³⁷⁹

[105] *O*-((6a*R*,8*R*,9*R*,9a*R*)-8-(4-acetamido-2-oxopyrimidin-1(2*H*)-yl)-9-cyano-2,2,4,4-tetraisopropyltetrahydro-6*H*-furo[3,2-*f*][1,3,5,2,4]trioxadisilocin-9-yl) *S*-ethyl carbonodithioate



Crude **[103]** (5.48 g, 9.92 mmol) and DMAP (0.05 g, 0.45 mmol) were dissolved in CH₂Cl₂ (60 mL) and the vessel was flushed with Argon. The yellowish solution was cooled in an ice-cold bath. Ethyl dithiochloroformate **[109]** (1.81 g, 12.90 mmol) was diluted with anhydrous dichloromethane (4 mL) and added to the reaction mixture in a steady stream, followed by the dropwise addition of triethylamine (2.07 mL, 14.85 mmol). The mixture was stirred 1 hour with cooling and a further 1 hour at room temperature. Water was added (33 mL) and the organic phase was separated. The aqueous phase was extracted with CH₂Cl₂ (33 mL), the combined organics were washed with brine (50 mL), dried over Na₂SO₄, filtered and evaporated to yield a crude (5.92 g, 9.03 mmol) that was used in the following reaction without purification.³⁷⁹

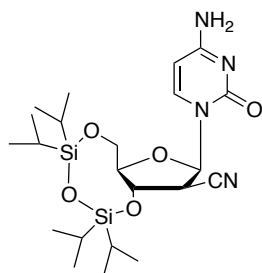
[106] *N*⁴-Acetyl-1-[3,5-*O*-(tetraisopropylidisiloxanyl)-β-*D*-erythro-*n*-pentofuran-2-β-cyano]cytosine



Crude **[104]** (5.92 g, 9.03 mmol), was dissolved in isopropyl alcohol (65 mL), 2,4,6-collidine (1.55 mL, 11.74 mmol) was added, and the mixture was degassed under vacuum. Lauroyl peroxide (2.39 g, 6.00 mmol) was added in three portions over 20 minutes and the vessel flushed with Argon. The reaction was refluxed at 100 °C. After 1 hour a second portion of lauroyl peroxide (0.78 g, 2.00 mmol) was added and the reaction mixture was stirred at 100 °C for another hour. The mixture was cooled to room temperature, the solvent was removed *in vacuo* and the residue was triturated with cold *n*Hex and filtered to afford the product as a white solid (3.78 g, 78%). Overall yield (4 steps) 60%. (Lit. mp = 209-211 °C).³⁶⁹

¹H NMR (500 MHz, CDCl₃) δ_H 10.50 (br s, 1H, NH), 8.08 (d, *J* = 7.5 Hz, 1H, H6), 7.46 (d, *J* = 7.5 Hz, 1H, H5), 6.36 (d, *J* = 6.7 Hz, 1H, H1'), 4.64 (dd, *J* = 8.7 Hz, 8.2 Hz, 1H, H3'), 4.18 (dd, *J* = 13.1 Hz, 2.8 Hz, 1H, H5'), 4.09 (dd, *J* = 13.1 Hz, 3.3 Hz, 1H, H5'), 3.91 (ddd, *J* = 8.0 Hz, 3.3 Hz, 2.8 Hz, 1H, H4'), 3.75 (dd, *J* = 8.7 Hz, 6.7 Hz, 1H, H2'), 2.29 (s, 3H, Ac), 1.15-1.03 (m, 28H, *i*Pr).

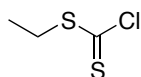
[107] 3',5'-O-(tetraisopropylidisiloxanyl)-2'-C-cyano-2'-deoxy-1-β-D-arabino-pentofuranosylcytosine



*N*⁴-Acetyl-1-[3,5-*O*-(tetraisopropylidisiloxanyl)-β-D-erythro-*N*-pentofuran-2-β-cyano]cytosine [**106**] (3.78 g, 7.04 mmol) was dissolved in anhydrous THF (20 mL) under argon atmosphere, zirconocene hydrochloride (Schwartz reagent) (3.63 g, 14.08 mmol) was added and the yellow mixture was stirred for 1 hour at room temperature. A second portion of the Schwartz reagent (1.82 g, 7.04 mmol) was added and the reaction was stirred for a further 2 hours. The reaction was quenched by addition of water (5 mL) and the aqueous solution was extracted with EtOAc (2 x 25 mL) to afford the product as a white solid (2.61 g, 75%).^{369,379}

¹H NMR (500 MHz, CDCl₃) δ_H 7.64 (d, *J* = 7.6 Hz, 1H, H6), 7.59 (br s, 1H, NH₂), 6.30 (d, *J* = 6.8 Hz, 1H, H1'), 6.00 (br s, 1H, NH₂), 5.85 (d, *J* = 7.6 Hz, 1H, H5), 4.64 (dd, *J* = 8.8, 7.9 Hz, 1H, H3'), 4.15-4.03 (m, 2H, H5'), 3.86-3.81 (m, 1H, H4'), 3.68 (dd, *J* = 7.9, 6.8 Hz, 1H, H2'), 1.15-1.01 (m, 28H, iPr).

[109] Ethyl chlorodithioformate

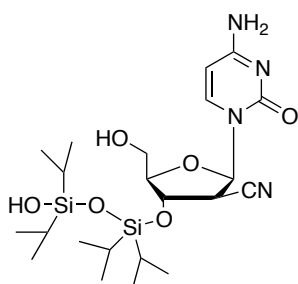


A solution of the ethanethiol (25.5 mL, 353.48 mmol) in toluene (75 mL) at 10 °C was added dropwise to a stirred solution of thiophosgene (62.1 g, 0.54 mol) in toluene (50 mL) maintaining the temperature at 10 °C. The reaction mixture was stirred for 16 hours in an ice bath. The solvent was removed and the product fractionated. The title compound was isolated at a temperature of 63 °C, and a pressure of 5.8 mmHg, as a dark orange liquid (4.89 g, 65%).³⁸⁶

¹H NMR (500 MHz, CDCl₃) δ_H 3.23 (q, *J* = 7.5 Hz, CH₂CH₃), 1.40 (t, *J* = 7.5 Hz, CH₂CH₃).

¹³C NMR (125 MHz, CDCl₃) δ_C 197.30 (C=S), 35.06 (CH₂CH₃), 11.82 (CH₂CH₃).

[110] 3',5'-O-(tetraisopropylidisiloxanyl)-2'-C-cyano-2'-deoxy-1-β-D-arabino-pentofuranosylcytosine



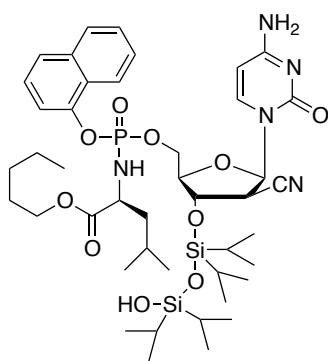
3',5'-*O*-(tetraisopropylidisiloxanyl)-2'-*C*-cyano-2'-deoxy-1-β-D-*arabino*-pentofuranosylcytosine [**107**] (3.03 g, 6.12 mmol) was dissolved in anhydrous THF (4 mL), and cooled to 0 °C in an ice-cold bath. Trifluoroacetic acid (1 mL) and water (1 mL) were added dropwise, and the mixture was stirred at 0 °C for 5 hours.

The volatiles were evaporated and the mixture was purified by column chromatography (eluent EtOAc/nHex 5-25%), affording the title compound as a white solid (1.94 g, 62%).

$^1\text{H NMR}$ (500 MHz, CDCl_3) δ_{C} 7.64 (d, $J = 7.6$ Hz, 1H, H6), 7.59 (br s, 1H, NH_2), 6.30 (d, $J = 6.8$ Hz, 1H, H1'), 6.00 (br s, 1H, NH_2), 5.85 (d, $J = 7.6$ Hz, 1H, H5), 4.64 (dd, $J = 8.8, 7.9$ Hz, 1H, H3'), 4.15-4.03 (m, 2H, H5'), 3.86-3.81 (m, 1H, H4'), 3.68 (dd, $J = 7.9, 6.8$ Hz, 1H, H2'), 1.15-1.01 (m, 28H, iPr).

9.5.17 Synthesis of CNDAC ProTides

[111a] 3'-*O*-(tetraisopropylidisiloxanyl)-2'-*C*-cyano-2'-deoxy-1- β -*D*-arabino-pentofuranosylcytosine-5'-*O*-naphth-1-yl-(pentyl-1-oxy-*L*-leucinyl)] phosphate

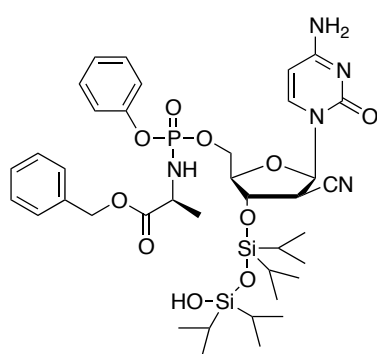


Prepared according to procedure F_1 using 3'-*O*-(tetraisopropylidisiloxanyl)-2'-*C*-cyano-2'-deoxy-1- β -*D*-arabino-pentofuranosylcytosine [110] (0.10 g, 0.19 mmol), in THF (4 mL), *t*BuMgCl (0.50 mL, 0.50 mmol), naphth-1-yl-(pentyl-1-oxy-*L*-leucinyl) phosphorochloridate [17f] (0.24 g, 0.57 mmol), in THF (2 mL). After evaporation, the crude was purified by Biotage Isolera One (10g SNAP cartridge KP-SIL, 12 mL/min, using a gradient elution of 1-12% $\text{CH}_3\text{OH}/\text{CH}_2\text{Cl}_2$ over 10 CV, 12% $\text{CH}_3\text{OH}/\text{CH}_2\text{Cl}_2$ over 5 CV), yielding the title compound as a white solid (0.103 g, 60%).

$^{31}\text{P NMR}$ (202 MHz, CD_3OD) δ_{P} 4.32, 4.27.

$^1\text{H NMR}$ (500 MHz, CD_3OD) δ_{H} 8.24-8.19 (m, 1H, Nap), 7.94-7.89 (m, 1H, Nap), 7.86 (d, 0.5H, $J = 7.3$ Hz, H6), 7.83 (d, 0.5H, $J = 7.3$ Hz, H6), 7.75-7.71 (m, 1H, Nap), 7.59-7.50 (m, 3H, Nap), 7.47-7.41 (m, 1H, Nap), 6.22 (d, 0.5H, $J = 5.9$ Hz, H1'), 6.21 (d, 0.5H, $J = 6.1$ Hz, H1'), 5.89 (d, 0.5H, $J = 7.6$ Hz, H5), 5.84 (d, 0.5H, $J = 7.6$ Hz, H5), 4.95-4.92 (m, 1H, H3'), 4.62-4.48 (m, 1.5H, H5'), 4.46-4.40 (m, 0.5H, H5'), 4.32-4.24 (m, 1H, H4'), 4.01-3.97 (m, 2H, $\text{CH}_2\text{CH}_2\text{CH}_2\text{CH}_2\text{CH}_3$ *n*-Pen), 3.95-3.91 (m, 2H, H2', $\text{CHCH}_2\text{CH}(\text{CH}_3)_2$ L-Leu), 1.71-0.71 (m, 46H, $\text{CH}_2\text{CH}_2\text{CH}_2\text{CH}_2\text{CH}_3$ *n*-Pen, $\text{CHCH}_2\text{CH}(\text{CH}_3)_2$ L-Leu, $\text{OSi}(i\text{Pr})_2\text{OSi}(i\text{Pr})_2\text{OH}$).

[111b] 3'-O-(tetraisopropylidisiloxanyl)-2'-C-cyano-2'-deoxy-1-β-D-arabino-pentofuranosylcytosine-5'-O-phenyl-(benzyloxy-L-alaninyl)] phosphate



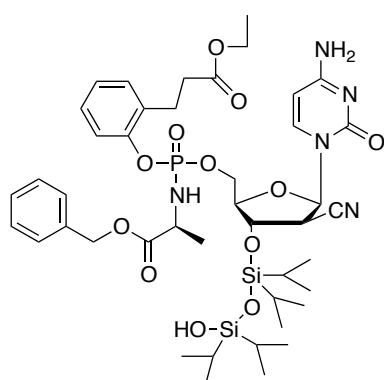
Prepared according to procedure **F₁** using 3'-O-(tetraisopropylidisiloxanyl)-2'-C-cyano-2'-deoxy-1-β-D-arabino-pentofuranosylcytosine [**110**] (0.10 g, 0.19 mmol), in THF (4 mL), *t*BuMgCl (0.50 mL, 0.50 mmol), naphth-1-yl (benzyloxy-L-alaninyl) phosphorochloridate [**17a**] (0.20 g, 0.57 mmol), in THF (2 mL). After evaporation, the crude

was purified by Biotage Isolera One (10g SNAP cartridge KP-SIL, 12 mL/min, using a gradient elution of 2-20% CH₃OH/CH₂Cl₂ over 10 CV, 20% CH₃OH/CH₂Cl₂ over 5 CV), yielding the title compound as a white solid (0.10 g, 63%).

³¹P NMR (202 MHz, CD₃OD) δ_P 3.64, 3.59.

¹H NMR (500 MHz, CD₃OD) δ_H 7.85 (d, 0.5H, *J* = 7.5 Hz, H6), 7.80 (d, 0.5H, *J* = 7.6 Hz, H6), 7.39-7.30 (m, 7H, Ph), 7.27-7.18 (m, 3H, Ph), 6.22 (d, 0.5H, *J* = 6.1 Hz, H1'), 6.19 (d, 0.5H, *J* = 6.1 Hz, H1'), 5.92 (d, 0.5H, *J* = 7.65 Hz, H5), 5.88 (d, 0.5H, *J* = 7.45 Hz, H5), 5.18-5.10 (m, 2H, CH₂Ph), 4.96-4.93 (m, 1H, H3'), 4.53-4.45 (m, 1H, H5'), 4.43-4.33 (m, 1H, H5'), 4.28-4.21 (m, 1H, H4'), 4.08-4.00 (m, 1H, CHCH₃ L-Ala), 3.93 (dd, *J* = 6.1, 3.4 Hz, 0.5H, H2'), 3.92 (dd, *J* = 6.1, 3.4 Hz, 0.5H, H2'), 1.39-1.35 (m, 3H, CHCH₃ L-Ala), 1.13-0.87 (m, 28H, OSi(*i*Pr)₂OSi(*i*Pr)₂OH).

[111c] 3'-O-(tetraisopropylidisiloxanyl)-2'-C-cyano-2'-deoxy-1-β-D-arabino-pentofuranosylcytosine-[ethyl 3-(2-hydroxyphenyl)propanoyl (benzyloxy-L-alaninyl)] phosphate



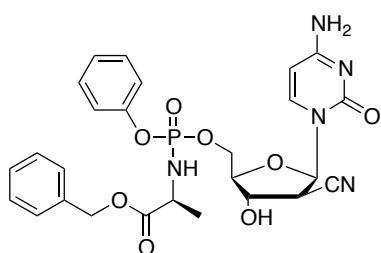
Prepared according to procedure **F₁** using 3'-O-(tetraisopropylidisiloxanyl)-2'-C-cyano-2'-deoxy-1-β-D-arabino-pentofuranosylcytosine [**110**] (0.10 g, 0.19 mmol), in THF (4 mL), *t*BuMgCl (0.50 mL, 0.50 mmol), ethyl 3-(2-hydroxyphenyl)propanoyl (benzyloxy-L-alanin-*N*-yl) phosphorochloridate [**17v**] (0.26 g, 0.57 mmol), in THF (2 mL). After evaporation, the crude

was purified by Biotage Isolera One (10g SNAP cartridge KP-SIL, 12 mL/min, using a gradient elution of 2-10% CH₃OH/CH₂Cl₂ over 10 CV, 10% CH₃OH/CH₂Cl₂ over 5 CV), yielding the title compound as a white solid (0.11 g, 70%).

³¹P NMR (202 MHz, CD₃OD) δ_P 3.73, 3.56.

$^1\text{H NMR}$ (500 MHz, CDCl_3) δ_{H} 7.83 (d, $J = 7.5$ Hz, 0.5H, H6), 7.78 (d, 0.5H, $J = 7.5$ Hz, H6), 7.38-7.28 (m, 7H, Ph), 7.16-7.07 (m, 2H, Ph), 6.21 (d, 0.5H, $J = 6.0$ Hz, H1'), 6.18 (d, 0.5H, $J = 6.0$ Hz, H1'), 5.92 (d, 0.5H, $J = 7.5$ Hz, H5), 5.89 (d, 0.5H, $J = 7.5$ Hz, H5), 5.19-5.00 (m, 2H, CH_2Ph), 4.94-4.89 (m, 1H, H3'), 4.54-4.33 (m, 2H, H5'), 4.28-4.16 (m, 1H, H4'), 4.12-4.02 (m, 3H, $\text{CH}_2\text{CH}_2\text{CO}_2\text{CH}_2\text{CH}_3$, CHCH_3 L-Ala), 3.94-3.89 (m, 1H, H2'), 3.05-2.89 (m, 2H, $\text{CH}_2\text{CH}_2\text{CO}_2\text{CH}_2\text{CH}_3$), 2.67-2.54 (m, 2H, $\text{CH}_2\text{CH}_2\text{CO}_2\text{CH}_2\text{CH}_3$), 1.45-1.07 (m, 34H, $\text{CH}_2\text{CH}_2\text{CO}_2\text{CH}_2\text{CH}_3$, CHCH_3 L-Ala, $\text{OSi}(i\text{Pr})_2\text{OSi}(i\text{Pr})_2\text{OH}$).

[112b] 2'-C-cyano-2'-deoxy-1- β -D-arabino-pentofuranosylcytosine-5'-O-phenyl-(benzoxy-L-alaninyl) phosphate



Compound **111b** (0.04 g, 0.05 mmol) was dissolved in THF (2 mL), and treated with KF (0.028 g, 0.3 mmol) and 18-crown-6 (0.004 g, 0.015 mmol), and stirred at room temperature. After 3 hours, the mixture was filtered and the solids washed with THF. The filtrate was concentrated, re-dissolved in ethyl acetate (15 mL), washed with water (15 mL) and brine (15 mL), dried over Na_2SO_4 , filtered and evaporated. The product was purified by flash chromatography (eluent system 0-7% $\text{CH}_3\text{OH}/\text{CH}_2\text{Cl}_2$), to afford the title compound as a white solid (5 mg, 17%).

[Alternative procedure] Compound **111b** (0.04 g, 0.05 mmol) was dissolved in EtOAc (1.5 mL), pyridine (20 μL , 0.23 mmol) and the mixture was cooled to 0 °C. Then HF·pyridine (70% HF, 6 μL , 0.22 μmol) was added. The progress of the reaction was monitored by HPLC. After stirring for six hours another portion of pyridine (20 μL , 0.23 mmol) and HF·pyridine (70% HF, 6 μL , 0.22 μmol) was added to the reaction mixture. After stirring for 23 hours an additional portion of pyridine (20 μL , 0.23 mmol) and HF·pyridine (70% HF, 6 μL , 0.22 μmol) was added and the stirring was continuing up to a total of 24 hours. After addition of TMSOMe (0.21 mL, 1.54 mmol) and stirring for one hour, the solution was evaporated and the crude purified by flash column chromatography (eluent 0-7% $\text{CH}_3\text{OH}/\text{CH}_2\text{Cl}_2$), and preparative TLC (500 μm , 5% $\text{CH}_3\text{OH}/\text{CH}_2\text{Cl}_2$) to yield the title compound as a white solid (8 mg, 30%).³⁹³

$^{31}\text{P NMR}$ (202 MHz, CD_3OD) δ_{P} 3.85, 3.69.

$^1\text{H NMR}$ (500 MHz, CD_3OD) δ_{H} 7.76 (d, 0.5H, $J = 7.5$ Hz, H6), 7.70 (d, 0.5H, $J = 7.6$ Hz, H6), 7.40-7.31 (m, 7H, Ph), 7.27-7.19 (m, 3H, Ph), 6.27 (d, 0.5H, $J = 7.0$ Hz, H1'), 6.23 (d, 0.5H, $J = 7.0$ Hz, H1'), 5.91 (d, 0.5H, $J = 7.65$ Hz, H5), 5.87 (d, 0.5H, $J = 7.65$

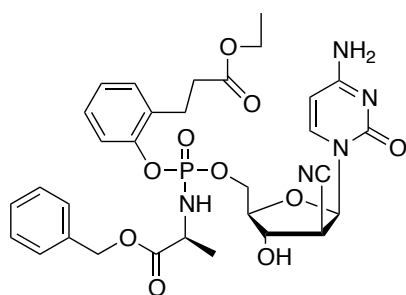
Hz, H5), 5.20-5.11 (m, 2H, CH_2Ph), 4.58-4.51 (m, 1H, H3'), 4.49-4.26 (m, 2H, H5'), 4.09-4.01 (m, 2H, CHCH_3 L-Ala, H4'), 3.81-3.75 (m, 1H, H2'), 1.40-1.35 (m, 3H, CHCH_3 L-Ala).

^{13}C NMR (125 MHz, CD_3OD) δ_{C} 174.87 (d, $^3J_{\text{CP}} = 3.75$ Hz, CO), 174.64 (d, $^3J_{\text{CP}} = 3.75$ Hz, CO), 167.83 (C4), 167.80 (C4), 152.16 (C2), 152.10 (C2), 141.88 (C6), 141.78 (C6), 137.43 (C-Ar), 137.25 (C-Ar), 130.90 (CH-Ar), 130.12 (CH-Ar), 129.39 (CH-Ar), 129.37 (CH-Ar), 129.34 (CH-Ar), 129.26 (CH-Ar), 129.24 (CH-Ar), 129.64 (CH-Ar), 129.55 (CH-Ar), 126.34 (CH-Ar), 126.29 (CH-Ar), 123.84 (CH-Ar), 121.61 (CH-Ar), 121.48 (CH-Ar), 121.44 (CH-Ar), 117.64 (CN), 117.62 (CN), 96.58 (C5), 96.51 (C5), 85.64 (C1'), 85.42 (C1'), 84.47 (d, $^3J_{\text{CP}} = 8.1$ Hz, C4'), 84.37 (d, $^3J_{\text{CP}} = 3.7$ Hz, C4'), 74.45 (C3'), 74.07 (C3'), 68.04 (CH_2Ph), 67.66 (CH_2Ph), 65.83 (d, $^2J_{\text{CP}} = 4.6$ Hz, C5'), 65.57 (d, $^2J_{\text{CP}} = 4.4$ Hz, C5'), 51.86 (CHCH_3 L-Ala), 51.66 (CHCH_3 L-Ala), 44.50 (C2'), 44.45 (C2'), 20.45 (d, $^3J_{\text{CP}} = 7.1$ Hz, CHCH_3 L-Ala), 20.30 (d, $^3J_{\text{CP}} = 7.2$ Hz, CHCH_3 L-Ala).

HPLC Reverse-phase HPLC eluting with $\text{H}_2\text{O}/\text{CH}_3\text{CN}$ from 90/10 to 0/100 in 30 minutes, $F = 1$ mL/min, $\lambda = 254$ nm, showed two peaks with tR 12.52 min, 12.75 min.

MS (ES+) m/z found 570.2 [$\text{M}+\text{H}^+$], 592.2 [$\text{M}+\text{Na}^+$], $\text{C}_{26}\text{H}_{28}\text{N}_5\text{O}_8\text{P}$ required m/z 569.50 [M].

[112c] 2'-C-cyano-2'-deoxy-1- β -D-arabino-pentofuranosylcytosine-5'-O-phenyl-[ethyl 3-(2-hydroxyphenyl)propanoyl (benzyloxy-L-alaninyl)] phosphate



Compound **111c** (0.11 g, 0.12 mmol) was dissolved in EtOAc (4.8 mL), pyridine (48 μL , 0.55 mmol) and the mixture was cooled to 0 °C. Then HF·pyridine (70% HF, 14.4 μL , 0.53 μmol) was added. The progress of the reaction was monitored by HPLC. After stirring for six hours another portion of pyridine (48 μL , 0.55 mmol)

and HF·pyridine (70% HF, 14.4 μL , 0.53 μmol) was added to the reaction mixture. After stirring for 23 hours an additional portion of pyridine (48 μL , 0.55 mmol) and HF·pyridine (70% HF, 14.4 μL , 0.53 μmol) was added and the stirring was continuing up to a total of 24 hours. After addition of TMSOMe (0.50 mL, 3.70 mmol) and stirring for one hour, the solution was evaporated purified by flash column chromatography (eluent 0-7% $\text{CH}_3\text{OH}/\text{CH}_2\text{Cl}_2$), and preparative TLC (500 μm , 5% $\text{CH}_3\text{OH}/\text{CH}_2\text{Cl}_2$) to yield the title compound as a white solid (0.009 g, 11%).

^{31}P NMR (202 MHz, CD_3OD) δ_{P} 3.73, 3.56.

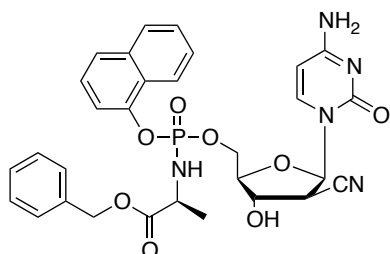
¹H NMR (500 MHz, CD₃OD) δ_H 7.61 (d, *J* = 7.5 Hz, 0.5H, H6), 7.53 (d, 0.5H, *J* = 7.5 Hz, H6), 7.32-6.99 (m, 7H, Ph), 7.16-7.07 (m, 2H, Ph), 6.13 (d, 0.5H, *J* = 7.3 Hz, H1'), 6.09 (d, 0.5H, *J* = 7.3 Hz, H1'), 5.78 (d, 0.5H, *J* = 7.5 Hz, H5), 5.73 (d, 0.5H, *J* = 7.7 Hz, H5), 5.09-4.96 (m, 2H, CH₂Ph), 4.69-4.51 (m, 1H, H3'), 4.44-4.39 (m, 1H, H4'), 4.37-4.07 (m, 2H, H5'), 4.00-3.89 (m, 3H, CHCH₃ L-Ala, CH₂CH₂CO₂CH₂CH₃), 3.70-3.59 (m, 1H, H2'), 2.91-2.80 (m, 2H, CH₂CH₂CO₂CH₂CH₃), 2.54-2.46 (m, 2H, CH₂CH₂CO₂CH₂CH₃), 1.33-1.26 (m, 3H, CH₂CH₂CO₂CH₂CH₃), 1.12-1.00 (m, 3H, CHCH₃ L-Ala).

¹³C NMR (125 MHz, CD₃OD) δ_C 174.59 (C=O), 174.06 (C=O), 167.78 (C4), 150.50 (C2), 150.44 (C2), 141.85 (C6), 141.75 (C6), 137.26 (C-Ar), 133.02 (C-Ar), 132.96 (C-Ar), 131.72 (CH-Ar), 131.70 (CH-Ar), 129.72 (CH-Ar), 129.62 (CH-Ar), 129.38 (CH-Ar), 129.35 (CH-Ar), 129.32 (CH-Ar), 129.24 (CH-Ar), 129.21 (CH-Ar), 128.85 (CH-Ar), 128.83 (CH-Ar), 128.64 (CH-Ar), 126.30 (CH-Ar), 126.29 (CH-Ar), 121.00 (CH-Ar), 120.98 (CH-Ar), 117.61 (CN), 117.58 (CN), 96.54 (C5), 96.47 (C5), 85.68 (C1'), 85.46 (C1'), 84.39 (d, ³*J*_{CP} = 7.6 Hz, C4'), 84.34 (d, ³*J*_{CP} = 7.6 Hz, C4'), 74.57 (C3'), 74.34 (C3'), 68.06 (CH₂Ph), 62.26 (C5'), 62.22 (C5'), 62.21 (C5'), 61.65 (CH₂CH₂CO₂CH₂CH₃), 51.86 (CHCH₃ L-Ala), 51.73 (CHCH₃ L-Ala), 44.47 (C2'), 35.38 (CH₂CH₂CO₂CH₂CH₃), 35.33 (CH₂CH₂CO₂CH₂CH₃), 26.71 (CH₂CH₂CO₂CH₂CH₃), 26.76 (CH₂CH₂CO₂CH₂CH₃), 20.56 (d, ³*J*_{CP} = 6.4 Hz, CHCH₃ L-Ala), 20.37 (d, ³*J*_{CP} = 6.4 Hz, CHCH₃ L-Ala), 14.54 (CH₂CH₂CO₂CH₂CH₃).

HPLC Reverse-phase HPLC eluting with H₂O/CH₃CN from 90/10 to 0/100 in 30 minutes, F = 1 mL/min, λ = 254 nm, showed one broad peak with t_R 15.41 min.

MS (ES+) m/z found 670.2 [M+H⁺], 692.2 [M+Na⁺], C₃₁H₃₆N₅O₁₀P required m/z 669.62 [M].

[112d] 2'-C-cyano-2'-deoxy-1-β-D-arabino-pentofuranosylcytosine-5'-O-naphth-1-yl-(benzyloxy-L-alaninyl)]phosphate



Compound **111d** was prepared according to procedure **F1** using **110** (0.10 g, 0.19 mmol), in THF (4 mL), *t*BuMgCl (0.50 mL, 0.50 mmol), naphth-1-yl(benzyloxy-L-alanin-*N*-yl)]phosphorochloridate (0.23 g, 0.57 mmol), in THF (2 mL). After evaporation, the crude was purified by Biotage

Isolera One (50g SNAP cartridge KP-SIL, 100 mL/min, using a gradient elution of 2-10% CH₃OH/CH₂Cl₂ over 10 CV, 10% CH₃OH/CH₂Cl₂ over 5 CV). The crude (0.065 g) was dissolved in EtOAc (2.8 mL), pyridine (28 μL, 0.32 mmol) and the mixture was cooled to 0 °C. Then HF·pyridine (70% HF, 8.5 μL, 0.31 μmol) was added. The progress of the

reaction was monitored by HPLC. After stirring for six hours another portion of pyridine (28 μL , 0.32 mmol) and HF·pyridine (70% HF, 8.5 μL , 0.31 μmol) was added to the reaction mixture. After stirring for 23 hours an additional portion of pyridine (28 μL , 0.32 mmol) and HF·pyridine (70% HF, 8.5 μL , 0.31 μmol) was added and the stirring was continuing up to a total of 24 hours. After addition of TMSOMe (0.29 mL, 2.18 mmol) and stirring for one hour, the solution was evaporated and the crude purified by flash column chromatography (eluent 0-7% $\text{CH}_3\text{OH}/\text{CH}_2\text{Cl}_2$), and preparative TLC (500 μm , 5% $\text{CH}_3\text{OH}/\text{CH}_2\text{Cl}_2$) to yield the title compound as a white solid (0.004 mg, 3% two steps).

^{31}P NMR (202 MHz, CD_3OD) δ_{P} 4.26, 4.22.

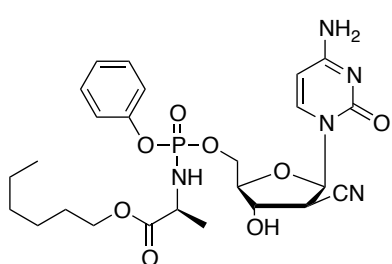
^1H NMR (500 MHz, CD_3OD) δ_{H} 8.11-8.04 (m, 1H, Ar), 7.81-7.78 (m, 1H, Ar), 7.64-7.60 (m, 1H, Ar), 7.56 (d, 0.5H, $J = 7.5$ Hz, H6), 7.53 (d, 0.5H, $J = 7.6$ Hz, H6), 7.46-7.36 (m, 3H, Ar), 7.33-7.28 (m, 1H, Ar), 7.22-7.17 (m, 5H, Ar), 6.11 (d, 0.5H, $J = 6.0$ Hz, H1'), 6.09 (d, 0.5H, $J = 6.5$ Hz, H1'), 5.65 (d, 0.5H, $J = 7.5$ Hz, H5), 5.61 (d, 0.5H, $J = 7.6$ Hz, H5), 5.01-4.97 (m, 2H, CH_2Ph), 4.46-4.42 (m, 1H, H3'), 4.42-4.36 (m, 1H, H5'), 4.29-4.24 (m, 1H, H5'), 4.02-3.96 (m, 1H, CHCH_3 L-Ala), 3.95-3.91 (m, 1H, H4'), 3.67-3.61 (m, 1H, H2'), 1.26-1.19 (m, 3H, CHCH_3 L-Ala).

^{13}C NMR (125 MHz, CD_3OD) δ_{C} 173.35 (C=O), 167.71 (C4), 167.64 (C4), 152.27 (C2), 141.79 (C6), 136.33 (C-Ar), 130.54 (C-Ar), 130.49 (C-Ar), 129.61 (CH-Ar), 129.60 (CH-Ar), 129.36 (CH-Ar), 129.32 (CH-Ar), 128.94 (CH-Ar), 127.93 (CH-Ar), 127.91 (CH-Ar), 127.68 (CH-Ar), 127.62 (CH-Ar), 126.60 (CH-Ar), 126.16 (CH-Ar), 126.13 (CH-Ar), 122.76 (CH-Ar), 122.70 (CH-Ar), 116.32 (CN), 116.29 (CN), 96.45 (C5), 96.43 (C5), 85.69 (C1'), 85.49 (C1'), 84.39 (C4'), 84.19 (C4'), 74.39 (C3'), 74.33 (C3'), 68.01 (CH_2Ph), 65.95 (C5'), 65.89 (C5'), 51.93 (CHCH_3 L-Ala), 51.79 (CHCH_3 L-Ala), 44.45 (C2'), 20.45 (CHCH_3), 20.39 (CHCH_3).

HPLC Reverse-phase HPLC eluting with $\text{H}_2\text{O}/\text{CH}_3\text{CN}$ from 90/10 to 0/100 in 30 minutes, $F = 1$ mL/min, $\lambda = 254$ nm, showed one broad peak with $t_{\text{R}} 15.48$ min.

MS (ES+) m/z found 620.2 [$\text{M}+\text{H}^+$], 642.2 [$\text{M}+\text{Na}^+$], $\text{C}_{30}\text{H}_{30}\text{N}_5\text{O}_8\text{P}$ required m/z 619.56 [M].

[112e] 2'-C-cyano-2'-deoxy-1-β-D-arabino-pentofuranosylcytosine-5'-O-phenyl-(hexyl-1-oxy-L-alaninyl)]phosphate



Compound **111e** was prepared according to procedure **F₁** using **110** (0.10 g, 0.19 mmol), in THF (4 mL), *t*BuMgCl (0.50 mL, 0.50 mmol), phenyl (hexyl-1-oxy-L-alanin-*N*-yl)] phosphorochloridate (0.20 g, 0.57 mmol), in THF (2 mL). After evaporation, the crude was purified by Biotage Isolera One (50g SNAP cartridge KP-SIL, 100 mL/min, using a gradient elution of 1-10% CH₃OH/CH₂Cl₂ over 10 CV, 10% CH₃OH/CH₂Cl₂ over 5 CV). The crude (0.068 mg) was dissolved in EtOAc (2.0 mL), pyridine (28 μL, 0.32 mmol) and the mixture was cooled to 0 °C. Then HF·pyridine (70% HF, 8.5 μL, 0.31 μmol) was added. The progress of the reaction was monitored by HPLC. After stirring for six hours another portion of pyridine (28 μL, 0.32 mmol) and HF·pyridine (70% HF, 8.5 μL, 0.31 μmol) was added to the reaction mixture. After stirring for 23 hours an additional portion of pyridine (28 μL, 0.32 mmol) and HF·pyridine (70% HF, 8.5 μL, 0.31 μmol) was added and the stirring was continuing up to a total of 24 hours. After addition of TMSOMe (0.29 mL, 2.18 mmol) and stirring for one hour, the solution was evaporated and the crude purified by flash column chromatography (eluent 0-7% CH₃OH/CH₂Cl₂), and preparative TLC (500 μm, 5% CH₃OH/CH₂Cl₂) to yield the title compound as a white solid (0.002 g, 2% two steps).

³¹P NMR (202 MHz, CD₃OD) δ_P 3.92, 4.01.

¹H NMR (500 MHz, CD₃OD) δ_H 7.66 (d, 0.5H, *J* = 7.7 Hz, H6), 7.60 (d, 0.5H, *J* = 7.7 Hz, H6), 7.31-7.24 (m, 2H, Ph), 7.19-7.08 (m, 3H, Ph), 6.16 (d, 0.5H, *J* = 7.0 Hz, H1'), 6.13 (d, 0.5H, *J* = 7.2 Hz, H1'), 5.81 (d, 0.5H, *J* = 7.5 Hz, H5), 5.76 (d, 0.5H, *J* = 7.5 Hz, H5), 4.47-4.22 (m, 3H, H3', H5'), 4.02-3.94 (m, 3H, CH₂CH₂CH₂CH₂CH₂CH₃ *n*-Hex, H4'), 3.91-3.83 (m, 1H, CHCH₃ L-Ala), 3.69-3.64 (m, 1H, H2'), 1.55-1.46 (m, 2H, CH₂CH₂CH₂CH₂CH₂CH₃ *n*-Hex), 1.28-1.16 (m, 7H, CH₂CH₂CH₂CH₂CH₂CH₃ *n*-Hex, CHCH₃ L-Ala), 1.02-0.95 (m, 2H, CH₂CH₂CH₂CH₂CH₂CH₃ *n*-Hex), 0.81-0.76 (m, 3H, CH₂CH₂CH₂CH₂CH₂CH₃ *n*-Hex).

¹³C NMR (125 MHz, CD₃OD) δ_C 175.18 (d, ³*J*_{CP} = 5.0 Hz, C=O), 174.97 (d, ³*J*_{CP} = 5.0 Hz, C=O), 167.84 (C4), 167.81 (C4), 157.67 (C-Ar), 157.03 (C-Ar), 152.44 (C2), 152.12 (C2), 141.85 (C6), 141.75 (C6), 130.90 (CH-Ar), 126.34 (CH-Ar), 126.29 (CH-Ar), 121.48 (CH-Ar), 121.46 (CH-Ar), 121.44 (CH-Ar), 121.43 (CH-Ar), 117.61 (CN), 117.59 (CN), 96.55 (C5), 96.47 (C5), 85.59 (C1'), 85.40 (C1'), 84.48 (d, ³*J*_{CP} = 8.1 Hz, C4'), 84.38 (d, ³*J*_{CP} = 8.1 Hz, C4'), 74.40 (C3'), 74.04 (C3'), 66.54 (CH₂CH₂CH₂CH₂CH₂CH₃ Hex), 66.52

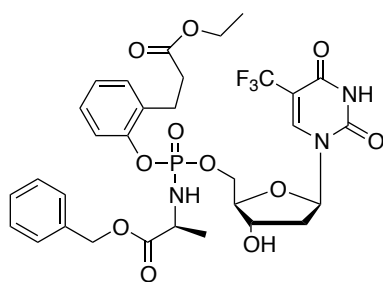
(CH₂CH₂CH₂CH₂CH₂CH₃ Hex), 65.78 (d, ²J_{CP} = 5.4 Hz, C5'), 65.56 (d, ²J_{CP} = 5.4 Hz, C5'), 51.80 (CHCH₃ L-Ala), 51.63 (CHCH₃ L-Ala), 44.49 (C2'), 44.46 (C2'), 32.62 (CH₂CH₂CH₂CH₂CH₂CH₃ *n*-Hex), 32.61 (CH₂CH₂CH₂CH₂CH₂CH₃ *n*-Hex), 29.68 (CH₂CH₂CH₂CH₂CH₂CH₃ *n*-Hex), 26.66 (CH₂CH₂CH₂CH₂CH₂CH₃ *n*-Hex), 23.63 (CH₂CH₂CH₂CH₂CH₂CH₃ *n*-Hex), 20.57 (d, ³J_{CP} = 7.12 Hz, CHCH₃ L-Ala), 20.42 (d, ³J_{CP} = 7.12 Hz, CHCH₃ L-Ala), 14.39 (CH₂CH₂CH₂CH₂CH₂CH₃ *n*-Hex).

HPLC Reverse-phase HPLC eluting with H₂O/CH₃CN from 90/10 to 0/100 in 30 minutes, F = 1 mL/min, λ = 254 nm, showed one broad peak with tR 16.09 min.

MS (ES+) m/z found 564.3 [M+H⁺], 586.3 [M+Na⁺], C₂₅H₃₄N₅O₈P required m/z 563.54 [M].

9.5.18 Synthesis of TFT ProTides

[114a] 5-Trifluoromethyl-2'-deoxyuridine-5'-[ethyl-3-(2-hydroxyphenyl)propanoyl (benzyloxy-L-alanin-N-yl)]phosphate



Prepared according to general procedure F₂ using trifluorothymidine (0.05 g, 0.17 mmol) in THF (2 mL), ethyl 3-(2-hydroxyphenyl)propanoyl (benzyloxy-L-alanin-N-yl)] phosphorochloridate [17v] (0.23 g, 0.51 mmol) in THF (1 mL), and *N*-methylimidazole (67 μL, 0.84 mmol).

The solvent was evaporated and the crude was dissolved in CH₂Cl₂ (25 mL) and washed with 0.5 M aqueous HCl solution (5 mL). The organic phase was dried over Na₂SO₄, filtered, evaporated and purified by silica gel column chromatography (eluent system 0-6% CH₃OH /CH₂Cl₂) and by preparative TLC (500 μM, eluent system 5% CH₃OH /CH₂Cl₂) to give the title compound as a white solid (0.013 g, 11%).

³¹P NMR (202 MHz, CD₃OD) δ_P 3.95, 3.54.

¹H NMR (500 MHz, CD₃OD) δ_H 8.20 (s, 0.5H, H6), 8.16 (s, 0.5H, H6), 7.40-7.30 (m, 6H, Ar), 7.28-7.24 (m, 1H, Ar), 7.22-7.09 (m, 2H, Ar), 6.17 (dd, *J* = 7.3, 6.2 Hz, 0.5H, H1'), 6.11 (dd, *J* = 7.3, 6.2 Hz, 0.5H, H1'), 5.19-5.08 (m, 2H, CH₂Ph), 4.47-4.42 (m, 0.5H, H3'), 4.39-4.28 (m, 2H, H3', H5'), 4.26-4.20 (m, 0.5H, H5'), 4.17-3.97 (m, 4H, H4', CH₂CH₂CO₂CH₂CH₃, CHCH₃ L-Ala), 3.00-2.89 (m, 2H, CH₂CH₂CO₂CH₂CH₃), 2.65-2.53 (m, 2H, CH₂CH₂CO₂CH₂CH₃), 2.40-2.33 (m, 1H, H2'), 2.24-2.17 (m, 0.5H, H2'), 2.14-

2.07 (m, 0.5H, H^{2'}), 1.41-1.36 (m, 3H, CHCH₃ L-Ala), 1.24-1.18 (m, 3H, CH₂CH₂CO₂CH₂CH₃).

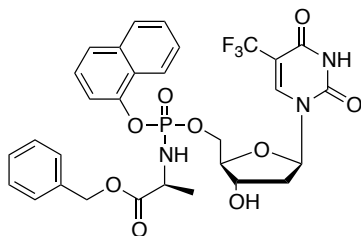
¹³C NMR (125 MHz, CD₃OD) δ_C 174.79 (d, ³J_{C-P} = 4.5 Hz, C=O), 174.56 (C=O), 174.52 (C=O), 174.47 (d, ³J_{C-P} = 5.2 Hz, C=O), 161.13 (C4), 151.12 (C2), 151.02 (C2), 150.39 (d, ²J_{CP} = 7.5 Hz, C-Ar), 150.37 (d, ²J_{CP} = 7.5 Hz, C-Ar), 143.04 (q, ³J_{CF} = 6.2 Hz, C6), 142.91 (q, ³J_{CF} = 6.2 Hz, C6), 137.24 (C-Ar), 137.18 (C-Ar), 132.87 (d, ³J_{C-P} = 7.5 Hz, C-Ar), 132.09 (d, ³J_{C-P} = 7.5 Hz, C-Ar), 131.64 (CH-Ar), 131.55 (CH-Ar), 129.64 (CH-Ar), 129.61 (CH-Ar), 129.43 (CH-Ar), 129.39 (CH-Ar), 129.37 (CH-Ar), 128.77 (CH-Ar), 128.71 (CH-Ar), 126.25 (CH-Ar), 123.81 (q, ¹J_{CF} = 267.5 Hz, CF₃), 120.91 (d, ³J_{CP} = 2.5 Hz, CH-Ar), 120.89 (d, ³J_{CP} = 2.5 Hz, CH-Ar), 105.20 (q, ²J_{CF} = 32.5 Hz, C5), 105.19 (q, ²J_{CF} = 32.5 Hz, C5), 88.59 (C1'), 88.31 (C1'), 87.22 (d, ³J_{CP} = 7.5 Hz, C4'), 87.16 (d, ³J_{CP} = 7.5 Hz, C4'), 72.24 (C3'), 72.17 (C3'), 68.04 (CH₂Ph), 67.70 (d, ²J_{CP} = 7.5 Hz, C5'), 67.65 (d, ²J_{CP} = 7.5 Hz, C5'), 61.62 (CH₂CH₂CO₂CH₂CH₃), 61.61 (CH₂CH₂CO₂CH₂CH₃), 51.77 (CHCH₃ L-Ala), 51.68 (CHCH₃ L-Ala), 41.47 (C2'), 41.45 (C2'), 35.29 (CH₂CH₂CO₂CH₂CH₃), 35.21 (CH₂CH₂CO₂CH₂CH₃), 26.75 (CH₂CH₂CO₂CH₂CH₃), 26.63 (CH₂CH₂CO₂CH₂CH₃), 20.47 (d, ³J_{CP} = 6.2 Hz, CHCH₃ L-Ala), 20.35 (d, ³J_{CP} = 6.2 Hz, CHCH₃ L-Ala), 14.52 (CH₂CH₂CO₂CH₂CH₃).

¹⁹F NMR (470 MHz, CD₃OD) δ_F 64.34, 64.35.

MS (ES+) m/z found 736.2 [M+Na⁺], 714.2 [M+H⁺], C₃₁H₃₅F₃N₃O₁₁P required m/z 713.59 [M].

HPLC Reverse-phase HPLC eluting with H₂O/CH₃CN from 100/10 to 0/100 in 30 minutes, F = 1 mL/min, λ = 254 nm, showed one peak with t_R 20.87 min.

[114b] 5-Trifluoromethyl-2'-deoxyuridine-5'-naphth-1-yl-(benzyloxy-L-alaninyl)phosphate



Prepared according to generale procedure F₂ using trifluorothymidine (0.05 g, 0.17 mmol), in THF (2 mL), naphth-1-yl(benzyloxy-L-alaninyl)phosphorochloridate [17a] (0.14 g, 0.34 mmol) in THF (1 mL), and *N*-methylimidazole (67 μL, 0.84 mmol). The solvent was

evaporated and the crude was dissolved in CH₂Cl₂ (25 mL) and washed with 0.5 M aqueous HCl solution (5 mL). The organic phase was dried over Na₂SO₄, filtered, evaporated and purified by silica gel column chromatography (eluent system 0-6% CH₃OH /CH₂Cl₂) and by preparative TLC (500 μM, eluent system CH₃OH /CH₂Cl₂ = 5/95) to give the title compound as a white solid (0.035 g, 31%).

³¹P NMR (202 MHz, CD₃OD) δ_P 4.47, 4.03.

¹H NMR (500 MHz, CD₃OD) δ_H 8.16-8.08 (m, 2H, H₆, Ar), 7.81-7.87 (m, 1H, Ar), 7.73, 7.68 (m, 1H, Ar), 7.57-7.45 (m, 2H, Ar), 7.44-7.35 (m, 1H, Ar), 7.34-7.27 (m, 6H, Ar), 6.07-6.01 (m, 1H, H1'), 5.13-5.03 (m, 2H, CH₂Ph), 4.42-4.23 (m, 3H, H3', H5'), 4.15-4.11 (m, 1H, H4'), 4.11-4.02 (m, 1H, CHCH₃ L-Ala), 2.30-2.24 (m, 0.5H, H2'), 2.23-2.17 (m, 0.5H, H2'), 1.93-1.87 (m, 0.5H, H2'), 1.76-1.69 (m, 0.5H, H2'), 1.36-1.31 (m, 3H, CHCH₃ L-Ala).

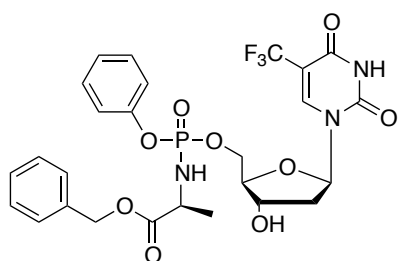
¹³C NMR (125 MHz, CD₃OD) δ_C 174.82 (d, ³J_{CP} = 4.0 Hz, C=O), 174.50 (d, ³J_{CP} = 4.0 Hz, C=O), 161.08 (C4), 161.07 (C4), 150.91 (C2), 150.88 (C2), 147.93 (d, ³J_{CP} = 7.4 Hz, C-Ar), 147.83 (d, ³J_{CP} = 7.4 Hz, C-Ar), 142.91 (q, ³J_{CF} = 6.0 Hz, C6), 142.63 (q, ³J_{CF} = 6.0 Hz, C6), 137.15 (C-Ar), 137.13 (C-Ar), 136.27 (C-Ar), 129.60 (CH-Ar), 129.55 (CH-Ar), 129.39 (CH-Ar), 129.34 (CH-Ar), 129.32 (CH-Ar), 128.94 (CH-Ar), 128.90 (CH-Ar), 127.85 (CH-Ar), 127.55 (CH-Ar), 123.80 (q, ¹J_{CF} = 268.7 Hz, CF₃), 123.76 (q, ¹J_{CF} = 268.7 Hz, CF₃), 126.49 (d, J_{CP} = 3.4 Hz, CH-Ar), 126.48 (d, J_{CP} = 3.4 Hz, CH-Ar), 126.16 (CH-Ar), 126.09 (CH-Ar), 116.28 (CH-Ar), 105.32 (q, ²J_{CF} = 32.7 Hz, C5), 88.61 (C1'), 88.44 (C1'), 87.46 (d, ³J_{CP} = 7.8 Hz, C4'), 87.22 (d, ³J_{CP} = 7.8 Hz, C4'), 72.33 (C3'), 72.22 (C3'), 68.02 (CH₂Ph), 67.82 (d, ²J_{CP} = 5.4 Hz, C5'), 67.78 (d, ²J_{CP} = 5.4 Hz, C5'), 51.84 (CHCH₃ L-Ala), 51.76 (CHCH₃ L-Ala), 41.42 (C2'), 41.40 (C2'), 20.37 (d, ³J_{CP} = 7.6 Hz, CHCH₃ L-Ala), 20.31 (d, ³J_{CP} = 7.6 Hz, CHCH₃ L-Ala).

¹⁹F NMR (470 MHz, CD₃OD) δ_F -64.30, -64.33.

MS (ES+) m/z: Found: 686.2 [M+Na⁺], 664.2 [M+H⁺], C₃₀H₂₉F₃N₃O₉P required m/z 663.53 [M].

HPLC Reverse-phase HPLC eluting with H₂O/CH₃CN from 100/10 to 0/100 in 30 minutes, F = 1 ml/min, λ = 245 nm, showed two peaks with t_R 17.25 min. and t_R 17.51 min.

[114c] 5-Trifluoromethyl-2'-deoxyuridine-5'-phenyl-(benzyloxy-L-alaninyl)]phosphate



Prepared according to general procedure **F**₂ using trifluorothymidine (0.054 g, 0.18 mmol) in THF (3 mL), phenyl(benzyloxy-L-alaninyl)phosphorochloridate [**17s**] (0.13 g, 0.36 mmol) in THF (1 mL) and *N*-methylimidazole (72 μL, 0.90 mmol). The solvent was evaporated and the crude was dissolved in CH₂Cl₂ (25 mL) and washed with 0.5 M aqueous HCl solution (5 mL). The organic phase was dried over Na₂SO₄, filtered,

evaporated and purified by silica gel column chromatography (eluent system 0-6% CH₃OH /CH₂Cl₂) to give the title compound as a white solid (0.05 g, 45%).

³¹P NMR (202 MHz, CD₃OD) δ_P 4.12, 3.56.

¹H NMR (500 MHz, CD₃OD) δ_H 8.17 (s, 0.5H, H6), 8.15 (s, 0.5H, H6), 7.39-7.28 (m, 7H, Ar), 7.24-7.15 (m, 3H, Ar), 6.17 (dd, *J* = 7.6, 6.2 Hz, 0.5H, H1'), 6.12 (dd, *J* = 7.6, 6.2 Hz, 0.5H, H1'), 5.18-5.08 (m, 2H, CH₂Ph), 4.45-4.41 (m, 0.5H, H3'), 4.40-4.22 (m, 2.5H, H3', H5'), 4.17-4.12 (m, 1H, H4'), 4.05-3.94 (m, 1H, CHCH₃ L-Ala), 2.42-2.29 (m, 1H, H2'), 2.14-2.07 (m, 0.5H, H2'), 2.03-1.94 (m, 0.5H, H2'), 1.37-1.31 (m, 3H, CHCH₃ L-Ala).

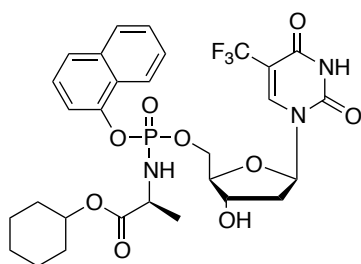
¹³C NMR (125 MHz, CD₃OD) δ_C 174.87 (d, ³*J*_{CP} = 5.0 Hz, C=O), 174.75 (d, ³*J*_{CP} = 5.0 Hz, C=O), 161.07 (C4), 152.06 (d, ²*J*_{CP} = 6.2 Hz, C-Ar), 152.05 (d, ²*J*_{CP} = 6.2 Hz, C-Ar), 151.07 (C2), 151.01 (C2), 142.90 (q, ³*J*_{CF} = 6.02 Hz, C6), 142.76 (q, ³*J*_{CF} = 6.02 Hz, C6), 137.22 (C-Ar), 137.14 (C-Ar), 130.84 (CH-Ar), 129.66 (CH-Ar), 129.64 (CH-Ar), 129.47 (CH-Ar), 129.42 (CH-Ar), 129.38 (CH-Ar), 126.34 (CH-Ar), 126.27 (CH-Ar), 123.87 (q, ¹*J*_{CF} = 267.5 Hz, CF₃), 121.42 (CH-Ar), 121.38 (CH-Ar), 105.50 (q, ²*J*_{CF} = 32.5 Hz, C5), 105.39 (q, ²*J*_{CF} = 32.5 Hz, C5), 88.50 (C1'), 88.17 (C1'), 87.40 (d, ³*J*_{CP} = 8.2 Hz, C4'), 87.21 (d, ³*J*_{CP} = 8.2 Hz, C4'), 72.31 (C3'), 72.22 (C3'), 68.06 (CH₂Ph), 67.66 (d, ²*J*_{CP} = 16.2 Hz, C5'), 67.54 (d, ²*J*_{CP} = 16.2 Hz, C5'), 51.79 (CHCH₃ L-Ala), 51.63 (CHCH₃ L-Ala), 41.62 (C2'), 41.55 (C2'), 20.52 (d, ³*J*_{CP} = 7.0 Hz, CHCH₃ L-Ala), 20.40 (d, ³*J*_{CP} = 7.0 Hz, CHCH₃ L-Ala).

¹⁹F NMR (470 MHz, CD₃OD) δ_F -64.11, -64.15.

MS (ES+) m/z found 636.1 [M+Na⁺], 614.1 [M+H⁺], C₂₆H₂₇F₃N₃O₉P required m/z 613.48 [M].

HPLC Reverse-phase HPLC eluting with H₂O/CH₃CN from 100/10 to 0/100 in 30 minutes, F = 1 mL/min, l = 254 nm, showed one peak with t_R 15.69 min.

[114d] 5-Trifluoromethyl-2'-deoxyuridine-5'-[naphth-1-yl-(cyclohexyloxy-L-alaninyl)] phosphate



Prepared according to general procedure F₂ using trifluorothymidine (0.05 g, 0.178 mmol) in THF (3 mL), naphth-1-yl(cyclohex-1-yloxy-L-alaninyl) phosphorochloridate [17c] (0.17 g, 0.51 mmol) in THF (1 mL) and *N*-methylimidazole (70 μL, 0.85 mmol). The

solvent was evaporated and the crude was dissolved in CH₂Cl₂ (25 mL) and washed with 0.5 M aqueous HCl solution (5 mL). The organic phase was dried over Na₂SO₄, filtered,

evaporated and purified by silica gel column chromatography (eluent system 0-6% CH₃OH /CH₂Cl₂) to give the title compound as a white solid (0.048 g, 41%).

³¹P NMR (202 MHz, CD₃OD) δ_P 4.40, 4.10.

¹H NMR (500 MHz, CD₃OD) δ_H 8.17-8.10 (m, 2H, H6, Nap), 7.91-7.87 (m, 1H, Nap), 7.74-7.69 (m, 1H, Nap), 7.56-7.48 (m, 3H, Nap), 7.45-7.39 (m, 1H, Nap), 6.09-6.02 (m, 1H, H1'), 4.73-4.66 (m, 1H, CH(CH₂)₅ cHex), 4.47-4.30 (m, 3H, H3', H5'), 4.20-4.14 (m, 1H, H4'), 4.03-3.95 (m, 1H, CHCH₃ L-Ala), 2.31 (ddd, *J* = 13.9 Hz, 6.2 Hz, 3.0 Hz, 0.5H, H2'), 2.20 (ddd, *J* = 13.9 Hz, 6.2 Hz, 3.0 Hz, 0.5H, H2'), 2.03-1.95 (m, 0.5H, H2'), 1.81-1.65 (m, 4.5H, H2', CH(CH₂)₅ cHex, CHCH₃ L-Ala), 1.57-1.48 (m, 1H, CH(CH₂)₅ cHex), 1.42-1.23 (m, 8H, CH(CH₂)₅ cHex).

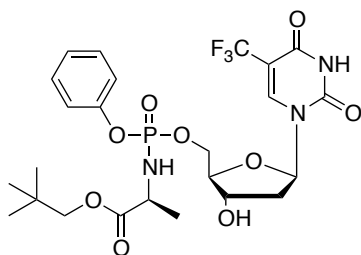
¹³C NMR (125 MHz, CD₃OD) δ_C 174.50 (d, ³*J*_{CP} = 4.7 Hz, C=O), 174.22 (d, ³*J*_{CP} = 4.7 Hz, C=O), 161.05 (C4), 161.02 (C4), 150.95 (C2), 150.87 (C2), 147.99 (d, ²*J*_{C-P} = 7.1 Hz, C-Ar), 147.90 (d, ²*J*_{C-P} = 7.1 Hz, C-Ar), 143.00 (q, ³*J*_{CF} = 5.7 Hz, C6), 142.59 (q, ³*J*_{CF} = 5.7 Hz, C6), 136.31 (C-Ar), 128.94 (CH-Ar), 127.87 (CH-Ar), 127.85 (CH-Ar), 127.54 (CH-Ar), 127.52 (CH-Ar), 126.50 (CH-Ar), 126.15 (CH-Ar), 126.08 (CH-Ar), 123.83 (q, ³*J*_{CF} = 268.8 Hz, CF₃), 123.76 (q, ³*J*_{CF} = 268.8 Hz, CF₃), 122.58 (CH-Ar), 122.55 (CH-Ar), 116.27 (d, ³*J*_{C-P} = 2.9 Hz, CH-Ar), 116.22 (d, ³*J*_{C-P} = 2.9 Hz, CH-Ar), 105.43 (q, ³*J*_{CF} = 32.6 Hz, C5), 105.35 (q, ³*J*_{CF} = 32.6 Hz, C6), 88.66 (C1'), 88.51 (C1'), 87.54 (d, ³*J*_{CP} = 8.3 Hz, C4'), 87.22 (d, ³*J*_{CP} = 8.3 Hz, C4'), 75.02 (CH(CH₂)₅ cHex), 74.99 (C3'), 67.87 (d, ²*J*_{CP} = 5.3 Hz, C5'), 67.80 (d, ²*J*_{CP} = 5.3 Hz, C5'), 51.88 (CHCH₃ L-Ala), 41.43 (C2'), 41.37 (C2'), 32.41 (CH(CH₂)₅ cHex), 32.38 (CH(CH₂)₅ cHex), 32.36 (CH(CH₂)₅ cHex), 32.33 (CH(CH₂)₅ cHex), 24.88 (CH(CH₂)₅ cHex), 20.64 (d, ³*J*_{CP} = 6.3 Hz, CHCH₃ L-Ala), 20.56 (d, ³*J*_{CP} = 6.3 Hz, CHCH₃ L-Ala).

¹⁹F NMR (470 MHz, CD₃OD) δ_F -64.23, -64.30.

MS (ES+) m/z found 678.2 [M+Na⁺], 656.2 [M+H⁺], C₂₉H₃₃F₃N₃O₉P required m/z 655.56 [M].

HPLC Reverse-phase HPLC eluting with H₂O/CH₃CN from 100/10 to 0/100 in 30 minutes, F = 1 mL/min, l = 254 nm, showed two peaks with t_R 18.38 min. and t_R 18.63 min.

[114e] 5-Trifluoromethyl-2'-deoxyuridine-5'-phenyl-(neopentyloxy-L-alaninyl)]phosphate



Prepared according to general procedure **F₂** using trifluorothymidine (0.05 g, 0.178 mmol) in THF (3 mL), phenyl(neopentyloxy-L-alaninyl)phosphorochloridate [**17t**] (0.17 g, 0.51 mmol) in THF (1 mL) and *N*-methylimidazole (70 μ L, 0.85 mmol). The solvent was evaporated and the

crude was dissolved in CH₂Cl₂ (25 mL) and washed with 0.5 M aqueous HCl solution (5 mL). The organic phase was dried over Na₂SO₄, filtered, evaporated and purified by silica gel column chromatography (eluent system 0-6% CH₃OH /CH₂Cl₂) to give the title compound as a white solid (0.029 g, 27%).

¹H NMR (500 MHz, CD₃OD) δ_{H} 8.19 (s, 0.5H, H6), 8.18 (s, 0.5H, H6), 7.39-7.33 (m, 2H, Ph), 7.26-7.18 (m, 3H, Ph), 6.20-6.12 (m, 1H, H1'), 4.48-4.30 (m, 3H, H3', H5'), 4.20-4.14 (m, 1H, H4'), 4.04-3.95 (m, 1H, CHCH₃ L-Ala), 3.87-3.84 (m, 1H, CH₂*t*Bu Neop), 3.80-3.73 (m, 1H, CH₂*t*Bu Neop), 2.44-2.38 (m, 0.5H, H2'), 2.37-2.31 (m, 0.5H, H2'), 2.24-2.18 (m, 0.5H, H2'), 2.06-1.99 (m, 0.5H, H2'), 1.39-1.35 (m, 3H, CHCH₃ L-Ala), 0.96 (s, 4.5H, CH₂*t*Bu Neop), 0.95 (s, 4.5H, CH₂*t*Bu).

¹³C NMR (125 MHz, CD₃OD) δ_{C} 175.06 (d, ³*J*_{CP} = 4.9 Hz, C=O), 174.72 (d, ³*J*_{CP} = 4.9 Hz, C=O), 161.07 (C4), 160.9 (C4), 152.06 (d, ²*J*_{CP} = 6.2 Hz, C-Ar), 152.05 (d, ²*J*_{CP} = 6.2 Hz, C-Ar), 151.09 (C2), 143.01 (q, ³*J*_{CF} = 6.2 Hz, C6), 142.77 (q, ³*J*_{CF} = 6.2 Hz, C6), 136.70 (C-Ar), 130.80 (CH-Ar), 126.31 (CH-Ar), 126.22 (CH-Ar), 123.70 (q, ¹*J*_{CF} = 267.5 Hz, CF₃), 121.38 (d, ²*J*_{CP} = 4.6 Hz, CH-Ar), 121.36 (d, ²*J*_{CP} = 4.6 Hz, CH-Ar), 105.15 (q, ²*J*_{CF} = 32.3 Hz, C5), 88.59 (C1'), 88.27 (C1'), 87.48 (d, ³*J*_{CP} = 8.1 Hz, C4'), 87.24 (d, ³*J*_{CP} = 8.1 Hz, C4'), 75.46 (CH₂C(CH₃)₃ Neop), 72.36 (C3'), 72.23 (C3'), 67.72 (d, ²*J*_{CP} = 4.6 Hz, C5'), 67.59 (d, ²*J*_{CP} = 4.6 Hz, C5'), 51.73 (CHCH₃ L-Ala), 51.65 (CHCH₃ L-Ala), 41.58 (C2'), 41.46 (C2'), 28.05 (CH₂C(CH₃)₃ Neop) 26.70 (CH₂C(CH₃)₃ Neop), 20.70 (d, ³*J*_{CP} = 6.3 Hz, CHCH₃ L-Ala), 20.56 (d, ³*J*_{CP} = 6.3 Hz, CHCH₃ L-Ala).

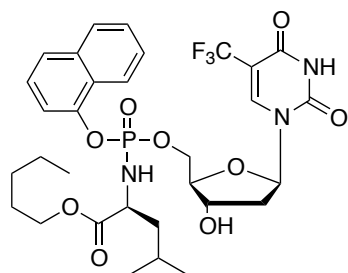
³¹P NMR (202 MHz, CD₃OD) δ_{P} 4.06, 3.71.

¹⁹F NMR (470 MHz, CD₃OD) δ_{F} -64.32, -64.24.

MS (ES⁺) *m/z* found 616.2 [M+Na⁺], 594.2 [M+H⁺], C₂₄H₃₁F₃N₃O₉P required *m/z* 593.49 [M].

HPLC Reverse-phase HPLC eluting with H₂O/CH₃CN from 100/10 to 0/100 in 30 minutes, F = 1 mL/min, λ = 254 nm, showed one peak with *t*_R 16.56 min.

[114f] 5-Trifluoromethyl-2'-deoxyuridine-5'-naphth-1-yl-(pentyl-1-oxy-L-alaninyl)]phosphate



Prepared according to general procedure **F₂** using trifluorothymidine (0.05 g, 0.17 mmol) in THF (3 mL), naphth-1-yl(pentyl-1-oxy-L-leucinyl)phosphorochloridate [**17f**] (0.22 g, 0.51 mmol) in THF (1 mL) and *N*-methylimidazole (70 μ L, 0.85 mmol). The solvent was

evaporated and the crude was dissolved in CH₂Cl₂ (25 mL) and washed with 0.5 M HCl solution (5 mL). The organic phase was dried over Na₂SO₄, filtered, evaporated and purified by silica gel column chromatography (eluent system 0-6% CH₃OH /CH₂Cl₂) and by prepTLC (1000 μ M, 5% CH₃OH in CH₂Cl₂) to give a white solid (0.03 g, 26%).

³¹P NMR (202 MHz, CD₃OD) δ_P 4.79, 4.23.

¹H NMR (500 MHz, CD₃OD) δ_H 8.19-8.11 (m, 2H, H6, Nap), 7.93-7.87 (m, 1H, Nap), 7.74-7.89 (m, 1H, Nap), 7.58-7.48 (m, 3H, Nap), 7.45-7.38 (m, 1H, Nap), 6.11-6.05 (m, 1H, H1'), 4.50-4.43 (m, 0.5H, H3'), 4.42-4.29 (m, 2.5H, H3', H5'), 4.20-4.10 (m, 3H, H4', CH₂CH₂CH₂CH₂CH₃ *n*-Pen), 3.97-3.89 (m, 1H, CHCH₂CH(CH₃)₂ L-Leu), 2.36-2.29 (m, 0.5H, H2'), 2.27-2.19 (m, 0.5H, H2'), 2.03-1.95 (m, 0.5H, H2'), 1.85-1.44 (m, 5.5H, H2', CHCH₂CH(CH₃)₂ L-Leu, CH₂CH₂CH₂CH₂CH₃ *n*-Pen), 1.41-1.36 (m, 2H, CH₂CH₂CH₂CH₂CH₃ *n*-Pen), 1.32-1.25 (m, 2H, CH₂CH₂CH₂CH₂CH₃ *n*-Pen), 0.99-0.91 (m, 6H, CHCH₂CH(CH₃)₂ L-Leu), 0.88-0.83 (m, 3H, CH₂CH₂CH₂CH₂CH₃ *n*-Pen).

¹³C NMR (125 MHz, CD₃OD), δ_C 175.42 (d, ³*J*_{C-P} = 2.5 Hz, C=O), 174.95 (d, ³*J*_{C-P} = 2.5 Hz, C=O), 161.04 (C4), 161.00 (C4), 150.96 (C2), 150.93 (C2), 147.97 (d, ²*J*_{CP} = 7.1 Hz, C-Ar), 147.90 (d, ²*J*_{CP} = 7.1 Hz, C-Ar), 143.00 (q, ³*J*_{CF} = 5.6 Hz, C6), 142.68 (q, ³*J*_{CF} = 5.6 Hz, C6), 136.32 (C-Ar), 128.93 (CH-Ar), 128.91 (CH-Ar), 127.84 (CH-Ar), 127.82 (CH-Ar), 127.52 (CH-Ar), 127.49 (CH-Ar), 126.48 (CH-Ar), 126.15 (CH-Ar), 126.02 (CH-Ar), 125.93 (q, ¹*J*_{CF} = 269.5 Hz, CF₃), 125.88 (q, ¹*J*_{CF} = 269.5 Hz, CF₃), 122.66 (CH-Ar), 122.61 (CH-Ar), 116.44 (d, ³*J*_{CP} = 3.5 Hz, CH-Ar), 116.10 (d, ³*J*_{CP} = 3.5 Hz, CH-Ar), 105.44 (q, ²*J*_{CF} = 33.5 Hz, C5), 88.61 (C1'), 88.31 (C1'), 87.45 (d, ³*J*_{CP} = 7.9 Hz, C4'), 87.17 (d, ³*J*_{CP} = 7.9 Hz, C4'), 72.30 (C3'), 72.24 (C3'), 67.89 (d, ²*J*_{CP} = 5.4 Hz, C5'), 67.81 (d, ²*J*_{CP} = 5.4 Hz, C5'), 66.37 (CH₂CH₂CH₂CH₂CH₃ *n*-Pen), 54.77 (CHCH₂CH(CH₃)₂ L-Leu), 44.19 (d, ³*J*_{CP} = 7.5 Hz, CHCH₂CH(CH₃)₂ L-Leu), 43.88 (d, ³*J*_{CP} = 7.5 Hz, CHCH₂CH(CH₃)₂ L-Leu), 41.38 (C2'), 41.32 (C2'), 29.33 (CH₂CH₂CH₂CH₂CH₃ *n*-Pen), 29.31 (CH₂CH₂CH₂CH₂CH₃ *n*-Pen), 25.70 (CHCH₂CH(CH₃)₂ L-Leu), 25.43 (CHCH₂CH(CH₃)₂ L-Leu), 23.30 (CH₂CH₂CH₂CH₂CH₃ *n*-Pen), 23.16 (CHCH₂CH(CH₃)₂ L-Leu), 22.97 (CHCH₂CH(CH₃)₂ L-Leu), 22.03 (CH₂CH₂CH₂CH₂CH₃ *n*-Pen), 21.65

(CH₂CH₂CH₂CH₂CH₃ *n*-Pen), 14.24 (CH₂CH₂CH₂CH₂CH₃ *n*-Pen), 14.23
(CH₂CH₂CH₂CH₂CH₃ *n*-Pen).

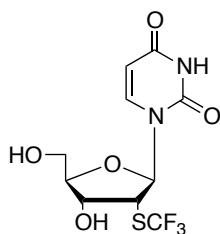
¹⁹F NMR (470 MHz, CD₃OD) δ_F -64.32, -64.23.

MS (ES+) *m/z* found 708.2 [M+Na⁺], 686.2 [M+H⁺], C₃₁H₃₉F₃N₃O₉P required *m/z* 685.63 [M].

HPLC Reverse-phase HPLC eluting with H₂O/CH₃CN from 100/10 to 0/100 in 30 minutes, F = 1 mL/min, l = 245 nm, showed one broad peak with t_R 21.58 min.

9.5.19 Synthesis of 2'-SCF₃-2'-deoxyuridine and 2'-SH-2'-deoxyuridine

[115] 2'-Trifluoromethylthio-2'-deoxyuridine



2'-Mercapto-2'-deoxyuridine [119] (0.54 g, 2.07 mmol) was dissolved in CH₃OH (15 mL) and the solution was cooled to -78 °C under argon atmosphere. 3,3-Dimethyl-1-(trifluoromethyl)-1,2-benziodoxole (Togni Reagent) (0.76 g, 2.5 mmol) was dissolved in CH₃OH (5 mL) in a second flask and cooled to -78 °C under argon atmosphere. The solution was added via a syringe to the initial solution, the second flask was washed with CH₃OH (1 mL) and the solution added to the first flask. The reaction mixture was allowed to stir at -78 °C for 10 minutes and then at room temperature for 5 hours. The mixture was evaporated and the crude purified via Biotage Isolera One (50g SNAP cartridge KP-SIL, 75 mL/min, using a gradient elution of 2-20% CH₃OH/CH₂Cl₂ over 10 CV, 20% CH₃OH/CH₂Cl₂ over 5 CV) to yield the title compound as a white solid (0.52 g, 76%).⁴³⁷

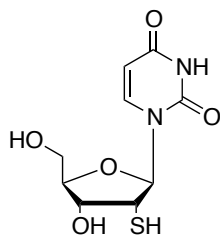
¹H NMR (CD₃OD) δ_H 7.99 (d, *J* = 7.9 Hz, 1H, H6), 6.32 (d, *J* = 9.2 Hz, 1H, H1'), 5.78 (d, *J* = 8.2 Hz, 1H, H5), 4.43 (dd, *J* = 5.1 Hz, 1.1 Hz, H3'), 4.11 (tt, *J* = 4.6 Hz, 1.1 Hz, 1H, H4'), 4.03 (dd, 9.1 Hz, 5.3 Hz, 1H, H2'), 3.789 (dd, 17.9 Hz, 12.0 Hz, 1H, H5'), 3.783 (dd, 17.9 Hz, 12.0 Hz, 1H, H5').

¹³C NMR (CD₃OD) δ_C 165.73 (C4), 152.57 (C2), 142.23 (C6), 132.37 (q, ¹*J*_{C-F} = 305.0 Hz, SCF₃), 103.83 (C5), 89.87 (C1'), 88.63 (C4'), 74.62 (C3'), 63.11 (C5'), 52.06 (C2').

¹⁹F NMR (CD₃OD) δ_F - 41.60.

MS (ES+) *m/z* found 351.2 [M+Na⁺], C₁₀H₁₁F₃N₂O₅S required *m/z* 328.26 [M].

HPLC Reverse-phase HPLC eluting with H₂O/CH₃OH 100/0 to 75/25 in 30 min, λ = 254 nm, F = 1 mL/min, showed one peak with t_R 18.51 min.

[119] 2'-Mercapto-2'-deoxyuridine

2'-*S*-acetyl-3',5'-di-*O*-acetyluridine [126] (1.0 g, 2.59 mmol) was dissolved in EtOH (20 mL) and cooled to 0 °C in a ice bath. An aqueous solution of KOH (2N, 20 mL) was added dropwise and the mixture was stirred for 15 minutes. Keeping the flask in the cool bath, the reaction solution was neutralised with HCl 2N aqueous solution and the volatiles evaporated. The crude was packed in a silica slurry and purified by Biotage Isolera One (25g SNAP cartridge C-18 KP-SIL, 25 mL/min, using water as eluent solvent over 30 minutes) to yield the desired product as a white solid (0.59 g, 87%).

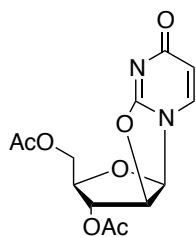
(Lit. mp: 174-175 °C).⁴⁴⁵

¹H NMR (CD₃OD) δ_H 7.94 (d, *J* = 7.8 Hz, 1H, H6), 5.99 (d, *J* = 8.7 Hz, 1H, H1'), 5.76 (d, *J* = 8.1 Hz, 1H, H5), 4.22 (dd, *J* = 5.1 Hz, 1.9 Hz, H3'), 4.08 (tt, *J* = 2.6 Hz, 1.9 Hz, 1H, H4'), 3.779 (dd, 20.5 Hz, 11.9 Hz, 1H, H5'), 3.772 (dd, 20.5 Hz, 11.9 Hz, 1H, H5'), 3.53 (dd, *J* = 8.6 Hz, 5.3 Hz, 1H, H2').

¹³C NMR (CD₃OD) δ_C 164.64 (C=O), 151.18 (C=O), 141.28 (C6), 102.00 (C5), 88.83 (C1'), 86.80 (C4'), 72.31 (C3'), 61.45 (C5'), 56.68 (C2').

MS (ES⁺) *m/z* found 299.0 (M+K⁺), 283.0 (M+Na⁺), 557.1 (2M+K⁺) C₉H₁₂N₂O₅S required *m/z* 260.05.

HPLC Reverse-phase HPLC eluting with H₂O/CH₃OH 100/0 to 75/25 in 30 min, λ = 280 nm, F = 1 mL/min, showed one peak with t_R 8.26 min.

[125] 3',5'-Bis-*O*-acetyl-2,2'-anhydrouridine

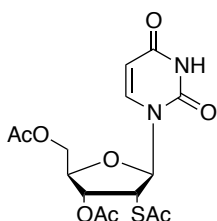
2,2'-Anhydrouridine (1.0 g, 4.42 mmol) was suspended in CH₃CN (20 mL) at room temperature and DMAP (0.22 g, 1.77 mmol) was added in one portion, followed by the dropwise addition of Ac₂O (1.67 mL, 17.68 mmol) and triethylamine (2.46 mL, 17.68 mmol). The solution was stirred at room temperature for 16 hours, the solvent evaporated and the crude

was dissolved in water (20 mL) and washed once with Et₂O (20 mL) and the desired compound was extracted from the aqueous solution with CH₂Cl₂ (20 mL x 3 times). The CH₂Cl₂ solution was dried over Na₂SO₄, filtered and evaporated to yield the desired compound as a white solid (1.33 g, 97%). (Lit. mp: 178-179 °C).⁴⁴⁸

¹H NMR (CDCl₃) δ_H 7.37 (d, *J* = 7.4 Hz, 1H, H6), 6.32 (d, *J* = 5.9 Hz, 1H, H1'), 6.07 (d, *J* = 7.5 Hz, 1H, H5), 5.47-5.44 (m, 1H, H2'), 5.42-5.40 (m, 1H, H3'), 4.52 (m, 1H, H4'), 4.33 (dd, *J* = 3.8 Hz, 12.6 Hz, 1H, H5'), 4.05 (dd, *J* = 3.5 Hz, 12.5 Hz, 1H, H5'), 2.18 (s, 3H, CH₃CO), 2.08 (s, 3H, CH₃CO).

^{13}C NMR (CDCl_3) δ_{C} 171.37 (C2), 170.53 (CH_3CO), 169.62 (CH_3CO), 159.60 (C4), 134.37 (C5), 110.66 (C6), 90.68 (C1'), 86.46 (C2'), 85.67 (C3'), 78.02 (C4'), 63.52 (C5'), 20.59 (CH_3CO), 20.51 (CH_3CO).

[126] 2'-*S*-Acetyl-3',5'-di-*O*-acetyluridine



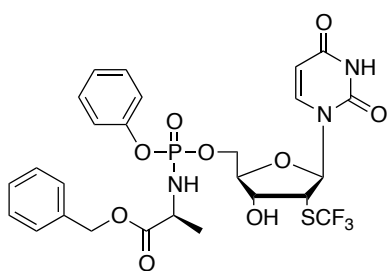
3',5'-Bis-*O*-acetyl-2,2'-anhydrouridine [125] (3.5 g, 11.28 mmol) was suspended in anhydrous dioxane (30 mL) at room temperature and thioacetic acid (19.25 mL, 270.7 mmol) was added dropwise. The reaction was refluxed for 12 hours, then allowed to reach room temperature and the solvent evaporated. The crude was suspended in water (50 mL) and washed with Et_2O (50 mL); the compound was extracted with CH_2Cl_2 (50 mL) from the aqueous solution, and the CH_2Cl_2 solution was dried over Na_2SO_4 , filtered and evaporated. The crude was purified by Biotage Isolera One (25g SNAP cartridge KP-SIL, 75 mL/min, using a gradient elution of 15-100% $\text{EtOAc}/n\text{Hex}$ over 8 CV, 100% $\text{EtOAc}/n\text{Hex}$ over 7 CV) to yield the title compound as a white solid (2.68 g, 73%). (Lit. mp: 124-126 $^\circ\text{C}$).^{445,446}

^1H NMR (CDCl_3) δ_{H} 8.63 (br s, 1H, NH), 7.32 (d, $J = 8.2$ Hz, 1H, H6), 6.29 (d, $J = 9.8$ Hz, 1H, H1'), 5.84 (d, $J = 8.2$ Hz, 1H, H5), 5.32-5.29 (m, 1H, H3'), 4.51 (dd, $J = 13.4$ Hz, 4.6 Hz, 1H, H5'), 4.34-4.27 (m, 3H, H4', H2', H5'), 2.37 (s, 3H, CH_3COS), 2.23 (s, 3H, CH_3CO_2), 2.17 (s, 3H, CH_3CO_2).

^{13}C NMR (CDCl_3) δ_{C} 192.99 (CH_3COS), 170.07 (OCOCH_3), 169.77 (OCOCH_3), 162.11 (C2), 150.33 (C4), 138.68 (C6), 103.61 (C5), 86.51 (C1'), 81.98 (C4'), 74.38 (C3'), 63.83 (C5'), 46.75 (C2'), 30.40 (CH_3COS), 20.78 (OCOCH_3), 20.63 (OCOCH_3).

9.5.20 Synthesis of 2'-SCF₃-2'-dU ProTides

[128a] 2'-Trifluoromethylthio-2'-deoxyuridine-5'-phenyl-(benzyloxy-L-alaninyl)phosphate



Prepared according to general procedure F_2 using 2'-trifluoromethylthio-2'-deoxyuridine [115] (0.025 g, 0.076 mmol) in THF (2 mL), phenyl(benzyloxy-L-alaninyl)phosphorochloridate [17s] (0.054 g, 0.152 mmol) in THF (0.5 mL) and *N*-methylimidazole (30 μL , 0.38 mmol). The mixture was evaporated, dissolved in CH_2Cl_2 (5mL) and washed with HCl

aqueous 0.5N (3 x 1.5 mL), the organic phase dried over Na₂SO₄, filtered and evaporated. The crude was purified via Biotage Isolera One (10g SNAP cartridge KP-SIL, 36 mL/min, using a gradient elution of 1-14% CH₃OH/CH₂Cl₂ over 10 CV, 14% CH₃OH/CH₂Cl₂ over 2 CV), to yield the title compound as a white solid (0.043 g, 87%).

³¹P NMR (CD₃OD, 202 MHz) δ_P 3.75, 4.04.

¹H NMR (CD₃OD, 500 MHz) δ_H 7.67 (d, *J* = 8.0 Hz, 0.5H, H6), 7.59 (d, *J* = 8.0 Hz, 0.5H, H6), 7.41-7.28 (m, 7H, Ph), 7.26-7.19 (m, 3H, Ph), 6.31 (t, *J* = 9.6 Hz, 1H, H1'), 5.73 (d, *J* = 8.0 Hz, 0.5H, H5), 5.66 (d, *J* = 8.0 Hz, 0.5H, H5), 5.19-5.12 (m, 2H, CH₂Ph), 4.49 (dd, *J* = 5.6 Hz, 1.4 Hz, 0.5H, H3'), 4.47 (dd, *J* = 5.6 Hz, 1.4 Hz, 0.5H, H3'), 4.35-4.31 (m, 1H, H5'), 4.30-4.27 (m, 1H, H5'), 4.23-4.18 (m, 1H, H4'), 4.08-4.00 (m, 1H, CHCH₃ L-Ala), 3.94 (dd, *J* = 5.5 Hz, 9.15 Hz, 0.5 H, H2'), 3.91 (dd, *J* = 5.5 Hz, 9.15 Hz, 0.5 H, H2'), 1.41-1.33 (m, 3H, CHCH₃ L-Ala).

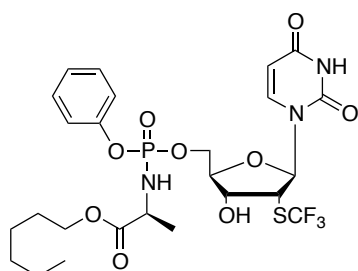
¹³C NMR (CD₃OD, 125 MHz) δ_C 174.93 (d, ³*J*_{CP} = 3.7 Hz, C=O), 174.57 (d, ³*J*_{CP} = 3.7 Hz, C=O), 165.56 (C2), 165.50 (C2), 152.37 (C4), 152.33 (C4), 152.09 (d, *J*_{CP} = 2.5 Hz, C-Ar), 152.04 (d, *J*_{CP} = 2.5 Hz, C-Ar), 141.87 (C6), 141.75 (C6), 137.22 (C-Ar), 137.21 (C-Ar), 132.28 (q, ¹*J*_{C-F} = 303.7 Hz, SCF₃), 132.22 (q, ¹*J*_{C-F} = 303.7 Hz, SCF₃), 130.98 (CH-Ar), 130.92 (CH-Ar), 129.66 (CH-Ar), 129.44 (CH-Ar), 129.42 (CH-Ar), 129.38 (CH-Ar), 129.36 (CH-Ar), 126.38 (CH-Ar), 121.36 (CH-Ar), 121.33 (CH-Ar), 121.30 (CH-Ar), 104.13 (C5), 104.10 (C5), 89.97 (C1'), 89.83 (C1'), 86.06 (d, ³*J*_{CP} = 8.1 Hz, C4'), 85.90 (d, ³*J*_{CP} = 8.1 Hz, C4'), 73.65 (C3'), 73.53 (C3'), 68.09 (CH₂Ph), 67.65 (d, ²*J*_{CP} = 9.1 Hz, C5'), 67.60 (d, ²*J*_{CP} = 9.1 Hz, C5'), 51.90 (CHCH₃ L-Ala), 51.74 (CHCH₃ L-Ala), 51.54 (C2'), 51.45 (C2'), 20.43 (d, ³*J*_{CP} = 6.1 Hz, CHCH₃ L-Ala), 20.18 (d, ³*J*_{CP} = 6.1 Hz, CHCH₃ L-Ala).

¹⁹F NMR (CD₃OD, 470 MHz) δ_F -41.37 -41.26.

MS (ES⁺) *m/z* found 668.2 [M+Na⁺], C₂₆H₂₇F₃N₃O₉PS required *m/z* 645.12 [M].

HPLC Reverse-phase HPLC eluting with H₂O/CH₃CN 90/10 to 0/100 in 30 min, λ = 254 nm, F = 1 ml/min, showed two peaks with t_R = 17.36, 17.48 min.

[128b] 2'-Trifluoromethylthio-2'-deoxyuridine-5'-phenyl-(hex-1-yloxy-L-alaninyl) phosphate



Prepared according to general procedure F₂ using 2'-trifluoromethylthio-2'-deoxyuridine [115] (0.025 g, 0.076 mmol), THF (2 mL), phenyl(hex-1-yloxy-L-alaninyl) phosphorochloridate [17u] (0.05 g, 0.152 mmol) in 0.5 mL of THF and *N*-methylimidazole (30 μL, 0.38 mmol). The

compound was then dissolved in CH_2Cl_2 (5mL) and washed with HCl 0.5N (3 x 1.5 mL), the organic phase dried over Na_2SO_4 , filtered and evaporated to dryness. Purification was performed *via* Biotage Isolera One (10g SNAP cartridge KP-SIL using a gradient elution of 1-10% $\text{CH}_3\text{OH}/\text{CH}_2\text{Cl}_2$ over 10 CV, 10% $\text{CH}_3\text{OH}/\text{CH}_2\text{Cl}_2$ over 5 CV), yielding the title compound as a white solid (0.027 g, 56%).

^{31}P NMR (CD_3OD , 202 MHz) δ_{P} 3.84, 4.07.

^1H NMR (CD_3OD , 500 MHz) δ_{H} 7.59 (d, $J = 8.5$ Hz, 0.5H, H6), 7.48 (d, $J = 8.0$ Hz, 0.5H, H6), 7.31-7.19 (m, 2H, Ph), 7.18-7.07 (m, 3H, Ph), 6.22 (d, $J = 9.1$ Hz, 0.5H, H1'), 6.19 (d, $J = 9.3$ Hz, 0.5H, H1'), 5.64 (d, $J = 8.0$ Hz, 0.5H, H5), 5.55 (d, $J = 8.0$ Hz, 0.5H, H5), 4.40 (dd, $J = 5.5$ Hz, 1.2 Hz, 0.5H, H3'), 4.36 (dd, $J = 5.5$, 1.2 Hz, 0.5H, H3'), 4.29-4.19 (m, 2H, H5'), 4.16-4.10 (m, 1H, H4'), 4.01-3.95 (m, 2H, $\text{CH}_2\text{CH}_2\text{CH}_2\text{CH}_2\text{CH}_2\text{CH}_3$ *n*-Hex), 3.89-3.76 (m, 2H, CHCH_3 L-Ala, H2'), 1.55-1.47 (m, 2H, $\text{CH}_2\text{CH}_2\text{CH}_2\text{CH}_2\text{CH}_2\text{CH}_3$ *n*-Hex), 1.29-1.14 (m, 9H, $\text{CH}_2\text{CH}_2\text{CH}_2\text{CH}_2\text{CH}_2\text{CH}_3$ *n*-Hex, CHCH_3 L-Ala), 0.82-0.74 (m, 3H, $\text{CH}_2\text{CH}_2\text{CH}_2\text{CH}_2\text{CH}_2\text{CH}_3$ *n*-Hex).

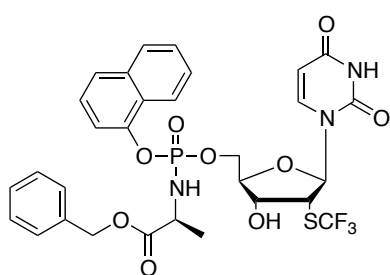
^{13}C NMR (CD_3OD , 125 MHz) δ_{C} 173.82 (d, $^3J_{\text{CP}} = 3.8$ Hz, C=O), 174.17 (d, $^3J_{\text{CP}} = 3.8$ Hz, C=O), 164.16 (C2), 164.10 (C2), 150.96 (C4), 150.91 (C4), 150.69 (d, $J_{\text{CP}} = 12.7$ Hz, C-Ar), 150.55 (d, $J_{\text{CP}} = 12.7$ Hz, C-Ar), 140.51 (C6), 140.30 (C6), 130.89 (q x 2, $^1J_{\text{CF}} = 303.5$ Hz, CF3), 129.67 (CH-Ar), 129.59 (CH-Ar), 129.52 (CH-Ar), 129.21 (CH-Ar), 124.99 (CH-Ar), 124.27 (CH-Ar), 120.33 (CH-Ar), 120.29 (CH-Ar), 119.97 (CH-Ar), 119.93 (CH-Ar), 119.89 (CH-Ar), 102.72 (C5), 102.71 (C5), 88.47 (C1'), 88.28 (C1'), 84.68 (d, $^3J_{\text{CP}} = 8.5$ Hz, C4'), 84.54 (d, $^3J_{\text{CP}} = 8.5$ Hz, C4'), 72.31 (C3'), 72.20 (C3'), 66.28 (d, $^2J_{\text{CP}} = 11.5$ Hz, C5'), 66.19 (d, $^2J_{\text{CP}} = 11.5$ Hz, C5'), 65.17 ($\text{CH}_2\text{CH}_2\text{CH}_2\text{CH}_2\text{CH}_2\text{CH}_3$ *n*-Hex), 65.14 ($\text{CH}_2\text{CH}_2\text{CH}_2\text{CH}_2\text{CH}_2\text{CH}_3$ *n*-Hex), 50.43 (CHCH_3 L-Ala), 50.26 (CHCH_3 L-Ala), 50.12 (C2'), 50.06 (C2'), 31.24 (CH_2 *n*-Hex), 31.21 (CH_2 *n*-Hex), 28.30 (CH_2 *n*-Hex), 28.28 (CH_2 *n*-Hex), 25.30 (CH_2 *n*-Hex), 25.25 (CH_2 *n*-Hex), 22.25 (CH_2 *n*-Hex), 22.22 (CH_2 *n*-Hex), 19.46 (d, $^3J_{\text{CP}} = 6.0$ Hz, CHCH_3 L-Ala), 19.44 (d, $^3J_{\text{CP}} = 6.12$ Hz, CHCH_3 L-Ala), 19.20 ($\text{CH}_2\text{CH}_2\text{CH}_2\text{CH}_2\text{CH}_2\text{CH}_3$ *n*-Hex), 19.15 ($\text{CH}_2\text{CH}_2\text{CH}_2\text{CH}_2\text{CH}_2\text{CH}_3$ *n*-Hex).

^{19}F NMR (CD_3OD , 470 MHz) δ_{F} -41.16, -41.26.

MS (ES+) m/z found 662.2 [$\text{M}+\text{Na}^+$], $\text{C}_{25}\text{H}_{33}\text{F}_3\text{N}_3\text{O}_9\text{PS}$ required m/z 639.16 [M].

HPLC Reverse-phase HPLC eluting with $\text{H}_2\text{O}/\text{CH}_3\text{CN}$ 90/10 to 0/100 in 30 min, $\lambda = 254$ nm, $F = 1$ mL/min, showed two peaks with $t_{\text{R}} = 20.08, 20.26$ min.

[128c] 2'-Trifluoromethylthio-2'-deoxyuridine-5'-naphth-1-yl-(benzyloxy-L-alaninyl) phosphate



Prepared according to general procedure **F₂** using 2'-trifluoromethylthio-2'-deoxyuridine [**115**] (0.015 g, 0.046 mmol), THF (2 mL), naphth-1-yl(benzyloxy-L-alaninyl) phosphorochloridate [**17a**] (0.054 g, 0.137 mmol) in THF (0.5 mL) and *N*-methylimidazole (17 μ L, 0.23 mmol). The compound was then dissolved in CH₂Cl₂ (5 mL) and

washed with HCl 0.5N (3 x 1.5 mL), the organic phase dried over Na₂SO₄, filtered and evaporated to dryness to yield a white solid. The mixture was evaporated and the desired product isolated via Biotage Isolera One (SNAP Ultra 10g, 36 mL/min, 1-10% CH₃OH/CH₂Cl₂ 10CV, 10% 5 CV) to yield the title compound as a white solid (0.013 g, 42%).

³¹P NMR (CD₃OD, 202 MHz) δ_P 4.45, 4.22.

¹H NMR (CD₃OD, 500 MHz) δ_H 8.18-8.14 (m, 1H, Ar), 7.94-7.90 (m, 1H, Ar), 7.77-7.72 (m, 1H, H6), 7.59-7.49 (m, 4H, Ar), 7.46-7.40 (m, 1H, Ar), 7.35-7.28 (m, 5H, Ar), 6.30 (d, $J = 9.0$ Hz, 0.5H, H1'), 6.27 (d, $J = 9.0$ Hz, 0.5H, H1'), 5.58 (d, $J = 8.0$ Hz, 0.5H, H5), 5.52 (d, $J = 8.0$ Hz, 0.5H, H5), 5.11 (s, 1H, CH₂Ph), 5.10 (ABq, $J = 12.0$ Hz, 1H, CH₂Ph), 4.47 (dd, $J = 6.0, 1.5$ Hz, 1H, H3'), 4.42-4.29 (m, 2H, H5'), 4.22-4.18 (m, 1H, H4'), 4.14-4.04 (m, 1H, CHCH₃ L-Ala), 3.88-3.81 (m, 1H, H2'), 1.37-1.33 (m, 3H, CHCH₃ L-Ala).

¹³C NMR (CD₃OD, 125 MHz) δ_C 173.49 (d, $^3J_{CP} = 3.6$ Hz, C=O), 173.10 (d, $^3J_{CP} = 3.6$ Hz, C=O), 164.08 (C2), 164.05 (C2), 150.90 (C4), 150.87 (C4), 146.51 (C-Ar), 146.45 (C-Ar), 146.39 (C-Ar), 146.28 (CH-Ar), 140.25 (C6), 140.26 (C6), 135.73 (C-Ar), 134.95 (C-Ar), 130.76 (2 x q, $^1J_{CF} = 304.1$ Hz, CF₃), 128.19 (CH-Ar), 127.97 (CH-Ar), 127.92 (CH-Ar), 127.90 (CH-Ar), 127.63 (CH-Ar), 127.59 (CH-Ar), 126.55 (CH-Ar), 126.53 (CH-Ar), 126.26 (CH-Ar), 126.17 (CH-Ar), 125.19 (CH-Ar), 125.18 (CH-Ar), 125.12 (CH-Ar), 124.77 (CH-Ar), 121.20 (CH-Ar), 121.04 (CH-Ar), 114.70 (d, $^3J_{CP} = 3.4$ Hz, CH-Ar), 114.66 (d, $^3J_{CP} = 3.4$ Hz, CH-Ar), 102.64 (C5), 102.60 (C5), 88.53 (C1'), 88.43 (C1'), 84.59 (d, $^3J_{CP} = 8.0$ Hz, C4'), 84.44 (d, $^3J_{CP} = 8.0$ Hz, C4'), 72.03 (C3'), 71.96 (C3'), 66.65 (CH₂Ph), 66.27 (d, $^2J_{CP} = 4.9$ Hz, C5'), 66.23 (d, $^2J_{CP} = 4.9$ Hz, C5'), 50.58 (CHCH₃ L-Ala), 50.44 (CHCH₃ L-Ala), 50.08 (C2'), 50.02 (C2'), 18.95 (d, $^3J_{CP} = 6.5$ Hz, CHCH₃ L-Ala), 18.74 (d, $^3J_{CP} = 6.5$ Hz, CHCH₃ L-Ala).

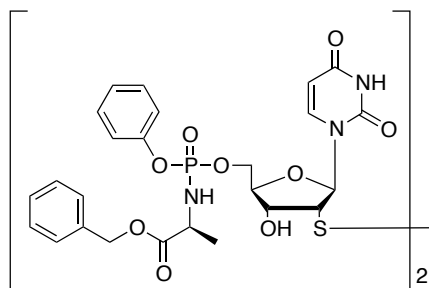
¹⁹F NMR (CD₃OD, 470 MHz) δ_F -41.11 -41.15.

MS (ES⁺) m/z found 718.1 [M+Na⁺], C₃₀H₂₉F₃N₃O₉PS required m/z 695.60 [M].

HPLC Reverse-phase HPLC eluting with H₂O/CH₃CN 90/10 to 0/100 in 30 min, λ = 254 nm, F = 1 mL/min, showed two peaks with t_R = 22.15, 22.23 min.

9.5.21 Synthesis of 2'-SH-2'-dU ProTide dimers

[129a] Bis-(5'-[phenyl(benzyloxy-L-alaninyl)phosphate]-2'-deoxyuridine-2'-yl)disulfide



Prepared according to general procedure **F**₂ using 2'-mercapto-2'-deoxyuridine [**119**] (0.05 g, 0.19 mmol), anh. THF (5 mL), phenyl(benzyloxy-L-alaninyl)phosphorochloridate [**17s**] (0.14 g, 0.38 mmol) in THF (1 mL) and *N*-methylimidazole (76 μ L, 0.95 mmol). The compound was then dissolved in CH₂Cl₂

(5mL) and washed with HCl aqueous 0.5N (3 x 1.5 mL), the organic phase dried over Na₂SO₄, filtered and evaporated to dryness. Purification was performed *via* Biotage Isolera One (10g SNAP cartridge KP-SIL using a gradient elution of 1-10% CH₃OH/CH₂Cl₂ over 10 CV, 10% CH₃OH/CH₂Cl₂ over 5 CV), yielding the title compound as a white solid (0.046 g, 21%).

³¹P NMR (CD₃OD, 202 MHz) δ_P 3.94, 3.62, 3.58.

¹H NMR (CD₃OD, 500 MHz) δ_H 7.456 (d, *J* = 8.0 Hz, 0.25H, H6), 7.453 (d, *J* = 8.0 Hz, 0.25H, H6), 7.43 (d, *J* = 8.0 Hz, 0.25H, H6), 7.42 (d, *J* = 8.0 Hz, 0.25H, H6), 7.26-7.16 (m, 7H, Ph), 7.13-7.03 (m, 3H, Ph), 6.18 (d, *J* = 8.0 Hz, 0.25H, H1'), 6.17 (d, *J* = 8.0 Hz, 0.25H, H1'), 6.158 (d, *J* = 8.0 Hz, 0.25H, H1'), 6.153 (d, *J* = 8.0 Hz, 0.25H, H1'), 5.57-5.51 (m, 1H, H5), 5.07-4.98 (m, 2H, CH₂Ph), 4.32-4.27 (m, 1H, H3'), 4.22-4.10 (m, 2H, H5'), 4.02-3.87 (m, 2H, H4', CHCH₃ L-Ala), 3.56 (dd, *J* = 8.0 Hz, 6.1 Hz, 0.25H, H2'), 3.53 (dd, *J* = 8.0 Hz, 6.1 Hz, 0.25H, H2'), 3.41 (dd, *J* = 8.0 Hz, 6.1 Hz, 0.25H, H2'), 3.37 (dd, *J* = 8.0 Hz, 6.1 Hz, 0.25H, H2'), 1.26-1.20 (m, 3H, CHCH₃ L-Ala).

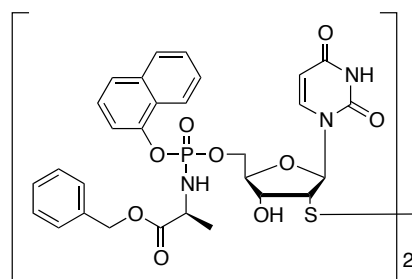
¹³C NMR (CD₃OD, 125 MHz) δ_C 175.05 (d, ³*J*_{CP} = 3.7 Hz, C=O), 175.01 (d, ³*J*_{CP} = 3.7 Hz, C=O), 174.75 (d, ³*J*_{CP} = 4.8 Hz, C=O), 165.68 (C2), 152.45 (d, *J*_{CP} = 2.5 Hz, C-Ar), 152.40 (d, *J*_{CP} = 2.5 Hz, C-Ar), 152.13 (C4), 152.08 (C4), 152.07 (C4), 142.24 (C6), 142.19 (C6), 142.08 (C6), 142.03 (C6), 137.21 (C-Ar), 137.19 (C-Ar), 130.94 (CH-Ar), 129.66 (CH-Ar), 129.43 (CH-Ar), 129.40 (CH-Ar), 129.34 (CH-Ar), 128.96 (CH-Ar), 126.44 (CH-Ar), 126.33 (CH-Ar), 121.43 (CH-Ar), 121.39 (CH-Ar), 103.86 (C5), 103.84 (C5), 103.81 (C5), 103.77 (C5), 89.99 (C1'), 89.62 (C1'), 85.85 (d, ³*J*_{CP} = 7.5 Hz, C4'), 85.79 (d, ³*J*_{CP} = 7.5 Hz, C4'), 85.64 (d, ³*J*_{CP} = 7.5 Hz, C4'), 85.61 (d, ³*J*_{CP} = 7.5 Hz,

C4'), 73.48 (C3'), 73.37 (C3'), 73.26 (C3'), 73.21 (C3'), 68.16 (CH₂Ph), 68.17 (CH₂Ph), 68.12 (CH₂Ph), 67.62 (C5'), 67.58 (C5'), 67.54 (C5'), 57.52 (C2'), 57.42 (C2'), 57.31 (C2'), 57.27 (C2'), 51.84 (CHCH₃ L-Ala), 51.69 (CHCH₃ L-Ala), 20.55 (d, ³J_{CP} = 6.2 Hz, CHCH₃ L-Ala), 20.53 (d, ³J_{CP} = 6.2 Hz, CHCH₃ L-Ala), 20.40 (d, ³J_{CP} = 6.2 Hz, CHCH₃ L-Ala), 20.34 (d, ³J_{CP} = 6.2 Hz, CHCH₃ L-Ala).

MS (ES+) m/z: found: 1175.3 [M+Na⁺]. C₅₀H₅₄N₆O₁₈P₂S₂ required m/z 1152.24 [M].

HPLC Reverse-phase HPLC eluting with H₂O/CH₃CN 90/10 to 0/100 in 30 min, λ = 254 nm, F = 1 mL/min, showed two broad peaks with t_R = 19.27, 19.44 min.

[129b] Bis-(5'-[naphth-1-yl(benzyloxy-L-alaninyl)phosphate]-2'-deoxyuridine-2'-yl)disulfide



Prepared according to general procedure F₂ using 2'-mercapto-2'-deoxyuridine [**119**] (0.10 g, 0.38 mmol), anh. THF (10 mL), naphthyl(benzyloxy-L-alaninyl)phosphorochloridate [**17a**] (0.46 g, 1.15 mmol) in 3 mL of anh. THF and *N*-methylimidazole (143 μL, 1.9 mmol). The compound was then dissolved in CH₂Cl₂

(5 mL) and washed with HCl 0.5N (3 x 1.5 mL), the organic phase dried over Na₂SO₄, filtered and evaporated to dryness. Purification was performed via Biotage Isolera One (10g SNAP cartridge Ultra, 36 mL/min, gradient elution of 1-14% CH₃OH/CH₂Cl₂ over 10 CV, 14% over 5 CV), yielding the title compound as a white solid (0.053 g, 11%).

³¹P NMR (CD₃OD, 202 MHz) δ_P 4.42, 4.40, 4.09, 4.05.

¹H NMR (CD₃OD, 500 MHz) δ_H 7.97-7.91 (m, 1H, Ar), 7.69-7.62 (m, 1H, Ar), 7.51-7.44 (m, 1H, H₆), 7.35-7.26 (m, 3H, Ar), 7.20-7.02 (m, 7H, Ar), 6.06-5.99 (m, 1H, H1'), 5.27 (d, *J* = 8.5 Hz, 0.25H, H₅), 5.25 (d, *J* = 8.5 Hz, 0.25H, H₅), 5.20 (d, *J* = 8.5 Hz, 0.25H, H₅), 5.19 (d, *J* = 8.5 Hz, 0.25H, H₅), 4.94-4.84 (m, 2H, CH₂Ph), 4.18-4.01 (m, 3H, H₃', H₅'), 3.95-3.83 (m, 2H, H₄', CHCH₃ L-Ala), 3.20 (dd, *J* = 8.0 Hz, 6.0 Hz, 0.25H, H₂'), 3.13 (dd, *J* = 8.0 Hz, 6.0 Hz, 0.25H, H₂'), 3.05 (dd, *J* = 8.0 Hz, 6.0 Hz, 0.25H, H₂'), 2.98 (dd, *J* = 8.0 Hz, 6.0 Hz, 0.25H, H₂'), 1.20-1.12 (m, 3H, CHCH₃ L-Ala).

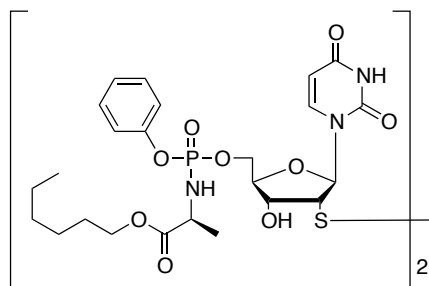
¹³C NMR (CD₃OD, 125 MHz) δ_C 173.70 (C=O), 173.69 (C=O), 173.67 (C=O), 173.36 (C=O), 173.33 (C=O), 173.23 (C=O), 173.20 (C=O), 164.16 (C₂), 164.09 (C₂), 150.97 (C₄), 150.93 (C₄), 146.56 (C-Ar), 146.51 (C-Ar), 146.45 (C-Ar), 146.39 (C-Ar), 140.51 (C₆), 140.44 (C₆), 140.20 (C₆), 140.13 (C₆), 135.70 (C-Ar), 134.89 (C-Ar), 128.22 (CH-Ar), 128.18 (CH-Ar), 127.97 (CH-Ar), 127.95 (CH-Ar), 127.93 (CH-Ar), 127.91 (CH-Ar), 127.83 (CH-Ar), 127.70 (CH-Ar), 127.67 (CH-Ar), 126.61 (CH-Ar), 126.59 (CH-Ar),

126.57 (CH-Ar), 126.30 (CH-Ar), 126.28 (CH-Ar), 125.25 (CH-Ar), 125.19 (CH-Ar), 124.86 (CH-Ar), 121.25 (CH-Ar), 121.21 (CH-Ar), 115.07 (CH-Ar), 115.04 (CH-Ar), 115.03 (CH-Ar), 115.00 (CH-Ar), 114.81 (CH-Ar), 114.79 (CH-Ar), 102.39 (C5), 88.24 (C1'), 88.21 (C1'), 87.89 (C1'), 87.86 (C1'), 84.46 (d, $^3J_{CP} = 8.9$ Hz, C4'), 84.38 (d, $^3J_{CP} = 8.9$ Hz, C4'), 84.20 (d, $^3J_{CP} = 8.9$ Hz, C4'), 84.13 (d, $^3J_{CP} = 8.9$ Hz, C4'), 72.05 (C3'), 71.94 (C3'), 71.87 (C3'), 71.82 (C3'), 66.82-66.89 (m, CH₂Ph), 66.39-66.18 (m, C5'), 55.61 (C2'), 55.54 (C2'), 55.42 (C2'), 50.49 (CHCH₃ L-Ala), 50.44 (CHCH₃ L-Ala), 19.14 (CHCH₃ L-Ala), 19.08 (CHCH₃ L-Ala), 19.02 (CHCH₃ L-Ala), 18.96 (CHCH₃ L-Ala), 18.95 (CHCH₃ L-Ala).

MS (ES⁺) m/z found: 1305.33 (M+Na⁺) C₆₀H₆₄N₆O₁₈P₂S₂ required m/z 1282.34 [M].

HPLC Reverse-phase HPLC eluting with H₂O/CH₃CN 90/10 to 0/100 in 30 min, λ = 254 nm, F = 1 mL/min, showed three broad peaks with tR = 22.18, 22.31, 22.58 min.

[129c] Bis-(5'-[phenyl(hexyl-1-oxy-L-alaninyl)phosphate]-2'-deoxyuridine-2'-yl)disulfide



Prepared according to general procedure **F₂** using 2'-mercapto-2'-deoxyuridine [**119**] (0.05 g, 0.19 mmol), anh. THF (5 mL), phenyl(hex-1-yloxy-L-alaninyl)phosphorochloridate [**17u**] (0.013 g, 0.38 mmol) in THF (1 mL) and *N*-methylimidazole (76 μL, 0.95 mmol). The compound was then dissolved in

CH₂Cl₂ (5 mL) and washed with HCl aqueous 0.5N (3 x 1.5 mL), the organic phase dried over Na₂SO₄, filtered and evaporated to dryness. Purification was performed *via* Biotage Isolera One (30g ZIP cartridge KP-SIL, gradient elution of 1-10% CH₃OH/CH₂Cl₂ over 10 CV, 10/90 over 5 CV), yielding the title compound as a white solid (0.011 g, 5%).

³¹P NMR (CD₃OD, 202 MHz) δ_P 3.97, 3.70, 3.66.

¹H NMR (CD₃OD, 500 MHz) δ_H 7.62 (d, *J* = 8.0 Hz, 0.25H, H6), 7.61 (d, *J* = 8.0 Hz, 0.25H, H6), 7.59 (d, *J* = 8.0 Hz, 0.25H, H6), 7.58 (d, *J* = 8.0 Hz, 0.25H, H6), 7.41-7.35 (m, 2H, Ph), 7.30-7.19 (m, 3H, Ph), 6.32 (d, *J* = 8.0 Hz, 0.5H, H1'), 6.30 (d, *J* = 8.0 Hz, 0.25H, H1'), 6.28 (d, *J* = 8.0 Hz, 0.25H, H1'), 5.72-5.66 (m, 1H, H5), 4.46-4.41 (m, 1H, H3'), 4.38-4.27 (m, 2H, H5'), 4.19-4.07 (m, 3H, H4', CH₂CH₂CH₂CH₂CH₂CH₃ Hex), 4.04-3.95 (m, 1H, CHCH₃ L-Ala), 3.75-3.64 (m, 0.5H, H2'), 3.57-3.48 (m, 0.5H, H2'), 1.68-1.59 (m, 4H, CH₂CH₂CH₂CH₂CH₂CH₃ Hex), 1.41-1.27 (m, 7H, CH₂CH₂CH₂CH₂CH₂CH₃ Hex, CHCH₃ L-Ala), 0.94-0.88 (m, 3H, CH₂CH₂CH₂CH₂CH₂CH₃ Hex).

¹³C NMR (CD₃OD, 125 MHz) δ_C 174.57 (C=O), 174.15 (C=O), 151.01 (C2), 140.87 (C6), 140.83 (C6), 140.73 (C6), 140.69 (C6), 129.55 (CH-Ar), 125.53 (CH-Ar), 125.08 (CH-Ar), 125.02 (CH-Ar), 124.93 (CH-Ar), 124.61 (CH-Ar), 124.58 (CH-Ar), 120.02 (CH-Ar), 120.00 (CH-Ar), 119.98 (CH-Ar), 119.97 (CH-Ar), 102.49 (C5), 102.47 (C5), 102.43 (C5), 102.40 (C5), 102.38 (C5), 88.61 (C1'), 88.57 (C1'), 88.20 (C1'), 88.19 (C1'), 84.66-84.06 (m, C4'), 72.15 (C3'), 72.06 (C3'), 72.04 (C3'), 71.94 (C3'), 66.27-66.00 (m, C5'), 65.20 (CH₂CH₂CH₂CH₂CH₂CH₃ Hex), 56.03 (CHCH₃ L-Ala), 55.77 (CHCH₃ L-Ala), 31.19 (CH₂CH₂CH₂CH₂CH₂CH₃ Hex), 30.73 (CH₂CH₂CH₂CH₂CH₂CH₃ Hex), 28.28 (CH₂CH₂CH₂CH₂CH₂CH₃ Hex), 28.26 (CH₂CH₂CH₂CH₂CH₂CH₃ Hex), 25.26 (CH₂CH₂CH₂CH₂CH₂CH₃ Hex), 25.24 (CH₂CH₂CH₂CH₂CH₂CH₃ Hex), 22.20 (CH₂CH₂CH₂CH₂CH₂CH₃ Hex), 19.34-18.38 (m, CHCH₃ L-Ala), 12.96 (CH₂CH₂CH₂CH₂CH₂CH₃ Hex).

MS (ES+) m/z found: 1193.4 [M+Na⁺] C₅₀H₇₂N₆O₁₈P₂S₂ required m/z 1170.38 [M].

HPLC Reverse-phase HPLC eluting with H₂O/CH₃CN 90/10 to 0/100 in 30 min, λ= 254 nm, F = 1 Lmin, showed three broad peaks with tR = 23.96, 24.06, 24.28 min.

10 References

1. Davies DB. Conformation of nucleosides and nucleotides. *Progr. Nucl. Magn. Res. Sp.* **1978**;12:135-235.
2. Berg J, Tymoczko J, Stryer L. Biochemistry. 5th ed. Freeman NYWH, edition **2002**.
3. Baldwin SA, Mackey JR, Cass CE, Young JD. Nucleoside transporters: molecular biology and implications for therapeutic development. *Mol. Med. Today.* **1999**;5(5):216-24.
4. Shryock JC, Belardinelli L. Adenosine and adenosine receptors in the cardiovascular system: biochemistry, physiology, and pharmacology. *Am. J. Cardiol.* **1997**;79(12, Supplement 1):2-10.
5. Fajardo AM, Piazza GA, Tinsley HN. The role of cyclic nucleotide signaling pathways in cancer: targets for prevention and treatment. *Cancers (Basel).* **2014**;6(1):436-58.
6. Khakh BS, Burnstock G. The double life of ATP. *Sci. Am.* **2009**;301(6):84-92.
7. Idzko M, Ferrari D, Eltzschig HK. Nucleotide signalling during inflammation. *Nature.* **2014**;509(7500):310-7.
8. De la Fuente IM, Cortés JM, Valero E, Desroches M, Rodrigues S, Malaina I. On the dynamics of the adenylate energy system: homeorhesis vs homeostasis. *PLoS One.* **2014**;9(10):e108676.
9. Jordheim LP, Durantel D, Zoulim F, Dumontet C. Advances in the development of nucleoside and nucleotide analogues for cancer and viral diseases. *Nat. Rev. Drug Discov.* **2013**;12(6):447-64.
10. Ewald B, Sampath D, Plunkett W. Nucleoside analogs: molecular mechanisms signaling cell death. *Oncogene.* **2007**;27(50):6522-37.
11. De Clercq E. Strategies in the design of antiviral drugs. *Nat. Rev. Drug Discov.* **2002**;1(1):13-25.
12. Gerber L, Welzel TM, Zeuzem S. New therapeutic strategies in HCV: polymerase inhibitors. *Liver International.* **2013**;33:85-92.
13. Powdrill MH, Bernatchez JA, Götte M. Inhibitors of the hepatitis C virus RNA-dependent RNA polymerase NS5B. *Viruses.* **2010**;2(10):2169-95.
14. Cappellacci L, Franchetti P, Vita P, Petrelli R, Lavecchia A, Jayaram HN, Saiko P, Graser G, Szekeres T, Grifantini M. Ribose-modified purine nucleosides as ribonucleotide reductase inhibitors. Synthesis, antitumor activity, and molecular modeling of N⁶-substituted 3'-C-methyladenosine derivatives. *J. Med. Chem.* **2008**;51(14):4260-9.
15. Flotho C, Claus R, Batz C, Schneider M, Sandrock I, Ihde S, Plass C, Niemeyer CM, Lübbert M. The DNA methyltransferase inhibitors azacitidine, decitabine and zebularine exert differential effects on cancer gene expression in acute myeloid leukemia cells. *Leukemia.* **2009**;23(6):1019-28.
16. Kicska GA, Long L, Hörig H, Fairchild C, Tyler PC, Furneaux RH, Schramm VL, Kaufman HL. Immucillin H, a powerful transition-state analog inhibitor of purine nucleoside phosphorylase, selectively inhibits human T lymphocytes. *PNAS* **2001**;98(8):4593-8.
17. Longley DB, Harkin DP, Johnston PG. 5-Fluorouracil: mechanisms of action and clinical strategies. *Nat. Rev. Cancer.* **2003**;3(5):330-8.
18. Avendaño C, Menéndez JC. Chapter 2 - Antimetabolites. In: Avendaño C, Menéndez JC, editors. Medicinal Chemistry of Anticancer Drugs. Amsterdam: Elsevier; **2008**. p. 9-52.
19. Damaraju VL, Damaraju S, Young JD, Baldwin SA, Mackey J, Sawyer MB, Cass CE. Nucleoside anticancer drugs: the role of nucleoside transporters in resistance to cancer chemotherapy. *Oncogene.* **2003**;22(47):7524-36.
20. Zhang J, Visser F, King K, Baldwin S, Young J, Cass C. The role of nucleoside transporters in cancer chemotherapy with nucleoside drugs. *Cancer Metastasis Rev.* **2007**;26(1):85-110.

21. Deville-Bonne D, El Amri C, Meyer P, Chen Y, Agrofoglio LA, Janin J. Human and viral nucleoside/nucleotide kinases involved in antiviral drug activation: Structural and catalytic properties. *Antiviral Res.* **2010**;86(1):101-20.
22. Van Rompay AR, Johansson M, Karlsson A. Substrate specificity and phosphorylation of antiviral and anticancer nucleoside analogues by human deoxyribonucleoside kinases and ribonucleoside kinases. *Pharmacol. Ther.* **2003**;100(2):119-39.
23. Van Rompay AR, Norda A, Lindén K, Johansson M, Karlsson A. Phosphorylation of uridine and cytidine nucleoside analogs by two human uridine-cytidine kinases. *Mol. Pharmacol.* **2001**;59(5):1181-6.
24. Van Rompay AR, Johansson M, Karlsson A. Phosphorylation of nucleosides and nucleoside analogs by mammalian nucleoside monophosphate kinases. *Pharmacol. Ther.* **2000**;87(2-3):189-98.
25. Zhu C, Johansson M, Karlsson A. Incorporation of nucleoside analogs into nuclear or mitochondrial DNA is determined by the intracellular phosphorylation site. *J. Biol. Chem.* **2000**;275(35):26727-31.
26. Deville-Bonne D, Sellam O, Merola F, Lascu I, Desmadril M, Véron M. Phosphorylation of nucleoside diphosphate kinase at the active site studied by steady-state and time-resolved fluorescence. *Biochemistry.* **1996**;35(46):14643-50.
27. Laliberté J, Momparler RL. Human cytidine deaminase: purification of enzyme, cloning, and expression of its complementary DNA. *Cancer Res.* **1994**;54(20):5401-7.
28. Cristalli G, Costanzi S, Lambertucci C, Lupidi G, Vittori S, Volpini R, Camaioni E. Adenosine deaminase: Functional implications and different classes of inhibitors. *Med. Res. Rev.* **2001**;21(2):105-28.
29. Chapman AG, Miller AL, Atkinson DE. Role of the adenylate deaminase reaction in regulation of adenine nucleotide metabolism in Ehrlich ascites tumor cells. *Cancer Res.* **1976**;36(3):1144-50.
30. Hunsucker SA, Spychala J, Mitchell BS. Human cytosolic 5'-nucleotidase I: characterization and role in nucleoside analog resistance. *J. Biol. Chem.* **2001**;276(13):10498-504.
31. Anderson JP, Daifuku R, Loeb LA. Viral error catastrophe by mutagenic nucleosides. *Annu. Rev. Microbiol.* **2004**;58(1):183-205.
32. Sampath D, Rao VA, Plunkett W. Mechanisms of apoptosis induction by nucleoside analogs. *Oncogene.* **2003**;22(56):9063-74.
33. <https://www.medicinescomplete.com/mc/bnf/current/PHP532-antimetabolites.htm>.
34. Galmarini CM, Mackey JR, Dumontet C. Nucleoside analogues and nucleobases in cancer treatment. *The Lancet Oncology.* **2002**;3(7):415-24.
35. Karran P. Thiopurines, DNA damage, DNA repair and therapy-related cancer. *Br. Med. Bull.* **2006**;79-80(1):153-70.
36. van Laar JAM, Rustum YM, Ackland SP, van Groeningen CJ, Peters GJ. Comparison of 5-fluoro-2'-deoxyuridine with 5-fluorouracil and their role in the treatment of colorectal cancer. *Eur. J. Cancer.* **1998**;34(3):296-306.
37. Lamont EB, Schilsky RL. The oral fluoropyrimidines in cancer chemotherapy. *Clin. Cancer Res.* **1999**;5(9):2289-96.
38. Mini E, Nobili S, Caciagli B, Landini I, Mazzei T. Cellular pharmacology of gemcitabine. *Ann. Oncol.* **2006**;17(suppl 5):v7-v12.
39. Robak T, Lech-Maranda E, Korycka A, Robak E. Purine nucleoside analogs as immunosuppressive and antineoplastic agents: mechanism of action and clinical activity. *Curr. Med. Chem.* **2006**;13(26):3165-89.
40. Galmarini CM, Mackey JR, Dumontet C. Nucleoside analogues: mechanisms of drug resistance and reversal strategies. *Leukemia.* **2001**;15(6):875-90.
41. Zhenchuk A, Lotfi K, Juliusson G, Albertioni F. Mechanisms of anti-cancer action and pharmacology of clofarabine. *Biochem. Pharmacol.* **2009**;78(11):1351-9.
42. Cooper TM. Role of nelarabine in the treatment of T-cell acute lymphoblastic leukemia and T-cell lymphoblastic lymphoma. *Ther. Clin. Risk Manag.* **2007**;3(6):1135-41.

43. Stresemann C, Lyko F. Modes of action of the DNA methyltransferase inhibitors azacytidine and decitabine. *Int. J. Cancer*. **2008**;123(1):8-13.
44. <https://www.medicinescomplete.com/mc/bnf/current/PHP3742-antiviral-drugs.htm>.
45. De Clercq E. Anti-HIV drugs: 25 compounds approved within 25 years after the discovery of HIV. *Int. J. Antimicrob. Agents*. **2009**;33(4):307-20.
46. De Clercq E. Antiviral drugs in current clinical use. *J. Clin. Virol*. **2004**;30(2):115-33.
47. Franssen RME, Meenhorst PL, Koks CHW, Beijnen JH. Didanosine, a new antiretroviral drug. *Pharm. Weekbl*. **1992**;14(5):297-304.
48. De Clercq E. Antiviral drugs: current state of the art. *J. Clin. Virol*. **2001**;22(1):73-89.
49. Sacks S, Wilson B. Famciclovir/Penciclovir. In: Mills J, Volberding P, Corey L. Antiviral Chemotherapy 5. Advances in Experimental Medicine and Biology. 458: Springer US; 1999. p. 135-47.
50. Graci JD, Cameron CE. Mechanisms of action of ribavirin against distinct viruses. *Rev. Med. Virol*. **2006**;16(1):37-48.
51. Committee on Infectious Diseases. Use of ribavirin in the treatment of respiratory syncytial virus infection. *Pediatrics*. **1993**;92(3):501-4.
52. De Clercq E. Selective anti-Herpesvirus agents. *Antiviral Chem. Chemother*. **2013**;23(3):93-101.
53. De Clercq E. Clinical potential of the acyclic nucleoside phosphonates Cidofovir, Adefovir, and Tenofovir in treatment of DNA virus and retrovirus infections. *Clin. Microbiol. Rev*. **2003**;16(4):569-96.
54. Khungar V, Han S-H. A systematic review of side effects of nucleoside and nucleotide drugs used for treatment of chronic Hepatitis B. *Curr. Hepat. Rep*. **2010**;9(2):75-90.
55. Fung J, Lai C-L, Seto W-K, Yuen M-F. Nucleoside/nucleotide analogues in the treatment of chronic hepatitis B. *J. Antimicrob. Chemother*. **2011**;66(12):2715-25.
56. Arts EJ, Wainberg MA. Mechanisms of nucleoside analog antiviral activity and resistance during human immunodeficiency virus reverse transcription. *Antimicrob. Agents Chemother*. **1996**;40(3):527-40.
57. Damaraju VL, Damaraju S, Young JD, Baldwin SA, Mackey J, Sawyer MB, Cass CE. Nucleoside anticancer drugs: the role of nucleoside transporters in resistance to cancer chemotherapy. *Oncogene*. **2003**;22(47):7524-36.
58. Higashigawa M, Ido M, Nagao Y, Kuwabara H, Hori H, Ohkubo T, Kawasaki H, Sakurai M. Decreased DNA polymerase sensitivity to 1- β -D-arabinofuranosylcytosine 5'-triphosphate in P388 murine leukemic cells resistant to vincristine. *Leukemia Res*. **1991**;15(8):675-81.
59. Minami K, Shinsato Y, Yamamoto M, Takahashi H, Zhang S, Nishizawa Y, Tabata S, Ikeda R, Kawahara K, Tsujikawa K, Chijiwa K, Yamada K, Akiyama S, Pérez-Torras S, Pastor-Anglada M, Furukawa T, Yasuo T. Ribonucleotide reductase is an effective target to overcome gemcitabine resistance in gemcitabine-resistant pancreatic cancer cells with dual resistant factors. *J. Pharmacol. Sci*. **2015**;127(3):319-25.
60. Feng L, Achanta G, Pelicano H, Zhang W, Plunkett W, Huang P. Role of p53 in cellular response to anticancer nucleoside analog-induced DNA damage. *Int. J. Mol. Med*. **2000**; 5:597-1201.
61. Wagner CR, Iyer VV, McIntee EJ. Pronucleotides: Toward the in vivo delivery of antiviral and anticancer nucleotides. *Med. Res. Rev*. **2000**;20(6):417-51.
62. Mehellou Y, Balzarini J, McGuigan C. Aryloxy phosphoramidate triesters: a technology for delivering monophosphorylated nucleosides and sugars into cells. *ChemMedChem*. **2009**;4(11):1779-91.
63. Vertuani S, Baldisserotto A, Varani K, Borea PA, De Marcos Maria Cruz B, Ferraro L, Manfredini S, Dalpiaz A. Synthesis and in vitro stability of nucleoside 5'-phosphonate derivatives. *Eur. J. Med. Chem*. **2012**;54:202-9.

64. Efimtseva EV, Mikhailov SN, Meshkov S, Hankamaki T, Oivanen M, Lonnberg H. Dioxolane nucleosides and their phosphonate derivatives: synthesis and hydrolytic stability. *J. Chem. Soc., Perkin Trans. 1*. **1995**(11):1409-15.
65. Clercq ED, Holy A. Acyclic nucleoside phosphonates: a key class of antiviral drugs. *Nat. Rev. Drug Discov.* **2005**;4(11):928-40.
66. Meier C. Pro-Nucleotides - Recent advances in the design of efficient tools for the delivery of biologically active nucleoside monophosphates. *Synlett*. **1998**;09(03):233-42.
67. Pertusati F, McGuigan C, Serpi M. Symmetrical diamidate prodrugs of nucleotide analogues for drug delivery. *Curr. Protoc. Nucleic Acid Chem.*: John Wiley & Sons, Inc.; **2015**.
68. Zhang Y, Gao Y, Wen X, Ma H. Current prodrug strategies for improving oral absorption of nucleoside analogues. *Asian J. Pharm. Sci.* **2014**;9(2):65-74.
69. Sofia MJ. Chapter Two - Nucleotide prodrugs for the treatment of HCV infection. *Adv. Pharmacol.* Volume 67: Academic Press; **2013**. p. 39-73.
70. Hwang Y, Cole PA. Efficient synthesis of phosphorylated prodrugs with bis(POM)-phosphoryl chloride. *Org. Lett.* **2004**;6(10):1555-6.
71. Sastry JK, Nehete PN, Khan S, Nowak BJ, Plunkett W, Arlinghaus RB, Farquhar D. Membrane-permeable dideoxyuridine 5'-monophosphate analogue inhibits human immunodeficiency virus infection. *Mol. Pharmacol.* **1992**;41(3):441-5.
72. Pompon A, Lefebvre I, Imbach JL, Kahn S, Farquhar D. Decomposition pathways of the mono- and bis(pivaloyloxymethyl) esters of azidothymidine 5'-monophosphate in cell extract and in tissue culture medium: An application of the 'on-line ISRP-Cleaning' HPLC technique. *Antiviral Chem. Chemother.* **1994**;5(2):91-8.
73. Marcellin P, Chang T-T, Lim SG, Tong MJ, Sievert W, Shiffman ML, Jeffers L, Goodman Z, Wulfsohn MS, Xiong S, Fry J, Brosgart CL. Adefovir dipivoxil for the treatment of hepatitis B e antigen-positive chronic hepatitis B. *New Engl. J. Med.* **2003**;348(9):808-16.
74. Segovia MC, Chacra W, Gordon SC. Adefovir dipivoxil in chronic hepatitis B: history and current uses. *Expert Opin. Pharmacother.* **2012**;13(2):245-54.
75. Lai C-L, Ahn SH, Lee KS, Um SH, Cho M, Yoon SK, Lee JW, Park NH, Kweon YO, Sohn JH, Lee J, Kim JA, Han KH, Yuen MF. Phase IIb multicentred randomised trial of besifovir (LB80380) versus entecavir in Asian patients with chronic hepatitis B. *Gut*. **2014**;63(6):996-1004.
76. Fung J, Lai C-L, Yuen M-F. LB80380: a promising new drug for the treatment of chronic hepatitis B. *Exp. Opin. Invest. Drugs.* **2008**;17(10):1581-8.
77. Farquhar D, Khan S, Srivastva DN, Saunders PP. Synthesis and antitumor evaluation of bis[(pivaloyloxy)methyl] 2'-deoxy-5-fluorouridine 5'-monophosphate (FdUMP): A strategy to introduce nucleotides into cells. *J. Med. Chem.* **1994**;37(23):3902-9.
78. Fung HB, Stone EA, Piacenti FJ. Tenofovir disoproxil fumarate: A nucleotide reverse transcriptase inhibitor for the treatment of HIV infection. *Clin. Ther.* **2002**;24(10):1515-48.
79. Naesens L, Bischofberger N, Augustijns P, Annaert P, Van den Mooter G, Arimilli MN, Kim CU, De Clercq E. Antiretroviral efficacy and pharmacokinetics of oral bis(isopropylloxycarbonyloxymethyl)9-(2-phosphonylmethoxypropyl)adenine in mice. *Antimicrob. Agents Chemother.* **1998**;42(7):1568-73.
80. Puech F, Gosselin G, Lefebvre I, Pompon A, Aubertin A-M, Kirn A, Imbach JL. Intracellular delivery of nucleoside monophosphates through a reductase-mediated activation process. *Antiviral Res.* **1993**;22(2-3):155-74.
81. Jochum A, Schlienger N, Egron D, Peyrottes S, Périgaud C. Biolabile constructs for pronucleotide design. *J. Organomet. Chem.* **2005**;690(10):2614-25.
82. Périgaud C, Gosselin G, Lefebvre I, Girardet J-L, Benzaria S, Barber I. Rational design for cytosolic delivery of nucleoside monophosphates : "SATE" and "DTE" as enzyme-labile transient phosphate protecting groups. *Bioorg. Med. Chem. Lett.* **1993**;3(12):2521-6.
83. Gosselin G, Girardet JL, Périgaud C, Benzaria S, Lefebvre I, Schlienger N, Pompon A, Imbach JL. New insights regarding the potential of the pronucleotide approach in antiviral chemotherapy. *Acta Biochim. Pol.* **1996**;43(1):196-208.

84. Cinatl J, Gröschel B, Zehner R, Cinatl J, Périgaud C, Gosselin G. Human immunodeficiency virus resistance to AZT in MOLT4/8 cells is associated with a lack of AZT phosphorylation and is bypassed by AZT-monophosphate SATE prodrugs. *Antiviral Chem. Chemother.* **1997**;8(4):343-52.
85. Gouy M-H, Jordheim LP, Lefebvre I, Cros E, Dumontet C, Peyrottes S. Special feature of mixed phosphotriester derivatives of cytarabine. *Bioorg. Med. Chem.* **2009**;17(17):6340-7.
86. Beltran T, Egron D, Pompon A, Lefebvre I, Périgaud C, Gosselin G. Rational design of a new series of pronucleotide. *Bioorg. Med. Chem. Lett.* **2001**;11(13):1775-7.
87. Zhou X-J, Pietropaolo K, Chen J, Khan S, Sullivan-Bólyai J, Mayers D. Safety and pharmacokinetics of IDX184, a liver-targeted nucleotide polymerase inhibitor of Hepatitis C virus, in healthy subjects. *Antimicrob. Agents Chemother.* **2011**;55(1):76-81.
88. Sheridan C. Calamitous HCV trial casts shadow over nucleoside drugs. *Nat Biotech.* **2012**;30(11):1015-6.
89. Meier C. cycloSal phosphates as chemical trojan horses for intracellular nucleotide and glycosylmonophosphate delivery - chemistry meets biology. *Eur. J. Org. Chem.* **2006**;2006(5):1081-102.
90. Meier C, Lorey M, De Clercq E, Balzarini J. Cyclic saligenyl phosphotriesters of 2',3'-dideoxy-2',3'-didehydrothymidine (d4T) - a new pro-nucleotide approach. *Bioorg. Med. Chem. Lett.* **1997**;7(2):99-104.
91. Meier C, Lorey M, De Clercq E, Balzarini J. cycloSal-2',3'-dideoxy-2',3'-didehydrothymidine monophosphate (cycloSal-d4TMP): Synthesis and antiviral evaluation of a new d4TMP delivery system. *J. Med. Chem.* **1998**;41(9):1417-27.
92. Meier C, De Clercq E, Balzarini J. Nucleotide Delivery from cycloSaligenyl-3'-azido-3'-deoxythymidine monophosphates (cycloSal-AZTMP). *Eur. J. Org. Chem.* **1998**;1998(5):837-46.
93. Meier C, Balzarini J. Application of the cycloSal-prodrug approach for improving the biological potential of phosphorylated biomolecules. *Antiviral Res.* **2006**;71(2-3):282-92.
94. Bontemps F, Meier C, Delacauw A, Balzarini J, Galmarini C, Van Den Neste E. Study of the efficacy of a pronucleotide of 2-chloro-2'-deoxyadenosine in deoxycytidine kinase-deficient lymphoma cells. *Nucleos. Nucleot. Nucl.* **2006**;25(9-11):997-1000.
95. Marty FM, Winston DJ, Rowley SD, Vance E, Papanicolaou GA, Mullane KM. CMX001 to prevent Cytomegalovirus disease in hematopoietic-cell transplantation. *New Engl. J. Med.* **2013**;369(13):1227-36.
96. Lanier ER, Ptak RG, Lampert BM, Keilholz L, Hartman T, Buckheit RW. Development of hexadecyloxypropyl Tenofovir (CMX157) for treatment of infection caused by wild-type and nucleoside/nucleotide-Resistant HIV. *Antimicrob. Agents Chemother.* **2010**;54(7):2901-9.
97. Quenelle DC, Collins DJ, Pettway LR, Hartline CB, Beadle JR, Wan WB. Effect of oral treatment with (S)-HPMPA, HDP-(S)-HPMPA or ODE-(S)-HPMPA on replication of murine cytomegalovirus (MCMV) or human cytomegalovirus (HCMV) in animal models. *Antiviral Res.* **2008**;79(2):133-5.
98. Girard P-M, Pegram PS, Diquet B, Anderson R, Raffi F, Tubiana R. Phase II placebo-controlled trial of Fozivudine Tidoxil for HIV infection: pharmacokinetics, tolerability, and efficacy. *J. Acquired Immune Defic. Syndromes.* **2000**;23(3).
99. Erion MD, van Poelje PD, MacKenna DA, Colby TJ, Montag AC, Fujitaki JM, Linemeyer DL, Bullough DA. Liver-targeted drug delivery using HepDirect prodrugs. *J. Pharmacol. Exp. Ther.* **2005**;312(2):554-60.
100. Reddy KR, Matelich MC, Ugarkar BG, Gómez-Galeno JE, DaRe J, Ollis K, Sun Z, Craigo W, Colby TJ, Fujitaki JM, Boyer SH, van Poelje PD, Erion MD. Pradefovir: a prodrug that targets Adefovir to the liver for the treatment of Hepatitis B. *J. Med. Chem.* **2008**;51(3):666-76.
101. Ma B, Forbes W, Venook AP, Bissell DM, Peterson C, Niculae I. A phase I/II study to assess the safety, tolerability and pharmacokinetics (PK) of intravenous (IV) infusion of

MB07133 in subjects with unresectable hepatocellular carcinoma (HCC). *J. Clin. Oncol.* **2006**;24(18S):2054.

102. <http://www.businesswire.com/news/home/20070910005361/en/Metabasis-Announces-Orphan-Drug-Designation-Granted-MB07133> - .Ve7eg2RVhHw.

103. Abraham TW, Kalman TI, McIntee EJ, Wagner CR. Synthesis and biological activity of aromatic amino acid phosphoramidates of 5-fluoro-2'-deoxyuridine and 1- β -arabinofuranosylcytosine: evidence of phosphoramidase activity. *J. Med. Chem.* **1996**;39(23):4569-75.

104. Song H, Griesgraber GW, Wagner CR, Zimmerman CL. Pharmacokinetics of amino acid phosphoramidate monoesters of Zidovudine in rats. *Antimicrob. Agents Chemother.* **2002**;46(5):1357-63.

105. Serpi M, Madela K, Pertusati F, Slusarczyk M. Synthesis of phosphoramidate prodrugs: ProTide approach. *Curr. Protoc. Nucleic Acid Chem.*: John Wiley & Sons, Inc.; **2012**.

106. Cahard D, McGuigan C, Balzarini J. Aryloxy phosphoramidate triesters as Pro-Tides. *Mini Rev. Med. Chem.* **2004**;4(4):371-81.

107. McGuigan C, Tollerfield SM, Riley PA. Synthesis and biological evaluation of some phosphate triester derivatives of the anti-viral drug AraA. *Nucleic Acids Res.* **1989**;17(15):6065-75.

108. Hunston RN, Jones AS, McGuigan C, Walker RT, Balzarini J, De Clercq E. Synthesis and biological properties of some cyclic phosphotriesters derived from 2'-deoxy-5-fluorouridine. *J. Med. Chem.* **1984**;27(4):440-4.

109. McGuigan C, Shackleton JM, Tollerfield SM, Riley PA. Synthesis and evaluation of some novel phosphate and phosphinate derivatives of araA. Studies on the mechanism of action of phosphate triesters. *Nucleic Acids Res.* **1989**;17(24):10171-7.

110. McGuigan C, Nickson C, Petrik J, Karpas A. Phosphate derivatives of AZT display enhanced selectivity of action against HIV1 by comparison to the parent nucleoside. *FEBS Lett.* **1992**;310(2):171-4.

111. McGuigan C, Nicholls SR, O'Connor TJ, Kinchington D. Synthesis of some novel dialkyl phosphate derivatives of 3'-modified nucleosides as potential anti-AIDS drugs. *Antiviral Chem. Chemother.* **1990**;1(1):25-33.

112. McGuigan C, O'Connor TJ, Nicholls SR, Nickson C, Kinchington D. Synthesis and anti-HIV activity of some novel substituted dialkyl phosphate derivatives of AZT and ddCyd. *Antiviral Chem. Chemother.* **1990**;1(6):355-60.

113. McGuigan C, Kinchington D, Wang MF, Nicholls SR, Nickson C, Galpin S. Nucleoside analogues previously found to be inactive against HIV may be activated by simple chemical phosphorylation. *FEBS Lett.* **1993**;322(3):249-52.

114. McGuigan C, Pathirana RN, Mahmood N, Devine KG, Hay AJ. Aryl phosphate derivatives of AZT retain activity against HIV1 in cell lines which are resistant to the action of AZT. *Antiviral Res.* **1992**;17(4):311-21.

115. McGuigan C, Davies M, Pathirana R, Mahmood N, Hay AJ. Synthesis and anti-HIV activity of some novel diaryl phosphate derivatives of AZT. *Antiviral Res.* **1994**;24(1):69-77.

116. McGuigan C, Pathirana RN, Davies MPH, Balzarini J, De Clercq E. Diaryl phosphate derivatives act as pro-drugs of AZT with reduced cytotoxicity compared to the parent nucleoside. *Bioorg. Med. Chem. Lett.* **1994**;4(3):427-30.

117. McGuigan C, Pathirana RN, Mahmood N, Hay AJ. Aryl phosphate derivatives of AZT inhibit HIV replication in cells where the nucleoside is poorly active. *Bioorg. Med. Chem. Lett.* **1992**;2(7):701-4.

118.

<http://www.fda.gov/NewsEvents/Newsroom/PressAnnouncements/ucm418365.htm>

119. Cahn P RM, Gun AM, Ferrari I, Dibirdik I, Qazi S, D'Cruz O, Sahin K, Uckun F;. Preclinical and first-in-human Phase I clinical evaluation of Stampidine, a potent anti-HIV pharmaceutical drug candidate. *J AIDS Clinic Res.* **2012**;3:138.

120. Chang W, Bao D, Chun B-K, Naduthambi D, Nagarathnam D, Rachakonda S. Discovery of PSI-353661, a novel purine nucleotide prodrug for the treatment of HCV infection. *ACS Med. Chem. Lett.* **2011**;2(2):130-5.
119. Vernachio JH, Bleiman B, Bryant KD, Chamberlain S, Hunley D, Hutchins J. INX-08189, a phosphoramidate prodrug of 6-O-methyl-2'-C-methyl guanosine, is a potent inhibitor of Hepatitis C virus replication with excellent pharmacokinetic and pharmacodynamic properties. *Antimicrob. Agents Chemother.* **2011**;55(5):1843-51.
120. Ahmad T, Yin P, Saffitz J, Pockros PJ, Lalezari J, Shiffman M, Freilich B, Zamparo J, Brown K, Dimitrova D, Kumar M, Manion D, Heath-Chiozzi M, Wolf R, Hughes E, Muir AJ, Hernandez AF. Cardiac dysfunction associated with a nucleotide polymerase inhibitor for treatment of hepatitis C. *Hepatology.* **2015**;62(2):409-16.
121. <http://www.prnewswire.com/news-releases/newbiotics-presents-preliminary-data-of-thymectacintm-phase-i-clinical-trial-for-drug-resistant-colon-cancer-76923112.html>.
122. <http://www.nucanabiomed.com/acelarin.html>.
123. <http://www.nucanabiomed.com/NUC3373.html>.
124. Murakami E, Wang T, Park Y, Hao J, Lepist E-I, Babusis D, Ray AS. Efficient hepatic delivery by Tenofovir Alafenamide (GS-7340): implications for Hepatitis B virus therapy. *Antimicrob. Agents Chemother.* **2015**.
125. Mackman RL, Ray AS, Hui HC, Zhang L, Birkus G, Booramra CG. Discovery of GS-9131: Design, synthesis and optimization of amidate prodrugs of the novel nucleoside phosphonate HIV reverse transcriptase (RT) inhibitor GS-9148. *Biorg. Med. Chem.* **2010**;18(10):3606-17.
126. Murakami E, Tolstykh T, Bao H, Niu C, Steuer HMM, Bao D, Chang W, Espiritu C, Bansal S, Lam AM, Otto MJ, Sofia MJ, Furman PA. Mechanism of activation of PSI-7851 and its diastereoisomer PSI-7977. *J. Biol. Chem.* **2010**;285(45):34337-47.
127. Birkus G, Wang R, Liu X, Kutty N, MacArthur H, Cihlar T. Cathepsin A is the major hydrolase catalyzing the intracellular hydrolysis of the antiretroviral nucleotide phosphonoamidate prodrugs GS-7340 and GS-9131. *Antimicrob. Agents Chemother.* **2007**;51(2):543-50.
128. Birkus G, Kutty N, Frey CR, Shribata R, Chou T, Wagner C. Role of Cathepsin A and lysosomes in the intracellular activation of novel antipapillomavirus agent GS-9191. *Antimicrob. Agents Chemother.* **2011**;55(5):2166-73.
129. Ricci A, Brancale A. Density functional theory calculation of cyclic carboxylic phosphorus mixed anhydrides as possible intermediates in biochemical reactions: Implications for the Pro-Tide approach. *J. Comput. Chem.* **2012**;33(10):1029-37.
130. Michielssens S, Maiti M, Maiti M, Dyubankova N, Herdewijn P, Ceulemans A. Reactivity of amino acid nucleoside phosphoramidates: a mechanistic quantum chemical study. *J. Phys. Chem. A.* **2012**;116(1):644-52.
131. Maiti M, Michielssens S, Dyubankova N, Maiti M, Lescrinier E, Ceulemans A. Influence of the nucleobase and anchimeric assistance of the carboxyl acid groups in the hydrolysis of amino acid nucleoside phosphoramidates. *Chemistry-Eur. J.* **2012**;18(3):857-68.
132. Ora M, Ojanperä J, Lönnberg H. Hydrolytic reactions of thymidine 5'-O-phenyl-N-alkylphosphoramidates, models of Nucleoside 5'-monophosphate prodrugs. *Chemistry-Eur. J.* **2007**;13(30):8591-9.
133. Chou T-F, Baraniak J, Kaczmarek R, Zhou X, Cheng J, Ghosh B. Phosphoramidate pronucleotides: a comparison of the phosphoramidase substrate specificity of human and Escherichia coli histidine triad nucleotide binding proteins. *Mol. Pharm.* **2007**;4(2):208-17.
134. McGuigan C, Tsang H-W, Cahard D, Turner K, Velazquez S, Salgado A. Phosphoramidate derivatives of d4T as inhibitors of HIV: The effect of amino acid variation. *Antiviral Res.* **1997**;35(3):195-204.
135. Meppen M, Pacini B, Bazzo R, Koch U, Leone JF, Koeplinger KA. Cyclic phosphoramidates as prodrugs of 2'-C-methylcytidine. *Eur. J. Med. Chem.* **2009**;44(9):3765-70.

136. Jain HV, Kalman TI. Synthesis and study of cyclic pronucleotides of 5-fluoro-2'-deoxyuridine. *Bioorg. Med. Chem. Lett.* **2012**;22(14):4497-501.
137. Du J, Bao D, Chun B-K, Jiang Y, Ganapati Reddy P, Zhang H-R. β -d-2'- α -F-2'- β -C-methyl-6-O-substituted 3',5'-cyclic phosphate nucleotide prodrugs as inhibitors of hepatitis C virus replication: A structure-activity relationship study. *Bioorg. Med. Chem. Lett.* **2012**;22(18):5924-9.
138. Gupta SP. Cancer-causing viruses and their inhibitors, Chapter 3; CRC Press, 2014.
139. McGuigan C, Jones BCNM, Devine KG, Nicholls SR, Kinchington D. Attempts to introduce chemotherapeutic nucleotides into cells: studies on the anti-HIV agent FDT. *Bioorg. Med. Chem. Lett.* **1991**;1(12):729-32.
140. Kinchington D, Harvey JJ, O'Connor TJ, Jones BCNM, Devine KG, Taylor-Robinson D. Comparison of antiviral effects of Zidovudine phosphoramidate and phosphorodiamidate derivatives against HIV and ULV in vitro. *Antiviral Chem. Chemother.* **1992**;3(2):107-12.
141. McGuigan C, Madela K, Aljarah M, Bourdin C, Arrica M, Barrett E. Phosphorodiamidates as a promising new phosphate prodrug motif for antiviral drug discovery: application to anti-HCV agents. *J. Med. Chem.* **2011**;54(24):8632-45.
142. McGuigan C, Bourdin C, Derudas M, Hamon N, Hinsinger K, Kandil S. Design, synthesis and biological evaluation of phosphorodiamidate prodrugs of antiviral and anticancer nucleosides. *Eur. J. Med. Chem.* **2013**;70:326-40.
143. Serpi M, Madela K, Pertusati F, Slusarczyk M. Synthesis of phosphoramidate prodrugs: ProTide approach. *Curr. Protoc. Nucleic Acid Chem.* Chapter 15:Unit15.5; John Wiley & Sons, Inc.; **2013**.
144. Pradere U, Garnier-Amblard EC, Coats SJ, Amblard F, Schinazi RF. Synthesis of nucleoside phosphate and phosphonate prodrugs. *Chem. Rev.* **2014**;114(18):9154-218.
145. van Boom JH, Burgers PMJ, Crea R, Luyten WCMM, Vink ABJ, Reese CB. Phosphorylation of nucleoside derivatives with aryl phosphoramidochloridates. *Tetrahedron.* **1975**;31(23):2953-9.
146. Derudas M, Carta D, Brancale A, Vanpouille C, Lisco A, Margolis L, Balzarini J, McGuigan C. The application of phosphoramidate ProTide technology to acyclovir confers anti-HIV inhibition. *J. Med. Chem.* **2009**;52(17):5520-30.
147. Derudas M, Brancale A, Naesens L, Neyts J, Balzarini J, McGuigan C. Application of the phosphoramidate ProTide approach to the antiviral drug ribavirin. *Bioorg. Med. Chem.* **2010**;18(7):2748-55.
148. Gutsche CD, Oude-Alink BAM. The photoinduced alcoholysis of 3,4-dihydrocoumarin and related compounds. *J. Am. Chem. Soc.* **1968**;90(21):5855-61.
149. Bondada L, Detorio M, Bassit L, Tao S, Montero CM, Singletary TM. Adenosine dioxolane nucleoside phosphoramidates as antiviral agents for human Immunodeficiency and Hepatitis B viruses. *ACS Med. Chem. Lett.* **2013**;4(8):747-51.
150. Slusarczyk M, Lopez MH, Balzarini J, Mason M, Jiang WG, Blagden S, Thompson E, Ghazaly E, McGuigan C. Application of ProTide technology to gemcitabine: a successful approach to overcome the key cancer resistance mechanisms leads to a new agent (NUC-1031) in clinical development. *J. Med. Chem.* **2014**;57(4):1531-42.
151. McGuigan C, Murziani P, Slusarczyk M, Gonczy B, Vande Voorde J, Liekens S, Balzarini J. Phosphoramidate ProTides of the anticancer agent FUDR successfully deliver the preformed bioactive monophosphate in cells and confer advantage over the parent nucleoside. *J. Med. Chem.* **2011**;54(20):7247-58.
152. Congiatu C, Brancale A, Mason MD, Jiang WG, McGuigan C. Novel potential anticancer naphthyl phosphoramidates of BVdU: separation of diastereoisomers and assignment of the absolute configuration of the phosphorus center. *J. Med. Chem.* **2006**;49(2):452-5.
153. Uchiyama M, Aso Y, Noyori R, Hayakawa Y. O-selective phosphorylation of nucleosides without N-protection. *J. Org. Chem.* **1993**;58(2):373-9.
154. Jones BCNM, McGuigan C, O'Connor TJ, Jeffries DJ, Kinchington D. Synthesis and anti-HIV activity of some novel phosphorodiamidate derivatives of 3'-azido-3'-deoxythymidine (AZT). *Antiviral Chem. Chemother.* **1991**;2(1):35-9.

155. Yoshikawa M, Kato T, Takenishi T. Studies of phosphorylation. III. Selective phosphorylation of unprotected nucleosides. *Bull. Chem. Soc. Jpn.* **1969**;42(12):3505-8.
156. Buenz EJ, Bauer BA, Osmundson TW, Motley TJ. The traditional Chinese medicine *Cordyceps sinensis* and its effects on apoptotic homeostasis. *J. Ethnopharmacol.* **2005**;96(1-2):19-29.
157. Tuli HS, Sharma AK, Sandhu SS, Kashyap D. Cordycepin: A bioactive metabolite with therapeutic potential. *Life Sci.* **2013**;93(23):863-9.
158. Tuli HS, Sandhu SS, Sharma AK. Pharmacological and therapeutic potential of *Cordyceps* with special reference to Cordycepin. *3 Biotech.* **2014**;4(1):1-12.
159. Khan MAT, Mousumi; Dian-zheng Zhang; Han-chun Chen. *Cordyceps* mushroom: a potent anticancer nutraceutical. *Open Nutraceuticals J.* **2010**;3:179-83.
160. Baldwin SA, Yao SYM, Hyde RJ, Ng AML, Foppolo S, Barnes K. Functional characterization of novel human and mouse equilibrative nucleoside transporters (hENT3 and mENT3) located in intracellular membranes. *J. Biol. Chem.* **2005**;280(16):15880-7.
161. Holbein S, Wengi A, Decourty L, Freimoser FM, Jacquier A, Dichtl B. Cordycepin interferes with 3' end formation in yeast independently of its potential to terminate RNA chain elongation. *RNA.* **2009**;15(5):837-49.
162. Tsai Y-J, Lin L-C, Tsai T-H. Pharmacokinetics of adenosine and cordycepin, a bioactive constituent of *Cordyceps sinensis* in rat. *J. Agric. Chem.* **2010**;58(8):4638-43.
163. Mikhailopulo IA WH, Cramer F. Substrate specificity of adenosine deaminase: the role of the substituents at the 2'- and 3'-carbons of adenine nucleosides, of their configuration and of the conformation of the furanose ring. *Biochem. Pharmacol.* **1981**;30(9):1001-4.
164. Penman S, Rosbash M, Penman M. Messenger and heterogeneous nuclear RNA in HeLa cells: differential inhibition by cordycepin. *Proc. Natl. Acad. Sci. U. S. A.* **1970**;67(4):1878-85.
165. Müller WEG, Seibert G, Beyer R, Breter HJ, Maidhof A, Zahn RK. Effect of cordycepin on nucleic acid metabolism in L5178Y cells and on nucleic acid-synthesizing enzyme systems. *Cancer Res.* **1977**;37(10):3824-33.
166. Kondrashov A, Meijer HA, Barthet-Barateig A, Parker HN, Khurshid A, Tessier S. Inhibition of polyadenylation reduces inflammatory gene induction. *RNA.* **2012**;18(12):2236-50.
167. Imesch P, Goerens A, Fink D, Fedier A. MLH1-deficient HCT116 colon tumor cells exhibit resistance to the cytostatic and cytotoxic effect of the poly(A) polymerase inhibitor cordycepin (3'-deoxyadenosine) in vitro. *Oncol. Lett.* **2012**;3(2):441-4.
168. Nakamura K, Yoshikawa N, Yamaguchi YU, Kagota S, Shinozuka K, Kunitomo M. Antitumor effect of cordycepin (3'-deoxyadenosine) on mouse melanoma and lung carcinoma cells involves adenosine A3 receptor stimulation. *Anticancer Res.* **2006**;26(1A):43-7.
169. Yoshikawa N, Kunitomo M, Kagota S, Shinozuka K, Nakamura K. Inhibitory effect of cordycepin on hematogenic metastasis of B16-F1 mouse melanoma cells accelerated by adenosine-5'-diphosphate. *Anticancer Res.* **2009**;29(10):3857-60.
170. Jeong J-W, Jin C-Y, Park C, Hong SH, Kim G-Y, Jeong YK. Induction of apoptosis by cordycepin via reactive oxygen species generation in human leukemia cells. *Toxicol. In Vitro.* **2011**;25(4):817-24.
171. Kadomatsu M, Nakajima S, Kato H, Gu L, Chi Y, Yao J. Cordycepin as a sensitizer to tumour necrosis factor (TNF)- α -induced apoptosis through eukaryotic translation initiation factor 2 α (eIF2 α)- and mammalian target of rapamycin complex 1 (mTORC1)-mediated inhibition of nuclear factor (NF)- κ B. *Clin. Exp. Immunol.* **2012**;168(3):325-32.
172. Kim H, Naura AS, Errami Y, Ju J, Boulares AH. Cordycepin blocks lung injury-associated inflammation and promotes BRCA1-deficient breast cancer cell killing by effectively inhibiting PARP. *Mol. Med.* **2011**;17(9-10):893-900.
173. Kim HG, Shrestha B, Lim SY, Yoon DH, Chang WC, Shin D-J. Cordycepin inhibits lipopolysaccharide-induced inflammation by the suppression of NF- κ B through Akt and p38 inhibition in RAW 264.7 macrophage cells. *Eur. J. Pharmacol.* **2006**;545(2-3):192-9.
174. Jeong J-W, Jin C-Y, Kim G-Y, Lee J-D, Park C, Kim G-D, Kim WJ, Jung WK, Seo SK, Choi IW, Choi YH. Anti-inflammatory effects of cordycepin via suppression of

- inflammatory mediators in BV2 microglial cells. *Int. Immunopharmacol.* **2010**;10(12):1580-6.
175. Cho H-J, Cho JY, Rhee MH, Park H-J. Cordycepin (3'-deoxyadenosine) inhibits human platelet aggregation in a cyclic AMP-and cyclic GMP-dependent manner. *Eur. J. Pharmacol.* **2007**;558(1-3):43-51.
176. Sugar AM, McCaffrey RP. Antifungal activity of 3'-deoxyadenosine (Cordycepin). *Antimicrob. Agents Chemother.* **1998**;42(6):1424-7.
177. Vodnala SK, Ferella M, Lundén-Miguel H, Betha E, van Reet N, Amin DN, Oberg B, Andersson B, Kristensson K, Wigzell H, Rottenberg ME. Preclinical assessment of the treatment of second-stage african trypanosomiasis with cordycepin and deoxycoformycin. *PLoS Negl. Trop. Dis.* **2009**;3(8):e495.
178. Rosa LD, Da Silva AS, Gressler LT, Oliveira CB, Dambrós MGC, Miletto LC, França RT, Lopes ST, Samara YN, da Veiga ML, Monteiro SG. Cordycepin (3'-deoxyadenosine) pentostatin (deoxycoformycin) combination treatment of mice experimentally infected with *Trypanosoma evansi*. *Parasitology.* **2013**;140(05):663-71.
179. Rottenberg Martin E, Masocha W, Ferella M, Petitto - Assis F, Goto H, Kristensson K, McCaffrey R, Wigzell H. Treatment of african trypanosomiasis with cordycepin and adenosine deaminase inhibitors in a mouse model. *J. Infect. Dis.* **2005**;192(9):1658-65.
180. Becker Y. Antiviral agents from natural sources. *Pharmacol. Ther.* **1980**;10(1):119-59.
181. Ryu E, Son M, Lee M, Lee K, Cho JY, Cho S, Lee SK, Lee YM, Cho H, Sung GH, Kang H. Cordycepin is a novel chemical suppressor of Epstein-Barr virus replication. *Oncoscience.* **2014**;1(12):866-81.
182. Pridgen CL. Influenza virus RNA's in the cytoplasm of chicken embryo cells treated with 3'-deoxyadenosine. *J. Virol.* **1976**;18(1):356-60.
183. Chen Y-H, Wang J-Y, Pan B-S, Mu Y-F, Lai M-S, So EC, Wong TS, Huang BM. Cordycepin enhances cisplatin apoptotic effect through caspase/MAPK pathways in human head and neck tumor cells. *Onco Targets Ther.* **2013**;6:983-98.
184. Lee SY, Debnath T, Kim S-K, Lim BO. Anti-cancer effect and apoptosis induction of cordycepin through DR3 pathway in the human colonic cancer cell HT-29. *Food Chem. Toxicol.* **2013**;60(0):439-47.
185. Lee S-J, Moon G-S, Jung K-H, Kim W-J, Moon S-K. c-Jun N-terminal kinase 1 is required for cordycepin-mediated induction of G2/M cell-cycle arrest via p21WAF1 expression in human colon cancer cells. *Food Chem. Toxicol.* **2010**;48(1):277-83.
186. Chen Y, Chen Y-C, Lin Y-T, Huang S-H, Wang S-M. Cordycepin induces apoptosis of CGTH W-2 thyroid carcinoma cells through the calcium-calpain-caspase 7-PARP pathway. *J. Agric. Food. Chem.* **2010**;58(22):11645-52.
187. Chen LS, Stellrecht CM, Gandhi V. RNA-directed agent, cordycepin, induces cell death in multiple myeloma cells. *Br. J. Haematol.* **2008**;140(6):682-391.
188. Kodama EN, McCaffrey RP, Yusa K, Mitsuya H. Antileukemic activity and mechanism of action of cordycepin against terminal deoxynucleotidyl transferase-positive (TdT+) leukemic cells. *Biochem. Pharmacol.* **2000**;59(3):273-81.
189. Wehbe-Janek H, Shi Q, Kearney CM. Cordycepin/hydroxyurea synergy allows low dosage efficacy of cordycepin in MOLT-4 leukemia cells. *Anticancer Res.* **2007**;27(5A):3143-6.
190. Nakamura K, Konoha K, Yoshikawa N, Yamaguchi YU, Kagota S, Shinozuka K, Kunitomo M. Effect of cordycepin (3'-deoxyadenosine) on hematogenic lung metastatic model mice. *In Vivo.* **2005**;19(1):137-41.
191. <https://clinicaltrials.gov/ct2/show/NCT00003005>.
192. <https://clinicaltrials.gov/ct2/show/NCT00709215>.
193. Rodman LE, Farnell DR, Coyne JM, Allan PW, Hill DL, Duncan KKL, Tomaszewski JE, Smith AC, Page JG. Toxicity of cordycepin in combination with the adenosine deaminase Inhibitor 2'-deoxycoformycin in Beagle dogs. *Toxicol. Appl. Pharmacol.* **1997**;147(1):39-45.

194. Wei HP, Ye XL, Chen Z, Zhong YJ, Li PM, Pu SC, Pu SC, Li XG. Synthesis and pharmacokinetic evaluation of novel N-acyl-cordycepin derivatives with a normal alkyl chain. *Eur. J. Med. Chem.* **2009**;44(2):665-9.
195. Chang HM, Oakes, J., Olsson, A., Panaitescu, L., Britt, B.M., Kearney, C.M., Kane, R.R. . Synthesis and in vitro evaluation of adenosine deaminase resistant N-6 aminal and thioaminal prodrugs of cordycepin. *Lett. Drug Des. Discov.* **2005**;2:133– 6.
196. Kane RC, H-M, Compounds resistant to metabolic deactivation and methods of use. United States. 2006.
197. Meier C, Neumann JM, Andre F, Henin Y, Huynh Dinh T. O-Alkyl-5',5'-dinucleoside phosphates as prodrugs of 3'-azidothymidine and cordycepin. *J. Org. Chem.* **1992**;57(26):7300-8.
198. Ciuffreda P, Casati S, Santaniello E. The action of adenosine deaminase (E.C. 3.5.4.4.) on adenosine and deoxyadenosine acetates: the crucial role of the 5'-hydroxy group for the enzyme activity. *Tetrahedron.* **2000**;56(20):3239-43.
199. Iwashima A, Ogata M, Nosaka K, Nishimura H, Hasegawa T. Adenosine kinase-deficient mutant of *Saccharomyces cerevisiae*. *FEMS Microbiol. Lett.* **1995**;127(1-2):23-8.
200. Walton E, Nutt RF, Jenkins SR, Holly FW. 3'-Deoxynucleosides. I. A Synthesis of 3'-Deoxyadenosine. *Journal of the American Chemical Society.* 1964;86(14):2952-.
201. Ito Y, Shibata T, Arita M, Sawai H, Ohno M. Chirally selective synthesis of sugar moiety of nucleosides by chemicoenzymatic approach: L- and D-ribose, showdomycin, and cordycepin. *J. Am. Chem. Soc.* **1981**;103(22):6739-41.
202. McDonald FE, Gleason MM. Asymmetric synthesis of nucleosides via molybdenum-catalyzed alkynol cycloisomerization coupled with stereoselective glycosylations of deoxyfuranose Glycals and 3-amidofuranose glycals. *J. Am. Chem. Soc.* **1996**;118(28):6648-59.
203. Wang Z, Prudhomme DR, Buck JR, Park M, Rizzo CJ. Stereocontrolled syntheses of deoxyribonucleosides via photoinduced electron-transfer deoxygenation of benzoyl-protected rbo- and arabinonucleosides. *J. Org. Chem.* **2000**;65(19):5969-85.
204. Meier C, T H-D. Improved conversion of adenosine to 3'-deoxyadenosine. *Synlett.* **1991**;4:227-8.
205. Robins MJ, Wilson JS, Hansske F. Nucleic acid related compounds. 42. A general procedure for the efficient deoxygenation of secondary alcohols. Regiospecific and stereoselective conversion of ribonucleosides to 2'-deoxynucleosides. *J. Am. Chem. Soc.* **1983**;105(12):4059-65.
206. Ogilvie KK, Hakimelahi GH, Proba ZA, Usman N. Conversion of ribonucleosides to protected 3'-deoxynucleosides. *Tetrahedron Lett.* **1983**;24(9):865-8.
207. Halligan KN, V. A highly efficient procedure for the oxidation of the 5'-position of adenosine analogues. *ARKIVOC.* **2006**;2006(2):101-6.
208. Hakimelahi GH, Proba ZA, Ogilvie KK. Nitrate ion as catalyst for selective silylations of nucleosides. *Tetrahedron Lett.* **1981**;22(48):4775-8.
209. Hakimelahi GH, Proba ZA, Ogilvie KK. New catalysts and procedures for the dimethoxytritylation and selective silylation of ribonucleosides. *Can. J. Chem.* **1982**;60(9):1106-13.
210. Robins MJ, Hansske F, Low NH, Park JI. A mild conversion of vicinal diols to alkenes. Efficient transformation of ribonucleosides into 2'-ene and 2',3'-dideoxynucleosides. *Tetrahedron Lett.* **1984**;25(4):367-70.
211. Robins MJ, Wilson JS, Madej D, Low NH, Hansske F, Wnuk SF. Nucleic acid-related compounds. 88. Efficient conversions of ribonucleosides into their 2',3'-anhydro, 2'(and 3')-deoxy, 2',3'-didehydro-2',3'-dideoxy, and 2',3'-dideoxynucleoside analogs. *J. Org. Chem.* **1995**;60(24):7902-8.
212. Robins MJ, Mengel R, Jones RA, Fouron Y. Nucleic acid related compounds. 22. Transformation of ribonucleoside 2',3'-O-ortho esters into halo, deoxy, and epoxy sugar nucleosides using acyl halides. Mechanism and structure of products. *J. Am. Chem. Soc.* **1976**;98(25):8204-13.

213. Hansske F, J. Robins M. Regiospecific and stereoselective conversion of ribonucleosides to 3'-deoxynucleosides. A high yield three-stage synthesis of cordycepin from adenosine. *Tetrahedron Lett.* **1985**;26(36):4295-8.
214. Russell AF, Greenberg S, Moffatt JG. Reactions of 2-acyloxyisobutyryl halides with nucleosides. II. Reactions of adenosine. *J. Am. Chem. Soc.* **1973**;95(12):4025-30.
215. Mattocks AR. 371. Novel reactions of some α -acyloxy acid chlorides. *J. Chem. Soc. (Resumed)*. **1964**(0):1918-30.
216. Koole LH, Neidle S, Crawford MD, Krayevski AA, Gurskaya GV, Sandstroem A, Wu JC, Tong W, Chattopadhyaya J. Comparative structural studies of [3.1.0]-fused 2',3'-modified β -D-nucleosides by x-ray crystallography, NMR spectroscopy, and molecular mechanics calculations. *J. Org. Chem.* **1991**;56(24):6884-92.
217. McGuigan C, Bourdin C, Derudas M, Hamon N, Hinsinger K, Kandil S, Madela K, Meneghesso S, Pertusati F, Serpi M, Slusarczyk M, Chamberlain S, Kolykhalov A, Vernachio J, Vanpouille C, Introini A, Margolis L, Balzarini J. Design, synthesis and biological evaluation of phosphorodiamidate prodrugs of antiviral and anticancer nucleosides. *Eur. J. Med. Chem.* **2013**;70(0):326-40.
218. Choi S, Lim M-H, Kim KM, Jeon BH, Song WO, Kim TW. Cordycepin-induced apoptosis and autophagy in breast cancer cells are independent of the estrogen receptor. *Toxicol. Appl. Pharmacol.* **2011**;257(2):165-73.
219. Ko B-S, Lu Y-J, Yao W-L, Liu T-A, Tzean S-S, Shen T-L, Liou JY. Cordycepin regulates GSK-3 β / β -catenin signaling in human leukemia cells. *PLoS One.* **2013**;8(9):e76320.
220. Valente R. Design, synthesis and biological evaluation of nucleotide prodrugs as potential anticancer agents [PhD thesis]: Cardiff University; **2009**.
221. Monath TP. Treatment of yellow fever. *Antiviral Res.* 2008;78(1):116-24.
222. Barrett ADT, Higgs S. Yellow fever: a disease that has yet to be conquered. *Annu. Rev. Entomol.* **2006**;52(1):209-29.
223. Baron S FM, Albrecht T. Medical Microbiology. Viral Pathogenesis. Chapter 45. 4th edition. 1996.
224. Vodnala SK, Lundbäck T, Yeheskieli E, Sjöberg B, Gustavsson A-L, Svensson R, Olivera GC, Eze AA, de Konin HP, Hammarström LGJ, Rottenberg ME. Structure-activity relationships of synthetic cordycepin analogues as experimental therapeutics for african trypanosomiasis. *J. Med. Chem.* **2013**;56(24):9861-73.
225. Vial JM, Johansson NG, Vrang L, Chattopadhyaya J. Synthesis of 2'- and 3'-amino-substituted uridine, thymidine and adenosine, and their inhibitions of HIV replication. *Antiviral Chem. Chemother.* **1990**;1(3):183-202.
226. Krayevsky AA, Kukhanova MK, Atrazhev AM, Dyatkina NB, Papchikhin AV, Chidgeavadze ZG, Beabealashvilib RS. Selective inhibition of DNA chain elongation catalyzed by DNA polymerases. *Nucleos. Nucleot.* **1988**;7(5-6):613-7.
227. Estrov Z, Talpaz M, Ku S, Harris D, Van Q, Beran M, Hirsch-Ginsberg C, Huh Y, Yee G, Kurzrock R. Z-138: a new mature B-cell acute lymphoblastic leukemia cell line from a patient with transformed chronic lymphocytic leukemia. *Leukemia Res.* **1998**;22(4):341-53.
228. Al-Hajj M, Wicha MS, Benito-Hernandez A, Morrison SJ, Clarke MF. Prospective identification of tumorigenic breast cancer cells. *Proc. Natl. Acad. Sci.* **2003**;100(7):3983-8.
229. Kim CFB, Jackson EL, Woolfenden AE, Lawrence S, Babar I, Vogel S, Crowley D, Bronson RT, Jacks T. Identification of bronchioalveolar stem cells in normal lung and lung cancer. *Cell.* **2005**;121(6):823-35.
230. O'Brien CA, Pollett A, Gallinger S, Dick JE. A human colon cancer cell capable of initiating tumour growth in immunodeficient mice. *Nature.* **2007**;445(7123):106-10.
231. Collins AT, Berry PA, Hyde C, Stower MJ, Maitland NJ. Prospective Identification of Tumorigenic Prostate Cancer Stem Cells. *Cancer Res.* 2005;65(23):10946-51.
232. Szotek PP, Pieretti-Vanmarcke R, Masiakos PT, Dinulescu DM, Connolly D, Foster R, Dombkowski D, Preffer F, Maclaughlin DT, Donahoe PK. Ovarian cancer side population defines cells with stem cell-like characteristics and Mullerian Inhibiting Substance responsiveness. *Proc. Natl. Acad. Sci. U. S. A.* **2006**;103(30):11154-9.

233. Fang D, Nguyen TK, Leishear K, Finko R, Kulp AN, Hotz S. A tumorigenic subpopulation with stem cell properties in melanomas. *Cancer Res.* **2005**;65(20):9328-37.
234. Zhou B-BS, Zhang H, Damelin M, Geles KG, Grindley JC, Dirks PB. Tumour-initiating cells: challenges and opportunities for anticancer drug discovery. *Nat. Rev. Drug Discov.* **2009**;8(10):806-23.
235. Qiu H, Fang X, Luo Q, Ouyang G. Cancer stem cells: a potential target for cancer therapy. *Cell. Mol. Life Sci.* **2015**:1-14.
236. Nguyen LV, Vanner R, Dirks P, Eaves CJ. Cancer stem cells: an evolving concept. *Nat. Rev. Cancer.* **2012**;12(2):133-43.
237. Dean M, Fojo T, Bates S. Tumour stem cells and drug resistance. *Nat. Rev. Cancer.* **2005**;5(4):275-84.
238. Chen K, Huang Y-h, Chen J-l. Understanding and targeting cancer stem cells: therapeutic implications and challenges. *Acta Pharmacol. Sin.* **2013**;34(6):732-40.
239. Beck B, Blanpain C. Unravelling cancer stem cell potential. *Nat. Rev. Cancer.* **2013**;13(10):727-38.
240. Maccalli C, De Maria R. Cancer stem cells: perspectives for therapeutic targeting. *Cancer Immunol., Immunother.* **2015**;64(1):91-7.
241. Dean M. ABC Transporters, Drug resistance, and cancer stem cells. *J. Mammary Gland Biol. Neoplasia.* **2009**;14(1):3-9.
242. Gottesman MM, Fojo T, Bates SE. Multidrug resistance in cancer: role of ATP-dependent transporters. *Nat. Rev. Cancer.* **2002**;2(1):48-58.
243. Baumann M, Krause M, Hill R. Exploring the role of cancer stem cells in radioresistance. *Nat. Rev. Cancer.* **2008**;8(7):545-54.
244. Singh A, Settleman J. EMT, cancer stem cells and drug resistance: an emerging axis of evil in the war on cancer. *Oncogene.* **2010**;29(34):4741-51.
245. Rizzo S, Hersey JM, Mellor P, Dai W, Santos-Silva A, Liber D, uk L, Titley I, Carden CP, Box G, Hudson DL, Kaye SB, Brown R. Ovarian cancer stem cell-like side populations are enriched following chemotherapy and overexpress EZH2. *Mol. Cancer Ther.* **2011**;10(2):325-35.
246. Hamilton G, Olszewski U. Chemotherapy-induced enrichment of cancer stem cells in lung cancer. *J. Bioanal. Biomed.* **2013**;S9:003.
247. She M, Niu X, Chen X, Li J, Zhou M, He Y Le Y, Guo K. Resistance of leukemic stem-like cells in AML cell line KG1a to natural killer cell-mediated cytotoxicity. *Cancer Lett.* **2012**;318(2):173-9.
248. Horton SJ, Huntly BJP. Recent advances in acute myeloid leukemia stem cell biology. *Haematologica.* **2012**;97(7):966-74.
249. Peng G, Liu Y. Hypoxia-inducible factors in cancer stem cells and inflammation. *Trends Pharmacol. Sci.* **2015**;36(6):374-83.
250. Muz B, de la Puente P, Azab F, Luderer M, Azab AK. Hypoxia promotes stem cell-like phenotype in multiple myeloma cells. *Blood Cancer Journal.* **2014**;4:e262.
251. Axelson H, Fredlund E, Ovenberger M, Landberg G, Pählman S. Hypoxia-induced dedifferentiation of tumor cells – A mechanism behind heterogeneity and aggressiveness of solid tumors. *Semin. Cell Dev. Biol.* **2005**;16(4-5):554-63.
252. Keith B, Simon MC. Hypoxia-inducible factors, stem cells, and cancer. *Cell.* **2007**;129(3):465-72.
253. van Engeland M, Nieland LJW, Ramaekers FCS, Schutte B, Reutelingsperger CPM. Annexin V-affinity assay: a review on an apoptosis detection system based on phosphatidylserine exposure. *Cytometry.* **1998**;31(1):1-9.
254. MacDonald BT, Tamai K, He X. Wnt/ β -catenin signaling: components, mechanisms, and diseases. *Dev. Cell.* **2009**;17(1):9-26.
255. Wang Y, Krivtsov AV, Sinha AU, North TE, Goessling W, Feng Z, Zon LI, Armstrong SA. The Wnt/ β -catenin pathway is required for the development of leukemia stem cells in AML. *Science.* **2010**;327(5973):1650-3.
256. Ashihara E, Takada T, Maekawa T. Targeting the canonical Wnt/ β -catenin pathway in hematological malignancies. *Cancer Sci.* **2015**;106(6):665-71.

257. Zeng X, Tamai K, Doble B, Li S, Huang H, Habas R, Okamura H, Woodgett J, He X. A dual-kinase mechanism for Wnt coreceptor phosphorylation and activation. *Nature*. **2005**;438(7069):873-7.
258. Doble BW, Woodgett JR. GSK-3: tricks of the trade for a multi-tasking kinase. *J. Cell Sci.* **2003**;116(7):1175-86.
259. Ysebaert L, Chicanne G, Demur C, De Toni F, Prade-Houdellier N, Ruidavets JB, Mansat-De Mas V, Rigal-Huguet F, Laurent G, Payrastré B, Manenti S, Racaud-Sultan C. Expression of β -catenin by acute myeloid leukemia cells predicts enhanced clonogenic capacities and poor prognosis. *Leukemia*. **2006**;20(7):1211-6.
260. Saboulard D, Naesens L, Cahard D, Salgado A, Pathirana R, Velazquez S, McGuigan C, De Clercq E, Balzarini J. Characterization of the activation pathway of phosphoramidate triester prodrugs of stavudine and zidovudine. *Mol. Pharmacol.* **1999**;56(4):693-704.
261. Satoh Y KY, Oheda Y, Kuwahara J, Aikawa S, Matsuzawa F, Doi H, Aoyagi T, Sakuraba H, Itoh K. Microbial serine carboxypeptidase inhibitors-comparative analysis of actions on homologous enzymes derived from man, yeast and wheat. *J. Antibiot. (Tokyo)*. **2004**;57(5):316-25.
262. Schneider B, Xu YW, Janin J, Véron M, Deville-Bonne D. 3'-Phosphorylated nucleotides are tight binding inhibitors of nucleoside diphosphate kinase activity. *J. Biol. Chem.* **1998**;273(44):28773-8.
263. Cividini F, Filoni DN, Pesi R, Allegrini S, Camici M, Tozzi MG. IMP-GMP specific cytosolic 5'-nucleotidase regulates nucleotide pool and prodrug metabolism. *Biochim. Biophys. Acta* **2015**;1850(7):1354-61.
264. Bianchi V, Spychala J. Mammalian 5'-nucleotidases. *J. Biol. Chem.* **2003**;278(47):46195-8.
265. Krakowiak A, Pace HC, Blackburn GM, Adams M, Mekhalfia A, Kaczmarek R, Baraniak J, Stec WJ, Brenner C. Biochemical, crystallographic, and mutagenic characterization of Hint, the AMP-lysine hydrolase, with novel substrates and inhibitors. *J. Biol. Chem.* **2004**;279(18):18711-6.
266. Bahar FG, Ohura K, Ogihara T, Imai T. Species difference of esterase expression and hydrolase activity in plasma. *J. Pharm. Sci.* **2012**;101(10):3979-88.
267. McGuigan C, Gilles A, Madela K, Aljarah M, Holl S, Jones S, Vernachio J, Hutchins J, Ames B, Bryant KD, Gorovits E, Ganguly B, Hunley D, Hall A, Kolykhalov A, Liu Y, Muhammad J, Raja N, Walters R, Wang J, Chamberlain S, Henson G. Phosphoramidate ProTides of 2'-C-methylguanosine as highly potent inhibitors of Hepatitis C virus. Study of their in vitro and in vivo properties. *J. Med. Chem.* **2010**;53(13):4949-57.
268. Dalla Rosa L, Da Silva AS, Ruchel JB, Gressler LT, Oliveira CB, França RT, Lopes ST, Leal DB, Monteiro SG. Influence of treatment with 3'-deoxyadenosine associated deoxycoformycin on hematological parameters and activity of adenosine deaminase in infected mice with *Trypanosoma evansi*. *Exp. Parasitol.* **2013**;135(2):357-62.
269. Dickinson MJ, Holly FW, Walton E, Zimmerman M. 3'-Deoxynucleosides. V. 3'-Deoxy-2-fluoroadenosine. *J. Med. Chem.* **1967**;10(6):1165-6.
270. Baer H-P, Drummond GI, Duncan EL. Formation and deamination of adenosine by cardiac muscle enzymes. *Mol. Pharmacol.* **1966**;2(1):67-76.
271. Brockman RW, Schabel Jr FM, Montgomery JA. Biologic activity of 9- β -d-arabinofuranosyl-2-fluoroadenine, a metabolically stable analog of 9- β -d-arabinofuranosyladenine. *Biochem. Pharmacol.* **1977**;26(22):2193-6.
272. Gillerman I, Fischer B. Investigations into the origin of the molecular recognition of several adenosine deaminase inhibitors. *J. Med. Chem.* **2011**;54(1):107-21.
273. Montgomery J, Hewson K. Nucleosides of 2-fluoroadenine. *J. Med. Chem.* **1969**;12(3):498-504.
274. Schnebli HP, Hill DL, Bennett LL. Purification and properties of adenosine kinase from human tumor cells of type H. Ep. No. 2. *J. Biol. Chem.* **1967**;242(9):1997-2004.
275. Nicolaou KC, Ellery SP, Rivas F, Saye K, Rogers E, Workinger TJ, Schallenberger M, Tawatao R, Montero A, Hessell A, Romesberg F, Carson D, Burton D. Synthesis and

- biological evaluation of 2',4'- and 3',4'-bridged nucleoside analogues. *Biorg. Med. Chem.* **2011**;19(18):5648-69.
276. Bodamer GW, Kunin R. Behavior of ion exchange resins in solvents other than water - swelling and exchange characteristics. *Ind. Eng. Chem.* **1953**;45(11):2577-80.
277. Pietrzyk DJ. Ion-exchange resins in non-aqueous solvents—III: Solvent-uptake properties of ion-exchange resins and related adsorbents. *Talanta.* **1969**;16(2):169-79.
278. Pietrzyk DJ. Ion-exchange resins in non-aqueous solvents—I: Sorption rates of p-nitroaniline and the effects of small amounts of water. *Talanta.* **1966**;13(2):209-23.
279. Pietrzyk DJ. Ion-exchange resins in non-aqueous solvents—II: Sorption of P-nitroaniline and other weak bases in water-organic solvent mixtures. *Talanta.* **1966**;13(2):225-32.
280. Fier PS, Hartwig JF. Selective C-H fluorination of pyridines and diazines inspired by a classic amination reaction. *Science.* **2013**;342(6161):956-60.
281. Fier PS, Hartwig JF. Synthesis and late-stage functionalization of complex molecules through C-H fluorination and nucleophilic aromatic substitution. *J. Am. Chem. Soc.* **2014**;136(28):10139-47.
282. McConathy J, Owens MJ. Stereochemistry in drug action. *Prim. Care Companion to the J. Clin. Psychiatry.* **2003**;5(2):70-3.
283. Hutt AG, O'Grady J. Drug chirality: a consideration of the significance of the stereochemistry of antimicrobial agents. *J. Antimicrob. Chemother.* **1996**;37(1):7-32.
284. Pertusati F, McGuigan C. Diastereoselective synthesis of P-chirogenic phosphoramidate prodrugs of nucleoside analogues (ProTides) via copper catalysed reaction. *Chem. Commun.* **2015**;51(38):8070-3.
285. Chapman H, Kernan M, Prisbe E, Rohloff J, Sparacino M, Terhorst T, Yu, R. Practical synthesis, separation, and stereochemical assignment of the PMPA pro-drug GS-7340. *Nucleos. Nucleot. Nucl.* **2001**;20(4-7):621-8.
286. Sofia MJ, Bao D, Chang W, Du J, Nagarathnam D, Rachakonda S, Reddy PG, Ross BS, Wang P, Zhang HR, Bansal S, Espiritu C, Keilman M, Lam AM, Steuer HM, Niu C, Otto MJ, Furman PA. Discovery of a β -D-2'-deoxy-2'- α -fluoro-2'- β -C-methyluridine nucleotide prodrug (PSI-7977) for the treatment of Hepatitis C virus. *J. Med. Chem.* **2010**;53(19):7202-18.
287. Cho A, Zhang L, Xu J, Lee R, Butler T, Metobo S. Discovery of the first C-nucleoside HCV polymerase inhibitor (GS-6620) with demonstrated antiviral response in HCV infected patients. *J. Med. Chem.* **2014**;57(5):1812-25.
288. Congiatu C, Brancale A, Mason MD, Jiang WG, McGuigan C. Novel potential anticancer naphthyl phosphoramidates of BVdU: separation of diastereoisomers and assignment of the absolute configuration of the phosphorus center. *J. Med. Chem.* **2006**;49(2):452-5.
289. McGuigan C, Murziani P, Slusarczyk M, Gonczy B, Vande Voorde J, Liekens S, Balzarini J. Phosphoramidate proTides of the anticancer agent FUDR successfully deliver the preformed bioactive monophosphate in cells and confer advantage over the parent nucleoside. *J. Med. Chem.* **2011**;54(20):7247-58.
290. Pertusati F, Hinsinger K, Flynn ÁS, Powell N, Tristram A, Balzarini J, McGuigan, C. PMPA and PMEA prodrugs for the treatment of HIV infections and human papillomavirus (HPV) associated neoplasia and cancer. *Eur. J. Med. Chem.* **2014**;78:259-68.
291. Siccardi D, Gumbleton M, Omid Y, McGuigan C. Stereospecific chemical and enzymatic stability of phosphoramidate triester prodrugs of d4T in vitro. *Eur. J. Pharm. Sci.* **2004**;22(1):25-31.
292. Siccardi D, Kandalaf LE, Gumbleton M, McGuigan C. Stereoselective and concentration-dependent polarized epithelial permeability of a series of phosphoramidate triester prodrugs of d4T: an in vitro study in Caco-2 and Madin-Darby canine kidney cell monolayers. *J. Pharmacol. Exp. Ther.* **2003**;307(3):1112-9.
293. Mesplet N, Saito Y, Morin P, Agrofoglio LA. Liquid chromatographic separation of phosphoramidate diastereomers on a polysaccharide-type chiral stationary phase. *J. Chromatogr. A.* **2003**;983(1-2):115-24.

294. Chen C-L, Venkatachalam TK, Zhu Z-H, Uckun FM. In vivo pharmacokinetics and metabolism of anti-human immunodeficiency virus agent d4T-5'-[p-Bromophenyl methoxyalaninyl phosphate] (SAMPIDINE) in mice. *Drug Metab. Dispos.* **2001**;29(7):1035-41.
295. Allender CJ, Brain KR, Ballatore C, Cahard D, Siddiqui A, McGuigan C. Separation of individual antiviral nucleotide prodrugs from synthetic mixtures using cross-reactivity of a molecularly imprinted stationary phase. *Anal. Chim. Acta.* **2001**;435(1):107-13.
296. Perrin C, Coussot G, Lefebvre I, Périgaud C, Fabre H. Separation of 3-azido-2',3'-dideoxythymidine pronucleotide diastereoisomers in biological samples by CZE with cyclodextrin addition. *J. Chromatogr. A.* **2006**;1111(2):139-46.
297. Goossens JF, Roux S, Egron D, Perigaud C, Bonte JP, Vaccher C, Foulon C. Separation of nucleoside phosphoramidate diastereoisomers by high performance liquid chromatography and capillary electrophoresis. *Journal of Chromatography B.* **2008**;875(1):288-95.
298. Foulon C, Tedou J, Peyrottes S, Perigaud C, Bonte JP, Vaccher C, Goossens JF. Separation of diastereoisomers of Ara-C phosphotriesters using solid phase extraction and HPLC for the study of their decomposition kinetic in cell extracts. *J. Chromatogr. B.* **2009**;877(29):3475-81.
299. Foulon C, Vaccher C, Villard AL, Puy JY, Lefebvre I, Perigaud C, Bonte JP, Goossens JF. Diastereoisomeric resolution of a pronucleotide using solid phase extraction and high performance liquid chromatography: Application to a stereoselective decomposition kinetic in cell extracts. *J. Pharm. Biomed. Anal.* **2006**;42(2):245-52.
300. Pradere U, Amblard F, Coats SJ, Schinazi RF. Synthesis of 5'-methylene-phosphonate furanonucleoside prodrugs: application to D-2'-Deoxy-2'- α -fluoro-2'- β -C-methyl nucleosides. *Org. Lett.* **2012**;14(17):4426-9.
301. Zhu X-F, Williams HJ, Scott AI. Facile and highly selective 5'-desilylation of multisilylated nucleosides. *J. Chem. Soc., Perkin Trans. 1.* **2000**;15:2305-6.
302. Verma VA, Rossman R, Bennett F, Chen L, Gavalas S, Girijavallabhan V. Synthesis and SAR of geminal substitutions at the C5' carbosugar position of pyrimidine-derived HCV inhibitors. *Bioorg. Med. Chem. Lett.* **2012**;22(22):6967-73.
303. Beigelman L, Blatt L, Wang G, Alios BioPharma, Inc., USA . assignee. Preparation of nucleoside and nucleotide analog with protected phosphates for treating diseases such as viral infections, cancer, and/or parasitic diseases patent WO2010108140A1. 2010.
304. Verma V, Arasappan A, Njoroge FG, Chen KX. 5'-Substituted nucleoside analogs as antiviral agents. WO2013009737A1. **2013**.
305. Beigelman L, Blatt L, Wang G. Substituted nucleoside and nucleotide analogs. Google Patents; 2010.
306. Yakovlev GI, Bocharov AL, Moiseyev GP, Mikhaylov SN. Stereoelectronic effects in RNase-catalysed reactions of dinucleoside phosphate cleavage. *FEBS Lett.* **1985**;179(2):217-20.
307. Bzowska A, Kulikowska E, Shugar D. Purine nucleoside phosphorylases: properties, functions, and clinical aspects. *Pharmacol. Ther.* **2000**;88(3):349-425.
308. Grobosky CL, Lopez JB, Rennie S, Skopelitis DJ, Wiest AT, Bingman CA, Bitto E. Structural basis of substrate specificity and selectivity of murine cytosolic 5'-nucleotidase III. *J. Mol. Biol.* **2012**;423(4):540-54.
309. Pieters R, Veerman AJP. The role of 5'-nucleotidase in therapy-resistance of childhood leukemia. *Med. Hypotheses.* **1988**;27(1):77-80.
310. Brouwer C, Vogels-Mentink TM, Keizer-Garritsen JJ, Trijbels FJM, Bökkerink JPM, Hoogerbrugge PM, van Wering ER, Veerman AJ, De Abreu RA. Role of 5'-nucleotidase in thiopurine metabolism: enzyme kinetic profile and association with thio-GMP levels in patients with acute lymphoblastic leukemia during 6-mercaptopurine treatment. *Clinica Chimica Acta.* **2005**;361(1-2):95-103.
311. Hunsucker SA, Mitchell BS, Spychala J. The 5'-nucleotidases as regulators of nucleotide and drug metabolism. *Pharmacol. Ther.* **2005**;107(1):1-30.

312. Gray T, Morrey E, Gangadharan B, Sumter T, Spsychala J, Archer D, Spencer HT. Enforced expression of cytosolic 5'-nucleotidase I confers resistance to nucleoside analogues in vitro but systemic chemotherapy toxicity precludes in vivo selection. *Cancer Chemother. Pharmacol.* **2006**;58(1):117-28.
313. Gallier F, Lallemand P, Meurillon M, Jordheim LP, Dumontet C, Périgaud C, Lionne C, Peyrottes S, Chaloin L. Structural insights into the inhibition of cytosolic 5'-nucleotidase II (cN-II) by ribonucleoside 5'-monophosphate analogues. *PLoS Comput Biol.* **2011**;7(12):e1002295.
314. De Clercq E. The clinical potential of the acyclic (and cyclic) nucleoside phosphonates. The magic of the phosphonate bond. *Biochem. Pharmacol.* **2011**;82(2):99-109.
315. Pertusati F, Serpi M, McGuigan C. Medicinal chemistry of nucleoside phosphonate prodrugs for antiviral therapy. *Antiv. Chem. Chemother.* **2012**;22(5):181-203.
316. Hatse S, Naesens L, Degève B, Segers C, Vandeputte M, Waer M, De Clercq E, Balzarini J. Potent antitumor activity of the acyclic nucleoside phosphonate 9-(2-phosphonylmethoxyethyl)adenine in choriocarcinoma-bearing rats. *Int. J. Cancer.* **1998**;76(4):595-600.
317. Bubenik M, Rej R, Nguyen-Ba N, Attardo G, Ouellet F, Chan L. Novel nucleotide phosphonate analogues with potent antitumor activity. *Bioorg. Med. Chem. Lett.* **2002**;12(21):3063-6.
318. Pisarev VM, Lee S-H, Connelly MC, Fridland A. Intracellular metabolism and action of acyclic nucleoside phosphonates on DNA replication. *Mol. Pharmacol.* **1997**;52(1):63-8.
319. Nelson V, El Khadem HS, Whitten BK, Sesselman D. Synthesis of hypoxanthine, guanine, and 6-thiopurine nucleosides of 6-deoxy-D-allofuranose. *J. Med. Chem.* **1983**;26(7):1071-4.
320. David S, de Sennyey G. Syntheses of the two epimeric 5'-methylcytidines, their 5'-phosphates and [5-3H]-5'-pyrophosphates, and the two 5'-methyldeoxycytidines. A novel cytosine anhydro-nucleoside with two oxygen bridges between the base and the sugar. *J. Chem. Soc., Perkin Trans. 1.* **1982**(0):385-93.
321. Nelson V, El Khadem HS. Synthesis and antitumor activity of 7- and 9-(6'-deoxy- α -L-talofuranosyl)-hypoxanthine and 9-(6'-deoxy- α -L-talofuranosyl)-6-thiopurine. *J. Med. Chem.* **1983**;26(10):1527-30.
322. Ikeuchi H, Meyer ME, Ding Y, Hiratake J, Richards NGJ. A critical electrostatic interaction mediates inhibitor recognition by human asparagine synthetase. *Biorg. Med. Chem.* **2009**;17(18):6641-50.
323. Jansa P, Baszczyński O, Dračinský M, Votruba I, Zidek Z, Bahador G, Stepan G, Cihlar T, Mackman R, Holý A, Janeba Z. A novel and efficient one-pot synthesis of symmetrical diamide (bis-amidate) prodrugs of acyclic nucleoside phosphonates and evaluation of their biological activities. *Eur. J. Med. Chem.* **2011**;46(9):3748-54.
324. Hocková D, Holý A, Masojdková M, Keough DT, Jersey Jd, Guddat LW. Synthesis of branched 9-[2-(2-phosphonoethoxy)ethyl]purines as a new class of acyclic nucleoside phosphonates which inhibit Plasmodium falciparum hypoxanthine-guanine-xanthine phosphoribosyltransferase. *Biorg. Med. Chem.* **2009**;17(17):6218-32.
325. Baszczyński O, Janeba Z. Medicinal chemistry of fluorinated cyclic and acyclic nucleoside phosphonates. *Med. Res. Rev.* **2013**;33(6):1304-44.
326. Voet DV, J.; Pratt, C. V. . *Fundamental of Biochemistry*. 4th ed. ed: Wiley ed.; **2006**.
327. Langdon S, Langdon S. Growth inhibition by 8-chloro cyclic AMP of human HT29 colorectal and ZR-75-1 breast carcinoma xenografts is associated with selective modulation of protein kinase A isoenzymes. *Eur. J. Cancer.* **1995**;31A:969-73.
328. <http://clinicaltrials.gov/ct2/show/NCT00004902>.
329. Lange-Carter CA, Vuillequez JJ, Malkinson AM. 8-Chloroadenosine mediates 8-chloro-cyclic AMP-induced down-regulation of cyclic AMP-dependent protein kinase in normal and neoplastic mouse lung epithelial cells by a cyclic AMP-independent mechanism. *Cancer Res.* **1993**;53(2):393-400.

330. Dennison JB, Ayres ML, Kaluarachchi K, Plunkett W, Gandhi V. Intracellular succinylation of 8-chloroadenosine and its effect on fumarate levels. *J. Biol. Chem.* **2010**;285(11):8022-30.
331. <https://clinicaltrials.gov/ct2/show/NCT00714103>.
332. Robinson-White AJ, Bossis I, Hsiao H-P, Nesterova M, Leitner WW, Stratakis CA. 8-Cl-Adenosine Inhibits Proliferation and Causes Apoptosis in B-Lymphocytes via Protein Kinase A-Dependent and Independent Effects: Implications for Treatment of Carney Complex-Associated Tumors. *J. Clin. Endocrinol. Metab.* **2009**;94(10):4061-9.
333. Langeveld CH, Jongenelen CAM, Theeuwes JWM, Baak JPA, Heimans JJ, Stoof JC, Peters GJ. The antiproliferative effect of 8-chloro-adenosine, an active metabolite of 8-chloro-cyclic adenosine monophosphate, and disturbances in nucleic acid synthesis and cell cycle kinetics. *Biochem. Pharmacol.* **1997**;53(2):141-8.
334. Langeveld CH, Jongenelen CAM, Heimans JJ, Stoof JC. Growth inhibition of human glioma cells induced by 8-chloroadenosine, an active metabolite of 8-chloro cyclic adenosine 3':5'-monophosphate. *Cancer Res.* **1992**;52(14):3994-9.
335. Chen LS, Du-Cuny L, Vethantham V, Hawke DH, Manley JL, Zhang S, Zhang S, Gandhi V. Chain termination and inhibition of mammalian poly(A) polymerase by modified ATP analogues. *Biochem. Pharmacol.* **2010**;79(5):669-77.
336. Hirose Y, Manley JL. RNA polymerase II and the integration of nuclear events. *Genes Dev.* **2000**;14(12):1415-29.
337. Chen LS, Nowak BJ, Ayres ML, Krett NL, Rosen ST, Zhang S, Gandhi V. Inhibition of ATP synthase by chlorinated adenosine analogue. *Biochem. Pharmacol.* **2009**;78(6):583-91.
338. Balakrishnan K, Stellrecht CM, Genini D, Ayres M, Wierda WG, Keating MJ, Leoni LM, Gandhi V. Cell death of bioenergetically compromised and transcriptionally challenged CLL lymphocytes by chlorinated ATP. *Blood.* **2005**;105(11):4455-62.
339. Yang S-Y, Jia X-Z, Feng L-Y, Li S-Y, An G-S, Ni J-H, Jia HT. Inhibition of topoisomerase II by 8-chloro-adenosine triphosphate induces DNA double-stranded breaks in 8-chloro-adenosine-exposed human myelocytic leukemia K562 cells. *Biochem. Pharmacol.* **2009**;77(3):433-43.
340. Wang JC. Cellular roles of DNA topoisomerases: a molecular perspective. *Nat. Rev. Mol. Cell Biol.* **2002**;3(6):430-40.
341. Sondergaard Thomsen L. Synthesis, biological evaluation and mechanistic investigations of potential anticancer nucleotide phosphoramidates. Welsh School of Pharmacy, Cardiff University; **2011**.
342. Gandhi V, Chen W, Ayres M, Rhie J, Madden T, Newman R. Plasma and cellular pharmacology of 8-chloro-adenosine in mice and rats. *Cancer Chemoth. Pharm.* **2002**;50(2):85-94.
343. Gandhi V, Ayres M, Halgren RG, Krett NL, Newman RA, Rosen ST. 8-Chloro-cAMP and 8-Chloro-adenosine act by the same mechanism in multiple myeloma cells. *Cancer Res.* **2001**;61(14):5474-9.
344. McBrayer SK, Yarrington M, Qian J, Feng G, Shanmugam M, Gandhi V, Krett NL, Rosen ST. Integrative gene expression profiling reveals G6PD-mediated resistance to RNA-directed nucleoside analogues in B-cell neoplasms. *PLoS ONE.* **2012**;7(7):e41455.
345. Brentnall HJ, Hutchinson DW. Preparation of 8-chloroadenosine and its phosphate esters. *Tetrahedron Lett.* **1972**;13(25):2595-6.
346. Ikehara M, Ogiso Y, Maruyama T. Studies of nucleosides and nucleotides. 73. Chlorination of adenosine and its N6-methyl derivatives with *t*-butyl hypochlorite. *Pharm. Bull.* **1977**;25(4):575-8.
347. Ryu EK, MacCoss M. New procedure for the chlorination of pyrimidine and purine nucleosides. *J. Org. Chem.* **1981**;46(13):2819-23.
348. Ryu EK, Kim JN. The Oxidative chlorination of pyrimidine and purine bases, and nucleosides using acyl chloride-dimethyl-formamide-*m*-chloroperbenzoic acid system. *Nucleos. Nucleot.* **1989**;8(1):43-8.

349. Robins RK, Revankar GR, Chang Y. 8-Chloroadenosine 3', 5'-cyclic monophosphate preparations. US4861873 A; **1989**.
350. Ogilvie KK, Schifman AL, Penney CL. The synthesis of oligoribonucleotides. III. The use of silyl protecting groups in nucleoside and nucleotide chemistry. VIII. *Can. J. Chem.* **1979**;57(17):2230-8.
351. Hayakawa H, Tanaka H, Haraguchi K, Mayumi M, Nakajima M, Sakamaki T, Miyasaka T. Preparation of 8-chloropurine nucleosides through the reaction between their C-8 lithiated species and p-toluenesulfonyl chloride. *Nucleos. Nucleot.* **1988**;7(1):121-8.
352. Chen LS, Bahr MH, Sheppard TL. Effects of 8-chlorodeoxyadenosine on DNA synthesis by the klenow fragment of DNA polymerase I. *Bioorg. Med. Chem. Lett.* **2003**;13(9):1509-12.
353. Wuts PGM, Greene TW. Protection for the hydroxyl group, including 1,2- and 1,3-diols. *Greene's Protective Groups in Organic Synthesis*: John Wiley & Sons, Inc.; **2006**. p. 16-366.
354. Chandra T, Broderick WE, Broderick JB. Chemoselective deprotection of triethylsilyl ethers. *Nucleos. Nucleot. Nucl.* **2009**;28(11):1016-29.
355. Bergman AM, Pinedo HM, Talianidis I, Veerman G, Loves WJP, van der Wilt CL, PETERS, GJ. Increased sensitivity to gemcitabine of P-glycoprotein and multidrug resistance-associated protein-overexpressing human cancer cell lines. *Br. J. Cancer.* **2003**;88(12):1963-70.
356. Reid G, Wielinga P, Zelcer N, de Haas M, van Deemter L, Wijnholds J, Balzarini J, Borst P. Characterization of the transport of nucleoside analog drugs by the human multidrug resistance proteins MRP4 and MRP5. *Mol. Pharmacol.* **2003**;63(5):1094-103.
357. Endrizzi JA, Breddam K, Remington SJ. 2.8-Å structure of yeast serine carboxypeptidase. *Biochemistry.* **1994**;33(37):11106-20.
358. Davies DB. Conformations of nucleosides and nucleotides. *Prog. Nucl. Magn. Reson. Spectrosc.* **1978**;12(3):135-225.
359. Tavale SS, Sobell HM. Crystal and molecular structure of 8-bromoguanosine and 8-bromoadenosine, two purine nucleosides in the syn conformation. *J. Mol. Biol.* **1970**;48(1):109-23.
360. Uesugi S, Shida T, Ikehara M. Synthesis and properties of CpG analogs containing an 8-bromoguanosine residue. Evidence for Z-RNA duplex formation. *Biochemistry.* **1982**;21(14):3400-8.
361. Fujii S, Fujiwara T, Tomita K-i. Structural studies on the two forms of 8-bromo-2' , 3' -O-isopropylideneadenosine. *Nucleic Acids Research.* 1976;3(8):1985-96.
362. Walker GA, Bhatia SC, Hall JH. Theoretical calculations on adenine and adenosine and their 8-chloro-substituted analogs. *J. Am. Chem. Soc.* **1987**;109(25):7629-33.
363. Rios AC, Yu HT, Tor Y. Hydrolytic fitness of N-glycosyl bonds: comparing the deglycosylation kinetics of modified, alternative, and native nucleosides. *J. Phys. Org. Chem.* **2015**;28(3):173-80.
364. Garrett ER, Mehta PJ. Solvolysis of adenine nucleosides. I. Effects of sugars and adenine substituents on acid solvolyses. *J. Am. Chem. Soc.* **1972**;94(24):8532-41.
365. Kaburagi Y, Kishi Y. Operationally simple and efficient workup procedure for TBAF-mediated desilylation: application to halichondrin synthesis. *Org. Lett.* **2007**;9(4):723-6.
366. Nakajima M, Oda Y, Wada T, Minamikawa R, Shirokane K, Sato T, Chida N. Chemoselective reductive nucleophilic addition to tertiary amides, secondary amides, and N-methoxyamides. *Chem.-Eur. J.* **2014**;20(52):17565-71.
367. Spletstoser JT, White JM, Tunoori AR, Georg GI. Mild and selective hydrozirconation of amides to aldehydes using Cp₂Zr(H)Cl: scope and mechanistic insight. *J. Am. Chem. Soc.* **2007**;129(11):3408-19.
368. Morin J, Zhao Y, Snieckus V. Reductive cleavage of aryl O-carbamates to phenols by the Schwartz reagent. Expedient link to the directed ortho metalation strategy. *Org. Lett.* **2013**;15(16):4102-5.

369. Ferrari V, Serpi M, Pertusati F. Chemoselective *N*-deacetylation of protected nucleosides and nucleotides promoted by the Schwartz's reagent. *Nucleos. Nucleot. Nucl.* **2015**:accepted manuscript.
370. Matsuda A, Nakajima Y, Azuma A, Tanaka M, Sasaki T. Nucleosides and nucleotides. 100. 2'-C-Cyano-2'-deoxy-1- β -D-arabinofuranosylcytosine (CNDAC): design of a potential mechanism-based DNA-strand-breaking antineoplastic nucleoside. *J. Med. Chem.* **1991**;34(9):2917-9.
371. Azuma A, Nakajima Y, Nishizono N, Minakawa N, Suzuki M, Hanaoka K, Kobayashi T, Tanaka M, Sasaki T, Matsuda A. Nucleosides and nucleotides. 122. 2'-C-Cyano-2'-deoxy-1- β -D-arabinofuranosylcytosine and its derivatives. A new class of nucleoside with a broad antitumor spectrum. *J. Med. Chem.* **1993**;36(26):4183-9.
372. Yoshida T, Endo Y, Obata T, Kosugi Y, Sakamoto K, Sasaki T. Influence of cytidine deaminase on antitumor activity of 2'-deoxycytidine analogs in vitro and in vivo. *Drug Metab. Disposition.* **2010**;38(10):1814-9.
373. Matsuda A, Takenuki K, Tanaka M, Sasaki T, Ueda T. Nucleosides and nucleotides. 97. Synthesis of new broad spectrum antineoplastic nucleosides, 2'-deoxy-2'-methylidene cytidine (DMDC) and its derivatives. *J. Med. Chem.* **1991**;34(2):812-9.
374. Serova M, Galmarini CM, Ghoul A, Benhadji K, Green SR, Chiao J, Faivre S, Cvitkovic E, Le Tourneau C, Calvo F, Raymond E. Antiproliferative effects of sapacitabine (CYC682), a novel 2'-deoxycytidine-derivative, in human cancer cells. *Br. J. Cancer.* **2007**;97(5):628-36.
375. Obata T, Endo Y, Tanaka M, Matsuda A, Sasaki T. Development and biochemical characterization of a 2'-C-cyano-2'-deoxy-1- β -D-arabino-pentofuranosylcytosine (CNDAC)-resistant variant of the human fibrosarcoma cell line HT-1080. *Cancer Lett.* **1998**;123(1):53-61.
376. Azuma A, Huang P, Matsuda A, Plunkett W. 2'-C-cyano-2'-deoxy-1- β -D-arabino-pentofuranosylcytosine: a novel anticancer nucleoside analog that causes both DNA strand breaks and G2 arrest. *Mol. Pharmacol.* **2001**;59(4):725-31.
377. Matsuda A, Sasaki T. Antitumor activity of sugar-modified cytosine nucleosides. *Cancer Sci.* **2004**;95(2):105-11.
378. Liu X, Kantarjian H, Plunkett W. Sapacitabine for cancer. *Exper. Opin. Invest. Drugs* **2012**;21(4):541-55.
379. Kantarjian H, Faderl S, Garcia-Manero G, Luger S, Venugopal P, Maness L. Oral sapacitabine for the treatment of acute myeloid leukaemia in elderly patients: a randomised phase 2 study. *Lancet Oncology.* **2012**;13(11):1096-104.
380. Gavin Jeffrey Wood RW. Intermediate and processes involved in the preparation of 2'-cyano-2'-deoxy-N⁴-palmitoyl-1- β -arabinofuranoylcytosine, WO 2009/136162 A2009.
381. Zhong M, Strobel SA. Synthesis of the Ribosomal P-Site Substrate CCA-pcb. *Org. Lett.* **2006**;8(1):55-8.
382. Robins MJ, Wilson JS. Smooth and efficient deoxygenation of secondary alcohols. A general procedure for the conversion of ribonucleosides to 2'-deoxynucleosides. *J. Am. Chem. Soc.* **1981**;103(4):932-3.
383. Appell RB, Duguid RJ. New synthesis of a protected ketonucleoside by a non-cryogenic oxidation with TFAA/DMSO. *Org. Process Res. Dev.* **2000**;4(3):172-4.
384. Buff R, Hunziker J. 2'-Ethynyl-DNA: synthesis and pairing properties. *Helv. Chim. Acta.* **2002**;85(1):224-54.
385. Samano V, Robins MJ. Nucleic acid related compounds. 60. Mild periodinane oxidation of protected nucleosides to give 2'- and 3'-ketonucleosides. The first isolation of a purine 2'-deoxy-3'-ketonucleoside derivative. *J. Org. Chem.* **1990**;55(18):5186-8.
386. Camarasa MJ, Diaz-Ortiz A, Calvo-Mateo A, De las Heras FG, Balzarini J, De Clercq E. Synthesis and antiviral activity of 3'-C-cyano-3'-deoxynucleosides. *J. Med. Chem.* **1989**;32(8):1732-8.
387. Godt HC, Wann RE. The Synthesis of organic trithiocarbonates. *J. Org. Chem.* **1961**;26(10):4047-51.

388. Quiclet-Sire B, Zard SZ. A practical modification of the Barton-McCombie reaction and radical O- to S- rearrangement of xanthates. *Tetrahedron Lett.* **1998**;39(51):9435-8.
389. Liard A, Quiclet-Sire B, Zard SZ. A practical method for the reductive cleavage of the sulfide bond in xanthates. *Tetrahedron Lett.* 1996;37(33):5877-80.
390. Matsuda A, Takenuki K, Itoh H, Sasaki T, Ueda T. Radical deoxygenation of tert-alcohols in 2'-branched-chain sugar pyrimidine nucleosides: synthesis and antileukemic activity of 2'-deoxy-2'-(S)-methylcytidine. *Chem. Pharm. Bull. (Tokyo)*. **1987**;35(9):3967-70.
391. Kakefuda A, Yoshimura Y, Sasaki T, Matsuda A. Nucleosides and nucleotides. 120. Stereoselective radical deoxygenation of tert-alcohols in the sugar moiety of nucleosides: synthesis of 2',3'-dideoxy-2'-C-methyl- β -2'-C-ethynyl- β -D-threo-pentofuranosyl pyrimidines and adenine as potential antiviral and antitumor agents. *Tetrahedron*. **1993**;49(38):8513-28.
392. Yoshimura Y, Iino T, Matsuda A. Nucleosides and nucleotides. 102. Stereoselective radical deoxygenation of tert-propargyl alcohols in sugar moiety of pyrimidine nucleosides: synthesis of 2'-C-alkynyl-2'-deoxy-1- β -D-arabinofuranosylpyrimidines. *Tetrahedron Lett.* **1991**;32(42):6003-6.
393. Sultane PR, Mete TB, Bhat RG. Chemoselective N-deacetylation under mild conditions. *Org. Biomol. Chem.* **2014**;12(2):261-4.
394. Azuma A, Hanaoka K, Kurihara A, Kobayashi T, Miyauchi S, Kamo N, Tanaka M, Sasaki T, Matsuda A. Nucleosides and nucleotides. 141. Chemical stability of a new antitumor nucleoside, 2'-C-cyano-2'-deoxy-1- β -D-arabino-pentofuranosylcytosine (CNDAC) in alkaline medium: formation of 2'-C-cyano-2'-deoxy-1- β -D-ribo-pentofuranosylcytosine (CNDRC) and its antitumor activity. *J. Med. Chem.* **1995**;38(17):3391-7.
395. Chentsova A, Kapourani E, Giannis A. Synthesis of novel derivatives of 5-hydroxymethylcytosine and 5-formylcytosine as tools for epigenetics. *Beilstein J. Org. Chem.* **2014**;10:7-11.
396. López SE, Salazar J. Trifluoroacetic acid: Uses and recent applications in organic synthesis. *J. Fluorine Chem.* **2013**;156:73-100.
397. Kremisky JN, Sinha ND. Facile deprotection of silyl nucleosides with potassium fluoride/ 18-crown-6. *Bioorg. Med. Chem. Lett.* **1994**;4(18):2171-4.
398. Serpi M. unpublished results.
399. <https://clinicaltrials.gov/ct2/results?term=sapacitabine&Search=Search>.
400. Wang J, Fang P, Schimmel P, Guo M. Side chain independent recognition of aminoacyl adenylates by the Hint1 transcription suppressor. *J. Phys. Chem. B.* **2012**;116(23):6798-805.
401. Zhou X, Chou T-F, Aubol BE, Park CJ, Wolfenden R, Adams J, Carston R, Wagner. Kinetic mechanism of human histidine triad nucleotide binding protein 1 (Hint1). *Biochemistry*. **2013**;52(20):10.1021/bi301616c.
402. Heidelberger C, Parsons D, Remy DC. Syntheses of 5-Trifluoromethyluracil and 5-Trifluoromethyl-2'-Deoxyuridine. *J. Am. Chem. Soc.* **1962**;84(18):3597-8.
403. Heidelberger C, Parsons DG, Remy DC. Syntheses of 5-trifluoromethyluracil and 5-trifluoromethyl-2'-deoxyuridine. *J. Med. Chem.* **1964**;7(1):1-5.
404. Heidelberger C, Boohar J, Kampschroer B. Fluorinated pyrimidines: XXIV. In vivo metabolism of 5-trifluoromethyluracil-2-C¹⁴ and 5-trifluoromethyl-2'-deoxyuridine-2-C¹⁴. *Cancer Res.* **1965**;25(3 Part 1):377-81.
405. Reyes P, Heidelberger C. Fluorinated pyrimidines XXVI. Mammalian thymidylate synthetase: its mechanism of action and inhibition by fluorinated nucleotides. *Mol. Pharmacol.* **1965**;1(1):14-30.
406. Okayama T, Yoshisue K, Kuwata K, Komuro M, Ohta S, Nagayama S. Involvement of concentrative nucleoside transporter 1 in intestinal absorption of Trifluorothymidine, a novel antitumor nucleoside, in rats. *J. Pharmacol. Exp. Ther.* **2012**;340(2):457-62.
407. Pouremad R, Bahk KD, Shen Y-J, Knop RH, Wyrwicz AM. Quantitative ¹⁹F NMR study of trifluorothymidine metabolism in rat brain. *NMR Biomed.* **1999**;12(6):373-80.

408. Santi DV, Sakai TT. Thymidylate synthetase. Model studies of inhibition by 5-trifluoromethyl-2'-deoxyuridylic acid. *Biochemistry*. **1971**;10(19):3598-607.
409. Temmink OH, Hoebe EK, van der Born K, Ackland SP, Fukushima M, Peters GJ. Mechanism of trifluorothymidine potentiation of oxaliplatin-induced cytotoxicity to colorectal cancer cells. *Br. J. Cancer*. **2007**;96(2):231-40.
410. Fujiwara Y, Heidelberger C. Fluorinated pyrimidines: XXXVIII. The incorporation of 5-trifluoromethyl-2'-deoxyuridine into the deoxyribonucleic acid of Vaccinia Virus. *Mol. Pharmacol*. **1970**;6(3):281-91.
411. Fujiwara Y, Oki T, Heidelberger C. Fluorinated pyrimidines: XXXVII. Effects of 5-trifluoromethyl-2'-deoxyuridine on the synthesis of deoxyribonucleic acid of mammalian cells in culture. *Mol. Pharmacol*. **1970**;6(3):273-80.
412. Sakamoto K, Yokogawa T, Ueno H, Oguchi KEI, Kazuno H, Ishida K, Tanaka N, Osada A, Yamada Y, Okabe H, Matsuo K. Crucial roles of thymidine kinase 1 and deoxyUTPase in incorporating the antineoplastic nucleosides trifluridine and 2'-deoxy-5-fluorouridine into DNA. *Int. J. Oncol*. **2015**;46(6):2327-34.
413. Suzuki N, Nakagawa F, Nukatsuka M, Fukushima M. Trifluorothymidine exhibits potent antitumor activity via the induction of DNA double-strand breaks. *Exp. Ther. Med*. **2011**;2(3):393-7.
414. Dexter DL, Wolberg WH, Ansfield FJ, Helson L, Heidelberger C. The clinical pharmacology of 5-trifluoromethyl-2'-deoxyuridine. *Cancer Res*. **1972**;32(2):247-53.
415. Heidelberger C, King DH. Trifluorothymidine. *Pharmacol. Ther*. **1979**;6(3):427-42.
416. Carmine AA, Brogden RN, Heel RC, Speight TM, Avery GS. Trifluridine: A review of its antiviral activity and therapeutic use in the topical treatment of viral eye infections. *Drugs*. **1982**;23(5):329-53.
417. Temmink OH, Emura T, De Bruin M, Fukushima M, Peters GJ. Therapeutic potential of the dual-targeted TAS-102 formulation in the treatment of gastrointestinal malignancies. *Cancer Sci*. **2007**;98(6):779-89.
418. Fukushima M, Suzuki N, Emura T, Yano S, Kazuno H, Tada Y, Yamada Y, Asao T. Structure and activity of specific inhibitors of thymidine phosphorylase to potentiate the function of antitumor 2'-deoxyribonucleosides. *Biochem. Pharmacol*. **2000**;59(10):1227-36.
419. Temmink OH. Role of thymidine phosphorylase / platelet derived endothelial cell growth factor inhibition in the cytotoxicity of fluoropyrimidines. Amsterdam, The Netherlands: VU University Medical Center; **2007**.
420. Doi T, Ohtsu A, Yoshino T, Boku N, Onozawa Y, Fukutomi A, Hironaka S, Koizumi W, Sasaki T. Phase I study of TAS-102 treatment in Japanese patients with advanced solid tumours. *Br. J. Cancer*. **2012**;107(3):429-34.
421. Yoshino T, Mizunuma N, Yamazaki K, Nishina T, Komatsu Y, Baba H. TAS-102 monotherapy for pretreated metastatic colorectal cancer: a double-blind, randomised, placebo-controlled phase 2 trial. *The Lancet Oncology*. **2012**;13(10):993-1001.
422. Mayer RJ, Van Cutsem E, Falcone A, Yoshino T, Garcia-Carbonero R, Mizunuma N, Yamazaki, K, Shimada, Y, Tabertero, J, Komatsu, Y, Sobrero, A, Boucher, E, Peeters, M, Tran, B, Lenz, H-J, Zaniboni, A, Hochster, H, Cleary, JM, Prenen, H, Benedetti, F, Mizuguchi, H, Makris, L, Ito, M, Ohtsu, A. Randomized trial of TAS-102 for refractory metastatic colorectal cancer. *New Engl. J. Med*. **2015**;372(20):1909-19.
423. Temmink OH, Bijnsdorp IV, Prins H-J, Losekoot N, Adema AD, Smid K, Honeywell RJ, Ylstra B, Eijk PP, Fukushima M, Peters GJ. Trifluorothymidine resistance is associated with decreased thymidine kinase and equilibrative nucleoside transporter expression or increased secretory phospholipase A2. *Mol. Cancer Ther*. **2010**;9(4):1047-57.
424. Vande Voorde J, Liekens S, McGuigan C, Murziani PGS, Slusarczyk M, Balzarini J. The cytostatic activity of NUC-3073, a phosphoramidate prodrug of 5-fluoro-2'-deoxyuridine, is independent of activation by thymidine kinase and insensitive to degradation by phosphorolytic enzymes. *Biochem. Pharmacol*. **2011**;82(5):441-52.
425. De Bruin M, Van Capel T, Smid K, Fukushima M, Hoekman K, Pinedo HM, Peters GJ. The effect of fluoropyrimidines with or without thymidine phosphorylase inhibitor on the expression of thymidine phosphorylase. *Eur. J. Pharmacol*. **2004**;491(2-3):93-9.

426. Lee H, Oh S, Lee E, Chung J, Kim Y, Ryu J-S, Kim SY, Lee SJ, Moon DH, Kim TW. Positron emission tomography imaging of human colon cancer xenografts in mice with [^{18}F]fluorothymidine after TAS-102 treatment. *Cancer Chemoth. Pharm.* **2015**;75(5):1005-13.
427. Armstrong DK, Isaacs JT, Ottaviano YL, Davidson NE. Programmed cell death in an estrogen-independent human breast cancer cell line, MDA-MB-468. *Cancer Res.* **1992**;52(12):3418-24.
428. Bronckaers A, Balzarini J, Liekens S. The cytostatic activity of pyrimidine nucleosides is strongly modulated by Mycoplasma hyorhinis infection: Implications for cancer therapy. *Biochem. Pharmacol.* **2008**;76(2):188-97.
429. Emura T, Suzuki, N., Yamaguchi, M., Ohshimo, H., Fukushima, M. A novel combination antimetabolite, TAS-102, exhibits antitumor activity in FU-resistant human cancer cells through a mechanism involving FTD incorporation in DNA. *Int. J. Oncol.* **2004**;25(3):571-8.
430. Congiatu C, Brancale A, McGuigan C. Molecular modelling studies on the binding of some protides to the putative human phosphoramidase Hint1. *Nucleos. Nucleot. Nucl.* **2007**;26(8-9):1121-4.
431. Hobden JA, Kumar M, Kaufman HE, Clement C, Varnell ED, Bhattacharjee PS. In vitro synergism of trifluorothymidine and ganciclovir against HSV-1. *Invest. Ophthalm. Vis. Sci.* **2011**;52(2):830-3.
432. Woster P. Foye's Principles of Medicinal Chemistry. Chapter 38. Antiviral agents and protease inhibitors. 7th ed **2013**.
433. Cobb SL, Murphy CD. ^{19}F NMR applications in chemical biology. *J. Fluorine Chem.* **2009**;130(2):132-43.
434. Mounné R, Pasco M, Prost E, Lecourt T, Micouin L, Tisné C. Fluorinated diaminocyclopentanes as chiral sensitive NMR probes of RNA structure. *J. Am. Chem. Soc.* **2010**;132(38):13111-3.
435. Kreutz C, Kählig H, Konrat R, Micura R. A general approach for the identification of site-specific RNA binders by ^{19}F NMR spectroscopy: proof of concept. *Angew. Chem. Int. Ed.* **2006**;45(21):3450-3.
436. Jud L, Košutić M, Schwarz V, Hartl M, Kreutz C, Bister K, Bister K, Micura R. Expanding the scope of 2'-SCF₃ modified RNA. *Chemistry-Eur. J.* **2015**;21(29):10400-7.
437. Košutić M, Jud L, Da Veiga C, Frener M, Fauster K, Kreutz C, Ennifar, E, Micura R. Surprising base pairing and structural properties of 2'-Trifluoromethylthio-modified ribonucleic acids. *J. Am. Chem. Soc.* **2014**;136(18):6656-63.
438. Fauster K, Kreutz C, Micura R. 2'-SCF₃ Uridine-a powerful label for probing structure and function of RNA by ^{19}F -NMR spectroscopy. *Angew. Chem. Int. Ed.* **2012**;51(52):13080-4.
439. Egli M, Minasov G, Tereshko V, Pallan PS, Teplova M, Inamati GB, Lesnik EA, Owens SR, Ross BS, Prakash TP, Manoharan M. Probing the influence of stereoelectronic effects on the biophysical properties of oligonucleotides: comprehensive analysis of the RNA affinity, nuclease resistance, and crystal structure of ten 2'-O-ribonucleic acid modifications. *Biochemistry.* **2005**;44(25):9045-57.
440. Iltzsch MH, Uber SS, Tankersley KO, el Kouni MH. Structure-activity relationship for the binding of nucleoside ligands to adenosine kinase from Toxoplasma gondii. *Biochem. Pharmacol.* **1995**;49(10):1501-12.
441. Covès J, Le Hir de Fallois L, Le Pape L, Décout JL, Fontecave M. Inactivation of Escherichia coli ribonucleotide reductase by 2'-deoxy-2'-mercaptouridine 5'-diphosphate. Electron paramagnetic resonance evidence for a transient protein perthiyl radical. *Biochemistry.* **1996**;35(26):8595-602.
442. Reichard P. Interactions between deoxyribonucleotide and DNA synthesis. *Annu. Rev. Biochem.* **1988**;57(1):349-74.
443. Robins MJ, Samano MC, Samano V. Ribonucleotide reductase targets for chemotherapy; mechanistic aspects and biologically active agents. *Nucleos. Nucleot.* **1995**;14(3-5):485-93.

444. Robins MJ. Mechanism-based inhibition of ribonucleotide reductases: new mechanistic considerations and promising biological applications. *Nucleos. Nucleot.* **1999**;18(4-5):779-93.
445. Roy B, Chambert S, Lepoivre M, Aubertin A-M, Balzarini J, Décout J-L. Deoxyribonucleoside 2'- or 3'-mixed disulfides: prodrugs to target ribonucleotide reductase and/or to inhibit HIV reverse transcription. *J. Med. Chem.* **2003**;46(13):2565-8.
446. Imazawa M, Ueda T, Ukita T. Synthesis of 2'-deoxy-2'-mercaptouridine. *Tetrahedron Lett.* **1970**;11(55):4807-10.
447. Imazawa M, Ueda T, Ukita T. Nucleosides and Nucleotides. XII. Synthesis and properties of 2'-deoxy-2'-mercaptouridine and its derivatives. *Chem. Pharm. Bull. (Tokyo)*. **1975**;23(3):604-10.
448. Xu S, Held I, Kempf B, Mayr H, Steglich W, Zipse H. The DMAP-catalyzed acetylation of alcohols—a mechanistic study. *Chem.-Eur. J.* **2005**;11(16):4751-7.
449. Furukawa Y, Honjo M. A direct synthesis of 3', 5'-di-O-acetyl-O², 2'-cycloouridine. *Chem. Pharm. Bull. (Tokyo)*. **1968**;16(11):2286-8.
450. Kieltsch I, Eisenberger P, Togni A. Mild electrophilic trifluoromethylation of carbon- and sulfur-centered nucleophiles by a hypervalent Iodine(III)-CF₃ reagent. *Angew. Chem. Int. Ed.* **2007**;46(5):754-7.
451. Capone S, Kieltsch I, Flögel O, Lelais G, Togni A, Seebach D. Electrophilic S-trifluoromethylation of cysteine side chains in α - and β -Peptides: isolation of trifluoromethylated Sandostatin (Octreotide) derivatives. *Helv. Chim. Acta.* **2008**;91(11):2035-56.
452. Miller N, Fox JJ. Nucleosides. XXI. Synthesis of some 3'-substituted 2',3'-dideoxyribonucleosides of thymine and 5-methylcytosine. *J. Org. Chem.* **1964**;29(7):1772-6.
453. Cosstick R, Vyle J, Cosstick R, Vyle J. Synthesis and phosphorus sulfur bond-cleavage of 3'-thiothymidylyl-3',5'-thymidine. *J. Chem. Soc. – Chem. Comm.* **1988**; (15):992-3.
454. Reist EJ, Benitez A, Goodman L. The synthesis of some 5'-thiopentofuranosylpyrimidines. *J. Org. Chem.* **1964**;29(3):554-8.
455. Saito G, Swanson JA, Lee K-D. Drug delivery strategy utilizing conjugation via reversible disulfide linkages: role and site of cellular reducing activities. *Adv. Drug Del. Rev.* **2003**;55(2):199-215.
456. Caldarelli SA, Hamel M, Duckert J-F, Ouattara M, Calas M, Maynadier M, Wein S, Périgaud C, Pellet A, Vial HJ, Peyrottes S. Disulfide prodrugs of albitiazolium (T3/SAR97276): synthesis and biological activities. *J. Med. Chem.* **2012**;55(10):4619-28.
457. Butora G, Qi N, Fu W, Nguyen T, Huang H-C, Davies IW. Cyclic-disulfide-based prodrugs for cytosol-specific drug delivery. *Angew. Chem. Int. Ed.* **2014**;53(51):14046-50.
458. Vrudhula VM, MacMaster JF, Li Z, Kerr DE, Senter PD. Reductively activated disulfide prodrugs of paclitaxel. *Bioorg. Med. Chem. Lett.* **2002**;12(24):3591-4.
459. Johnson R, Reese CB, Zhang P-Z. Lability of glycosidic linkages of 2'-thio-ribonucleosides. *Tetrahedron.* **1995**;51(17):5093-8.
460. Singh Y, Palombo M, Sinko PJ. Recent trends in targeted anticancer prodrug and conjugate design. *Curr. Med. Chem.* **2008**;15(18):1802-26.
461. Zhang Q, He J, Zhang M, Ni P. A polyphosphoester-conjugated camptothecin prodrug with disulfide linkage for potent reduction-triggered drug delivery. *J. Mat. Chem. B.* **2015**;3(24):4922-32.
462. Gamcsik MP, Kasibhatla MS, Teeter SD, Colvin OM. Glutathione levels in human tumors. *Biomarkers.* **2012**;17(8):671-91.
463. Appenzeller-Herzog C. Glutathione- and non-glutathione-based oxidant control in the endoplasmic reticulum. *J. Cell Sci.* **2011**;124(6):847-55.
464. Le Hir de Fallois L, Decout J-L, Fontecave M. Synthesis of 2'-thio-uridine and -cytidine derivatives as potential inhibitors of ribonucleoside diphosphate reductase: thionitrites, disulfides and 2'-thiouridine 5'-diphosphate. *J. Chem. Soc., Perkin Trans. 1.* **1997**(17):2587-96.
465. Gerland B, Désiré J, Balzarini J, Décout J-L. Anti-retroviral and cytostatic activity of 2',3'-dideoxyribonucleoside 3'-disulfides. *Bioorg. Med. Chem.* **2008**;16(14):6824-31.

466. Lukesh JC, Palte MJ, Raines RT. A potent, versatile disulfide-reducing agent from aspartic acid. *J. Am. Chem. Soc.* **2012**;134(9):4057-9.
467. Govindaraj RG, Manavalan B, Lee G, Choi S. Molecular modeling-based evaluation of hTLR10 and identification of potential ligands in toll-like receptor signaling. *PLoS ONE.* **2010**; 5(9):e12713.
468. Endrizzi JA, Breddam K, Remington SJ. 2.8 A structure of yeast serine carboxypeptidase. *Biochemistry.* **1994**;33(37):11106-20.
469. Korb O, Stütze T, Exner TE. An ant colony optimization approach to flexible protein–ligand docking. *Swarm Intell.* **2007**;1:115-134.
470. Dey S, Garner P. Synthesis of *tert*-butoxycarbonyl (Boc)-protected purines. *J. Org. Chem.* **2000**;65(22):7697-9.
471. Chen L, Sheppard T. Synthesis and hybridization properties of RNA containing 8-chloroadenosine. *Nucleos. Nucleot. Nucl.* **2002**;21(8-9):2002.
472. Ogilvie KK, Beaucage SL, Schiffman AL, Theriault NY, Sadana KL. The synthesis of oligoribonucleotides. II. The use of silyl protecting groups in nucleoside and nucleotide chemistry. *Can. J. Chem.* **1978**;56(21):2768-80.
473. Meyer J-P, Probst KC, Trist IML, McGuigan C, Westwell AD. A novel radiochemical approach to 1-(2'-deoxy-2'-[¹⁸F]fluoro-β-d-arabinofuranosyl)cytosine (¹⁸F-FAC). *J. Labelled Compd. Radiopharm.* **2014**;57(11):637-44.